Green Energy and Technology

Miguel A. Sanz-Bobi *Editor*

Use, Operation and Maintenance of Renewable Energy Systems

Experiences and Future Approaches

Springer

Green Energy and Technology

For further volumes:
http://www.springer.com/series/8059

Miguel A. Sanz-Bobi
Editor

Use, Operation and Maintenance of Renewable Energy Systems

Experiences and Future Approaches

Springer

Editor
Miguel A. Sanz-Bobi
ICAI School of Engineering
Comillas Pontifical University
Madrid
Spain

ISSN 1865-3529 ISSN 1865-3537 (electronic)
ISBN 978-3-319-03223-8 ISBN 978-3-319-03224-5 (eBook)
DOI 10.1007/978-3-319-03224-5
Springer Cham Heidelberg New York Dordrecht London

Library of Congress Control Number: 2014939041

Printed on acid-free paper

Springer is part of Springer Science+Business Media (www.springer.com)

To my wife Holly and my sons Miguel A. and Manuel I.

Preface

The aim of this book is to put the reader in contact with real experiences, current and future trends in the context of the use, exploitation and maintenance of renewable energy systems around the world. Today the constant increase of production plants of renewable energy is guided by important social, economical, environmental and technical considerations. The substitution of traditional methods of energy production is a challenge in the current context. New strategies of exploitation, new uses of energy and new maintenance procedures are emerging naturally as isolated actions for solving the integration of these new aspects in the current systems of energy production. This book puts together different experiences in order to be a valuable instrument of reference to take into account when a system of renewable energy production is in operation.

Part I of the book is focused on different aspects about the operation and maintenance of renewable energy systems, and in particular, attention is paid to systems that produce electrical energy by wind, sun and biogas because these are the most extended types of plants using a renewable source of energy. Current practices of operation and maintenance at these plants will be described in order to know strategies for a better use of their life cycle.

"Condition Monitoring and Maintenance Methods in Wind Turbines" presents a review of the main principles supporting different strategies of maintenance. Later, a framework is presented which is able to integrate different aspects related to the life of a wind turbine. In particular, a method is proposed for the detection of abnormal behaviour with respect to the normal behaviour expected and a procedure to obtain failure mode risk indicators that can help apply maintenance in wind turbines precisely when it is needed. This will contribute to a better use of the life cycle of the wind turbines in a wind farm.

"Operation and Maintenance Methods in Solar Power Plants" describes the fundamentals about the operation and maintenance in solar power plants. In these plants, Operation and Maintenance (O&M) is becoming more and more important for improving the performance of the plant. Most of the solar power plants are located in remote places with unreliable communication infrastructure. This makes it very difficult to diagnose and rectify problems in a timely manner. System operations and maintenance (O&M) is a broad area, and it is the continuing focus of several industry/government/national laboratory working groups. This chapter will review their main results.

"Biological Biogas" will review briefly the most significant part of the history of biogas. Here an overview of the microbial process will be provided covering some of the different types of digesters and looking at building, starting and operating a simple type of digester, including fault finding.

"Development, Operation, and Future Prospects for Implementing Biogas Plants: The Case of Denmark" describes different concepts of biogas technology as understood in a Danish context. It emphasises how energy from production of biogas is distributed, either as biogas to regional combined heat and power plants (CHP) or as district heating (DH) to small-scale local networks. The chapter provides an overview of the political situation and a historical outline of the development of the Danish biogas sector, and it presents the biogas process and operational aspects. The chapter ends with a discussion of biogas in both global and European contexts.

"Operation and Maintenance Contracts for Wind Turbines" addresses the fundamental negotiating issues of wind turbine O&M contracts. It includes a conceptual mathematical framework to support the analysis and design of O&M contracts. This will make it possible to investigate mechanisms through which incentives perceived by O&M contractors can be aligned with the objectives of wind farm owners over both the short and the long terms.

Part II of the book addresses how new renewable energy systems can be integrated with traditional methods of energy production, and also, with a new smart environmental use of energy. Within this perspective the hybridation of systems must be considered.

"Grid Integration of Wind Power Generation" discusses how generator technology affects grid integration of wind generation. Wind generators based on squirrel cage and doubly fed induction machines and multi-pole synchronous machines will be reviewed. The performance with respect to stability, load frequency and reactive power–voltage control is discussed.

"Control Methods Applied in Renewable Energy Systems" introduces the control methods used in renewable energy sources. The control methods of power electronics used in renewable energy sources such as solar, wind, and fuel cells are comprehensively explained through the different sections of the chapter. The required circuit topologies of current control methods are explained with grid-connected and island-mode operations of a solar energy system. The rest of the chapter consists of a discussion concerning renewable energy systems based on wind turbines and fuel cells.

"Low-Cost Hybrid Systems of Renewable Energy" is focused on research and development of low cost technologies for attending small and medium energetic demands. The results of such development are related to the use of hybrid systems combining different sources of renewable energy. To obtain the lowest cost of a system it is necessary to obtain the smallest cost in each one of their parts and a better control strategy that integrates the operation of these parts. In this chapter the constituent elements of a hybrid system will be presented along with different technological alternatives. Also control strategies will be presented in order to obtain the maximum efficiency of these elements and connection arrangements.

"Design for Reliability of Power Electronics in Renewable Energy Systems" is focused on the design of reliability of power electronics in renewable energy systems. Typically power electronics are designed for 20–25 years of operation and in order to do this it is crucial to know about mission profile of the power electronics technology as well as how the technology is loaded in terms of temperature and other stressors relevant for lifetime prediction. Hence, this chapter will show the basic power electronics technology for renewable energy systems, describe the mission profile of the technology and demonstrate how the power electronics is loaded for different stressors. Further, some systematic methods to design the power electronics technology for reliability will be given and demonstrated with two cases—one is a wind turbine and another one is a photovoltaic application.

Part III of the book is oriented to describing some experiences about the use of energy coming from renewable energy sources in different fields of industry and society. This is a point of increasing interest that is constantly changing and which future trends show will play a main role in how society uses energy.

"Use of Renewable Energy Systems in Smart Cities" addresses the use of renewable energy systems on a small scale, oriented to distributed generation for households or districts, integrated in a smart city. In this context, the main renewable energies and companion technologies are reviewed, and their profitability investigated to highlight their current economic feasibility. A simplified architecture for the development of a smart city is presented, consisting of three interconnected layers: the intelligence layer, the communication layer and the infrastructure layer.

"Analysis of the Impact of Increasing Shares of Electric Vehicles on the Integration of RES Generation" analyses the medium-term operation of a power system in several future scenarios that differ according to the level of use of electric vehicles and how renewable energy sources can be safely integrated into them. The analysis is performed using different vehicle charging strategies (namely dumb, multi-tariff and smart).

The analysis is based on results produced by an operation model of the electric power system where the charging of electric vehicles is being considered. Vehicles are regarded as additional loads whose features depend on a mobility pattern. The operation model employed is a combination of an optimisation-based planning problem used to determine the optimal day-ahead system operation and a Monte Carlo simulation to consider the stochastic events that may happen after the initial planning step.

Contents

Part I
Operation and Maintenance

Condition Monitoring and Maintenance Methods in Wind Turbines

Rodrigo J. A. Vieira and Miguel A. Sanz-Bobi

Abstract Wind is an attractive source of renewable energy, and its use has become increasingly important over the last decades all around the world. After this explosion of installations of wind farms, an important concern has arisen concerning several topics in which the goals are to keep the value of the assets of the wind farms and to guarantee long life cycles. The continuous monitoring of the life of the wind turbines and a correct application of maintenance plan contribute to achieving these goals. This chapter first reviews the main principles supporting different strategies of maintenance, later a framework is presented integrating different aspects of the lives of the wind turbine, and finally some methods for the detection of abnormal behavior in wind turbines and for failure risk evaluation are presented applied to some real cases.

1 Introduction

Wind is an attractive source of energy, as can be seen by the growing number of installed wind farms all over the world and the future trends of new installations over the coming years [35, 41]. Furthermore, asset management is gaining attention from different perspectives in industry, including wind energy, due to the competitive context where current businesses are being developed. Of increasing interest in industry is the integration of information coming from different departments of a company, such as operation and maintenance, during the application of reliability-centered maintenance (RCM) techniques, the application of prediction techniques, and other new emerging proposals, to better reach objectives in asset management [134, 149, 169].

R. J. A. Vieira · M. A. Sanz-Bobi (✉)
Institute for Research in Technology, Comillas Pontifical University, Madrid, Spain
e-mail: masanz@upcomillas.es

M. A. Sanz-Bobi (ed.), *Use, Operation and Maintenance of Renewable Energy Systems*, Green Energy and Technology, DOI: 10.1007/978-3-319-03224-5_1,

The cost-effective and efficient use of available assets is crucial in the current context, due to the competitive framework where current businesses are being developed. Asset management techniques are being extended to all segments of the power industry: generation, transmission, and distribution. All these strategies require information about the life of the assets in order to make decisions for future use. In the context of power systems, many approaches have been developed throughout the last decades to analyze different aspects of the life of the equipment or assets used in the operation. Maximizing the life span of the asset is one of the measures currently being analyzed and applied in this field. Maintaining the asset when required helps to guarantee that this maximization is achieved.

New engineering systems are becoming increasingly complex and subject to more severe working conditions to reach the new operation demand and to respond to the required quality levels.

The need for having systems with higher levels of quality and low costs causes the development of equipment with new technologies and new maintenance strategies that enable the operation of these increasingly complex systems to address this growing demand.

These systems are composed of various components that work together in order to accomplish the mission of the system. This mission must be fulfilled in the best possible way, i.e., with high levels of efficiency, so as to ensure the "proper functioning" of the system. Much of this responsibility is attributed to the maintenance.

Maintaining a good efficiency and system conditions over a long period of time, in good health and with a minimal risk of failure, is a challenge. This involves having a system capable of detecting incipient failures, assessing the current health of the system, predicting its remaining useful life (RUL), and being suitable for launching maintenance actions when they are actually necessary.

Many maintenances methodologies have been developed over the past several years with the primary objective of maintaining the proper functioning of a system and/or component. Each has its merits, but in general, they focus primarily on internal features of the system or component under study, i.e., only directly related to their work environment factors.

The wind energy industry has long been adopting maintenance methods which typically focus on corrective maintenance, i.e., when a fault occurs, repairs, and preventive maintenance to be performed at fixed time intervals. More recently, predictive maintenance, that is, using data from monitoring or inspections to determine the best moment to perform maintenance actions, is being incorporated into the maintenance plans.

Preventive maintenance actions have a direct impact on the availability and reliability of equipment or components (e.g., gearboxes and generators) by improving their health condition or prolonging their life. All maintenance involves a cost and a benefit to consider. Maintenance is profitable when the cost outweighs the potential cost associated with the occurrence of a fault that it attempts to prevent.

For maintenance planning over short and medium terms, the vast majority do not consider working conditions to which the component was subjected throughout

its life, but rather plan their actions based on the occurrence of faults and repair actions made in the past.

Furthermore, it should also be noted that in recent years, the increasing application of continuous monitoring systems prompted the development of various diagnostic techniques. These techniques try to verify certain parameters and then analyze the possibility of a component failure in its current condition or with an estimated evolution. For that reason, there must be a history of failures with enough information to apply some statistical and probabilistic techniques that enable the diagnosis and identification of such unavailability.

For systems that do not have adequate and sufficient historical failure, physical models capable of simulating the behavior of an industrial process or component may be used. Such models can collect various effects and analyze the possible response of a component or manufacturing process to a solicitation or an event of a different nature. Physical models are very useful both in the design phase and the production phase, once failures have occurred and there is a need to investigate how they occurred.

At present, physical models are not being used continuously, and nor are they automatically embedded into a process of industrial diagnosis, but only when it is necessary to analyze specific aspects of behavior. One reason for this may be first noted by the absence of a methodology of failure diagnosis and evaluation of health condition using these physical models in an integrated way. Another reason is that these models have to be able to get results in a short enough time to make decisions before the situation has already changed and/or cannot be avoided or the impact of a failure reduced.

On the other hand, there are effective models to detect anomalies in real time. These models require prior knowledge of normal behavior situations or the absence of failure modes. These models are very useful to anticipate possible failure modes, diagnose the causes of anomalies, and even adjust the maintenance plan to the actual needs of the equipment or industrial processes according to its real life during process operation.

However, these models would be even more useful in addition to detecting the anomaly, if they could make a forecast of the effect over the short and medium terms that an anomaly would have in a component or industrial process. If this forecast could be made in real (or near real) time, processes recommendations could be made more efficient for the people in charge of production.

In this sense, observing the currently existing standards related to the topic, it can be concluded that areas such as data acquisition, signal processing, condition monitoring, and diagnostics are sufficiently developed [100]. In contrast, it is now time to concentrate research in the areas of forecasting and decision-making [9]. To achieve the objective of increasing investments in predictive intelligence techniques, maps are designed from relationships between variations in product quality and equipment degradation processes [77]. Furthermore, analysis of degradation should consider the work environment in which the equipment is inserted along their life cycle to make appropriate predictions [142].

On the other hand, it would be appropriate that maintenance methodologies were integrated with an asset management system to help in the decision-making process and thus perform maintenance actions more efficiently not only from the maintenance engineering point of view, but also from the "general system management" point of view, i.e., assessing associated risks, reducing costs, prolonging the life of the assets, and in the end providing a high-quality service and reliability [12, 134, 145]. However, strategies for the integration of all of this information are being developed, and the existing ones are being improved.

2 The Maintenance: A Review

This section presents a summarized review of the main maintenance concepts and applications in the field of wind turbines.

2.1 Asset Management in the Maintenance Context

"Maintenance" is defined as the combination of all technical, administrative, and managerial actions during the life cycle of an asset in order to "keep" or "to restore" the status that allows it to run the function for which it was designed [38]. Thus, it is very important that maintenance is integrated into the overall system management (asset management), i.e., to consider the impact of their decisions on the operational and financial management of the asset.

An asset can be defined as a unique and identifiable element or a group of elements that has a financial value and against which maintenance actions are performed. Asset management is the ability to model and compare operational, maintenance, and financing alternatives in order to find a global solution for the system. This solution must meet the required conditions of the system and look for the best trade-off between costs and benefits [59, 110].

In Fig. 1, the "asset life management wheel" is shown, where it can be observed the different areas (operation, maintenance, financial, quality, etc.) of an industrial asset with its different levels (execution and decision-making). From an input (system resources), the industrial asset generates or produces a product or service (system function output) plus some residues, e.g., in a thermo-electric power plant from the fuel (gas, oil, etc.), is expected to generate electrical energy and some residues such as smoke.

"Asset efficiency" is directly related to the well-being of the system function and the right balance between the resources inputs and outputs. All the different asset areas work (sometimes independently and sometimes together) to achieve the maximum system efficiency, centered on the asset needs.

Furthermore, in Fig. 1, two "data or communication rings" are highlighted. One ring is accessible by all (system data ring), and the other (general system data

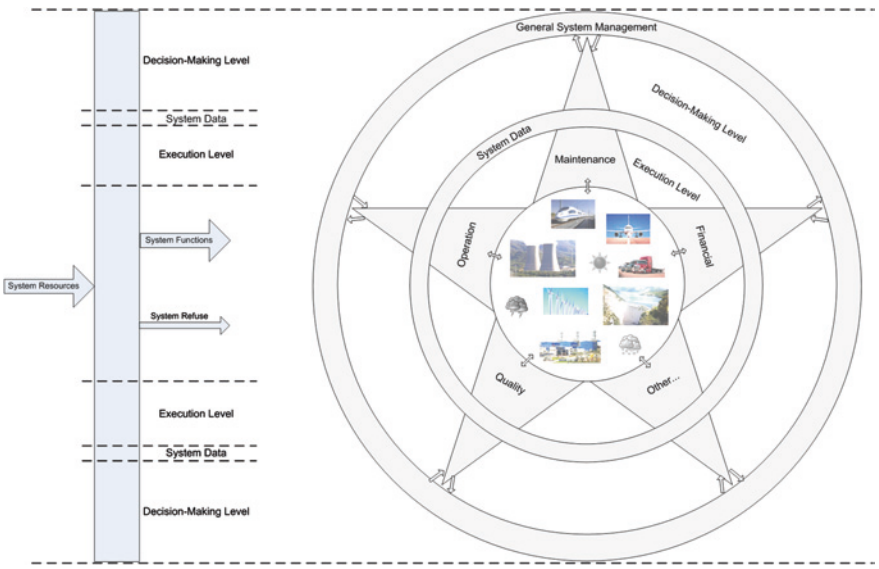

Fig. 1 Asset life management wheel

management ring) is only accessible by the senior managers of each area. In the ring are available storage system information and data. In the second ring, there is only shared strategic information related to the system/asset management within the environment in which it is inserted and where it acts.

Asset management and maintenance management represent a complex business area, including and requiring different processes and the integration of a wide range of knowledge (from technical and management to information and communication technologies, philosophies, management strategies, etc.) to provide an effective and satisfactory service to its customers. Over the last years, this integration is becoming more complex by increasing the amount of information to be processed [29].

The field of asset management is becoming increasingly professional. Knowledge related to the "practical application" of asset management exists in literature. However, this knowledge is less developed when compared to other areas [150]. Moreover, some models could be found in literature to formalize the knowledge and asset management practices, but sparingly and with only partial coverage of the very extensive and deep topic of asset management [56].

Asset management is nowadays a new and growing part of industry [128]. One of the facts that contributes to its growth is that asset management is witnessing the proliferation of various software [148], but each one is an independent solution within their expertise area (strategic planning, evaluation of the asset condition, inventory, etc.). Furthermore, not many software packages have been found with the potential ability to integrate data throughout the asset management cycle [57, 81, 114].

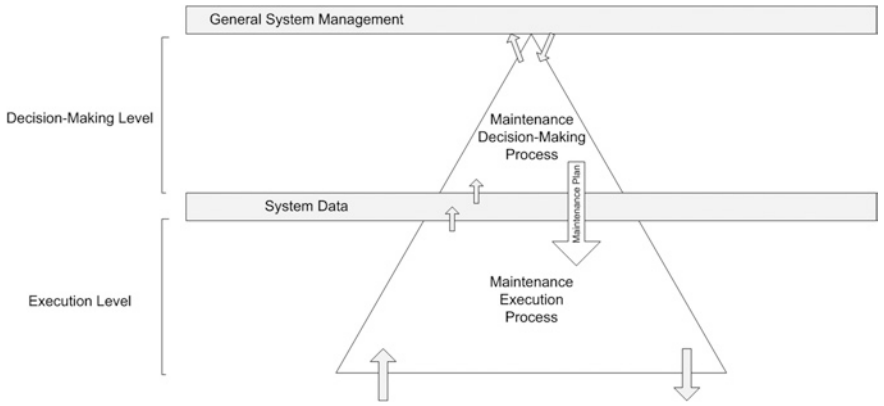

Fig. 2 General maintenance process

2.2 Maintenance Decision-Making Process Classification

Literature and maintenance-related knowledge can be found in the state of the art, according to different classifications proposed in some references such as [34, 48, 116, 146, 157]. These classifications are generally very long and complex; however, they are limited because in the end they cannot be easily applied to all literature related to maintenance.

In this section, a new maintenance process classification is proposed, supported by concepts related to asset management, i.e., according to the decision level that each method aims to address or contribute. Thus, the maintenance process is divided into two distinct parts (see Fig. 2), being one related to the execution process and the other related to the decision-making process in the same way as presented in other areas of the asset (system) in Fig. 1.

The "execution of maintenance" has the function to carry out the maintenance plan defined for the asset, i.e., it is the "physical" part referred to as the maintenance infrastructure (people, parts, working tools, etc.).

The other part is the maintenance decision-making process where three participation levels will be considered (described in detail in Sects. 2.3, 2.4, and 2.5): Maintenance Preprocessing, Maintenance Strategies, and Maintenance Management (Fig. 3).

This figure highlights the different levels of abstraction and interpretation of knowledge needed in the maintenance decision-making process, where the data represent the lowest level of interpretation or meaning in these levels. After the beginning of the interpretation process, the data are considered to be "information" and therefore knowledge.

The first level of the maintenance process in this classification is defined as maintenance pre-processing. The overall objective of this level is the conversion

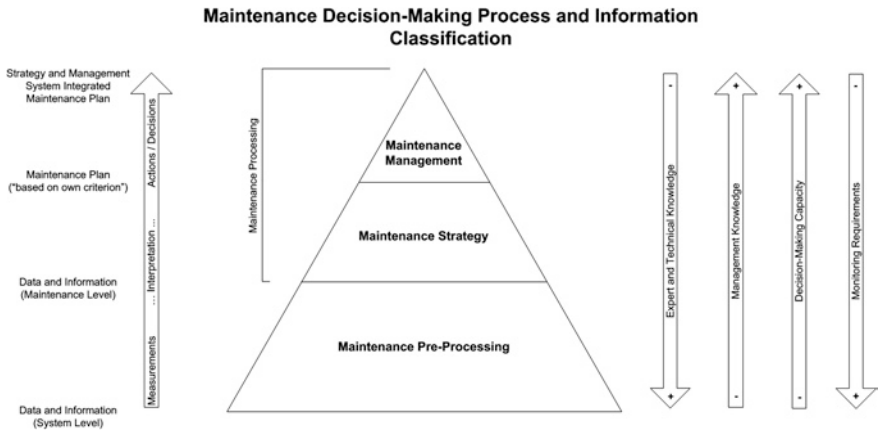

Fig. 3 Maintenance decision-making process

of the information or data available in the system to "treated" information to be used for the second level of this classification (maintenance strategies). In general, the methods are based on standard models or "expert" techniques supporting the maintenance strategies without the objective of making decisions with regard to the maintenance plan.

The other proposed classification level is called maintenance strategies, which are methodologies able to create and/or optimize a maintenance plan for the overall system using as input the information from the maintenance pre-processing level. At this level, the maintenance actions are planned and prioritized according to the criteria of each strategy.

The last classification level is formed by the support structures and methodologies in maintenance management that are responsible for integrating the proposed decisions from the maintenance strategies within them and with the restrictions and guidelines of the system. The final result of this level will be a maintenance plan set to the general interests of the system (operational, maintenance, financial, etc.) giving decision-making support within the asset management philosophy.

In Fig. 4, the three levels are presented in detail within the system structure. Thus, it is clear that the maintenance process of decision-making shall be as "final product" a maintenance plan integrated with the guidelines and strategies of the overall system. This maintenance plan, obtained from all available information in the system, will be executed by the other part of the maintenance process (execution level) shown in Fig. 2 and responsible for its implementation.

The following Sects. 2.3, 2.4, and 2.5 are three maintenance decision-making levels with the aim of defining the frontiers of knowledge as presented in the related literature and thus clarifying the main weaknesses, limitations, and future development trends.

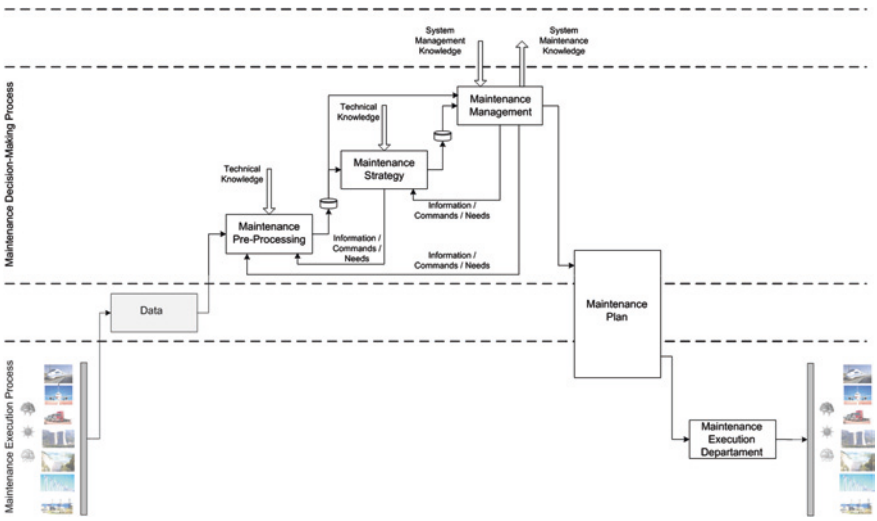

Fig. 4 Maintenance decision-making process (in detail)

2.3 Maintenance Preprocessing

Preprocessing maintenance plays a key role in the structure of maintenance planning and serves as a source of information (and treatment thereof) of all the following steps. This preprocessing is almost entirely made based on models and theories developed in several areas that are not actually part of maintenance. However, for a "complete" maintenance planning and with views over the operation of the system, the maintenance decision-making process must be ready to use all information in an efficient and integrated manner.

Some of the main models and theories used in maintenance preprocessing found in the literature are as follows: assessment and analysis of performance, efficiency, effectiveness, optimization, simulation, evaluation of criticality, cost, decision-making support, data transmission and storage, signal processing, condition monitoring, system diagnosis, anomaly detection, fault diagnosis, system prognosis, fault prognosis, system performance measurement, maintenance outsourcing performance evaluation, maintenance productivity index, life cycle cost analysis, reliability analysis, critical path method, failure root cause analysis, risk number probability, and balanced scorecard [1, 7, 14, 15, 18, 20, 50, 52, 62, 67–69, 75, 80, 86, 88, 94, 102, 118, 120, 140, 151–153, 158]. In general, the main functions of these models add value to the available information to be used by maintenance strategies and structures presented in the two upcoming sections.

From the analysis of the data from the events history (i.e., faults occurred and maintenance actions performed), mathematical models can be proposed, usually based on failure and repair rates.

Mathematical models are often used to obtain quantitative information of the component and to be able to associate reliability and maintenance. Usually, they are applied in fault models and in the evaluation of the maintenance effects, using deterministic or probabilistic approaches [17, 39, 40].

Reliability models traditionally determine the values of average failure rates for all components. With this simplification, that is, using average values, useful results can be obtained (very acceptable reliability prediction) and the paramount requirement is substantially reduced. However, the use of the average failure rate of the components in system reliability models is always limited and potentially misleading, mainly for short-to-medium term maintenance planning.

One way to process information and data from the past (events history) and estimate the reliability of the components is through the use of life distribution models. Among the many ways to estimate some parameters and evaluate and analyze reliability, parametric methods (e.g., based on discrete or continuous statistical laws) and nonparametric can be pointed out [123].

Another manner which is also widespread and used as a tool for events data processing is through techniques of qualitative and quantitative reliability analysis, in order to better estimate not only the parameters of the isolated components, but also the whole system [123].

In this sense, ideally, the life of each type of equipment can be characterized by an equation that calculates the failure rate as a function of critical parameters. For example, one wind turbine could be characterized based on its age, brand, size, and power, through its failure history, maintenance history, and inspection results history, but in most cases, the number of failure occurrences of these components is too small to generate an accurate model, and other approaches should be sought, such as models based on the measurements history as references for decision-making over the short-to-medium term.

When discussing the main models for analysis and evaluation of reliability, it is also important to know the maintenance models (see Sect. 2.4), because beyond the probability of failure is the life expectancy of the equipment used in the maintenance parameter models. This question cannot be easily addressed, because there are several parameters that influence its behavior throughout its life that are necessary to know or estimate, such as aging rates [43, 139]. Maintenance mathematical modeling has usually focused on the development of perfect or imperfect preventive maintenance strategies. The basic objectives pursued by these models consist of finding the optimal time interval between preventive maintenance actions scheduled at a minimal cost [8, 93, 104, 106].

“Cost models” utilize system and maintenance models information plus restrictions and/or budget targets to optimize costs [93]. The “service quality models” try to assess impact factors based on the occurrence of unavailability over the service quality and use these factors to help in maintenance planning.

In addition, other studies can be performed based on data measurements (for example in “real time”), which consist of the analysis of data obtained “continuously,” e.g., from inspections, condition monitoring systems, or any other source of information, by which the component behavior could be evaluated according

to the operating conditions to which it was subjected, detection of anomalies, and estimation of their health condition.

Many companies perform regular inspections of their equipment and have knowledge to relate information from inspections with the failure risks [17]. The integration of this information with reliability models of components and maintenance models can improve the accuracy of system models and extend their ability to reflect the maintenance effects [96].

One source of information that is becoming more common is the use of sensors along with the application of monitoring techniques and fault detection in order to supervise monitoring components. Based on the development of a failure mode and effects analysis (FMEA), techniques have emerged to monitor some variables related to failure modes of some components under the heading of condition monitoring (CM), which has been used for several years, mainly highlighting techniques associated with measured vibration signals. Its execution usually depends on measurement systems to provide information and experts who operate the equipment, because they physically work near this equipment and can directly assess its condition [52].

The condition of the equipment is defined through the processing of information, in order to detect anomalies and/or assess their health condition. Various methods can be used for "fault detection and isolation (FDI)," based on analytical redundancy, such as are the "first principles," "feature extraction and pattern recognition," and the normal behavior models [33, 52, 111]. Also, the process of incipient fault detection proposed by Isermann [66] based on the parameter estimation through physical models and comparing their results with measured values stands out as being one of the first methods.

After this, "parity equations" appeared along with the methods based on state observers as the "Kalman filters" where the modeling is made in system state variables [51]. Chow and Willsky [27] propose a process for fault detection and identification, divided into two stages: residual generation and decision-making. In this first stage, the idea is characterized as analytical redundancy based on parity relations, where the residue is generated in different ways to check for abnormal behavior within the components. Normal behavior models could be used to create an effective FDI.

The "statistical models" also can be used as a tool for the detection of anomalies. There are several approaches in the literature [153], which highlight the "principal component analysis (PCA)," the "partial least squares (PLS)," and the analysis that use classifiers (e.g., "Bayes classifiers"). In general, these approaches use well-known statistical techniques such as time series analysis, analysis of variance, and Gaussian distributions for data processing.

The effectiveness of fault detection algorithms can be qualitatively analyzed through the probability of a false alarm and the speed with which a fault is detected. In other words, the quality of the fault detection depends on how accurate the algorithm is and the amount of time needed for processing [117]. Unfortunately, these factors are inversely proportional, that is, the more sophisticated computational algorithms expend more time. Then, it is necessary to make a compromise of these factors with the costs and acceptable tolerance levels of each process.

Some of the available techniques used require a release from the equipment, and continuous measurements cannot be performed with which the condition measured through them is observed between periods usually long where big conditions changes may be observed. Nowadays, significant progresses in the condition monitoring field are being done to better understand the condition and health of the components.

The use of "intelligence" in condition monitoring can reduce the need for staff within the operation and may also minimize the damage caused by the non-detection of incipient failures. For model development and the use of "smart" methods, it is very important to have a large quantity of operation data, in order to identify and extract work features. Among the references that apply neural networks in condition monitoring of electrical components, we can highlight [49, 144, 163].

However, it is important to say that in general, the techniques discussed until now use the measurements history and do not directly address maintenance. They address the analysis of some values of variables to detect an anomaly or failure and suggest a correction, that is, without making any maintenance planning. Because of this, the condition monitoring cannot be defined as a predictive maintenance technique. It is a tool that tries to detect the failure, "saying" if the component is right or wrong. The adoption of maintenance policies based on measured parameters, and also with the function of making the diagnosis of incipient faults and evaluating the health condition of the system components, became possible and necessary over recent years due to the development and large application of continuous monitoring systems in industrial facilities.

Thereby, model-based methods were developed and can be divided into white-box, gray-box, and black-box models. The latter are used when there is no physical knowledge to determine its structure (e.g., models using neural networks).

However, to use black-box models and model the normal behavior of industrial equipment, it is necessary to use the available physical knowledge for the selection of output variables representing the behavior and health of the components and of the input variables that reflect the working condition of these components and influence the output variables of the models.

A normal behavior model makes it possible to estimate the normal evolution of the output variable and comparing it with the real one. If the difference or residue is significantly elevated, the conclusion is that there is an anomaly. To conclude that the residue is significantly elevated, confidence bands are defined that assume there is an error under normal operating conditions. Furthermore, this confidence band of normal operation considers the possible dependence of the residue variance with the input vector as a result of, for example, significant differences in the component behavior under various operating conditions as well as different precision levels depending on the model input vector [126].

The process of "building" a normal behavior model is divided into two stages. In the first, the components and their significant variables are chosen based on knowledge of "experts" on the equipment or process, and in the second stage, the models are trained so that the error between the value of the variable estimated and the corresponding real value is minimized.

With normal behavior models, the assessed equipment condition could be defined in this chapter as the level of degradation or aging suffered throughout its operating life. The key advantage of the assessment of the health condition of the components lies in to know continuously in real time. The actual needs of maintaining this equipment are a key factor for any predictive maintenance strategy that intends to establish not only what maintenance should be implemented but also the optimal time for applying them.

Likewise and also based on certain measured parameters, "manual measurement models" can be used as supplemental manners to assess the health condition of the component. These models are general models based on physical principles, experimental testing, external knowledge, etc., and these models together with the normal behavior models can help in the decision-making related to the development of the maintenance plan.

The "prognostic models" are the most recent and also the most prominent nowadays in the literature. To Byington [19], prognosis is the ability to predict the future condition of a system based on a current diagnosis in available component operating data and fault history. By this definition, in order to forecast, it is necessary to have information (events and measurements) about the component's life. For [42, 83], the prognosis must extrapolate to the future the current component health state, taking into account the present working conditions and future asset use. The future work conditions will be defined in a scenario composed by the future evolution of the data that will influence the degradation processes, failures, and maintenance actions.

2.4 Maintenance Strategies

In this section, important maintenance strategies found in literature are presented, such as corrective, preventive, condition-based, opportunistic, focused-on-reliability, and production strategies, among others discussed in this document. Maintenance strategies are the "heart" of the maintenance planning process. They are responsible for defining the "maintenance actions" based on information obtained from the system and preprocessed (see Sect. 2.3), i.e., the questions "When, What, Who, Where, Why, and How" are the system interventions that should be executed or not, in order to keep the system functions "alive."

Maintenance work usually consists of checks, measurements, replacements, adjustments, and repairs to extend the useful life of the equipment and facilities to their maximum level. In this sense, there is a need to establish and plan the maintenance actions to be carried out on the components and then create a system maintenance plan.

These actions, whenever possible, should attack the components failure modes. The success of these actions depends largely on the definition of the time of execution of the action, the priority of this action (this refers to the importance of it to maintain the system "functionality," reduce costs, and increase the service quality),

and the desired reliability. These three features are defined as the maintenance criteria.

In the maintenance plan, each failure mode must be associated, as far as possible, to a maintenance action to try to avoid a failure mode. The definition of this maintenance action involves knowing, as previously mentioned, the maintenance criteria. From the failure mode identification to the definition of the maintenance criteria and maintenance scheduling, there is a path that must be followed. This path is neither easy nor short.

One of the maintenance objectives is to reduce the failure occurrence, increase the availability, and extend the system life (or at least in the mean time until the next failure). However, even in a perfect maintenance plan, there can be some failures, such as those due to design and manufacturing errors that cannot be avoided before they occur. In the case of wind turbines, the maintenance plan could be improved to a certain limit in order for the system ability to resist "overloads" and external conditions changes [43].

The essence of the approach "run-to-failure" or corrective maintenance is to replace the component with a new one when it is not able to perform its function. This is a traditional maintenance strategy of companies that is still surprisingly popular nowadays [55]. The failures occur even when maintenance is trying to avoid them, so a system will always have to run corrective maintenance actions in times of an emergency to correct them. The big disadvantage is that this type of maintenance involves high maintenance downtime, lower customer satisfaction, and unscheduled actions. However, depending on the importance of the component criticality and how serious the consequences of failure are, corrective maintenance may be the most economical solution among the maintenance strategies [10].

Preventive maintenance consists of periodic maintenance actions and the replacement of components, scheduled at regular time intervals, independent of component wear or if it still executes its function satisfactorily [55]. Preventive maintenance has introduced a way to perform maintenance in companies with a certain level of control in a way that allows for an adjustment of this planning with production scheduling. In addition to the definitions of maintenance intervals and the activities to be carried out, budgets can be estimated. In this sense, if the intervals are not adjusted to the actual needs of the system, the traditional preventive maintenance will lead to a "poor" or "excessive" maintenance. To determine these intervals is necessary to have system operation experience and to be able to answer some questions in order to generate the maintenance plan (Fig. 5). Garg and Deshmukh [48] present an extensive review of perfect and imperfect preventive maintenance models based on optimization methods, simulation, probabilistic, "intelligence," etc. Nevertheless, it is important to point out that even though a preventive maintenance plan is launched, it may not be possible to avoid all components failures.

Preventive maintenance scheduling could be done using several strategies described in the available literature. The most common are usually with a minimal cost targets that are based on the budget allocation for maintenance in accordance with the system priorities [39, 123].

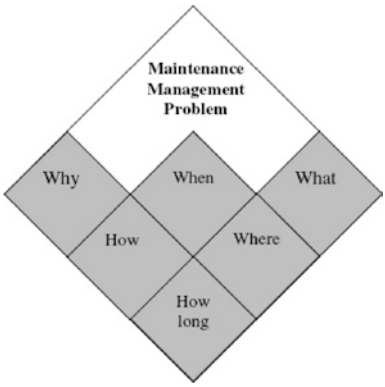

Fig. 5 Elements related to preventive maintenance actions Thomas et al. [143]

Many maintenance models have been proposed over a long period of time, normally centered on preventive maintenance models. One of the first well-known approaches [8] is based on performing preventive maintenance after a certain number of hours of continuous operation without failure or after a certain total number of hours, regardless of the number of intervening failures. Several preventive maintenance models were later proposed [36, 60, 71, 135]. These first maintenance models assume that the components, after preventive maintenance, were in conditions described either "as good as new" or "as bad as old." However, other maintenance models appeared, trying to be more realistic, where after a preventive maintenance action, the components' condition lies somewhere between "as good as new" and "as bad as old." These more realistic models are called imperfect maintenance models. Several proposals of imperfect maintenance models have been proposed [73, 92, 93, 104]. These models are based on the unavailability estimates, failure rates, and maintenance times.

More recently, important advances in measurement technology have allowed for the use of sensors to monitor some characteristics about the health condition of industrial components. There are many types of condition monitoring techniques [33, 126, 129], the results of which are used to propose maintenance strategies. The possibility to monitor in real time some important features of the life of an industrial component or system has originated new maintenance strategies that use this type of information, such as predictive maintenance, condition-based maintenance, or both [98].

According to [55], in order to rationalize the failure prevention, it is necessary to adopt the "condition-based maintenance (CBM)" where the physical variables that determine fault symptoms can be monitored. The CBM attempts to detect anomalies sooner, so that the impacts of interruptions on the operation are minimized, avoiding high costs and failures with unexpected consequences which significantly reduce maintenance costs [143]. The CBM often gets help from other techniques such as data acquisition systems, automated fault diagnosis, and prognosis [10], but overall, it is dependent on human intervention to define maintenance scheduling. Other similar terms which are widespread in the CBM field are

the "predictive maintenance" and "proactive maintenance" [72]. They are based on condition monitoring of components for maintenance decision-making, and also, they use predictive models in order to understand and predict how the monitored condition will evolve [132].

Thomas [143] explains that the conventional strategies of predictive maintenance can be difficult to apply to systems with many components. They are anticipative, allowing the maintenance expert to consider the possibility to do unplanned maintenance actions. However, they do not indicate in the case of more than one component to maintain, which one has priority in maintenance planning or how this selection can alter the costs of maintenance and the risk of unavailability. The answer to these questions led to the concept of opportunistic maintenance, therefore extending the preventive maintenance investigation to various components.

The evolutions of maintenance and diagnostic techniques have originated new wider frameworks where different maintenance strategies can coexist to reach a common objective in the elimination or mitigation of the possible consequences of a failure. Included in this type of framework are, for example, the well-known RCM [12, 90, 169] and total productive maintenance (TPM) [162].

"Reliability-centered maintenance (RCM)" was initially developed in the 1960s, but only over the last 10 years, it has begun to be effectively applied in the industry, thus concentrating the attention of maintenance on critical components system [48]. The RCM prioritizes maintenance actions in order to quantify the probability and the consequences of the effects of failures on the components or systems at any level of integration [99]. The RCM is another way to identify and rationally schedule the most appropriate tasks within a comprehensive action plan. The RCM is a method that relates reliability and preventive maintenance through a systematic qualitative procedure for organizing maintenance, i.e., it is a heuristic treatment that requires knowledge and experience about the process maintained. However, the method itself does not include the assessment of the benefits of maintenance on reliability and system costs. In this context, the reliability-centered asset maintenance (RCAM) [12] appeared, which is a method developed based on the RCM principles trying to more directly relate the impact on the maintenance costs into the system reliability through a quantitative ratio assessment which is both more effective and efficient [39, 43, 59, 149, 169].

Gabbar et al. [44] show an improvement in the RCM process through its integration into the computerized maintenance management system (CMMS) where the main parts of a RCM are identified and a prototype is integrated with several modules of CMMS. Wessels [160] proposes a scheduling optimization of the maintenance intervals where costs are used as constraints. Eisinger and Rakowsky [37] discuss a probabilistic treatment when modeling the RCM uncertainties and conclude that these uncertainties may be unacceptable in a decision-making process when using the RCM case studies, leading to the definition of a non-optimal maintenance strategy.

"Total productive maintenance (TPM)" was originally created in Japan in order to solve maintenance issues through strategies based on quality control processes. Nakajima [105] describes the main characteristics and concepts of TPM, which

tries to improve through autonomous and preventive maintenance the effectiveness of the equipment, processes, and plant. This philosophy involves all plant personnel. Before the TPM is implemented, two requirements need to be considered to obtain the desired improvement in the maintenance plan: increase motivation and competence of personnel who will be responsible for putting the changes in place and create a work environment that supports the systematic implementation of the TPM implementation program [11]. Some advantages of the TPM implemented in a company are, for example, a better understanding of the component performance and operation, the operational staff improvement, and fewer conflicts between operation and maintenance [156].

Various concepts and major maintenance requirements on the "effectiveness-centered maintenance (ECM)" and the determination of efficiency indexes of this strategy are reviewed in detail by Pun [119]. The ECM emphasizes the concept of "doing right things" instead of "doing things right." This strategy puts its focus on the functions of the system and the service provided to customers and also includes a number of features that are practical to increase the maintenance performance and cover the main concepts of quality management, the TPM and RCM. The ECM is more understandable when compared with TPM and RCM, incorporating the participation of the people involved and improving the quality and maintenance performance measurements.

Haddara and Khan [76] introduced the "risk-based maintenance (RBM)," in contrast to other strategies. The RBM strategy ensures proper maintenance to minimize the risk of unexpected failures and to define a profitable maintenance plan. The RBM is a quantitative strategy and consists of three main modules: risk estimate, risk assessment, and maintenance planning.

García [45] proposes a maintenance planning based on the health condition and current and real needs of the equipment or industrial system. A maintenance schedule is proposed as a final result coming from the evaluation of the components health condition and the incipient fault diagnosis [46]. Short-term scheduling is most appropriate to avoid or eliminate incipient failures and degradation in components. This scheduling is optimal with regard to a number of technical and economic criteria, such as the component failure risk, the components criticality, the appropriateness or effectiveness of the maintenance plan, the industrial equipment production planning, variable maintenance resource constraints, and maintenance costs incurred to these maintenance tasks implementing [47].

Lee [85] presents an important review about "prognostics and health management (PHM)" concepts. The PHM is focused on the incipient fault detection, the assessment of the current system health, and the prediction of the remaining useful life in a component. This approach has been accelerated by the fact that at present many systems, within their design, often include devices (sensors, controllers, software and intelligent algorithms) that enable the development of a methodology for maintenance scheduling with a certain level of automation and dynamism in terms of decision-making and with a better assessment of actual operating conditions. The PHM concept and structure have also been developed based on well-known maintenance strategies and diagnosis and prediction techniques, such

as preventive maintenance, RCM, and CBM. The PHM should eliminate preventive maintenance actions with high and unnecessary costs, optimizing the maintenance plan with the consequent reduction in the need for material for unscheduled substitutions.

The effectiveness of invested maintenance costs can vary drastically depending on the purpose and the coordination of their actions. Some of the maintenance strategies mentioned are based on the use of optimization techniques that maximize the effectiveness of maintenance actions under the restriction of economic resources, maintenance equipment assessment, and restrictive time intervals [96].

The goal of all these approaches is that maintenance contributes to keeping an optimal performance and availability in the industrial components according to the available budget. The maintenance plan must also be organized hierarchically in order to consider the ability of the people to perform the maintenance actions, the availability of necessary tools to perform the action, the information from storage and spare parts management, and any other information considered to be important. Improper maintenance can be avoided with the information and education of the people involved with the maintenance actions execution.

It is quite clear that wind farms maintenance scheduling is an optimization problem with complex constraints. The maintenance plan has a direct impact on system reliability. This planning can be classified as long, medium, and short terms, taking into account each different objective and also the sources of information. Thereby, maintenance strategies for different time scales can be incorporated and coordinated, resulting in a complete maintenance plan able to achieve a balance between cost optimization of the component life and system reliability [96].

In this section, the process of preparing and scheduling a maintenance plan and the main concepts related to it was described. Major theories which have been developed were discussed and highlighted from many years ago up to the present, as a way of clarifying the main objectives and constraints and developing a systematic process maintenance flow.

2.5 Maintenance Management

As discussed in previous sections, “maintenance management” integrates decisions concerning maintenance with strategic decisions about management. The integration between maintenance and the management system produces good results affecting the production, prevention, and quality system capacity [74]. Maintenance management should be integrated with other functional departments such as production and quality control. The computer-aided integrated maintenance management (CIMM) is required to integrate and control the production and maintenance as recommended in [48].

An important number of companies use the manufacturing resource planning (MRP II) isolated from the maintenance management activities. Therefore, strategies to integrate these two areas (maintenance and production) with a logical and

reasonable management are essential to actually get relevant advantages. An earlier study [64] suggests a MRP II system that incorporates integration with maintenance management through a model integration definition method (IDEF). In order to demonstrate the feasibility of this methodology, operation line producing lamps with sophisticated equipment was described and used as an example.

Tu et al. [147] present a case study of an electronics company that needed an adequate maintenance management system. Thereby, an integrated system was developed and implemented including maintenance-based audits, recording and analyzing costs, an RCM plan, and also condition monitoring and integrated control methods.

Research on total quality management (TQM), just in time (JIT), and total productive maintenance (TPM) is generally focused on the implementation and impact of these programs in an isolated form. Cua et al. [32] investigated the use of these three programs and demonstrated their compatibility.

Iravani and Duenyas [65] commented that a common practice of maintenance and production is making decisions separately which can be expensive, and therefore, they highlight the benefits of making them in an integrated manner. This demonstrated the operation of a system with both maintenance and production integrated using a Markov decision process that was validated by approximation methods.

Waeyenbergh and Pintelon [155] explain that more and more companies are looking for a concept of customized maintenance plan and describe a framework that provides guidelines for the development of this idea based on some existing concepts in the literature. An important feature of this structure is that it allows for the incorporation of all available information from the company from the experience of people in charge of maintenance to the data captured by modern information and communication technologies (ICT). The proposed structure is divided into five modules: start module, identification of critical systems and critical components module, maintenance policy decision module, performance measurement module, and the continuous improvement module.

Murthy et al. [103] detail the strategic maintenance management (SMM) with some example cases. This approach is considered to be a multidisciplinary case and overcomes some deficiencies of reliability-centered maintenance (RCM) and total productive maintenance (TPM), considering the working condition (load) of the system or equipment and its effect on the degradation process, the issue of long-term strategies, outsourcing of maintenance, etc. Moreover, it is also a quantitative treatment that uses mathematical models integrating technical, commercial, and operational aspects in order to manage the system.

Over the last decades, many companies have invested in the development and implementation of enterprise resource planning (ERP) systems. However, only a few of these installed systems develop or consider maintenance strategies. Nikolopoulos et al. [107] emphasize that the proper design and integration of maintenance management in an ERP system allow the company to effectively manage its production, planning, and scheduling. In this sense, Nikolopoulos et al. [107] present the design of an object-oriented maintenance management model and its integration with an ERP system.

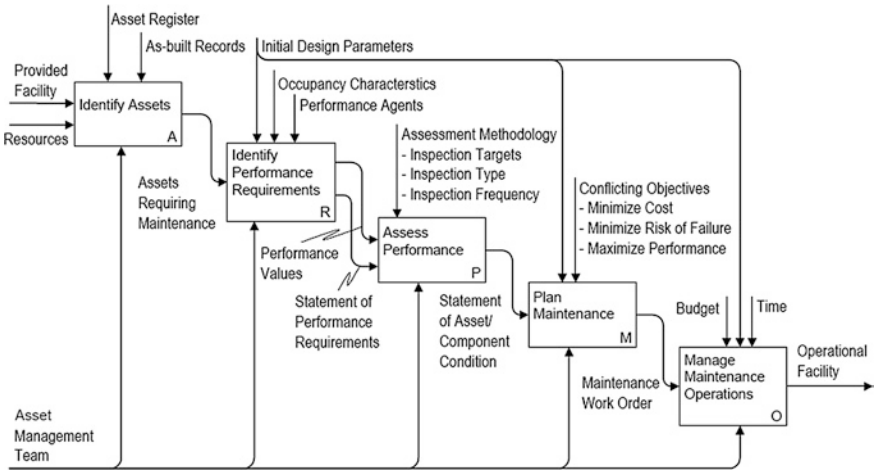

Fig. 6 Maintenance management model by Hassanain et al. [56]

Hassanein et al. [56] propose a model structure to formalize and standardize the process of asset maintenance management which is divided into five main sequential processes: asset identification, identification of the functional requirements of efficiency, evaluation of the asset performance, the maintenance plan, and the maintenance execution management. A number of support activities with their logical sequences and their information requirements are defined for each process. The structure was presented in the modeling diagrams language Integration Definition for Function Modeling (IDEF0), as shown in Fig. 6. In this structure, the outputs of some management processes are actually inputs of other subsequent processes in the hierarchy. The process model illustrates the interactions and dependencies between different sets of knowledge areas.

Tam and Price [141] presented a generic structure of asset management that integrates business decisions to optimize investment decisions related to maintenance. In physical assets management, the maintenance optimization is a concern, because in general, the assets deteriorate with use and as a result both the failure risk and cost increase. There are three levels of decision-making in the management of the annual costs of a company related to the maintenance cost of lost production, resource cost, and risk cost being the goal to minimize these costs.

Cigolini et al. [29] present the main recent trends regarding the use of maintenance management structures and production available for improving the efficiency and effectiveness of system operation, explaining the strategies and paths needed to pursue these trends.

Crespo et al. [31] define a generic model for maintenance management that integrates other models found in the literature. It consists of eight blocks of sequential management (Fig. 7). The first three blocks determine the maintenance effectiveness, the fourth and fifth blocks ensure the maintenance efficiency, the sixth and seventh blocks evaluate the asset maintenance and life cycle costs,

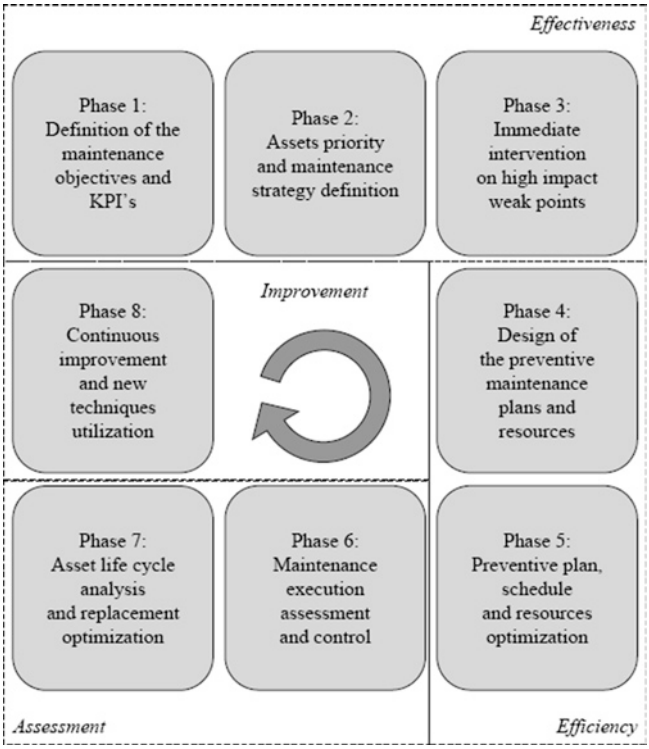

Fig. 7 Maintenance management model by Crespo et al. [31]

and finally the eighth block ensures continuous improvement of the maintenance management. With these blocks, Crespo et al. [31] characterize a "maintenance management structure," i.e., a support structure for the management process.

Hao et al. [55] present a support structure for decision-making in maintenance management systems, whose goal is the integration of maintenance, real-time management of projects, condition monitoring systems, and information models (Fig. 8). Basic processes for asset management, corrective maintenance, preventive maintenance, and condition-based maintenance are implemented in a Web prototype maintenance management based on Java. In this way, a complete system to support decision-making in both strategic management and operational management that provides a large-scale maintenance strategies optimization is presented.

2.6 The e-Technologies and Maintenance

In previous sections, different stages of a maintenance decision-making process and the necessary information to develop it have been presented. To efficiently and quickly manage all the information, "computer" tools that facilitate better communication and integration in the whole process are necessary.

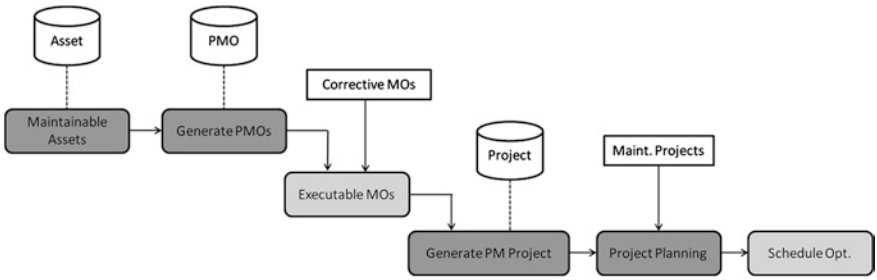

Fig. 8 Maintenance management model and scheduling process by Hao et al. [55]

At present, e-technologies are beginning to play a crucial role in supporting maintenance decision-making. The combination of preprocessing and modern communication tools provides the necessary technical support to remotely obtain the available information. This easy information transference among systems, environments, and different maintenance specialists provides a better jointly exchange of actions and decisions [70].

In summary, the e-technologies improve the possibilities to use data from multiple sources and of different types, to process a large volume of data, to make both forecasting and decision-making more reasonable, and to implement cooperative (or collaborative) activities. The benefit of implementing these e-technologies in the maintenance area is one of the primary reasons for the birth of e-maintenance [100].

The term e-maintenance emerged in the early part of this new century, and now, it is a very common term in the maintenance literature [87]. The concept of e-maintenance currently discusses concerns about the integration of information and communication technologies (ICT) with the strategies or maintenance plans, to face the new and emerging needs to support production (e-manufacturing), system management, and business (e-business) and what is expected by the "manufacturing renaissance" [167].

Muller et al. [100] define e-maintenance as a: "Support tool for maintenance that includes resources, services and management necessary for the implementation of a proactive decision process. This support includes e-technologies but also activities (operation and processes) of e-maintenance such as e-monitoring, e-diagnosis, e-prognosis, etc."

Muller et al. [100] also note that there is a considerable incentive for the development of specialized tools, methods, and systems, and therefore, many e-maintenance platforms were developed (ENIGMA, CASIP, ICAS-AME, Remote Data Sentinel, INTERMOR, INID, IPDSS, WSDF, MRPOS, PROTEUS, TELMA, etc.). These platforms are results from both the academic and industrial worlds and, in general, can be classified into individual platforms (e.g., ICAS), platforms developed for specific projects (e.g., PROTEUS), or platforms for research and education (e.g., TELMA).

More details of e-maintenance platforms and their integration with other tools that make up an industrial system can be seen in [54, 56, 57, 84].

2.7 Wind Turbines in the Maintenance Context

The current practice of maintenance applied to the existing wind turbines is based on periodic or preventive maintenance actions recommended by their manufacturers [8]. However, this typical approach does not pay attention to the real and local life of the wind turbines characterized by weather conditions at the location, stress by overload, hours continuously working, etc. These factors are crucial to knowledge of the specific conditions in which a wind turbine operates, and any type of maintenance has to be tailored to these conditions if one is to minimize costs or maximize the life span of the wind turbine.

The analysis of failed components and their causes in wind turbines is an important research area for improving their reliability and optimizing maintenance practices [121]. On the other hand, today it is very common for industrial processes to have monitoring systems that mainly assist the operators in the production process. The information collected normally is not connected directly to a maintenance plan. Strategies for the integration of all of this information coming during operation with a maintenance plan are being developed, and the existing ones are being improved.

Wind turbines rely on sensors to control their operation autonomously from a remote site. These sensors are useful not only from the operational point of view, but also from the maintenance point of view. In fact, these installed sensors, sometimes augmented with others, can be used for condition monitoring for the evaluation of the health condition of wind turbines [2, 53, 63, 78, 161]. Also, data mining and artificial intelligent techniques are being intensively used for this purpose [79, 136, 159]. The results of these techniques are the basis of new maintenance techniques such as predictive maintenance, condition-based monitoring (CBM), and prognostic and health management (PHM) [90, 98]. These techniques, based on fault diagnosis, continuous monitoring, predictive maintenance, artificial intelligence techniques, CBM, PHM, and others, are being studied and applied in general throughout many industrial fields and in particular in electrical generation systems using wind [3, 13, 16, 25, 26, 61, 89, 95, 108, 109, 124–126, 164, 166].

In general, supervisory control and data acquisition (SCADA) data are currently mostly used for backward analysis after fault occurrence to clarify the fault root cause, but not for condition monitoring on a large scale. For smaller and many older wind turbines, SCADA data are the only available information source. Yang and Jiang [165] pointed out that these data are the cheapest source for developing CMSs. Furthermore, there is a need to find expert systems capable of aiding operators in monitoring their assets and implementing their knowledge gained, combining all available information. However, technical details about the turbine or component design are seldom available to operators, formulating the need for self-learning algorithms with thresholds that are defined automatically. In the following paragraphs, some condition monitoring approaches that are highlighted by Schlechtingen [133] are presented.

Petersen [115] presents a knowledge-based approach to carry out a technical and economic assessment of smaller wind turbines, taking into account the

investment, operational costs, maintenance costs, and costs for lost production due to interruptions. The knowledge-based system allowed scheduling maintenance based on historical and on-site-monitored data as well as maintenance logs. Clayton et al. [30] add another possible source of information by developing a method to monitor the condition of composite rotor blades via an infrared technique. This was among the first monitoring methods especially suited for wind energy application. Many other monitoring methods were developed for other applications, e.g., methods to monitor turbine generators [30], machines with rolling element bearings [138], induction motors [28], or electric machines in general [112, 113].

However, except for the rotor blade CMS, none of these systems were applied to wind turbine generators (WTGs). Caselitz et al. [22] were the first to apply and combine several available condition monitoring methods to the special application in WTG in 1994. Their development project focused on the following main components: rotor, gearbox, generator, bearings, shafts, yaw system, tower, and WTG structure. In this context, the authors highlighted, reviewed, and investigated several different approaches [24, 137] to identify and isolate faults used in other applications (system identification approach, observer-based approach, signal analysis approach, expert system, and artificial intelligence approaches as fuzzy techniques and neural networks) and led to the conclusion that model-based approaches can, at best, be applied to single components of a WTG.

Caselitz et al. [23] started a field test with installations in several turbines of different manufacturers. Moreover, a fault classification system to combine information from different measurements based on fuzzy techniques was introduced. Figure 9 shows one general sensor scheme used for a WTG.

The system set up in this manner allowed for real-time analysis and monitoring, for example, including algorithms to monitor the overall turbine performance via a power curve analysis (power output vs. wind speed). In addition, gearbox and bearing faults can be monitored by an envelope curve analysis of the frequency spectra, etc. The idea is to create a CMS network in a wind power plant that optimizes the fault classification process by comparisons between WTGs operating under identical conditions and therefore significantly improving the efficiency of fault detection in new monitoring functions and the performance of each single WTG in a wind power plant. Caselitz and Giebhardt [21] present the results of the field test and the development of a processing unit.

However, the detailed knowledge of the component design parameters required to apply the developed CMS causes major problems in the practical application of this system, since this information is seldom available to operators. The particular advantage of independence of prior knowledge about the component or system leads to an increasing interest in neural network techniques for wind turbine applications once the limitation became evident [133].

In 2001, a comparative analysis of regression and artificial neural network models for wind turbine power curve estimation was published [91]. Verbruggen [154] published a final report of a project, reviewing different condition monitoring methods for wind turbine operation and maintenance that covered a large amount

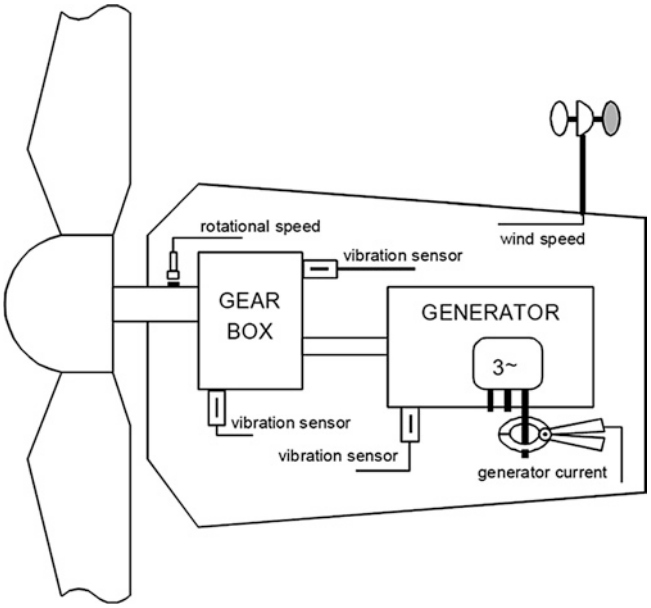

Fig. 9 Measurements for condition monitoring [23]

of wind turbine components and also included an experimental study. McArthur et al. [97] present an agent-based anomaly detection architecture for condition monitoring. As a result, in this system, individual agents perform different categories of functions and intercommunicate to implement the overall anomaly detection functionality.

Sanz-Bobi et al. [126] present an intelligent system for predictive maintenance (SIMAP) applied to the health condition of a wind turbine gearbox. This system makes use of back-propagation artificial neural networks to set up normal behavior models and to detect abnormal signal behavior and uses a number of different modules (agents) to evaluate the overall component condition. The system makes use of already available signals, e.g., component temperatures or digital operational signals. Zaher and McArthur [168] also apply the idea of a multiagent system for condition monitoring purposes to wind turbine signals. The development focused on processing and analyzing signals from the three main components: gearbox, generator, and rotor blades.

The literature review by Schlechtingen [133] reveals many research activities carried out over recent years, pointing in the direction of a global CMS to evaluate wind turbine performance and the condition of its components. In particular, for single wind turbine components, a large variety of monitoring methods are already available. These methods are either exclusively developed for wind turbine application or they are taken from other applications and adopted to the special wind turbine characteristics such as the dynamic load situation or variable-speed

operation. A number of research activities were undertaken to combine different measurements to gain an overall assessment of the system condition. They mainly differ in the input data used, required knowledge of the component design parameters as well as knowledge of how a fault manifests itself within in the data.

SIMAP is among the most advanced systems toward predictive and condition-based maintenance schemes. The system is still under development, and current research activities focus on the improvement of the link between health condition of the wind turbine and its required maintenance. Several methods for the characterization of a "virtual stress" of the wind turbine for different failure modes are currently under investigation, and efficiency evaluation of the executed maintenance actions is also a main objective.

3 The Framework

Today, several sources of information exist within a wind farm that can assist in decision-making during an asset management process, but sometimes they are not sufficiently integrated to facilitate the analysis of all the information available. This section describes a new maintenance framework in which several tools are integrated in order to assist the process of asset management in a wind farm. These tools are oriented to identify the more critical assets according to a combination of the following criteria: reliability, exploitation requirements of the wind farm, and impact on the quality of service to the clients. There are two different sources of information that will be used by these tools: historical events information about unavailability and maintenance previously performed and real-time information or measurements history about significant monitored variables related to the health condition of important components [130].

Figure 10 shows the main elements of the framework developed.

As is shown in Fig. 10, the information coming from the events history will be used to develop models for predicting possible times when medium-/long-term failure modes could occur. This information is based on particular events that occurred during the life of a component or system and, in particular, when a failure was present or maintenance action was done, but the continuous life was missing. This is the reason why it is only possible to develop models for the prediction of times of failure for the medium/long term using this information. This allows for the identification of critical points in the wind farm system using different criteria or points of view such as the reliability level required, exploitation conditions, and social cost of failures. Also, from Fig. 10, it can be observed that if there is continuous information available from significant variables about the condition of a component or system, models for the characterization of the normal behavior can be developed in order to predict an incipient failure mode as soon as possible, if it is progressive. The measurements history collected is the basic foundation of these models. Once the models are fitted using real data, they can be used in real time in order to continuously monitor if the prediction of normal behavior for the

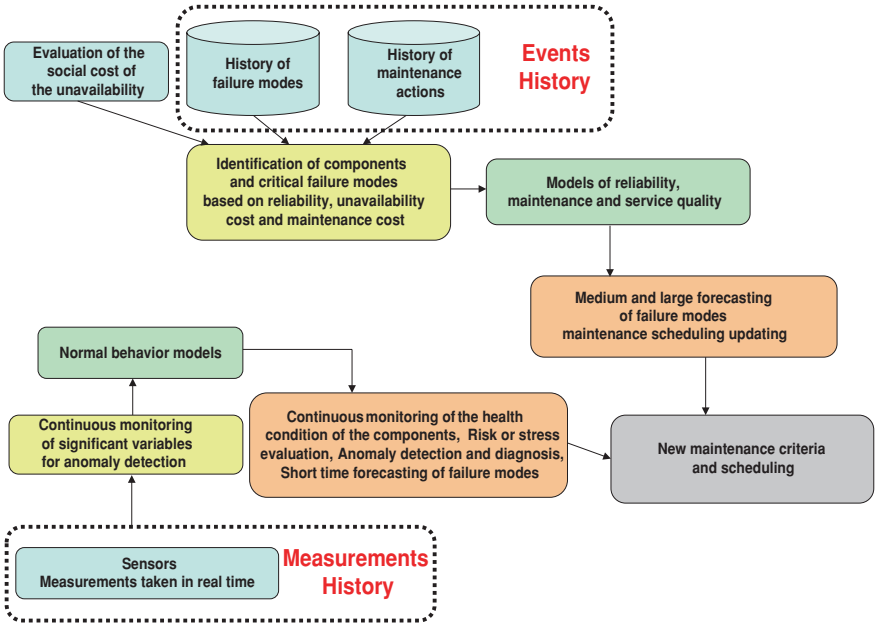

Fig. 10 Framework for the integration of information to assist in the process of maintenance planning in an asset management program

current working conditions corresponds with the real value observed. If there is not a suitable correspondence, a possible failure mode is in progress.

In general, the maintenance model represented in Fig. 10 is based on reliability models integrated with maintenance actions and also includes other important additional factors to improve the typical RCM plan, such as estimating the unavailability cost, the impact on the quality of service to the clients according to the service provided by the wind turbines of a wind farm, as well as budgetary or security limitations on certain components to maintain. In addition, this model considered data and cost constraints, resource constraints, and/or security, which make the results of this maintenance plan more reliable and adjusted to the equipment life over those in which personnel are responsible for performing maintenance based on their own decisions.

From the failure event historical information, failure rates of the components are estimated. Thus, probabilistic modeling of potential failure modes would be obtained, at least those considered to be the most representative. On the other hand, the maintenance events history is also needed. They will allow for identifying the main preventive maintenance actions to avoid the failure modes that were selected in the reliability analysis, in order to apply these actions at the most appropriate times from the reliability point of view. Finally, the costs (social and physical) of an interruption are in addition to technical and reliability features, important constraints for developing a maintenance plan. The social costs will

be evaluated based on the impact that unavailability has on customers, i.e., how the unavailability of a component affects the customers and as a consequence the company "image."

Based on the prediction of possible times of failure and times of execution of maintenance actions that try to avoid them, a maintenance plan will be proposed including a list of maintenance actions according to the expected failure mode reliability and its minimal acceptable confidence limits that should not be exceeded. In this sense, the events history only supplies knowledge about a few significant and specific moments of the life of a system or component, in particular, those related to unavailability occurred or when a maintenance action was applied. Associated with their analysis is an important uncertainty about the life of components or systems between periods of time when nothing is expected to occur.

If measurements history or real-time data are available, it could be better to refine the forecasts of possible times of failure with the actual component health condition. Therefore, the history of measurements could improve the application of maintenance actions, making it more effective and optimizing costs. Hence, this suggests the idea to integrate the previous historical information based on events with information coming from continuous monitoring systems supplying data about certain characteristics that can be important to know about the possible presence of a failure mode before it arises.

The continuously collected information about the life of components is the centerpiece in the component "health" monitoring, as described in the lower half of Fig. 10. In this framework, the normal behavior models will facilitate the prediction of important variables to detect anomalies based on the real work conditions of the components. The anomaly detection and the failure mode risk evaluation (see Sect. 4) will help in the identification of a failure cause and in scheduling of a maintenance action when it is really needed.

Finally, the analysis of the events history through the models created, the analysis of the measurements history through the normal behavior models, and the prediction resulting from all of them are very convenient instruments to efficiently update maintenance scheduling according to the real life of the components, hence optimizing costs and applying maintenance actions only when they are required.

4 Estimation of Deviations in the Wind Turbine Condition

4.1 Condition Indicators

The key concept of this subsection is the definition of condition indicator based on the observed life of a wind turbine. It is defined as the deviation between the real behavior observed and expected as normal behavior in a component according to its present working condition. These deviations between real and expected behavior may be more or less severe for the component life, and they can be interpreted

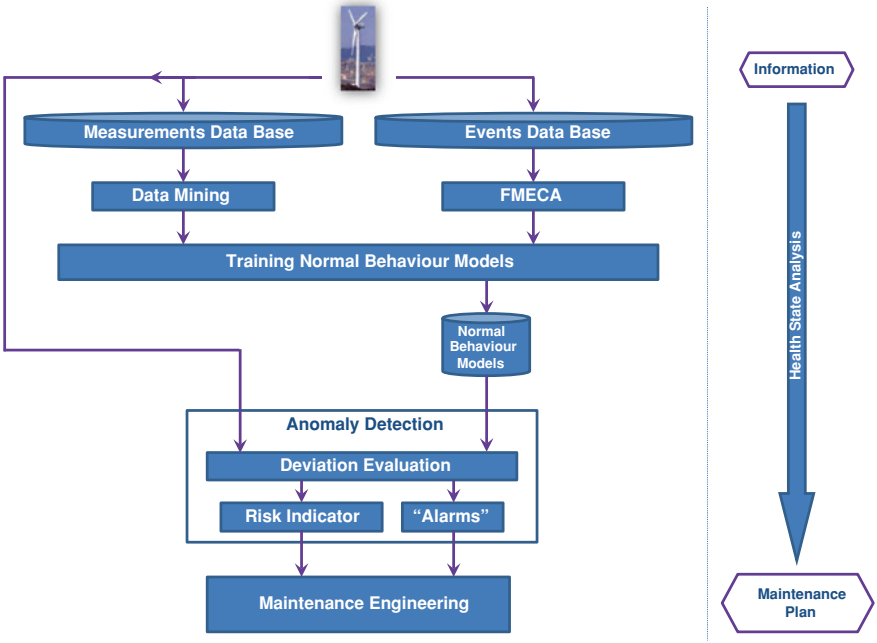

Fig. 11 Methodology to risk indicator evaluation

as symptoms leading to possible failure modes or not, but in any case, they create the appropriate seed for the development of possible failure modes.

The expected normal behavior is obtained from models, previously created, able to predict typical values of some variables based on other variables observed in the absence of other anomalies. The deviations observed from the expected normal behavior of a variable can be used to characterize certain qualitative indicators about the risk of appearing of a failure mode.

The aggregation of deviations observed of a possible failure mode risk over time makes it possible to define certain changes in the health condition of a component in a wind turbine and hence deduce if it is close or not to exceeding certain thresholds considered above in which the occurrence of a failure is most likely. The proximity to these thresholds will guide the maintenance rescheduling in such a way that it will be applied when it is really needed.

Figure 11 shows the general outline of the methodology developed for the determination of the health condition of a wind turbine. It includes all the information related to the historical events (faults and maintenance), continuous condition monitoring, prognostic, and associated maintenance plan of the wind turbine life cycle. The next subsections will explain more details about the different components of Fig. 11.

4.2 "Information Known": Preprocessing Step

The "failure modes effects and criticality analysis (FMECA)" is a systematic method to identify the critical "points" of a system with several components and helps to prevent failures (and possible consequences) that may affect or impact the main functions of the system under a given operation context. The FMECA aim is to identify and classify all the modes in which an asset of an industrial process can fail according to their occurrence, severity, and possible detection. Also, this method is able to identify the possible consequences or effects of the failure modes in terms of three basic criteria: human security, environment, and operation (production).

However, it is well known in industrial diagnosis that there are observable and unobservable failure modes. The observable ones can be detected by monitoring the values of one or more measured variables that characterize it and let set certain assumptions about how close the presence of the failure mode is. The unobservable failure modes are difficult to predict through condition monitoring in the absence of variables that betray them. Intermediate cases are those in which the failure modes are not observable, but through some variables, it is possible to know something about them indirectly.

In this chapter, a wind turbine has been divided into three main systems trying to group the most important parts from the point of view of its failure. These are generator, gearbox, and others (pitch control system, assembly rotor/blades/axle, etc.). The failure modes considered were as follows: electric generator fault, electric generator's high temperature, synchronization frequency fault in the electrical generator, gearbox's high temperature, gearbox oil's high temperature, gearbox bearing's high temperature, pitch drive's breakdown, synchronization speed fault in the axis rotor/generator, and other failures not related to the electrical generator and the gearbox.

As was mentioned before, the information collected by continuous monitoring from the operation of a wind turbine is the centerpiece for the estimation of the "health" component monitored according to the methodology proposed by the authors. The wind turbines have the advantage of having a great number of monitored variables in order to control different components of the wind turbine, but they can also be used to assess their diagnosis and condition.

Once the failure modes considered most important in a wind turbine have been identified, the variables that will be used to provide information about the presence of these possible failure modes can be identified too. They will be used for the development of the normal behavior models that later will be used for the estimation of behavior performance. The following are examples of some of them: ambient temperature, nacelle temperature, power generated, wind speed, rotor speed, pitch angle, gearbox oil temperature, gearbox temperature, gearbox bearing temperature, generator temperature, and generator winding temperature.

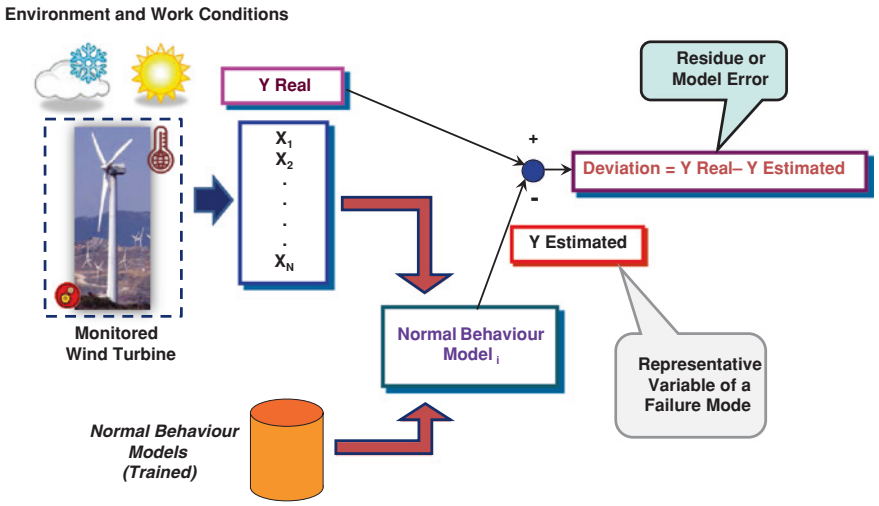

Fig. 12 Flow of information for the detection of anomalies or deviations with respect to the normal behavior expected

4.3 Normal Behavior Models

When a component performs the function for which it was designed under normal conditions, the effect of aging is often the most frequent cause of failures. However, in addition to this effect, in some situations, the component is "stressed" due to harsh working conditions, overload or extreme environmental conditions, or a combination of both. It is very important to characterize the expected normal behavior for a component through its different working conditions, because any deviation from this behavior can warn of the presence of a possible failure mode that could be developed [127].

The sooner the deviation is detected, the quicker the effect of a failure can be mitigated. In this way, information in real time is necessary to be used in order to follow the evolution of the main variables that can characterize the performance of a component [6, 126, 129].

In this context, normal behavior models were developed to predict the dynamic behavior of the variables continuously monitored that are important for the detection of potential failures. The normal behavior or baseline behavior has to take into account the different usual working and environmental conditions without failure symptoms and therefore no "stress."

Any incipient fault will cause a certain deviation between the estimated and the real value of some observed variables which have sensitivity to this failure mode. The detection as soon as possible of a possible failure mode will help to mitigate or prevent their effects when this is possible. Figure 12 illustrates the scheme for automatic evaluation of deviations based on the use of normal behavior models for comparing the real and estimated values of a variable that can be used for the detection of the failure mode.

The continuous analysis and trend of observed deviations from the expected normal behavior of the evolution of a variable can be used as an indicator of the health condition of a component.

The development of models of normal behavior includes the following significant steps:

- Analysis of the available information collected in real time from a wind turbine. Analysis of the time series of data and determination of relationships existing among the variables measured.
- Definition of the most representative failure mode features that can be detected using the previous information available.
- Normal behavior models formulation based on training data corresponding to periods without any anomaly.
- Model validation.

Two important concepts must be kept in mind when creating models. On the one hand, the data used for training have to correspond to the component working under normal operation conditions without anomalies. On the other hand, the quality of the model will depend on the ability to get the suitable input variables related to the output one with the lowest error.

After a normal behavior model has been trained and validated, it can be used with new real input values and its prediction will correspond to the normal behavior expected under the current working conditions. If there is a deviation between the real and estimated values of a variable, this deviation is assessed by recording not only the moment that occurred, but also its value in order to generate both an appropriate alarm about the possible presence of a failure mode and the re-evaluation of a risk indicator value (Fig. 11).

The models developed by the authors in the cases that will be described in the next subsections as case studies are based on information collected in real time from a wind farm. A total of 13 models of normal behavior were developed for each wind turbine.

As an example of the procedure followed for the development of normal behavior models, the creation of a model for the prediction of the gearbox temperature of a wind turbine will be presented. This model is able to predict the temperature of the gearbox of a wind turbine using information from three input variables: the total power generated, the nacelle temperature, and the gearbox oil temperature. The first input variable gives an idea about the amount of work developed by the wind turbine, the second one gives an idea about the conditions of the working environment of the gearbox, and the third one includes the effect of the cooling system of the gearbox.

A training data corresponding to selected time periods of normal behavior were selected. In addition, the selected data covered a wide range of typical working conditions. As an example, the training set for the development of the normal behavior model of the gearbox temperature consists of 8 months over a 1-year period covering different operation conditions of a wind turbine throughout the four seasons, i.e., 2 months for each season.

The most part of the normal behavior models developed by the authors of this chapter are based on different architectures of neural networks multilayer perceptrons [101]. They are able to characterize the relationships between a set of input

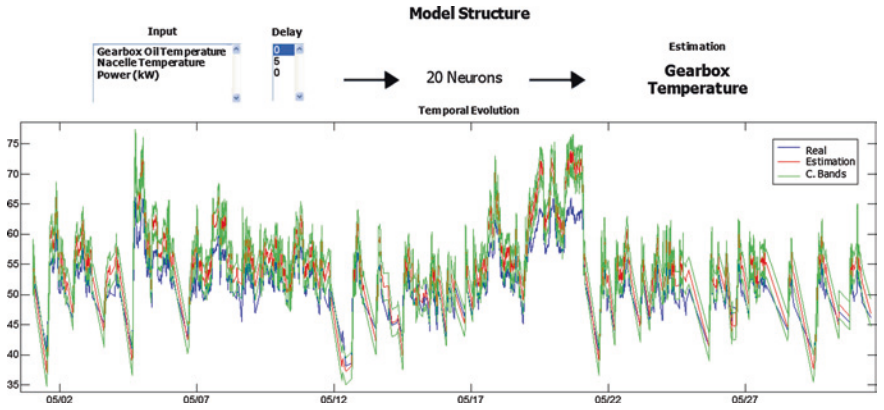

Fig. 13 Normal behavior validation to the gearbox temperature of a wind turbine to the anomaly detection

variables and an output variable used to detect some anomaly or deviation with respect to the normal behavior in the component monitored. The relationships among variables modeled are characteristic of the normal behavior observed in a wind turbine component under different working conditions. The trained neural networks have only one hidden layer with a sigmoidal activation function. The output layer uses a linear activation function. The training algorithm used was the Levenberg–Marquardt back-propagation [58].

After training and testing of the normal behavior models, they are used to detect possible anomalies with respect to the expected behavior pattern passing through the recent data collected from the wind turbine operation. Figure 13 shows the estimated value resulting from the normal behavior model for the gearbox temperature when using new data collected (not used during training). In particular, a new 1-month period of data were used. As can be observed in the figure, the real and estimated values are very close and no abnormal behavior was observed during that period of time. This validates this model as representative of the normal behavior expected for the gearbox temperature.

The structure of this example of a normal behavior model is presented on the top of Fig. 13. The estimation error obtained during training from the model is used to define a confidence band that will be used to decide whether the real and estimated values are similar or not.

4.4 Evaluation of Normal Behavior Deviation

Normal behavior models are used in real time to detect the presence of possible deviations from the normal behavior expected [131] by estimating the value that should have its output variable based on the inputs that the model receives. There will be normal behavior if the output estimated by the model is quite close to the

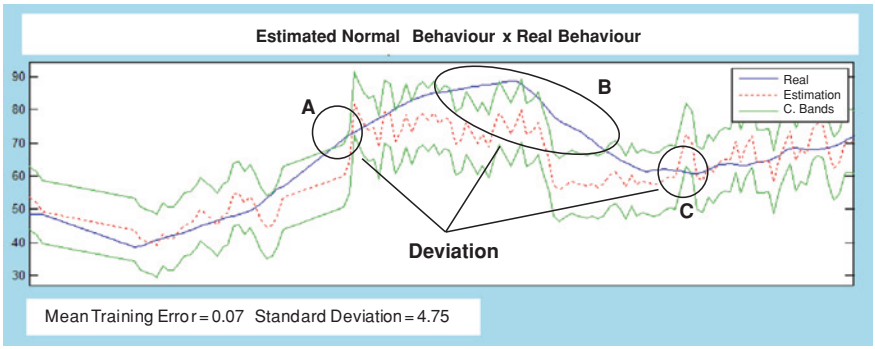

Fig. 14 Example of anomaly detection to the gearbox temperature

actual measured value. In contrast, if the values are not close, a possible anomaly is present and should be monitored and investigated. A deviation is detected when the actual output variable is outside the range of its expected estimation. The deviation is calculated as a ratio of distances between the value of the real variable and the estimated confidence band to its normal behavior value. The confidence bands are defined for each model as roughly twice the standard deviation of the model training error.

Figure 14 presents an example of how the gearbox temperature reaches values which are too high compared with those estimated by the model (points "A" and "B"). These points are detected as anomalies. In particular, for the case of point "C," the deviation will be considered to be zero because the real temperature is lower than the estimated temperature, meaning that the current situation will not cause stress in the component.

When a component is "stressed" due to harsh working conditions and overloaded conditions, a possible development of failure modes can occur if no action is taken to prevent or mitigate it. Likewise, accelerating natural aging thereof is also provided.

Figure 15 shows through the comparison between the structure of a failure mode and the structure of an iceberg, how the failure mode can be characterized based on observed symptoms or indicators. One of the symptoms, usually monitored by several methods of condition monitoring, is the occurrence of anomalies, i.e., when the calculated deviation exceeds a certain "threshold" and the failure mode is already present in the component causing an increasing deviation on its expected behavior. So if the actual value of the output variable of the model is inside its confidence bands, there is no anomaly present and the model is labeled with a "green" label in an application developed for that objective. If the actual value measured is outside the confidence bands, the model is labeled as "yellow" because there is not yet sufficient evidence of the permanent presence of a symptom of anomaly. However, when many deviations in a very short period of time are continuously tagged as yellow, the label changes to "red" and the presence of an abnormal behavior is confirmed.

Fig. 15 Main observations of a failure mode

Another symptom is the assessment of the level of degradation of the component against a particular failure mode, i.e., the failure mode has not yet caused a large component behavior deviation, but it is known that this component has been "stressed," and as a consequence, the failure mode risk increased. In general, when an anomaly is detected, there is an underlying degradation process that can cause the development of a failure mode. The evaluation of the degradation level versus the occurrence of failure modes in the wind turbine components is performed through a method able to estimate a failure mode risk indicator (FMRI).

5 Wind Turbines Risk Evaluation

5.1 Failure Mode Risk Indicator

Usually, it is difficult to predict the exact moment when a failure mode can cause unavailability or a catastrophic failure in an essential function of a wind turbine. However, the observation of the evolution of some characteristics of its performance over time can be valuable instruments to configure an idea about the health condition of the wind turbine and, in particular, if some important functions can be at risk of being lost due to symptoms that are usually not observed during normal operation.

For example, a failure mode with thermal nature developing inside a power transformer at an electrical substation of a wind farm would cause an increase in the measured temperatures above the normal temperatures expected for its working conditions in the windings, oil, or both. If this is not too severe, the deviation, observed when compared to the normal value expected, normally does not cause an immediate catastrophic failure, but in any case, this deviation causes a certain amount of stress in the component. If more deviations with respect to the normal behavior expected to occur, greater possibilities will exist of reaching a condition in the component that causes unavailability.

5.1.1 Definition of Failure Mode Risk Indicator

The continuous monitoring of deviations with respect to the normal behavior expected of significant variables for the life of a component in a wind turbine can provide important information about its health condition. This information is similar to an indirect indicator of a risk that a failure mode can cause unavailability, and for this reason, it could be used as a risk indicator of a failure mode. In [4], the authors describe an approach able to estimate this indicator (FMRI) of which the main features are included in this section. It makes it possible to better know the health condition of a wind turbine and to suggest how to reschedule its applied maintenance.

It is possible to assert that in general, the failure mode j of the component i will be a weighted function of the evolution of its observable symptoms. These symptoms can be based on measurements of deviations with respect to the normal behavior expected. In fact, these deviations would suggest that the failure mode is already present or at least that there are some contextual circumstances present that can facilitate it. In mathematical terms, the FMRI can be expressed by Eq. 1 as an accumulation of observed deviations with respect to the normal behavior over a period of time.

$$\mathrm{FMRI}_{ij}(t) = \int_0^t \mathrm{DEV}_{ij}(t)\mathrm{d}t. \tag{1}$$

where

- FMRI_{ij} is the risk indicator for the failure mode j in the component i during the period of time t.
- DEV_{ij} is the deviation when compared to the normal behavior expected for component i and failure mode j. The normal behavior expected is calculated by a model of normal behavior able to detect a failure mode. At each sample collected, DEV_{ij} has a value different from 0 when the difference between predicted and real value for the output of a model of normal behavior overpasses two times the standard deviation of the error of the model observed for the current working conditions and this was observed for at least two out of three consecutive samples.

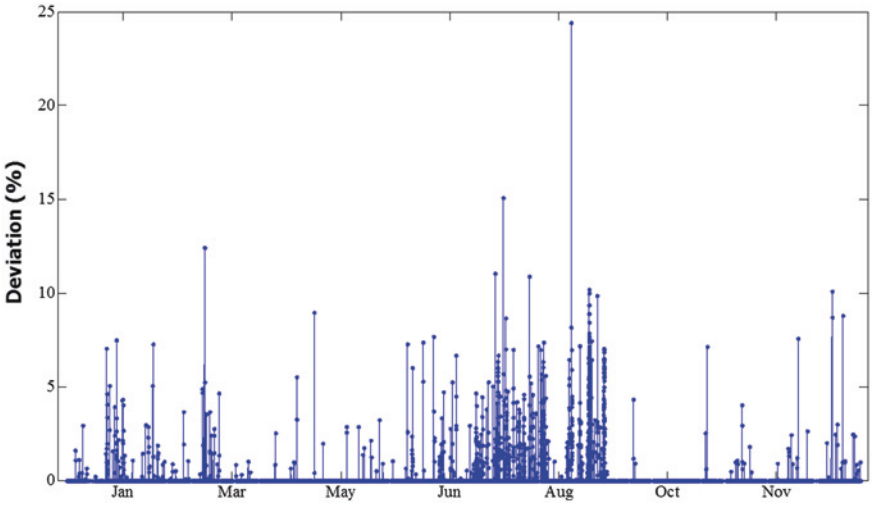

Fig. 16 Deviations over a 1-year period with respect to the expected gearbox temperature of a wind turbine using a normal behavior model that predicts its value under similar working conditions

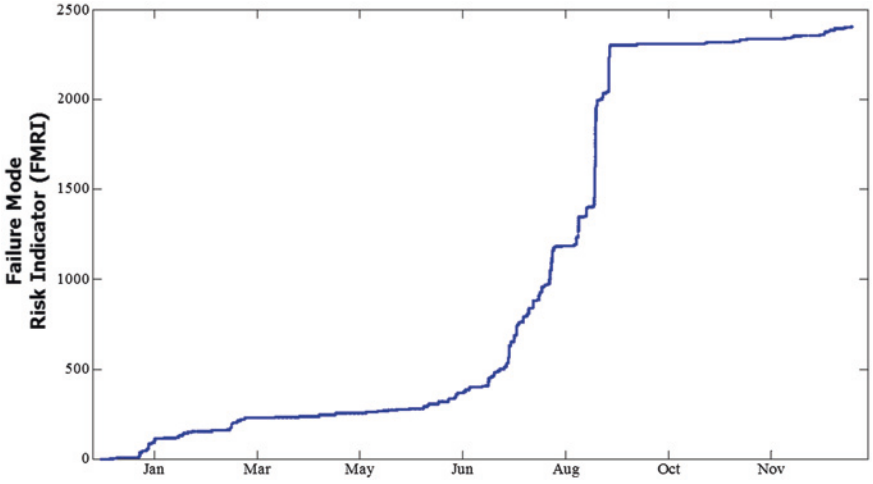

Fig. 17 FMRI estimated over a 1-year period for the gearbox temperature of a wind turbine

In order to illustrate the estimation of the FMRI, Fig. 16 shows the observed deviations over a 1-year period with respect to the expected gearbox temperature of a wind turbine using a normal behavior model that predicts its value under similar working conditions. Using the information included in Fig. 16, the values of the FMRI are estimated for this case using Eq. 1. The representation of these values in Fig. 17 is for a 1-year period using the normal behavior model for the gearbox temperature able to detect abnormal values of temperature in the gearbox.

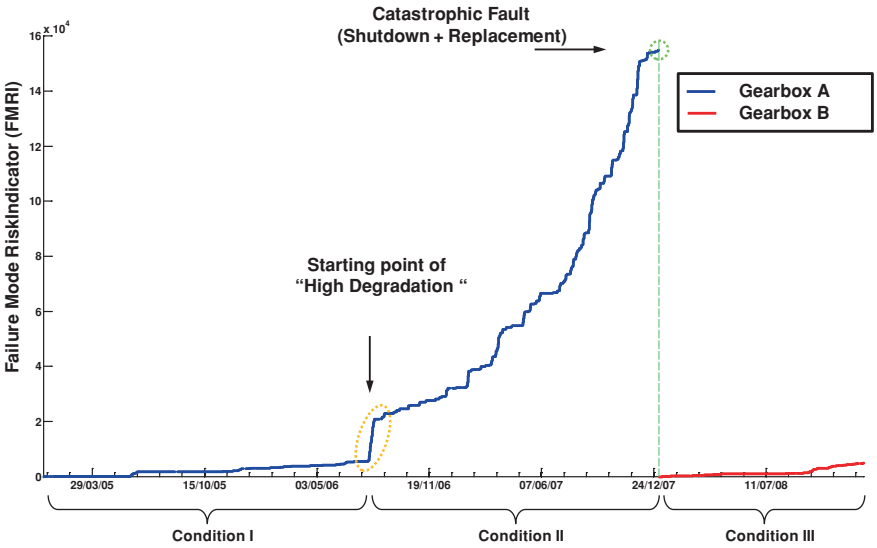

Fig. 18 Evolution of the FMRI over a period of 4 years by monitoring deviations in the gearbox temperature

Figure 18 shows the evolution of an example of FMRI over a period of 4 years (2005–2008) for the FMRI corresponding to the gearbox temperature of a wind turbine (gearbox A in the figure). At the beginning of the period considered ("Condition I"), the gearbox did not have relevant deviations in its normal behavior expected (small values of FMRI were observed). However, around August 2006, something happened in the gearbox, which caused high values of deviations and an important change in the value of the FMRI. An amount of stress for this failure mode appeared. A process of rapid degradation was observed ("Condition II") from this moment with a progressive increase in FMRI values and also the slope of the curve represented. Finally, at the beginning of 2008, the gearbox had a general fault causing it to go out of service and be replaced by a new gearbox (gearbox B). Once the new gearbox was in operation, and reset to 0 the value of FMRI ("Condition III"), the evolution of the FMRI was similar to that during the period of "Condition I" as expected because the new gearbox is now working under normal conditions without the degradation that caused "Condition II."

In the case that failure mode j in the component i can be observed from different models of normal behavior through the corresponding deviations, the definition of FMRI in Eq. 1 can be extended in Eq. 2 as such

$$\mathrm{FMRI}_{ij}(t) = \gamma_1 \mathrm{FMRI}_{M1ij}(t) + \cdots + \gamma_k \mathrm{FMRI}_{M1kj}(t) + \cdots + \gamma_n \mathrm{FMRI}_{Mnij}(t). \tag{2}$$

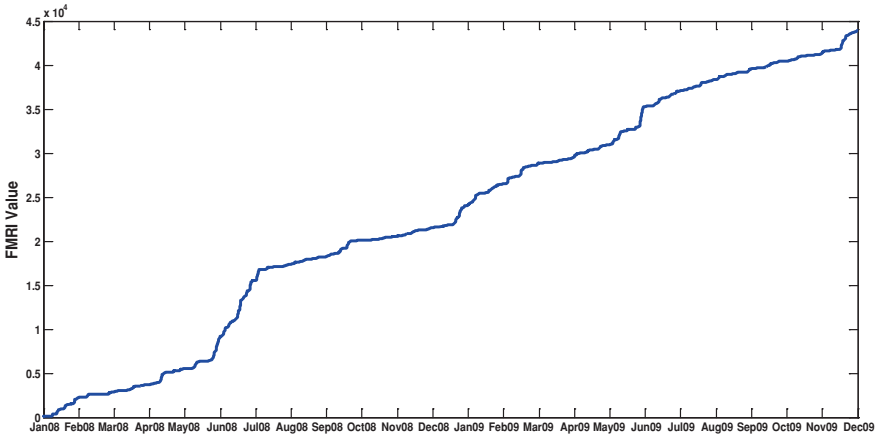

Fig. 19 Observed FMRI for the gearbox failure mode of a wind turbine over a period of 2 years

where

- FMRI_{Mkij} is the estimated FMRI by the normal behavior model k that monitors failure mode j in the component i. The different failure mode risk indicators are elaborated using different models of normal behavior able to qualitatively evaluate the same failure mode from different relationships among variables.
- γ_k is the weight that model k has in the weighted composition of FMRI for failure mode j in the component i with $0 \leq \gamma_k \leq 1$, k from 1 to n, n being the total number of normal behavior models for failure mode j in the component i. Additionally, the following relationship is required among all the γ_k weights:

$$\sum_{k=1}^{k=n} \gamma_k = 1$$

Figure 19 shows an example of the use of Eq. 2 estimating the FMRI for the case of the failure mode "gearbox fault" of a wind turbine over a period of 2 years. This FMRI has been obtained by Eq. 3, which is a particular case of Eq. 2.

$$\text{FMRI}_{\text{GF}}(t) = \gamma_1 \text{FMRI}_{M1\text{GF}}(t) + \gamma_2 \text{FMRI}_{M2\text{GF}}(t) + \gamma_3 \text{FMRI}_{M3\text{GF}}(t). \tag{3}$$

where

- FMRI_{GF} is the observed FMRI for the failure mode ***fault*** of the ***gearbox*** of a wind turbine.
- $\text{FMRI}_{Mk\text{GF}}$ is the FMRI estimated from the normal behavior model k that monitors the failure mode ***fault*** in the component ***gearbox***, $k = 1$–4.

$\text{FMRI}_{M1\text{GF}}$ is the observed FMRI obtained from the deviations between the expected and real value of the gearbox temperature. This temperature is estimated

by a normal behavior model of which the inputs are the nacelle temperature and the generated power.

$FMRI_{M2GF}$ is the observed FMRI obtained from the deviations between the expected and real value of the gearbox temperature. This temperature is estimated by a normal behavior model of which the inputs are the nacelle temperature, the generated power, and the gearbox cooling oil temperature.

$FMRI_{M3GF}$ is the observed FMRI obtained from the deviations between the expected and real value of the gearbox temperature. Now, this temperature is estimated by a different normal behavior model whose inputs are the nacelle temperature, the generated power, and the rotor speed. This model is in part redundant to the model used for estimating $FMRI_{M2GF}$; however, it is based on different variables, and therefore, it is expected that their complement reinforces the reliability of the estimated FMRI for the fault of the electrical generator.

γ_k is the weight that the model k has in the composition of FMRI for the failure mode ***fault*** of the electrical generator of the wind turbine. These γ_k weights are obtained based on the quality of the normal behavior model and its ability to reproduce the normal behavior that it is predicting.

When a normal behavior model is formulated, the different failure modes of a component (or system) are considered, and also, the variables that are continuously measured and that can supply some information about symptoms of the failure modes are to be considered. The importance or quality of a normal behavior model for the detection of an anomaly will depend on the variable to be predicted, how it can contribute to the detection of a failure mode, and how good the approximation between real and predicted value was during the training of the model. All of this information is used for assigning a value of γ_k to all the models that try to detect the same failure mode. In this example, the values for γ_1, γ_2, and γ_3 are the same and equal to 1/3 because the FMRI that they are weighing is closely related to the failure mode fault of the gearbox.

5.1.2 Relationship Between FMRI and Applied Maintenance

Figure 19 shows an example of FMRI observed over a period of 2 years for a particular wind turbine and a set of normal behavior models related to its gearbox. However, during this period of time, preventive maintenance was applied to the wind turbine. It is necessary to consider how the applied maintenance can impact the FMRI, and for this reason, a model integrating both factors has been developed. Its main features are described in the next lines. More details about this model can be found in [4].

The first maintenance models in the literature assumed that after preventive maintenance, the components were either “as good as new” or “as bad as old.” A more realistic view of the effect of maintenance on components corresponds to the imperfect maintenance models [104], whereas after a preventive maintenance action, usually the result lies somewhere between “as good as new” and “as bad as old,” coinciding in some cases with either of these extremes.

The model proposed considers that the execution of a maintenance action to prevent a failure mode in a component will reduce the level of FMRI for this failure mode. This reduction can be full or partial, and it will be calculated using Eq. 4, which expresses a reduction in the FMRI or residual of FMRI due to the execution of a maintenance action.

$$\text{Res\_RI}_{ij}(t_n) = (1 - \alpha_{ij}) \times \text{RI}_{ij}(t_n). \tag{4}$$

α_{ij} is a factor with real values in [0, 1] that represents the effectiveness of the application of the preventive maintenance action PM_{ij} to eliminate or reduce the value of FMRI in a component i for the failure mode j to a residual value Res_FMRI_{ij} remaining in t_n just after the maintenance action was applied.
The definition of residual FMRI, taking into account the maintenance applied, causes a redefinition of FMRI itself given in Eq. 1, expressed by Eq. 5. The meaning of this equation is that the value of FMRI observed over an interval of time will depend on the amount of FMRI over this interval plus the FMRI existing (if it is applicable) at the beginning of the interval of time considered just after maintenance was performed.

$$\text{FMRI}_{ij}(t) = \int_{t_{n-1}}^{t} \text{DEV}_{ij}(t)\text{d}t + \text{Res\_FMRI}_{ij}(t_{n-1}). \tag{5}$$

In order to complete the final definition of FMRI, a new term has to be added to Eq. 5. This term is difficult to express in mathematical terms; however, its concept is related to the natural aging of a component throughout its life. The most complete definition of FMRI is given in 6, taking into consideration all the effects mentioned.

$$\text{FMRI}_{ij}(t) = \int_{t_{\text{n - 1}}}^{t} \text{DEV}_{ij}(t)\text{d}t + \text{Res\_FMRI}_{ij}(t_{n-1}) + \beta_{ij} \times T(t). \tag{6}$$

where all the terms in Eq. 6 have the same meaning as in Eq. 5 and additionally:

- $\text{T}(t)$ is the length of the total life of the component till t, expressed in general by a function of the age of the component.
- β_{ij} is a factor that weighs by unit of time, the operational age of the component in the RI evaluation, and takes into account how the asset is used throughout its life.

Different laws of influence of aging in the FMRI can be considered in order to more exactly reflect this effect over that which was proposed in Eq. 6, but in this case, a simplified alternative has been chosen only for taking into account the concept and not for an exact modeling of this aspect in FMRI.

The relation between applied maintenance and FMRI expressed by Eq. 5 will be used in the case of FMRI presented in Fig. 19 for the gearbox failure mode. This figure shows the evolution of FMRI for this failure mode without taking into consideration the effect of scheduled maintenance. For simplicity,

three main components were identified in a wind turbine: gearbox, electrical generator, and other main components. Associated with these main components, the following three types of scheduled preventive maintenance actions have been considered:

- Maintenance actions performed in the wind turbine gearbox (MGear).
- Maintenance actions focused on the electrical generator (MGen), which obviously either are not related to the gearbox or are related to it very weakly.
- Maintenance actions carried out on other wind turbine components (MWT), some of which are directly or indirectly related to the gearbox to some degree.

Each type of maintenance action consists of a set of tasks and tests designed specially to develop the preventive capability of maintenance in a wind turbine. Other maintenance actions exist, but they were not considered in this analysis because they are less relevant.

According to the experience of the maintenance personnel, the effectiveness of the MGear actions on the gearbox failure mode was evaluated as 20 %, meaning that the value for α in Eq. 4 was 0.2. In the case of the MWT actions, the value for α was 0.15 and that for α was 0 for the MGen actions.

The β coefficients in Eq. 6 were considered null because the period of time analyzed was not very long, estimating the FMRI as indicated by Eq. 5.

Over a period of 2 years analyzed in Fig. 19 for the FMRI of the gearbox failure mode, the exact dates when preventive maintenance actions were performed are known. On these dates, and according to the type of maintenance performed, Eq. 5 was used for estimating the residual FMRI. Figure 20 shows the results of this estimation of the observed FMRI corrected according to the maintenance performed. The dates when sets of maintenance actions were applied are presented in Fig. 20 as vertical lines with different symbols according to the type of maintenance performed, such as $\diamond$, $\square$, and $+$ in Fig. 20, which correspond, respectively, to the maintenance types: MGen, MWT, and MGear. Observe that sometimes several symbols coincide because various maintenance action types are performed at the same time.

Also, Fig. 20 includes the FMRI of Fig. 19 (upper curve). This comparison shows the effect of maintenance on the evolution of the observed FMRI as an important instrument for limiting the continuous increase in the observed FMRI.

5.1.3 Use of the FMRI in Maintenance Modeling

Using the information supplied by the FMRI discussed in the previous subsections, a maintenance model can be formulated based on continuous monitoring of the life of the wind turbine components. The authors called this maintenance model as MACOL, an acronym whose initials correspond to maintenance model adapted to the continuous observed life of industrial components.

The essential feature of the MACOL model is based on scheduling preventive maintenance not at equally spaced intervals of time, but precisely when

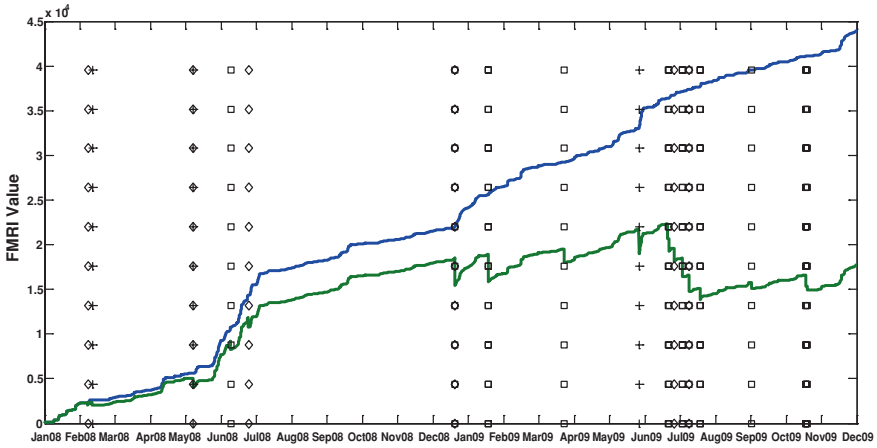

Fig. 20 Observed FMRI for the gearbox failure mode of a wind turbine with and without correction (*lower and upper lines*) of the applied maintenance. Type of maintenance actions: MGear (*plus sign*), MGen (*diamond*), and MWT (*square*)

a predefined value of FMRI is reached according to the observed life of the component. This will schedule the maintenance to be carried out when the component reaches or is close to a similar FMRI level each time. This means that according to this maintenance model, the FMRI value reached between two consecutive maintenance actions has to be kept under FMRI_T or equivalently $0 \leq \text{FMRI}_{ij}(t) \leq \text{FMRI}_T$ in $t_{i-1} \leq t \leq t_i$.

FMRI_T is a threshold for the value of FMRI that is not desirable to overpass because failures were experienced when this was reached, or this is the typical value of FMRI when preventive maintenance actions were performed and no failures appeared.

As an example, a hypothetical case of maintenance rescheduling for the MGear actions will be presented. Using the information about corrected observed FMRI calculated by Eq. 5 and represented in Fig. 20, it is possible to determine a possible value for the threshold FMRI_T as the maximum value of FMRI reached without any fault appearing. This is a conservative strategy based on the current effect of the maintenance applied.

Once FMRI_T was determined using the observed FMRI without correction by applied maintenance as presented in Fig. 20, it is possible to redefine the scheduled dates for applying the maintenance type MGear. The other types of maintenance previously considered were unaltered. The results are presented in Fig. 21 where the observable corrected FMRI is under the threshold FMRI_T at any moment and the number of MGear maintenance actions has been reduced from 6 to 4 during the period of time considered keeping the same level of reliability and availability using MACOL rather than using a strategy of maintenance based on equal intervals of time. This can save costs and requires less handling of components inside the wind turbines reducing the risk of fault by a human error.

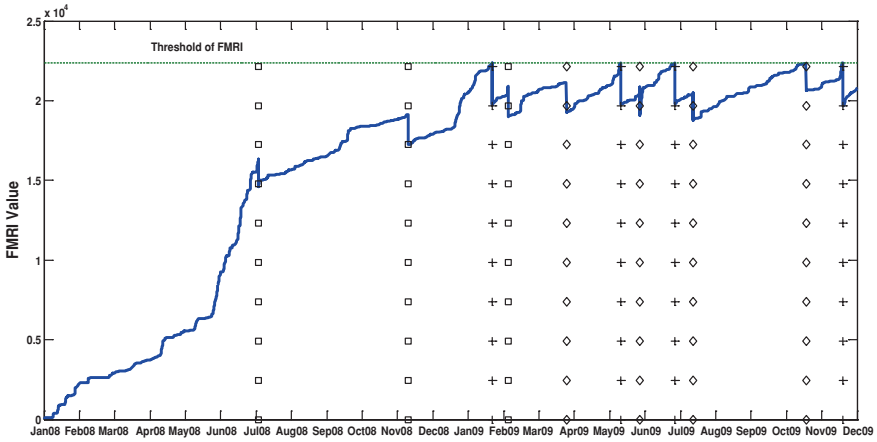

Fig. 21 The new time scheduling for the maintenance type MGear according to the MACOL model

5.2 Performance of Risk Indicator

A performance risk indicator (PRI) is defined as a value able to evaluate the performance of a system in order to verify whether it corresponds or not to what is expected. A non-correspondence is usually due to a possible fault or malfunction due to several causes overlapped at the same time. This indicator is very useful for a global assessment and for scheduling maintenance. The PRI is clearly different from the FMRI described in the previous section because the latter one is focused on particular failure modes of components.

Several models of PRI can be defined, but in this section, a case example will be briefly described based on the power curve of a wind turbine [5].

The wind speed–power curve of a wind turbine is one of the most valuable sources of information to understand its overall behavior, and it is one of the main inputs in condition monitoring programs [82]. The power curve indicates the amount of power that can be generated by a wind turbine as a function of the wind speed, and it is also generally used to estimate the analytic average energy production and to monitor the power production.

The PRI used in this section for illustrative purposes is based on a model named linear hinge model (LHM). This is a piece-wise linear regression model which has proved to be robust and effective in different regression problems [122]. Its main characteristics are as follows: flexibility, accuracy, simplicity, and computational efficiency for modeling data observed from a physical process. The LHM is able to adapt its complexity to the quality and availability of the data, being able to produce adequate models in many different situations. The LHM is completely defined by a set of K internal knots or hinges, plus two external nodes that specify the boundary conditions.

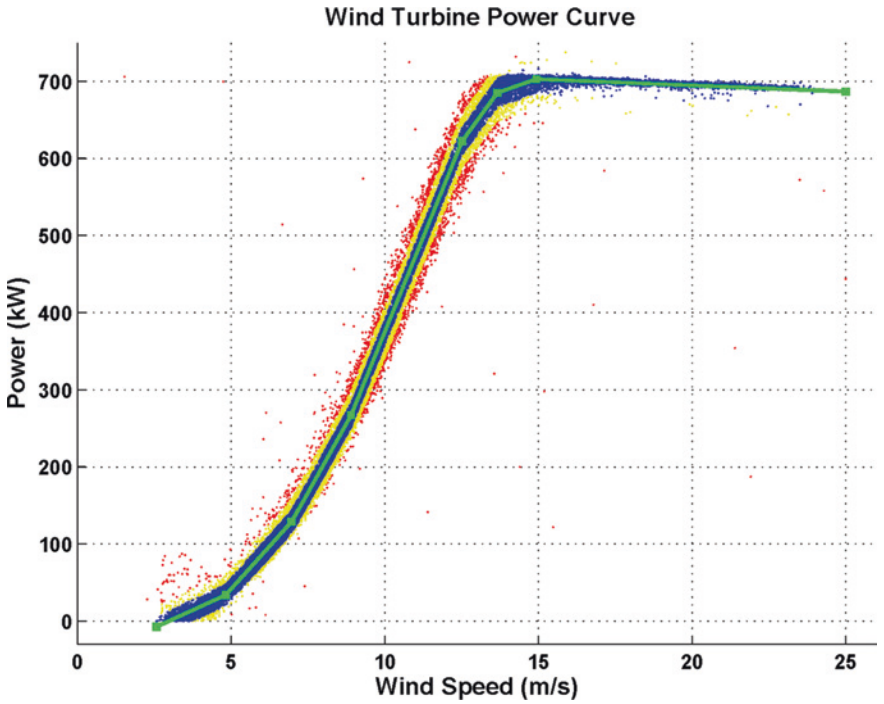

Fig. 22 Fitted power curve using LHM

Here, the LHM was used to model the power curve of a wind turbine according to the real data collected in real time for power and wind speed from a wind turbine. The resulting model (green line) is presented in Fig. 22. Also, the figure includes three regions:

- The blue region represents data collected that are inside a confidence band of the model LHM. It is one standard deviation in distance from the model obtained (green line).
- The yellow region represents data between one and two standard deviations away from the model.
- The red region includes data farther than two standard deviations away from the model.

Both standard deviation values and number of LHM linear segments change, depending on the dispersion and nonlinearity of the data included in the training data set. The model was fitted using data from one full year, and it is the reference power curve in the proposed methodology to evaluate the PRI.

The PRI can be defined as the difference between the reference power curve obtained previously from data over 1-year period and the power curve obtained from data collected from the wind turbine in a different and later period of time. The PRI tries to detect any difference in the performance of a wind turbine through

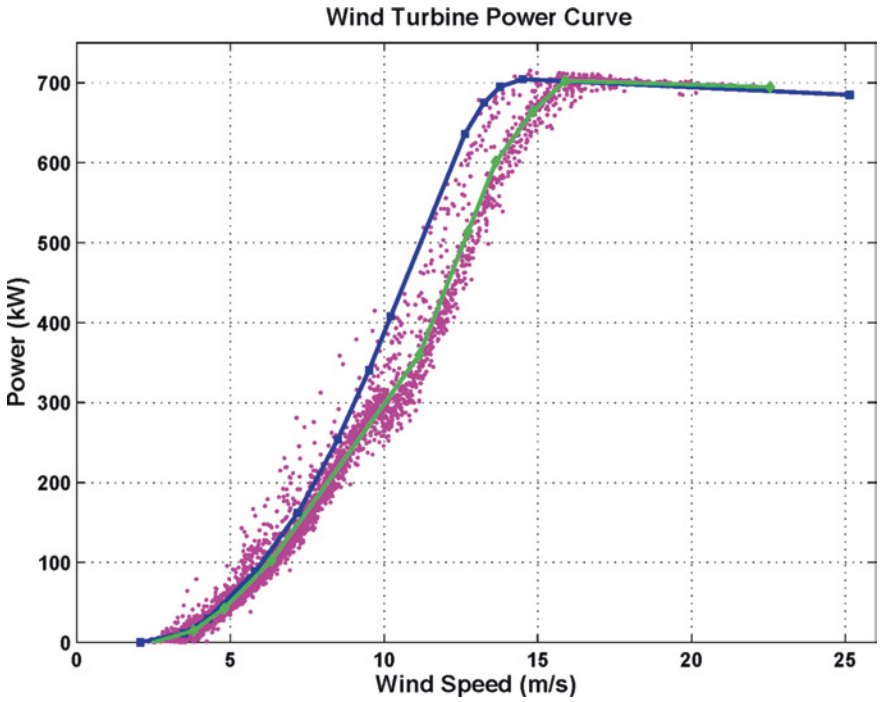

Fig. 23 Reference (*blue*) and updated (*green*) power curves for the initial period of time considered as reference and another one later than the first one

the continuous monitoring of the power curve in sequential periods of time because any significant difference means there is degradation or malfunction, and in any case, there are income losses due to energy not produced for the wind farm owner.

Figure 23 shows an example of the difference between two estimated power curves: the one used as reference (in blue) and another one (green line) corresponding to a period of time later than that which was used for the estimation of the reference power curve. The difference between the two is important especially in the region of high production of electricity.

In order to obtain a robust diagnosis, the comparison between power curves is made according to different ranges of wind speeds and areas below the power curve. A wind turbine can keep the same profile of power curve over time, but under different wind distribution profiles, its performance may be better under one condition than under another; for this reason, wind distribution has to be considered in the calculation of the PRI.

Wind distribution is calculated by adding the number of occurrences observed in each wind range i considered and dividing them by the total number of samples collected. The number of wind ranges to be taken into account will depend on the behavior expected in the design of the wind turbine. For example, in the present case, the total range of wind was divided into two regions (low and high wind speed ranges).

The lower wind speed region is defined from 3 to 10 m/s and the higher wind speed region from 10 to 20 m/s. The two wind speed ranges represent the operational speed range of the machine, from the cut-in to the cut-out speeds. The wind distribution (WD_i^T) parameter represents the percentage of wind occurrences in region i during the window of time considered.

Once the power curves and wind distribution are established, it is possible to quantify the differences of areas under the power curves (reference and current) for each range of wind speed and finally to obtain the PRI. The areas under the curves are divided into n regions such as the wind distributions, and the differences in areas in the regions are calculated. A performance risk indicator by region (PRI_i) is obtained as a ratio of the difference in areas to the total area of the region according to Eq. 7:

$$PRI_i = \frac{S_i^T - S_i^R}{S_i^R} \tag{7}$$

where S_i^T and S_i^R are the current and reference areas of region i, respectively. There are different ways to estimate the areas of the curve such as the trapezoidal rule or the Simpson's rule. The PRI_i will be negative if the area under the current curve is smaller than the area under the reference curve, and this will indicate a degradation of performance.

Therefore, by knowing the PRI_i for each region, it is reasonable to assert that the overall wind turbine PRI should be defined as a weighted average of PRI_i as presented in Eq. 8:

$$PRI = \sum_{i=1}^{n} \left(WD_i^T \cdot PRI_i \right). \tag{8}$$

The PRI is able to determine the performance of the wind turbine itself over time, meaning the gain between the current and reference power curves. Figure 24 shows regions considered for the estimation of the PRI.

Figure 25 shows an analysis of data corresponding to 5 years of operation of a wind turbine. The left part of the figure shows the electrical power output as a function of wind speed; the blue line and the red dashed lines are the reference power curve (first year analyzed) and its confidence bands, respectively; the pink points represent the "last" current period of time analyzed; the green line and turquoise dashed lines are the current fitted power curve and its confidence bands, respectively. The confidence bands in both cases are two times the standard deviation of the data set evaluated. The differences in behavior observed suggest that as the wind turbine is getting older, the power curve shifts to the right, i.e., it needs a higher wind speed to generate the same amount of electrical power.

The right side of Fig. 25 contains seven subplots corresponding to seven significant variables (i.e., points) of the hinge model of the fitted power output ($P1$, $P2$, etc.) versus time for seven specific wind speed levels ($L1$, $L2$, etc.). This makes it possible to reduce all the information of the training set of data to these seven variables able to represent the wind turbine power curve behavior over time.

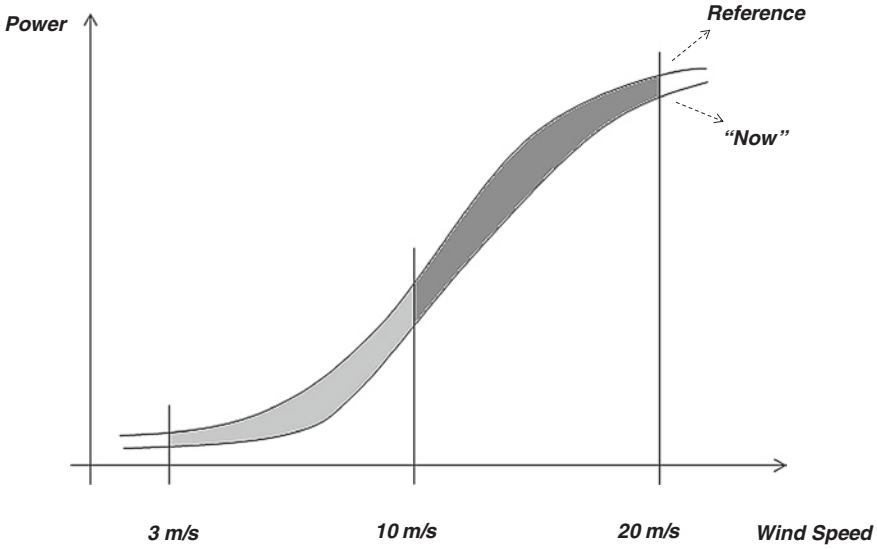

Fig. 24 Regions used for the calculation of PRI

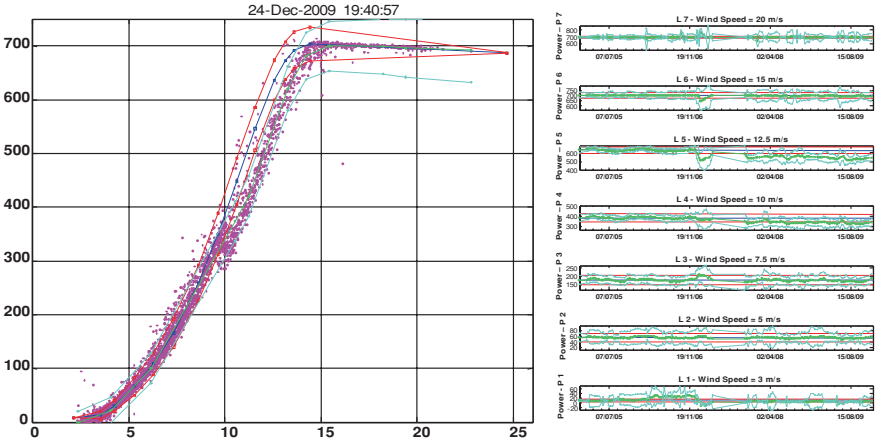

Fig. 25 Power curve modeling and PRI estimation over the period 2005–2009

Figure 26 shows a more detailed explanation of the contents for five subplots on the left side of Fig. 25. Here, some periods of power curve deviations are identified.

Figure 27 displays the evolution of the PRI for a wind turbine over the period of time analyzed. It can suggest the health condition of the wind turbine, as well as its aging. As can be observed, the value of PRI in this case is negative, i.e., the performance of the wind turbine is decreasing over the period of time analyzed

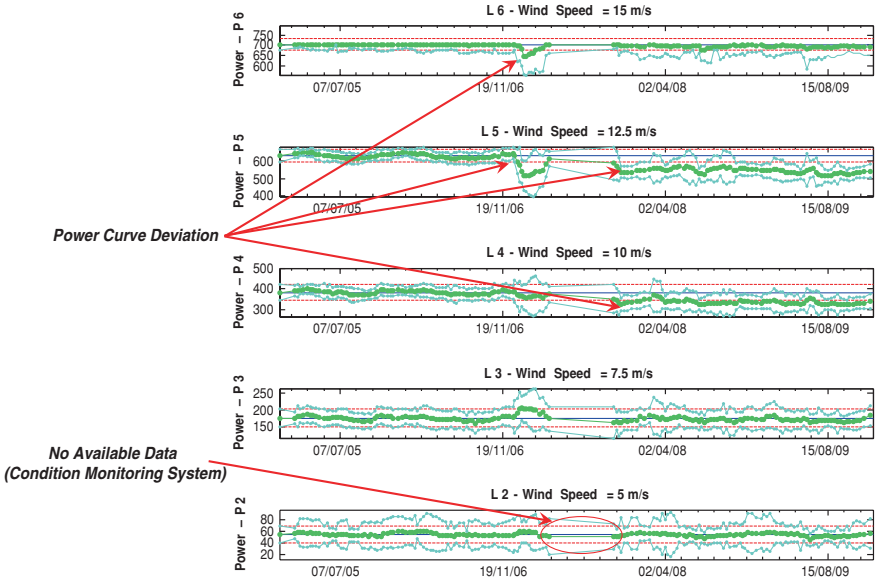

Fig. 26 Detailed information of the five central variables of the power curve model

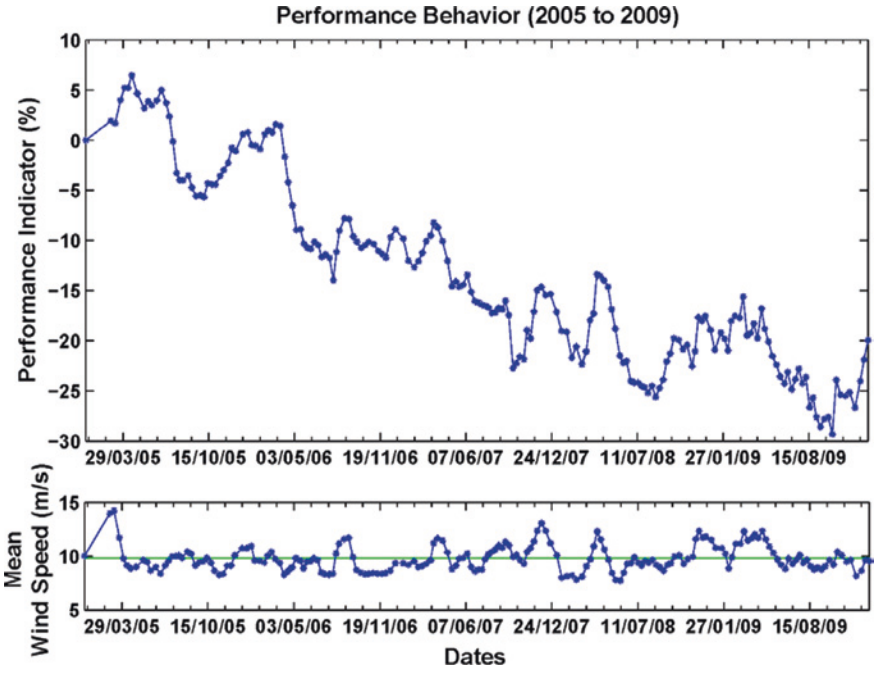

Fig. 27 Evolution of the PRI over the period 2005–2009

around 25 % less than the reference taken 5 years before. The PRI follows a negative trend, which may indicate a process of degradation due to aging or the effect triggered by a problem in an internal component (electrical generator, gearbox, etc.). Thereby, it is important to monitor the PRI slope because if an unexpected change in its value occurs, then a specific failure/degradation cause or event could be present. The mean wind speed during the interval of time analyzed is shown at the bottom of Fig. 27 where important variations were not observed in its profile that could explain the degraded wind turbine performance.

As was demonstrated in this section, the PRI is a valuable tool used to assess the process of taking decisions about maintenance, life cycle, and new investments in a wind farm.

6 Conclusions

This chapter has presented a complete and thorough review of the state of the art concerning the operation, diagnosis, and maintenance of industrial processes focusing in particular in wind turbines. This review shows the important interest in this field both in research and in industry. Wind energy is actually a key contribution in the production of energy in a large part of the world, and the correct operation and maintenance of wind farms is a focus of main attention from different perspectives such as life cycle, asset management, quality of service, investment and operational cost, and reliability. Also, this chapter has described the essential features of a method used to evaluate the health condition of a wind turbine based on continuous monitoring of its behavior. This behavior is characterized by models of normal behavior able to predict the values expected for particular variables under different working conditions. The deviations with respect to the normal behavior expected are the main inputs for the evaluation of the FMRI. The definition of this concept and the development of a methodology for its calculation have been described in this chapter. Finally, a performance indicator about the general condition of a wind turbine has been outlined. All the methods presented are feasible samples of real experiences that demonstrate how it is possible to better know the life of the wind turbines and how their operation and maintenance can be improved.

References

1. Al-Najjar B, Alsyouf I (2004) Enhancing a company's profitability and competitiveness using integrated vibration-based maintenance: a case study. Eur J Oper Res 157(3):643–657
2. Amirat Y, Benbouzid MEH, Bensaker B, Wamkeue R (2007) Condition monitoring and fault diagnosis in wind energy conversion systems: a review. In: Proceedings of 2007 IEEE international electric machines and drives conference, vol 2, pp 1434–1439
3. Amirat Y, Benbouzid MEH, Bensaker B, Wamkeue R (2007) Generators for wind energy conversion systems: state of the art and coming attractions. J Electr Syst 3–1:26–38

4. Andrade Vieira RJ, Sanz-Bobi MA (2013) Failure risk indicators for a maintenance model based on observable life of industrial components with an application to wind turbines. IEEE Trans Reliab 62(3):569–582
5. Andrade Vieira RJ, Sanz-Bobi MA, Kato S (2013) Wind turbine condition assessment based on changes observed in its power curve. In: 2nd international conference on renewable energy research and applications—ICRERA 2013, Madrid, Spain
6. Arranz AL, Cruz A, Sanz-Bobi MA, Ruíz P, Coutiño J (2008) DADICC: intelligent system for anomaly detection in a combined cycle gas turbine plant. Expert Syst Appl 34–4:2267–2277
7. Arts RHPM, Knapp GMJ, Lawrence M (1998) Some aspects of measuring maintenance performance in the process industry. J Qual Maintenance Eng 4(1):6–11
8. Barlow RE, Hunter L (1960) Optimal preventive maintenance policies. Oper Res 8:90–100
9. Bengtsson M (2004) Condition based maintenance system technology—where is development heading? In: Proceedings of the 17th European maintenance congress Euromaintenance, Barcelona, Spain
10. Bengtsson M (2004) Condition based maintenance systems: an investigation of technical constituents and organizational aspects. In: Citeseer
11. Bengtsson M, Jackson M (2004) Important aspect to take into considerations when deciding to implement condition based maintenance. In: Proceeding from the 17th conference of condition monitoring and diagnostic management, England, Cambridge: The Central Printing Services, University of Birmingham, UK
12. Bertling L, Allan R, Eriksson R (2005) A reliability-centered asset maintenance method for assessing the impact of maintenance in power distribution systems. IEEE Trans Power Syst 20(1):1–8
13. Bin L, Yaoyu L, Xin W, Zhongzhou Y (2009) A review of recent advances in wind turbine condition monitoring and fault diagnosis. In: Proceedings of IEEE power electronics machines in wind applications (PEMWA), pp 1–7
14. Birolini A (1994) Quality and reliability of technical systems. Springer, Berlin
15. Birolini A (2004) Reliability engineering: theory and practice, 4th edn. Springer, Berlin
16. Bouno T, Yuji T, Hamada T, Hideaki T (2005) Failure forecast diagnosis of small wind turbine using acoustic emission sensor. KIEE Int Trans Electr Mach Energy Convers Syst 5-B(1):78–83
17. Brown RE, Frimpong G et al (2004) Failure rate modeling using equipment inspection data. IEEE Trans Power Syst 19(2):782–787
18. Buczkowski PS, Hartmann ME, Kulkarni VG (2005) Outsourcing prioritized warranty repairs. Int J Qual Reliab Manag 22(7):699–714
19. Byington CS, Roemer MJ, Galie T (2002) Prognostic enhancements to diagnostic systems for improved condition-based maintenance. In: IEEE aerospace conference proceedings
20. Campbell JD, Jardine AKS (2001) Maintenance excellence. Marcel Dekker, New York
21. Caselitz P, Giebhardt J (1999) Advanced condition monitoring for wind energy converters. In: Proceedings of the European wind energy conference, Nizza, France, 1–5 Mar 1999
22. Caselitz P, Giebhardt J, Mevenkamp M (1994) On-line fault detection and prediction in wind energy converters. In: Proceedings of the European wind energy conference, Thessaloniki, Greece, 10–14 Oct 1994, pp 623–627
23. Caselitz P, Giebhardt J, Mevenkamp M (1997) Application of condition monitoring systems in wind energy converters. In: Proceedings of the European wind energy conference, Dublin, Ireland, 6–9 Oct 1997, pp 579–582
24. Caselitz P, Giebhardt J, Krüger T, Mevenkamp M (1996) Development of a fault detection system for wind energy converters. In: Proceedings of the European wind energy conference, Goteborg, Sweden, 20–24 May 1996, pp 1004–1007
25. Chen C, Sun C, Zhang Y, Wang N (2005) Fault diagnosis for large-scale wind turbine rolling bearing using stress wave and wavelet analysis. In: Proceedings of 8th international conference on electrical machines and systems, vol 3, pp 2239–2244
26. Chenglong M, Bin D (2011) Design and application of wind farm fault diagnosis system. In: Proceedings of IEEE power energy engineering conference (APPEEC), Asia-Pacific, pp 1–4

27. Chow EY, Willsky AS (1984) Analytical redundancy and the design of robust failure detection systems. IEEE Trans Autom Control 29(7):603–614
28. Chow MY, Mangum PM, Yee SO (1991) A neural network approach to real time condition monitoring of induction motors. IEEE Trans Industr Electron 38(6):448–454
29. Cigolini R, Fedele L, Garetti M, Macchi M (2008) Recent advances in maintenance and facility management. Prod Plan Control 19(4):279–286
30. Clayton BR, Dutton AG, Aftab N, Bond LJ, Irving AD, Lipman NH (1990) Development of structural condition monitoring techniques for composite wind turbine blades. In: Proceedings of European community wind energy conference, Madrid, Spain, 10–14 Sept 1990, pp 10–14
31. Crespo A, Moreu P, Gómez JF, Parra C, López M (2009) The maintenance management framework: a practical view to maintenance management. J Qual Maint Eng 15(2):167–178
32. Cua KO, McKone KE, Schroeder RG (2001) Relationships between implementation of TQM, JIT, and TPM and manufacturing performance. J Oper Manage 19(6):675–694
33. Davies A (1998) Handbook of condition monitoring. Chapman & Hall, London
34. Dekker R, Scarf PA (1998) On the impact of optimization models in maintenance decision making: the state of the art. Reliab Eng Syst Saf 60(2):111–119
35. DOE (2008) 20 % Wind energy by 2030: increasing wind energy's contribution to U.S. electricity supply. DOE/GO-102008-2578 2008 [Online]. Available: http://www1.eere.energy.gov/wind/pdfs/42864.pdf. Accessed May 2012
36. Duffuaa SO, Raouf A, Campbell JD (1999) Planning and control of maintenance system: modeling and analysis. Wiley, Hoboken
37. Eisinger S, Rakowsky UK (2001) Modeling of uncertainties in reliability centered maintenance—a probabilistic approach. Reliab Eng Syst Saf 71(2):159–164
38. EN 13306: 2001 (2010) Maintenance Terminology (Replaced by EN 13306: 2010)
39. Endrenyi J, Aboresheid S et al (2001) The present status of maintenance strategies and the impact of maintenance on reliability. IEEE Trans Power Syst 16(4):638–646
40. Endrenyi J, Anders GJ et al (1998) Probabilistic evaluation of effect of maintenance on reliability—an application. IEEE Trans Power Syst 13(2):576–583
41. EWETP (2008) Strategic research agenda: market deployment strategy from 2008 to 2030, European wind energy technology platform 2008 [Online]. Available: http://www.windplatform.eu/fileadmin/ewetp_docs/Bibliography/Synopsis_2008.pdf. Accessed May 2012
42. Farrar CR, Lieven NAJ (2007) Damage prognosis: the future of structural health monitoring. Philos Trans R Soc A 365:623–632
43. Franzén A, Bertling L (2007) State of the art—life time modeling and management of transformers. Royal Institute of Technology, KTH, Stockholm
44. Gabbar HA, Yamashita H, Suzuki K, Shimada Y (2003) Computer-aided RCM-based plant maintenance management system. Robot Comput-integr Manufact 19(5):449–458
45. García MC (2004) Planificación y Medida de la Efectividad del Mantenimiento predictivo aplicado a un proceso industrial basándose en el uso de técnicas de modelado de su comportamiento y inteligencia artificial. In: Tesis del departamento de electrónica y automática, Universidad Pontificia Comillas, Madrid
46. García MC, Sanz-Bobi MA (2003) Planificación dinámica del mantenimiento industrial mediante algoritmos genéticos. Mantenimiento 161(42):49
47. García MC, Sanz-Bobi MA, Pico J (2006) Técnicas de inteligencia artificial aplicadas al mantenimieto predictivo de aerogeneradores. Mantenimiento 137:5–16
48. Garg A, Deshmukh SG (2006) Maintenance management: literature review and directions. J Qual Maint Eng 12(3):205–238
49. Gebraeel N, Lawley MA (2008) A neural network degradation model for computing and updating residual life distributions. IEEE Trans Autom Sci Eng 5:154–163
50. Gertler J (1988) Survey of model-based failure detection and isolation in complex plants. IEEE Control Syst Mag 8(6):3–11
51. Gertler J (1991) Analytical redundancy methods in fault detection and isolation. In: IFAC fault detection, supervision and safety for technical process

52. Grimmelius H, Meiler TP, Maas H et al (1999) Three state-of-the-art methods for condition monitoring. IEEE Trans Ind Electron 46(2):407–416
53. Hameed Z, Hong YS, Cho YM, Ahn SH, Song CK (2009) Condition monitoring and fault detection of wind turbines and related algorithms: a review. Renew Sustain Energy Rev 13(1):1–39
54. Han T, Yang B-S (2006) Development of an e-maintenance system integrating advanced techniques. In: Comput Ind [special issue on e-maintenance] 57(6):569–80
55. Hao Q, Xue Y, Shen W, Jones B, Zhu J (2010) A Decision support system for integrating corrective maintenance, preventive maintenance, and condition-based maintenance
56. Hassanain MA, Froese TM, Vanier DJ (2003) Framework model for asset maintenance management. J Perform Constructed Facil 17:51
57. Hassanain MA, Froese TM, Vanier DJ (2003) Implementation of distributed model-based integrated asset management system. J Inf Technol Constr 8:119–134
58. Haykin S (1994) Neural networks: a comprehensive foundation. IEEE Press, New York
59. Hilber P (2008) Maintenance optimization for power distribution systems. Royal Institute of Technology, KTH, Stockholm
60. Huang J, Miller CR, Okogbaa OG (1995) Optimal preventive-replacement intervals for the Weibull life distribution: solutions and applications. In: Proceedings of annual reliability and maintainability, pp 370–377
61. Huang Q, Jiang D, Hong L, Ding Y (2008) Application of wavelet neural networks on vibration fault diagnosis for wind turbine gearbox. Lecture notes in computer science, vol 5264, LNCS, n PART 2, advances in neural networks. In: Proceedings of 5th international symposium on neural networks, pp 313–320
62. Huang S, Kok KT (2009) Fault detection and diagnosis based on modeling and estimation methods. IEEE Trans Neural Netw 20(5):872–881
63. Hyers RW, McGowan JG, Sullivan KL, Manwell JF, Syrett BC (2006) Condition monitoring and prognosis of utility scale wind turbines. Energy Mater 1(3):187–203
64. Ip WH, Kwong CK, Fung R (2000) Design of maintenance system in MRPII. J Qual Maint Eng 6(3):177–191
65. Iravani SMR, Duenyas I (2002) Integrated maintenance and production control of a deteriorating production system. IIE Trans 34(5):423–435
66. Isermann R (1984) Process fault detection based on modeling and estimation methods—a survey. Int Fed Autom Control 20(4):387–404
67. Isermann R (1993) Fault diagnosis of machines via parameter estimation and knowledge processing-tutorial paper. Automatica 29(4):815–835
68. Isermann R (1997) Supervision, fault-detection and fault-diagnosis methods-an introduction. Control Eng Pract 5(5):639–652
69. Isermann R (2005) Model-based fault-detection and diagnosis—status and applications. Ann Rev Control 29(1):71–85
70. Iung B (2003) From remote maintenance to MAS-based E-maintenance of an industrial process. J Intell Manuf 14(1):59–82
71. Jardine AK, Tsang AH (2006) Maintenance, replacement, and reliability: theory and applications. CRC Taylor & Francis, Boca Raton
72. Jardine A, Lin D, Banjevic D (2006) A review on machinery diagnostics and prognostics implementing condition-based maintenance. Mech Syst Sig Process 20(7):1483–1510
73. Jayabalan V, Chaudhuri D (1992) Cost optimization of maintenance scheduling for a system with assured reliability. IEEE Trans Rel R-41:21–25
74. Jonsson P (1999) Company-wide integration of strategic maintenance: an empirical analysis. Int J Prod Econ 60–61:155–164
75. Kaplan RS, Norton DP (1992) The balanced scorecard—measures that drive performance. Harv Bus Rev 70(1):71–79
76. Khan FI, Haddara MM (2003) Risk based maintenance: a quantitative approach for maintenance/inspection scheduling and planning. J Loss Prev Process Ind 16(6):563–573

77. Koc M, Ni J, Lee J, Bandyopadhyay P (2003) Introduction of e-manufacturing. In: Proceedings of the 31st North American manufacturing research conference (NAMRC), Hamilton, Canada
78. Kusiak A, Li WY (2011) The prediction and diagnosis of wind turbine faults. Renew Energy 36(1):16–23
79. Kusiak A, Verma A (2011) Prediction of status patterns of wind turbines: a data-mining approach. ASME J. Solar Eng 133(1):011008-1–011008-10
80. Kutucuoglu KY, Hamali J, Irani Z, Sharp JM (2001) A framework for managing maintenance using performance measurement systems. Int J Oper Prod Manag 21(1):173–194
81. Kyle BR, Vanier DJ, Kosovac B, Froese TM (2000) Information needs towards service life asset management. In: Proceedings of 17th international conference of the committee on data for science and technology, CODATA, Baveno, Italy, pp 15–19
82. Lapira E, Brisset D, Davari Ardakari H, Siegel D, Lee J (2012) Wind turbine performance assessment using multi-regime modeling approach. Renew Energy 45:86–95
83. Lebold M, Thurston M (2001) Open standards for condition-based maintenance and prognostic systems. In: 5th annual maintenance and reliability conference (MARCON 2001), Gatlinburg, USA
84. Lee J (2001) A framework for next-generation E-maintenance system. In: Proceedings of the second international symposium on environmentally conscious design and inverse manufacturing, Tokyo, Japan
85. Lee J (2010) Design of self-maintenance and engineering immune systems for smarter machines and manufacturing systems. In: 1st IFAC workshop on advanced maintenance engineering, services and technology, Lisbon, Portugal, 1–2 July 2010
86. Lee J, Elmeligy S, Ghaffari M (2010) Transformation from prognostics to engineering immune systems. In: 1st IFAC workshop on advanced maintenance engineering, services and technology, Lisbon, Portugal, 1–2 July 2010
87. Lee J, Ni J, Djurdjanovic D, Qiu H, Liao H (2006) Intelligent prognostics tools and e-maintenance. Comput Ind Spec issue e-maint 57(6):476–489
88. Lee J, Wu F, Zhao W, Ghaffari M, Liao L, Siegel D (2010) Prognostics and health management design for rotary machinery systems—reviews, methodology and applications. Mech Syst Signal Process 42(1–2):314–334. http://www.sciencedirect.com/science/journal/08883270/42/1
89. Lekou DJ, Mouzakis F, Anastasopoulos A, Kourousis D (2009) Emerging techniques for health monitoring of wind turbine gearboxes and bearings. In: Proceedings of EWEC 2009, scientific track—operation and maintenance, Marseille, France, pp 16–19
90. Levitt J (2009) Handbook of maintenance management. Industrial Press, South Norwalk
91. Li S, O'Hair E, Giesselmann MG (1997) Using neural networks to predict wind power generation. In: Proceedings of the international solar energy conference, Washington, DC, pp 415–420
92. Lie CH, Chun YH (1986) An algorithm for preventive maintenance policy. IEEE Trans Rel R-35(1):71–75
93. Lin D, Zuo M, Yam R (2001) Sequential imperfect preventive maintenance models with two categories of failure models. Naval Res Logistics 48:172–183
94. Lofsten H (2000) Measuring maintenance performance—in search for a maintenance productivity index. Int J Prod Econ 63(1):47–58
95. Lu B, Li Y, Wu X, Yang Z (2009) A review of recent advances in wind turbine condition monitoring and fault diagnosis. In: Power electronics and machines in wind applications. PEMWA 2009. IEEE, p 1
96. MaCalley J, Jiang Y et al (2006) Automated integration of condition monitoring with an optimized maintenance scheduler for circuit breakers and power transformers. In: Power systems engineering research center, PSERC
97. McArthur SDJ, Booth CD, McFadyen IT (2005) An Agent based anomaly detection architecture for condition monitoring. IEEE Trans Power Syst 20(4):1675–1682

98. Mobley RK, Higgins LR, Wikoff DJ (2008) Maintenance engineering handbook. Mc-Graw-Hill, New York
99. Moubray J (1997) Reliability centred maintenance, 2nd edn. Butterworth-Heinemann, Boston
100. Muller A, Crespo A, Iung B (2008) On the concept of e-maintenance: review and current research. Reliab Eng Syst Saf 93(8):1165–1187
101. Muñoz A, Sanz-Bobi MA (1998) An incipient fault detection system based on the probabilistic radial basis function network: application to the diagnosis of the condenser of a coal power plant. Neurocomputing 23:177–194
102. Murthy DN, Asgharizadeh E (1999) Optimal decision making in a maintenance service operation. Eur J Oper Res 116(2):259–273
103. Murthy DNP, Atrens A, Eccleston JA (2002) Strategic maintenance management. J Qual Maint Eng 8(4):287–305
104. Nakagawa T (1988) Sequential imperfect preventive maintenance policies. IEEE Trans Reliab 37:295–298
105. Nakajima S (1988) Introduction to TPM, 1st edn. Productivity Press, Cambridge
106. Nguyen DG, Murthy DN (1981) Optimal preventive maintenance policies for repairable systems. Oper Res 29(6):1181–1194
107. Nikolopoulos K, Metaxiotis K, Lekatis N, Assimakopoulos V (2003) Integrating industrial maintenance strategy into ERP. Ind Manag Data Syst 103(3):184–191
108. Nilsson J (2006) Maintenance management of wind power systems—cost effect analysis of condition monitoring systems. Master's thesis, KTH, Stockholm, Sweden
109. Nilsson J, Bertling L (2007) Maintenance management of wind power systems using condition monitoring systems—life cycle cost analysis for two case studies. IEEE Trans Energy Convers 22(1):223–229
110. Ostergaard J, Jensen AN (2001) Can we delay the replacement of this component?—an asset management approach to the question. In: CIRED, paper no. 482, Amsterdam
111. Patton RJ, Frank PM, Clark RN (2000) Issues of fault diagnosis for dynamic systems. Springer, Berlin
112. Penman CM, Yin J (1994) Feasibility of using unsupervised learning, artificial neural networks for the condition monitoring of electrical machines. IEE Proc Electr Power Appl 141(6):317–323
113. Penman J, Tavner TJ (1989) Condition monitoring of electrical machines. Research Studies Press Ltd., Wiley, New York
114. Peters F, Meissner U (1995) Object-oriented composition of a framework for integrative facility management. In: Proceedings of CIB-W78/TG10: modeling of buildings through their life cycle, Stanford University, Palo Alto, California, CIB Publication No. 180, CIB, Rotterdam, The Netherlands, pp 111–118
115. Petersen KE (1993) Reliability based maintenance systems; a knowledge based approach. In: Proceedings of the 4th Scandinavian conference on artificial intelligence electrum, Stockholm, Sweden, 4–7 May 1993, pp 409–410
116. Pintelon L, Puyvelde FV (1997) Maintenance performance reporting systems: some experiences. J Qual Maint Eng 3(1):4–15
117. Pouliezos A, Stavrakakis G, Lefas C (1989) Fault detection using parameter estimation. Qual Reliab Eng Int 5:283–290
118. Provan G. (2003) Prognosis and condition-based monitoring: an open systems architecture. In: 5th IFAC symposium on fault detection, supervision and safety of technical processes, Washington, USA, pp 57–62
119. Pun K, Chin K, Chow M, Lau HCW (2002) An effectiveness-centered approach to maintenance management: a case study. J Qual Maint Eng 8(4):346–368
120. Raouf A, Ben-Daya M (1995) Total maintenance management: a systematic approach. J Qual Maint Eng 1(1):6–14
121. Ribrant J, Bertling LM (2007) Survey of failures in wind power systems with focus on Swedish wind power plants during 1997–2005. IEEE Trans Energy Convers 22(1):167–173

122. Sanchez-Ubeda EF, Wehenkel L (1998) The Hinges model: a one-dimensional continuous piecewise polynomial model. In: IPMU'98, Paris, France, pp 878–885
123. Sanz-Bobi MA (1992) Metodología de mantenimiento predictivo basada en análisis espectral y temporal de la historia de los equipos industriales y enfoque de su aplicación a un sistema experto. In: E.T.S. de Ingenieros Industriales, Universidad Politécnica de Madrid, Madrid
124. Sanz-Bobi MA, Andrade Vieira RJ (2011) A method for estimating stress of a failure mode in a component due to abnormal behavior observed in a wind turbine. In: Proceedings of 24th international congress condition monitoring diagnostics engineering management, Stavanger, Norway, pp 989–998
125. Sanz-Bobi MA, Andrade Vieira RJ, Montilla X (2011) Failure risk analysis and maintenance effectiveness in a wind turbine according to its history of unavailability and applied maintenance. In: Proceedings of European safety and reliability association conference—ESREL 2011, Troyes, France, pp 853–860
126. Sanz-Bobi MA, del Pico J, Garcia MC (2006) SIMAP: intelligent system for predictive maintenance application to the health condition monitoring of a wind turbine gearbox. Comput Ind 57(6):552–568
127. Sanz-Bobi MA, Garcia AC, Palacios R, Villar J, Rolan J, Moran B (1997) Experiences learned from the on-line internal monitoring of the behaviour of a transformer. In: IEEE—IEMDC'97 international electric machines and drive conference, USA
128. Sanz-Bobi MA, Palacios R, Pérez EM (2009) Estado actual y tendencias de la Gestión de activos (asset management) en las empresas de transporte y distribución de energía eléctrica. Mantenimiento 229:30–38
129. Sanz-Bobi MA, Palacios R, Muñoz A, García-Escudero R, Pérez M, Matesanz AL (2002) ISPMAT: intelligent system for predictive maintenance applied to trains. In: Proceedings of EUROMAINTENANCE, Helsinki, Finland
130. Sanz-Bobi MA, Palacios R, Vieira RJA, Nicolau G, Ferrarons P (2010) Assisting tools for a new maintenance planning in a power distribution system. In: IEEE power engineering society general meeting, USA
131. Sanz-Bobi MA, Vieira RJA, Brighenti C, Palacios R, Nicolau G, Ferrarons P, Vieira P (2010) Component stress evaluation in an electrical power distribution system using neural networks. In: 23rd international conference on industrial, engineering and other applications of applied intelligent systems, Spain
132. Scarf PA (2007) A framework for condition monitoring and condition based maintenance. Qual Technol Quant Manag 4(2):301–312
133. Schlechtingen M (2013) A global condition monitoring system for wind turbines. In: PhD thesis, Department of Mechanical Engineering—Solid Mechanics, Technical University of Denmark, Denmark
134. Schneider J, Gaul A, Neumann C, Hogräfer J, Wellssow W, Schwan M, Schnettler A (2006) Asset management techniques. Electr Power Energy Syst 28(9):643–654
135. Sheliga DJ (1981) Calculation of optimum preventive maintenance intervals for electric equipment. IEEE Trans Ind Appl 1A-17(5)
136. Shulian Y, Wenhai L, Canlin W (2008) The intelligent fault diagnosis of wind turbine gearbox based on artificial neural network. In: Proceedings of IEEE international conference on condition monitoring diagnosis (CMD 2008), pp 1327–1330
137. Sorsa T, Koivo HN (1991) Application of artificial neural networks in process fault diagnosis. Proc Saveprocess 91(2):133–138
138. Sturm A, Billhardt S (1991) Envelope curve analysis of machines with rolling-element bearings. Proc Saveprocess 91(2):275–279
139. Sumereder C (2008) Statistical lifetime of hydro generators and failure analysis. IEEE Trans Dielectr Electr Insul 15(3):678–685
140. Swanson L (2001) Linking maintenance strategies to performance. Int J Prod Econ 70(3):237–244
141. Tam ASB, Price JWH (2006) A generic maintenance optimization framework. In: 7th Asia pacific industrial engineering and management systems conference, Bangkok, Thailand

142. Tao B, Ding H, Xion YL (2003) IP sensor and its distributed networking application in e-maintenance. In: Proceedings of the 2003 IEEE international conference on systems, man and cybernetics, vol 4. Washington, DC, USA, pp 3858–63
143. Thomas E, Levrat E, Iung B, Cocheteux P (2009) Opportune maintenance and predictive maintenance decision support. In: 13th IFAC symposium on information control problems in manufacturing, Moscow, Russia
144. Tian Z (2009) An artificial neural network approach for remaining useful life prediction of equipments subject to condition monitoring. In: 8th international conference on reliability, maintainability and safety, pp 143–148
145. Tor O, Shahidephpour M (2006) Power distribution asset management. In: IEEE power engineering society general meeting
146. Tsang AHC, Jardine AKS, Kolodny H (1999) Measuring maintenance performance: a holistic approach. Int J Oper Prod Manag 19(7):691–715
147. Tu PVL, Yam R, Tse P, Sun AO (2001) An integrated maintenance management system for an advanced manufacturing company. Int J Adv Manuf Technol 17(9):692–703
148. Vanier DJ (2001) Why industry needs asset management tools. J Comput Civ Eng 15(1):35–43
149. Vatland S, Gundersen LS, Sande G, Bugge J, Asbjomsen T, Lund T (2004) Utility systems integration. In: Distribution and asset management conference
150. Velasquez J (2011) Intelligent monitoring and diagnosis of power transformers in the context of an asset management model. In: Universitat Politècnica de Catalunya UPC, Barcelona
151. Venkatasubramanian V, Rengaswamy R, Kavuri SN, Yin K (2003) A review of process fault detection and diagnosis. Part III. Process history based methods. Comput Chem Eng 27(3):327–346
152. Venkatasubramanian V, Rengaswamy R, Kavuri SN (2003) A review of process fault detection and diagnosis. Part II. Qualitative models and search strategies. Comput Chem Eng 27(3):313–326
153. Venkatasubramanian V, Rengaswamy R, Yin K, Kavuri SN (2003) A review of process fault detection and diagnosis. Part I. Quantitative model-based methods. Comput Chem Eng 27(3):293–311
154. Verbruggen TW (2003) Wind turbine operation and maintenance based on condition monitoring. In: ECN-C-03-047
155. Waeyenbergh G, Pintelon L (2002) A framework for maintenance concept development. Int J Prod Econ 77(3):299–313
156. Wang FK, Lee W (2001) Learning curve analysis in total productive maintenance. Omega 29(6):491–499
157. Wang H (2002) A survey of maintenance policies of deteriorating systems. Eur J Oper Res 139(3):469–489
158. Wang P, Vachtsevanos G (1999) Fault prognosis using dynamic wavelet neural networks. In: AAAI spring symposium in equipment maintenance service and support, Polo Alto, USA
159. Wenxian Y, Tavner PJ, Wilkinson M (2008) Wind turbine condition monitoring and fault diagnosis using both mechanical and electrical signatures. In: Proceedings of IEEE/ASME international conference on advanced intelligent mechatronics, pp 1296–1301
160. Wessels RW (2003) Cost optimized scheduled maintenance interval for reliability centered maintenance. In: Proceedings annual reliability and maintainability symposium, IEEE, pp 412–416
161. Wilkinson MR, Spinato F, Tavner PJ (2007) Condition monitoring of generators and other subassemblies in wind turbine drive trains. In: Proceedings of 2007 IEEE international symposium on diagnostics for electric machines, power electronics and drives, pp 388–392
162. Wireman T (2004) Total productive maintenance. Industrial Press, South Norwalk
163. Wu S, Gebraeel N, Lawley MA (2007) A neural network integrated decision support system for condition-based optimal predictive maintenance policy. IEEE Trans Syst Man Cybern 37(2):226–236

164. Yang S, Li W, Wang C (2008) The intelligent fault diagnosis of wind turbine gearbox based on artificial neural network. In: Proceedings of international conference on condition monitoring and diagnosis, pp 1327–1330
165. Yang W, Jiang J (2011) Wind turbine condition monitoring and reliability analysis by SCADA information. In: Second international conference on mechanic automation and control engineering (MACE), Blyth, UK, 15–17 July 2011, pp 1872–1875
166. Yang W, Tavner PJ, Wilkinson MR (2009) Condition monitoring and fault diagnosis of a wind turbine synchronous generator drive train. IET Renew Power Gener 3(1):1–11
167. Yoshikawa H (1995) Manufacturing and the 21st century—intelligent manufacturing systems and the renaissance of the manufacturing industry. Technol Forecast Soc Change 49(2):165–213
168. Zaher AS, McArthur SDJ (2007) A multi-agent fault detection system for wind turbine defect recognition and diagnosis. In: Proceedings of IEEE Lausanne POWERTECH, pp 22–27
169. Zhang X, Gockenbach E (2008) Reliability centered asset management for power distribution systems. In: Proceedings of IEEE international symposium on electrical insulation—ISEI

Operation and Maintenance Methods in Solar Power Plants

Mustapha Hatti

Abstract As in any power plant, a solar power plant in operation requires maintenance. Also, as the solar power plant becomes older, operation and maintenance (O&M) becomes more and more important for improving or keeping the performance of the plant. Another aspect to be taken into account is that usually the solar power plants are in remote locations with unreliable communication infrastructure [1]. Most of the remote monitoring systems need an Internet connection, and in the absence of a reliable connection, there could be problems of lack of data logging for long periods of time [6]. This makes it very difficult to diagnose and rectify problems in a timely manner. System O&M is a broad area and is the continuing focus of several industry/government/national laboratory working groups. These groups will better define the issues and develop consensus O&M approaches over the next few years. This chapter reviews the main principles of solar generation from a perspective of O&M of these plants.

1 Introduction

The principle of solar power plants is extremely simple. They consist of a field of solar photovoltaic modules connected them in series or in parallel and connected to one or more inverters. Energy is directly transformed into electricity panels and password then in the electric network to the nearest city. Like in any power plant, a solar power plant in operation requires maintenance. As the solar power plant becomes older, operation and maintenance (O&M) becomes more and more important for improving the performance of the plant. Most of the

M. Hatti (✉)
Unité de Développement des Equipements Solaires, EPST-CDER, Centre de Développement des Energies Renouvelables, 11 Route Nationale, B.P, 386-42415 Bou Ismail, Tipaza, Algeria
e-mail: musthatti@ieee.org

M. A. Sanz-Bobi (ed.), *Use, Operation and Maintenance of Renewable Energy Systems*, Green Energy and Technology, DOI: 10.1007/978-3-319-03224-5_2,

solar power plants are located in remote places with unreliable communication infrastructure [1]. Most of the remote monitoring systems need an Internet connection, and in the absence of a reliable connection, there could be problems of lack of data logging for long periods of time [6]. This makes it very difficult to diagnose and rectify problems in a timely manner. System O&M is a broad area and is the continuing focus of several industry/government/national laboratory working groups. These groups will better define the issues and develop consensus O&M approaches over the next few years. In this, chapter is assembled and collected into different kinds of operations and methods to maintain solar power plants existing in literature and notices of manufacturers.

2 Concentrating Systems

The most part of the techniques for generating electrical energy to warm water or another fluid requires high temperatures to reach rational efficiencies. The produced temperatures of non-concentrating sun collectors are restricted to temperatures below 250 °C. Consequently, concentrating systems should be used to generate higher temperatures. Due to their higher expenses, lenses and flaming glasses are not generally used for large-scale power plants, and more lucrative alternatives are used, as well as reflecting concentrators.

The reflector, which concentrates the rays to a focal row or central point, has a parabolic profile; such a reflector should perpetually be tracked. In common terms, a difference can be accomplished between one-axis and two-axis tracking: One-axis tracking systems focus the solar light onto an absorber cylinder in the focal row, while two-axis tracking systems do so onto a quite undersized absorber area close to the central point. The theoretical highest concentration issue is 46,211. It is prearranged since the sun is not truly a spot emission source.

The highest theoretical absorption temperature that can be achieved is the sun's surface temperature of about 5,800 °C; if the focus ratio is lower, the highest reachable heat decreases. On the other hand, genuine systems do not achieve these speculative maxima. This is because, on the one hand, it is not feasible to build an extremely accurate system, and on the other, the practical systems that transfer heat to the consumer also decrease the recipient temperatures. If the temperature transfer process stops, while, the recipient can attain significantly elevated temperatures [11].

3 Solar Thermal Power Plant

Parabolic ditch power plant is the only type of solar thermal power plant technology presented as viable working systems until 2010. In power terms, approximately 350 MWe of electrical power are installed in California, and a large amount of new plants are at present in the scheduling process in further places.

The parabolic ditch collector comprises a large shapely mirror, which concentrate the sunlight by a factor of 70 or more to a focal point. Parallel collectors make up a 250–600-m lengthy collector line, and a huge amount of parallel lines form the solar collector field. The two-axis tracked collectors pursue the sun.

The collector field can be produced from very lengthy lines of parallel Fresnel collectors. In the central line of these is a metal absorber cylinder, which is typically implanted in an evacuated glass cylinder that reduces temperature sufferers. A particular high-temperature, resistive discerning covering, moreover, reduces energy warm losses [11].

In the Californian systems, thermo-oil flows through the absorber cylinder. This tube heats up the oil to nearly 400 °C, and a heat exchanger transfers the heat of the thermal oil to a water steam cycle (also called Rankine cycle). A feed water pump then puts the water under pressure. Finally, an economizer, vaporizer, and super heater together produce superheated steam. This steam expands in a two-stage turbine; between the high-pressure and low-pressure parts of this turbine is a reheater, which heats the steam again. The turbine itself drives an electrical generator that converts the mechanical energy into electrical energy; the condenser behind the turbine condenses the steam back to water, which closes the cycle at the feed water pump.

It is also possible to produce superheated steam directly using solar collectors. This makes the thermo-oil unnecessary and also reduces costs because the relatively expensive thermo-oil and the heat exchangers are no longer needed. However, direct solar steam generation is still in the prototype stage.

3.1 Storage Capacity

In contrast to photovoltaic systems, solar thermal power plants can guarantee capacity. During periods of bad weather or during the night, a parallel, fossil fuel burner can produce steam; this parallel burner can also be fired by climate-compatible fuels such as biomass, or hydrogen produced by renewable. With thermal storage, the solar thermal power plant can also generate electricity even if there is no solar energy available.

A proven form of storage system operates with two tanks. The storage medium for high-temperature heat storage is molten salt. The excess heat of the solar collector field heats up the molten salt, which is pumped from the cold to the hot tank. If the solar collector field cannot produce enough heat to drive the turbine, the molten salt is pumped back from the hot to the cold tank and heats up the heat transfer fluid.

4 Solar Power Plants

The operation of solar thermal power plants is based on the following steps: (1) mirrors capture solar radiation at a point so as to generate very high temperatures (400–1,000 °C). (2) The obtained heat transforms the water in a steam boiler.

(3) Pressurized steam rotates a turbine which drives an alternator. (4) The generator produces an alternating electrical current [11].

There are three types of solar plants, according to the method of focusing the solar rays: Central cylindrical collectors: long mirrors rotate about a horizontal axis to follow the sun's path. The rays are focused on a tube in which the fluid used to transport the heat to the center. The central tower: fields of steerable mirrors located on the ground reflect the sun rays on a boiler at the top of a tower. Central parabolic collector: solar radiation is focused on the focal length of parables in which directional mini power station is. There are also other systems quite surprising to see incredible create electricity from solar energy, for domestic and industrial applications.

5 Trough Power Plant Efficiencies

The efficiency of a solar thermal power plant is the product of the collector efficiency, field efficiency, and steam-cycle efficiency. The collector efficiency depends on the angle of incidence of the sunlight and the temperature in the absorber tube and can reach values up to 75 %. Field losses are usually below 10 %. Altogether, solar thermal trough power plants can reach annual efficiencies of about 15 %; the steam-cycle efficiency of about 35 % has the most significant influence. Central receiver systems such as solar thermal tower plants can reach higher temperatures and therefore achieve higher efficiencies [11].

6 Solar Thermal Tower Power Plants

The solar power tower, also known as "central tower" power plants or "heliostat." In solar thermal tower power plants, hundreds or even thousands of large two-axis tracked mirrors are installed around a tower. These slightly curved mirrors are also called heliostats; a computer calculates the ideal position for each of these, and a motor drive moves them into the sun. The system must be very precise in order to ensure that sunlight is really focused on the top of the tower. It is here that the absorber is located, and this is heated up to temperatures of 1,000 °C or more.

Hot air or molten salt then transports the heat from the absorber to a steam generator; superheated water steam is produced there, which drives a turbine and electrical generator, as described above for the parabolic trough power plants. Only two types of solar tower concepts will be described here in greater detail. The potential for solar thermal power plants is enormous: For instance, about 1 % of the area of the Sahara desert covered with solar thermal power plants would theoretically be sufficient to meet the entire global electricity demand. Therefore, solar thermal power systems will hopefully play an important role in the world's future electricity supply [11].

7 Open Volumetric Air Receiver Concept

The first type of solar tower is the open volumetric receiver concept. A blower transports ambient air through the receiver, which is heated up by the reflected sunlight. The receiver consists of wire mesh or ceramic or metallic materials in a honeycomb structure, and air is drawn through this and heated up to temperatures between 650 and 850 °C. On the front side, cold incoming air cools down the receiver surface.

Therefore, the volumetric structure produces the highest temperatures inside the receiver material, reducing the heat radiation losses on the receiver surface. Next, the air reaches the heat boiler, where steam is produced. A duct burner and thermal storage can also guarantee capacity with this type of solar thermal power plant [11].

8 Pressurized Air Receiver Concept

The volumetric pressurized receiver concept offers totally new opportunities for solar thermal tower plants. A compressor pressurizes air to about 15 bars; a transparent glass dome covers the receiver and separates the absorber from the environment. Inside the pressurized receiver, the air is heated to temperatures of up to 1,100 °C, and the hot air drives a gas turbine. This turbine is connected to the compressor and a generator that produces electricity. The waste heat of the gas turbine goes to a heat boiler and in addition to this drives a steam-cycle process. The combined gas and steam turbine process can reach efficiencies of over 50 %, whereas the efficiency of a simple steam turbine cycle is only 35 %. Therefore, solar system efficiencies of over 20 % are possible [12].

9 Tower and Trough Systems

In contrast to the parabolic trough power plants, no commercial tower power plant exists at present. However, prototype systems—in Almería, Spain, in Barstow, California, US, and in Rehovot, Israel—have proven the functionality of various tower power plant concepts. The minimum size of parabolic trough and solar tower power plants is in the range of 10 MWe. Below this capacity, installation and O&M costs increase and the system efficiency decreases so much that smaller systems cannot usually operate efficiently. In terms of costs, the optimal system size is in the range of 50–200 MWe [4].

10 Dish–Stirling Systems

A parabolic concave mirror (the dish) concentrates sunlight; the two-axis tracked mirror must follow the sun with a high degree of accuracy in order to achieve high efficiencies. In the focus is a receiver which is heated up to 650 °C. The absorbed

Fig. 1 Solar oven, diameter 50 m, 3,000 °C (Algiers)

heat drives a Stirling motor, which converts the heat into motive energy and drives a generator to produce electricity. If sufficient sunlight is not available, combustion heat from either fossil fuels or biofuels can also drive the Stirling engine and generate electricity. Dish–Stirling systems can be used to generate electricity in the kilowatts range.

The system efficiency of Dish–Stirling systems can reach 20 % or more. Some Dish–Stirling system prototypes have been successfully tested in a number of countries. However, the electricity generation costs of these systems are much higher than those for trough or tower power plants, and only series production can achieve further significant cost reductions for Dish–Stirling systems (Fig. 1) [4].

11 Solar Chimney Power Plants

A solar chimney power plant has a high chimney (tower), with a height of up to 1,000 m, and this is surrounded by a large collector roof, up to 130 m in diameter, that consists of glass or resistive plastic supported on a framework (see artist's impression). Toward its center, the roof curves upward to join the chimney, creating a funnel. The sun heats the air inside the greenhouse, so the air rises up through the shaft. The turbine starts spinning, generating electricity for a nearby town. The excess heat is absorbed by the water within the dark solar panels (built on the floor of the greenhouse). During the night when there is no sun shining, the water releases the heat keeping the turbine spinning.

The sun heats up the ground and the air underneath the collector roof, and the heated air follows the upward incline of the roof until it reaches the chimney. There, it flows at high speed through the chimney and drives wind generators at its bottom. The ground under the collector roof behaves as a storage medium and can

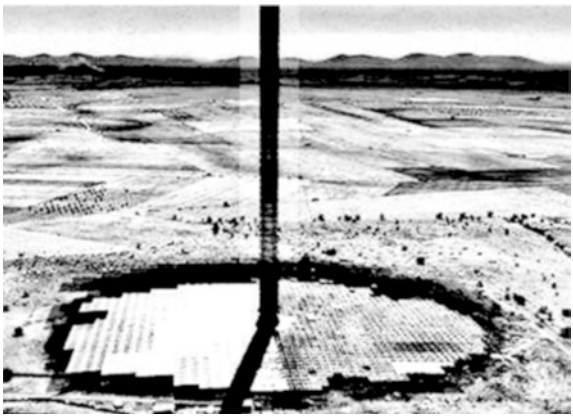

Fig. 2 Sketch of a solar chimney power plant

even heat up the air for a significant time after sunset. The efficiency of the solar chimney power plant is below 2 % and depends mainly on the height of the tower, and so these power plants can only be constructed on land which is very cheap or free. Such areas are usually situated in desert regions (Fig. 2).

However, the whole power plant is not without other uses, as the outer area under the collector roof can also be utilized as a greenhouse for agricultural purposes. As with trough and tower plants, the minimum economical size of solar chimney power plants is also in the multi-megawatt range[5].

12 Electricity Generation Costs

Due to the reduced part-load conduct of solar thermal power, plants should be installed in regions with a minimum of around 2,000 full-load hours. This is the case in regions with a direct normal irradiance more than 2,000 kWh/m^2 or a global irradiance more than 1,800 kWh/m^2. These irradiance values can be found in the earth's sunbelt; however, thermal storage can increase the number of full-load hours significantly. The specific system costs are between €2,000 and €5,000/kW depending on the system size, system concept, and storage size. Hence, a 50 MWe solar thermal power plant will cost €100–250 million. At very good sites, today's solar thermal power plants can generate electricity in the range of €0.15/kWh, and series production could soon bring down these costs below €0.10/kWh [10].

13 Qualified Personnel

The staffs are competent as "One who has expertise and knowledge related to the construction and operation of the electrical equipment and installations and has acknowledged security instructions to distinguish and keep away from the hazards

Fig. 3 Qualified person in maintenance activities

involved." Technicians can be experienced for some maintenance and service tasks but still be incompetent for others. Whether someone is a "qualified person" habitually depends on the specifics of the task at hand. Qualification is produced by both direct on-the-job training under qualified supervision and through instruction programs offered by certified educational establishments or manufacturers.

Many testing and maintenance activities necessitate two people to be completed safely and efficiently. An employee, who is being trained for a task, demonstrates the ability to perform duties related to that task safely and is under the direct supervision of a qualified person who is usually considered to be a qualified person (Fig. 3).

Additionally, in order to be considered a qualified person for solar power plant service and maintenance, a person must be trained in and familiar with: the skills and techniques necessary to identify exposed live parts from other parts of electrical equipment, the skills and techniques necessary to determine the nominal voltage of exposed live parts, the clearance distances specified by OSHA in the code of federal regulations (CFR) Part 1910.333(c) ("working on or near energized parts") and the corresponding voltages to which the qualified person will be exposed, the pertinent sections of the *NEC*, the characteristics of photovoltaic sources and hardware typically used in PV systems, and the characteristics of the hardware used in the photovoltaic system the person is working on [4, 7].

It is strongly recommended that anyone working around energized PV systems completes a minimum of the 20-h construction industry training program. Local jurisdictions may specify the necessary training, skills, certifications, or licenses required to perform the work in solar power plant area. One indicator that a person

may be qualified to work on many types of photovoltaic systems is to confirm that the person is a certified energy practitioner who has met the qualifications for and passed a certification exam.

14 Safety Necessities

Safety initiates with tolerable scheduling and research. Valuable safety strategies must be in state, human resources and contractors have to be familiar with (and devoted to) safety procedures in order to avoid accident or damage. Most important safety necessities during solar power plant operating consist of the proper use of Lockout/Tagout procedures, the exploit of personal protective equipment (PPE) procedures for securely disconnecting live paths, and appropriate examination and in conformity with the entire solar power installations specific system signage and warnings.

14.1 Lockout/Tagout Procedures

Lockout/Tagout procedures are designed to ensure safe working practices and must be strictly followed whenever systems are de-energized prior to servicing. Lockout/Tagout procedures are covered by CFR, under 29 CFR 1910.147. Lockout/Tagout procedures are required when energized equipment is serviced or maintained; safety guards are removed or bypassed; a worker has to place any part of his or her body in the equipment's point of operation, or hazardous energy sources are present.

Lockout/Tagout procedure steps include: notify others that the equipment will be shut down, perform a controlled shutdown to power down the equipment, open all of the energy isolating devices identified on the equipment's specific procedure, lock and tag all energy isolating devices, dissipate or restrain stored or residual energy, verify that the equipment is completely de-energized by attempting to cycle it, and verify that the equipment is completely de-energized by testing for voltage with a voltmeter.

Proper procedure labeling includes: name of the person placing the procedure and the date placed, details regarding the shutdown procedure for specific equipment, a list of all of the energy sources and isolating devices, and labels indicating the nature and magnitude of stored potential or residual energy within the equipment.

The lock placed on equipment during servicing should be removed only by the person who placed it. The lockout devices, such as padlocks, shall be approved for Lockout/Tagout procedures applications. OSHA provides variations in Lockout/Tagout procedures that may be used depending on an approved energy control program. Safety protocols need to be followed when re-energizing equipment, including notifying others that the system is about to be energized [5].

14.2 PPE and Other Safety Equipment

Service personnel must know what PPE is required for a specific task and wear it while completing the task. PPE includes fall protection, arc flash protection, fire-rated clothing, hot gloves, boots, and protective eyewear, among other items. PPE is designed to help minimize exposure to inherent system hazards. Identification of potential hazards is crucial to the process of selecting the appropriate PPE for the task at hand. All personnel working on or near photovoltaic systems should be trained to recognize hazards and choose the appropriate PPE to eliminate or reduce those hazards.

Rubber-insulating gloves, often referred to as "hot gloves," are the first line of defense against electric shock. They should always be worn with protective leather gloves over them and inspected before each use. Additionally, OSHA requires the gloves to be re-certified or replaced at regular intervals, beginning 6 months after they are placed in service. Insulated hand tools provide an additional layer of shock protection.

As solar power plant systems get larger and direct current operating voltages up to 1,000 V become increasingly common, arc flash requirements are a growing concern and it is more common to see arc flash warning labels on combiner boxes and disconnects. Unfortunately, for maintenance personnel, many existing solar power systems have been installed without labels warning of arc flash hazard.

Service personnel needs to be able to perform on-site evaluations to determine when a higher category of PPE is required to perform the work. Tasks such as performing thermal imaging on operating inverters with opened coverings or doors or verifying voltages in switchgear commonly require arc flash-rated PPE.

Even when not required by statute or regulations, general industrial safety equipments such as hardhats, safety glasses, boots, fire-rated clothing, and safety vests are strongly recommended when working on construction sites or around live electrical equipment. The jobsite also must be equipped with appropriate fire extinguisher sand first aid supplies, and all personnel must have proper training in their use. Lastly, at least two qualified people trained in cardiopulmonary resuscitation (CPR) should be on-site at all times [10].

14.3 Safe Operation of Electrical Disconnects

Switching on or off an electrical contactor or disconnect is a process often taken for granted as safe, but it can be one of the more dangerous tasks involved in maintaining a photovoltaic system. Workers must wear proper PPE when operating disconnects, and care should be taken to use the proper technique for throwing switches.

Some of the switches used to control the dc circuits of photovoltaic systems are not rated for load-break operation. Non-load-break-rated switches, which must be labeled as non-load-break-rated, must never be opened while the system is operating. Before opening a dc switch that is not rated for load break, the system should be shut down by turning off the connected inverter.

The pivots of most disconnect switches are on the left side of the switch, and the handles are on the right. A recommended safety protocol is to follow the left-hand rule, which involves standing to the right side of the switch and using the left hand to throw the switch. This ensures that the worker's body is not in front of the switch should an arc flash occur.

The proper technique for safely throwing an electrical disconnect includes: wear proper PPE, shut the system off at the inverter, stand to the right of the switch, grab the handle with the left hand, turn body and face away from the switch, close eyes, take a deep breath and hold it (to avoid breathing in flames if an arc flash occurs), throw (operate) the disconnect lever, use a properly rated voltmeter to confirm that no voltage is present on the disconnected circuit, and use Lockout/Tagout procedures methods to ensure the switch remains off.

15 PV-Specific Signage and Warnings

Article 690 of the *NEC* [8, 9] covers the requirements for PV-specific signage and warnings that must be present on every solar power system. Additional signage may also be required by the local jurisdiction or utility. These placards and warnings need to be visible to those working on or near the systems and should never be covered or painted over.

Early solar power systems often operated with maximum system voltages less than 50 Vdc. Today, 600 Vdc systems are common, and 1,000 Vdc systems are allowed by code in commercial and large-scale installations. Qualified personnel must use properly rated equipment and be trained for servicing the higher voltage systems.

Particular care must be taken to observe and follow warning labels reading "DO NOT DISCONNECT UNDER LOAD" located on module connections, combiner boxes, disconnects, and some inverter switches not designed as a load-break switch. Failure to heed these warning labels can lead to instrument malfunction, arcing, fires, and personnel injuries.

Although it is impossible to compile a list of universally applicable safety guidelines, the authors suggest the following steps as crucial to safe work: Before operating the solar power system, read all instructions for each product. All system components must be assumed to be energized with maximum dc voltages (up to 1,000 V) until personnel verify that the voltage has been removed. All enclosure doors should remain closed with latches tightened, except when they must be open for maintenance or testing.

Only qualified personnel who meet all local and governmental code requirements for licensing and training for the installation of electrical power systems with alternating current (ac) and dc voltages up to 1,000 V (or 600 V, when applicable) should perform solar power system servicing. To reduce the risk of electric shock, only qualified persons should perform servicing other than that specified in the installation instructions [4]. In order to remove all sources of voltage from the inverter, the incoming power must be de-energized at the source. This may be done by opening the ac disconnect and the dc disconnect.

Follow manufacturer guidelines for specifics of how to de-energize the inverter. In addition, allow a minimum of 5 min for the dc bus capacitors to discharge after disconnecting the power, always testing that voltage is reduced to touch-safe levels (30 Vdc) before working on the system. Always follow Lockout/Tagout procedures. Always check for ground faults. If there is a ground mistake, there may be a voltage potential between the inverter and ground. Further, check that the normally grounded pole is properly grounded and has not been energized by a fault.

Do not work alone when servicing solar power equipment. A team of two is required until the equipment is properly de-energized, locked out, and tagged out. Verify with a meter that the equipment is de-energized. Do not open a string (also known as a source circuit) combiner fuse holder without first confirming that there is no current flowing on the circuit. Do not disconnect (unplug) module leads, jumpers, or home run wires under load.

16 General Site Annual Inspections

Preventive maintenance is the planned maintenance of plant infrastructure and equipment with the goal of improving equipment life by preventing excess depreciation and impairment. This maintenance includes, but is not limited to, adjustments, cleaning, lubrication, repairs, replacements, and the extension of equipment life. At least once a year, O&M personnel should conduct a general inspection of the solar power installation site. During this inspection, technicians should: Ensure roof penetrations are watertight, if applicable, ensure roof drainage is adequate, roof drains are not clogged, and confirm that there are no signs of water pooling in the vicinity of the array, check for vegetation growth or other new shade items such as a satellite dish, check for ground erosion near the footings of a ground mount system, confirm proper system signage is in place, confirm appropriate expansion joints are used where needed in long conduit runs, confirm electrical enclosures are only accessible to authorized personnel who are secured with padlocks or combination locks and have restricted access signage, check for corrosion on the outside of enclosures and the racking system, check for cleanliness throughout the site—there should be no debris in the inverter pad area or elsewhere, check for loose hanging wires in the array, and check for signs of animal infestation under the array.

17 Detailed Visual Inspection

The installation should be inspected regularly for issues that impact the physical integrity or performance of the PV system. A visual inspection should include the following actions: inspect the inverter/electrical pad to make sure it does not show excessive cracking or signs of wear. The inverter should be bolted to the pad at all mounting points per the manufacturer installation requirements. Depending on the size, location, and accessibility of the system to unqualified

personnel, the inverters, combiner boxes, and disconnect switches should require tools or have locks to prevent unauthorized access to the equipment.

Look for warning placards including arc flash or PPE requirements for accessing equipment. Be sure to comply with all warning placards. If no placards are present, or if some placards are missing, make a note of it and install the missing placards during the maintenance visit. Consult the *NEC* and Underwriters Laboratories (UL) standards as well as the site host to determine signage requirements [4]. Inspect PV modules for defects that can appear in the form of burn marks, discoloration, delamination, or broken glass.

Check modules for excessive soiling from dirt buildup or animal droppings. Ensure that the module wiring is secure and not resting on the roof, hanging loose and exposed to potential damage, bent to an unapproved radius, or stretched across sharp or abrasive surfaces. Inspect racking system for defects including rust, corrosion, sagging, and missing or broken clips or bolts. If sprinklers are used to spray the array, check that the water is free of minerals (demineralized) as these minerals can cause gradual performance degradation. Inspect conduits for proper support, bushings, and expansion joints, where needed. In roof-mounted systems, check the integrity of the penetrations. In ground-mounted systems, look for signs of corrosion near the supports. Open combiner boxes and check for torque marks on the connections. Torque marks are made when lugs have been tightened to the proper torque value.

Ideally, they are applied during initial installation, but if not, the technician can mark the lug after torquing during a maintenance visit. A proper torque mark is made with a specialized torque marking pen. The mark is a straight line through the lug and the housing.

Over time, if the line separates between the lug and the housing, it shows that the lug has moved and needs to be retorqued. Look for debris inside the boxes and any evidence of damaging water intrusion. Look for discoloration on the terminals, boards, and fuse holders. Open the door to disconnect and look for signs of corrosion or damage. Check to make sure whether cabinet penetrations are properly sealed and there is no evidence of water ingress. Check for torque marks on the terminals. Perform a visual inspection of the interior and exterior of the inverter. Look for signs of water, rodent, or dust intrusion into the inverter. Check for torque marks on the field terminations.

If a weather station is present, ensure that the sensors are in the correct location and at the correct tilt and azimuth. A global horizontal irradiance sensor should be flat, and a plane of array irradiance sensor should be installed to the same pitch and orientation as the array. Irradiance sensors should be cleaned to remove dirt and bird droppings.

18 Manufacturer-Specific Inverter Inspection

Each inverter manufacturer will have specific requirements for inspection, testing, services, and documentation to meet its warranty obligations. Typical requirements for inverter inspections include: Record and validate all voltages and production values from the human machine interface (HMI) display, record last logged system

Fig. 4 Inverter inspection

error, clean filters, clean the inside of the cabinet, test fans for proper operation, check fuses, check torque on terminations, check gasket seal, confirm warning labels are in place, look for discoloration from excessive heat buildup, check integrity of lightning arrestors, check continuity of system ground and equipment grounding, check mechanical connection of the inverter to the wall or ground, check internal disconnect operation, verify that current software is installed, contact installer and/or manufacturer about any issues found, document findings for all work performed (Fig. 4) [4].

19 Manufacturer-Specific Tracker Inspection

Tracker manufacturers will have specific requirements for inspections, testing, service, and documentation to meet their warranty obligations. Typical maintenance or startup requirements for tracker systems include: lubricate tracker by inserting grease with grease gun into appropriate grease caps per manufacturer maintenance recommendation, check voltages inside the controller box, use a digital level to check the calibration and positioning of the inclinometers, check array for signs of parts hitting or rubbing other parts, remove vegetation that is near the drive shaft or moving components, check wind-stow operation [2].

Use appropriate (volt, ohm, dc clamp-on) meters to test: continuity of the equipment grounding at the inverter, combiner boxes, and disconnects, continuity of all system fuses at the combiner boxes, disconnects, and inside the inverters, open-circuit voltage (Voc) of all strings with the inverter off, and maximum power current (Imp) of all strings with the inverter on and at specified or recorded levels of power.

Additional testing (used when problems are identified or required by contract terms) may include: thermal images of combiner boxes (opened and closed), disconnects, inverters (external and internal at a specified operating point for a specified period of time), and modules, short-circuit (Isc) testing of strings, current-voltage (IV) curve testing of strings, insulation resistance tests of conductors at specified voltage, and comparison of a weather-corrected performance calculation of expected output to actual output of the system.

20 Manufacturer-Specific Data Acquisition System Inspection

Data acquisition system (DAS) manufacturers will have specific requirements for inspections, testing, service, and documentation to meet their warranty obligations. Typical maintenance or startup requirements for DASs include: taking voltage readings of power supplies, validating current transducer readings by comparing to calibrated equipment, and validating sensor reading by comparing to calibrated equipment. To confirm proper functionality of the DAS, the values measured by the DAS must be verified against values from devices with traceable calibration records.

Comparing the irradiance, temperature, and power measurements recorded by the DAS to values obtained from calibrated instruments will help identify sensor calibration issues that could result in the DAS data being incorrect.

The solar power industry as a whole is getting better at DAS installation and documentation, but it is still typical for DAS plans to be omitted or insufficiently detailed. As a result of such an omission, plan checkers often do not check for errors in the DAS design and inspectors have nothing to compare the as-built with for compliance. If the DAS will be tied into the building information technology system, O&M personnel should be aware that building networking upgrades or routine maintenance can cause connectivity issues.

21 General Isolation Procedures

21.1 Energized Components

Some testing and maintenance activities may require the system to be energized while workers are working on or near the equipment—string current testing is one example. Another common testing practice is to use an insulation resistance meter

to induce voltage to wiring or other components in an effort to identify signs of damage to insulation or resistance/leakage from other sources such as loose connections.

Guidance for what must be done in order to work safely on energized systems is as follows: Only qualified employees can work on electric circuits or equipment that has not been de-energized using Lockout/Tagout procedures, qualified employees must be able to work safely on energized circuits, the qualified employee must be familiar with the proper use of special precautionary techniques, PPE, insulating and shielding materials, and insulated tools. Employees working in areas where there are potential electrical hazards must be provided with and use electrical protective equipment that is appropriate for the specific parts of the body to be protected and for the work to be performed.

21.2 Inverter Pad Equipment

Use the following procedures for disconnecting a single inverter from the grid: If applicable, follow the inverter manufacturer guidelines for a controlled shutdown using the HMI keypad to pilot and select a shutdown, if the inverter has an on/off switch, turn it to off, turn the ac disconnect switch on the inverter off, turn the dc disconnect switch on the inverter off, turn any remaining external disconnect switches connected to the inverter off, install lockout devices on all disconnects, locking them in the open or off position, and repeat for all inverters and switches to completely isolate the entire solar power system from the grid and the inverters from the solar power source.

21.3 Transformer Isolation

Use the following procedures for transformer shutdown: For inverters connected to the transformer, turn the on/off switch to off, turn the ac disconnect off for the inverters connected to the transformer, turn the dc disconnect off for the inverters connected to the transformer, install lockout devices on the disconnects, turn off the transformer switch, which is either a dedicated stand-alone switch or is located in the switchgear, install a lockout device on the transformer switch, repeat for all transformers to completely isolate them from the switchgear.

22 Failure Response

22.1 Emergency Shutdown

In an emergency situation: If the inverters have Emergency Stop buttons, push them in on each inverter; if the inverter has an on/off switch, turn it to the off position (this may require a key). Each inverter should be manually turned to the off

position. This will immediately open the internal ac and dc contactors (if present) inside the inverter. Note that some inverters do not have an on/off switch or an Emergency Stop button. For these inverters, it will be necessary to turn the systems off using the disconnect switches attached to or located near the inverters. Do not open switches that are specifically labeled "Do not disconnect under load" until a load-break switch has been opened and current flow is stopped.

Generally, the first available upstream load-break ac switch or circuit breaker is safer to operate first (before the dc switch), because the inverter instantly shuts down the transistor bridge when ac voltage is removed. Once the system is off, the remaining switches can be opened, and the system can be locked out until the fault condition is repaired or it is safe to turn it back on.

22.2 Isolation Procedure: Inverter Pad Equipment

To isolate the inverter pad safely: Shut the inverters off through a controlled shutdown, turn off all dc and ac disconnects that feed the pad, follow the procedure in the Lockout/Tagout section for opening electrical disconnects, use Lockout/Tagout procedures to ensure the system remains off, always wear appropriate PPE and test for voltages with a properly rated meter to confirm the system is completely isolated.

22.3 Isolation Procedure: Field Combiner Box

To isolate field combiner boxes: Turn off the inverters as described above, operate the switch of the combiner by turning the handle to the off position, use a dc clamp on the meter to confirm there is no current passing through the ungrounded conductors in the combiner box, and then open all of the fuses, if further isolation of the box is needed, use the string diagrams to locate the homeruns (end connectors of the PV strings), use a clamp-on dc current meter to confirm that the homerun does not have any current passing through it, and then disconnect the string by opening the homerun positive and negative connectors and putting caps on the source circuit connectors, go back to the combiner box and use a voltmeter to confirm that each string has been successfully disconnected [7].

22.4 Isolation Procedure: Modules and String Wiring

After turning off the inverter, switches, and combiner boxes and isolating the combiner boxes from the array, disconnect individual modules from the string: Before disconnecting any string, use a dc clamp-on meter to confirm there is no current passing through the string, use the appropriate connector unlocking tool to disengage

the module connector, repeat for each module to be isolated from the system, if modules are removed from a system, even temporarily, technicians must ensure that the equipment grounding system remains intact for the remaining modules.

23 Inverter Troubleshooting and Service

There is an understandable focus on maximizing return on investments and system production. System uptime and availability is a key objective of O&M. Inverters that are offline can have a dramatic negative impact on the return on investments of a PV installation. Inverter failure rates are important to return on investments, but even more important than how often an inverter goes offline is how quickly it can be placed back into service.

The type of inverter fault often dictates how quickly it can be placed back into service. Inverters with known failure modes need a failure response procedure. This may include stocking critical parts that have long supply lead times so that the system is not left offline because of a lack of spare parts.

23.1 Inverter Troubleshooting

When an inverter goes offline, technicians must determine why and correct the error as quickly as possible. They can check the HMI for reported errors and then follow the actions noted in the table jointed. Some inverter faults will clear automatically when the fault condition returns to normal, but some fault conditions require a manual reset of the inverter. The ground fault fuse and even AC fuses can be nonstandard items that are difficult to purchase. Keep replacements on hand, especially if there are multiple inverters of the same size on site or in the portfolio. Having qualified technicians available and properly equipped with common replacement parts helps maximize system uptime [4].

23.2 Inverter Service Procedures

Some inverter service actions require that the system be shut down for safe inspection. Always begin with an examination of the equipment as described in the routine scheduled preventive maintenance table and further inspect subassemblies, wiring harnesses, contacts, and major components.

The following sample inverter service checklist applies to larger inverters in industrial scale and is not intended to be complete for all models from all manufacturers: Check insulated gate bipolar transistors and inverter boards for discoloration. Use inspection mirror if necessary. Check input dc and output ac capacitors for signs

of damage from overheating, record all voltage and current readings from the front display panel, check appearance/cleanliness of the cabinet, ventilation system, and insulated surfaces, check for corrosion/overheating on terminals and cables, torque terminals, connectors, and bolts as needed, record ambient weather conditions, including the temperature and whether the day is cloudy or sunny, check the appearance of both the ac and dc surge suppressors for damage or burn marks, check the operation of all safety devices (emergency stop devices, door switches, ground fault detector interrupter), inspect (clean or replace) air filter elements, correct any detected deficiencies, complete maintenance schedule card, complete written inspection report, if manufacturer-trained personnel are available on-site, install and perform any recommended engineering field modifications, including software upgrades [3].

24 Diagnosing and Testing for Low Power Production

Low power production also impacts return on investment, and O&M personnel need effective strategies for identifying and correcting problems quickly. System operators or owners may become conscientious of a PV installation's underperformance through one of the following means: A predefined DAS alert, which may be weather-related, a result of comparison with other systems in the range, or a result of comparison with other monitored parts of the system at a site with multiple inverters, a manual review of the DAS data through online gateway that indicates performance anomalies, a comparison of present performance with performance test results from preceding maintenance visits, and customer or external individual reports of a potential problem, often because of an unexpected boost in a monthly schedule.

24.1 Diagnostic Overview

Once the underperformance is confirmed, personnel must determine what is causing it. Steps to diagnosing power production deficiencies include: During routine maintenance and when diagnosing an underperforming system, the first and most important components to check are the fuses. Fuses generally must be removed from their holders to determine whether they have blown, perform a system performance data review using the DAS or a program such as the PV Watts calculator [10] to calculate the expected system output based on weather conditions and system size to compare actual to modeled systems production, dispatch a field technician to the site to do the following: Check that on-site performance meters have similar values.

Often systems will have revenue grade performance monitoring that can be compared against the inverter display totals, if there is a difference in the values,

then ideally the technician can log into the DAS system (when available) to investigate, a phase that has a different output than the others could be the result of a bad current transformer or a blown fuse in the current transformer circuit (i.e., an instrumentation problem), if there is no difference in recorded values, then use the inverter operator display/interface to identify the inverter error log. See inverter diagnostics for errors that may have caused the inverter to perform at less than 100 % power [1].

Verify that the array maximum power point voltage is in the maximum power point tracking window of the inverter, using an IV curve tracer on a sample string or group of strings. Modules will degrade over time and an array that begins service at the lower end of the inverter maximum power voltage window may degrade until its maximum power voltage no longer falls within this range, further compounding the effects of module degradation.

Look for external causes of the production drop, such as unexpected shade on the array. Vegetation growth is the most common form of shading, but it is not unusual to find a satellite dish or other object shading the array that was not present when the system was built.

Take photographs of the installation during commissioning and keep a visual record of any noticeable differences during maintenance visits. Perform general system checks as necessary to identify problems by to: Check all fuses at the inverter and work out to the combiner boxes, perform Voc string testing, perform Imp string testing, validate weather sensors, look for soiling. If soiling might be the problem, test an individual string (Voc, Imp, IV curve) and then clean the string and retest, perform IV curve tracing, take infrared (IR) images of the PV cells [3].

24.2 Diagnostic Testing

Operation and maintenance staff can exploit a number of diagnostic procedures to determine the causes of power deficiencies in a PV installation as:

24.2.1 Infrared Image Procedure

This procedure describes how to properly achieve field diagnostics of a PV installation using an IR camera to detect abnormal heat signatures, within the test conditions as: IR imaging should be completed with the system operating at peak levels if possible, do not open or work in electrical boxes, during rainy or wet conditions under safety considerations: Ensure all OSHA and environmental health and safety requirements are met, especially if working on angled roofs and/or at heights greater than 6 ft, safety precautions should also be taken when working near active high voltage systems or near surfaces that may be very hot to the touch, contact local health, security, safety, and environment personnel for questions and access to pertinent documentation [3].

24.2.2 Infrared Imaging Procedure

Prior to opening the IR scan, verify that the PV array is working, because temperature differences in modules are not apparent when the system is not operational, check inverter display for instantaneous kilowatt output, check current on each string in combiner box to ensure that it is operational, if the inverter or any of the strings are not operational, these must be corrected before the test can be conducted [3].

24.2.3 Infrared Camera Settings

Set the IR camera to "auto-scaling" rather than manual scaling. This will allow for automatic adjustment of the temperature scale. The IR camera does not capture shiny surfaces such as polished metals well due to their low emissivity value. However, for most active components on a solar module such as cells, J-Box, and cables, a value of 0.95 will be sufficient. Set temperature units to Celsius. Set color palette to Iron or Rainbow. "A thermal imager interprets IR-radiated or reflected heat by assigning a visible graduated color or gray scale to a radiated portrait of the scene. The color palette displays hot spots as white with diminishing temperatures through red-orange-yellow-green-blue-indigo-violet to black being cold" [3].

24.2.4 Infrared Inspection

When sunlight is present and camera settings are properly set, point the lens at the object of interest. In the case of solar modules in operation, looking through the glass onto the active cells is the most common inspection technique. Ensure that the picture is focused, either manually or automatically. For best results, position the camera as close to the module as possible without shading it or creating a reflection in the glass surface. If possible, the distance between the camera and the surface to be measured should not exceed 3 m [3].

This will depend on the camera's minimum focal distance and other specifications. Some temperature differences will not be picked up if the camera is too far away from the module. For best results, position the camera as perpendicular as possible to the object being measured. Hot spots will be easier to see if the image is taken perpendicular to the module surface. Image quality will degrade at camera angles other than normal (i.e., perpendicular) incidence. Care should be taken to avoid shading any part of the module while capturing images. Record module serial number, time, date, picture number, and module location in the array for all issues.

24.2.5 Infrared Testing Procedure

Turn system off at the inverter, post "High Voltage," "Testing in progress," "Stay clear of photovoltaic array!" signs around all entry points to array, use LOTO procedures, record test conditions including ambient temperature and irradiance,

open disconnect switch on combiner box. If there is no switch at the combiner box, open the applicable disconnect or fuse at the inverter to isolate the combiner box circuit. Isolate the output-circuit-grounded conductor (negative in a negative-grounded system, positive in a positive-grounded system) by removing the cable from its termination, remove any surge protection devices from circuits being tested (if testing at more than 50 Vdc).

Visually inspect box for signs of damage, as heat discoloration, corrosion, water intrusion, and conductors rubbing against metal in enclosure or other insulation damage. Use dc current meter to confirm there is no current present in the combiner box, open all fuse holders, and use ohmmeter to verify continuity of the box enclosure to ground.

If enclosure is not metal, verify ground wire connection to ground, test Voc of all strings to confirm proper polarity and voltage of each string [3].

24.2.6 Megohmmeter Testing

Megohmmeter or "megger" testing is a valuable way to identify weakened conductor insulation and loose wiring connections. These tests are often used in system acceptance and commissioning procedures but not often used in general maintenance unless a scrupulous troubleshooting of a fault condition is needed. The insulation resistance tester (IRT) applies a voltage to the circuit under test and measures return current to determine the insulation resistance and reliability. IRTs have various test voltage settings, such as 50, 100, 250, 500, and 1,000 V.

Generally, the higher voltage settings are better for detecting high-impedance shorts in the wiring than lower-voltage settings. However, some newer low-voltage equipment has sophisticated filtering that enables effective measurements even on circuits with PV modules. All 600-V-rated wire and PV modules should be capable of being tested at 1,000 Vdc, because they are factory proof tested at twice the maximum rated voltage plus 1,000 V—this adds up to 2,200 V for 600 V cable and PV modules. This test is short-term and will not damage the wire or module insulation.

To test specific products, including strings of modules, it is best to confirm that the testing (high voltage) will not void the warranties of those materials. It is best to get written permission for testing procedures from the module manufacturer if they do not already have approved megohmmeter testing guidelines. Some manufacturers explicitly disallow megohmmeter testing on their modules. Although it is true that some products may not allow this testing, the most common location of ground faults in PV systems is in the module wiring and modules [7].

Testing using the 500-Vdc setting may be appropriate for some modules. Lower voltages are often necessary when the system includes surge protection devices within the combiner boxes. Insulation testers are now available with 50-Vdc settings that will not damage the surge protectors. If these are used, it is important to ensure that they have filtering capable of compensating for the array capacitance. The added benefit of a low-voltage insulation test is that it can detect problems

with surge protectors. Leaking surge protectors are a common fault of older PV systems [7].

Tools used for such test include: IR tester megohmmeter, PPE rated for the appropriate voltages, screwdriver or combiner box key, dc clamp-on meter, dc voltmeter, electrical tape, system drawings—string wiring diagram, warning signs: "High Voltage—Testing in progress—Stay clear of photovoltaic array!," and recording device (pen and paper, laptop or tablet preferred).

Safety considerations and test conditions are that do not open or work in electrical boxes, in wet conditions. Also, shock hazard, live voltages present, fall hazard, combiner boxes are often elevated, need for proper PPE for electrical voltage testing, recognition that normally de-energized circuits may be energized in fault conditions, and requirement for two qualified people trained.

24.2.7 Fuse Checks

Fuses blow for a reason. Whenever a blown fuse is found, investigate why the fuse blew. When replacing fuses, it is essential to source the appropriate size, type, and rating. Do not assume that the fuse being replaced was the correct size, type, and rating, because an incorrect rating or size could be the reason the fuse blew. It may be necessary to consult the product manual to ensure the correct fuse is sourced. It is common to come across operating systems with incorrect fuses in place.

24.2.8 Fuse Testing Procedure and Safety Considerations

Confirm system is de-energized with a voltmeter, use Lockout/Tagout procedures and use an ohmmeter to test the continuity of the fuse. It may be possible to get voltage through a fuse that has not completely blown but is about to blow. For this reason, having voltage only on the load side of the fuse is not enough, set ohmmeter on a brawny surface, remove the fuse to be tested from the fuse holder unless it is clear that no alternative continuity paths can exist that would provide a false reading, use meter and test the fuse by placing a lead on each end of the fuse and listening for the meter to beep confirming continuity [3].

If the beep continuity reading is not constant while still holding the leads on each end of the fuse, then look at the ohm settings for a measurement of the resistance, make sure your fingers are not touching each end of the fuse as this will give a resistance reading for an open fuse that can be confusing, look at the fuse and confirm the size, type, and rating of the fuse. If the fuse fails the test or is not the properly rated size or type, replace the fuse with the correct fuse, always test replacement fuses before installing to confirm the fuse was good when it was placed in service, fuses should never be replaced or tested while the circuit is energized. Shut the system down prior to servicing fuses. Wear proper PPE for electrical voltage testing, at least until no voltage has been verified and the source has been locked out, if applicable.

24.2.9 DC System Voc Checks

Dc voltage checks are done with the system off, but "depending on the system size" voltages of up to 1,000 Vdc may be present. Ideally, test in stable sunlight of more than 750 W/m^2. However, stable conditions more than 200 W/m^2 still allow for simple comparisons among strings do not open or work in electrical boxes; in wet conditions, perform testing at the combiner boxes.

Safety considerations and tools include: Shock hazard, live voltages present, fall hazard, combiner boxes are often elevated, proper PPE for electrical voltage testing, recognition that normally de-energized circuits may be energized in fault conditions, and requirement for two qualified people trained to use dc voltmeter, PPE, irradiance meter, temperature sensor, screwdriver or combiner box key, and recording device (pen and paper, laptop, or tablet preferred).

Voltage testing procedure is resumed as turn system off at the inverter, use Lockout/Tagout procedures, record test conditions including ambient temperature and irradiance, open disconnect switch on combiner box, if applicable. Visually inspect box for signs of damage, heat discoloration, corrosion, water intrusion, and conductors rubbing against metal in enclosure or other insulation damage. Open all fuse holders, attach red lead to red terminal on tester, and attach black lead to black terminal on tester, use ohmmeter to verify continuity of the box enclosure to ground. If enclosure is not metal, verify ground wire connection to ground, use dc clamp-on ammeter to test for current in the equipment grounding conductor.

If current is present, stop this procedure and proceed to the ground fault troubleshooting procedure. Use voltmeter to test equipment, grounding conductor to ground. If voltage is present, find source of problem before placing combiner box back into service. Test ungrounded conductors one at a time by removing them from the bussing. Wear PPE and use insulated tools to remove ungrounded conductors under a fault condition, ideally, use an alligator clip meter cable for the black lead, connect to ground, and take the red lead and individually test from the line side of the open fuse holder for the ungrounded conductor.

Record results, making a note of voltage and polarity of each string, and if polarity is incorrect, find the source of problem before placing back into service, if reverse polarity is observed, do not just switch it without further investigation to identify the problem. Re-identify and properly label conductors if a switch is made. A change to the as-built plans may also be necessary. All voltages should be within 10 % of each other. If one string is the equivalent of the Voc of one module (roughly 30–40 V depending on the module) less than the average and one string is 30–40 V more than the average, it is a good indication that the stringing is incorrect for both strings. Given the same example of 40 Voc, if one string is 10–20 V less, then there may be an issue with one of the modules, and further investigation may be necessary (such as performing IV curve tracing).

If Imp testing is going to be carried out in the same combiner box, it is best to plan the box for the Imp testing. Ensure all terminations are properly torqued. Pull on conductors to ensure a large enough loop for the current meter to attach to. If necessary, cut zip ties, close fuse holders, close disconnect, plane of array

irradiance: Ensure location is not shaded, use inclinometer and compass to ensure it is in the same pitch and orientation as the array, clean with a cloth and mild soap solution if necessary, log into DAS program, place cleaned and recently calibrated handheld sensor in same pitch and orientation, compare results, if outside of acceptable range, replace sensor, noting the serial number of the new sensor for as-built updates. For ambient temperature sensor make a same procedure as here above, rather than risk damaging the module, leave the sensor in place and install the new sensor in the middle of the next closest cell.

Also for the anemometer, current transducers, voltage reference, and revenue meter have to log into DAS program, navigate program to compare programmed CT ratio to the ratio listed on the CTs, look at power factor of all three phases to confirm it is close to one with the system operating, note that power factor may be low at startup or in low-light conditions of less than 250 W/m^2, confirm good phase rotation with system running, compare revenue grade data with inverter data, noting differences [3].

Finally, the inverter direct, the maintainer has to log into DAS program, confirm system is checking in accurately, and look at system history to confirm data is not intermittent. Intermittent data from inverters can be the result of noise induced by the inverter; thus, check that the recommended shielded cable is used for communication wiring, check route of communication wiring to ensure it is away from voltage carrying conductors, confirm shield is only landed in one spot; best to do this at the DAS enclosure, confirm appropriate resistor or termination is installed in the last inverter in the chain (if required).

24.2.10 Combiner Box Level Monitoring Procedure

Log into DAS program, confirm that all boxes are visible, compare results to Imp string test results, and confirm communication to all devices, shade individual modules to confirm module mapping is accurate. Ensure location of global horizontal irradiance sensor is not shaded, use level to make sure it is level, clean with a cloth and mild soap solution if necessary, log into DAS program, place cleaned and recently calibrated handheld sensor in same pitch and orientation, compare results and if outside of acceptable range, replace sensor, noting serial number of the new sensor for as-built updates.

24.2.11 Array Washing Procedure

Depending on the site conditions, an annual or even quarterly cleaning may pay for itself in gained production. Some sites have more accumulation of dirt and other buildup than other sites. Depending on the tilt of the array and amount of seasonal rainfall, the soiling can have a dramatic impact on the overall production of the system. Most module manufacturers have specific guidelines about how not to clean modules, such as not using high-pressure water, not using harmful

chemicals, and even not using cold water when the module glass temperature is hot or using hot water to clean cold modules. Thermal shock from the difference in temperature between the glass surface temperature and the water temperature can result in fracturing or breaking of the glass [11].

Safety considerations must be taken as wear rubber sole shoes with good traction to prevent slips and falls, never walk on the modules, use non-conductive extended reach broom and hose handles to reach modules and a lift may be needed to access the array. Follow a serial lift safety procedures, including wearing a harness if required.

24.2.12 Before Washing Modules

Walk the site to confirm that there are no broken modules (shattered glass). Never spray broken modules with water. Perform a safety evaluation of the site looking for safety hazards such as trip hazards or areas that will become excessively slippery when wet, plan for water runoff. If the site has a storm water prevention plan in place, determine how the used water will be collected and disposed of. If harmful chemicals are not used during the cleaning process, drain guards can be used to filter out sediments. Be aware of trip hazards introduced by having hoses spread throughout the property, cone off area if needed. Determine whether the module cover glass is too hot and will be damaged by coming into contact with cool water.

Depending on the local climate and time of year, it may be best to limit washing activities to the morning or evening hours. Identify the water source to be used. Ideally, there will be a source of water near the array. If not, it may be necessary to bring in water from an outside source, which will involve a tank or water truck. Determine the best method of getting water to the modules. Typically, a 3/4-inch garden hose is used to connect to a spigot near the array. Set up hoses and tools. If required, block or install drain guards for filtration or water capture purposes. Take a baseline production reading of the system, noting both kilowatt-hour (kWh) output of each of the inverters and weather conditions including temperature and irradiance.

24.2.13 Washing Modules

De-ionized water is preferred to prevent spotting and calcium buildup. Normal water pressure is recommended; do not use high-pressure washers. If high-pressure washers are necessary, hold the pressure source far enough away from the modules to prevent damage. As a rule of thumb, if the stream is too strong to comfortably hold one's hand in, it is too much pressure for the modules, spray the modules with water, use a soft-bristled brush to get stubborn dirt off, if needed, use a non-damaging soap, use extensions with tools to be able to reach extended distances, if needed, squeegee modules dry.

24.2.14 After Washing Modules

After the system returns to steady-state temperature (i.e., there is no remaining impact from the cooling effect of wash water), take another production reading of the system, noting both kWh output of each of the inverters and weather conditions including temperature and irradiance, clean up tools, remove any drain guards or blocks, record the washing in the maintenance log, compare production of the clean system to the previous production values.

24.2.15 Vegetation Management

Vegetation management is particularly important in ground mount systems, but is a concern for all solar installations. Vegetation can grow into and cause problems with trackers, can cause problems with array wiring, and can cause shading, which will definitely impact production but could also cause damage to an operating system. Vegetation should also be controlled around the inverter pad and other areas where electrical equipment is present. Note: PV arrays are often home to snakes, bees, and venomous animals of all kinds. Wear protective clothing and be alert for possible encounters.

Safety considerations must be taken into account as wear rubber-soled shoes with good traction to prevent slips and falls, wear PPE to prevent bites and stings from insects, snakes, and vermin. Mowing or weed trimming vegetation around a ground mount can lead to problems if the mowing or weed trimming kicks up debris that can break the glass or cause general soiling those results in underperformance [4]. Poisoning weeds can lead to environmental and health problems.

Permanent abatement at the time of installation is the ideal way to deal with vegetation management. During inspections, note the amount of vegetation growth and document it through pictures. Work with the site owners to come up with a specific vegetation management plan that involves carefully removing or cutting back vegetation that is currently shading or will eventually grow to shade parts of the array.

24.2.16 System Warranties

It is important to know and understand the warranty requirements of the specific products used in a solar power plant. Not all warranties are created equal. The O&M personnel should have a very clear understanding of the warranty terms from the suppliers. They also need to know the type of defects or problems that are covered under warranty, the duration of the warranty and also the key personnel from the supplier with whom warranty claims can be taken up and enforced in a timely manner.

Warranty requirements not followed, including documenting regularly conducted preventive maintenance, can result in a voided warranty. Typical warranty

requirements are strict regarding the tasks that must be performed. However, the tasks are often simple and serve to protect the products and ensure greater long-term reliability.

25 Solar Power Plant Monitoring

Solar power plant needs to be monitored to detect breakdown and optimize their operation. Several solar power plants' monitoring strategies are depending on the output of the installation and its nature. Monitoring can be performed on site or remotely. It can measure production only, retrieve all the data from the inverter or retrieve all of the data from the communicating equipment (probes, meters, etc.). PV monitoring is the cornerstone of the o and m of a solar power plant. Monitoring includes inspection, supervision, sending signals and messages, and receiving signals from the environment [1].

The performance of monitoring depends on the performance and availability of solar power. It is therefore essential to bring in an expert organization, human, and material resources necessary to ensure effective monitoring and appropriate quality. Monitoring tools can be dedicated to supervision only or offer additional functions. Individual inverters and battery charge controllers may include monitoring using manufacturer-specific protocols and software [2]. Energy metering of an inverter may be of limited accuracy and not suitable for revenue metering purposes. A third-party DAS can monitor multiple inverters, using the inverter manufacturer's protocols, and also acquire weather-related information. Independent smart meters may measure the total energy production of a PV array system [1].

Separate measures such as satellite image analysis or a solar radiation meter can be used to estimate total insulation for comparison. Data collected from a monitoring system can be displayed remotely over the World Wide Web. For example, the open solar outdoors test field (OSOTF) is a grid-connected photovoltaic test system, which continuously monitors the output of a number of photovoltaic modules and correlates their performance to a long list of highly accurate meteorological readings. The OSOTF is organized under open-source principles—all data and analyses are being made freely available to the entire photovoltaic community and the general public. The Fraunhofer Center for Sustainable Energy Systems maintains two test systems, one in Massachusetts, and the outdoor solar test field OTF-1 in Albuquerque, New Mexico, which opened in June 2012.

Monitoring can be performed on site or remotely. It can measure production only, retrieve all the data from the inverter, or retrieve all data communicating equipment (probes, meters, etc.). Monitoring tools can be dedicated to supervision only or offer additional features. There are several technical solutions for monitoring different photovoltaic systems, depending on the type and accuracy of the information provided as well as their prices.

The first category is the first to have emerged since it comes from one of the major players in the solar system, the inverter. These solutions have the advantage

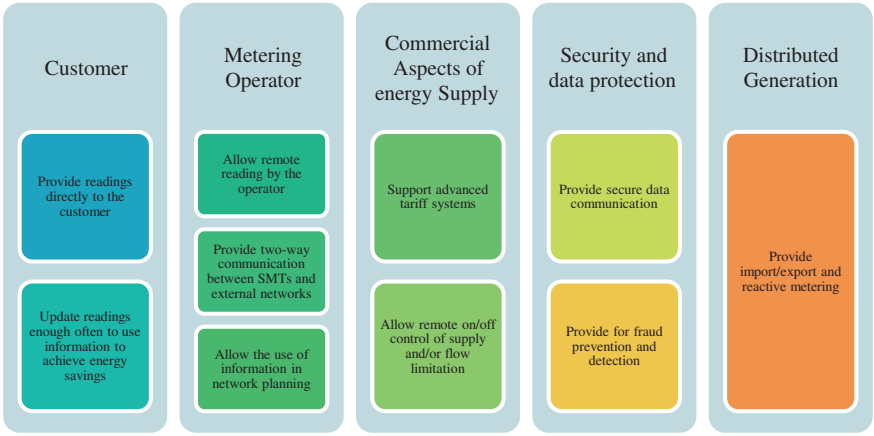

Fig. 5 Common minimum functional requirements for smart metering technologies

of back up information from the inverter and to provide a local display or transmit on the Internet, especially alerts the inverter itself (temperature, loss of connection with networks, etc.) [6]. Yet they remain expensive for single inverter, and installations are of course linked to an inverter brand. Moreover, the energy metering (kWh) is performed by the inverters more or less precise depending on the model. All major manufacturers of inverters have a data acquisition box.

The "universal" solutions connected inverters allow to overcome the major drawback of solutions inverter manufacturers, they are compatible with many brands (more or less depending on model). These data acquisition boxes connect the series connection of inverters in accordance with the protocol of each manufacturer. Universal solutions are generally more affordable than those of UPS manufacturers. The data transmission is most often an ADSL connection, but also GSM /GPRS or PSTN. According to the manufacturers, other communicating devices can be connected to these boxes. In particular, the weather sensors (cells pyranometer, anemometers, thermometers) and optionally safety devices. Note that some controllers can play the role of universal acquisition unit (Fig. 5) [2].

The last category is the most recent in the photovoltaic world. It consists of information for energy production directly back (kWh) without using the inverter. Today, there are two possibilities, each with their advantages. The first is to connect the ICT output electric meters; the second is to provide an electric meter communicating. These solutions are used to monitor production alone. To overcome the lack of information related to single monitor production, some companies offer cross-production data with a measure of sunlight (radiation in Wh/m^2) obtained by analysis of satellite images.

The measurement of radiation is essential to ensure precise control of the performance of a facility. Without this measure, impossible to verify the performance ratio (PR) of a facility. There are different solutions to track irradiance data. Either one uses one or more sensors installed adjacent photovoltaic panels or satellite

data is used. With the information on the installation position, the inclination, and orientation of the panels, satellites data provide information about the radiation received by a photovoltaic system.

If these two options are compared for acquiring information, the advantage of satellite data is a lower price for sufficient accuracy. In addition, this solution requires no additional installation (and therefore no maintenance). For consequence, the data collected with pyranometers have the advantage of being more accurate. Depending on the class of pyranometer, and therefore its price, accuracy may be up to 1 % or below. Some solutions using monitoring control cells for monitoring the operation of the generator. This solution is less accurate than using a pyranometer but more economical addition as the latter [1].

Today, most monitoring systems work with photovoltaic sensors. Solutions using satellite images are fewer.

All the solutions mentioned above have either online portals or local software assigned to supervision. UPS manufacturers have almost all set up a portal data recovery, provided free with the purchase of their DAS. However, some manufacturers offer more industrial supervision software locally installed. Offer emerges publisher's specialized software for data processing, regardless of the acquisition system. These software are being developed and are beyond simple monitoring of production, should provide further diagnosis, that is to say, a more precise analysis of data. Publishers' monitoring solutions for energy meters also offer their Web software.

26 Incident Rate on Photovoltaic Installations

Think that photovoltaic installations require no maintenance over their entire life is a legend still very persistent in the solar power industry. The reality is quite different and solar power systems like any other technical equipment have abnormalities in their production and should be checked and technically framed. For this, DIN-EN standards set for regular examinations maintaining operating rules [4].

27 Efficiency Gap by Continuous Quality Assurance

Comparing the performance data of photovoltaic installations that are either collected directly on counter or recovered by a professional monitoring, we find that photovoltaic installations without blame or servicing yield losses of 5.7 %. The average ratio of performance facilities subjects to either a remote monitoring system, or a regular servicing by a technician stood at 76.8 %. Photovoltaic systems that are framed professionally by a manager or a company that specializes in solar power plant have an average ratio of performance 81.4 %.

Obviously, there are facilities that produce unframed without malfunction, but in the majority cases, small or large efficiency losses are identified much later and

the operator records a decline in production. Conversely, there are facilities that despite has a performance below the average. However, this can be explained in general by major technical errors that affect negative on the performance of the installation. Most photovoltaic installations with supervision or service distinguished by the fact that the predicted total returns.

In general, it results in a difference in the PR of the order of 4.6 % and thus a relative decrease yield of 5.7 %. An operator this means that photovoltaic system that could achieve a specific annual yield of 950 kWh/kWp reached frameless an annual yield of only 896 kWh/kWp. This leads to the operator of a facility with a capacity of 10 kWc (with purchase price of 0.195 €/kWh) a financial loss of € 106 per year [10]. Individual yield loss can obviously be even higher. The research institute Fraunhofer ISE had already reached this conclusion in a study from 2008: loss of service quality performance without plants was 4.3 %.

28 Defect Classification

The defects are classified into five different categories: on the malfunctioning of the entire solar power system due to power failures or well tripping protection, decoupling of the inverter, a temporary malfunction of the UPS, a failure of the chain of modules, a problem of communication data. All events on solar power installations are based on the total number of plants examined, and then, there is an average of 5 per year reported failures that need to be analyzed systematically. Most often these are technical problems that appear on the inverter, two-thirds of malfunctions on solar power installations are assigned to the inverter.

Nearly 40 % of failures are disruptions in the operation of inverters, there are such cuts due to low insulation resistance due to cable failure or modules, or due to a shadow which leads to a decrease inverter efficiency. About a quarter of alerts are caused by failures of the inverter. Therefore, for string inverter is done in general with their replacement and central inverters to return to service is done on site by teams of specialists. Disruptions in the communication of data are about 20 % identified by the remote monitoring system errors.

These disturbances do not affect performance because only the data transfer is canceled. However, we cannot identify any failure of a technical component when perturbations in the data transmission. The judgment of the entire solar power system represents only 10 % of the cases analyzed, which is not much, but it happens more often on small plants than for large solar power plants. The reason is that, for example, in small- and medium-sized facilities, the general circuit breaker can be triggered so that the installation is disconnected from the network in case of technical problems. Failures on a single-channel module are relatively rare with only 2 % of cases and rarely contribute to the failure of solar power installations.

They represent more than 55 % yield losses. Decoupling a single inverter is about 40 % yield loss. We also note that the inverter malfunctions are the most common but they represent only 6 % of losses. It is for this reason that without a

system of remote monitoring and services such failures are often not detected and lead to a long-term sensitive yield losses. Losses resulting from normal faults, in particular, failures on strings of modules do not cause major losses [1].

29 Balance Sheet

On average, a photovoltaic installation can have around 5 incidents per year that can cause a loss performance requiring detailed analysis. Operators are self-maintenance, and a permanent monitoring should expect an average yield loss 5.7 % per year. This could be avoided by the use of a service system and central station. The alerts analysis 2-year operation showed that the inverters are responsible for two-thirds of failures on solar power installations. Control both the performance of the entire system that each inverter is essential in order to identify defects before and resolve them quickly. Otherwise operator risk significant yield losses that depreciate the investment in the solar power plant.

30 Reliability in Photovoltaic Installation

As part of their marketing photovoltaic modules must be certified from standardized tests (IEC 61215 for crystalline modules, IEC 61646 for thin modules and IEC 62108 diapers modules concentration). In addition, to establish the dependability of these, the tests of IEC 61730 must also be made. However, it should be noted that the test sequences described in these standards are too short to determine the lifetime of a photovoltaic module [4].

However, manufacturers still ensure the strength of their products over a very long period (80 % of the initial power after 20 or 25 years depending on the manufacturer) only by the standards mentioned above. A reliability study would allow manufacturers to determine the warranty on their modules with more certainty and evaluate the risks they take to ensure their products as they do now. Moreover, the thermal regulation RT 2012 requires the integration of a renewable energy source. Thus, for the solar photovoltaic or a permanent solution used, it is important to understand its reliability and lifetime [11].

30.1 Potential Failures of Photovoltaic Panels

Thanks to various technical publications on the subject, possible failures of a crystalline photovoltaic module are known, and it is possible to reproduce accelerated testing. A module is considered failed when its power is less than 80 % of its original power according to manufacturers' warranties. Two failure modes have been studied in detail and highlighted, discoloration of the encapsulant which causes a

significant loss of the power of the photovoltaic module and which can be reproduced by an UV exposure test, corrosion in the photovoltaic module that can be reproduced by a damp heat test. For each failure mode, an accelerated degradation test and simulation tool atmospheric conditions developed during the procedure can be used to determine the reliability curve of the photovoltaic module in real conditions of use [10].

Finally, when the reliability curve is defined for each failure mode, the total reliability of the photovoltaic module can be determined as well as its average lifespan. With this methodology, the manufacturer may specify precisely the average life of its photovoltaic modules and be able to define the proportion of modules that is likely to be defective during the warranty period.

31 Conclusions

The importance of O&M is often ignored by many developers. Considering the fact that the plant has to generate returns over a period of 25 years, a good O&M contractor, a good monitoring system and above all, a very good O&M process is very critical for the success of the solar power plant. The implementation of preventive maintenance procedures presented is a vital part of efforts promoting safe practices in the solar power plant.

References

1. Arianfar AH, Mehraban Jahromi MH, Mosalanejad M, Dehghan B (2009) Design and modeling remote monitoring system for solar power plant. IEEE Int Conf Comput Electr Eng pp 81--99
2. Camacho EF, Berenguel M, Rubio F (1994) Application of gain scheduling generalized predictive controller to a solar power plant. Control Eng Pract 2(2):227–237
3. Fluke Corporation (2006, 2008) Infrared thermal imagers: a primer for HVAC technicians
4. Haney J, Burnstein A (2013) Solar America Board for Codes and Standards Report, 2013. www.solarabcs.org. Accessed Jan 2014
5. Mehraban Jahromi MH, Shabaninia F (2007) Introducing effective parameters in tele-operation system assessment. Iran J Eng Educ 9(36):111–132
6. Munir S, Book WJ (2002) Internet-based teleoperation using wave variables with prediction. IEEE/ASME Trans Mechatron 7(2):16
7. Mync P, Berdner J (2009) PV system ground faults. SolarPro. Issue 2.5. http://solarprofessional.com/articles/operations-maintenance/pv-system-ground-faults. Accessed on Jan 2014
8. National Fire Protection Association (NFPA) (2011a) National Electrical Code® (NEC), NFPA 70®. Article 100
9. National Fire Protection Association (NFPA) (2011b) National Electrical Code® (NEC), NFPA 70®. Article 690
10. National Renewable Energy Laboratory (NREL) (2012) PVWatts calculator. www.nrel.gov/rredc/pvwatts/. Accessed Jan 2014
11. Quaschning V (2003) Technology fundamentals: solar thermal power plants. Renew Energy World 6(06):109–113
12. Sherwood L (2013) U.S. Solar Market Trends 2012. Interstate Renewable Energy Council. www.irecusa.org/wp-content/uploads/IRECSolarMarketTrends-2012-Web-8-28-12.pdf

Biological Biogas

Paul Harris

Abstract There is some confusion between "biogas" and "producer gas", "syngas", "pyrolysis gas" and similar gaseous products obtained from biological or organic materials by thermal processes. (1) Biogas (a mixture of methane (CH_4—natural gas) and carbon dioxide (CO_2), also known as marsh gas) is obtained from moist organic material by microbial processes, in fact it is so natural it occurs in our own stomachs as well as in other animal's digestive systems (particularly ruminants like cattle), marshes, mud, the Arctic Tundra and even volcanoes—anywhere air is absent. (2) Thermal processes can also be used to gasify combustible material in reduced oxygen, resulting in a mixture of gases that often includes carbon monoxide (CO)—a very toxic gas. Gasification is better applied to dry materials like wood and was used in World War Two, when petrol was rationed, to power vehicles by fitting a "gasifier" to the car/truck to make "producer gas". In this chapter, we will look briefly at the long history of biogas, take an overview of the microbial process, cover some of the different types of digesters and look at building, starting and operating a simple type of digester, including fault finding.

1 History of Biogas

The biogas flame has been known a long time and may even be responsible for the "will o' the wisp" and dragon legends (when methane from marshes or in dinosaur breath was ignited by fire or lightning).

During the tenth century BC, biogas was used in Assyria for heating bath water [4]. There were natural gas well in Asia as early as 615 AD, and in 900 AD, the Chinese are recorded as using bamboo pipes to transfer biogas for lighting [3].

P. Harris (✉)
Australian Biogas Group, University of Adelaide, Adelaide, Australia
e-mail: paul.harris@adelaide.edu.au

M. A. Sanz-Bobi (ed.), *Use, Operation and Maintenance of Renewable Energy Systems*, Green Energy and Technology, DOI: 10.1007/978-3-319-03224-5_3,

Modern biogas began with the observation of flammable gases emitted from decaying vegetable matter by Van Helmont in 1630, and Volta determined the direct correlation between matter decayed and gas produced in 1776, and in 1786, the chemistry of methane was studied by Berthollet. In 1808, Davey observed methane in gas from decomposing cattle manure [3–5].

Mumbai, India, is credited as the site of the "first" digester, built at a leper colony in 1859 [4] and powering a gas engine by 1897 [3].

In 1896, biogas recovered from a "carefully designed" sewage treatment plant was fuelling street lamps in Exeter, England [3, 4]. From these beginnings, biogas adoption began to accelerate.

In Essen, municipal users were supplied by pipeline by 1925 [3], and by the 1930s, bottled biogas was being used in Germany to fuel cars [4].

As the science of microbiology developed in the 1930s, people like Barker and Buswell identified anaerobic bacteria and the conditions required for methane production [1], bringing some rigour to digester design and operation.

The 1930s also saw the beginning of the Chinese biogas program, which progressed slowly until Chairman Mao's "Great Leap Forward" in the 1950s, and also Indian biogas work from about 1937. Both these programs have been through several stages of improvement and have resulted in hundreds of thousands of household digesters being built, although not all the early digesters were successful due to quality problems.

High-rate digesters were developed to process more waste and get more gas from a smaller unit. The anaerobic filter was developed by McCarty and co-workers at Stanford University in the 1960s, and in 1970, the Agricultural University at Wageningen developed the upflow anaerobic sludge blanket (UASB) digester.

Interest in biogas, fuelled in part by the energy crises of the 1970s, resulted in press items, books for the popular press, scientific papers and technical books being published by a number of people.

Various other methods of keeping the microbes in the digester, such as packed bed digesters and suspended growth digesters, have since been used to allow faster waste throughput and shorter retention time (RT).

2 The Microbial Process

Biogas is formed from readily degradable biological material by a process called anaerobic digestion (AD), which occurs in a number of steps.

In the "hydrolysis" step, extracellular enzymes released by microbes begin to break down large organic molecules so they can be taken into the microbial cell as a food source. Within the cell, further breakdowns release energy for the cell and result in smaller molecules and CO_2 being released as waste, so we have an "acidogenesis" step. This smaller molecule is then used as energy in the next step, called "acetogenesis" as the end result is acetic acid and CO_2 as the waste products.

The final "methanogenesis" step is what we are interested in, where both acetic acid (CH_3COOH) and CO_2 are used by different groups of methanogens to produce methane. Acetic acid produces methane (CH_4) and carbon dioxide (CO_2) while the CO_2 path produces just CH_4 and water (H_2O).

For successful digestion, each step has to occur at an appropriate rate as the waste of one stage can inhibit the following stage and lack of waste will result in poor performance. As the breakdown is sequential, the whole process can only proceed at a rate determined by the limiting process, often considered to be methanogenesis but hydrolysis may be limiting for some substrates.

3 Types of Digester

At the simplest level, digesters can be either "batch" operation or "continuous flow". Both batch and continuous-flow digesters can use either liquid wastes, that can be pumped, or solid wastes, that can be shovelled—but some moisture is necessary. Most people consider "digesters" to be the conventional liquid variety, but municipal solid waste (MSW) is now processed in a number of facilities worldwide.

With batch operation, a container is filled with digestible material (either liquid or solid), usually with some already digested material as inoculum to put the right microbes into the system. Some care has to be taken with filling, as too much substrate and not enough inoculum may result in the digester going "sour" due to a build-up of acetic acid, much like a silage heap (but that is usually lactic acid). The first gas will always be CO_2, as initial oxygen present is used up to get to anaerobic conditions, but then anaerobes take over and biogas will be produced. Initially, the gas production rate will increase, as the microbes build up, but then as the substrate is used, the gas production rate will fall to insignificant levels over a period of weeks (depending on operating temperature). To get continuous gas flow from a batch operation, you need at least two units, so one is always operating at full capacity while the other is finishing, being reloaded and starting up.

Continuous-flow digesters tend to be of the liquid variety and give a steady flow of gas if fed and managed consistently. Smaller sizes are really semi-continuous, fed at intervals of 24 h or less, as some wastes are difficult to pump continuously at low rates because they will clog small pipes or settle in larger ones.

The simplest liquid digester is a sealed tank with an inlet and outlet for digestate and a gas line to take the biogas to its use point. Gas is kept in the digester by having the internal inlet and outlet openings below the liquid surface. Common examples are the Chinese (Fig. 1) and Indian (Fig. 2) designs (around since the 1930s) and the plug-flow digester. These types of digester are commonly used in household systems in developing countries, but larger versions can serve a community. More recently, the plug-flow (Fig. 3) digester has been adapted to household use, largely by Dr Reg Preston at the University of Tropical Agriculture Foundation.

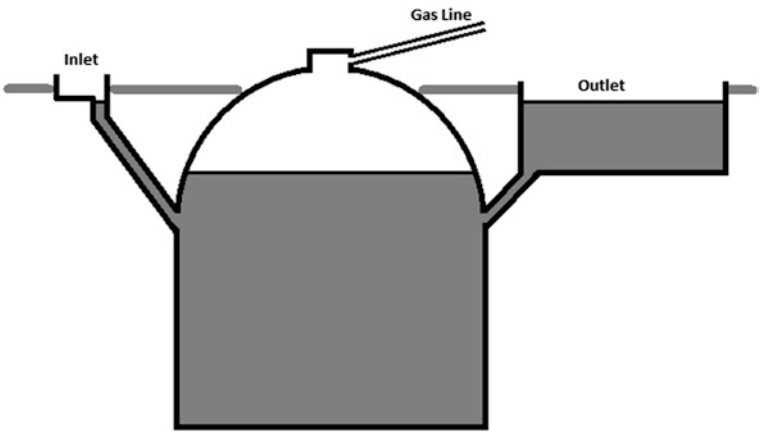

Fig. 1 Chinese-type fixed dome digester

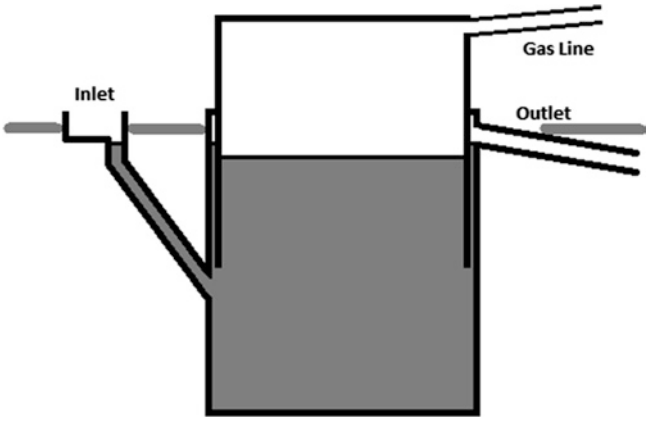

Fig. 2 Indian floating drum digester

Fig. 3 Plug-flow digester

To get better performance, the continuous-flow stirred tank (CFST) (Fig. 4) was developed and usually has heating to maintain a steady temperature close to 35 °C (Mesophylic) or sometimes 55 °C (Thermophylic) as well as a stirring system.

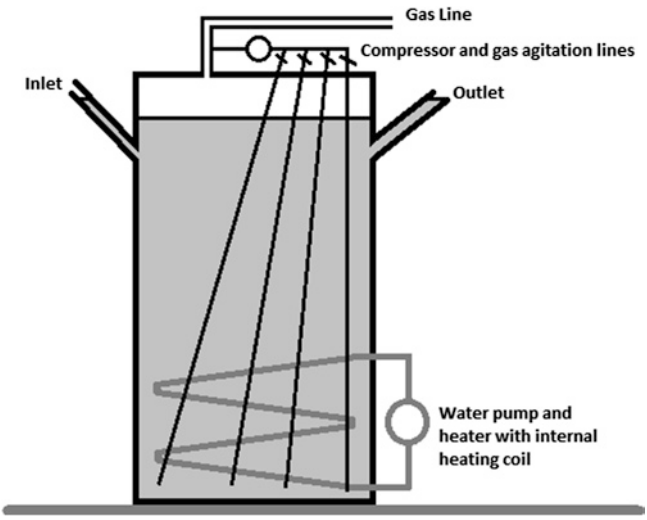

Fig. 4 Continuous-flow stirred-tank (CFST) digester

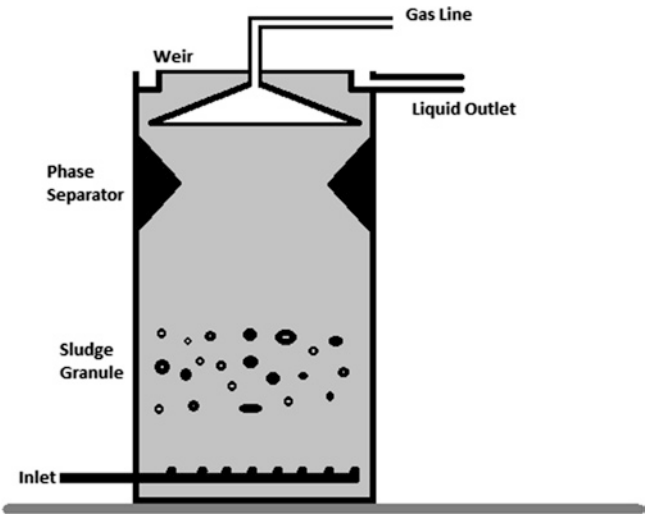

Fig. 5 Upflow anaerobic sludge blanket (UASB) digester

Sometimes the heating and agitation systems are combined, taking digester contents and using an external heat exchanger before returning the digestate as agitation. Other alternatives are mechanical or gas mixing (sometimes using draft tubes to give greater flow) and either an internal heating coil or heating through the digester wall. CFST digesters are commonly found on intensive animal farms, industrial sites or sewage treatment plants.

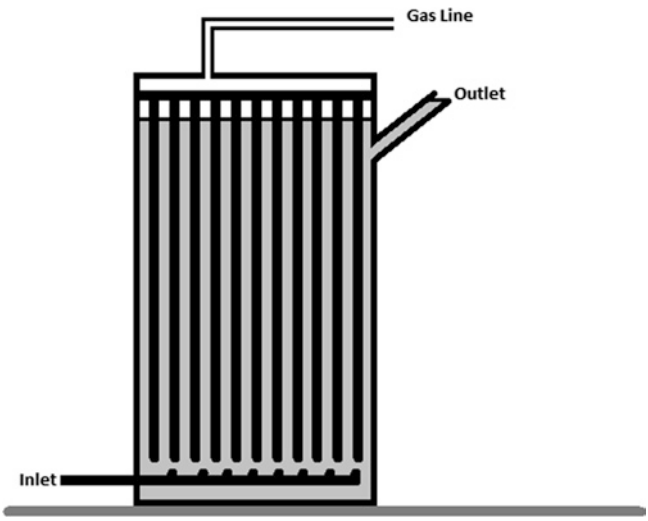

Fig. 6 Suspended growth digester

With the simple and CFST digesters, microbial growth rate determines the RT and hence the size of digester to treat a given amount of waste because of wash out of microbes. To enable more rapid treatment of waste, high-rate digesters such as the anaerobic filter, UASB (Fig. 5), packed bed and suspended growth digesters (Fig. 6) have been developed, where microbes are retained in the digester or attach to a support structure. Some of these designs are only suited to soluble wastes, as particles will clog the internal passages.

4 Building a Simple Digester

To learn how a digester works or try out a particular waste, a small digester is a good project—how small depends in part on what you want to do with the gas. As an initial trial, plastic drink bottles, as in Fig. 7, provide a good basis for a batch unit but do not produce much gas. To get an amount of gas useful to boil some water, if you have access to a suitable waste supply, a 200-L unit is a reasonable size, see Figs. 8 and 9.

4.1 Mini Digester Instructions

You need two sizes of bottle (I had two 350 ml? and one 500 ml? bottle) with lids, some small plastic tube, some silicone or similar sealant and a tee (as you get from an aquarium shop). I found some 25-mm PVC pipe that just fitted over the two lids to join them. I cut the top of the larger bottle so the smaller one just fits

Fig. 7 Mini digester (Indian type batch unit)

4 m of clear polyethylene layflat tube Inlet tube (100mm PVC pipe, 40 cm long) 0.4 m of ~19mm dia PVC pipe 0.4 m of 13mm dia black poly tube 2 m of 12 mm dia flexible poly tube 1 13mm poly Tee piece 1 burner (See below) Small plastic container for water trap Rubber strip (from push bike tube?) Insulating/plastic Tape	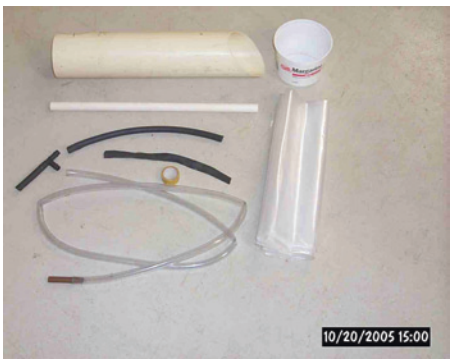

Fig. 8 Parts for 200-L plug-flow digester

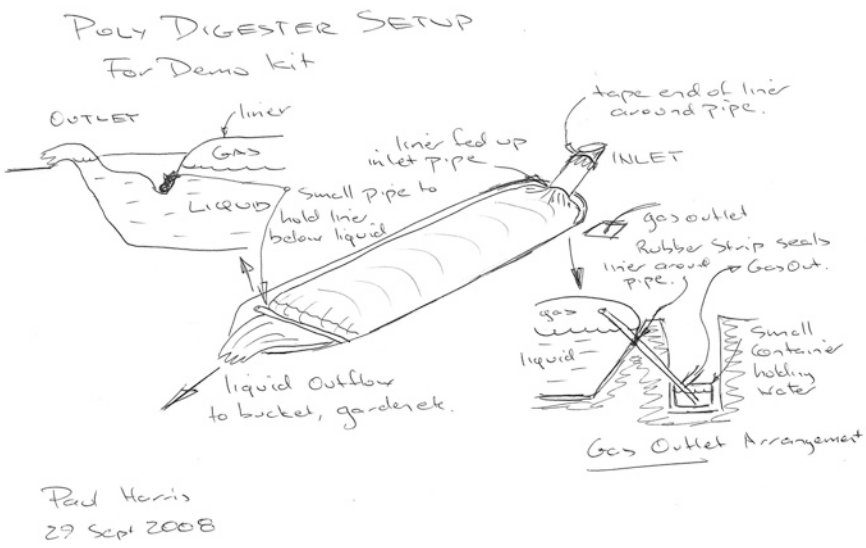

Fig. 9 Sketch of 200-L plug-flow set-up

through (as a guide) and used this offcut as the support for the inverted "digester" bottle. You also cut of the top of one smaller bottle to be the gas storage, inverted in the larger bottle. Join two of the lids (to fit the digester bottle and the support) back to back with some sealant between and make holes a little smaller than the tube in the joined lids and the larger bottle. Push the tube through the holes so it reaches to the top of each bottle (the "headspace") and join in the tee piece and you are ready for filling—I suggest you to use water firs and check for leaks.

You would be best to fill the digester with cattle, horse or pig manure if you can get it, as they all have the right bacteria already present so the digester will start itself. Dilute the manure with water, cattle manure 1 manure to 1.2 water, pig 1 to 1 or horse 1 manure to 3.7 water. The first gas will be carbon dioxide, but after a few days (depending on temperature), you should start to get biogas containing methane.

4.2 DIY Poly Digester

4.2.1 What Is Needed

See Fig. 8.

4.2.2 Sketch of Arrangement

A 200-L digester was constructed as part of a biogas course run in Cameroon.

4.2.3 What You Need to Supply

1. A hole in the ground (i.e. shovel and energy to dig same!)—0.9 m top width, 0.3 m deep width, 0.3 m bottom width and length to suit digester (see Introduction) with provision for gas outlet and effluent outlet (or some other way of containing the digester, like a trough).
2. Buckets for loading/unloading
3. Waste material for digestion
4. Water
5. Weight to develop burner pressure
6. Matches (or other means of igniting gas)
7. Patience
8. Scissors and/or sharp knife for cutting plastic, tape, rubber and tube.

4.2.4 Extras You May Need

1. Some pieces of wood or bricks to hold back soil?
2. A fence to keep out animals?
3. A roof for protection from the sun?
4. Support for the burner?
5. Container to boil water in.

4.2.5 To Consider

The basic concept is that the layflat tube be cut in half (that is half the length, not split down the middle to make a sheet!) and used as a double thickness to make the digester more durable and to have the gas storage in the digester, but you may want a longer (or shorter) digester or a separate gas storage so you may vary the length to suit. Follow the steps below, in order.

See [2] for more background information.

4.2.6 The Hole

Mark out the main hole 0.9 m wide and 2 m long (for the standard digester) and excavate to 30 cm deep with 1:1 side slopes to give 30 cm bottom width and 1.4 m bottom length, with a level bottom (if you are on a hill put the digester along the contour). At the inlet end, which can be shaped to support the inlet pipe, make a small area in one sidewall to take the gas outlet (you may need some wood or bricks to hold back the soil), and at the outlet end, make a hole that the outlet bucket can sit in (more wood/bricks?), Fig. 10 gives an idea of the requirements.

Ensure that there are NO sharp objects in the hole, so the digester would not get punctured.

Fig. 10 The hole used in Cameroon, a bit deeper than necessary

4.2.7 The Digester

Lay the plastic layflat tube in the hole and fold the inlet end to facilitate feeing through the inlet pipe. Put some insulating tape around the end if the inlet pipe to protect the poly sheet from sharp edges (see Fig. 11 for some of the steps). Once the poly is through the inlet pipe, fold the end back, trim excess sheet and tape as shown in Fig. 11. Lay the inlet pipe on the bank of the hole and support with some soil if necessary.

To construct the gas outlet, make a small hole in one of the folds of plastic near the inlet pipe, push the black poly pipe through so the end will sit above water level (the hole should be below final water level) and wrap the area tightly with rubber strip and hold rubber in place with insulating tape.

Spread the layflat tube out in the trench, making sure it is properly centred and the base is laid out flat. It may help to put a couple of centimetres of water in the digester at this point (It will also stop the plastic blowing away!).

At the outlet end, arrange the PVC pipe so the plastic sheet fed under the pipe will be below liquid level. The bottom of the plastic sheet must rise higher than the bottom of the PVC pipe by at least 50 mm (2″) to hold the operating gas pressure. The operating level in the digester will be lower than the outflow level by the amount of pressure in the digester, and the inlet pipe end needs to be a little higher than the outflow level.

The last thing to do in construction is to put the tee in the end of the poly pipe (you may be able to cut 75 mm (3″) off the black poly pipe first, or use 100 mm of flexible pipe on the other end of the tee) and the flexible poly pipe on the middle of the tee. You now need to arrange the small container so the short piece of

Fig. 11 Steps in making a poly plug-flow digester. **a** Folded layflat tube. **b** Inlet completed. **c** Fitting gas outlet tube

pipe sits in it as a water drain point (and to relieve excess pressure!) and fill the container up to the tee junction with water (to keep gas in the digester). Put the free end of the flexible pipe into the small container as well, making sure the end will stay fully submerged, to stop gas escaping. The completed Cameroon digester is shown in Fig. 12.

4.2.8 Testing

At this stage, you may like to fill the digester with enough water to seal the inlet and outlet pipes. You can then inflate the digester and check for gas and water leaks and make sure the gas outlet is functional. A motorcycle exhaust has been suggested for inflating (just make sure the gas has cooled, by running the connection tube through some water), but an air compressor, hand pump or just your lungs will do the trick. Soapy water is a good way of finding gas leaks, as you may need to do if damage occurs during operation. If you are unfortunate enough to have a leak, just dry the area and apply an "insulating tape" patch. It is much more pleasant doing this with water rather than effluent in the digester, so an initial test is recommended.

4.2.9 Filling

Now you can fill the digester to operating level with effluent. If you are using poultry manure, kitchen scraps or any waste that may not have methanogens present, you will need to add some inoculum as well—cattle or pig manure will be fine, or you may be able to get some sludge from another anaerobic digester (maybe your local sewerage works).

Once filled, you will need some patience, as it will be at least a few days before you get much gas, and the first gas will be mainly carbon dioxide, so would not burn. Let the digester get going properly before commencing feeding, perhaps this will take a week or two (depending on operating temperature and how many bacteria were introduced).

Fig. 12 The completed digester in Cameroon

4.2.10 Burning Biogas

When you want to try the "biogas" being produced, you may need to place some weight on the gas storage (probably the digester itself) to develop about 2 cm (1″) water pressure—if you hold the flexible tube end about this far below the water surface, gas will bubble out. If the digester has built up its own pressure by pushing effluent out, weights will not be needed.

Push the copper "burner" into the end of the flexible tube (you can just kink the tube to stop gas flow while you do this), let the gas flow, light a match and see if the gas ignites. If the match blows out, you have too much carbon dioxide, so let the gas escape and wait a few more days for pressure to build up again. If

you have waited a few weeks and still have no flame, you probably do not have methanogens, so will have to inoculate the digester and wait a bit longer.

The simple burner is just a piece of 12-mm-diameter copper tube or other metal tube (about 10 cm long) with the supply end closed down and drilled to 1 mm diameter as a gas jet.

For more ambitious cooking projects, a commercial BBQ/camping burner will do the job, but you will probably find you need to drill out the gas jet (or even remove it entirely) to get a satisfactory flame with the low gas pressure from the digester.

Once you are getting enough gas to keep the flame alight 5–10 min, you may like to see how much water you can heat up.

4.2.11 Feeding

Once you are getting combustible gas, you may start feeding waste into the digester. You will only need to add 8 L (2 gallons) of waste every second day. If you find the biogas is not burning, stop feeding the digester until combustible gas is produced again and then reduce the feeding rate—either feed less each time or wait longer between feedings.

As you add effluent, you should find treated material flowing out the other end, this is very good organic fertiliser.

4.2.12 Next

Now you have an operating digester, the rest is your own—you may like to vary the type of waste treated or the amount fed to the digester to see what happens to biogas production, but if you feed too much, the gas quality will fall and the flame would not burn properly.

Have fun!

4.3 Start-Up

Once the digester is constructed, it is a good idea to fill it with water to check that all components work properly and there are no leaks (it is much easier to work with water than with effluent/waste!). If you start with all openings closed off, make sure that there is some means of pressure relief or the water may displace enough gas to burst the digester!

When all systems have been checked, add about half the digester volume of waste, with inoculum if necessary, then wait (im)patiently for gas production to occur. You may get a burst of gas initially as oxygen is used up and converted to CO_2, which will extinguish a test flame. Depending on temperature and initial microbial population, methane should be produced within a week or so. Wait until biogas volume (and quality) has stabilised before starting feeding, initially at

half the design rate. Again give the digester time to adjust (remember it is a living organism and does not like rapid change—the microbes have to adjust!) before stepping up to full feeding rate. Continue to monitor performance carefully and at any drop in gas quality or volume, stop feeding, or at least reduce the rate, and try to work out what may have caused a difficulty for your microscopic workers.

4.4 Operation

With regular and consistent feeding and monitoring to pick up potential problems, a digester should work reliably, giving a gas flow of relatively constant rate and quality.

To assist in fault finding and early detection of possible problems, daily recording of major parameters is a good idea, or in larger facilities, a data logger may be used to keep records at shorter intervals. Obviously, gas volume and quality are important, as they have already been mentioned above as things to watch. Digester temperature is also important as it shows up heater problems or, if the digester is unheated, may indicate that reduced feeding is required in cooler weather. If pumps are used, monitoring their electricity consumption can indicate changes in amount fed or agitator operation.

Sometimes really simple ideas may be a huge help. On a digester, I was involved with a float, visible from well down the driveway, let me determine what my first task may be. If the float was not visible, I knew either gas pressure was low or a valve had stuck open (usually indicated near the top of the drive by a grey flood) so I had some checking to do. On the other hand if the float was high, I was fairly sure my first task was to find and clear a blockage, as the liquid level was too high. A normal float level meant I could go and start my routine checks, measurements and tasks and hopefully get back to other things without too much delay.

4.5 Fault Finding

If maintenance is carried out regularly and no sudden changes are made to the amount or composition of feed to the digester or the operating temperature, faults will be minimised. Regular monitoring of performance and components will allow early detection of possible problems, as prevention is definitely much better than cure when considering a digester.

As with all fault finding, it is best to start with simple things first and try to isolate where the problem may be. For example, if gas production is down but feeding and temperature have not changed, a probable cause is a gas leak. Immediately ensure that there is no source of ignition in the area and warn others of the hazard. The easiest check is a visual inspection for broken pipes if the pressure is low, followed by a check to see if the area of leakage can be located by smell or gas detector. If nothing can be found or for a smaller scale leak, work by a process

of elimination—if there is a separate storage try isolating the storage from the digester to determine which is leaking. Once you know which side of the isolation the leak is try to work on smaller sections if possible, looking at likely leak points such as joints, valve glands and other weak points.

If a leak cannot be found, it may be necessary to check that the input has really been consistent. In a piggery situation, for example, maybe a tap has been left on and the effluent is more dilute than normal or perhaps antibiotics or disinfectants have got into the digester.

Apart from gas leaks and equipment malfunctions, which will depend on what ancillary equipment is required for a particular digester and the maintenance carried out on this equipment, the other main fault is in the microbiology of the digester. If the digester has gone acid (sour), it may be possible to raise the pH by adding sodium or potassium hydroxide, but this needs to be done gradually to avoid over correcting and feeding should be stopped. If this is not possible (or does not work), it may be necessary to empty and restart the digester. Lack of methane may indicate that the correct microbes are not present, so inoculation will be necessary.

4.6 Safety

Like most of life, there are risks associated with anaerobic digestion. Often manures are involved, with their associated microbial populations, and the digester itself relies on a consortium of microbes which may affect some individuals.

Because we are dealing with a fuel gas, there are flammability issues to consider. The explosive limits for methane in air are 6–12 %, so minimising leaks, using appropriate rated equipment to eliminate ignition sources and having adequate ventilation are important. It is important to warn people of the possible hazards and to ensure that there is no smoking or naked flames near the gas equipment and that no sparks are generated by ferrous tools or electrical equipment, including switches and commutator motors used in power tools.

Biogas itself will displace air, reducing the oxygen available for respiration. The CO_2 component is generally heavier than air, so will tend to collect at lower levels and in pits while CH_4, which is lighter than air, will tend to rise and be trapped in roof apexes or dissipate. CH_4 is about 23 times worse than CO_2 as a greenhouse gas, so every effort should be made to collect the biogas and flare off any excess to minimise emissions.

The other safety consideration with a digester is the trace gases also produced as part of the digestion process. Some of the volatile organics may be odorous (a benefit) but may also cause health problems, and hydrogen sulphide (H_2S) and ammonia (NH_3) may also be produced. Both H_2S and NH_3 cause physiological damage at quite low levels, affecting breathing and the nervous system, and H_2S destroys the olfactory nerves so becomes odourless before it causes unconsciousness and death at higher levels. Detectors for flammable limits, H_2S and NH_3, are available to warn of possible problems.

Of course, the normal hazards of electricity, water, slips and falls are also present, possibly to a greater extent in a digester context.

5 Conclusion

It is possible to make a small anaerobic digester quite cheaply and use it for small tasks to learn about the process or to try different substrates available in your area. Any digestate generated makes good organic compost and could also be used to inoculate or seed other digesters. It is important to be aware of possible hazards and problems so your digestion experience can be as enjoyable and successful as possible.

References

1. Buysman E (2009) Anaerobic digestion for developing countries with cold climates. Master thesis, Faculty of Environmental Sciences, Sub-department of Environmental Technology, University of Wageningen
2. Harris P (2014) Beginners guide to biogas. http://www.adelaide.edu.au/biogas. Accessed Jan 2014
3. Klass DL (1989) Biomass for renewable energy, fuels, and chemicals. Academic Press, San Diego
4. Sabonnadiere JC (2009) Renewable energy technologies. ISTA/Wiley, London
5. Tietjen C (1975) From biodung to biogas—a historical review of European experience. In: Jewell WJ (ed) Energy, agriculture, and waste management. Proceedings of the 1975 cornell agricultural waste management conference. Ann Arbor Science Publishers, Ann Arbor, pp 207–260

Development, Operation, and Future Prospects for Implementing Biogas Plants: The Case of Denmark

Rikke Lybæk

Abstract This chapter elaborates on different concepts of biogas technology understood in a Danish context. It emphasizes how energy from production of biogas is distributed, either as biogas to regional combined heat and power plants (CHP) or as district heating (DH) to small-scale local networks. The chapter provides an overview of the political situation and a historical outline of the development of the Danish biogas sector, and it presents the biogas process and operational aspects (e.g., the production of biogas, use of manure and industrial waste as gas boosters). Advantages of biogas technology are emphasized; its capacity as a *renewable energy* and *GHG-avoiding technology*, and as a *waste processing* and *environmental technology*. It is argued that biogas can provide a future platform for the use of household waste and other types of organic materials (gas boosters) to enhance gas yield, as is the case of biomass from nature conservation, straw and deep litter, etc. Further, the chapter discusses whether or not biogas technology can create new job opportunities in rural areas that lack development. Economic results from operating centralized biogas plants in Denmark now also stress the importance of developing new gas boosters in order to support a further development of the biogas sector. This chapter ends with a discussion about new trends in biogas production, for example, how new organizational models can be designed as well as how the use of alternative boosters—like blue biomass—can be applied. Finally, biogas is discussed in global and European contexts, and emphasis is given to the need for digesting organic waste in combination with manure to provide valuable nutrients to farmland and also for enhancing the energy services provided by the biogas technology.

R. Lybæk (✉)
Department of Environmental, Social and Spatial Change (ENSPAC), House 9.2,
University of Roskilde, Universitetsvej 1, 4000 Roskilde, Denmark
e-mail: rbl@ruc.dk

M. A. Sanz-Bobi (ed.), *Use, Operation and Maintenance of Renewable Energy Systems*, Green Energy and Technology, DOI: 10.1007/978-3-319-03224-5_4,

1 What is Biogas?

Biogas consists of approximately 2/3 methane (CH_4), 1/3 carbon dioxide (CO_2), small amounts of hydrogen sulfide (H_2S) as well as hydrogen (H_2). The gasses are formed by the decomposition of animal manure and organic waste from industry and households, etc., in anaerobic (i.e., oxygen free) reactor tanks where it is heated. The organic materials remain in the reactor for about 2–3 weeks after which the resultant gas can be used for electricity and heat production. In the reactor, a biological decomposition takes place in which microorganisms produce methane (biogas). Biogas is, however, also produced naturally by the decomposition of organic materials in the natural world, for instance in bogs, in which swamp gas is developed. In principle, all organic material can be converted into biogas.

Methane is thus a by-product from the respiration of microorganisms' decomposition of different types of organic materials. The type of organic materials being decomposed determines the amount of methane that is produced, i.e., fatty or greasy organic materials lead to a high gas production, whereas materials primarily containing carbohydrates such as glucose and other simple sugars as well as high-molecular such as cellulose and hemicelluloses lead to a lower gas production. The combustible part of the biogas consists of methane and hydrogen. It is an odorless and colorless gas with a boiling point of −162 °C, and it burns with a blue flame. Methane has a density of 0.75 kg/m^3 at normal pressure and temperature, and an upper calorific value of 39.8 MJ/m^3, corresponding to a potential energy production of up to 11 kWh per m^3 biogas [13].

In the commercial production of biogas, it is common to utilize manure (a mix of slurry and solid animal waste) from livestock, sludge from wastewater treatment, residues from agriculture and industrial biomass waste from, for example, the food industry. Animal manure is therefore, at least in a Danish context, the main ingredient when producing biogas. Industrial organic waste is thus added to increase the gas yield. In some other countries, biogas is mainly produced on landfills where it develops naturally when the organic parts of the garbage decomposes. Biogas is thus extracted directly within the landfill site by gas pipes for energy production. In other countries, again, biogas is mainly produced by organic waste from households without animal manure. The dry matter in manure consists, among other things, of carbon, and the digesting process transforms this carbon into biogas, whereas the nutrients are left in the manure providing a valuable soil fertilizer.

1.1 Status and Development Path

1.1.1 Status

Today (2014), there are 23 large-scale *centralized biogas plants* and 60 smaller *farm biogas plants* in operation in Denmark, located as shown in Fig. 1. The figure does not show all the plants established, but more interestingly indicates in which parts of

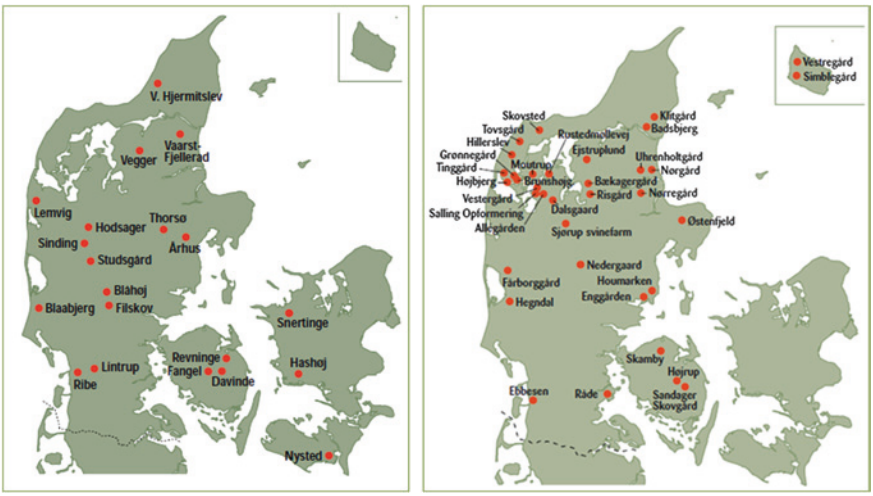

Fig. 1 Location of centralized and farm biogas plants in Denmark [48]

Denmark the livestock density is highest, primarily in Jutland in the western part of Denmark (mainland connected to Germany). Several new plants are, however, under construction or scheduled to be so in the near future. Other already established plants have planned to expand their current production.

Existing biogas plants—including a number of plants located in connection with wastewater treatment plants digesting sludge and landfill gas—account for only approximately 5 % of the total manure potential (manure and organic waste). This corresponds to around 4 PJ, or 0.5 % of the Danish energy consumption of 800 PJ.

The estimated total available manure potential is, however, much higher and could provide an energy production of 40 PJ, equal to 5 % of the current energy consumption [33]. Reaching this level of energy production requires the implementation of approximately 50 new large-scale centralized biogas plants or a large number of relatively smaller farm plants. It is also necessary to develop new gas boosters, substituting scarce industrial biomass waste, to secure the plant economy and make the utilization of the full manure potential viable. The Danish Government is aware of the biogas potentials and has formulated several political goals for the biogas sector in recent years. In 2008, the 'Energy Deal' stated that 30 % of the manure potentials should be digested by 2025, corresponding to 12 PJ. Later in 2009, the 'Green Growth Strategy' was formulated requiring 50 % of the manure to be digested by 2020, corresponding to 20 PJ [6].

Renewable energy, as such, must contribute to 30 % of the energy production in Denmark by 2020 [24]. A long-term goal of a carbon-free energy sector before the year 2050 is envisioned [5]. A transition from an energy supply, primarily based on fossil fuels, such as coal, oil, and natural gas (close to 80 % of the primary energy consumption in 2012), to a future with the supply of renewable energy only, is thus planned to take place within the next 35–40 years. Polluting

fossil-fuel-based energy will thus be substituted with wind energy as base load, in which liquid biofuels (such as syngas and biogas) are used as reserve and peak load capacity when wind energy is insufficient for covering the electricity demand. Other solutions than biomass, wind and smart grid technologies will also be used in such future energy supply, for example solar, geothermal energy, heat pumps (ibid.).

Today, biogas is regarded as an important fuel providing a flexible capacity supplementing a massive future use of fluctuating wind energy. The production of biogas is thus an important way to reduce the Danish greenhouse gas (GHG) emissions, as the technology has multiple advantages: It increases energy supply security by diversifying the supply of renewable energy, it reduces negative environmental impacts from Danish agriculture leaching nitrogen to the aquatics, it helps avoid emissions of CH_4 and N_2O from farmers storage of manure and use of undigested manure on farmland, and it provides a high-value fertilizer substituting expensive industrial products [34]. It is therefore important to increase the use of the manure potential—in combination with new gas boosters—to pursue the implementation of as many biogas plants as possible. Only then will it be possible to fully exploit the benefits which can be gained from biogas technology.

1.1.2 The Danish Biogas Development Path

The implementation of the earliest Danish biogas plants must be viewed in the light of the political context of the late 1970s energy crisis, caused by the oil embargo on Denmark. The purpose of the technology at that time was to generate renewable energy and thus to increase energy security. Attention to the environmental benefits of co-thinking biogas and the agriculture did not exist at the time. During the 1980s, however, environmental concerns were raised as far as nitrogen and phosphorous pollution from agricultural production, which happened as a consequence of the use of animal manure as fertilizer. Hence, this problem significantly increased with the growing number of pigs. Danish agriculture therefore faced stricter environmental regulation, especially relating to the handling and storage of manure. The focus of the early Danish biogas research therefore changed, and priority was now given to develop technology that could assist farmers in reducing emissions of nitrogen and phosphorous. The shift illustrates how the early biogas technology was shaped by changing policy regimes, shifting from focusing on energy security to primarily focusing on environmental protection.

Thus, the first Danish biogas research program was phased out in 1986 and the focus shifted from small-scale farm biogas plants toward smaller centralized biogas plants. The development of the centralized biogas plants took place parallel to the ongoing development of the farm plants and thus kept two separated development paths alive. Political support and university research, however, mainly targeted innovation on the centralized plants, whereas farm plants mainly continued their life due to sporadic grassroot activities and a track record of better performing plants [22].

Important university research, primarily conducted at the Danish Technical University (DTU), was undertaken in research programs in the 1990s, leading to a better understanding of the biogas process, for example residence time, gas mix, gas yield, and the behavior of different organic materials together with manure. This research was targeted to support the development path of large centralized plants. Research on farm plants was only conducted on the basis of individual grants given to specific activities at farm plants already established and as such proved very fragmented and with lack of focus. During the same period, the technology applied at the centralized plants was improved, but the profitability of the plants was, however, still low. During the late 1990s, the Danish biogas research programs continued to focus on the larger plants. Several of these plants started to mix manure from livestock with organic industrial waste in order to boost the gas production. The biogas plants thereby shifted focus from solely being a technology applied to agriculture, but also to integrate the industry as far as organic waste. University research continued to refine the technology in close collaboration with the centralized plants by improving the understanding of digestion processes and by optimizing the process technology [22].

A period of almost a decade followed in which the biogas technology was almost abandoned as far as governmental support was concerned. No research programs were initiated and the framework conditions for the technology were relatively poor. Low electricity prices and construction grants hampered a further development of the technology [27]. In the decade that followed, however, new targets for biogas were formulated in energy and environmental protection plans, now attaching a dual policy objective to the biogas development programs: promotion of renewable energy and limitation of nutrient loads to the aquatic environment. In 2009, the Danish government presented a new strategy for agriculture: the 'Green Growth Strategy' (mentioned earlier). This strategy intended to improve the competitiveness of the agricultural sector, enhance environmental protection, and increase energy production from biogas significantly. The strategy also underlined the integration of the energy, agricultural, and environmental policy. Biogas therefore holds a strong position in this governmental plan (for thorough analyses of the Danish biogas innovation history, see [22] and also [27]).

Today, the technical level of the two biogas concepts is relatively mature, but a further implementation of the technology is currently hampered by lack of industrial biomass waste, which means that alternatives must be developed. For the centralized biogas plants, problems connected with identification of appropriate sites for the location of such plants are also present. Many communities become opponents of plans for implementing biogas plants in their local area, due to noise, odor, and visual pollution from these plants. This calls for alternative solutions and will be presented later on in this book chapter (see Sect. 4.2). Other barriers hampering a further development of the biogas sector are, for example, the extremely long period in which the authorities have to work with approving biogas plants, before actual implementation can take place. Financial opportunities have also posed problems for the sector in recent years, as financial institutions have been reluctant to provide loans for new biogas projects. Finally, a future issue could be

the lack of appropriate manure in Denmark, due to the export of small pigs to for example Germany, caused by unfavorable framework conditions for the Danish swine sector. This means that primarily sow manure will be available for biogas production, providing a relatively low dry matter content and thus a low gas yield.

1.2 Two Types of Plant Concepts

1.2.1 Centralized Biogas Plants

Plant concept: Large-scale centralized biogas plants are the most common type of biogas plants in Denmark, as far as quantity of manure digested. Such plants, first saw light in Denmark in the mid-1980s with the establishment of the Vester Hjermitslev biogas plant and later, among others, the Vegger plant [19]. The size and numbers of such plants have increased steadily over the years, and currently 23 centralized biogas plants are in operation digesting between 50 and 600 m^3 manure per day corresponding to between 18,250 and 219,000 tonnes annually. The plants have increased from having a handful to several hundred farms connected to them. These deliver manure to be digested at the plants. The number of connected farms will, however, be even larger on some of the new biogas plants which have been planned. This also underlines the structural development of Danish agriculture evolving toward even larger and more centralized production. The ownership of such type of plants can be quite different. The owner might be an independent institution or a business foundation where neither farmers nor heat consumers are included. The owner might also be a limited liability company owned by external investors and farmers, as well as a municipal-owned utility, the latter not currently seen in Denmark. The most widespread form of ownership is that in which farmers and heat consumers are joint owners, this category includes farmer and consumer-owned cooperatives, farmer-owned cooperatives, and consumer-owned cooperatives [34].

Use of biomass: Many centralized biogas plants digest manure from several types of farms, i.e., cattle and pig farms, as well as mink and poultry farms. The nutrients in the manure thereby undergo a favorable redistribution when it is returned to farmers and used as a nutrient-rich fertilizer on the fields. As mentioned, large quantities of organic biomass waste are commonly added to the process enhancing the gas yield and thus the electricity and heat production. This will influence the income from the sale of gas or electricity and heat and thus the plant economy. On Bånlev biogas plant near Århus (see Fig. 2 below), beet and deep litter as well as silage grass are added to the manure with a distribution of 35,000 and 120,000 per year, respectively. This 12 % additional biomass contributes to a gas production of 7 million m^3 biogas annually, as well as to a production of fertilizer equal to 155,000 tonnes for redistribution among farmers [42].

Economy: The use of additional biomass is significant for the plant economy, so the motivation to develop alternatives to the previously used industrial waste is

Fig. 2 Bånlev centralized biogas plant (*Photo* by Videncenter for Landbrug, [46])

high [42]. Lack of traditional gas booster is thus hampering the economy of many plants today, and the use of alternatives seems difficult to adopt on several plants. On Bånlev biogas plant, the 12 % biomass added contributes to almost twice as much gas, as the supply of the 88 % manure would lead to, that is 3.7 million m^3 of gas compared to 2 million m^3 of gas, respectively. In total, they generate 18,000 MWh of electricity and 19,000 MWh of heat per year, which is distributed on the power grid and sold to the local district heating (DH) network [42].

1.2.2 Farm Biogas Plants

Plant concept: The most common type of plant concept when looking at the number of plants installed is farm biogas plants, which have a history dating back to the mid 1970s, when the first plant was established as a result of the oil crisis in Denmark [22, 23]. There are currently 60 farm plants in operation in Denmark digesting between 5 and 50 m^3 of manure per day, corresponding to between 1,850 and 18,250 tonnes of manure per year. The manure is from the farm's own production of cattle or pigs, etc. A farm plant can be operated and jointly owned by up to five agricultural-based and/or horticultural-based farms, but must be established on the land registered to one of the parties involved [34].

In recent years, there has not been any significant development in farm biogas, whereas some improvements have happened on centralized plants. One single organic farm biogas plant has, however, been implemented, and recent applications for governmental grants to establish farm plants indicate that several new organic farm plants will be implemented in Denmark in coming years [40].

Fig. 3 Torsø farm biogas plant. "Blacksmith plant" with horizontal steel reactor (*Photo* by Landbrugets Rådgivnings-center, [48])

Use of biomass: Farm plants have a long tradition for adding different biomass to boost gas production and hence energy production. Some of the former concepts, for instance the early 'blacksmith biogas plant' (see Fig. 3), were actually sold as a concept including contracts with industrial waste suppliers to ensure a high gas yield and thus a favorable plant economy [19]. Previously, farm plants used large amounts of glycerin, bleaching earth, fish and slaughterhouse residues, etc., to boost gas production. These types of waste are almost impossible to obtain today, due to the large demand and hence competition within the sector. Another explanation is that the manufacturing industry has increased their resource efficiency leading to lower amounts of industrial biomass waste being generated in general. The main supply of the gas boosters applied today is thus industrial waste of lower quality (lower gas yield) and energy crops such as maize and grass silage.

Economy: As described above, the competition for good quality gas boosters is very high, and many smaller farm plants therefore have difficulties raising the necessary quantity to be able to increase the gas yield, which affects the plant economy. Therefore, many farmers are interested in the possibility of using alternative gas boosters, such as agricultural crop residues, energy crops, or silage grass.

1.3 Utilization and Distribution of Energy

Biogas can be used in several different ways which depend on the capabilities and needs of the local community. The widespread implementation of combined heat and power plants (CHP) in Denmark makes it relatively easy to use biogas for energy purposes. Biogas can also be stored, mixed, and distributed in the natural

gas pipelines throughout the country and hence used for heating in households and industry. This requires upgrading to natural gas standard, and thus extraction of CO_2 and removal of moisture, etc., from the biogas. Upgraded biogas can also be used for transportation purposes, which are the case in, for example Sweden where favorable taxation has supported the 16,000 cars that run on biogas and implementation of more than 150 service stations. Hence, upgrading has so far been too expensive in Denmark due to unfavorable framework conditions, but new technologies will most likely emerge making this process more economically feasible in the future [23]. Presently, the energy from biogas plants is used as follows on centralized and farm biogas plants in Denmark.

At the plant facility, a motor/generator converts the biogas into power and heat at a ratio of approximately 35–40 % electricity, 45–50 % heat (related to the lower calorific value of methane), and 15 % losses due to for example motor friction. On centralized and farm biogas plants, the electricity produced is normally sold to the local power company for a fixed price defined by the government. For a period, the price amounted to 77 øre/kWh (equals to approx. 10 euro cent), but with the 2012 'Energy Deal,' it grew to 115 øre/kWh. On centralized plants, the generated heat is either sent to a smaller local DH network in the community, or distributed on a larger DH network in the area providing energy services to a larger geographical area. On centralized plants, some of the generated heat is also used to heat up reactor tanks to the temperature required in order to digest the manure and biomass applied. The temperature level determines the residence time in the reactor tank. On farm plants, the generated heat is also used to heat up the reactor tank, but often also to warm up stables and the farmhouse, etc. Sometimes a neighbor's house, or an institution, such as a school, nursing home, etc., can also receive heat from the plant. Alternatively, the farm biogas plant distributes the biogas to a nearby CHP plant, which then converts the gas to electricity and heat, but most often the motor/generator is implemented in connection with the farm plant.

2 Operational and Economic Aspects of Biogas Plants

2.1 The Biogas Process

The biogas process is depictured in Fig. 4, here emphasized by a centralized biogas plant, comprising the following steps:

Before the manure is pumped to the ***receiving unit***, it is collected from the individual farms connected to the biogas plant, which can be up to several hundred farmers to only a handful on the smallest plants. Manure, as well as biomass from other sources such as organic kitchen waste, industrial residues and maize, etc., is then mixed together with the collected manure in the receiving unit. This ensures a homogenous biomass that later can be pumped to the pre-storage tank. A macerator sometimes assists in fine separating the biomass to achieve a biomass that is pumpable

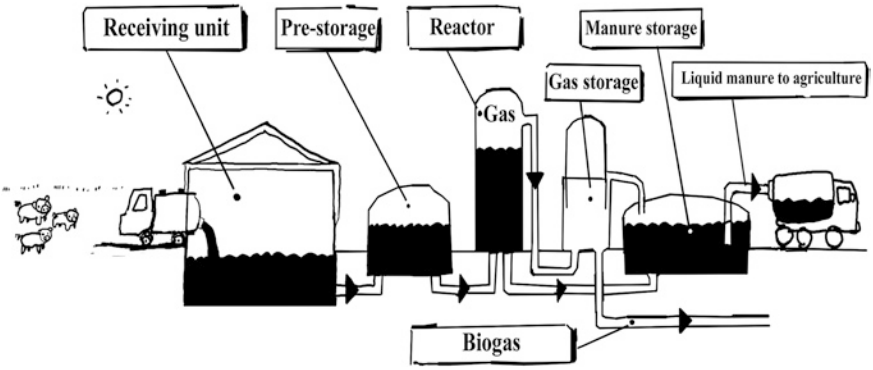

Fig. 4 The biogas process [49]

Fig. 5 Truck leaving the receiving unit at Hashøj biogas plant after delivering manure. It will return to the farms with digested manure (*Photo* by author, 2009)

and homogenous. The receiving unit is thus fully stirred to prevent formation of hard layers on the top and sometimes also heated to ensure that fatty parts stay liquid [13]. Besides receiving and mixing the biomass, the receiving unit holds an important role in providing quality control of the biomass that enters the plant and thus check, account, and verify the supplied organic materials. After delivering manure to the receiving unit, the trucks return to farmers with digested manure (Fig. 5).

After obtaining a homogeneous composition in the receiving unit, the manure is pumped to the ***pre-storage tank*** where it is stored until pumped to the reactor tank. Before the different biomass enters the pre-storage tank, it may pass a hygenization tank, where it is heated to 70 °C for at least one hour to avoid the spreading of various diseases. The biomass is continuously stirred in the pre-storage tank.

Table 1 Gas potentials of different organization materials [48]

Organic materials	Amount of gas per tonnes manure and per m^3 organic waste	Equal to liter fuel oil
Pig manure	22	14
Cattle manure	22	14
Solid waste from poultry	50–100	33–65
Intestinal contents slaughterhouses	40–60	26–39
Greasy waste from slaughterhouses	>100	>65
Fish oil residues	100–1,000	65–650

A visual check of each truck load is thus applied as well as weight registration, where after various data are recorded: supplier date, quantity, type of biomass, processes of origin, and quality. This includes, for instance, measurement of the dry matter content of the supplied manure, important for the registration of the collaborating farmers contribution to the biogas plant [38]. Manure from mother pigs (sows) does not provide a high gas production compared to, for instance, pig and cow manure, hence the first providing a lower gas yield per dry matter unit. Cow manure in general contains high dry matter, but due to the digestion process in the stomachs of the cow, the end result is manure providing a lower gas yield per dry matter unit.

Thus, pigs and cows contribute to the same amount of gas yield per dry matter unit, even though the cow manure initially contains higher dry matter (see Table 1). Bad housekeeping at the farms, where too much water is mixed with manure, can also lower the dry matter content of manure. When recording data special attention is for example given to biomass classified as 'wastes,' for which it may be necessary to fulfill regulatory obligations (depending on the waste category), as well as legal and administrative conditions [29]. In some cases, organic industrial waste is placed in smaller receiving units in order to be able to add the right quantity to the remaining biomass waste [13].

On centralized biogas plants, the ***reactor tanks*** are normally large vertical steel or concrete tanks between 500 and 7,000 m^3 and on smaller farm plants, horizontal steel tanks are the norm (see Figs. 2 and 3). The walls of the reactor are insulated and contain heating coils which keep the biomass at the desired temperature by using excess heat from the motor/generator. Today, the reactor tanks are all designed as a continued process—as opposed to a batch process—in which biomass is added at the top, and the same amount tapped from the bottom. The reactors are fully stirred to avoid hard layers and to provide a good heat distribution and thus bacteria activity. The reactor is a fully closed environment in which the microorganisms reside and digest the organic materials.

Methane-producing bacteria enjoy a temperature variation from 5 to 70 °C. Some bacteria strains enjoy the best growing conditions in the psykrofile temperature area from 5 to 20 °C, and others in the mesophile area from 30 to 40 °C, and again others in the thermofile area from 50 to 60 °C. The fastest digestion is in the thermofile temperature area, but the process is here often more unstable. In the mesophile temperature area, the process is, on the contrarily, more stable

Fig. 6 Manure storage tank (*front*) and gas storage facility at Hashøj biogas plant (*Photo* by author, [47])

and most organic materials will be digested within a few weeks. The mesophile temperature area used to dominate how biogas plants were operated during the last decades, but plants operated with thermofile temperature levels have now become more widespread. This is primarily due to hygenization of organic industrial waste requiring higher temperatures, but also to speed up the process of extracting gas from the biomass [44]. As different bacteria are active at different temperature levels, it is not possible to change the temperature without a long adjustment period where new bacteria are cultivated and become the domination strain. If the temperatures are kept steady, the process is also relatively stable, especially in the mesophile temperature area as mentioned [19].

The biomass remains in the reactor for several weeks depending upon the temperature level, but until at least half of the dry matter has been transformed into usable biogas. The remaining dry matter is more difficult to digest, and it is not economically feasible to extend the residence time even further, and it is therefore pumped to the ***manure storage tank*** shown in Fig. 6. Even after the biomass leaves the reactor, significant biogas production can take place, as the biomass cannot be fully digested in the reactor tank. Thus, in the manure storage tank, the manure will be digested further [21]. Besides collecting additional gas, the purpose of the closed manure storage tank is also to prevent losses of ammonia to the atmosphere [13].

From the manure storage tank, the digested manure are transported back to the collaborating farmers where it is stored in the farm's manure storage tanks and later used as liquid fertilizer. Additional to the manure storage tank, some plants also have a ***gas storage facility***, also shown in Fig. 6, with capacity of up to 24 h gas production in order to even out an unequal daily gas production [13].

2.2 Economic Results

The economy of Danish biogas is exemplified by the economic performance of seven centralized biogas plants, having proved a feasible plant economy within recent years. As larger centralized plants mainly will be the backbone of the future biogas implementation, they are relevant for exemplification of the economic results of biogas. The results are based on a recent report elaborated by Deloitte and Blue Planet Innovation [7] for the Danish Energy Agency. Thus, the following seven plant cases are used for highlighting the more 'successful plant' economy, which are compared with other 'less successful' and 'average plants':

Bånlev Biogas A/S
Lemvig Biogasanlæg A.m.b.A.
Linkogas A.m.b.A.
Ribe Biogas A/S, Thorsø Miljø- og Biogasanlæg A.m.b.A.
GrønGas
Hashøj Biogas.

The economic results are shown in Table 2. The Table indicates that the seven more 'successful plants' have displayed a positive result after financial expenses for repaying debt. The interest cover for these plants is 2.1, which is seen as satisfactory. The plants are on the other hand relatively indebted with a debt ratio of 4.9, but compared to 'less successful plants' centralized plants with a debt ratio of 25.4, and 'average plants' with a debt ratio of 5.7, these results are positive. The average equity ratio is 0.24 which is quite favorable compared to the 'average plants,' which are 0.09 [7]. Thus, the company equity is three times higher than the 'average plant.'

It is further shown that the more 'successful plants' have an average return on investment (ROI) of 5.9 %, as well as an operating margin of 9.5 %. The operating margin is the result before interests as a share of the turnover. These plants also show a positive result on the return on equity corresponding to 13.9 %, which is far more than the 'less successful plants' showing negative results (−17 %). It can be concluded that some centralized biogas plants in Denmark have managed to obtain a favorable plant economy, which can be seen in approximately half of the total plants implemented. Thus, under good management and stable process conditions, it is possible to make a profit running these types of plants [7].

The relatively mixed economic results on Danish centralized biogas plants are primarily due to the lack of organic industrial waste, which previously was used extensively to boost the gas production. Some plants have managed this transition better than others, leaving certain plants with limited options for adding organic materials contributing positively to the plant economy. Many plants are thus designed to digest manure in a combination with organic waste from, for example, slaughterhouses alone. If this supply fails, technical challenges can occur when digesting (storing, handling, mixing, pumping, etc.) other types of boosters with another structure and higher dry matter, such as maize, beet, or deep litter.

Table 2 Economic results of centralized biogas plants in Denmark (own calculations based on data from: [7])

1,000 Euro			
Biogas plants	Successful	Average	Less successful
Result			
Turnover	2,436.40	2,169.20	1,367.87
Total operating costs	−1,276.80	−1,258.40	−1,148.40
Margin	970.53	711.73	258.80
Result before interest, tax, and depreciation	600.27	415.73	157.33
Depreciation	−362	−365.53	−300.80
Result before interest, tax	238.27	79.20	−143.47
Ledger net	−104.27	−138.80	−187.33
Result before tax	137.07	−53.33	−319.87
Result	123.20	−59.87	−316.13
Balance			
Fixed assets	2,843.87	3,59.40	4,635.47
Land and buildings	1,061.87	1,113.60	1,186.00
Current assets	718.00	919.60	1,201.87
Equity	1,012	571.20	143.07
Capital	733.33	498.00	321.60
Long-term debt	1,576.27	2,385.73	3,519.07
Short-term debt	1,133.73	1,539.73	2,108.27
Total balance	3,652.40	4,562.80	5,837.33
Ration (median)			
Interest cover	0.28	0.16	−0.08
Debt ratio	0.65	0.76	3.39
Operating margin	9.5 %	n/a	−9.0 %
ROI	5.9 %	2.9 %	−1.8 %
Return on equity	13.9 %	n/a	−17.0 %
Equity ration	0.032	0.012	0.00

This emphasizes the importance of identifying alternative gas boosters and in general increasing the knowledge in the Danish biogas sector of how to handle such alternative but very important gas boosters.

Another issue hampering around half of the centralized plants from obtaining a better economic result is the roof set on how high an income these types of plants must achieve, called “hvile-i sig-selv” in Danish, translated to “break-even.” Thus, only a limited economic surplus can be obtained, favoring, for example, heat consumers being a part of the owner circle. Only a “reasonable” economic surplus must be obtained corresponding to a return on the invested capital of maximum 8 %, [7]. This of course leaves the plants in a situation in which possible profitable investments could be hampered. On the positive side, it will however be interesting to follow how the increased government guaranteed price on electricity (from 77 to 115 øre/kWh), as a result of the 2012 “Energy Deal,” will impact the feasibility of some of the biogas plants currently suffering from an unfavorable plant economy.

3 Environmental Advantages of Biogas Production

3.1 Renewable Energy and GHG Avoidance

Biogas is regarded as a renewable energy being CO_2 neutral as the amount of carbon dioxide emitted when combusting the gas is the same, as once used by the photosynthesis when the organic materials were formed. Thus, biogas also contributes to CO_2 emissions, but as opposed to fossil fuels, this carbon was only recently trapped from the atmosphere and the release is much less concentrated. The carbon cycle is therefore closed within a short period of time, for example between one and several years [29]. Biogas displaces the use of fossil fuels such as coal, gas, and oil from energy production and transport and thus reduces emissions of CO_2, and particle emissions from use of these fuels are avoided. Biogas can be combusted on CHP plants for power and heat production; it can be stored and distributed to households and industry through the natural gas network and used for water and space heating. It can be upgraded and compressed and used in vehicles for transport. As mentioned earlier, biogas is also regarded as an important fuel for integrating fluctuating wind energy in the future Danish energy supply, due to its reserve and peak load capacity.

The production of biogas from the agriculture also significantly reduces emissions of methane (CH_4) and nitrous oxide (N_2O) from farmer's storage of manure and use of untreated animal manure as fertilizer. The GHG potential of methane has a CO_2 equivalent of 21 and an equivalent of 300 for that of nitrous oxide [29]. It is therefore important to digest the full manure potential to avoid these emissions, as it will contribute to global warming (GW). Newer studies indicate that the 2009 emissions of CH_4 and N_2O from Danish pigs and cows (calculated as CO_2 equivalents) were reduced by 15.12 kg CO_2 per tonnes cow manure and 22.37 kg CO_2 per tonnes pig manure, due to the manure being digested in biogas plants [10]. Thus, as outlined above, the biogas technology is clearly a *renewable energy technology,* but also a *GHG-avoiding technology* that helps prevent emissions of very strong climate gasses from the agriculture (and e.g., from blue biomass like seaweed discussed in Sect. 4.1.5).

3.2 Environmental Benefits

Apart from the benefits achieved through the production of renewable energy, as described above, there are several other important benefits that should be mentioned, which emphasize the relevance of the biogas plant being a valuable technology in the forthcoming transition of the Danish energy supply.

First, biogas production has the ability to transform organic waste materials into valuable resources for society by utilizing waste from animal livestock or organic waste from household, industry, etc. The amount of waste is an increasing problem

within the EU and problems associated with overproduction of organic wastes from industry, agriculture, and household are commonly seen [29]. The Lemvig centralized biogas plant digests the following agricultural products emphasizing the plants capability as a waste processor: rape oil and seed, soy bean, corn residues, fruit and vegetables residues. Furthermore, the following industrial waste products are processed in the plant: fish residues, different waste from food industries, flotation grease, and intestinal contents from slaughterhouses [18]. Other plants, for instance Hashøj centralized plant, also digest organic source-separated food waste from kitchens and canteens in Copenhagen. The organic waste is thus recycled in the biogas plant together with manure, etc. [41]. Thus, the biogas technology can assist in getting nutrients from the organic waste back to the soil, instead of being incinerated, which is very common in Denmark, or dumped in landfill, which is commonly applied in several European countries, for example the UK. Thus, the volume of the total waste will decrease just like nutrients will be recycled which will increase the fertility of the soil.

Second, nutrients in the fertilizer are more directly available for the farm crops, as the chemical form shifts to ammonium. An 80 % uptake of nitrogen is observed for digested manure, as opposed to 70 % for untreated manure. This means that the risk of nutrient pollution to rivers, lakes, and groundwater reservoirs decreases. Third, unpleasant odors connected with distribution of manure on the fields also decrease, by as much as 30 %. Forth, as the digested manure receives a declaration of its content of nitrogen, phosphorous, and potassium, it enhances the options for regulating the distribution of nutrients on farmland [13].

Fifth, the manure also undergoes a sanitation process in the reactor tank meaning that pathogen organisms, germ, and seeds are eliminated, reducing the risks of spreading diseases between farms. Also, degradation of hazardous substances, for instance, polyaromatic hydrocarbons (PAH), which increase the risk of cancer, is genotoxic, can damage fetus and the ability of having children, can be significant reduced by the biogas process [11]. Almost 100 % degradation of such substances was found through experiments made at Lemvig centralized biogas plant in Denmark, but the general knowledge of the behavior of these pollutants are, however, very low [13]. Thus, the biogas technology is also a *waste processing* and *environmental technology*.

3.3 Other Benefits

Increased production of biogas from centralized and farm biogas plants in Denmark could potentially provide new job opportunities, more or less skilled. Manpower is needed for production, collection, and transport of, organic waste boosters such as source-separated household waste, silage grass, or hay from natural areas. Technical equipment, construction, operation and maintenance of the plants, also provide jobs; some short term such as jobs associated with the construction phase, and some permanent such as those associated with daily

maintenance and operation, for example supply of biomass. In the construction phase, around 3.71 direct jobs (temporary) are connected with each MW_{total} installed. The daily operation and maintenance of biogas plants normally corresponds to 2.28 direct jobs (permanent) per MW_{total} installed [12, 14]. Biomass technology is, compared to other renewable energy technologies, more labor intensive and thus creates the most jobs both directly and indirectly (Ibid.). More biogas plants in Denmark would thus develop the national biogas sector further and contribute to the establishment of new companies, some with significant economic potential, increase the income in rural areas, and create new above.

Apart from the benefits outlined above, another potential advantage could be the economic robustness that farmers, engaged in economically profitable biogas plants, can obtain. This means that market conditions for the sale of crops and meat can vary throughout the year, but the income support from the biogas production provides a buffer, leaving the farmer less sensitive to shifting world market prices, etc. This will be the case especially on farm plants and, for instance, acts as a buffer for the shifting fossil fuel prices. Being self-sufficient in a secondary production (energy and fertilizer)—heat to stables and farmhouse and in producing a high-quality fertilizer—leaves the farmer less sensitive toward external factors potentially hampering his primary production of livestock.

4 New Trends in Biomass Utilization and Plant Organization

4.1 Energy Crops and Other Biomass Resources

Due to lack of industrial biomass waste, some, especially large-scale biogas plants, have begun to utilize energy crops, such as maize and beet, to boost gas production, and thus to secure the plant economy. From the political side, however, a roof has been applied to how much Danish agriculture may use energy crops; thus, from 2012 to 2017, it is, for example, possible to use 25 % maize (compared to total weight), which is reduced to 12 % from year 2018–2020. Hence, after 2020, new solutions will have to be applied, which, for example, could be a requirement that up to 60 % of the domestic organic waste should be digested [45]. Thus, grass, biomass harvested from nature conservation, straw, deep litter, as well as organic waste from households and commerce, will mean that most probably there will be substantial use of such organic materials in the future. An important advantage of using biomass as gas boosters, as opposed to, for instance, organic waste, is the option for a seasonal regulation of the gas production. To increase the production of DH on the CHP plants during the winter periods, the biogas plants can regulate production by adding pre-stored biomass (silage) to the manure.

4.1.1 Maize, Beet, and Grass from Agriculture

It is estimated that 30 PJ of energy can be produced from biomass in Denmark on approximately 150,000 ha or on 6 % of the cultivated land. The energy potentials of manure are, as mentioned earlier, 40 PJ [6]. Manure and biomass together could thus cover approximately 7 % of the current energy consumption in Denmark, and with the expected energy savings in coming years, this could add up to 10 % in the future [31]. There is, however, still limited experience with the use of biomass gas boosters in Denmark. The perspectives of using maize, grass, and beet will briefly be highlighted below.

Energy crops such as maize and beets are extensively used on German biogas plants where a large proportion of the maize applied to biogas plants in the northern part of Germany are actually produced in Denmark. Also, grass such as clover grass is widely used often stored and applied as silage grass. From Germany, it is thus possible to obtain experience in the use of energy crops, where particularly the handling of beet has challenged Danish biogas plants. The conditions under which these crops are received at the plants must in general be improved if new and existing plants are to digest several different types of biomass in the future. Many different technologies will have to be applied in order to convert this biomass, such as extruders, hammer mills, and bio-mixer's, etc. Thus, various pre-treatment technologies are therefore needed, which increase the costs of using energy crops, just as expenses connected with storing the crops must be faced [42].

The supply security of energy crops is also an element that should be considered, since not all crops are available throughout the year. Here, the storage capacity is an opportunity to 'extend' the season for each crop. Supply security also includes that crop farmers only produce, for example, beet and maize for biogas purposes, if they are not able to earn more on the production of, for instance, grain. As soon as grain prices rise, farmers will typically convert to grain production, meaning that the price of energy crops will increase [42]. On smaller plants, these costs can hardly be borne by the limited plant economy, so alternative resources will have to be considered.

Maize is the crop that will be most profitable for Danish biogas plants with a production prize of 0.25–0.29 €/m^3 methane (depending on the soil). Experiences from Germany show that maize is relatively easy to grow and quite unproblematic for biogas plants to handle in their pre-treatment and biogas process. Beet is, on the contrary, more problematic when it comes to handling and storage [42], but the gas yields are quite high due to sugar content. If both top and root are included, the yield is approximately 1/3 higher than maize. The production price is higher than maize and add up to 0.27 to 0.35 €/m^3 methane. Grass can be harvested from natural areas as a cover crop and from intensively cultivated farmland as well. The latter will give a yield of 12 tonnes dry matter/hectare, with a production prize a little higher than maize [31].

Thus, from a production price and crop handling perspective, maize is attractive, but requires both fertilizer and pesticides. New research, however, indicates that emissions of GHGs from manure containing digested maize are far from beneficial,

as it lead to high emissions of N_2O. Thus, it is actually problematic to use maize for biogas production [16]. Grass—especially when grown on natural areas—has several environmental benefits including nitrogen fixation. Beet on the other hand require both fertilizer and pesticides which are difficult to handle, but have the highest yield per hectare. It is, however, possible to combine the production of fodder and biogas using beet. This type of system integration—the production of crops for human food or animal fodder, as well as the production of renewable energy based on the green tops—is important for a sustainable future agricultural sector in Denmark.

4.1.2 Biomass from Nature Conservation

Biomass from nature conservation could also have a great potential for biogas in Denmark and currently corresponds to 338,000 ha consisting of fresh meadow, moor land, marsh, grassland and bogs, etc. In these areas, there is a need for nature conservation in the form of animal grazing or straw harvesting, and it is estimated that potentially between 236,000 and 366,000 tonnes of dry matter could be harvested annually. In addition to these biomass resources, 210,000–666,000 tonnes of dry matter are situated in the immediate vicinity consisting of extensively as well as intensively cultivated farmland. The potentials are thus relatively high, and the technologies used for harvesting this biomass are well-known equipment. On more wet areas, however, it will be necessary to deploy new technology in the form of belt drive vehicles and perhaps robots, etc. The cost of harvesting in these areas will therefore be higher than in the more easily accessible areas [4].

It is difficult for the biogas plants to utilize the harvested hay since the biogas technology is based on pumpable organic materials immediately. It will therefore have to be pre-treated in the same relatively costly way as traditional straw, in which an extruder can be utilized. It breaks the cells of the straw using two snail screws operated under high pressure, which leaves it wetter and with a much larger surface [26]. Bånlev centralized biogas plant uses a low-cost method, which seems promising. The straw is first chopped in a shredder to approximately 10 cm in length, whereafter a snail moves it into the receiving unit where it is stirred to ensure a good mix with the manure and other types of biomass applied [38]. As increased use of hay harvesting from natural areas, roadsides, etc., will contribute to reduced pollution with nutrients, it could be considered whether biogas plants should receive a form of gate fee. Thus, the biogas technology can protect society from a number of unpleasant problems related to the leaching of nutrients, damaging lakes, streams, inland waters, and ultimately groundwater resources.

4.1.3 Straw and Deep Litter

The current consumption of straw on Danish CHP plants, substituting coal and natural gas, etc., will most likely decline in the future as the plants will convert to wood chips. This means that there will be more biomass resources available in

the future for biogas plants. It is estimated that the potentials of straw in Denmark corresponds to 2–3 million tonnes of dry matter [4], equal to 100 PJ of energy [32]. It is presently possible to use approximately 10 % straw (of total weight) in the biogas plants without any special pre-treatment technologies that only would add cost to the process. The residence time in the reactor must, however, be increased to a total of 60 days, since the structure of the straw requires a longer digestion period [25]. It will not cause any problem on farm plants already operating at mesophile temperature level, whereas on modern large-scale centralized plants operated at the thermophile temperature level (higher temperatures), this cannot easily be done, since the residence time is correspondingly shorter in this type of plants.

Also, deep litter could in the long run play a much larger role in the production of biogas than it has today. The proportion of deep litter used in biogas plants is limited, but intensified regulation from EU regarding animal welfare will increase the proportion of farms established with stables containing deep litter in the future. In this way, farmers could increase their supply of deep litter for biogas plants from such facilities in the future [40]. It is estimated that there are approximately 1 million tonnes of deep litter (in dry matter) available from Danish agriculture today [4] having a gas potential that are at least 10 times higher than manure, indicating that it should be utilized for biogas production [25]. If the biogas plants could add straw, in combination with deep litter, and at the same time increase the dry matter of pig manure to about 6.6—from approximately 6.1—it would be possible for the biogas sector to completely avoid the use of energy crops, etc., as gas boosters (ibid.). On smaller farm plants, this would clearly be an advantage, as the cost of acquiring such gas boosters is relatively higher than on large plants.

4.1.4 Organic Waste from Households, Institutions, Kitchens, etc.

In Denmark, approximately 500,000 tonnes of organic food waste is discharged annually from a population of nearly 6 million people [35]. Most of this waste will be incinerated at the waste incineration plants, contributing to electricity and heat production. The energy in the organic waste could, however, be used more efficiently when digested in biogas plants due to its wet consistence, just as the nutrients' in the waste would be recycled to the farmland. One tonne of source-separated food waste has a potential of up to 180 m^3 biogas, which equals 1,100 kWh, but most often around 130 m^3 is achieved. To compare, 1 tonne of average animal manure has a gas potential of 20 m^3. Only 12 % of Danish municipalities recycle food waste in biogas plants, and only 20 % provide citizens with an option of source separating their wastes. As mentioned earlier, some centralized plants in Denmark digest organic waste from public kitchens, canteens from, for instance, hospitals, old people's home, kindergartens, etc., but not to the extent possible.

In Norway and Sweden, however, biogas plants based on organic food waste are very common, especially in non-animal dense areas [36]. Technically, these plants are operated satisfactory and seldom face operational problems. Digesting

organic household waste has historically never been very successful in Denmark, due to technical problems with pre-treating the waste at the biogas plants [19]. But in the municipality of Billund in Jutland, organic households waste has been digested successfully for many years. In this case, the technology was designed to treat sludge, household waste, and industrial biomass waste right from the beginning [35]. Thus, based on the experiences from Norway, Sweden, and the municipality of Billund in Denmark, organic household wastes should preferably be digested in biogas plants instead of being incinerated.

The challenge is to source separate the household waste by the citizens, in order to avoid the use of costly and advanced pre-treatment technology. In Billund, two waste bins are provided to household, one for organic and one for non-organic waste, which are collected every 2 weeks alternately. The bag for the green bin is made of strong paper, which decomposes together with the organic waste at the biogas plant. The citizens of Billund are good at separating the waste at source, indeed the percentage of mal-sorted waste in below 1 % [35]. Thus, an alternative to industrial biomass waste, and crops such as beet and maize, could be source-separated household waste in the future. As shown, the biogas potentials from household waste are high, but the municipalities will need to provide the households with options for actually source separating their garbage and enhance the use of this waste together with manure in biogas plants throughout Denmark.

4.1.5 Blue Biomass

Blue biomass—or third-generation biofuels—means biomass from the aquatics such as algae (micro) and seaweed (macro). The benefit of using such biomass for biogas production, as opposed to maize and beet, etc., is that it does not compete with animal or human food, which leaves out an ethical discussion of its relevance for energy production. This biomass could be algae harvested from the sea or cultivated on land, combined with carbon capture and wastewater used as growing nutrients. Different research projects have been established in Denmark, for example, at the Algae Center Denmark, to gain knowledge about the energy potentials of algae [2]. The results from several projects with on land farming of micro-algae's (green filamentous algae) in ponds indicate that approximately 18 tonnes of dry matter per hectare can be harvested with an eight-month season [17].

Another type of blue biomass that could have future potentials in Denmark and within the EU is seaweed, which currently plays an important role in a new centralized biogas plant on Zealand in Solrød municipality, just commissioned for bidding medio 2013. This biogas project exemplifies the positive impacts of using blue biomass resources, but also emphasizes biogas technologies' capability as a *renewable energy* and *GHG-avoiding technology* and a *waste processing* and *environmental technology*, as discussed in Sect. 3.

The project idea originally came from a pollution problem at the bay of Køge, where large amounts of decomposing, and thus bad-smelling casted seaweed, covered the beach. To clean up this problem and make the beach accessible,

local citizens came up with the idea of implementing a biogas plant to digest the seaweed. Together with the municipality, the ideas evolved further, and plans of digesting manure from local farmers and other types of organic waste from the community were developed. Industrial biomass waste from the local industry CP Kelco producing pectin, which leaves a by-product based on citrus shells, was considered. Thus, approximately 22,000 tonnes of seaweed will be used annually together with by-products from CP Kelco corresponding to 79,400 tonnes and animal manure equal to 52,800 tonnes annually. Besides this, the plant will also digest horse manure, weed cutting from lakes and streams, etc. The plant will also be designed to digest, for instance, deep litter and energy crops. [9, 37].

The energy and environmental benefits associated with the implementation of the Solrød biogas plant are, besides a clean and non-smelling beach, the reduction of nutrients into the bay of Køge. The removal of nitrogen from coastal waters will be lowered by 62 tonnes annually, which is equal to 70 % of the reduction requirement for the area. Also, leaching of phosphorous will be a result corresponding to 9 tonnes annually, which thus fulfills the total requirements for the areas. In addition, nitrogen leaching from the farms will decrease, as they utilize digested manure being more accessible for farm crops. Avoided emissions of CH_4 from seaweed *not* decomposing on the beach will be 568 tonnes, equal to 11,928 tonnes of CO_2 equivalent. Emissions of CO_2 from avoided use of fossil fuels for electricity and heat generation amount to 40,500 tonnes annually, corresponding to 60 % of the municipal target in 2025. On top of these energy and environmental related benefits, approximately 4 permanent jobs will be created in maintaining and operating the plant [9, 37, 43].

It should be noted that no studies so far have covered the potentials from avoiding GHG emissions from cast seaweed in Denmark. As the figure shows, the emissions derive from a strong GHG (CH_4), having a high CO_2 equivalent, providing favorable options for reducing the GW potentials from such gas. Thus, this aspect needs to be examined further.

4.2 New Organizational Setups

4.2.1 The Ringkøbing-Skjern Model

The organizational model developed by Ringkøbing-Skjern municipality is based on a desire to digest manure and organic materials as close to the source as possible. The municipality has therefore launched a strategy where approximately 60 small-scale biogas plants will be decentralized placed on local farms and additionally receive manure from neighboring farms. The biogas produced is then distributed in approximately 200 km pipelines into urban CHP plants, where electricity and heat are produced efficiently for the local market. The model also includes one or two large biogas plants for the treatment of more difficult biomass waste, such as organic waste from household, commerce, and

fiber fractions from manure. This more decentralized organizational model contributes to a low transport need, in which only the valuable biogas is moved over greater distances in pipes, and not the more aqueous manure from farmers. The newly established public- and private-owned company BioEnergy Vest will undertake the planning, construction, and operation of biogas plants as well as gas pipelines. The first five farm plants with associated gas pipeline are planned to be establish just south of the city of Skjern and will provide the CHP plant in the city with biogas. This system will act as a demonstration project, before the full master plan is launched in the remaining parts of the municipality [28].

The energy production of the Ringkøbing-Skjern model is expected, at full extension, to reach 2 PJ. The biogas produced will, in the short term, replace the municipality's current consumption of natural gas used in several CHP plants, corresponding to the same amount of energy. In the long-term energy savings, achieved as implementation of buildings with low energy consumption, and by energy renovation of buildings, etc., will enable the municipality to export biogas to other municipalities in the region such as to the Esbjerg area located south of Ringkøbing-Skjern [39].

4.2.2 The Danish Energy Agency Model

The Danish Energy Agency has also outlined some visions in order to achieve a high utilization of the Danish manure potential, and imagine a utilization of more than 90 % of the manure potentials in 2030. At full extension, approximately 50–100 large-scale centralized biogas plants will need to be established, as well as 900 very large farm plants. It is envisioned that a local and overall infrastructure for biogas will be established, where manure from small farms will be piped to large-scale farm plants. Here, the manure is digested and the biogas piped to a local 'consumption site' distributing the energy further. In Jutland, there could thus be up to 100 'consumption sites,' each associated with a local biogas pipeline that is interconnected. Large biogas plants will thus produce the gas which is distributed in pipes to a local 'consumption sites.' With construction of, for instance 40 'consumption sites,' it is necessary to establish around 1,300 km of biogas pipes to be able to connect these sites. At the 'consumption sites,' the biogas can either be used for CHP production or be upgraded to natural gas and thus distributed on the natural gas network or used for transportation purposes [39].

Such an organizational model for biogas will primarily be useful in Jutland, where the majority of livestock units are located (1,860 million animal units, against 2,101 nationwide), meaning that the largest biogas potential of course is located there. With a utilization of manure potentials corresponding to approximately 90–95 %, this equals an energy production of up to 42 PJ when energy crops, straw, organic waste, etc., are added to the process [39].

4.2.3 Alternative Models

Besides the models outlined above, this section will also present some possibilities for implementing other types of organizational models which could be developed in areas where the number of livestock units are less dense. In such areas, it is also beneficial to utilize the manure potentials if Denmark is to undergo a full transition of the energy supply as envisioned. The suggestions below firstly depart in establishing smaller farm plants in areas where the implementation of large centralized plants is unfeasible. Secondly, the suggestions focus on substituting an existing consumption of oil on the farm for heat generation by means of fossil fuels, with a supply of heat from biogas production. Below the different models are outlined.

Neighbor model: This model takes its point of departure in distribution of either manure or gas between two neighboring farms, where the purpose is to reduce the construction costs associated with implementing two biogas plants; one at each farm, see Fig. 7. In Option A, manure is distributed from farm #1 to farm #2 in manure pipes connecting the two farms. If farm #1 is to benefit from the generated heat, it is necessary to establish heat pipes between the farms. The manure is thus digested at farm #2 where the actual implementation of the digester, technical house with motor/generator, gas storage, etc., are placed. The heat is used for heating up the reactor tank, stables, and farmhouse at farm # 2, and by means of heat pipes, stables and farmhouse at farm #1.

Option B would be to distribute manure from farm #1 to farm # 2 without receiving energy services (heat) in return, which would lower the cost of the scheme but also the economic and environmental benefits by subsidizing fossil fuels. Depending on the size of farm #1, the manure can either be piped or transported by means of vehicle between the two farms. Option C is to distribute biogas from farm #1 to farm #2 after which the gas simply is converted into electricity and heat on the latter. This model requires a bigger investment at farm #1 that needs to establish digester and gas blower, to distribute the gas to farm #2. The generated heat can thereafter be distributed to farm #1 through heat pipes, as in Option A.

All options will, however, reduce the construction costs connected with establishing separate farm biogas plants and may lead to that manure—otherwise not being used for energy purposes—actually are being utilized. Such cooperation will also mean that the degree of heat utilization can be optimized, as the total area of stables and farmhouse requiring heat increases. The neighbor model can thus contribute to a better use of the manure potentials in Denmark. On cattle livestock farms that cannot alone fulfill the conditions for an economically viable plant, it will, for instance, be possible to cooperate with a nearby pig farm to establish a shared farm biogas plant. The model also makes it possible for smaller farms with relatively scarce amounts of manure to use the resources for energy production. In any specific case, it is of course necessary to calculate the costs connected with establishing manure and gas pipes, as well as heat pipes, etc., between the two farms.

Star model: This model works with some of the same components as the models from the Danish Energy Agency and the Ringkøbing-Skjern model discussed

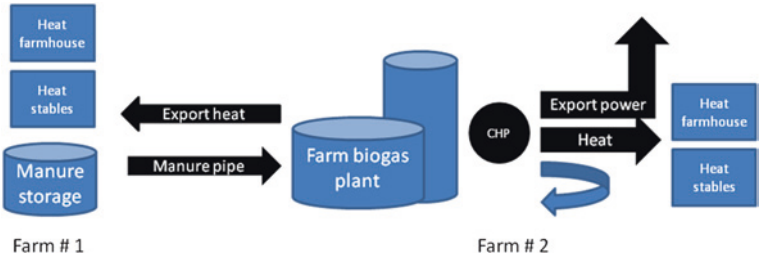

Fig. 7 'Neighbor model' showing Option A (*Figure* by author, 2013)

above. The idea is that up to 20 farmers join together and distribute manure to a central placed facility (hence the name 'star model'), which then digest the manure and convert the gas to energy as electricity and heat. The economies of scale therefore lie in the efficient conversion of energy and that the individual farmer does not convert manure into gas, but simply delivers the manure. Expenses connected with motor/generator, gas storage, connection to the grid, etc., are thus not faced by the individual farms [30]. As seen in Fig. 8, the generated heat is used to warm up reactor tanks and send to a local heat market as DH, and electricity exported to the power grid. Farms with a large heat demand, as for instance pig farms, will, however, not be able to substitute the oil consumption with biogas heat from this model. In such cases, the neighbor model as described above or an individual solution may be a better option.

As for the neighbor model, this organization of the biogas production prevents extensive road transportation with consequences such as road wear and noise pollution in the local community. The saved costs of road transport should be used to establish and maintain a pipeline system for manure with associated pumping stations, etc. The star model also allows smaller farms with limited amounts of manure to utilize these resources for energy production. Both large and small farms will be able to join this manure network, providing a more favorable mix of pig and cattle manure with an optimal relationship between phosphorus and potassium. This is caused by the fact that pig manure is rich in phosphorus and low in potassium, where the opposite holds for cattle manure.

Institutional model: This model is based on a farm plant producing electricity and heat for sale depicted in Fig. 9. This will typically be a pig farm with a swine herd producing a steady amount of manure year round. At the same time, it will be able to consume parts of the generated heat from the biogas plant by heating up the reactor tank, pig stables all year round and farmhouse during winter periods. This will thus replace the cost of heating oil. Within a reasonable distance, the plant can also distribute energy to a nearby institution, being a continuation school, a public swimming pool, sports facility, nursing homes, etc., typically substituting heat generated by means of fossil fuels. A farm plant that treats approximately 20,000 tonnes of manure annually can produce about 100,000 m^3 of biogas, which roughly corresponds to 400,000 kWh of electricity and

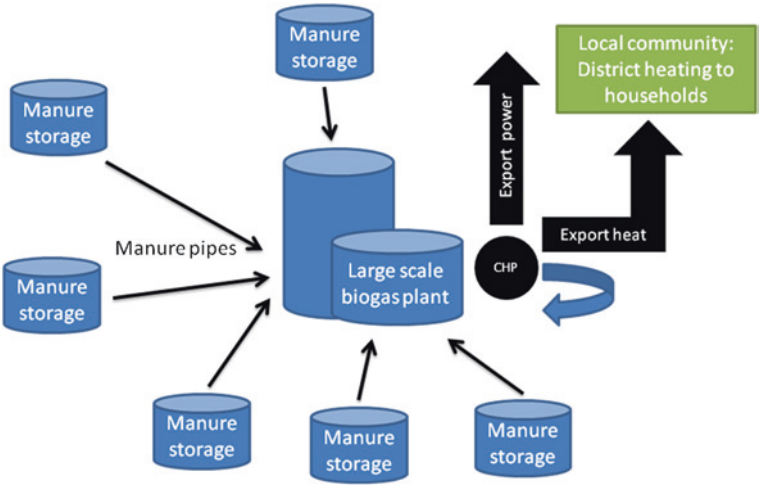

Fig. 8 'Star model' (*Figure* by author, 2013)

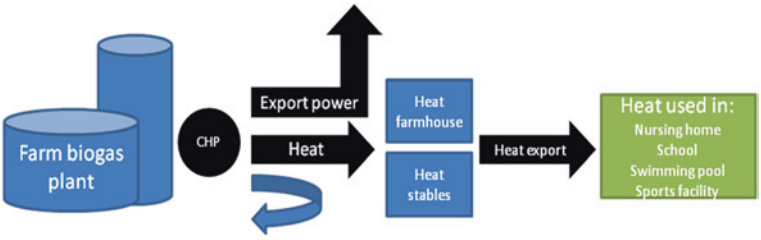

Fig. 9 'Institutional model' (*Figure* by author, 2013)

500,000 kWh heat annually. The latter is equivalent to 50,000 liters fuel oil and could therefore bring substantial income if a local heat market can be identified in the community [40].

4.2.4 Organic Biogas Plants

As mentioned earlier, there is only one organic farm biogas plant in Denmark, but the construction of new plants is scheduled in the near future [40]. The Danish Organic Farming Association and the Ministry of Agriculture and Food have, however, developed a strategy that will phase out the use of conventional manure on organic farmland by the year 2021. This means that within a few years, alternative solutions to the nutrient requirements on organic farmland must be identified, which organic biogas plants could help solve. Thus, organic biogas plants could therefore indirectly mean that conventional crop farmers convert to organic crop farming. However, it is problematic to establish biogas plants on organic plant materials alone, which otherwise would be an ideal opportunity to produce organic

soil fertilizer. A mix with manure from livestock is thus a prerequisite for an optimal biogas process and a good quality soil fertilize, emphasized below.

On organic biogas plants, it is important not to add too much nitrogen and easily degradable organic materials, as the biogas process will be hampered due to acidification. The methane production will simply stop when there are too many organic acids, which the microorganisms not are capable of converting. A solution is to add manure in order to obtain a better balance, which acts as a buffer and neutralize any surplus amount of acids [15]. For organic farmers, it will therefore clearly be beneficial if manure- and crop-based farmers work together around a biogas production, so that the composition of biomass does not hinder an optimal biogas process. As indicated above, implementation of biogas plants in non-manure dense areas of Denmark (mainly in the eastern part of Denmark on Zealand) will primarily take place as a collaboration between smaller farms being crop farms and livestock farms (cattle and pig). In this way, an organic production of nutrients for crop farmers is established, and the reliability of the process is ensured.

5 Biogas Throughout the World

5.1 Biogas in Denmark

The development of the Danish biogas sector is quite different from the biogas development in other European countries, as for instance Germany which has a very large biogas sector. Here, many small-scale farm biogas plants are primarily operated to supply renewable electricity to the grid using a combination of animal manure and biomass (mainly maize and beet). The drivers for the implementation of the biogas technology in Denmark has, as illustrated earlier, mainly been connected to the handling of large quantities of manure from primarily pig farms, which are used to fertilize the agricultural soil. This extensive use of manure in Danish agriculture has caused severe problems for the aquatic environment and the risk of groundwater pollution, etc. The development of the biogas sector in Denmark has therefore historically primarily been driven by a ‘waste’ problem, rather than a way of producing renewable energy. The latter is of course much more in focus today.

Another difference in comparison with the German biogas context is the strong Danish emphasis on using the generated energy as efficient as possible. Thus, Danish biogas plants’ emphasis on CHP production (co-production of power and heat) has historically been very strong, and the identification of local heat markets for appropriate use of heat has been a strong focus all along the technology’s development path. This focus has been supported by the Danish government as far as the relatively low feed in tariffs for electricity sold on the grid—compared to Germany—requiring plant owners to look for heat markets to create an income selling heat as well.

Table 3 Installed capacity of biogas (in ktoe) within the EU (Biogas barometer 2012)

2010					2011			
Country	Landfill gas	Sewage sludge gas	Other gas	Total	Landfill gas	Sewage sludge gas	Other gas	Total
Germany	232.5	402.6	6,034.5	6,669.6	149.0	504.2	4,414.2	5,067.6
UK	1,492.6	258.0	0.0	1,750.6	1,482.4	282.4	0.0	1,764.8
Italy	349.6	8.1	149.8	507.5	755.6	16.2	323.9	1,095.7
France	236.7	44.1	53.2	334.0	249.7	41.9	58.0	349.6
Netherland	36.7	50.2	206.5	293.4	31.5	51.5	208.3	291.3
Spain	29.5	35.9	111.3	176.7	31.8	38.8	179.9	249.6
Czech Rep.	119.6	12.4	66.7	198.7	148.1	15.3	82.6	246.0
Austria	5.1	22.3	144.2	171.6	4.3	16.4	138.8	159.5
Poland	43.3	63.3	8.0	114.6	47.5	67.8	20.1	135.4
Belgium	41.9	14.6	70.9	127.4	41.9	14.6	70.9	127.4
Sweden	35.7	60.7	14.8	111.2	12.4	68.9	37.9	119.3
Denmark	8.1	20.1	74.0	102.2	5.2	19.6	73.2	98.1
Greece	51.7	15.0	1.0	67.7	55.4	16.1	1.4	72.8
Ireland	44.2	9.6	4.6	58.4	43.8	8.2	5.6	57.6
Slovakia	0.8	9.5	1.8	12.2	3.0	13.6	29.3	45.8
Portugal	28.2	1.7	0.8	30.7	42.3	1.8	0.9	45.0
Finland	22.7	13.2	4.5	40.4	23.9	13.4	4.8	42.0
Slovenia	7.7	2.8	19.9	30.4	7.1	2.7	26.2	36.0
Hungary	2.6	12.3	19.3	34.2	7.3	6.4	15.5	29.1
Latvia	7.9	3.3	2.2	13.3	7.8	2.4	11.8	22.0
Luxembourg	0.1	1.2	11.7	13.0	0.1	1.4	11.3	12.8
Lithuania	2.0	3.0	5.0	10.0	5.9	3.1	2.1	11.1
Estonia	2.7	1.1	0.0	3.7	2.2	1.1	0.0	3.3
Romania	0.0	0.0	3.0	3.0	0.0	0.0	3.0	3.0
Cyprus	0.0	0.0	1.0	1.0	0.0	0.0	1.0	1.0
EU	2,801.7	1,065.0	7,008.8	10,875.4	3,157.9	1,208.0	5,719.3	10,085.8

5.2 Biogas Within the EU

The European biogas sector includes thousands of biogas installations, and especially countries such as Germany, Austria, Holland, Italy, and Denmark are technical forerunners having the largest number of modern biogas plants. Table 3 outlines the installed capacity within the EU countries. As seen, around 10.1 Mtoe were generated in 2011, equal to an electricity production of 35.9 TWh, as shown in Table 4. As noted, not all the installed capacity is based on digesting manure from livestock, which is mainly the case in the Northern part of Europe, for example in Denmark, Germany, Holland, and Austria. Other European countries have an extensive production of biogas from landfill, and from sludge from wastewater treatment plants (sewage). This is especially significant in the UK, but also to a lesser extent in Poland and Sweden. Germany is the leading energy producers of biogas from animal manure in the EU, but at the same time produces large amounts of energy from landfill.

Table 4 Gross electricity production from biogas in Europe (GWh) (Biogas barometer 2012)

2010				2011		
Country	Electricity plants	CHP plants	Total	Electricity plants	CHP plants	Total
Germany	14,847.0	1,358.0	16,205.0	10,935.0	8,491.0	19,426.0
UK	5,137.0	575.0	5,712.0	5,098.0	637.0	5,735.0
Italy	1,451.2	602.9	2,054.1	1,868.5	1,536.2	3,404.7
France	756.0	297.0	1,053.0	780.0	337.0	1,117.0
Netherland	82.0	946.0	1,028.0	69.0	958.0	1,027.0
Spain	536.0	117.0	653.0	709.0	166.0	875.0
Czech Rep.	361.0	275.0	636.0	535.0	394.0	929.0
Austria	603.0	45.0	648.0	555.0	70.0	625.0
Belgium	149.0	417.0	566.0	158.0	442.0	600.0
Poland	0.0	398.4	398.4	0.0	430.0	430.0
Denmark	1.0	352.0	353.0	1.0	342.0	343.0
Ireland	184.0	22.0	206.0	181.0	22.0	203.0
Greece	190.5	31.4	221.9	37.6	161.7	199.3
Hungary	75.0	21.0	96.0	128.0	55.0	183.0
Portugal	90.0	11.0	101.0	149.0	11.0	160.0
Slovenia	7.2	90.2	97.4	5.7	121.0	126.7
Slovakia	1.0	21.0	22.0	39.0	74.0	113.0
Latvia	5.9	50.8	56.7	0.0	105.3	105.3
Finland	51.5	37.8	89.2	53.6	39.4	93.0
Luxembourg	0.0	55.9	55.9	0.0	55.3	55.3
Lithuania	0.0	31.0	31.0	0.0	37.0	37.0
Sweden	0.0	36.4	36.4	0.0	33.0	33.0
Romania	0.0	1.0	1.0	0.0	19.1	19.1
Estonia	0.0	10.2	10.2	0.0	17.0	17.0
EU	24,528.2	5,803.0	30,331.2	21,302.4	14,554.1	35,856.4

One challenge connected with existing landfill gas is that the nutrients composed in the organic materials forming the gas cannot be recycled as valuable fertilizer. It is thus a closed cycle in which the nutrients' are lost. On already established landfill sites, it is obvious that the developed biogas should be used, but in the future alternative means of waste management should be emphasized. As mentioned earlier, it is therefore important to collect organic fractions from households, kitchens, etc., to begin a more cyclic utilization of our resources by means of digestion in biogas plants and thus to enhance the technology's capability as a waste processer and environmental technology.

On the other hand, applying sewage sludge on farmland could potentially lead to future environmental problems, such as heavy metal pollution and the spread of hormone disturbing substances to our food supply. This is an issue that draws more and more attention in Denmark, currently especially from a large diary company, which is setting up new standards for farmers to follow if supplying milk to the company, emphasized in the following report [1].

The issue concerning the difference between Danish and German biogas production, as far as electricity and heat production, is illustrated in Table 4. Around

2/3 of the energy production on biogas plants in Europe anno 2011 is based on electricity only; thus, it does not include combined heat and power (CHP). The data for 2010 imply that as much as 4/5 of the total energy production was based on electricity only. As the data indicates, the trend is to emphasize CHP in future installations. This conclusion should, however, be taken with caution, as data from Germany dominates the picture. The increase in CHP is primarily due to a new method in calculating the cogeneration share of electricity production on small-scale installations. Thus, the share of CHP has not changed significantly in Europe within the period shown [3]. Therefore, the majority of the energy is still produced as electricity only, meaning that the actual resources not are utilized satisfactory.

Thus, emphasis on biogas as CHP plants should be promoted more strongly in Europe, increasing the energy efficiency of the plants, diversifying their energy supply, and providing less dependence to imported fossil fuels. Some of the ideas that I mention in the section about new organizational models hence emphasize how to identify local heat markets, which could make a CHP production feasible. Thus, more focus on this issue will enhance the biogas technology as far as being a *renewable energy technology*.

5.3 Biogas in Developing Countries and Emerging Markets

It is estimated that around 18 million rural households in China had installed biogas plants in 2006, and the total Chinese biogas potential is estimated to be of 145 billion m^3. Approximately 5 million small-scale biogas plants currently are under operation in India. Other countries such as Nepal and Vietnam, as well as Thailand, have also implemented numerous small-scale family owned biogas plants [29]. These plants are often privately initiated and financed, or implemented as part of a governmental program or by means of donor support from developing countries. Again, other plants have received financial support through the Clean Development Mechanism (CDM), where a carbon trade from developing countries to developed country takes place [8]. Many biogas plants in Asia are applied as relatively simple technology that are easy to design and reproduce, but within certain of the CDM supported projects, also more advanced technologies are applied. This is, for instance, the case on modern pig farms and within industry in Thailand where mature and reliable biogas technology is required for a stable and continuous supply of energy [20]. In Latin America, a more developed and modern biogas sector is currently under development, in which favorable political frameworks are implemented alongside to support this development [29].

6 Conclusion

The Danish biogas sector has evolved throughout the last 40–45 years first focusing on small-scale biogas plants providing a solution to the energy scarcity during the energy crises in the 1970s, developing further to becoming a sector with focus

on primarily large-scale centralized biogas plants and the handling of manure from farmers. The biogas technology holds many potential benefits and can thus be interpreted as a *renewable energy* and *GHG-avoiding technology*, as well as a *waste processing* and *environmental technology*. The plants generate renewable energy diversifying the supply of energy by the production of both electricity *and* heat providing a substitute to polluting imported fossil fuel. The gas can also be utilized for transport purposes when upgraded, be stored, and distributed in the natural gas network and thus used for heating and energy production in industry and household. The biogas are regarded very important for a future transition of the energy supply, due to its reserve and peak load capacity being capable of adjusting to the fluctuating wind energy, which will be the backbone of the future Danish energy supply.

Biogas technology impacts the environment in several ways including providing a valuable fertilizer leading to lower nitrogen and phosphorous pollution to the aquatic environment, resulting in less odors when spreading the digested manure on farmland, as well as benefits related to the sanitation process that it undergoes preventing spreading of diseases. The technology also helps avoid emissions of CH_4 and N_2O from farmer's storage of manure and from the use of non-digested manure as fertilizer, which are very strong GHGs with a high GW potential. It is also possible to get a declaration of the manure (the specific content of nutrients) after being digested, which facilitates a proper distribution of nutrients. Biogas plants also provide a platform for digesting organic materials such as organic waste from households, kitchens, and institutions which currently are being incinerated in Denmark, and can therefore help to close the nutrient cycle by returning the waste to farmland. Biomass resources such as weed cuttings from streams and lakes, as well as seaweed, could also be applied and significantly reduce nitrogen pollution to the aquatics. I recommend that this is emphasized more strongly in the future as it would also provide a solution for the lack of gas boosters currently hampering a further evolution of the biogas sector.

Thus, a further development of biogas in Denmark depends on the identification of alternatives to the traditional gas boosters (fish and slaughterhouse waste, etc.), where for instance grain straw, grass, deep litter, organic waste from households, etc., as mentioned above, are emphasized. The use of maize and beet is not recommendable as it competes with human and animal food, but in a transition period, I believe it can be beneficial for the plant economy. In the future, however, resources such as blue biomass, for example algae and seaweed, as well as biomass from nature conservation should be applied in biogas plants together with manure. Using biomass, preventing nitrogen leaching is also recommendable, as for instance scheduled on a new centralized biogas plant on Zealand. To overcome the challenges connected with unfavorable economic results on the average Danish centralized biogas plants, it is important to speed up the knowledge and utilization of such resources.

The implementation of biogas plants can also provide potential jobs in more remote areas of Denmark, which lack options for further development. Biomass technologies, as opposed to other renewable energy technologies, can provide

relatively more jobs per MW_{total} installed. Thus, further experience must be gained of how to handle, store, digest, pump, etc., alternative gas boosters, as they will typically have another structure and a higher dry matter content. Knowledge regarding energy crops as maize, beet, and grass are currently available in Germany, and in Sweden and Norway extensive know-how regarding the production of biogas from household waste exists.

To utilize the manure potentials in Denmark and to overcome some of the location barriers, I suggest several alternative organizational models that focus on smaller plants also in manure scarce areas. The models emphasize the distribution of biogas from smaller plants to larger facilities producing and distributing the energy further (Ringkøbing-Skjern model and Danish Energy Agency model). Other models look more into local solutions where gas or manure is pumped between two neighboring farms, or from several farms to a larger biogas plant producing the energy (Neighbor model and Star model). It is important to develop such alternative models in the future if the energy potential from biogas is to be fully utilized, and the biogas technology is to become an important means of reaching the envisioned transition of the Danish energy supply.

Biogas is widely applied within the EU, but most definitely applied in developing countries as less mature and easily reproducible technology. A challenge within the EU is to use the organic fractions, previously dumped in landfills or in waste bins for incineration, for the production of biogas and thus recycle the nutrients on farmland. Another important issue that I would like to emphasize is the relatively scares share of biogas being converted by means of CHP in a European context. Using biogas for both electricity and heat production limits the pressure on fossil fuels necessary to import, and diversifies the supply of renewable energy. Thus, heat markets must be identified and new plants should live up to CHP standards.

References

1. Arla (2012) Quality assurence program Arlagården. Report at http://www.arla.com/Images/arla.com/PDF/arlagaarden/Kvalitetsprogrammet-Arlagaarden_UK.pdf. Accessed 25 Aug 2013
2. Alge Center Danmark (2013) Research in Algae Center Denmark. Information at http://www.algecenterdanmark.dk. Accessed 12 Aug 2013
3. Biogas Barometer—EU Observer (2012) Report at http://www.eurobserv-er.org/pdf/baro212biogas.pdf. Accessed the 14 Sept 2013
4. Birkmose T, Hjort-Gregersen K, Stefanek K (2013) Biomasser til biogasanlæg i Danmark—På kort og lang sigt. AgroTech, Institut for Jordbrugs- og Fødevareinnovation, Denmark
5. Climate Commission (2010) Grøn energi—Vejen mod et dansk energisystem uden fossile brændsler. Danish Climate Commission, Keen Press and DEA, Copenhagen
6. Danish Government (2009). Green growth strategy. Schultz Distribution, Albertslund
7. Deloitte, Blue Planet Innovation (2013) Afdækning af muligheder for at fremme investeringer i biogas—Status, muligheder og betingelser i forbindelse med finansiering af biogasanlæg. Copenhagen
8. Fenhann J, Hinostroza ML (2011) CDM information and guidebook. Technical University of Denmark and Risø National Laboratory for Sustainable Energy, Roskilde

9. Fredenslund A, Christensen TB, Kjær T, Danielsen S, Møller H, Kjær LL, Fafner K (2011) Utilization of cast seaweed and waste from pectin production for anaerobic digestion. In: Proceedings of 13th international waste management and landfill symposium, CITA Publisher, Sardinia, Italy 2011
10. Fredenslund A, Kjær T (2012) Vurdering af energiproduktion, miljøeffekter og økonomi for biogasanlæg. Roskilde Universitet, ENSPAC, Roskilde
11. Informationscenter for Miljø og Sundhed (2013) PAH. Information at http://www.forbrugerkemi.dk/kemi-info/stofgrupper/pah. Accessed the 12 Sept 2013
12. International Energy Agency (2005) Bioenergy Task 29: socio-economic drivers in implementing bioenergy projects. ExCo56, Dublin
13. Jørgensen PJ (2009) Biogas—green energy. PlanEnergi and Faculty of Agricultural Science, Århus University, Århus
14. Kjær T (2006) Socio-economic and regional benefits—employment assessment. REGENERGY, ENSPAC, University of Roskilde, Denmark
15. Krog LT (2012) Kan afgasset gødning fra økologisk biogas erstatte konventionel husdyrgødning og samtidig sikre vækst i det økologiske areal?. Det Natur -og Biovidenskabelige Fakultet, Københavns Universitet, Denmark
16. Hauggaard-Nielsen H, Østergård H (2012) Bioenergi kan støtte bæredygtig landbrugsproduktion. Forskning i Bioenergi (FIB), Særnummer: Robust og bæredygtig bioenergi, Biopress Risskov, Denmark
17. Laurentius S (2012) Algedyrkning—teori og praksis. forskning i bioenergi (FIB), nr. 40, Biopress Risskov, Denmark
18. Lemvig biogas plant (2013). Produkter. Information at http://www.lemvigbiogas.com/produkter.htm. Accessed the 15 Aug 2013
19. Lybæk R, Møller P (1999) Teknologisk innovative- og markedsunderstøttende strategier for fremme af gårdbiogasanlæg. Master thesis. University of Roskilde, ENSPAC, Roskilde
20. Lybæk R (2009) How to enhance the sustainable development contribution of future CDM projects in Asia—experience from Thailand. Post doctoral dissertation. University of Roskilde, ENSPAC, Roskilde
21. Lybæk R (2012) Biogas technology optimization opportunities—lessons learned from Denmark. IEEE, APPEEC Shanghai Proceedings. vol. IEEE Catalog nr: CFP12PEE-CDR IEEE
22. Lybæk R, Christensen TB, Kjær T (2013a) Governing innovation for sustainable development in the Danish Biogas sector—an historical overview and analysis of innovation. J Sustain Dev 21 (3):171–182
23. Lybæk R, Christensen TB, Kjær T (2013b) Enhancing the transition capability of Danish biomass technology by applying a futures study backcasting methodology on the biogas sector. Eur J Sustain Dev 2(4):37–50
24. Ministry of Climate and Energy (2010). National renewable energy action plan. Ministry of Climate and Energy, Copenhagen
25. Møller H, Jørgen PJ (2013) Dybstrøelse hører hjemme i biogasanlæg. Forskning i Bioenergi (FIB), Nr. 45, Biopress Risskov, Denmark
26. PlanEnergi (2013). Praktisk anvendelse af dybstrøelse som substrat til biogasanlæg—Kommende som eksisterende. Skørping, Denmark
27. Raven RPJM, Gregersen KH (2007) Biogas plants in Denmark: Successes and setbacks. Renew Sustain Energy Rev 11 (1):116–132
28. Ringkøbing-Skjern (2013) Energi2020. Information at http://www.energi2020.dk. Accessed the 16 Jan 2013
29. Seadi AT, Rutz D, Prassl N, Költtner M, Finsterwalder T, Volk S, Janssen R (2008) Biogas handbook. University of Souther Denmark, Esbjerg
30. Skadborg O (1992) Nye Bogaskoncepter; Skals Biogasanlæg. Viborgegnens miljø -og Energikontor, Viborg
31. Skøtt T. (2010) Gylle og energiafgrøder kan dække 10 % af energiforbruget. Forskning i Bioenergi (FIB), Nr. 31, Biopress Risskov, Denmark

32. Skøtt T (2013) Behandling af biomass: ikke én vinderteknologi. Forskning i bioenergi (FIB), Nr. 44, Biopress Risskov, Denmark
33. Tafdrup S (2009) Stort behov for udvikling af biogasprocessen. Forskning i bioenergi, FIB, Nr. 3, Biopress Risskov, Denmark
34. Tybirk K (2012) Kogebog for etablering af biogas med 12 faktaark. Agro Business Park/ Innovationsnetværket for Biomasse, Skejby
35. Vetter K (2013) Danmark har kedelig førsteplads. Bioenergy magasinet, Nr. 2, Vmarketing, Vejen
36. Vetter K (2013) Teknologien findes. Bioenergy magasinet, Nr. 2, Vmarketing, Vejen
37. Vetter K (2013) Biogas i udbrud. Bioenergy magasinet, Nr. 3, Vmarketing, Vejen

Interviews/Guided Tours/Presentations

38. Bånlev centralised biogas plant (2013). Information provided at the guided tour, Århus the 16 Jan 2013
39. Danish Energy Agency, DEA (2013). Hvad kan opnås med lokale biogasnet. Oral presentation by B. Harder at the Biogas Workshop, Skejby the 16 Jan 2013
40. Gregersen KH (2013) Biogas expert at AgroTech, Interview, Skejby, 17 Jan 2013
41. Hashøj biogas plant (2009). Information provided at the guided tour, Hashøj the 2 Sept 2009
42. Jensen A (2013) CEO at Bånlev centralized biogas plant, Interview, Århus the 16 Jan 2013
43. Kjær T (2012) Samlede miljøeffekter. Oral presentation at Roskilde University, Roskilde the 14 Jan 2013
44. Lundsgaard E (2009) CEO at Hashøj centralized biogas plant, Interview, Hashøj the 2 Sept 2009
45. Sander B (2012) Energy crops. Oral presentation at the Biogas Workshop, Skejby the 20 Jan 2012

Photos/Drawing

46. Bånlev plant (2013). Videnscenter for Landbrug. At https://www.landbrugsinfo.dk/Energi/Biogas/Sider/Billeder.aspx
47. Lybæk R (2009) Photos taken by the author at Hashøj biogas plant, Plant visit the 2 Sept 2009
48. Torsø plant, Landbrugets Rådgivnings-center (2001) Skejby
49. Rask J (2013) Drawing by student at TekSam. University of Roskilde, Denmark

Operation and Maintenance Contracts for Wind Turbines

Rafael S. Ferreira, Charles D. Feinstein and Luiz A. Barroso

Abstract Owners of wind parks often outsource operation and maintenance (O&M) of their assets. This chapter addresses the fundamental negotiating issues of wind turbine O&M contracts. We develop a conceptual mathematical framework to support the analysis and design of O&M contracts. The framework is used to investigate mechanisms through which incentives perceived by O&M contractors can be aligned with the objectives of wind park owners in both the short and the long terms. This alignment ensures that the negotiated contracts are part of a general strategy for maximizing the value extracted from wind turbines over their lifetime.

1 Introduction

In the wind power industry, the expression *operation and maintenance* (O&M) is often used in reference to a broad set of activities, including insurance, land rental, and administration.

R. S. Ferreira · L. A. Barroso (✉)
PSR, Praia de Botafogo 228/1701 A, 22250-906 Rio de Janeiro, RJ, Brazil
e-mail: luiz@psr-inc.com

R. S. Ferreira
e-mail: ferreira@psr-inc.com

C. D. Feinstein
Santa Clara University, Santa Clara, CA 95053, USA
e-mail: cdfvmn@comcast.net

C. D. Feinstein
VMN Group LLC, Redwood City, CA 94062, USA

M. A. Sanz-Bobi (ed.), *Use, Operation and Maintenance of Renewable Energy Systems*, Green Energy and Technology, DOI: 10.1007/978-3-319-03224-5_5,

In this chapter, we employ a narrower definition of O&M, including preventive and corrective maintenance, servicing, provision of consumables and spare parts, and performance and condition monitoring. These activities are commonly included in the scope of O&M contracts for wind turbines. Expenditures associated with these activities typically account for 7–15 % of the levelized energy cost of wind power plants, suggesting their relevance as cost drivers.

Clearly, this definition focuses on the *maintenance* part of O&M. Maintenance involves technical and administrative actions that keep a system in (or return it to) a state in which its function can be performed. The general objectives of such actions involve ensuring system availability, preserving equipment lifetime, and ensuring safety and human well-being [6]. Therefore, maintenance is fundamental for power systems in general and for wind parks in particular. For a park owner: (1) preserving equipment lifetime in this capital-intensive business is crucial to obtain adequate return on investment; and (2) ensuring asset availability is necessary for capturing revenue streams that depend on the actual output of the generator. Thus, the fundamental incentives an owner perceives to ensure that maintenance is executed relate to asset availability, either in the short or in the long term.

Decisions about O&M activities that aim at ensuring asset availability are made under uncertainty because of the stochastic nature of equipment failure processes. Failures represent relevant operational risks to wind park owners, and the ability to manage these risks via contractual instruments is one of the reasons owners may opt to outsource O&M. The specialization of the contractor and his ability to execute O&M at lower costs than those an owner would incur are also among the reasons for outsourcing.

O&M contractors usually offer owners a range of contractual options, which differ with respect to the allocation of costs, revenues, and risks among the parties. This chapter deals with decision-making about O&M contracts from the owner's viewpoint and has three main objectives: (i) to present the main characteristics of O&M contracts for wind turbines; (ii) to introduce a mathematical framework for decision-making for the design of O&M contracts, taking into account the economic behavior of owners and contractors; and (iii) to analyze incentive mechanisms that aim at aligning potentially conflicting objectives of the contracting parties in both the short and the long terms.

The remainder of this chapter is organized as follows. Section 2 develops the definition of O&M used in this text. Section 3 presents an overview of incentive mechanisms that motivate wind park owners to ensure adequate availability of their facilities. Section 4 presents an overview of O&M contracts for wind turbines, with emphasis on performance incentives for contractors. A theoretical framework for assessing O&M contracts is introduced in Sect. 5, in which we analyze the case of a single non-renegotiable contract whose term equals the design lifetime of the wind turbines. In Sect. 6, the analysis is extended to the situation in which an owner is given an option to engage in renegotiation of the O&M contract within the turbine lifetime. Conclusions are presented in Sect. 7. At the end of this chapter, references are listed.

2 Operation and Maintenance Activities

The definition of O&M we employ includes solely activities that may be within the scope of O&M contracts for wind turbines, such as:

- *Preventive maintenance and servicing*: periodic and condition-based maintenance, replacement of consumables, cleaning, calibration of sensors and actuators, etc.
- *Corrective maintenance*: unscheduled maintenance routines needed to restore failed equipment to the functioning state, including repair and replacement routines.
- *Condition inspection and performance monitoring*: gathering of data, diagnosis of equipment condition, monitoring of plant output, identification of events that trigger preventive maintenance, etc.
- *Provision of consumables and spare parts*: sourcing and stockholding of spare parts and consumables.
- *Maintenance planning and optimization*: analysis of historical data, identification of critical components and failure modes, forecasting of environmental conditions for the purposes of short-term scheduling, planning for logistic challenges, assurance of compliance to warranty requirements, devising maintenance strategies for achieving long-term objectives, etc.
- *Other items*: such as workforce training, documentation, etc.

The costs associated with many of these activities—preventive maintenance and servicing, condition inspection and performance monitoring, and maintenance planning—are essentially deterministic and can be controlled and even predicted with some accuracy.

The process of failure of components of wind turbines is stochastic in nature. Hence, the costs of corrective maintenance, including repair and replacement of failed components, are also stochastic. These costs may be substantial: the current purchase prices of a replacement gearbox and a replacement generator are, respectively, around 10 and 5 % of the upfront capital expenditures of an installed onshore wind turbine. Further, the total costs of equipment failure include lost revenues due to interruption of power generation. The downtime of a typical wind turbine due to failure of critical components, such as gearboxes or generators, may reach several days, so the lost revenues may be considerable.

Therefore, component failures are a significant source of operational risk for wind park owners. O&M contracts may be interpreted as instruments for operational risk management, in combination with insurance contracts and warranties from the wind turbine manufacturer. The importance of O&M contracts as risk management instruments is indicated by the fact that they are a common prerequisite for project finance for wind parks [15].

Obviously, outsourcing O&M is not necessarily the best choice for wind park owners. Experienced owners with a significant portfolio of projects may have capabilities that make in-house provision of O&M attractive. Nonetheless, the considerable growth in the number of active service suppliers in the course of the last decade suggests that O&M contracts can be an attractive choice.

3 Performance Incentives for Wind Park Owners

In the following, we present the mechanisms through which owners are incentivized to ensure adequate levels of availability of their facilities. These *performance incentives* may be formally defined as mechanisms that make the owner's revenues conditional on the availability[1] of the wind turbines.[2]

The need to ensure the availability of generation facilities, as well as other classes of assets, is clear: only available assets can contribute to maintaining continuity and adequacy of power supply. The exact value of the availability of any given generation facility for the power system, however, depends on various factors: the availability of potentially non-storable primary energy resources, the ability of a generator to provide ancillary services, the possibility of transporting energy through the electrical network, etc.

Power systems differ not only with respect to the factors mentioned above, but also with respect to the design of institutions such as markets and regulatory frameworks. Therefore, performance incentives for wind park owners may take many different forms. In this section, we present two categories of performance incentives, providing examples of mechanisms that fit each of them. The two categories are: (1) performance incentives based solely on energy output; and (2) performance incentives based on energy output and prices. This categorization aims solely at facilitating our discussion and is not exhaustive.

The two basic characteristics of the mathematical framework we employ to describe the performance incentives are:

- *Time dependence of performance incentives*: The value of the availability of a generation facility for the power system varies in time and so do the performance incentives for wind park owners. In this chapter, time is treated as a discrete quantity.
- *Stochasticity of performance incentives*: The randomness of equipment failure processes makes the availability of wind turbines a stochastic variable. Because performance incentives depend on the availability of facilities (and eventually on other random quantities), these are also stochastic variables.

The following notation convention is employed throughout this chapter: unless otherwise stated, we use Greek letters to denote stochastic quantities (parameters or

[1] Many of the mechanisms mentioned in this chapter consist of incentives that also affect other desired attributes of wind parks as generation facilities. Our focus on availability is justified by the object of this chapter being O&M contracts.

[2] The expression *availability of the wind turbines* means the availability of the energy conversion facilities only, without consideration of the availability of primary energy resources (wind energy). Though O&M can be executed with the goal of ensuring that conversion facilities are available when there are primary energy resources to be converted, O&M services do not influence the availability of the energy resources per se.

decision variables that, because of being conditioned to the occurrence of stochastic phenomena, are also stochastic in nature), and Latin letters to denote deterministic variables.

I. *Performance incentives based solely on energy output (PIEN)*:

The simplest category considered here is that in which the performance incentive depends on only one time-dependent stochastic variable, the energy production of the wind park. The energy production, in turn, depends both on the availability of the energy conversion facilities and on the availability of the primary kinetic energy of wind.

The performance incentive at a given time period t may be based solely on the output in that same period, or on the output within a past time window. We consider the former case first, and may write:

$$\eta_t = \eta_t(\kappa_t, \varepsilon_t) \tag{1}$$

where

t is an index for the time period;
η_t is the performance incentive perceived by the owner in t, in \$;
κ_t is the wind park available conversion capacity in t, in MW;
ε_t is the net convertible energy available in t, in MWh.

As κ_t is determined by the availability of the wind turbines, this stochastic variable depends on the O&M of the wind park. Even though the incentive perceived by the owner at a given time period depends solely on the production in that same period, the decision process that this incentive influences is not *decoupled* in time. This will become clear in Sect. 5.1, when the dependence of κ_t on the history of maintenance actions is presented.

Equation (1) merely states that the performance incentive is a function of the time-dependent stochastic variables κ_t and ε_t, but it does not specify the functional form. Considering that the performance incentives of interest are monetary quantities, a possible functional form for the performance incentive is:

$$\eta_t = \min(\kappa_t \cdot d_t, \varepsilon_t) \cdot \pi = \gamma_t \cdot \pi \tag{2}$$

where

γ_t is the output of the wind park in t, in MWh;
d_t is the duration of t, in hours;
π is a constant, in \$/MWh.

In (2) and the remainder of this chapter, we assume that κ_t is constant during period t.

In some jurisdictions, performance incentives are dependent not only on the current output of a wind park, but also on its production within a limited window in the past. In this case, the incentive can be generally defined as:

$$\eta_t = \eta_t(\{(\kappa_h, \varepsilon_h) | h \in [t - H, t]\}) \tag{3}$$

where

h is an index for the time period;
H is the number of past time periods considered for the calculation of the incentive;
$[t - H, t]$ is the compact notation employed for the set $\{t - H, \ldots, t - 1, t\}$.

The purpose of including historic data for the calculation of the incentive is to make the current remuneration dependent on a statistic of the historic production of the wind park—commonly, the sample average. Usually, the sample statistic is employed as an approximation of the output which the park can reliably supply (the exact definition of the term *reliably* varies according to the jurisdiction and certainly affects the choice of the sample statistic to be used).

We now provide examples of mechanisms that may be characterized as PIENs, considering either only the plant's current production or some set of historic measurements.

Feed-in tariffs:

Feed-in tariffs (FIT) are equivalent to long-term purchase agreements in which the entire production of a project is remunerated at a price that is either fixed or that varies slowly according to a pre-defined profile. An owner whose remuneration depends solely on the park's current production and on the fixed FIT experiences a PIEN analogous to Eq. (1). The ideal scenario for the owner is that all turbines are available at all times. However, full availability is not generally possible, because facilities must be taken out of service for preventive maintenance and random failures may occur. When subject to PIENs, the wind park owner will seek to ensure that the facilities are *operable* when the maximum amount of primary energy resources is available—for instance, by ensuring that preventive maintenance actions are scheduled for times of low wind speeds.

Long-term imbalances settlement for Reserve Energy Auctions (REA) in Brazil:

An example of a PIEN based on both current and historic production is the mechanism employed for the settlement of long-term imbalances for winners of reserve energy auctions (REA) in Brazil. These are pay-as-bid, technology-specific auctions, in which participants compete for long-term *reserve energy contracts*. These contracts specify a *reference energy quantity* to be delivered yearly at a fixed price. Each participant in the REA bids a price and an energy quantity, and the auction winners are those with the lowest price bids, stacked up until the auction demand is met [4].

Presently, capacity constraints are not as significant for the Brazilian security of supply as energy constraints. This justifies the fact that reserve energy contracts establish performance incentives that are calculated based on the historical production averaged over long time intervals. Simply put, the performance incentives correspond to imbalance settlement mechanisms in which surpluses and deficits of

actual yearly generation with respect to the *reference energy quantity* are valued at prices that correspond to pre-defined percentages of the fixed contract price. Deficits are penalized at more than 100 %, and surpluses are valued at less than 100 %, of the contract price.

II. *Performance incentives based on energy output and prices (PIEP)*:

The time-dependent arguments of the function that describes the second category of performance incentives include not only the output of the wind park, but also the price at which this output is valued. Again, incentives may depend solely on the current value of these variables, or also on historical data. Incentives that depend solely on current values may be described by:

$$\eta_t = \eta_t(\kappa_t, \varepsilon_t, \pi_t) \tag{4}$$

where
π_t is the price at which the output of the wind park is valued in t, in \$/MWh.

Assuming that the wind generator is a price taker, π_t is a stochastic parameter from the owner's standpoint. Though we refer to π_t simply as a price, it is more properly described as the equivalent multiplicative coefficient for calculating the revenue associated with the production of the wind park; e.g., it may be simply the spot price, or a compound of the day-ahead price and the price of the short-term imbalances settling mechanism. A possible exact form for the performance incentive is:

$$\eta_t = \min(\kappa_t \cdot d_t, \varepsilon_t) \cdot \pi_t = \gamma_t \cdot \pi_t \tag{5}$$

As long as the variation of π_t in time reflects the marginal value of the output of the wind park to the power system, there is a conceptual advantage, from a systemic viewpoint, in employing a PIEP instead of a PIEN. Under both mechanisms, a rational owner will seek to manage his resources in order to ensure that the conversion facilities are available when the most revenue can be captured. Under a PIEN, this is when the wind is blowing stronger, because prices are constant. Under a PIEP, this may be in times of comparatively weaker winds but higher prices, when the marginal value of the output of the wind park has greater value for the system.

We now consider the situation in which the remuneration of the owner in period t depends on the actual output of the park and the time-dependent price in this same period, but the possible choices of actions of the owner in period t are somehow limited by a statistic of the historic production data. A general form for such performance incentives is:

$$\eta_t = \eta_t(\pi_t, \{(\kappa_h, \varepsilon_h) | h \in [t - H, t]\}) \tag{6}$$

The limitation of the range of actions eligible by the owner in period t will typically refer to the choice of markets to which the output of the park can be committed, thus indirectly dictating the value of π_t perceived by the owner.

In the following, we provide examples of mechanisms that are either characterized as PIEPs or that are generally used in conjunction with PIEPs.

Participation in energy markets:

The obvious example of a PIEP is the revenue arising from the participation of wind generators in spot markets, as the production of the plant is valued at a price that closely fits the description of π_t and the revenue in period t is well described by (5).

The participation of wind parks in forward markets also results in incentives that may be categorized as PIEPs. However, the form of the performance incentive associated with the participation in forward markets is more complex than (5). As forward markets involve some kind of imbalance settlement mechanism, the incentive of the owner to maintain the facility available at period t is properly described as a function of both the forward price and the price employed for settling imbalances. Furthermore, the imbalance depends on the actual production at period t and on the quantity sold before gate closure. Thus, a possible format for the performance incentive associated with the participation in forward markets is:

$$\eta_t = \acute{\gamma}_t \cdot \acute{\pi}_t - \max\left[\acute{\gamma}_t - \min(\kappa_t \cdot d_t, \varepsilon_t), 0\right] \cdot \pi_t + \max\left[\min(\kappa_t \cdot d_t, \varepsilon_t) - \acute{\gamma}_t, 0\right] \cdot l \cdot \pi_t \tag{7}$$

where

$\acute{\gamma}_t$ is the energy sold at the forward market, in MWh;
$\acute{\pi}_t$ is the forward price for t, in \$;
π_t is, in Eq. (7), the settlement price for negative imbalances in t, in \$/MWh;
$l \cdot \pi_t$ is the settlement price for positive imbalances in t, in \$/MWh.

Several markets [1] employ an asymmetric procedure for imbalance settlement, in which negative imbalances are valued at higher prices than positive ones. This is the reason for the parameter l in Eq. (7).

The complexity of Eq. (7), compared with (4), follows from a characteristic shared by all general functional forms of performance incentives presented in this chapter: they provide the reader only with a description of the main functional dependences. Actual incentives may be more complex than suggested by the general functional forms presented in this section. However, we expect that the reader will generally be able either to assign any actual incentive to one of the categories presented here or to represent it as a combination of categories.

Feed-in premiums (FIP):

A FIP consists of a fixed premium, in \$/MWh, that is added to the market price. These mechanisms are usually associated with a cap on the equivalent selling price resulting from the sum of the market price and the premium. Assuming, for simplicity, that the owner sells the park's output in the spot market, whose price is π_t, the performance incentive perceived under a FIP mechanism is given by:

$$\eta_t = \min(\kappa_t \cdot d_t, \varepsilon_t) \cdot \min(\pi_t + \text{FIP}, \overline{\pi}) = \gamma_t \cdot \pi'_t \tag{8}$$

where
$\overline{\pi}$ is the cap for the sum of the market price and the FIP, in \$/MWh.

Depending on the values of the FIP and of $\overline{\pi}$, the pattern of variation of the equivalent capped price π_t' may differ significantly from the behavior of π_t, losing resemblance to the marginal value of the output of the wind park for the operation of the power system.

Tax credits:

Some policies for fostering the development of renewable energy include introducing tax credits equal to a fixed monetary amount awarded per MWh generated—e.g., the North American Renewable Electricity Production Tax Credit [7]. The value of the tax credit does not vary in time (at least not with a periodicity that affects short- and medium-term decisions on O&M). Hence, they consist basically of a fixed premium over the market price. However, we make reference to tax credits at this point because they never consist of the sole mechanism through which the wind park owner is remunerated; i.e., they are used in combination with other remuneration mechanisms, often sales in the short-term market. Hence, tax credits are similar to FIP. The difference between these mechanisms is that caps are usually not imposed on the sum of the market price and the tax credit.

Participation of wind power in PJM's Reliability Pricing Model:

This is an example of a performance incentive whose definition is consistent with Eq. (6). The reliability pricing model (RPM), implemented by PJM in 2007, consists of the main element in its forward capacity market. The RPM consists of a sequence of auctions for the procurement of capacity, which are carried out on a yearly basis. The first auction takes place three years before the delivery year and is called the Base Residual Auction. The auction results in a capacity clearing price, in \$/(MW·day), which determines the daily remuneration of the procured capacity in the delivery year. This remuneration is complementary to that achieved by participation in other markets [13].

Our discussion focuses exclusively on the participation of existing wind parks in the RPM—particularly, plants that exist for at least 3 years. The capacity value that can be bid by these plants in the RPM is bounded by the product of the plant maximum capacity by the average capacity factor verified during the summer peak hours of the 3 years that immediately precede the auction.

This rule results in a performance incentive of the form of Eq. (6). Maintaining the availability of the energy conversion facilities during the time window considered for the calculation of the average capacity factor during summer peak hours is relevant for determining the capacity value that can be bid into the RPM. This ultimately determines the potential revenue captured by wind power plants via capacity payments, which complement the revenue obtained by participation in energy markets.

4 An Overview of O&M Contracts for Wind Turbines

The recent growth in the market for O&M services was accompanied by a diversification of the contractual options available for wind park owners. Contracts may differ with respect to the allocation of costs, revenues, and risks among the parties. We now present the basic elements of contracts for *post-warranty O&M*; i.e., O&M services provided after the termination of the original equipment warranty provided by the turbine manufacturer.

I. *Scope of services*:

The scope of services provided by the O&M contractor includes the activities listed in Sect. 2. While many activities listed in Sect. 2, notably those related to preventive and corrective maintenance, are usually considered *standard services*, which are continuously supplied by the contractor and covered by the basic remuneration mechanism specified in the contract, other tasks may be categorized as *additional services*, whose execution is subject to individual quotations and separate payment mechanisms.

II. *Payment*:

A common option for the remuneration of the O&M contractor is the association of a base fee, fixed except for indexing, and a variable payment for the execution of additional services, subject to event-based quotations. These are typically combined with performance incentives (described in III below).

The fixed fee is usually paid in advance by the wind park owner, in periodic installments. The contract may establish a specific condition for the payment schedule, e.g., lower payments in the first contract years. The payment for additional services is calculated individually for each event. Contracts may either specify pricing parameters for these services (prices for replacement parts, labor fees) or establish that the prevailing prices of the O&M contractor are used for calculating them [12].

The choice of which services are covered by the base fee and which are subject to individual quotation may vary among contracts. A single O&M supplier may offer different contractual options, ranging from those resembling time-and-materials contracts, in which virtually every maintenance service is quoted individually, to those resembling all-inclusive contracts, in which virtually all activities, with the exception of those relating to the *exceptional events* listed in IV below, are covered by the base fee.

III. *Performance incentives for O&M contractors*:

The expression *performance incentives* is used here in reference to all mechanisms that make the profit of the O&M contractor conditional on the actual costs of the O&M activities and on the availability of the wind turbines.

Note that O&M contracts in which both preventive and corrective maintenance are remunerated via a fixed base fee, in contrast to time-and-materials contracts, provide the contractor with implicit incentives not only to be efficient in the

execution of services, but also to balance preventive and corrective maintenance costs in an optimal way. The costs of corrective maintenance tend to be substantial, especially when replacement of failed equipment is required. Contractors will thus seek to reduce the frequency of failures that lead to these costs by carrying out preventive maintenance and servicing actions. This generally contributes to the availability of the turbines, because the downtime associated with corrective maintenance following equipment failure is typically longer than the downtime required for most servicing and preventive maintenance actions.

Yet, owners do not have to rely solely on the implicit incentive mechanism described above: O&M contracts usually include explicit performance incentives for contractors. In the following, we discuss the most common of these explicit incentive mechanisms, grouping them in three categories: *performance guarantees*, *upsides sharing,* and *production-based pricing*. Presently, *performance guarantees* are the most commonly used incentives, and mechanisms of the two latter categories are frequently employed in combination with them.

Performance guarantees:

Performance guarantees consist of minimum performance thresholds that, if not met, entitle the owner to a compensation for *liquidated damages*, paid by the contractor. The monetary amount of liquidated damages is calculated according to contractual provisions. In many jurisdictions, it is a legal requirement that the rules for calculating liquidated damages lead to values commensurate with the monetary losses incurred by the owner; i.e., liquidated damages should function primarily as compensation for losses, rather than as penalties for the contractor.

Performance guarantees commonly found in O&M contracts can be categorized either as *minimum availability thresholds* or as *minimum energy conversion ratio thresholds*:

- A *minimum availability threshold* consists of a minimum value for the equivalent available conversion capacity within a given measurement interval, usually expressed in percentage of the nominal value, which is guaranteed either for each turbine separately or for the whole set of turbines in the park.
- A *minimum energy conversion ratio threshold*, often termed *minimum energy-based availability*, consists of a minimum level for the ratio of the energy effectively generated and the total amount of energy that could have been generated within a given measurement interval, which is guaranteed either for each wind turbine separately or for the whole set of turbines in the park. The denominator of this ratio is calculated according to a procedure specified in the contract, for which the inputs usually are measured wind data and reference conversion efficiencies.

Annual or semiannual measurement periods are commonly used for the calculation of the actual availability and energy conversion ratios, which are benchmarked against the minimum thresholds mentioned above.

Contracts usually contain a list of *exceptional events* that, if resulting in turbine unavailability, are not considered for the calculation of the actual availability

or energy conversion ratios. The assets are deemed available during the downtime associated with these events, and contractual provisions specify if calculations are made under assumption of full availability or if historical levels of availability are considered for hours of deemed availability. Examples of exceptional events are provided in IV below.

The total volume of liquidated damages for which the O&M supplier is responsible is capped at a value defined in the contract. This cap is usually defined as a percentage of the total remuneration corresponding to the fixed base fee due to the contractor within a given period. The *cap on liquidated damages* associated with performance incentives is typically defined separately from cap for the aggregate liability of the O&M contractor, though the latter usually indirectly constrains the former.

Considering the above, performance incentives based on *minimum availability thresholds* can be generally defined as:

$$\iota_t = \iota_t\left(\{\kappa_h | h \in [t-H, t-1]\}, q, \underline{A}, \bar{\mathrm{I}}, T_{\mathrm{msr}}\right) \tag{9}$$

where

ι_t is the performance incentive perceived by the contractor in t, in \$;
H is the number of past periods considered for calculating the historical availability;
$\underline{A}$ is the minimum availability threshold, in *per unit*;
$\bar{\mathrm{I}}$ is the cap on liquidated damages, in \$;
T_{msr} is the set of periods at which the historical availability is measured and at which liquidated damages are paid;
q is the coefficient for calculating the liquidated damages, in \$.

Equation (9) indicates the most relevant functional dependences of the performance incentive, but offers little insight on the actual procedure for its calculation. Though the exact expression for calculating ι_t varies from contract to contract, a possible definition is:

$$\iota_t = \begin{cases} \max\left\{-q \cdot \max\left\{\left[\underline{A} - \sum_{h=t-H}^{t-1} \kappa_h \cdot d_t \big/ \kappa^{\mathrm{nom}} \cdot d_t\right], 0\right\}, -\bar{\mathrm{I}}\right\}, & t \in T_{\mathrm{msr}} \\ 0, & t \notin T_{\mathrm{msr}} \end{cases} \tag{10}$$

where

κ^{nom} is the wind park nominal conversion capacity, in MW.

Analogously, performance incentives based on *minimum energy conversion ratio thresholds* may be defined as:

$$\iota_t = \iota_t\left(\{(\kappa_h, \varepsilon_h) | h \in [t-H,\ t-1]\}, q, \underline{\mathrm{ECR}}, \bar{\mathrm{I}}, T_{\mathrm{msr}}\right) \tag{11}$$

where

$\underline{\mathrm{ECR}}$ is the minimum availability threshold, in *per unit.*

And an example of the exact expression for calculating the incentive is:

$$\iota_t = \begin{cases} \max\left\{-q \cdot \max\left\{\left[\underline{\mathrm{ECR}} - \sum_{h=t-H}^{t-1} \kappa_h \cdot \varepsilon_h \cdot d_t \Big/ \sum_{h=t-H}^{t-1} \kappa^{\mathrm{nom}} \cdot \varepsilon_h \cdot d_t\right], 0\right\}, -\bar{\mathrm{I}}\right\}, & t \in T_{\mathrm{msr}} \\ 0, & t \notin T_{\mathrm{msr}} \end{cases} \tag{12}$$

The incentives described by (9) and (11) are necessarily non-positive.

Upsides sharing:

While performance guarantees translate into *negative* incentives for the O&M contractor, upsides sharing mechanisms result in *positive* ones.

A possible design for an upside sharing mechanism consists in defining a *reference threshold* either for the availability or for the energy conversion ratio of a wind plant, and establishing an additional, variable component of the contractor's remuneration that is conditioned to the measured availability or energy conversion ratio being above the reference threshold. The additional remuneration will be typically proportional to the positive difference between the verified availability or energy conversion ratio and the reference threshold.

The mechanism described in the previous paragraph is conceptually symmetric to the negative incentives associated with performance guarantees. However, the symmetry is typically not mathematically perfect, mainly due to two factors. First, the *reference threshold* for upsides sharing is usually higher than the *minimum threshold* for performance guarantees. Second, while liquidated damages are usually calculated in such a way to make their value commensurate with an estimate of the losses incurred due to *below-the-minimum availability,* the rules for calculating the additional remuneration due to *above-the-reference availability* result in values corresponding to a small part of the additional gains captured by the owner. This is consistent with the notion of *sharing* the upsides of an above-the-reference availability between owner and contractor.

Upsides sharing mechanisms can also be implemented by defining a reference threshold for the operating revenues of the project, and indicating a proportion of the positive difference between the actual operating revenues and the reference threshold to which the O&M contractor is entitled. This mechanism can be represented in general terms as:

$$\iota_t = \iota_t\left(\{\eta_h | h \in [t-H, t-1]\}, g, \overline{\mathrm{OR}}, T_{\mathrm{msr}}\right) \tag{13}$$

where

$\underline{g}$ is a multiplicative factor (with $g < 1$), in *per unit*;
$\overline{\mathrm{OR}}$ is the reference threshold for operating revenues, in $.

We assume that the operating revenues of the owner coincide exactly with the performance incentives η_t defined in Sect. 3, for simplicity. An example of the exact expression for calculating the performance incentive is:

$$\iota_t = \begin{cases} g \cdot \max\left\{\left[\left(\sum_{h=t-H}^{t-1} \eta_h\right) - \overline{\mathrm{OR}}\right], 0\right\}, & t \in T_{\mathrm{msr}} \\ 0, & t \notin T_{\mathrm{msr}} \end{cases} \tag{14}$$

The definition of reference thresholds for upside sharing mechanisms depends on project-specific variables and on economic interests of the involved parties.

Production-based pricing:

This third class includes incentive mechanisms based on defining the remuneration of the O&M supplier as the product of a rate (in $/MWh) multiplied by the actual energy produced (MWh) within a measurement period. The O&M contractor still receives the fixed base fee, but this is now augmented by the production-based remuneration.

$$\iota_t = \iota_t(\kappa_t, \varepsilon_t, e) = \min(\kappa_t \cdot d_t, \varepsilon_t) \cdot e \tag{15}$$

where
e is the rate at which the production is valued, in $/MWh.

For the definition of (15), we neglect the fact that the remuneration of the contractor only occurs at specific time periods $t \in T_{msr}$. This highlights a fundamental difference between this mechanism and previous ones. For the previous performance incentives, a quantity depending on the availability of the facilities is either accumulated or averaged over a time interval and then compared to a threshold. For this latter incentive mechanism, the quantity depending on the availability is also accumulated over an interval. However, no comparison to a pre-defined threshold is required to determinate the monetary value of the incentive, and thus the accumulation over time has the sole effect of delaying the collection of revenues.

The rate at which the production is valued is typically fixed *ex ante* in the O&M contract and may be changed only under special conditions; e.g., when factors outside the control of the contractor and not predictable when the contract was signed, such as the construction of structures adjacent to the wind park, fundamentally affect the expectancy of the average energy production of the park in the long term.

Contrary to the incentive mechanisms discussed previously, production-based pricing results in essentially symmetric negative and positive performance incentives for O&M contractors. Also, production-based pricing mechanisms result not only in changes in the allocation of operational risk due to equipment failure and unavailability, but also in the reallocation of the risk associated to medium-term variability in wind speeds. Some argue that the primary value of this mechanism for owners is indeed associated with the reallocation of the latter risk factor, with owners specially appreciating the smoothing effect of the variable O&M expenditures on profits, as costs decrease in periods of low production and vice versa. Naturally, the rate in $/MWh paid to the O&M contractor is considerably lower than the energy price captured by the wind park owner.

IV. *Exceptional events*:

O&M contracts typically contain a list of events that are treated as *exceptions*, such that their occurrence relieves the contractor either from the obligation to perform specific services or from the applicability of negative performance incentives. This list typically comprises *force majeure* events, including natural

catastrophes and vandalism; interference of third parties (including other service suppliers) with the facilities; events related to failures originated at the electrical network to which the wind park is connected; and impossibility of carrying out services due to severe environmental conditions.

V. *Contract term and termination*:

O&M contractors may offer owners various options regarding the term of the contract. Currently, most offers refer to initial contracts that extend from 5 to 10 years, with the possibility of subsequent renewals, subject to renegotiation.

In case project financing is employed for a wind park, the owner's choice of the contract term may be constrained by requests imposed by the financing institution, which may seek to ensure either that the term of O&M contract is at least as long as the loan amortization period or that the possibility of contract renewal is explicitly mentioned in the contract.

The conditions for the termination of the O&M contract prior to the expiration of the contract term do not typically differ significantly from those found in other industries, and include *force majeure* events and major unilateral defaults. The owner may be allowed to terminate the contract for his convenience, provided that certain conditions, including remuneration of the contractor for expected loss of future profits, are met.

5 Assessing O&M Contracts: Static Contractual Relationship

We present basic notions of decision-making in planning of O&M services in Sect. 5.1. These basic notions are required for the introduction of a mathematical framework for assessing O&M contracts in Sect. 5.2.

5.1 Planning the Operation and Maintenance of Wind Turbines

Decision-making for O&M of wind parks involves a hierarchy of problems, which starts at system design and goes as far as short-term scheduling of maintenance actions. Here, we focus on contracts for post-warranty O&M services. Therefore, we do not discuss decisions required at initial phases of project development, such as those made by project developers when designing the wind park. Rather, we consider decisions regarding O&M actions executed after the wind park starts operation.

These may be grouped into two classes: *strategic* and *operational* decisions. Strategic decisions are those that can and should be planned in advance, may require considerable time or significant capital expenditures to be implemented, and constrain the choice of short-term decisions. Strategic decisions result from

an analysis of the fundamental uncertainties that govern the operations of the wind farm. They refer to the development of maintenance capacity (with respect to workforce, infrastructure, technology, and stocks levels of spares and consumables), determination of maintenance protocols (specification of which actions shall be executed to which assets under which conditions, either with certain regularity or when specific events, including major equipment failures, occur) and scheduling of extraordinary, yet predictable, actions (those of major costs and significant lead times). Operational decisions are those related to the actual implementation of strategic decisions. Hence, they are constrained by maintenance protocols. Operational decisions include short-term scheduling and implementation of preventive maintenance and servicing actions, real-time management of stock of spare parts and consumables, and the execution of corrective maintenance actions.

We now develop a mathematical framework for decision-making in O&M planning. We first introduce the notion of the *condition* of component i of wind turbine r at a given time period t, $\varphi_{i,r,t}$. The physical properties relevant for determining the condition differ among the components of a wind turbine. Nevertheless, there are monitoring and inspection techniques that allow at least partially observing the condition of a number of components; e.g., acoustic emission measurements for bearings and gearboxes, and oil and debris analysis for bearings. The relevant features of the *condition* of a given component, for the purposes of this chapter, are that:

- The value of both the failure rate function and the repair rate function[3] for any given component at any given time period is a function of its physical condition at that period. These rates also depend on variables other than the condition of the equipment.
- The condition of a given component varies in time, due to deterioration with aging, to the history of physical stressing due to operating conditions, and to the history of maintenance actions to which the equipment was subject.

The former considerations may be summarized in the following mathematical model[4]:

$$\lambda_{i,r,t} = \lambda_{i,r,t}\left(\varphi_{i,r,t}, \omega_{i,r,t}\right), \quad \forall\, i \in I_r, r \in R, t \in T \tag{16}$$

$$\mu_{i,r,t} = \mu_{i,r,t}\left(\varphi_{i,r,t}, \omega_{i,r,t}\right), \quad \forall\, i \in I_r, r \in R, t \in T \tag{17}$$

$$\varphi_{i,r,t} = \varphi_{i,r,t}\left(\varphi_{i,r,t-1}, \delta_{i,r,t-1}, \nu_{i,r,t}\right), \quad \forall\, i \in I_r, r \in R, t \in T \tag{18}$$

where

i is an index for the component;
r is an index for the wind turbine;
I_r is the set of components of r;

[3] The reader is assumed to be familiar with basic concepts of reliability engineering. See [2].

[4] To avoid notational complexity, we suppress the dependence of $\varphi_{i,r,t}$ on the history of component operation, which may result in physical stressing of components.

R is the set of turbines in the wind park;
T is the set of all time periods in the planning horizon;
$\varphi_{i,r,t}$ is the physical condition of $\{i, r\}$ at the beginning of t;
$\lambda_{i,r,t}$ is the value of the failure rate function of $\{i, r\}$ at the beginning of t, in *per unit*;
$\mu_{i,r,t}$ is the value of the repair rate function of $\{i, r\}$ at the beginning of t, in *per unit*;
$\delta_{i,r,t}$ indicates the operational decisions referring to actions executed to $\{i, r\}$ during t;
$v_{i,r,}$t is an exogenous random parameter that affects the evolution of the condition of {i, r} from the beginning of period t − 1 to the beginning of period t;
ωi,r,t is an exogenous random parameter that affects the failure and repair rate functions of $\{i, r\}$ within period t.

The model of condition deterioration corresponding to Eq. (18) indicates that, given the condition of the component at the beginning of period $t - 1$, its condition at the beginning of period t depends both on the O&M actions executed in period $t - 1$, $\delta_{i,r,t\text{-}1}$, and on an exogenous, stochastic parameter, $v_{i,r,t}$. Thus, the evolution of component condition is governed by a dynamic stochastic model. In order to provide the reader with insight on the role of $v_{i,r,t}$, we may consider concrete examples. An electrical failure leading to a converter malfunction in the course of a given time period $t - 1$ may lead to stressing of the mechanical drive train and ultimately result in deterioration, resulting in the component being in a worse condition at the beginning of t. The probability of failure would be higher for a drive train in a worse condition. Also, severe structural loading due to wind turbulence during period $t - 1$ may result in deterioration of the condition of blades from the beginning of $t - 1$ to the beginning of t. These examples suggest that the mathematical modeling of the random variable $v_{i,r,t}$ is rather complex, not only due to the underlying physical nature of the phenomena causing deterioration, but also due to the possible correlation with other random parameters in the problem; e.g., wind speeds relate not only to structural loading that can cause condition deterioration, but also to the net convertible wind energy available at a given time period t, ε_t. The mechanism through which O&M actions result in improvement of equipment condition is typically straightforward; e.g., greasing is done in order to improve the condition of the main bearing.[5]

We now discuss the model for $\lambda_{i,r,t}$ and $\mu_{i,r,t}$ in Eqs. (16)–(17). These functions depend not only on the equipment condition at the beginning of the time period, but also on the exogenous random parameter $\omega_{i,r,t}$. This parameter allows the modeling of environmental conditions that affect failure rates (for instance due to lightning activity that may affect the electronics of the turbine control system) and/or repair rates (for instance due to the feasibility of physical access to the asset).

We direct the reader's attention to an important assumption of the model presented above. Equation (16) indicates that the value of the failure and repair rate functions can be satisfactorily estimated without requiring any past information *once* the information on the asset condition at the beginning of t is known. That is, if $\varphi_{i,r,t}$ were directly and perfectly observable (it generally is not, because monitoring

[5] However, it should be noted that procedural errors or latent failures in replaced parts may result in deterioration of the condition of a given component (and thus an increase in the failure rate) as a result of maintenance and servicing actions.

and inspection routines only provide incomplete information on $\varphi_{i,r,t}$), the value of the failure and repair rate functions could be satisfactorily estimated without requiring any past information. This assumption allows the construction of models of the effects of maintenance on stochastic failure and repair processes that are particularly suitable for use in optimization problems—see, for instance [8] and [9].

It should be clear, however, that even under this model, the failure and repair rate functions implicitly depend on the history of both O&M decisions and on the realization of exogenous stochastic parameters. This can be easily seen when (18) is rewritten as:

$$\varphi_{i,r,t} = \varphi_{i,r,t}\left(\varphi_{i,r,t^1}, \delta_{i,r,[t^1+1,t-1]}, \nu_{i,r,[t^1+1,t]}\right), \quad \forall\, i \in I_r, r \in R, t \in T \tag{19}$$

where

t^1 is the first time period of the horizon for planning O&M services[6];
$[t, t']$ is the compact notation employed for the set $\{t, t+1, \ldots, t'-1, t'\}$.

Note that the possibility of observing $\varphi_{i,r,t}$ depends on O&M decisions. The decisions to install condition monitoring systems and build up technical capability through workforce training to be able to implement *condition-based maintenance* are *strategic*, whereas the decisions to execute inspection routines are *operational* in nature. If the direct observation of $\varphi_{i,r,t}$ for a specific component via condition monitoring and inspection is not carried out, the entity executing O&M will either determine maintenance protocols that are implicitly based on its a priori belief on $\varphi_{i,r,t}$ (such as *periodic maintenance* routines based on recommendations of the manufacturer), or simply employ a *run-to-failure* maintenance scheme for a given component.

We now develop the model of availability of turbines. Recall that $\lambda_{i,r,t.}$ and $\mu_{i,r,t}$ are random variables in our formulation, because they depend on the realizations of the random parameters $\nu_{i,r,t}$ and $\omega_{i,r,t}$. Yet, even if $\lambda_{i,r,t}$ and $\mu_{i,r,t}$ were known with certainty, it would not be possible to state with certainty whether component i was *failed* or *intact* in t. This is because $\lambda_{i,r,t}$ and $\mu_{i,r,t}$ are parameters that describe the stochastic failure and repair process of component $\{i, r\}$, and the best information that we can derive from them is the *probability* that the component is intact (or failed) at period t:

$$\rho_{i,r,t} = \rho_{i,r,t}\left(\lambda_{i,r,t}, \mu_{i,r,t}\right), \quad \forall\, i \in I_r, r \in R, t \in T \tag{20}$$

where

$\rho_{i,r,t}$ is the probability that component $\{i, r\}$, is intact in t, in *per unit*.

The variable that will be fundamentally important for the model of decision-making in O&M is the *available capacity of wind turbine r in period t*. A given wind turbine may be unavailable due to failure and subsequent non-scheduled maintenance, but also due to the execution of scheduled preventive maintenance

[6] In (19), the variable indicating operational decisions is indexed by $\left[t^1+1, t-1\right]$ and not by $\left[t^1, t-1\right]$, because we assume that no operational decisions are taken at period 1. As we discuss below, no maintenance protocols are available before t^1, preventing any operational decisions to be taken.

or servicing routines. Hence, even if a component is *intact* in period t, it does not mean that it is *operable*, as the plant may be shut down for the execution of scheduled O&M actions. Therefore, we employ the following model:

$$\kappa_{r,t} = \kappa_{r,t}\left(\left\{\left(\rho_{i,r,t}, \delta_{i,r,t}, \theta_{i,r,t}\right) | i \in I_r\right\}\right), \quad \forall\, r \in R, t \in T \tag{21}$$

$$\kappa_{r,t} = \kappa_{r,t}\left(\left\{\left(\lambda_{i,r,t}, \mu_{i,r,t}, \delta_{i,r,t}, \theta_{i,r,t}\right) | i \in I_r\right\}\right), \quad \forall\, r \in R, t \in T \tag{22}$$

where

$\theta_{i,r,t}$ is a random parameter, uniformly distributed in [0, 1], that indicates if $\{i, r\}$ is intact or failed in period t;

$\kappa_{r,t}$ is the available capacity of turbine r in period t, in MWh.

Equation (22) differs from Eq. (21) because the dependence of $\kappa_{r,t}$ on $\lambda_{i,r,t}$ and $\mu_{i,r,t}$ has been indicated directly in (22), which follows from $\lambda_{i,r,t}$ and $\mu_{i,r,t}$ being the sole parameters of $\rho_{i,r,t}$ in (20).

Note that component $\{i, r\}$ is intact at period t if $\theta_{i,r,t} \leq \rho_{i,r,t}$, and failed otherwise. We assume that all physical phenomena relevant for the determination of the failure process are modeled either through the endogenous variable $\varphi_{i,r,t}$ (which in turn depends on the exogenous parameter $\nu_{i,r,t}$) or by the exogenous parameter $\omega_{i,r,t}$. Thus, all relevant physical phenomena that may result in changes in the probabilities of a component being *intact* or *failed* are already captured by $\rho_{i,r,t}$. Hence, to determine whether the component will actually be intact or failed in a realization of the time period t, it suffices to sample a number from a uniform distribution between [0, 1] and compare it to $\rho_{i,r,t}$.

Finally, it is necessary to consider that the wind park available capacity in period t depends on the maximum energy conversion capacity of each turbine r:

$$\kappa_t = \kappa_t\left(\left\{\kappa_{r,t} | r \in R\right\}\right), \quad \forall\, t \in T \tag{23}$$

We now proceed to the mathematical formulation of the decision problem faced by the entity responsible for carrying out O&M of the wind park. In Sect. 5.1, we assume that the owner is the entity responsible for O&M. In Sect. 5.2, we consider the situation in which O&M is the responsibility of the contractor.

We recall the distinction between strategic and operational decisions made at the beginning of this section, and note that all O&M decisions that appeared in the equations of this section to this point are operational. These are the decisions that result in the actual execution of O&M actions. Strategic decisions, not yet considered in the equations of this section, relate to the development of maintenance capacity, determination of protocols (rules that will determine operational decisions), and general scheduling of extraordinary O&M actions (whose execution will also correspond to an operational decision).

We now consider the relationship between strategic and operational decisions. For that, it is necessary to introduce the notion that decision-making in O&M can be thought as a multistage stochastic programming problem with recourse.[7] Figure 1

[7] The reader is assumed to be familiar with basic concepts of stochastic programming. See, for example [3] and [14].

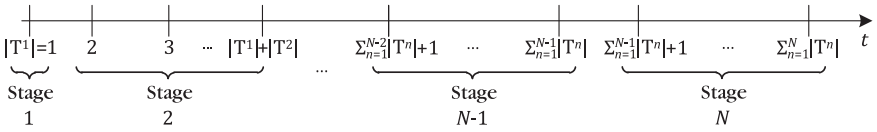

Fig. 1 Relationship between stages and periods in multistage stochastic program

indicates the relationship between stages and time periods for this multistage stochastic program.

From Fig. 1, it is clear that one stage may comprise several time periods. We denote the set of sequential time periods associated with each stage n by T^n. Notice that $\bigcup_{n=1}^{N} T^n = T$. We will denote the last period of each stage n by t^n. In our formulation, a stage is a time interval at the end of which *strategic* decisions are made and implemented, and the strategic decisions made at the end of each stage constrain the operational decisions made at each time period of the following stage. Naturally, considering that strategic decisions are made and implemented precisely at the end of each stage is a simplifying assumption. We consider that the first stage is prior to any operational O&M decisions and therefore any O&M actions, because maintenance capacity and protocols will only be developed as a result of the strategic decisions made at this first stage.

Operational decisions are made at each time period of each stage (except the first one). We consider that strategic decisions result in rules for the execution of short-term maintenance actions that determine exactly which operational decisions will be made under every possible realization of the stochastic parameters of the problem. That is to say, operational decisions are completely determined by strategic decisions and the realizations of stochastic variables, and the implementation of O&M never diverges from the strategic rules. This requires that the rules arising from strategic decisions are exhaustive, indicating the actions to be taken in the event of every possible realization of the uncertain parameters.[8] We can thus write:

$$\boldsymbol{\delta}_t = \boldsymbol{\delta}_t\left(\boldsymbol{\varphi}_t, \boldsymbol{\chi}^{n-1}, \boldsymbol{\xi}_t\right), \quad \forall\, t \in T^n \tag{24}$$

where

- n is an index for the stage;
- T^n is the set of all time periods that form n;
- $\boldsymbol{\chi}^n$ is the vector with all *strategic decisions* made at the end of n;
- $\boldsymbol{\delta}_t$ is the vector with all *operational decisions* referring to actions executed during t;
- $\boldsymbol{\varphi}_t$ is the vector with the physical condition of all components of all turbines in the wind park at the beginning of t;
- $\boldsymbol{\xi}_t$ is the vector with the realization of all relevant random parameters in period t, including $\omega_{i,r,t}$, $\nu_{i,r,t}$ and $\theta_{i,r,t}$ for all components and all turbines in the park.

[8] This simplifying assumption becomes more restrictive as the total duration of a stage in the problem increases.

However, it is clear from Eq. (19) that we have:

$$\boldsymbol{\varphi}_t = \boldsymbol{\varphi}_t\left(\boldsymbol{\varphi}_{t^1}, \boldsymbol{\delta}_{[t^1+1,t-1]}, \boldsymbol{\xi}_{[t^1+1,t]}\right), \quad \forall\, t \in T^n \tag{25}$$

The condition of the assets at the first stage of the planning horizon, $\boldsymbol{\varphi}_{t^1}$, is a vector of known, deterministic variables. Recalling the assumption that the operational decisions $\boldsymbol{\delta}_t$ are completely determined by the strategic decisions of the previous stage and the realization of the stochastic variables, we may write:

$$\boldsymbol{\varphi}_t = \boldsymbol{\varphi}_t\left(\boldsymbol{\varphi}_{t^1}, \boldsymbol{\chi}^{[1,n-1]}, \boldsymbol{\xi}_{[t^1+1,t]}\right), \quad \forall\, t \in T^n \tag{26}$$

where
$[n, n']$ is the compact notation employed for the set $\{n, n+1, \ldots, n'-1, n'\}$.

Considering the functional dependences indicated above to rewrite Eq. (24), we get:

$$\boldsymbol{\delta}_t = \boldsymbol{\delta}_t\left(\boldsymbol{\varphi}_{t^1}, \boldsymbol{\chi}^{[1,n-1]}, \boldsymbol{\xi}_{[t^1+1,t]}\right), \quad \forall\, t \in T^n \tag{27}$$

We now present the expression for the net present value (NPV) of the total profit obtained by the wind park owner during stage n. This is given by:

$$\begin{aligned}\Pi^n = &\left\{\sum_{t \in \mathrm{T}^n} a_t \cdot \left[\eta_t(\boldsymbol{\delta}_t, \boldsymbol{\xi}_t) - \alpha_t(\boldsymbol{\delta}_t, \boldsymbol{\xi}_t)\right]\right\} \\ &- a_{t^n} \cdot \sigma^n\left(\boldsymbol{\chi}^n, \boldsymbol{\varphi}_{t^n}, \boldsymbol{\xi}^n\right), \quad \forall\, n \in \{1 \ldots N\}\end{aligned} \tag{28}$$

where

Π^n is the NPV of the total profit obtained by the owner during n, in \$;
$\boldsymbol{\xi}^n$ is the vector with the realization of all random parameters in all periods of stage n;
a_t is a discount factor for calculating the NPV, in *per unit*;
η_t is the variable component of the revenue received by the owner at t, in \$;
α_t is the cost of implementing the operational decisions at t, in \$;
σ^n is the cost of implementing the strategic decisions made at stage n, in \$.

In (28), we ignore any other fixed or variable costs incurring in stage n that are not related to O&M of the wind park. Also, we consider that the remuneration of the owner has no fixed components and simply equals the performance incentives he receives. It is straightforward to include fixed remuneration components in the above expression, if needed.

Because $\kappa_t = \kappa_t(\boldsymbol{\delta}_t)$, from (21) to (23), $\eta_t(\boldsymbol{\delta}_t, \boldsymbol{\xi}_t)$ corresponds to the performance incentives described in Sect. 3 if the stochastic parameters relevant for the calculation of the performance incentives—for instance, ε_t and π_t—are included in vector $\boldsymbol{\xi}_t$.

Considering that the terms $\eta_t(\boldsymbol{\delta}_t, \boldsymbol{\xi}_t)$ and $\alpha_t(\boldsymbol{\delta}_t, \boldsymbol{\xi}_t)$ are summed over all time periods within stage n in Eq. (28), we may rewrite this equation in a simplified form that emphasizes the dependence on problem variables and parameters:

$$\Pi^n = \Pi^n\left(\boldsymbol{\varphi}_{t^1}, \boldsymbol{\chi}^{[1,n]}, \boldsymbol{\xi}^{[2,n]}\right), \quad \forall\, n \in \{1 \ldots N\} \tag{29}$$

The previous equation emphasizes the dependence of the profits Π^n on the history of O&M actions and on the realization of uncertainties up to stage n.

Naturally, the strategic decisions made at the end of a given stage are influenced by the strategic decisions made at the end of previous stage. Consider, for instance, decisions on the acquisition of lifting equipment: the costs to expand the number of cranes in the possession of the contractor to any given quantity naturally depend on the number of cranes owned in the previous stage. Moreover, it is clear from Eqs. (16)–(17) that the condition of the assets at any given period depends on the realization of the stochastic data process—namely the parameters $\omega_{i,r,t}$, $\nu_{i,r,t}$, and $\theta_{i,r,t}$—up to that period. Therefore, the strategic decisions made at a period at the very end of any given stage will depend on the realization of uncertainties up to that period. Thus, the feasible space for the strategic decisions $\boldsymbol{\chi}^n$ can be represented by the multivalued function $\boldsymbol{X}^n\left(\boldsymbol{\varphi}_{t^1}, \boldsymbol{\chi}^{[1,n-1]}, \boldsymbol{\xi}^{[2,n]}\right)$:

$$\boldsymbol{\chi}^n \in \boldsymbol{X}^n\left(\boldsymbol{\varphi}_{t^1}, \boldsymbol{\chi}^{[1,n-1]}, \boldsymbol{\xi}^{[2,n]}\right), \quad \forall\, n \in \{1 \ldots N\} \tag{30}$$

In order to avoid notational complexity, we will suppress the dependence on the vector of deterministic variables $\boldsymbol{\varphi}_{t^1}$ in the following equations. Considering Eqs. (29)–(30), we may define the objective function of the multistage stochastic program corresponding to the decision-making process of the owner responsible for carrying out O&M:

$$\begin{aligned}\mathcal{P}\left(\grave{\boldsymbol{\chi}}^{[1,N]*}\right) = \max_{\boldsymbol{\chi}^1 \in \boldsymbol{X}^1} -\sigma^1\left(\boldsymbol{\chi}^1\right) + \mathrm{E}_{\boldsymbol{\xi}^2}\Bigg[\max_{\boldsymbol{\chi}^2 \in \boldsymbol{X}^2\left(\boldsymbol{\chi}^1, \boldsymbol{\xi}^2\right)} \Pi^2\left(\boldsymbol{\chi}^{[1,2]}, \boldsymbol{\xi}^2\right) \\ + \mathrm{E}_{\boldsymbol{\xi}^3|\boldsymbol{\xi}^2}\Bigg[\cdots + \mathrm{E}_{\boldsymbol{\xi}^N|\boldsymbol{\xi}^{[2,N-1]}}\Bigg[\max_{\boldsymbol{\chi}^N \in \boldsymbol{X}^N\left(\boldsymbol{\chi}^{[1,N-1]}, \boldsymbol{\xi}^{[2,N]}\right)} \Pi^N\left(\boldsymbol{\chi}^{[1,N]}, \boldsymbol{\xi}^{[2,]}\right)\Bigg]\Bigg]\Bigg]\end{aligned} \tag{31}$$

where

$\grave{\boldsymbol{\chi}}^{[1,N]*}$ is the optimal O&M policy;
$\mathcal{P}\left(\grave{\boldsymbol{\chi}}^{[1,N]}\right)$ is the expected NPV of the profit of the owner under policy $\grave{\boldsymbol{\chi}}^{[1,N]}$;
$\mathrm{E}_{\boldsymbol{\xi}^n|\boldsymbol{\xi}^{[2,n-1]}}$ is the operator that indicates expectation with respect to $\boldsymbol{\xi}^n$ given the realization of the vector of stochastic variables in all previous stages.

We use the grave accent in $\grave{\boldsymbol{\chi}}^{[1,N]}$ to denote that the solution of (31) provides the owner with a *policy* of strategic decisions, also called a *contingent strategy*; i.e., a single set of strategic decisions for stage 1 and a decision rule for the following stages, which associates a single sequence of strategic decisions to each realization of the vector of uncertain parameters up to that point.

Equation (31) corresponds to a nested formulation of the multistage stochastic program. The constraints of this program are implicitly represented by $\boldsymbol{\chi}^n \in \boldsymbol{X}^n\left(\boldsymbol{\chi}^{[1,n-1]}, \boldsymbol{\xi}^{[1,n]}\right)$. The basic constraints correspond to (16)–(18), (22)–(24). Additional constraints that apply to specific problems, such as budget constraints, are also considered to be implicitly represented by $\boldsymbol{\chi}^n \in \boldsymbol{X}^n\left(\boldsymbol{\chi}^{[1,n-1]}, \boldsymbol{\xi}^{[1,n]}\right)$.

Embedded in Eq. (31) is the assumption that, at each stage of the decision problem, the owner carrying out O&M makes strategic decisions in order to maximize the *expected value* of his profits from that point in time on. This corresponds to

the behavior of a *risk-neutral* owner. A more realistic situation is that in which the owner is risk-averse, and his preferences are represented by a concave utility function U. In this case, we rewrite (31) for the more general case:

$$\check{\mathcal{P}}\left(\grave{\boldsymbol{\chi}}^{[1,N]*}\right) = \max_{\boldsymbol{\chi}^1 \in \boldsymbol{X}^1} -\sigma^1\left(\boldsymbol{\chi}^1\right) + \mathrm{CE}_{\boldsymbol{\xi}^2}\left[\max_{\boldsymbol{\chi}^2 \in \boldsymbol{X}^2(\boldsymbol{\chi}^1, \boldsymbol{\xi}^2)} \Pi^2\left(\boldsymbol{\chi}^{[1,2]}, \boldsymbol{\xi}^2\right) + \mathrm{CE}_{\boldsymbol{\xi}^3|\boldsymbol{\xi}^2}\left[\cdots + \mathrm{CE}_{\boldsymbol{\xi}^N|\boldsymbol{\xi}^{[2,N-1]}}\left[\max_{\boldsymbol{\chi}^N \in \boldsymbol{X}^N(\boldsymbol{\chi}^{[1,N-1]}, \boldsymbol{\xi}^{[2,N]})} \Pi^N\left(\boldsymbol{\chi}^{[1,N]}, \boldsymbol{\xi}^{[2,N]}\right)\right]\right]\right] \tag{32}$$

where

$\check{\mathcal{P}}\left(\grave{\boldsymbol{\chi}}^{[1,N]}\right)$ is the risk-adjusted NPV of the profit of the owner under policy $\grave{\boldsymbol{\chi}}^{[1,N]}$;

$\mathrm{CE}_{\boldsymbol{\xi}^n|\boldsymbol{\xi}^{[2,n-1]}}$ is the operator that indicates the certainty equivalent with respect to $\boldsymbol{\xi}^n$ given the realization of the vector of stochastic variables in all previous stages.

The certainty equivalent is the *certain* quantity whose utility equals the expected utility of a random variable. Mathematically, it is defined as:

$$U(\mathrm{CE}[\xi]) = \mathrm{E}[U(\xi)] \tag{33}$$

where

U is the (von Neumann–Morgenstern) utility function;

ξ is a random variable.

For more details on risk-averseness, utility functions, and the certainty equivalent, the reader may refer to [11]. Notice that Eqs. (31) and (32) are identical when the utility function is linear; i.e., for a risk-neutral entity. The general nature of the certainty equivalent will be useful when we consider the definition of similar problems in this chapter.

5.2 *A Mathematical Framework for Decision-Making for the Design of O&M Contracts*

After presenting the benchmark situation in which the owner is responsible for executing O&M, we now proceed to the situation in which this responsibility is allocated to a service provider by means of a contract. We first analyze this situation under the assumption that the parties enter a single static bilateral O&M contract whose term coincides with the operational lifetime of the wind turbines.

The general model of physical phenomena described in Sect. 5.1 and summarized in Eqs. (16)–(18), (22), and (23) also applies when the entity responsible for the execution of the O&M is a contractor. We maintain the assumption that protocols resulting from strategic decisions are exhaustive in defining operational decisions in response to every possible realization of the stochastic parameters, and therefore, the relationship indicated by (24) also still applies.

It is important, however, to understand the differences between the decision-making processes of the O&M contractor and of the wind park owner. We may begin the analysis of these differences by comparing Eq. (28) to the following expression for the profit of the O&M contractor in stage n:

$$\begin{aligned}\Psi^n &= \left\{\sum_{t\in \mathrm{T}^n} b_t \cdot \left[F_t(\boldsymbol{y}) + \iota_t(\boldsymbol{\delta}_t, \boldsymbol{\xi}_t, \boldsymbol{y}) - \beta_t(\boldsymbol{\delta}_t, \boldsymbol{\xi}_t, \boldsymbol{y})\right]\right\} - b_{t^n} \cdot \zeta^n\left(\boldsymbol{\chi}^n, \boldsymbol{\varphi}_{t^n}, \boldsymbol{\xi}^n, \boldsymbol{y}\right) \\ &= \Psi^n\left(\boldsymbol{\chi}^{[1,n]}, \boldsymbol{\xi}^{[2,n]}, \boldsymbol{y}\right), \quad \forall n \in \{1 \ldots N\}\end{aligned} \tag{34}$$

where

Ψ^n is the NPV of the total profit obtained by the contractor during n, in \$;
b_t is a discount factor for calculating the NPV, in *per unit*;
F_t is the fixed component of the revenue received by the contractor at t, in \$;
ι_t is the variable component of the revenue received by the contractor at t, in \$;
β_t is the cost of implementing the operational decisions at t, in \$;
ζ^n is the cost of implementing the strategic decisions made at stage n, in \$;
$\boldsymbol{y}$ is the vector of provisions and parameters of the O&M contract.

In the above expression, we assume that ι_t corresponds to revenues obtained via one of the incentive mechanisms described in Sect. 4—or, correspondingly, to deductions to the base fixed fee in the case of negative performance incentives. Costs of additional services may be captured through β_t or ζ^n, depending on their nature.

In (34), we emphasize that the revenues and costs perceived by the contractor depend on the provisions and parameters of the contract, $\boldsymbol{y}$. We assume that a single set of contractual parameters, defined before the beginning of the planning horizon and thus deterministic, applies for the whole time in which the contractor provides O&M services—an assumption that will be lifted in Sect. 6.

In the following, we present the nested formulation of the multistage stochastic programming problem faced by the contractor planning its activities. The notation is analogous to that previously employed in Sect. 5.1 to represent the decision-making process of the owner responsible for carrying out O&M:

$$\begin{aligned}\check{\mathcal{W}}\left(\grave{\boldsymbol{\chi}}^{[1,N]*}, \boldsymbol{y}\right) &= \max_{\grave{\boldsymbol{\chi}}^{[1,N]}} \check{\mathcal{W}}\left(\grave{\boldsymbol{\chi}}^{[1,N]}, \boldsymbol{y}\right) \\ &= \max_{\boldsymbol{\chi}^1 \in \boldsymbol{X}^1} -\zeta^1\left(\boldsymbol{\chi}^1, \boldsymbol{y}\right) + \mathrm{CE}_{\boldsymbol{\xi}^2}\left[\max_{\boldsymbol{\chi}^2 \in \boldsymbol{X}^2(\boldsymbol{\chi}^1, \boldsymbol{\xi}^2, \boldsymbol{y})} \Psi^2\left(\boldsymbol{\chi}^{[1,2]}, \boldsymbol{\xi}^2, \boldsymbol{y}\right) + \mathrm{CE}_{\boldsymbol{\xi}^3|\boldsymbol{\xi}^2}\left[\cdots\right.\right. \\ &\quad \left.\left. + \mathrm{CE}_{\boldsymbol{\xi}^N|\boldsymbol{\xi}^{[2,N-1]}}\left[\max_{\boldsymbol{\chi}^N \in \boldsymbol{X}^N(\boldsymbol{\chi}^{[1,N-1]}, \boldsymbol{\xi}^{[2,N]}, \boldsymbol{y})} \Psi^N\left(\boldsymbol{\chi}^{[1,N]}, \boldsymbol{\xi}^{[2,N]}, \boldsymbol{y}\right)\right]\right]\right]\end{aligned} \tag{35}$$

where

$\check{\mathcal{W}}\left(\grave{\boldsymbol{\chi}}^{[1,N]}, \boldsymbol{y}\right)$ is the risk-adjusted NPV of the profit of the contractor under policy $\grave{\boldsymbol{\chi}}^{[1,N]}$.

As in Sect. 5.1, all constraints are implicitly represented by

$$\boldsymbol{\chi}^n \in \boldsymbol{X}^n\left(\boldsymbol{\chi}^{[1,n-1]}, \boldsymbol{\xi}^{[2,n]}, \boldsymbol{y}\right).$$

We now approach the problem of the wind park owner.[9] The owner still receives the performance incentives η_t. However, he now does not incur the actual costs of O&M actions. The owner's O&M expenditures now correspond to the remuneration of the contractor. Thus, the NPV of the profit obtained by the owner during stage n is given by:

$$\begin{aligned}\Pi^n &= \left\{\sum_{t\in T^n} a_t \cdot \left[\eta_t(\boldsymbol{\delta}_t, \boldsymbol{\xi}_t) - F_t(\boldsymbol{y}) - \iota_t(\boldsymbol{\delta}_t, \boldsymbol{\xi}_t, \boldsymbol{y})\right]\right\} \\ &= \Pi^n\left(\boldsymbol{\chi}^{[1,n]}, \boldsymbol{\xi}^{[2,n]}, \boldsymbol{y}\right), \quad \forall\, n \in \{1 \ldots N\}\end{aligned} \tag{36}$$

Clearly, both the revenues and the costs of the owner are affected by the decisions of the contractor. The choice of contractual provisions and parameters $\boldsymbol{y}$ is now the means by which the owner can influence the O&M of his facilities. The problem faced by the owner is thus now one of contractual design. Basically, the owner must determine $\boldsymbol{y}$ such that his returns are maximized, given that the contractor, who is responsible for O&M services, acts to maximize his own returns. The two basic elements of a problem of incentive design, conflicting objectives and asymmetrical information [10], are found in this setup.

Insight on the conflict of objectives may be gained by analyzing Eqs. (34) and (36). It is clear that improving the availability of assets in order to increase the remuneration of the owner generally requires incrementing the actual costs of O&M services and thus the expenditures of the contractor. In fact, if the term ι_t, which represents the variable remuneration of the contractor due to performance incentives, were eliminated from Eq. (34), the optimal strategy for the contractor would be simply not to carry out any O&M actions and thus incur no costs. This indicates the importance of designing contractual incentives in order to align the objectives of the parties.

Information asymmetry is also present in the problem of contracting O&M services. The very specialized knowledge of the contractor that makes the option of outsourcing O&M services potentially attractive to the owner also results in information asymmetry. For instance, prior to contract signature, a contractor with experience in the field may possess information on the expected behavior of component failure and on the actual costs of maintenance actions that an inexperienced owner may not have. Also, information about the efficiency of the contractor in executing

[9] We neglect operational expenditures incurred by the owner but not related to the items referring to O&M of wind turbines, such as land rental and administration. Effects of taxation are also neglected.

the O&M services will usually be kept private. Furthermore, the importance of the dependence of asset condition on the history of O&M actions poses difficulties with respect to the observability of the performance of the contractor. Even when the actions of the contractor ensure an adequate level of asset availability at a given moment in time—which can be observed by the owner at that very moment—the owner may not have the expertise to determine whether these actions are optimal with respect to the evolution of the equipment failure and repair rate functions in the long term.

The above characterization suggests that the theory of incentives may provide an adequate framework for analyzing the problem of designing O&M contracts. This is in fact the theoretical framework we adopt for approaching this problem. In particular, we employ a principal–agent model [10], in which the role of the principal is attributed to the wind park owner, who acts first and determines an incentive mechanism (the contractual provisions and parameters $\boldsymbol{y}$) that aims at eliciting the actions of the agent that will maximize the principal's payoff. The role of the agent is attributed to the contractor, who chooses whether or not to accept the contract under the proposed incentive mechanism and, upon acceptance, acts to maximize his own returns. We assume that the payoff of both agents is properly represented by the risk-adjusted NPV of their profits—this model allows accommodating specific von Neumann–Morgenstern utility functions of both parties when calculating the risk-adjusted NPV using the certainty equivalent.

It is worth discussing the adherence of this model to the actual negotiation of O&M contracts. The assumption that the owner, in his role as the principal, acts first and determines the contractual provisions and parameters is a simplification of the negotiation process, which actually involves extensive debate between the parties. The negotiation power attributed to the contractor under this assumption is lower than that found in many real-life situations. In fact, it is very common that O&M contractors, particularly those that are also turbine manufacturers, present the owner with a collection of standard contractual alternatives, from within which the final choice of contract must be made—and even in this case, the value of parameters such as the fixed base fee or the caps on liquidated damages is extensively discussed by the parties. In order to (at least partially) model this common situation in which the contractor offers a set of standard contractual formats to the owner, we assume that the owner must choose $\boldsymbol{y}$ from a pre-defined set $\boldsymbol{Y}$. The resulting model still represents the negotiation process in a simplified manner, which will be sufficient for discussing the phenomena relevant for this chapter.

An extensive analysis of the problem of contracting O&M services in the light of all relevant aspects of incentive theory, and particularly of the principal–agent model, would exceed the purposes and the intended length of this chapter. We thus borrow only selected aspects of this theoretical framework. This renders our analysis incomplete with respect to incentive theory, while allowing the discussion of a wide range of practical phenomena. We focus on the assessment of the most common performance incentives for wind park owners and O&M service suppliers, as described, respectively, in Sects. 3 and 4, and address the effects of information asymmetry in the design of these mechanisms only qualitatively.

After providing the reader with this background, we may present the mathematical model of the problem of contract design faced by the owner:

$$\breve{\mathcal{P}}(\boldsymbol{y}^*) = \max_{\boldsymbol{y}} \mathrm{CE}^o \left[\sum_{n=2}^{N} \Pi^n \left(\boldsymbol{\chi}^{[1,n]*}, \boldsymbol{\xi}^{[2,n]}, \boldsymbol{y} \right) \right] \tag{37}$$

$$\text{s.t.} \qquad \grave{\boldsymbol{\chi}}^{[1,N]*} = \arg \left[\max_{\grave{\boldsymbol{\chi}}^{[1,N]}} \breve{\mathcal{W}} \left(\grave{\boldsymbol{\chi}}^{[1,N]}, \boldsymbol{y} \right) \right] \tag{38}$$

$$\breve{\mathcal{W}} \left(\grave{\boldsymbol{\chi}}^{[1,N]*}, \boldsymbol{y} \right) \geq \underline{\breve{\mathcal{W}}} \tag{39}$$

$$\boldsymbol{y} \in \boldsymbol{Y} \tag{40}$$

where

$\breve{\mathcal{P}}(\boldsymbol{y})$ is the risk-adjusted NPV of the profit of the owner under the set of contractual parameters and provisions $\boldsymbol{y}$;
$\underline{\breve{\mathcal{W}}}$ is the *reservation utility* of contractor, in \$;
CE^o is the notation for the certainty equivalent calculated with the utility function of the owner[10];
$\boldsymbol{Y}$ is the set of possible combinations of contractual provisions and parameters offered by the contractor to the owner.

The objective function (37) states that the owner chooses $\boldsymbol{y}$ in order to maximize the risk-adjusted NPV of his profits throughout the contract term. The choice of $\boldsymbol{y}$ occurs prior to the provision of O&M services and thus prior to any of the stages of the O&M planning problem depicted in Fig. 1. The reader may think of the choice of $\boldsymbol{y}$ as a *decision in stage* 0.

Constraint (38) states that, given a set of contractual provisions and parameters $\boldsymbol{y}$, the policy of O&M decisions is defined by the contractor and corresponds to that which maximizes the risk-adjusted NPV of his profits. Constraint (39) states that, in order for the contractor to accept the contract, the risk-adjusted NPV of the profits obtained under $\boldsymbol{y}$ must at least equal a minimum monetary value, to which we refer as the *reservation utility* of the contractor. Constraint (40) models our assumption that the owner is required to choose $\boldsymbol{y}$ from a set previously defined by the contractor.

In the following, we discuss specific aspects of the problem of contractual design faced by the owner with the help of the mathematical formulation presented above.

First, it is necessary to notice that, as the problem (37)–(40) is formulated and solved by the owner, the solution is determined by his assumptions on the following: (1) the probability distributions of the stochastic parameters relevant for the problem;

[10] We use the superscript o to emphasize that the utility function of the owner is potentially different from that of the contractor, which is used in Eq. (35).

(2) the models of physical phenomena such as the effects of aging and maintenance actions over the condition of assets and consequently over their failure rates; (3) the structure of the cost functions of the contractor; and (4) the utility function, the discount rate, and the requisites of return on invested capital of the contractor.

The specialization of the contractor puts him in a better position to model the physical phenomena and to estimate the probability distributions of many of the stochastic parameters relevant for the problem. The information asymmetry with respect to his operational efficiency (which reflects on the actual costs of O&M) and his preferences (utility function, discount rate) is also obvious. It is thus useful to consider here two situations that may occur when the owner is solving the problem (37)–(40). The first situation is that in which the owner's assumptions lead to a choice of $\boldsymbol{y}$ that results in the O&M supplier not accepting the contract. Despite the fact that constraint (39) is satisfied *under the owner's assumptions* on the items described in the previous paragraph, the actual value of the risk-adjusted NPV of the contractor's profits is lower than his actual reservation utility, when the contractor's private information is considered. This case would likely lead to renegotiation of the contract, with the owner revising his assumptions and solving problem (37)–(40) again. The second situation is that in which the owner's assumptions lead to a choice of $\boldsymbol{y}$ with which the contractor is able to obtain a risk-adjusted NPV of profits that is higher than his actual reservation utility. The difference between the actual risk-adjusted NPV of profits and the actual reservation utility is thus a rent that the contractor is able to obtain from the owner due to possessing relevant private information—an *informational rent*.[11]

Having stated this important observation, we may deepen the discussion on the alignment of incentives perceived by the owner, η_t, and by the contractor, ι_t.

First, consider the unlikely situation in which the performance incentives perceived by the contractor perfectly match those perceived by the owner, with $\eta_t(\boldsymbol{\delta}_t, \boldsymbol{\xi}_t) = \iota_t(\boldsymbol{\delta}_t, \boldsymbol{\xi}_t, \boldsymbol{y})$ for all time periods in Eq. (36). This effectively means that the owner is transferring all his revenues to the contractor, who is now renting the wind power plant and absorbing all risks. This situation can only be economically meaningful if the fixed remuneration $F_t(\boldsymbol{y})$ is strictly negative; i.e., the contractor now pays a fixed rent to the owner. The NPV of the owner's profits is now certain,[12] because it is determined solely by this fixed rent. Recall that we are dealing with post-warranty O&M and the capital expenditures in the original installation of the wind park have already been made. Provided that the fixed rent now received by the owner is sufficient to cover these capital expenditures, this situation could be economically optimal, for instance, in the case of a risk-neutral O&M contractor and an extremely risk-averse owner. For a risk-neutral contractor, the risk-adjusted NPV

[11] The theory of incentives deals with techniques for analyzing the trade-off between informational rent extraction and allocative efficiency. A discussion of the many different results on rent extraction and allocative efficiency would exceed the objectives of this chapter and require changes to the model of contracting employed here. We thus limit our observation to the fact that informational rents exist, and direct the interested reader to [10] and [5] for further details.

[12] We have to either neglect other operational expenditures such as insurance, land rental, and O&M of electrical connection facilities or assume that these are also absorbed by the contractor.

and the expected value of the NPV of the profits coincide. The risk-premium required by the contractor, which is given by the difference between the expected value and the risk-adjusted value of the NPV of its profits, is now zero. If the risk-averse owner were receiving the stochastic remuneration η_t, he would require a positively valued risk-premium for the operation of the plant. Thus, the optimal allocation of risk is that in which all risks are transferred to the risk-neutral entity: the contractor.

The situation described in the former paragraph is an extreme one. In real situations, the contractor will likely not be risk neutral nor will the risk aversion of the owner be so high as to lead to such an economically optimal allocation of revenues and risks. In a situation in which both entities are risk-averse, the optimal design of contractual incentives will result in some risk being allocated to each of them. This allocation will depend on $\boldsymbol{y}$, due to the fixed remuneration, $F_t(\boldsymbol{y})$, and the performance incentives, $\iota_t(\boldsymbol{\delta}_t, \boldsymbol{\xi}_t, \boldsymbol{y})$, through which Eqs. (34) and (36) are linked.

Consider the mechanism of performance guarantees described in Sect. 4. Under this mechanism, the contractor partially absorbs the risks associated with foregone revenues when the unavailability of facilities exceeds a given threshold. Note that these risks are not entirely reallocated to the contractor, for two reasons: first, because of the caps on liquidated damages and second because the coefficient for calculating the liquidated damages—q in Eqs. (9) and (11)—is typically a parameter calculated *ex ante* and not coupled to energy prices verified *ex post*. Nevertheless, performance guarantees are important from the point of view of risk allocation, and this is the reason why they are frequently used as an incentive mechanism.

In fact, whenever other mechanisms, such as upsides sharing and production-based pricing, are employed as incentives, this is usually done in combination with performance guarantees. Arguably, upsides sharing mechanisms do not aim primarily at risk reallocation, because these mechanisms alone do not result in the contractor absorbing any negative remuneration shocks due to low availability. Production-based pricing does result in the contractor absorbing a parcel of remuneration shocks due to low availability, but the value at which production is remunerated—e in Eq. (15)—is significantly lower than market prices, which makes the parcel of remuneration shocks absorbed by the contractor also low.

Another important topic for the alignment of performance incentives for contractors and owners relates to the exogenous stochastic parameters upon which each incentive depends. The variable remuneration of the owner may depend on the availability of kinetic wind energy and on prices that vary in time, as discussed in Sect. 3. Making the parameters upon which the incentives perceived by the owner and by the contractor coincide can elicit efficient behavior from the contractor. For instance, an owner whose remuneration depends on a PIEP may benefit from establishing an *upsides sharing* mechanism for the O&M contractor, since the contractor will be incentivized to keep the facilities available when the output of the wind park is valued at high prices. On the other hand, it suffices for an owner whose remuneration corresponds to a PIEN to establish incentives for his O&M contractor that depend solely on the plant production. The determination of the fixed and

variable components of the contractor's remuneration always involves a trade-off between incentivizing operational efficiency (by exposing the contractor to the same stochastic variables upon which the remuneration of the owner depends) and reallocating risks in such a way to ensure that the risk-premium required by the contractor is not excessive. The optimal trade-off between incentivizing operational efficiency and reallocating risks may be determined precisely by the solution of problem (37)–(40) if there is no information asymmetry between the parties. However, as information asymmetries usually do exist,[13] the remuneration of the contractor will also include an informational rent, as noted above.

The specialization of the contractor leads to genuine technological advantages, resulting in lower costs of executing O&M actions. Economies of scale and scope are also relevant for establishing cost advantages for the contractor. O&M suppliers that provide services for a number of different wind parks will typically experience economies of scale that allow them to more efficiently allocate workforce, monitor equipment condition, procure spare parts, and manage stocks. Economies of scale related to the simultaneous supply of services to several wind parks are also relevant for the perception of risk of the O&M contractor, as long as the stochastic failure processes of wind turbines of different parks are essentially independent.[14] In order to understand the potential role of economies of scope, we may consider the case of O&M contractors that are also wind turbine manufacturers. This may allow them to capture economies of scope that are not experienced by independent service providers; e.g., those related to the procurement of spare parts. Also, manufacturers have incentives to place high value on O&M contracts: (1) they may be able to create business models in which the long-term revenues of O&M services are considered simultaneously with the turbine sales when calculating returns and (2) the provision of O&M services may allow them to retain skilled workforce in periods of declining turbine sales.

6 Renegotiation in Long-Term O&M Contracts and Alignment of Incentives for Owners and Contractors

In the previous section, we presented a mathematical framework for the problem of designing O&M contracts, taking into account the behavior of owners and contractors. Throughout Sect. 5.2, we adopted the assumption that the parties entered a single non-renegotiable O&M contract whose term coincides with the operational lifetime of the wind turbines. Though there are currently examples of actual O&M contracts with a 20-year term, which closely matches the design lifetime of wind

[13] Experienced owners may have better information than O&M contractors with respect to at least one stochastic parameter relevant for the contracting: the time-varying market prices.

[14] Which may not always be the case; e.g., high wind speeds and turbulence may lead to simultaneous failures in neighboring projects.

turbines, most O&M offerings refer to initial contracts with a term between 5 and 10 years. Thus, the situation in which contracts are renegotiated within the lifetime of the wind turbines is of interest. In this section, we address this situation.

As in Sect. 5.2, we start by developing a mathematical model of the economic behavior of the owner and the contractor and then use this model as a tool for qualitatively discussing relevant aspects of the problem. For the sake of conciseness, we will discuss the situation in which there is only one renegotiation of the O&M contract in the course of the relationship between the parties.[15]

In this situation, the parties enter at most two contracts from the moment the post-warranty O&M services start until the end of the operational lifetime of the assets: the *original* contract and the *renegotiated* contract. Naturally, it may be that no renewal of the O&M contract occurs after the termination of the original contract. We assume that the renegotiation occurs at the end of stage M, and the set of renegotiated contractual provisions and parameters are known starting in stage $M + 1$. This means that the *original contract* applies up to stage M, and the *renegotiated contract* after that. Thus, the NPV of the profits of the contractor during stages 1 to M is given by:

$$\begin{aligned}\Psi^n &= \left\{ \sum_{t \in \mathrm{T}^n} b_t \cdot \left[F_t(\boldsymbol{y}) + \iota_t(\boldsymbol{\delta}_t, \boldsymbol{\xi}_t, \boldsymbol{y}) - \beta_t(\boldsymbol{\delta}_t, \boldsymbol{\xi}_t, \boldsymbol{y}) \right] \right\} - b_{t^n} \cdot \zeta^n\left(\boldsymbol{\chi}^n, \boldsymbol{\varphi}_{t^n}, \boldsymbol{\xi}^n, \boldsymbol{y}\right) \\ &= \Psi^n\left(\boldsymbol{\chi}^{[1,n]}, \boldsymbol{\xi}^{[2,n]}, \boldsymbol{y}\right), \quad \forall\, n \leq M \end{aligned} \tag{41}$$

where
M is the stage at the end of which the renegotiation of the contract occurs.

The parameters of the original contract, $\boldsymbol{y}$, are known with certainty by the contractor at stage 1. Thus, rigorously, we could write the simplified expression for Ψ^n without using $\boldsymbol{y}$ as an argument. We maintain $\boldsymbol{y}$ as an argument of Ψ^n, because emphasizing this functional dependence will facilitate the understanding of the problem faced by the wind park owner.

We refer to the set of renegotiated contractual provisions and parameters as $\boldsymbol{\upsilon}$. The value of $\boldsymbol{\upsilon}$ is not known by the contractor from stages 1 to M. For simplicity, we assume that the set of options of contractual parameters offered by the contractor to the owner, $\boldsymbol{Y}$, does not change in time. Hence, just as $\boldsymbol{y} \in \boldsymbol{Y}$, we can write $\boldsymbol{\upsilon} \in \boldsymbol{Y}$. Notice that it is not required that all parameters are discrete variables—parameters such as the fixed base fee or caps on liquidated damages may be continuous, but the interval within which the owner will be allowed to choose them when renegotiating the contract will be the same within which he could choose the parameters of the original contract.

[15] The extension of the mathematical framework to the situation in which multiple renegotiations are allowed is relatively straightforward, basically corresponding to allowing the problem faced by the owner to be a multistage stochastic program, rather than a two-stage problem.

At the occasion of contract renegotiation at the very end of stage M, the stochastic process $\boldsymbol{\xi}^{[2,M]}$ will already have unfolded—i.e., a specific sequence of random events will have happened, leading all assets in the system to a certain condition $\boldsymbol{\varphi}^M$ and affecting the expectation of owner and contractor about the future probability distribution of events (i.e., the probability distribution of future events conditioned to a particular realization of $\boldsymbol{\xi}^{[2,M]}$). The condition of the assets and the specification of the probability distribution of events clearly affect the renegotiation of the contract. We should thus expect the parties to arrive at different sets of contractual parameters $\boldsymbol{\upsilon}$ for different realizations of the stochastic process up stage M.

However, because the parameters of the renegotiated contract are known by the contractor only after stage M, he perceives $\boldsymbol{\upsilon}$ as a stochastic variable whose distribution is conditioned to the evolution of events from stages 1 to M. The NPV of the profits of the contractor in stages $n > M$ can thus be written as:

$$\begin{aligned}\Psi^n &= \left\{\sum_{t\in \mathrm{T}^n} b_t \cdot \left[F_t(\boldsymbol{\upsilon}) + \iota_t(\boldsymbol{\delta}_t, \boldsymbol{\xi}_t, \boldsymbol{\upsilon}) - \beta_t(\boldsymbol{\delta}_t, \boldsymbol{\xi}_t, \boldsymbol{\upsilon})\right]\right\} - b_{t^n} \cdot \zeta^n\left(\boldsymbol{\chi}^n, \boldsymbol{\varphi}_{t^n}, \boldsymbol{\xi}^n, \boldsymbol{\upsilon}\right) \\ &= \Psi^n\left(\boldsymbol{\chi}^{[1,n]}, \boldsymbol{\xi}^{[2,n]}, \boldsymbol{\upsilon}\right), \quad \forall n > M\end{aligned} \tag{42}$$

where
$\boldsymbol{\upsilon}$ is the set of renegotiated contractual provisions and parameters.

And the problem of the contractor can thus be written as:

$$\begin{aligned}\check{\mathcal{V}}\left(\grave{\boldsymbol{\chi}}^{[1,N]*}, \boldsymbol{y}, \boldsymbol{\upsilon}\right) &= \max_{\grave{\boldsymbol{\chi}}^{[1,N]}} \check{\mathcal{V}}\left(\grave{\boldsymbol{\chi}}^{[1,N]}, \boldsymbol{y}, \boldsymbol{\upsilon}\right) \\ &= \max_{\boldsymbol{\chi}^1 \in \boldsymbol{X}^1} -\zeta^1\left(\boldsymbol{\chi}^1, \boldsymbol{y}\right) + \mathrm{CE}_{\boldsymbol{\xi}^2}\left[\max_{\boldsymbol{\chi}^2 \in \boldsymbol{X}^2(\boldsymbol{\chi}^1, \boldsymbol{\xi}^2, \boldsymbol{y})} \Psi^2\left(\boldsymbol{\chi}^{[1,2]}, \boldsymbol{\xi}^2, \boldsymbol{y}\right) + \mathrm{CE}_{\boldsymbol{\xi}^3|\boldsymbol{\xi}^2}[\cdots\right. \\ &\quad + \mathrm{CE}_{\{\boldsymbol{\xi}^{M+1}, \boldsymbol{\upsilon}\}|\boldsymbol{\xi}^{[2,M]}}\left[\max_{\boldsymbol{\chi}^{M+1} \in \boldsymbol{X}^{M+1}(\boldsymbol{\chi}^{[1,M]}, \boldsymbol{\xi}^{[2,M+1]}, \boldsymbol{\upsilon})} \Psi^{M+1}\left(\boldsymbol{\chi}^{[1,M+1]}, \boldsymbol{\xi}^{[2,M+1]}, \boldsymbol{\upsilon}\right)\right. \\ &\quad + \mathrm{CE}_{\boldsymbol{\xi}^{M+2}|\{\boldsymbol{\xi}^{[2,M+1]}, \boldsymbol{\upsilon}\}}[\cdots \\ &\quad \left.\left.\left.\left.\left.+ \mathrm{CE}_{\boldsymbol{\xi}^N|\{\boldsymbol{\xi}^{[2,N-1]}, \boldsymbol{\upsilon}\}}\left[\max_{\boldsymbol{\chi}^N \in \boldsymbol{X}^N(\boldsymbol{\chi}^{[1,N-1]}, \boldsymbol{\xi}^{[2,N]}, \boldsymbol{\upsilon})} \Psi^N\left(\boldsymbol{\chi}^{[1,N]}, \boldsymbol{\xi}^{[2,N]}, \boldsymbol{\upsilon}\right)\right]\right]\right]\right]\right]\end{aligned} \tag{43}$$

Notice that $\boldsymbol{y}$ and $\boldsymbol{\upsilon}$ are not decision variables in the problem of the contractor—rather, they are parameters. The fact the contractor perceives $\boldsymbol{\upsilon}$ as a stochastic parameter has impacts for the determination of his optimal policy, $\grave{\boldsymbol{\chi}}^{[1,N]*}$. Suppose, for instance, that one of the possible realizations of $\boldsymbol{\upsilon}$ considered by the contractor is a scenario in which the owner terminates the contract after the end of stage M. In this scenario, irrespective of the condition in which the assets are at the end of M, the contractor would capture no revenues (and also incur no costs) for all stages $n > M$. Because of the dependence of asset condition on the history of O&M

actions indicated in Eq. (19), preventive maintenance and servicing actions have impacts on the availability of assets not only in the short term, but also in the long term. Therefore, if the contractor foresees a scenario in which the contract is terminated at stage M, his optimal strategy may be to reduce the efforts with respect to preventive maintenance in stages prior to M: after all, the contractor will perceive no impacts of the assets arriving at $M+1$ in a poor condition. The situation is further complicated by the fact that the probability distribution of the stochastic parameter $\boldsymbol{\upsilon}$ is conditional on the actions of the contractor in previous stages. The reader may gain insight on this by considering the case in which the contractor has had an extraordinarily good performance up to M, increasing the probability that the owner will feel inclined to renew the contract.

We ask the reader to keep the above observations in mind when we consider the implications of the contractor perceiving $\boldsymbol{\upsilon}$ as a stochastic parameter. First, it is necessary to address the problem of the owner. The NPV of the profits of the owner in each stage n is given by the following equations:

$$\begin{aligned}\Pi^n &= \left\{ \sum_{t \in \mathrm{T}^n} a_t \cdot \left[\eta_t(\boldsymbol{\delta}_t, \boldsymbol{\xi}_t) - F_t(\boldsymbol{y}) - \iota_t(\boldsymbol{\delta}_t, \boldsymbol{\xi}_t, \boldsymbol{y}) \right] \right\} \\ &= \Pi^n \left(\boldsymbol{\chi}^{[1,n]}, \boldsymbol{\xi}^{[2,n]}, \boldsymbol{y} \right), \quad \forall\, n \leq M \end{aligned} \tag{44}$$

$$\begin{aligned}\Pi^n &= \left\{ \sum_{t \in \mathrm{T}^n} a_t \cdot \left[\eta_t(\boldsymbol{\delta}_t, \boldsymbol{\xi}_t) - F_t(\boldsymbol{\upsilon}) - \iota_t(\boldsymbol{\delta}_t, \boldsymbol{\xi}_t, \boldsymbol{\upsilon}) \right] \right\} \\ &= \Pi^n \left(\boldsymbol{\chi}^{[1,n]}, \boldsymbol{\xi}^{[2,n]}, \boldsymbol{\upsilon} \right), \quad \forall\, n > M \end{aligned} \tag{45}$$

Considering our model of contractual negotiation in which the owner is the principal and the contractor the agent, the owner is the one to determine the value of $\boldsymbol{\upsilon}$. However, when negotiating the *original contract*, the owner does not need to define deterministically a single set of provisions and parameters of the *renegotiated contract*. In fact, the renegotiation of the contract at a future point in time is a *recourse decision* by the owner. This means that a single set of provisions and parameters $\boldsymbol{y}$ is to be defined for the original contract, but the owner will consider the possibility of choosing different sets of contractual parameters $\boldsymbol{\upsilon}$ for different realizations of the stochastic process of O&M activities up to M. Thus, from the point of view of the owner, a *policy* of optimal contractual parameters, $\grave{\boldsymbol{\upsilon}}$, is defined for the renegotiated contract. The problem of contract design faced by the owner is thus a two-stage stochastic program.

The fact that the owner aims at defining a policy of decisions for contractual provisions and parameters of the renegotiated contract, while the contractor perceives these as stochastic parameters whose probability distribution is conditioned to his own policy of O&M decisions, brings about modeling difficulties.

One possibility for formulating the problem faced by the owner would be to assume that he is able to produce estimates of the conditional probability

distributions that the contractor perceives, and to formulate a stochastic problem in which the model of economical behavior of the contractor up to stage M is implicitly determined by these assumed conditional probability distributions. This is an assumption that we do not adopt, not only because of the difficulties in justifying it[16] but also because it leads to a mathematical formulation whose complexity would significantly hinder the qualitative discussions of this section. Rather, in our model, the owner simply assumes, while representing the behavior of the contractor, that the conditional probability distributions perceived by the contractor are similar enough to the actual policy of contractual parameters to justify treating the parameters of the renegotiated contract simply as the policy determined by the owner. This leads to the owner adopting the following approximate model for the behavior of the contractor:

$$\begin{aligned}
\breve{\mathcal{W}}\left(\grave{\boldsymbol{\chi}}^{[1,N]*}, \boldsymbol{y}, \grave{\boldsymbol{\upsilon}}\right) &= \max_{\grave{\boldsymbol{\chi}}^{[1,N]}} \breve{\mathcal{W}}\left(\grave{\boldsymbol{\chi}}^{[1,N]}, \boldsymbol{y}, \grave{\boldsymbol{\upsilon}}\right) \\
&= \max_{\boldsymbol{\chi}^1 \in \boldsymbol{X}^1} -\zeta^1\left(\boldsymbol{\chi}^1, \boldsymbol{y}\right) \\
&\quad + \mathrm{CE}_{\boldsymbol{\xi}^2}\left[\max_{\boldsymbol{\chi}^2 \in \boldsymbol{X}^2(\boldsymbol{\chi}^1, \boldsymbol{\xi}^2, \boldsymbol{y})} \Psi^2\left(\boldsymbol{\chi}^{[1,2]}, \boldsymbol{\xi}^2, \boldsymbol{y}\right) + \mathrm{CE}_{\boldsymbol{\xi}^3|\boldsymbol{\xi}^2}\left[\cdots\right.\right. \\
&\quad + \mathrm{CE}_{\boldsymbol{\xi}^{M+1}|\boldsymbol{\xi}^{[2,M]}}\left[\max_{\boldsymbol{\chi}^{M+1} \in \boldsymbol{X}^{M+1}(\boldsymbol{\chi}^{[1,M]}, \boldsymbol{\xi}^{[2,M+1]}, \boldsymbol{\upsilon})} \Psi^{\boldsymbol{M}+1}\left(\boldsymbol{\chi}^{[1,M+1]}, \boldsymbol{\xi}^{[2,M+1]}, \boldsymbol{\upsilon}\right)\right. \\
&\quad + \mathrm{CE}_{\boldsymbol{\xi}^{M+2}|\boldsymbol{\xi}^{[2,M+1]}}\left[\cdots + \mathrm{CE}_{\boldsymbol{\xi}^N|\boldsymbol{\xi}^{[2,N-1]}}\right. \\
&\quad \left.\left.\left.\left.\left.\times \left[\max_{\boldsymbol{\chi}^N \in \boldsymbol{X}^N(\boldsymbol{\chi}^{[1,N-1]}, \boldsymbol{\xi}^{[2,N]}, \boldsymbol{\upsilon})} \Psi^N\left(\boldsymbol{\chi}^{[1,N]}, \boldsymbol{\xi}^{[2,N]}, \boldsymbol{\upsilon}\right)\right]\right]\right]\right]\right]
\end{aligned} \tag{46}$$

where $\grave{\boldsymbol{\upsilon}}$ is the policy determined by the owner.

The problem of contractual design faced by the owner is then given by:

$$\begin{aligned}
\breve{\mathcal{P}}\left(\boldsymbol{y}^*, \grave{\boldsymbol{\upsilon}}^*\right) = \max_{\boldsymbol{y}} \mathrm{CE}^o_{\boldsymbol{\xi}^{[2,M]}}\left[\left[\sum_{n=2}^{M} \Pi^n\left(\boldsymbol{\chi}^{[1,n]*}, \boldsymbol{\xi}^{[2,n]}, \boldsymbol{y}\right)\right]\right. \\
\left. + \max_{\boldsymbol{\upsilon} \in \boldsymbol{\Upsilon}^{M+1}(\boldsymbol{y}, \boldsymbol{\xi}^{[2,M]})} \mathrm{CE}^o_{\boldsymbol{\xi}^{[M+1,N]}|\boldsymbol{\xi}^{[2,M]}}\left[\sum_{n=M+1}^{N} \Pi^n\left(\boldsymbol{\chi}^{[1,n]*}, \boldsymbol{\xi}^{[2,n]}, \boldsymbol{\upsilon}\right)\right]\right]
\end{aligned} \tag{47}$$

$$\text{s.t.} \quad \breve{\mathcal{W}}\left(\grave{\boldsymbol{\chi}}^{[1,N]*}, \boldsymbol{y}, \grave{\boldsymbol{\upsilon}}\right) \geq \underline{\breve{\mathcal{W}}} \tag{48}$$

[16] Namely, the assumption that *the owner estimates that the contractor estimates that the owner will take the actions with a certain probability* is rather heroic.

$$\grave{\boldsymbol{\chi}}^{[1,N]*} = \arg\left[\max_{\grave{\boldsymbol{\chi}}^{[1,N]}} \grave{\mathcal{W}}\left(\grave{\boldsymbol{\chi}}^{[1,N]}, \boldsymbol{y}, \grave{\boldsymbol{\upsilon}}\right)\right] \tag{49}$$

$$\boldsymbol{y} \in \boldsymbol{Y}; \grave{\boldsymbol{\upsilon}} \in \boldsymbol{Y} \tag{50}$$

Equation (47) indicates that the problem of the owner is now a two-stage stochastic program. A single, deterministic decision on the set of provisions and parameters of the original contract, $\boldsymbol{y}$, is made at the beginning of the problem horizon. Uncertainty then unfolds until the end of stage M. A policy of contractual decisions, $\grave{\boldsymbol{\upsilon}}$, determines the set of provisions and parameters for the renegotiated contract to be adopted for each possible realization of $\boldsymbol{\xi}^{[2,M]}$.

We can discuss fundamental issues related to long-term incentives for the O&M contractor with the help of this model. Reconciling potentially conflicting objectives of the contracting parties under information asymmetries is, as in Sect. 5.2, an important concern in contract design. The evolution of these information asymmetries over time is an important phenomenon in repeated contractual relationships. From the initial stage of the problem until the moment of contract renegotiation, the owner is able to observe both the behavior of exogenous stochastic parameters relevant for the problem and the behavior of the contractor, thus reducing the information asymmetry. This offers the owner the possibility to renegotiate the contract in such a way to decrease the informational rent obtained by the contractor. The possibility to reduce the informational rents is not transparent in the formulation of problem (47)–(50)—which is due to this being the formulation of the problem *seen* by the owner when designing the original contract. The reader must consider, however, that when designing the renegotiated contract, the owner will face a problem equivalent to that indicated by (37)–(40), but with information that better reflects that possessed by the contractor.

The possibility of reducing informational rents at the occasion of contract renegotiation, however, comes at the cost of removing the certainty of the contractor about the provisions and parameters that will rule the long-term relationship between the parties. Suppose, for the sake of argumentation, that one of the optimal decisions in policy $\grave{\boldsymbol{\upsilon}}$ involves terminating the relationship between the parties after the term of the original contract.[17] This may lead to an optimal policy of O&M decisions by the contractor that includes *running down* the assets: reducing efforts in preventive maintenance in order to increase profits. This would lead to a faster deterioration of the asset's condition, increasing failure rates in the long term. Formulation (47)–(50) can be used to determine whether the long-term impacts of contract termination and consequent running down of assets are so significant that this is not the optimal decision under any scenario. This is an extreme

[17] In this case, either another O&M supplier would be contracted or the owner would assume the responsibility for O&M. This need to hand over the responsibility of O&M should be included in (47)–(50). This can be done by considering constraints analogous to (48) and (49) for other parties potentially considered as candidates for assuming the responsibility of O&M.

scenario—but one that illustrates that uncertainty over long-term remuneration conditions may lead the contractor to make decisions that negatively affect the long-term value of the assets for the owner.

These factors need to be considered when contemplating the term of the contract. The owner will evaluate whether it is better: (1) to sign a non-renegotiable contract with a term that matches the design lifetime of the assets and give up any possibility of reducing the informational rent captured by the contractor at the occasion of renegotiation; or (2) to sign a shorter-term contract with the possibility of renewal after renegotiation and possibly expose the contractor to incentives to run assets down. Again, this is a trade-off between the extraction of informational rents and incentives to operational efficiency.

The mathematical framework presented in this chapter provides the reader with tools for evaluating which option is better for each specific contractual relationship. For instance, suppose a decision must be made between entering a contract for the whole remaining design lifetime of a wind park—say, 18 years—or entering a 10-year contract with the possibility of renewal for the remaining 8 years after renegotiation. If this is the case, solving the problems presented in Sects. 5 and 6 will allow not only determining the optimal set of contractual provisions and parameters, but also determining the risk-adjusted NPV of the owner's profits for each option. The owner would then choose the option (non-renegotiable contract for design lifetime or contract with shorter term but possibility of renegotiation) that leads to the higher risk-adjusted NPV.

We note that model (47)–(50) is a generalization of model (37)–(40). A single contract for the design lifetime of a wind park can be modeled with (47)–(50) simply by setting $M = N$ and equaling N to the design lifetime.

7 Conclusions

In this chapter, we presented the main characteristics of O&M contracts for wind turbines and developed a conceptual mathematical model to support the analysis and design of these contracts, from the point of view of wind park owners.

The nature of O&M contracts as instruments for managing operational risks associated with failures of wind turbines was extensively discussed. Outsourcing O&M to an experienced contractor offers owners the possibility of reducing the likelihood of equipment failure and decreasing the cost of maintenance services, and contractual arrangements may be designed to provide insurance against potentially high repair and replacement costs and lost revenues due to interruption of power generation.

The problem of O&M contract design was modeled as a principal–agent problem, in which the roles of the principal and the agent are associated, respectively, with the owner and the contractor. The developed model was employed as a tool for (1) discussing how the choice of contractual parameters and provisions affects the alignment of the performance incentives perceived by the owner and the

contractor, in an uncertain environment and (2) indicating the trade-off between allocative efficiency and informational rent extraction faced by the contractor, due to the existence of informational asymmetries.

References

1. Aparicio N, MacGill I, Abbad J, Beltran H (2012) Comparison of wind energy support policy and electricity market design in Europe, the United States, and Australia. IEEE Trans Sustain Energ 3–4:809–818
2. Billinton R, Allan RN (1983) Reliability evaluation of engineering systems: concepts and techniques. Plenum Press, New York, pp 245–247
3. Blischke WR, Murthy DP (2011) Reliability: modeling, prediction, and optimization, vol 767. Wiley, New York
4. BMME-Brazilian Ministry of Mines and Energy (2013) Portaria Nº 132, Apr (in Portuguese)
5. Bolton P, Dewatripont M (2005) Contract theory. The MIT Press, Cambridge
6. Dekker R (1996) Applications of maintenance optimization models: a review and analysis. Reliab Eng Syst Saf 51(3):229–240
7. DSIREUSA (2013) Renewable electricity production tax credit (PTC). http://dsireusa.org/incentives/incentive.cfm?Incentive_Code=US13F. Accessed Aug 2013
8. Endrenyi J, Anders GJ, Leite da Silva AM (1998) Probabilistic evaluation of the effect of maintenance on reliability. An application [to power systems]. IEEE Trans Power Syst 13(2):576–583
9. Feinstein CD, Morris PA (2010) The role of uncertainty in asset management. In: IEEE T&D conference and exposition, Apr 2010
10. Laffont JJ, Martimort D (2009) The theory of incentives: the principal-agent model. Princeton University Press, Princeton
11. Luenberger DG (1998) Investment science. Oxford University Press, Oxford
12. London T, Metzger D, Steadman T, Mulqueen M (2012) Operation and maintenance agreement issues for wind turbines. Briefing note by Clifford Chance, Feb 2012
13. PJM (2013) PJM manual 18: PJM capacity market, Revision 19
14. Shapiro A, Dentcheva D, Ruszczyński AP (2009) Lectures on stochastic programming: modeling and theory, vol 9. SIAM, Philadelphia
15. Turner G, Roots S, Wiltshire M et al (2013) Profiling the risks in solar and wind: a case for new risk management approaches in the renewable energy sector. Swiss Reinsurance, Zurich

Part II
Integration of Renewable Energy in Traditional Energy Systems

Grid Integration of Wind Power Generation

L. Rouco

Abstract Wind power generation has become a significant component of the generation portfolio in a number of power systems worldwide. Moreover, the development of wind generation will be continued as the implementation of policies aimed at fighting the climate change requires the increase of use of renewable energy sources in power generation. Grid integration is a major issue that affects the massive development of wind generation. This chapter discusses how generator technology affects grid integration of wind generation. Wind generators based on squirrel cage and doubly fed induction machines and multi-pole synchronous machines will be reviewed. The performance with respect to stability, load-frequency and reactive power–voltage control is discussed.

1 Introduction

Wind power generation has become a significant component of the generation portfolio in a number of power systems worldwide. Moreover, the development of wind generation will be continued as the implementation of policies aimed at fighting the climate change requires the increase of use of renewable energy sources in power generation.

Grid integration is a major issue that affects the massive development of wind generation. Precisely, the successful grid integration of wind power generation requires addressing a number of problems: stability and active power–frequency and reactive power–voltage controls [4]. Those aspects are very much affected by the specific features of the electromechanical conversion devices used in wind generation. In contrast with hydro and thermal-based generation that makes use of synchronous generators (SGs) of constant speed, wind generation employs both induction machines (squirrel cage and doubly fed) and variable speed (multi-pole) synchronous machines.

L. Rouco (✉)
Comillas Pontifical University, Madrid, Spain
e-mail: rouco@upcomillas.es

M. A. Sanz-Bobi (ed.), *Use, Operation and Maintenance of Renewable Energy Systems*, Green Energy and Technology, DOI: 10.1007/978-3-319-03224-5_6,

This chapter discusses how generator technology affects grid integration of wind generation. Wind generators based on squirrel cage and doubly fed induction machines and multi-pole synchronous machines will be reviewed. The performance with respect to stability, load-frequency and reactive power–voltage control is discussed.

Grid integration requirements have been addressed by transmission system operators (TSOs) through Grid Codes. Grid Codes have legal value in the country when they apply. As Grid Codes requirements vary from one country to another, the need of Grid Code harmonization has been requested by many players of wind power generation industry [17, 18]. The European Network of Transmission System Operators for Electricity (ENTSO–E), by the mandate of the European Commission, has developed a proposal of European Code that defines the requirements for connecting any generator to the grid [3].

Despite the specific features of the electromechanical energy conversion used by wind generators, the chapter shows that they can fulfil grid integration requirements. Specific requirements of the ENTSO–E Grid Code proposal will be considered and discussed.

The chapter is organized as follows. Section 2 reviews the features of three wind generator technologies. Section 3 investigates the large-disturbance stability of wind generators. It also discusses the impact of wind power generation on the small-disturbance stability of power systems. Section 4 addresses the active power–frequency control problem with special emphasis on primary frequency control and stability. Section 5 discusses the reactive power–voltage control problem from both steady-state and transient perspectives. Section 6 provides the conclusion of the chapter. Finally, the end of this chapter contains references.

2 Wind Generator Technology

First, wind generators were based on fixed speed squirrel cage induction machines. Variable speed wound rotor (doubly fed) induction machines were subsequently developed allowing the wind turbine to operate at its maximum efficiency point for each wind speed. Variable speed synchronous (multi-pole) machines were introduced to avoid the gear box used by both squirrel-cage and doubly fed induction machines to couple wind turbine low-speed rotor with induction machine high-speed rotor. Variable speed drives of doubly fed induction and multi-pole synchronous machines make use of power electronic converters that provides continuous reactive power generation/consumption capability.

2.1 Squirrel Cage Induction Generators

Squirrel-cage induction generators (SCIGs) are still used because of their simplicity. The wind turbine is coupled to the electrical machine through a gear box. Figure 1 displays the scheme of a SCIG. The rotor speed is determined by the wind speed and

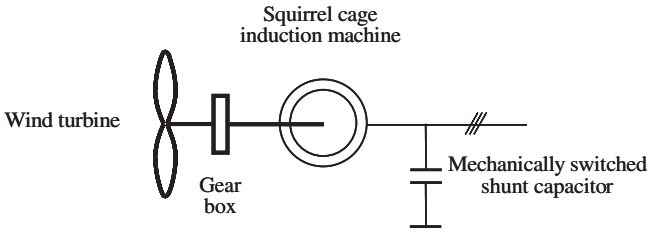

Fig. 1 Squirrel cage induction generator

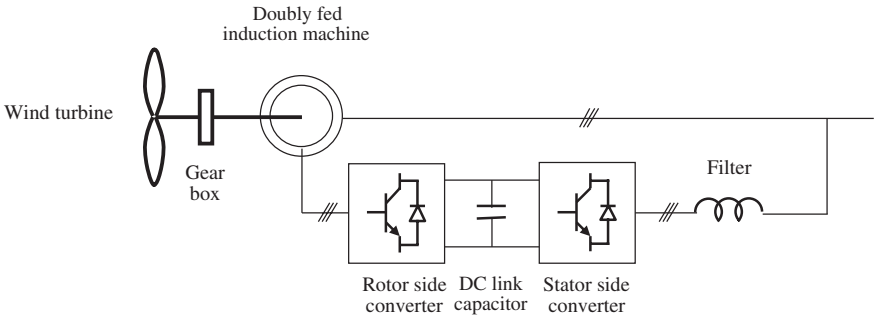

Fig. 2 Doubly fed induction generator

the characteristic curves of both the wind turbine and the induction machine. The wind turbine does not operate, in general, at its maximum efficiency point.

As induction machines consume reactive power, reactive power compensation must be provided. Reactive power compensation is usually provided with mechanically switched shunt capacitors at generator terminals and substation MV bus bars.

2.2 Doubly Fed Induction Generators

Doubly fed induction generators (DFIGs) are the most widespread electromechanical energy conversion devices used in wind power generation due to their speed regulating capability and the lower rating of their power electronic converters. It allows them to operate in the optimal operating point (maximum efficiency) of the wind turbine. In addition, the network-side power electronic converter can be used to provide continuous reactive power compensation capability.

Figure 2 displays the scheme of a DFIG. The rotor windings are fed by a three-phase voltage source converter with pulse-width modulation that provides a three-phase voltage system of variable frequency. The variation of the frequency

of rotor currents results in a variation of the rotor speed. Assuming that the stator frequency f_1 is constant, a variation of the rotor frequency f_2 results in a change of rotor speed n according to:

$$s = \frac{n_1 - n}{n_1} = \frac{f_2}{f_1}$$

The power electronic converter is actually built of two converters coupled through a dc-link capacitor. The rotor converter is used to control either the torque or the rotor speed and the rotor reactive power [9]. The component in the d-axis of the rotor current in a reference system solid with the stator flux is the excitation current and allows controlling the machine reactive power. The usual strategy is to set it to zero. The component in the q-axis of rotor current in a reference system solid with stator flux is the torque current and allows controlling the electromagnetic torque.

The stator or network-side converter is used to control the overall unit reactive power and the capacitor voltage. The component in the d-axis of the stator converter current determines the active power through the stator converter and allows controlling the capacitor voltage. The component in the q-axis of the stator converter current determines the reactive power provided by the stator converter.

2.3 Multi-pole Synchronous Generators

Wind generators based on multi-pole synchronous generators (MSGs) have the advantage that do not require the gear box used in wind generators based on either squirrel cage or DFIGs that use to be two pole pair machines. MSGs equipped with voltage source power electronic converters have speed regulating capability to be able to operate in the optimal operating point (maximum efficiency) of the wind turbine. As in DFIGs, the network-side power electronic converter provides them continuous reactive power compensation capability. A simpler scheme uses a thyristor converter at the machine side coupled through a LC filter with a voltage source converter at the network side. It should be noted that such scheme does not provide speed control capability.

Figure 3 displays the scheme of a MSG equipped with two voltage source converters. The machine stator windings are fed by a three-phase voltage source converter with pulse-width modulation that provides a three-phase voltage system of variable frequency. The variation of the frequency of stator voltages results in a variation of the rotor speed.

The electronic converter is built of two converters coupled through a dc-link capacitor. The stator converter is used to control either the torque or the rotor speed [5]. The excitation is controlled by the machine field current. It is assumed to be constant. The component in the q-axis of stator current is the torque current and allows controlling the electromagnetic torque.

The control strategy of the network-side converter is similar to the control strategy of the stator-side converter of a DFIG. The network-side converter is used to

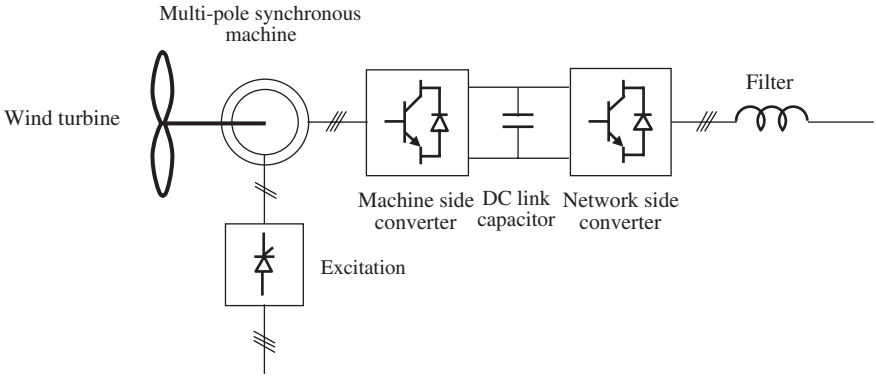

Fig. 3 Multi-pole synchronous generator

control the overall unit reactive power and the capacitor voltage. The component in the *d*-axis of the stator converter current (active current) determines the active power through the stator converter and allows controlling the capacitor voltage. The component in the *q*-axis of the stator converter current (reactive current) determines the reactive power provided by the stator converter.

3 Stability

Power system stability is concerned with the ability of the power system either to reach a new stable equilibrium point or to come back to the original stable equilibrium point after a disturbance [6, 7]. Power system stability phenomena are separated according to the size of the disturbance between large-signal and small-signal stability. Small-signal stability problems arise when the size of the disturbance allows linearizing the system differential equations to study the phenomenon of interest. In contrast, in large-signal stability problems, the size of the disturbance is such that the system non-linear differential equations must be considered to analyze the phenomenon of interest.

3.1 Large-Disturbance Stability

Wind power generation can affect the large-signal stability of power systems since a fault in the network results in a reduction of the supply voltage to a wind generator for a short period of time (voltage dip) and subsequently to its tripping due to the minimum voltage protections. When many wind farms are connected to the transmission network and the minimum voltage protections used to have settings

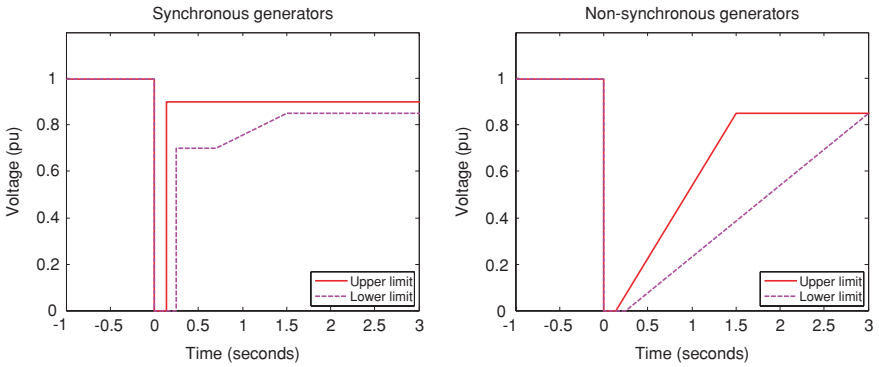

Fig. 4 ENTSO-E voltage ride through requirements for synchronous and non-synchronous generators

Fig. 5 Test system to evaluate the voltage ride through capability of synchronous and SCIGs

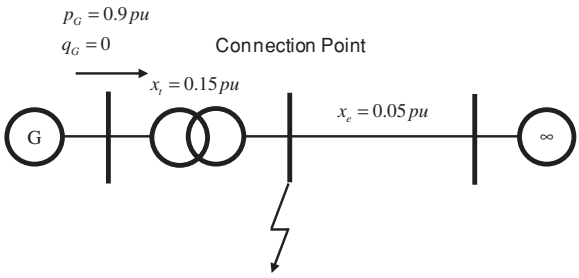

as tight as instantaneous tripping when the voltage is below 85 % of its nominal value, a fault in the transmission network can result in the tripping of a large amount of wind power generation and eventually to the system collapse [4].

The ability of generators to withstand a voltage dig without disconnecting from the grid or voltage ride through capability has been established as a time–voltage curve that the generator must sustain. Precisely, the time–voltage curve defines the fault duration and its severity. It also requires that the voltage is over the time–voltage curve after the fault clearing. Figure 4 shows the ENTSO–E voltage ride through requirements for synchronous (left) and non-synchronous generators (right). The fault duration is between 140 and 250 ms for both synchronous and SGs. However, the allowed time–voltage variation after the fault of non-synchronous generators is less demanding than the one of SGs.

The voltage ride through capability of wind generators depends on their technologies [10]. The capability of wind generators based on squirrel cage induction machines to withstand voltage dips, assuming identical operating conditions and connecting impedance (see Fig. 5), is highly affected by the inertia of the rotating masses. It should be emphasized that SCIGs are as vulnerable as SGs. Figure 6 displays the slip of a SCIG (left) and the speed deviation of a steam turbine SG

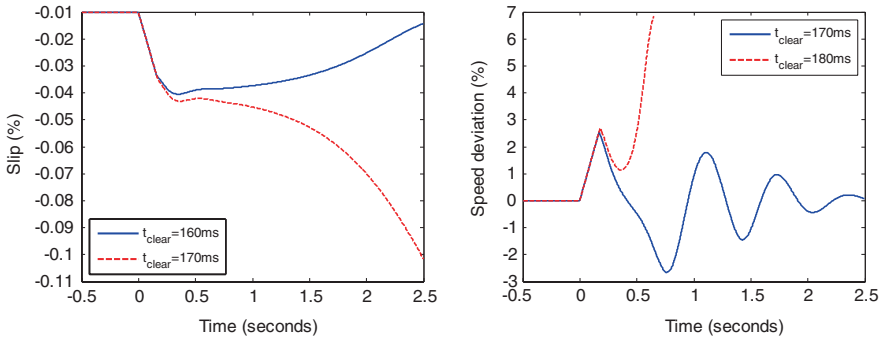

Fig. 6 Slip of a squirrel cage induction generator (*left*) and speed deviation of a steam turbine synchronous generator (*right*) to a voltage dip

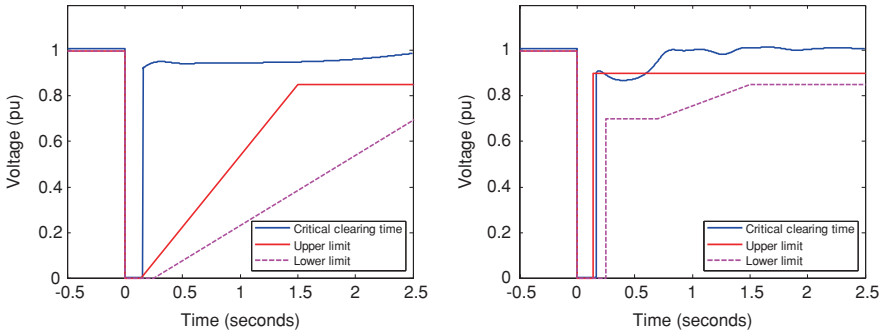

Fig. 7 Voltage of a squirrel cage induction generator (*left*) and a steam turbine synchronous generator (*right*) to a voltage dip

(right) in case of a solid fault at the point of connection to the grid and assuming that the rotor inertia of both machines is identical. The critical clearing time of the SG is slightly higher than the one of the SCIG. Figure 7 compares the voltage at the connection point of a SCIG (left) and of a steam turbine SG (right) in case of a solid fault. The voltage variation is compared with the upper and lower limits of the ENTSO–E requirements.

In contrast to SCIG, the response of wind generators based on doubly fed induction machines and multi-pole synchronous machines are determined by the power electronic converters capability to work with low voltages. Crowbar systems (thyristor-controlled resistances) have been added to the rotor of DFIGs to reduce the rotor overspeed while the fault is applied. Crowbars are also used to control the dc-link capacitor voltage of MSGs in case of fault.

The improvement of wind power generators capability to withstand voltage dips allows increasing the maximum admissible wind power generation as the amount of wind generation disconnection due to transmission network faults decreases.

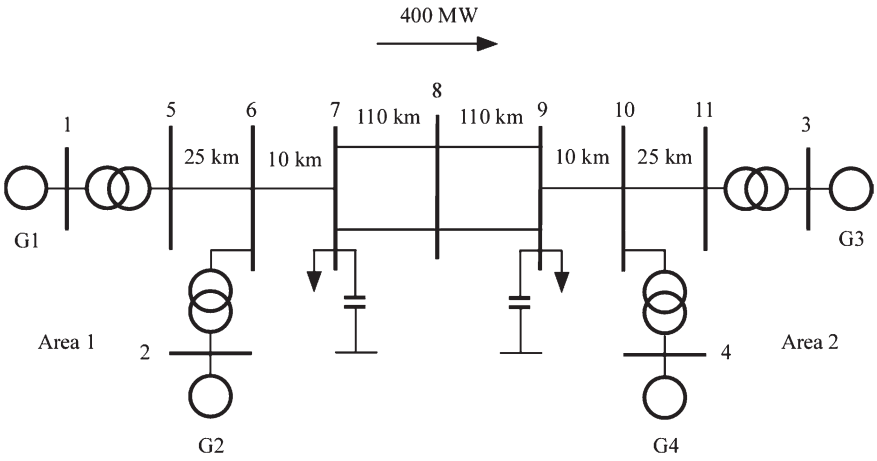

Fig. 8 Two-area test system

High penetration of wind power generation can also affect large-disturbance stability of multi-machine systems by reducing critical clearing times of some network faults. Such problem is illustrated in case of a solid three-phase fault in the mid-point bus (bus number 8) of the two-area test system shown in Fig. 8. The two-area test system consists of an exporting area (supplied by generators G1 and G2) and an importing area (supplied by generators G3 and G4) connected through a weak link. It was proposed for fundamental studies of power system stability and it is widely used [6].

The impact on the critical clearing of a fault at bus number 8 of substituting synchronous generation by wind generation is determined. Wind generators are represented by a response model that characterizes their response as required by ENTSO–E Grid Code [10]. If generators G2 and G4 are wind generators instead of SGs, the critical clearing time of a fault at bus number 8 is 480 ms instead of 680 m.

Figure 9 compares generator relative angles with respect to G3 angle in case of solid three-phase faults of 680 and 690 ms at bus number 8. The system is stable when the fault duration is 680 ms, whereas it is unstable when the fault duration is 690 ms. The instability occurs due to the fact that Area 1 generators (G1 and G2) loss synchronism with respect to Area 2 generators (G3 and G4).

If generators G2 and G4 become wind generators, the system is stable when the fault duration is 480 ms, whereas it is unstable when the fault duration is 490 ms. Figure 10 shows generator G1 relative angle with respect to G3 angle in case of solid three-phase faults of 480 and 490 ms at bus number 8. The system instability is due to the fact that generator G1 losses synchronism with respect to generator G2. Substituting synchronous generation by wind generation results in the reduction of the critical clearing time of a solid three-phase fault at the mid-point bus. The underlying physical phenomenon is the loss of rotational inertia due to the substitution

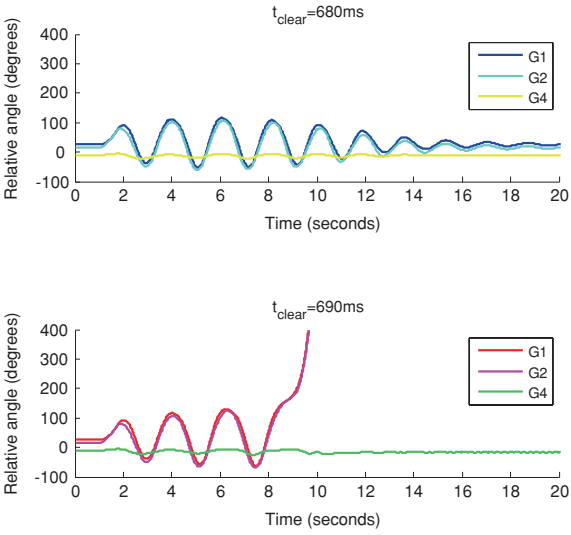

Fig. 9 Two-area test system when all generators are synchronous generators: generator relative angle with respect to G3

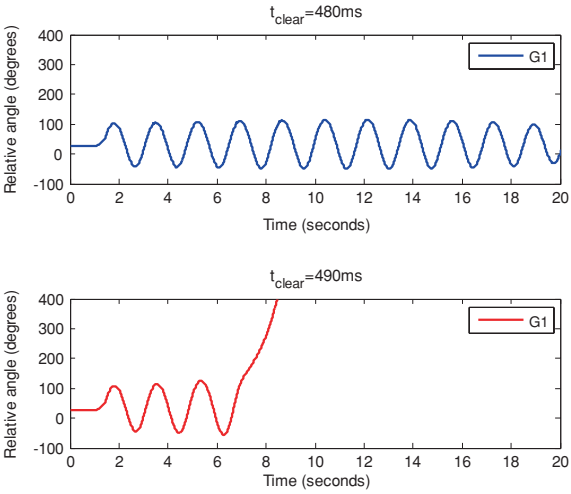

Fig. 10 Two-area test system when G1 and G3 are synchronous generators and G2 and G4 are wind generators: generator G1 relative angle with respect to G3

of synchronous generation by non-synchronous generation increases the SG rotor acceleration and the system separation takes earlier (lower clearing time).

It is worth investigating the impact of installing a STATCOM to increase the critical clearing time of a fault at bus number 8. The use of dynamic reactive power compensators has already been suggested for facilitating the grid integration of wind generation [1, 2, 8].

Several locations have been checked. The most effective STATCOM location for increasing the critical clearing time of a fault at bus number 8 is bus number 7.

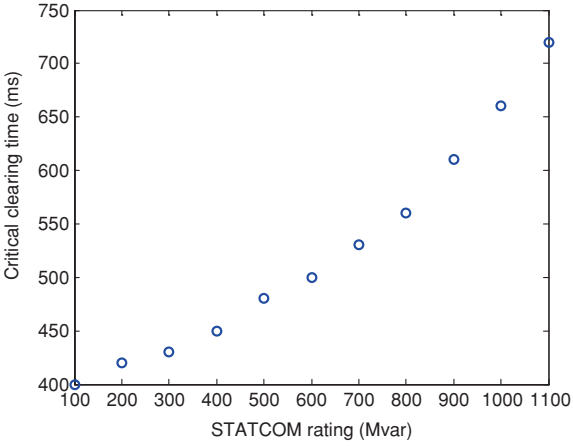

Fig. 11 Two-area test system when G1 and G3 are synchronous generators and G2 and G4 are wind generators: variation of the critical clearing time of a three-phase fault at bus number 8 as the rating of a STACOM installed at bus number 7 increases

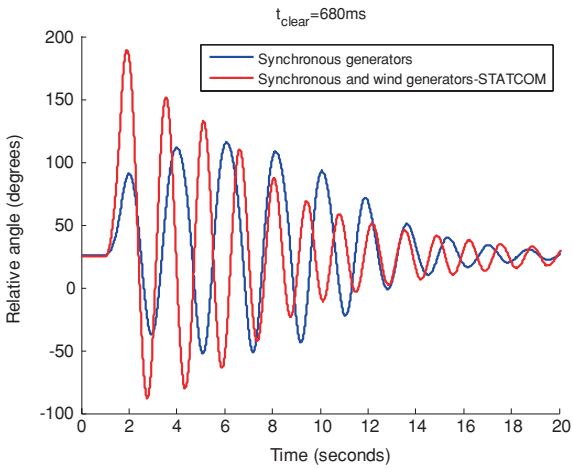

Fig. 12 Two-area test system when all generators are synchronous ones and when G1 and G3 are synchronous generators and G2 and G4 are wind generators, and a STACOM is installed in bus number 7: relative angle of generator G1 with respect to generator G3

Figure 11 shows the variation of the critical clearing time of a fault at bus number 8 with the STATCOM rating when generators G2 and G4 are wind generators. The critical clearing time would be 680 ms if a 1,025 Mvar STATCOM is installed at bus number 7. In other words, a system with high wind penetration can reach the performance of a system fully equipped with SGs if a STATCOM is installed in the appropriate bus.

Figure 12 compares relative angle of generator G1 with respect to generator G3 when all generators are synchronous ones and when G1 and G3 are SGs and G2 and G4 are wind generators, and a STACOM is installed in bus number 7 in case of the critical clearing time of a three-phase fault at bus number 8. The relative angle is greater when generators G2 and G4 are wind generators.

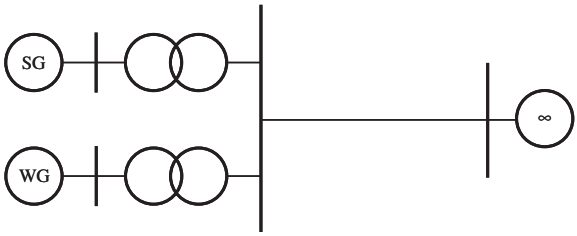

Fig. 13 Test system to investigate the impact of wind generation on power system small-signal stability

3.2 Small-Disturbance Stability

Small-signal stability is concerned with the damping of the natural oscillations of the power systems that lie in the frequency range between 0.1 and 2 Hz. Such oscillations are usually called electromechanical oscillation since they have their origin in the oscillation of SG rotors. Electromechanical oscillations are usually poorly damped in contrast to other natural oscillations of power systems. However, they can be damped out properly if supplementary controls (namely power system stabilizers) are added to synchronous excitation systems.

Although the small-signal stability problem is rather complex, it can be accurately characterized by the eigenvalues of the state matrix of the system linear model [11, 12, 15]. In addition, the right and left eigenvectors corresponding to the eigenvalues of interest are the basis of sensitivity tools to identify the relationships between variables and eigenvalues and, hence, to design power system damping controls.

The impact of wind generation on power system small-signal stability is discussed considering the power system example of Fig. 13 [13]. The variation of the damping and frequency of the electromechanical oscillation of a SG when wind generation increases while synchronous generation decreases is investigated. Figure 14 displays the SG electromechanical eigenvalue shift as the proportion of wind generation increases: the damping and the frequency of the SG generator electromechanical oscillation increase as the proportion of wind generation increases. This fact can be explained in terms of the lack of inertia of WGs: as WG increases, only SG inertia remains resulting in higher electromechanical oscillation frequency and damping. Figure 14 also displays the shift of the electromechanical eigenvalue if the WG is represented as a constant current load (CCL). It should be noted that the electromechanical eigenvalues obtained representing the WG as a CCL are closed to the electromechanical eigenvalues when the WG is either a DFIG or a MSG.

4 Active Power–Frequency Control

The mission of active power–frequency (*p–f*) control is to maintain the system frequency constant despite of the usual load variations. Moreover, *p–f* control systems should be able to deal with unscheduled variations of both generation and load.

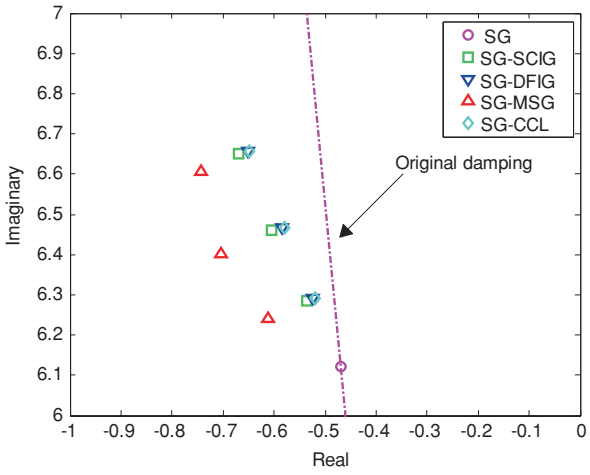

Fig. 14 Variation of the electromechanical mode of the synchronous generator of Fig. 13

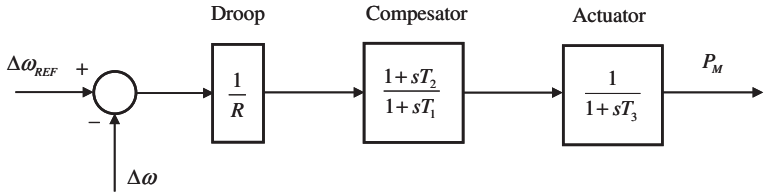

Fig. 15 Model of the primary frequency regulator of wind turbines

P–f control system is organized hierarchically at three levels acting at three timescales: primary, secondary and tertiary controls [16]. Primary regulation is an automatic control implemented at generator level. The output of the prime mover is controlled to maintain constant the generator speed. However, a steady-state error of frequency remains due to the permanent drop of governors needed to ensure the distribution of load variations among generators. Secondary regulation is a centralized automatic control system aimed at eliminating the steady-state error of the frequency and power interchange deviations. Tertiary regulation is a manual control system that ensures the level of primary and secondary regulating reserves.

The dominant actor in *p–f* control in large interconnected systems is secondary regulation as their large rotating inertia prevents large frequency excursions. In contrast, primary regulation is critical for the frequency stability of isolated systems.

This section illustrates how a DFIG wind generator (see Fig. 6) driven by a wind turbine with pitch control (Fig. 15) can perform primary frequency [14].

We have developed for this purpose two simple test systems (see Fig. 16). The test system I contains a single SG of 200 MVA feeding a load of 160 Mw and

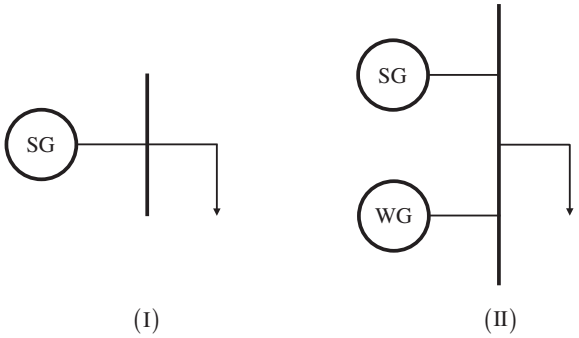

Fig. 16 Test systems to evaluate the impact of wind power generation on the frequency stability of synchronous generators

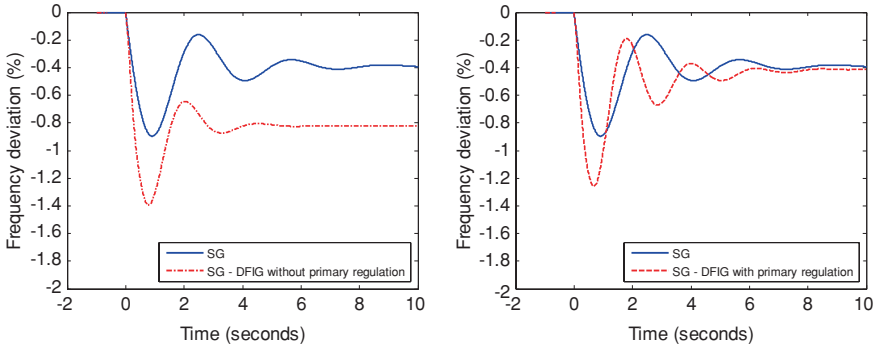

Fig. 17 Comparison of the frequency deviation in systems with synchronous generators and in systems with synchronous and DFIGs: DFIGs without (*left*) and with (*right*) primary frequency regulation

will be used as a reference. The test system II comprises of a SG and WG both of 100 MVA feeding a load.

The contribution of DFIGs to the frequency regulation is discussed. Figure 17 compares the frequency deviation of the SG in test systems I and II in case of the trip of 20 MW (10 % of the system rating). The left-hand-side plots correspond to the case in which the DFIG is not equipped with primary frequency regulation. The steady-state error of frequency when the system contains only a SG is $-0.04 \times 0.1 = -0.004$ pu $= -0.4$ %, and when the system includes both a SG and a DFIG becomes $-0.04 \times 0.2 = -0.008$ pu $= -0.8$ %. Not only the steady-state error of frequency changes due to the presence of a DFIG but also the transient response is affected. Precisely, the initial rate of change of the frequency in the first case results $-0.1/6 = -0.0167$ pu/s $= -1.67$ %/s, whereas in the second case becomes $-0.2/6 = -0.033$ pu/s $= -3.33$ %/s. It means that the frequency variation is only determined by the inertia of the SG. In other words, the inertia

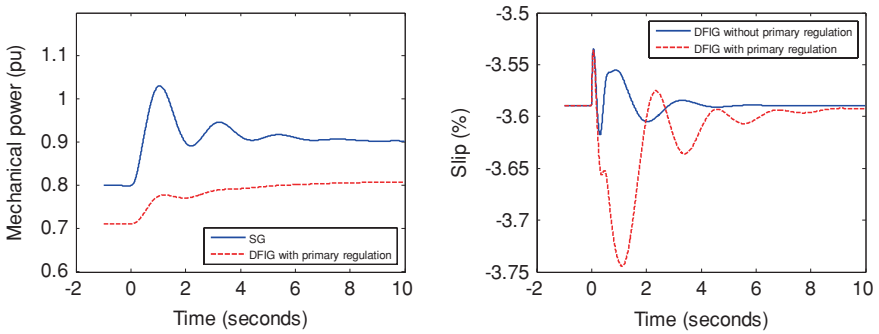

Fig. 18 Generator mechanical of synchronous and DFIGs (*left*) and comparison of the slip of the doubly fed induction generator without and with primary frequency regulation (*right*)

of the DFIG does not affect to the frequency of the SG. The right-hand-side plots correspond to the case in which the DFIG is equipped with primary frequency regulation. The steady-state error of frequency in the test system I is the same that in test system II. That is, the frequency error depends on the amount of generation that provides primary regulation no matter the type of generation. In addition, although the initial rate of change of frequency is the same in test systems I and II, the maximum frequency deviation is smaller in test system II than in test system I due to the action of the primary frequency regulation of the DFIG.

Figure 18 (left) shows the output of the SG and the DFIG when the DFIG includes primary frequency regulation. When the DFIG includes frequency regulation, both SG and DFIG increase their output to compensate the generation lost. Figure 18 (right) compares the slip of the DFIG in the cases when it does not and does include primary frequency regulation. The speed control loop of the DFIG ensures the speed despite of the increase of the output of the DFIG itself.

The study has shown that the initial rate of change of the frequency in case of a generator tripping is only determined by the inertia of the online SGs. In other words, wind generators do not contribute to the system inertia.

Variable speed wind generators (DFIGs and MSGs) can affect the initial rate of change of the frequency in case of a generator tripping by drawing transient kinetic energy of the turbine-generator rotor through the so-called synthetic inertia control. The synthetic inertia control is merely a differential control that acts upon the speed reference of the speed controller. The speed controller commands the component of the rotor current in the q-axis [11,12,15].

Figure 19 shows the frequency control by synthetic inertia of DFIGs. The controller input is the system frequency (SG speed) and the controller output is the slip reference of the slip control. Should the frequency deviation become constant, the variation of reference slip due to the output of synthetic inertia controller becomes zero. The performance of the synthetic inertia controller is investigated by comparing the frequency deviation in the test system II in three cases: DFIG without primary regulation, DGIG with primary regulation and DFIGs with synthetic inertia

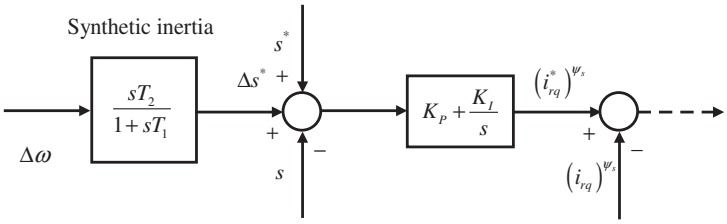

Fig. 19 Model of the synthetic inertia control in a doubly fed induction generator

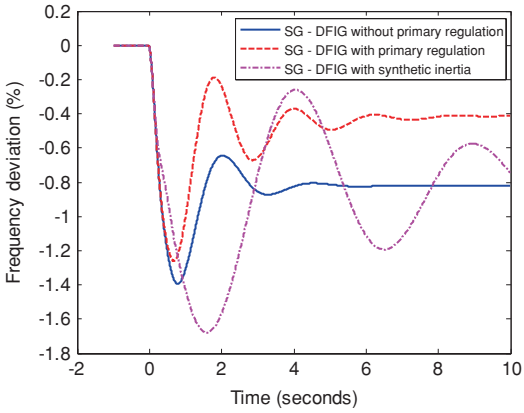

Fig. 20 Comparison of the frequency deviation in systems with synchronous and DFIGs: DFIGs without and with primary frequency regulation and with synthetic inertia

assuming $T1 = T2 = 1$ s. Figure 20 compares the frequency deviation in those three cases. Although the synthetic inertia control slightly affects the rate of change of frequency, the system response becomes less damped and the expected reduction of the maximum frequency excursion lost.

5 Reactive Power–Voltage Control

Reactive power–voltage (q–v) control in power system is aimed at maintaining the bus voltages within acceptable ranges. Generators are required either to produce or consume reactive power depending on transmission lines loading, reactive power demand and losses. The dynamic performance of the q–v control system relies basically on the response of the primary voltage regulation of the synchronous machines.

Reactive power requirements of wind farms have evolved with the development of wind generation: starting from power factor compensation to present required generation/consumption capability independent of the active power generation. Moreover, a fast transient response of q–v control system is also being required.

SCIGs cannot achieve fast transient response q–v control system when using mechanically switched shunt capacitors at both machine terminals and substation

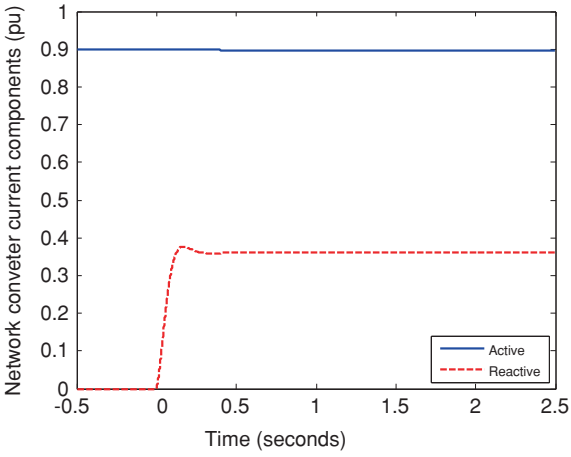

Fig. 21 Transient response of a multi-pole synchronous generator to a step in the q-axis component of the network-side converter current

MV busbar. In contrast, both DFIGs and MSGs, thanks to vector control of the network-side power electronic converter, are able to attain high-performance q–v control systems. Figure 21 shows the response of a MSG to a step at the reference of the reactive component of the network-side converter current that determines the reactive power supplied by the machine. Both supplied active and reactive current components are displayed. The machine was supplying 0.9 pu of active current at unity power factor. The machine is required to operate 0.95 lag power factor while supplying the same active current. The transient response of the reactive current component is very fast and is well damped as current controllers were properly designed. In addition, the active current component is not affected by the change of the reference of the reactive current component which confirms the success of vector control of network-side converter in controlling independently active and reactive currents.

Reactive power requirements at the grid connecting point of a wind farm can be fulfilled making use of the reactive power resources of wind farm generators. We discuss such approach in an actual wind farm located in the UK equipped with 9 wind generators of 1,670 kW connected to a 33-kV busbar as shown in Fig. 22. The 33-kV substation busbar is connected to the 132 kV connection point through a wind farm transformer.

Figure 23 (left) shows the ENTSO–E reactive power requirements (corresponding to the inner envelope) [3] at the connection point (bus number 20) as a function of the active generation at wind generator terminals and how they are fulfilled using the reactive power generation capability of 1,670 kW generators ($\pm$550 kvar). Extra reactive power generation capacity is required at high loads (1,300 kvar) to accomplish ENTSO–E requirements. Figure 23 (right) displays how ENTSO–E reactive power requirements are fully achieved at high loads with the proposed extra shunt capacitors connected at the 33-kV substation busbar.

The use of the reactive power capability of wind generators to accomplish the reactive power requirements at the wind farm connecting point to the network has

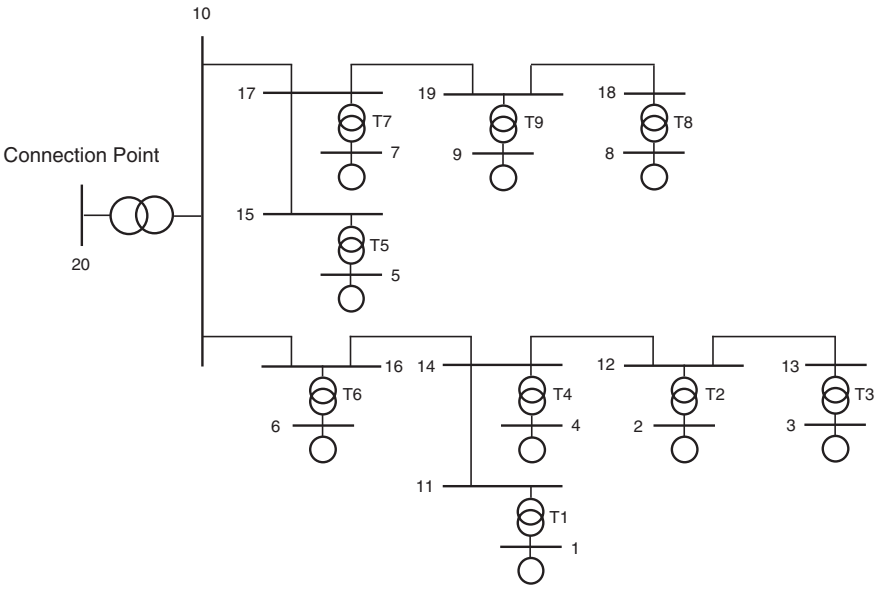

Fig. 22 Single-line diagram of an actual wind farm

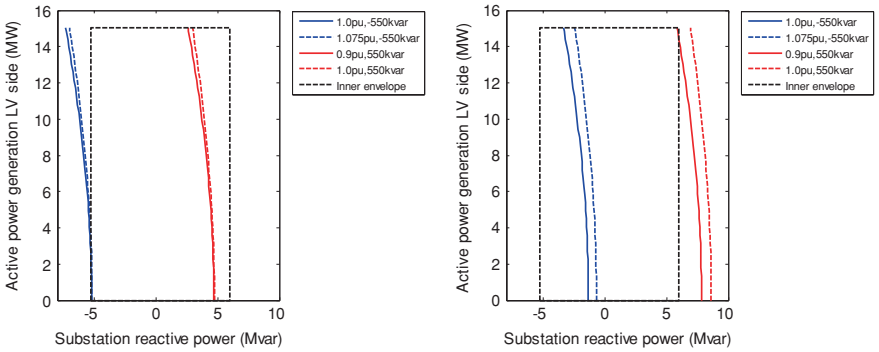

Fig. 23 Substation reactive power as a function of the active power generation at the LV side and the substation voltage: without (*left*) and with (*right*) shunt capacitor bank at 33-kV substation busbar

the disadvantage of increasing the losses through the circulation of reactive power through the wind farm network. Figure 24 shows the variation of the losses as a function of active power generation in the LV side for several scenarios of substation voltage and generator power factor. It confirms that the losses increase is not neglected. Hence, an alternative to reactive power supply based on a single source (i.e. a static var compensator) located at the substation busbar is worth. Such option would also allow reducing the rating of the network-side power electronic converter.

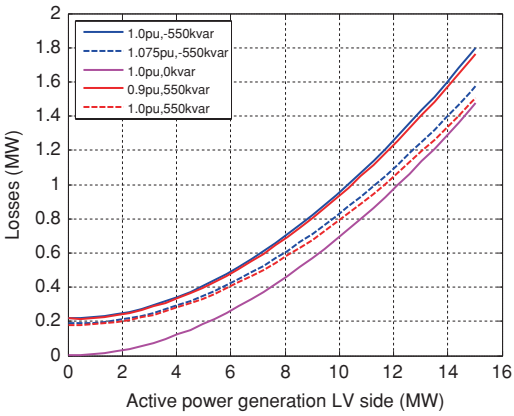

Fig. 24 Active power losses as a function of the active power generation in the LV side for several scenarios of substation voltage and generator power factor

6 Conclusions

Grid integration is a major issue that affects the massive development of wind generation. Precisely, the successful grid integration of wind power generation requires addressing a number of problems: stability and active load-frequency and reactive power–voltage controls. Those aspects are very much affected by the specific features of the electromechanical conversion devices used in wind generation. Wind generation makes use of fixed (squirrel cage) and variable (doubly fed) speed induction machines and variable speed (multi-pole) synchronous machines.

This chapter has discussed the performance of the SCIGs, DFIGs and MSGs with respect to large- and small-signal stability, primary load-frequency and reactive power–voltage controls. Despite the specific features of the electromechanical energy conversion used by wind generators, the chapter has shown that they can fulfil grid integration requirements. Of course, a number of aspects of the solutions adopted can be improved.

The broader problem of integrating wind generation in power systems (secondary frequency regulation, generation scheduling and security of supply) still requires much work.

References

1. ABB (2007) STATCOM for wind farm to meet grid code requirements. ABB Technical Note. Available from http://www05.abb.com/global/scot/scot232.nsf/veritydisplay/9cc1328c6b8e19f9c12576c50030add6/$file/statcom_meeting%20the%20grid%20code.pdf. Accessed Jan 2014
2. Chong H, Huang AQ, Baran ME, Bhattacharya S, Litzenberger W, Anderson L, Johnson AL, Edris AA (2008) STATCOM impact study on the integration of a large wind farm into a weak loop power system. IEEE Trans Energy Convers 23(1):226–233
3. ENTSO–E (2012) Network code for requirements for grid connection applicable to all generators. Available from https://www.entsoe.eu/fileadmin/user_upload/_library/consultations/Network_Code_RfG/120626_final_Network_Code_on_Requirements_for_Grid_Connection_applicable_to_all_Generators.pdf, 25/06/2012. Accessed Jan 2014

4. Eriksen PB, Ackerman T, Abildgaard H, Smith P, Winter W, Rodrígez-García J (2005) System operation with high wind penetration: the transmission challenges of Denmark, Germany, Spain, and Ireland. IEEE Power Energy Mag 3(6):65–74
5. Hünemörder S, Bierhoff M, Fuchs FW (2002) Drive with permanent magnet synchronous machine and voltage source inverter for wind power application. In: NORPIE 2002, Nordic workshop on power and industrial electronics, Stockholm, Sweden
6. Kundur P (1994) Power system stability and control. Mc Graw Hill, New York
7. Kundur P, Paserba J, Ajjarapu V, Andersson G, Bose A, Canizares C, Hatziargyriou N, Hill D, Stankovic A, Taylor C, Van Cutsem T, Vittal V (2004) Definition and classification of power system stability IEEE/CIGRE joint task force on stability terms and definitions. IEEE Trans Power Syst 19(3):1387–1401
8. Maibach P, Wernli J, Jones P, Obad M (2007) STATCOM technology for wind parks to meet grid code requirements, ABB Technical Note No. 3BHS237435 ZAB E01. Available from http://library.abb.com/global/scot/scot232.nsf/veritydisplay/50fab2bdc45be270c12572ea0050ae66/$File/STATCOM%20Technology%20for%20Wind%20Parks%20to%20Meet%20Grid%20Code.pdf. Accessed Jan 2014
9. Pena R, Clare JC, Asher GM (1996) Doubly fed induction generator using back-to-back PWM converters and its application to wind-energy generation. IEE Proc Electron Power Appl 143(3):231–241
10. Rodríguez-Bobada F, Ledesma P, Martínez S, Coronado L, Prieto E (2008) Simplified wind generator model for transmission system operator planning studies. In: 7th International workshop on large scale integration of wind power and on transmission networks for offshore wind farms, Madrid, Spain, 26–27 May 2008
11. Rouco L, Pérez M, Díez M (2006) Contribution of wind power generation to power system stabilization. In: 13th IFAC workshop on control applications of optimization, Paris-Cachan, France, 26–28 Apr 2006
12. Rouco L, Zamora JL, Diez M (2006) Dynamic patterns and model order reduction in small-signal models of doubly fed induction generators for wind power applications. In: 2006 IEEE/PES general meeting, Montreal, Canada, 18–22 June 2006
13. Rouco L, Fernández F, Zamora JL, García-González P (2006) Comparison of the dynamic response of wind power generators of different technologies in case of voltage dips. In: 41 Cigré session, paper A1–304, Paris, France, 27 Aug–1 Sep 2006
14. Rouco L, Zamora JL, Egido I, Fernández F (2008) Impact of wind power generators on the frequency stability of synchronous generators. In: 42 Cigré session, paper A1–203, Paris, France, 24–29 Aug 2008
15. Tabernero J, Rouco L (2007) Dynamic patterns in small-signal models of multi–pole synchronous generators for wind power applications. In: IEEE Power Tech 2007, Lausanne, Switzerland, 1–5 July 2007
16. UCTE (2013) Operational hand book. Available from https://www.entsoe.eu/publications/system-operations-reports/operation-handbook/. Accessed Jan 2014
17. Van Hulle F (2010) Grid codes: the manufacturer's nightmare. In: Proceedings of EWEC, Warsaw (Poland), 20–23 Apr 2010
18. Van Hulle F, Christensen W, Seman S, Schulz V (2010) European grid code development—the road towards structural harmonization. In: Proceedings of the 9th international workshop on large-scale integration of wind power into power systems as well as on transmission networks for offshore wind power plants, Québec City (Québec, Canada), 18–19 Oct 2010

Control Methods Applied in Renewable Energy Systems

Ilhami Colak and Ersan Kabalci

Abstract This chapter is dedicated to introducing the control methods used in renewable energy sources. The conventional and innovative energy generation methods are explained according to their historical background in the initial section. The power electronic circuits that are widely known by most of the readers are briefly analysed in Sect. 2 where the circuit topologies and design criteria are also addressed. The control methods of power electronics used in renewable energy sources such as solar, wind, and fuel cells are comprehensively explained in the following sections. The maximum power point tracking (MPPT) that is the essential part of solar power systems is introduced by means of software and hardware. On the other hand, the required circuit topologies of current control method are explained with grid-connected and island-mode operations of a solar energy system. The rest of the chapter consists of renewable energy systems based on wind turbine and fuel cells. The wind turbine dynamics are initially introduced to create a link through the power electronics and control methods. The control methods of fixed and variable wind turbines are explained regarding to current and voltage control requirements. The fuel cell-based renewable energy systems and control methods are also explained in the last section of the chapter.

I. Colak (✉)
Faculty of Technology, Department of Electrical and Electronics Engineering, Gazi University, Besevler, 06500 Ankara, Turkey
e-mail: icolak@gazi.edu.tr

E. Kabalci
Faculty of Engineering and Architecture, Department of Electrical and Electronics Engineering, Nevsehir University, 2000 Evler Mah. Zübeyde Hanım Cad, 50300 Nevsehir, Turkey
e-mail: kabalci@nevsehir.edu.tr

M. A. Sanz-Bobi (ed.), *Use, Operation and Maintenance of Renewable Energy Systems*, Green Energy and Technology, DOI: 10.1007/978-3-319-03224-5_7,

1 Introduction

An electrical power system consists of generator units, transformers, transmission and distribution lines, loads, and protection and control units. All these parts of a power system interact together to meet the demands of beneficiaries as the most important requirement for a power system. The power quality supplied to load is determined regarding to several factors such as stable voltage, frequency, power factor, balanced phase values, reduced harmonics, and pure sine waves [2, 49]. Besides these components of a power system, entire electrical network can be classified into four main infrastructures that are generation, transmission, distribution, and utilization. The conventional power generation substructure is based on hydroelectric, synchronous machinery, thermal-generating units, and distributed utilities such as micro turbines, fuel cells, and combustion turbines [25]. Although the conventional generation systems still cover the biggest part of the whole power generated, the distributed generation idea accelerated the innovative technologies that enable us to utilize variable renewable energy sources together [64]. The renewable energy utilization and dedicated technologies have experienced a great speedup in the last few decades. The limited reserves and increased cost of fossil or gas fuels and the hesitations on security issues of nuclear energy all promoted the increment of renewable energy sources. Furthermore, the emissions caused by fossil fuels and nuclear sources are also taken into account comparing the renewable sources on the sustainability arguments. Besides the scientific approaches, the modern lifestyle and ecological perspective enhanced by local residents, wherever they live, led to sensitivity on greenhouse effect and climate change. Since renewable sources are much more compatible with sustainability and environmental effects, almost all the nations revised their energy policies considering innovative technologies on renewable energy sources [64, 68]. Main expectations of energy policies are directed to similar issues as increasing the total energy of renewable sources, increasing the efficiency, reducing the emissions, and improving the quality of life.

On the other hand, energy security is as important as sustainability issue for all economies due to increased utilization of industrial equipments, lightning, electric-based vehicles, and data processing systems such as telecommunication or servers. Although the energy expenses of nations that are more industrial are around 5–10 %, some developing countries may have energy outcomes up to half of their total imports and cause more unsustainable and weak economic development. In the twenty-first century, some energy provider countries promoted the global energy usage up to ten times all over the world by adding the nuclear sources and natural gases in huge manners compared to last century [12, 45, 68]. However, the increased energy demand and industrialization level of countries made them much more foreign dependent that aggravates the medium- and long-term sustainability plans. These and similar developments encouraged the alternative energy sources to be integrated to distributed generation, DG stations. The renewable energy sources (RES) are becoming extensively studied and researched energy area as being the most widely used alternative energy sources.

Wind power, which is first used in Persia as early as 200 BC, was the preliminary RES that is known by human even before solar power. The first windmill used to generate electricity was constructed in 1888 that had a 12-kW direct-current (dc) generator. Although several individual researches were sustained up to 1900s, it was age of fossil fuel plants and centrally generated power. The first remarkable wind turbines were developed in Soviet Russia in 1931 named Balaclava with 100 kW rated power and 30 m diameter and the Andrea Enfield with 100 kW rated power and 24 m in the early 1950s in England. The next phase of wind turbines increased rated power to 200 kW with Gedser machine of Denmark in 1956 and to 1.1 MW with 35 m diameter by French in 1963. In those times, Ulrich Hütter, an Austrian engineer, first described the theoretical basis for the modern wind turbine in detail mathematically and constructed some novel turbine models that are light in weight. When the oil crisis occurred in 1973, wind energy gleamed again and extensive researches were initiated on non-fossil energy sources [12, 27, 44].

Alexandre-Edmund Becquerel firstly discovers the photovoltaic (PV) energy in 1839 in which he proved that the electrical current transported with light induces chemical reactions [18, 56]. Later on, a similar relation between electricity and light was observed with the invention of selenium that is assumed to be the first solid PV material. The developments in solid PV materials are followed up to 1940s, and a silicon PV cell with 6 % efficiency is implemented in those years. The material and structure inventions promoted solar cells to solar modules, and the total rated power and energy efficiency is increased to 20 %. Nowadays, several types of solar cells such as silicon, gallium arsenic $GaAs$, zinc oxide ZnO, and organic, inorganic, and polymer cells are industrially available [16, 34, 51]. Though several materials and connection opportunities are developed, the main research aim on PV is to obtain the maximum power output and the highest efficiency at minimum cost. Therefore, numerous electrical and mechanical control techniques are implemented.

Besides the wind and solar power sources, other renewable energy researches are seen in cogeneration sources such fuels and diesels that are intended to be replaced with their hydrogen, biomass, or biodiesel substitutes. Biomass, which mostly involves waste wood and horticultural materials, is much more widely available compared to fossil fuels and can be easily produced and utilized on electricity generation. The cogeneration or combined heat and power (CHP) concept defines a power station where heat energy is also obtained, while the plant is generating electricity. Biomass sources are utilized in the best way in CHP plants. In particular, the energy obtained is maximized from a few hundred kW electric power to one or two MW electric power in small power systems [11, 31, 61]. Furthermore, energy plants that are especially produced for energy instead of food were extensively researched as renewable bioenergy sources after oil crisis of 1970s [40].

Wilhelm Ostwald discovered the fuel cell, another remarkable renewable energy source, in 1894 by showing the importance of non-pollutant properties of the direct conversion of chemical energy into electricity. However, internal combustion engines dominated the twentieth century instead of fuel cells and batteries.

Christian Friedrich Schonbein started the preliminary studies on fuel cell in the early 1830s with electrolysis of diluted sulphuric acid and other matters. William R. Grove introduced the first electrolytic cell that consists of two platinum strips around closed tubes where the tubes contain sulphuric acid. The first commercial fuel cells were implemented in 1990s using alkaline, and then, several types of fuel cells that are based on proton-exchange (PEM), direct methanol (DM), molten carbonate fuel (MC), and solid oxide (SO) are developed as most widely known types. Fuel cells are assumed to be one of the key technologies for the future energy sources because of its ability to obtain zero carbon emission and to purchase hydrogen as an easily acquired raw material [4, 36, 42].

Additional to the sources indicated above, several innovative researches on RESs are still being extensively carried out by scientist and investors. The novel RESs can be classified as tidal or wave sources of oceans, solar updraft towers, ocean thermal energy, rain power, tornado wind power, and so on. All the renewable energy systems that use one or more RESs together should be properly controlled to obtain the maximum power output at the highest efficiency.

This chapter deals with control methods applied in renewable energy conversion systems in detail. An energy conversion system involves several power electronic devices that are supplied by a source or that are assumed to be the source of load sites. Although the main power electronics are similar to each other in any energy conversion system, some featured control methods and circuits are required to increase the efficiency of the complete system, depending on RES supplied to the system. The common power electronic circuits and topologies that perform the energy conversion from alternative current (ac) to direct current (dc) or vice versa are introduced in Sect. 2. The next section is dedicated to control methods of solar systems that include the estimation, prediction, and computation algorithms to increase the total efficiency obtained. A similar approach is realized for wind systems in the fourth section that analyses mechanical and electrical control methods. The control methods of fuel cells are analysed in Sect. 5.

2 Power Electronic at a Glance

The power electronic can be simply defined as energy conversion process that is performed by several circuits. The basic power semiconductors were rapidly developed since mid-1900s that are now able to control megavolt-amperes (MVA) in solid-state integrated circuits [10, 54]. The electrical energy is generated either in dc or in ac waveforms. Various power electronic circuits illustrated in Fig. 1 that are introduced in this section realize the conversion of these waveforms. The power electronic devices are named according to their energy conversion processes where dc–dc conversion is performed by converters, ac–dc by rectifiers, dc–ac by inverters, and ac–ac by cycloconverters [10, 54].

Although the rectifiers are widely known owing to its widespread utilization area, inverters and converters are used in power supplies in order to condition

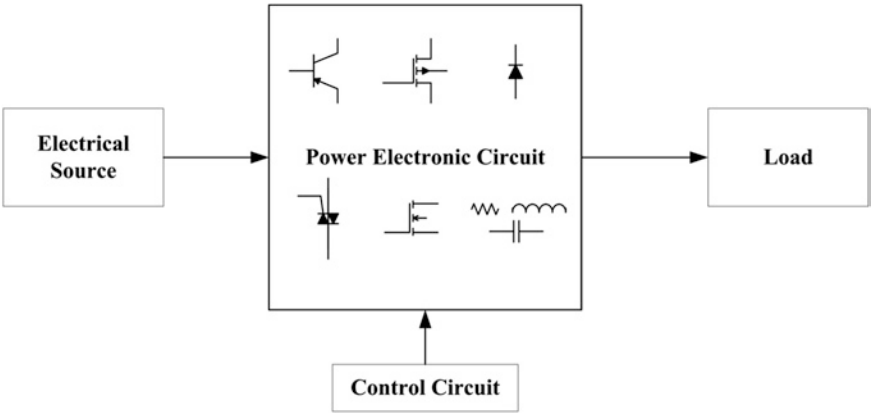

Fig. 1 Energy conversion with power electronic circuits

the electrical energy form. The cycloconverters are used to adjust amplitude and frequency of ac waveform to an intended upper or lower level [54]. However, all power electronic circuits manage the energy on the generating and consuming parts. The diode as being the first semiconductor device is the milestone in rectifier circuit. The developed semiconductor technology yielded power transistors, thyristor, gate turn-off thyristor (GTO), MOSFET, insulated gate bipolar transistor (IGBT) that allow to implement several circuit topologies [19]. Besides the developing semiconductor technology, modern power electronic is based on control methods that are performed by high-precision microprocessors. The lately improved control methods are researched to increase the efficiency and reliability of the complete power electronic system. The conventional power electronic was severely affected by conduction losses and was suffered efficiency even in the most basic usage purposes. On the other hand, modern control methods can be examined relating to developing software and algorithm approaches.

Since most of the readers are familiar to the basic power electronic circuits, they will not be analysed in detail. The most widely used power electronic circuits are introduced in the related subsections in order to make a connection through the control methods.

2.1 Rectifier Topologies

A rectifier circuit converting the ac waveform to dc waveform is constructed in two ways either in uncontrolled structure with diodes or in controlled structure with thyristors. There is another alternative configuration called semicontrolled that has not a wide utilization area. The uncontrolled rectifiers are based on the unidirectional conduction feature of diodes and are probably the most widely used circuit since they do not involve any control method. The unidirectional

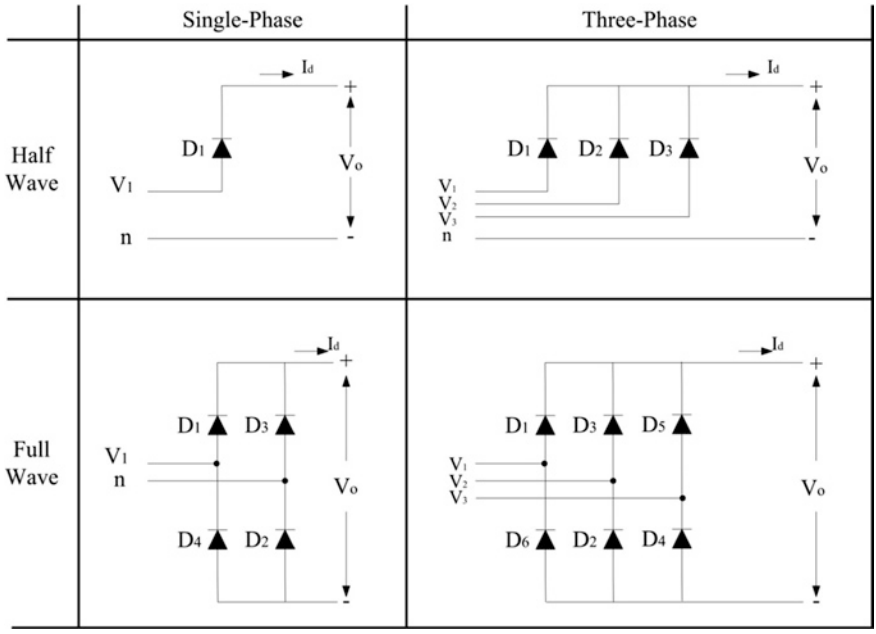

Fig. 2 General rectifier circuits arranged according to phase numbers

conduction of a diode is known as forward biasing that allows conducting the positive cycle from anode to cathode. On the other hand, handling the high-voltage stresses in the reverse biasing, namely high peak inverse voltage, is another prominent feature of a diode that makes uncontrolled rectifier powerful.

Since a period of an ac waveform consists of two sinusoidal cycles that oscillate from positive to negative peak continuously, rectifiers are constructed either to operate during the one half-cycle that is known as *half-wave rectifier* or to operate during the entire period that is known as *full-wave rectifier*. The general views of these circuits are shown in Fig. 2 where the columns are arranged according to single- and three-phase supplies [19, 43, 54]. The load connected to the output can be resistive R or resistive–inductive (RL), and the output line current is calculated using Ohm's law. The average dc output voltage V_{dc} supplied to load is calculated as given below:

$$V_{\mathrm{dc}} = \frac{1}{\mathrm{T}} \int_0^T V_{\mathrm{o}} \mathrm{d}t \tag{1}$$

In case single-phase half-wave rectifier is used, the T period is considered as 2π by remembering the negative cycle yields zero since diode is reverse-biased. The average dc voltage is obtained as given in Eq. (2), while the full-wave rectifier output is calculated as given in Eq. (3) [54].

$$\text{Half-wave } V_{\text{dc}} = \frac{V_{\text{m}}}{\pi} = 0.318\, V_{\text{m}} \tag{2}$$

$$\text{Full-wave } V_{\text{dc}} = \frac{2V_{\text{m}}}{\pi} = 0.636\, V_{\text{m}} \tag{3}$$

where V_{m} is the peak value of supply voltage. By assuming that the load is an R, the dc line currents (I_{dc}) are calculated as shown in Eqs. (4) and (5).

$$\text{Half-wave } I_{\text{dc}} = \frac{V_{\text{dc}}}{R} = \frac{0.318\, V_{\text{m}}}{R} \tag{4}$$

$$\text{Full-wave } I_{\text{dc}} = \frac{V_{\text{dc}}}{R} = \frac{0.636\, V_{\text{m}}}{R} \tag{5}$$

Although there are various three-phase rectifier circuits that can be built in several pulse levels as 6-ns pulses, the most widely used half- and full-wave rectifiers are considered in this section. The dc output voltage and currents of three-phase half-wave rectifier are shown in Eqs. (6) and (7), while the voltage and current equations are given in Eqs. (8) and (9), respectively.

$$\text{Half-wave } V_{\text{dc}} = \frac{3}{2\pi} \int_{\pi/6}^{5\pi/6} V_{\text{m}} \sin(\omega t) d(\omega t) = 0.827\, V_{\text{m}} \tag{6}$$

$$I_{\text{dc}} = \frac{0.827\, V_{\text{m}}}{R} \tag{7}$$

$$\text{Full-wave } V_{\text{dc}} = \frac{6}{2\pi} \int_{\pi/3}^{2\pi/3} \sqrt{3} V_{\text{m}} \sin(\omega t) d(\omega t) = 1.654\, V_{\text{m}} \tag{8}$$

$$I_{\text{dc}} = \frac{1.654\, V_{\text{m}}}{R} \tag{9}$$

The simulation results of a full-wave single-phase rectifier with RL load are shown in Fig. 3 where the upper axis illustrates the supply voltage and current, while the load voltage and current waveforms are given in the lower axis.

A single-phase controlled half-wave rectifier constituted a thyristor instead of a diode in the circuit given in the upper left cell of Fig. 2. The thyristor conducts on the positive half-cycles when a gate current is applied. The load voltage is controlled by thyristor referring to switching angle α that is known as phase delay on the generated switching pulses. The load voltage V_{dc} and current I_{dc} given in Eqs. (2) and (4) are rearranged by considering the angle α as given in Eqs. (10) and (11), respectively [5, 19, 43, 54, 60].

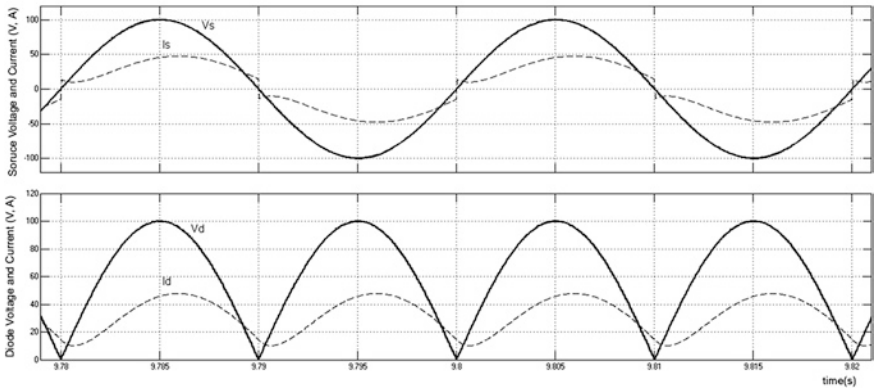

Fig. 3 Voltage and current waveforms of a full-wave single-phase rectifier at the supply and load sides

$$\text{Half-wave } V_{\text{dc}} = \frac{1}{2\pi}\int_{\alpha}^{\pi} V_{\text{m}} \sin(\omega t) d(\omega t) = \frac{V_{\text{m}}}{2\pi}(1 + \cos\alpha) \tag{10}$$

$$I_{\text{dc}}(\omega t) = \frac{1}{\omega L}\int_{\alpha}^{\omega t} V_{\text{L}}\, d\theta \tag{11}$$

where the load current I_{dc} is dependent on inductance voltage V_{L} in a *RL* load conduction. The V_{L} is calculated by substituting the resistor voltage V_{R} from source voltage V_{m} as shown in Eq. (12):

$$V_{\text{L}} = V_{\text{m}} - V_{\text{R}} = L\frac{\text{d}i}{\text{d}t} \tag{12}$$

It is obvious by referring to Eq. (11) that I_{dc} increases when V_{L} is positive and vice versa. The root mean square (rms) value of load current is calculated using Eq. (13):

$$I_{\text{rms}} = \frac{I_{\text{m}}}{2}\sqrt{1 - \frac{\alpha}{\pi} + \frac{\sin 2\alpha}{2\pi}} \tag{13}$$

$$I_{\text{m}} = \frac{V_{\text{m}}}{2\pi R}(1 + \cos\alpha) \tag{14}$$

The equations from 10 to 14 prove that the output voltage and current are controlled by the switching angle α. The increment occurred in angle α decreases the output voltage, whereas if the circuit is switched at $\alpha = 0°$, the circuit acts as a diode rectifier. In an RL-loaded thyristor rectifier as shown in Fig. 4, a shunt freewheeling diode is required to eliminate negative current ripple. Otherwise, load

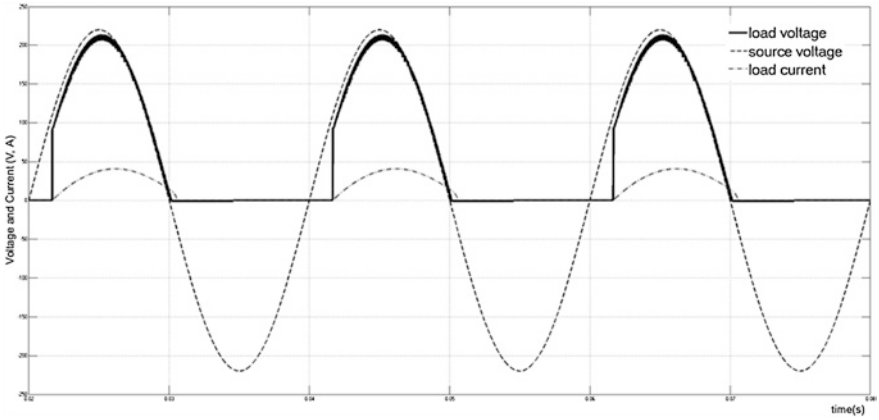

Fig. 4 Controlled half-wave rectifier waveforms, $\alpha = 30^{\circ}$

voltage and load current generate negative pulses in the reverse-biased half-cycles [19, 54, 60].

A single-phase controlled full-wave rectifier constituted four thyristors in H-bridge diagram that generates output voltage and current in each half-cycle. The average or dc output voltage and output current of pure R load are calculated referring to equations given below:

$$\text{Full-wave } V_{\text{dc}} = \frac{1}{\pi}\int_{\alpha}^{\pi+\alpha} V_{\text{m}} \sin(\omega t) d(\omega t) = \frac{V_{\text{m}}}{\pi}(1 + \cos\alpha) \tag{15}$$

$$I_{\text{dc}} = \frac{1}{\pi R}\int_{\alpha}^{\pi+\alpha} V_{\text{m}} \sin(\omega t) d(\omega t) = \frac{V_{\text{m}}}{\pi R}(1 + \cos\alpha) \tag{16}$$

If it is assumed that an inductive load is connected to output, the load voltage and rms current equations can be written as follows:

$$V_{\text{O}} = Ri_{\text{dc}} + L\frac{\text{d}i_{\text{dc}}}{\text{d}t} \tag{17}$$

$$I_{\text{rms}} = \frac{I_{\text{m}}}{\sqrt{2}}\sqrt{1 - \frac{\alpha}{\pi} + \frac{\sin 2\alpha}{2\pi}} \tag{18}$$

The load voltage and current waveforms of a full-wave controlled rectifier are shown in Fig. 5 on the same axis with source voltage shown in dotted line. The angle α is set to 30º in the simulation designed.

The controlled rectifiers introduced in this section are replaced with three-phase configuration when higher load power is required. The three-phase rectifier applications cover speed control of dc motors, general-purpose industrial power

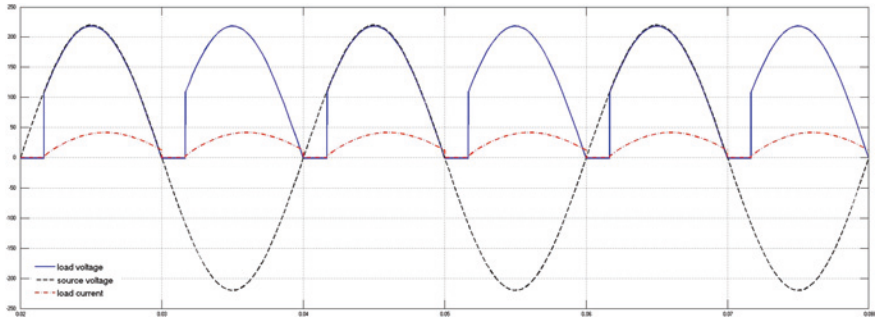

Fig. 5 Controlled full-wave rectifier waveforms, $\alpha = 30^{o}$

supplies, and high-voltage dc (HVDC) systems. Therefore, bidirectional switches as power transistors, IGBTs, and IGCTs are used in high-power rectifiers to perform four-quadrant operation. For those who are not familiar to rectifiers, further readings are recommended referring to [5, 10, 19, 43, 54, 60].

2.2 DC–DC Converters Used in Renewable Energy Sources

The dc–dc converters that are widely named as switch-mode power supplies (*SMPS)* are involved in modern power electronic to obtain high precision, lightweight, reliable, and efficient power supplies. In spite of existence of current dividers, most of the linear regulators are based on the principle of voltage dividing that causes to generate decreased output voltage that is lower than source voltage. On the other hand, the dc–dc converters are operated at higher switching frequencies and are able to increase the source voltage as well as decrease it. Although several converter topologies are implemented, either isolated or non-isolated, they can be limited to three basic categories such as buck *(step-down)*, boost *(step-up)*, and buck–boost *(step-down/step-up)* converters [46, 54, 60].

Buck converter, the circuit diagram for which is given in Fig. 6a, consists of a controllable switch *S*, a reverse-conducted diode *D*, a low-pass filter with inductor *L* and capacitor C besides the dc source, *V*s. The switching device preferred is usually a MOSFET owing to its high operating frequency. Filtering inductor and capacitor ensure to generate output voltage with a limited ripple ratio. The operating modes of a buck converter are determined by the inductor value that one is known as continuous conduction mode (CCM), while the other is discontinuous conduction mode (DCM). In the CCM, the value of inductor is fixed high enough to prevent inductor current to decrease down to zero. However, in case inadequate inductor values are used, the inductor current descents to zero for a while in each half-cycle that causes to operate in DCM. Separate analysis methods are required for CCM and DCM where the relation between these modes is described using boundary analysis method [43, 46, 54].

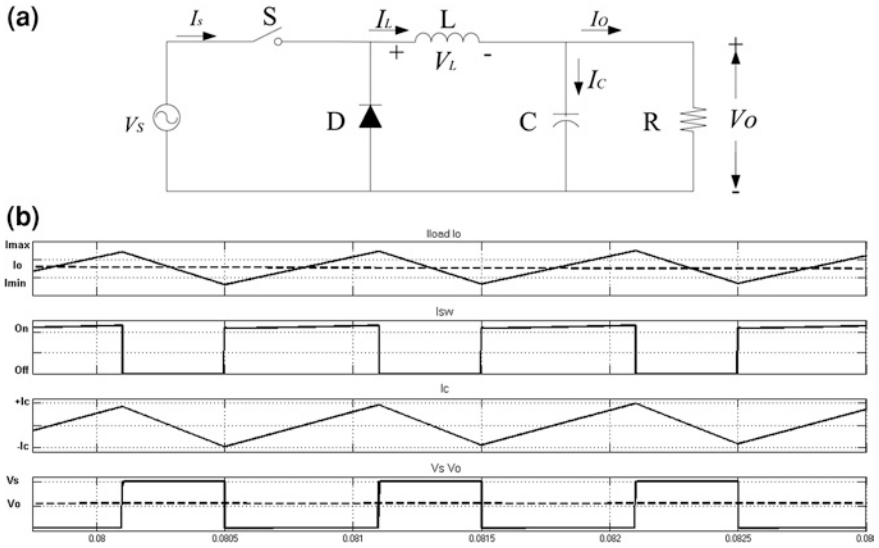

Fig. 6 Buck converter: **a** circuit diagram and **b** waveforms

The average output voltage of a buck converter is calculated as given in Eq. (19) regarding to duty cycle D that is the ratio of switching interval to entire period.

$$V_{\mathrm{O}} = \frac{1}{T}\int_0^T v_{\mathrm{O}}(t)\mathrm{d}t = \frac{1}{T}\left(\int_0^{t_{\mathrm{on}}} v_{\mathrm{S}}(t)\mathrm{d}t + \int_{t_{\mathrm{on}}}^{T} 0\,\mathrm{d}t\right)$$
$$\therefore\ V_{\mathrm{O}} = \frac{t_{\mathrm{on}}}{T}V_{\mathrm{S}} \tag{19}$$

Operating principle of the buck converter can be explained in detail referring to Fig. 6b in which the first axis indicates load current (I_{load}) and average output current (I_{o}). Continuous steady-state operation is dependent on periods of switch that increase the current and emf of inductor. When S is shifted to off period as shown in the second axis, inductor current and capacitor current begin to decrease in a previously calculated minimum limit in the CCM operation mode. The minimum inductor current which is higher than zero can be defined using Eq. (20):

$$L_{\mathrm{min}} = \left(\frac{TR}{2}\right)(1-D) \tag{20}$$

where the minimum inductor value depends to load resistance R, switching period T, and duty cycle D.

Figure 7a shows a boost (step-up) converter. This circuit configuration generates output voltage higher than supply voltage at all switching conditions that main applications include regenerative braking and regulated dc power supplies. When the switch is turned on, diode is reverse–biased, allowing us to increment inductor current

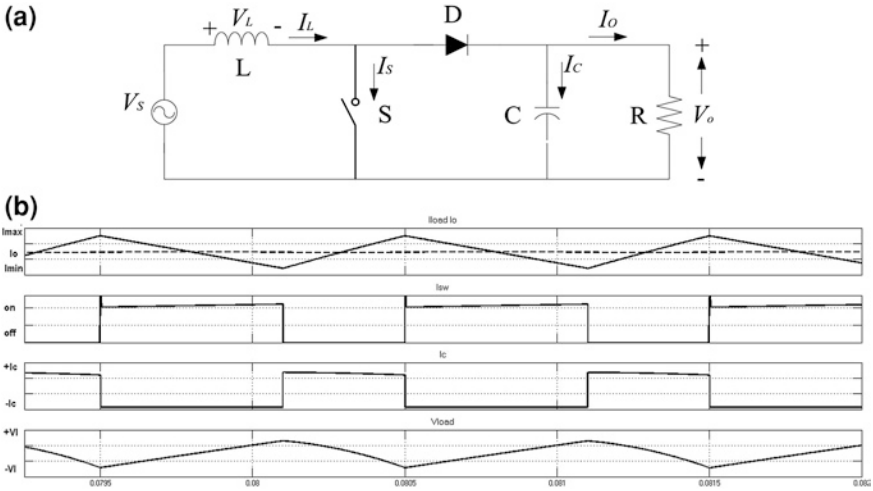

Fig. 7 Boost converter: **a** circuit diagram and **b** waveforms

I_L linearly. The inductor voltage V_L is equal to source voltage V_S during this interval defined as DT referring to duty cycle D and period T values as given in Eq. (21):

$$V_S = V_L = L\frac{dI_L}{dt} = L\frac{\Delta I_L}{T_{on}} = L\frac{\Delta I_L}{DT} \tag{21}$$

The charged energy of inductor is dumped in the switch off interval (1-D)T, and I_L continues to flow through the diode. At this interval, V_L yields $-V_O$ until the switch is turned on again. The inductor energy transferred to load is calculated as follows:

$$L\frac{dI_L}{dt} = V_S - V_O = -L\frac{\Delta I_L}{T_{off}} = -L\frac{\Delta I_L}{(1-D)T} \tag{22}$$

The current dumping ΔI_L of inductor is equal at each interval; therefore, eliminating ΔI_L in Eqs. (21) and (22) gives

$$\frac{DTV_S}{L} = \frac{(1-D)T}{L}(V_S - V_O) \tag{23}$$

and,

$$V_S = (1-D)V_O \tag{24}$$

Equating Eqs. (23) and (24), and rearranging the terms, yields the output voltage V_O definition of boost converter [5, 19, 43, 46, 60].

$$\begin{aligned} &V_S DT + (-V_O)(1-D)T = 0 \\ &\frac{V_O}{V_S} = \frac{D}{1-D} \\ &\therefore\ V_O = \frac{D}{1-D}V_S \end{aligned} \tag{25}$$

The maximum and minimum inductor currents are shown in the first axis of Fig. 7b in which switch current, capacitor current, and load voltage are also illustrated. Boost converter is analysed for CCM and DCM as well, and the relation between conduction modes is described using boundary analysis method. The minimum inductor value ensuring the converter to operate in CCM is expressed as follows in which capacitor voltage V_C equals load voltage V_O:

$$L = \frac{V_S \cdot (V_C - V_S) \cdot T}{\Delta I_L \cdot V_C} \tag{26}$$

Hence, the average output current in the boundary of CCM and DCM is written as follows:

$$I_{OB} = \frac{V_S \cdot T}{2L} D(1-D)^2 \tag{27}$$

From the information of the capacitor current, I_C, the peak-to-peak ripple voltage can be obtained, ΔV_o, which is shown in the last curve of Fig. 7b.

$$\begin{aligned} \Delta V_O = \Delta V_C &= \frac{1}{C} \int i_C(t)\, \mathrm{d}t \\ \therefore\ \Delta V_O &= \frac{V_O DT}{CR} \end{aligned} \tag{28}$$

The main application of buck–boost (step-up/step-down) converter includes the regulated dc power supply in which a negative polarity of source voltage at the output is required. Moreover, buck–boost converter can increase or decrease the output voltage with respect to source level. This circuit configuration illustrated in Fig. 8a is the one of the most widely used non-isolated converters since the isolation operation is electrically performed depending on diode *D*. The diode is reverse-biased during the conduction states, namely on the state of switch, and load is electrically isolated, while the energy flow is directed from source to inductor. When the switch *S* is turned off, the load current flows through inductor *L* and the charged energy is supplied to load in which the intervals depending on switching states are shown in the first axis of Fig. 8b, and at this stage, diode current I_D equals inductor current I_L. The inductor current is similar to boost mode during *on* state,

$$\frac{\mathrm{d}i_L}{\mathrm{d}t} = \frac{V_S}{L} \tag{29}$$

$$I_{Lmax} - I_{Lmin} = \left(\frac{V_S}{L}\right) DT \tag{30}$$

On the other hand, the inductor current is similar to buck mode during *off* state,

$$\frac{\mathrm{d}i_L}{\mathrm{d}t} = -\frac{V_O}{L} \tag{31}$$

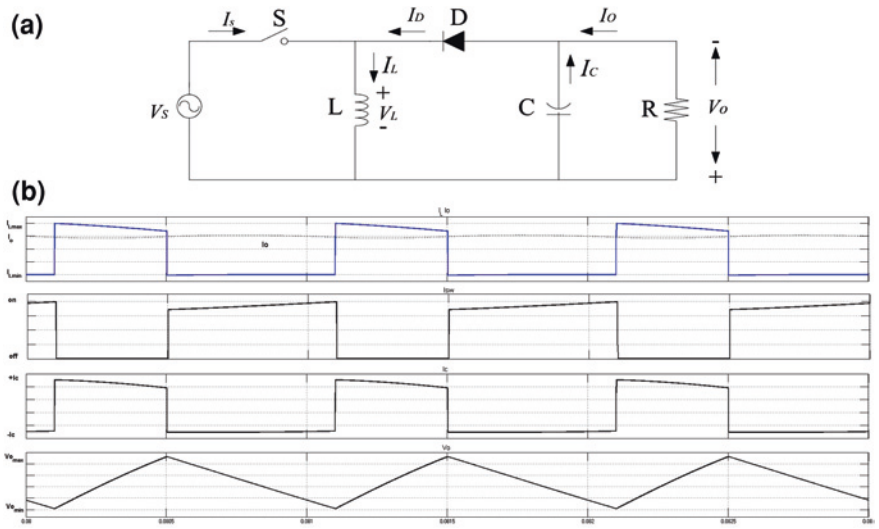

Fig. 8 Buck–boost converter: **a** circuit diagram and **b** waveforms

$$I_{\mathrm{Lmin}} - I_{\mathrm{Lmax}} = \left(-\frac{V_{\mathrm{O}}}{L}\right)(1-D)T \tag{32}$$

The output voltage equation is obtained by equating the variations in inductor currents as given in Eqs. (30) and (32) [5, 46, 54, 60]:

$$\begin{aligned} &\frac{V_{\mathrm{S}}DT}{L} - \frac{V_{\mathrm{O}}(1-D)T}{L} = 0 \\ &\therefore \ \frac{V_{\mathrm{O}}}{V_{\mathrm{S}}} = \frac{D}{1-D} \end{aligned} \tag{33}$$

The boundary of CCM and DCM operation modes is determined with respect to the value of inductor:

$$L_b = \frac{(1-D)^2 R}{2f} \tag{34}$$

A number of dc–dc converter topologies such as Sepic, Cuk, and Flyback are implemented to generate regulated dc power. However, these configurations are developed referring to the basic converters introduced in this section. Therefore, several power electronic books can provide detailed knowledge about these topologies [5, 10, 19, 43, 46, 54, 60].

2.3 Inverters Used in Renewable Energy Sources

The circuit supplying an ac load using dc power source is known as inverter where this operation is called inversion theory in power electronic. The adjustable speed drives (ASD), ac motor controllers, uninterruptable power supplies (UPS), and active power filters (APF) are the most widely known types of inverters among numerous applications. Inverters are designed to operate in single phase or in three phases owing to required power level. The dc power supply used assigns the inverter type where a dc current source forms a current source inverter (CSI), while a voltage source inverter (VSI) consists of a dc voltage source to generate ac output voltage. The input source and inverter connection are done over a serial inductor in CSI on the contrary of parallel capacitor in VSI configuration. The details of CSI and VSI can be found in textbooks about power electronics [10, 17, 19, 46, 54, 60, 75]. This section deals with the latest VSI topologies such as symmetrical and asymmetrical multilevel inverters (MLI), hybrid MLIs, modified sine wave MLIs, and grid-tie MLIS while the developing control methods are introduced as space vector, sinusoidal pulse width modulation (SPWM), third harmonic injection PWM, and hysteresis control.

Nabae introduced the MLI idea using neutral point clamping in the pioneer studies. In the initial studies, the third level was generated with the neutral point of dc power source in which the implemented topology was known as diode-clamped MLI as shown in Fig. 9a [17]. The most widely used MLI topologies in renewable energy applications are diode-clamped, flying capacitor and cascaded H-bridge, which are shown in Fig. 9a, c, respectively. The diode-clamped and cascaded H-bridge topologies provide the most proper involvement in wind turbine applications in which multi-megavolt-ampere (MVA) power handling is sought. The flying capacitor arrangement that is shown in Fig. 9b eliminates filtering requirement compared to diode-clamped topology. However, this circuit is not accepted as robust as cascaded H-bridge to obviate the harmonic contents and the cost issues. Several other MLI topologies such as grid-tied or string structures are implemented depending on the power ratings in solar energy application.

The MLI configuration provides lower common-mode voltage, lower voltage, and current increment ratio to decrease the harmonic orders, lower voltage stress on power switches, and flexible control opportunities. Several other MLI topologies are implemented using the existing supply or switch methodology. In case of asymmetrical supply voltage applied to H-bridge cells, the obtained topology is named asymmetric hybrid inverter in which the switches used in the cells are also different. On the other hand, the hybrid topology means that the cells only consist of different switches such as IGBT and GTO [17, 46, 75]. Some novel inverter topologies known as asymmetrical hybrid MLIs are arranged by cascading various inverter types or different switches together in the same topologies. Since the DC-MLI and cascaded H-bridge MLIs are the most proper inverter types used in wind energy systems, the asymmetrical hybrid inverters involving the combination of these two are illustrated in Fig. 10a.

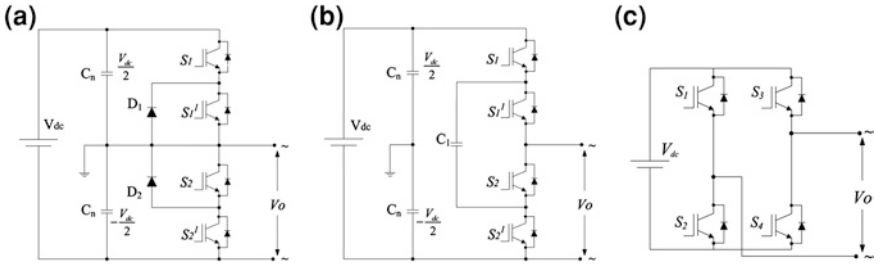

Fig. 9 MLI topologies: **a** three-level diode clamped, **b** three-level flying capacitor, and **c** three-level cascaded H-bridge

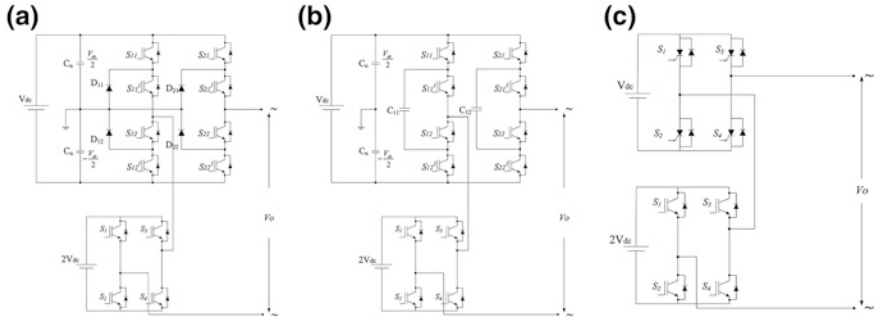

Fig. 10 Asymmetrical hybrid MLI topologies: **a** three-level diode clamped with H-bridge, **b** three-level flying capacitor with H-bridge, and **c** three-level cascaded H-bridges

The notion of asymmetrical hybrid inverters emphasizes that the inverter is designed in a cascaded connection through the several cells, and the voltage level of each cell is multiple of the previous cell. This kind of a design generates increased output voltage or current level while decreasing the required cell number compared to ordinary MLI topologies in order to obtain same output levels. Each power module of a hybrid MLI can operate at different dc voltage levels and switching frequencies that improve the efficiency and total harmonic distortion (THD) characteristics of inverter. However, conventional PWM strategies generating pulses at fundamental frequency cannot be appropriately used for asymmetrical hybrid MLIs since the switches in the higher-voltage modules should only be operated at high frequencies during some limited intervals. Hybrid modulation methods have been proposed that provide to get high-power cells switched at low frequency and low-power cells switched at high frequency in order to manage the required control strategy [17, 47, 55, 70]. The asymmetrical inverter shown in Fig. 10b consists of flying capacitor and cascaded H-bridge topologies together.

This arrangement is not preferred as much as the previous one because precharge control is required in order to condition the dc voltage shared in dc bus capacitors. Another arrangement of asymmetrical topology is shown in Fig. 10c in which the cascaded H-bridges constituted GTOs and IGBTs.

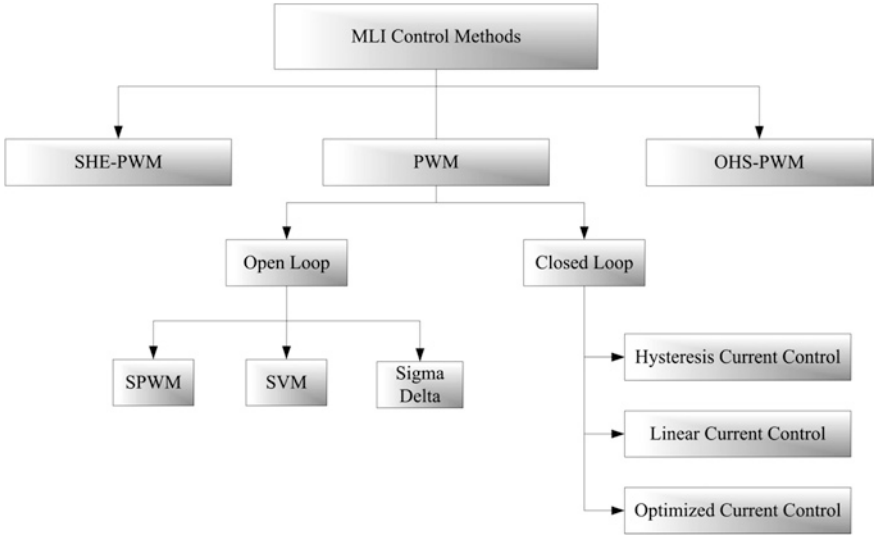

Fig. 11 MLI control methods

The efficiency indicators such as switching losses and harmonic reduction of an MLI are principally dependent on the control methods applied to the inverter. The control methods based on modulation types are known as fundamental switching frequency and high switching frequency. Besides this classification, another widely used definition for the modulation methods is open-loop and closed-loop strategies that are illustrated in Fig. 11.

The outstanding control methods are selective harmonic elimination pulse width modulation (SHE-PWM), regular PWM, and optimized harmonics stepped pulse width modulation (OHS-PWM). The regular PWM method can be applied in both open-loop and closed-loop strategies owing to its control strategy. The open-loop PWM techniques are SPMW, space vector PWM, and sigma-delta modulation, while closed-loop current control methods are defined as hysteresis, linear, and optimized current control techniques. SHE-PWM is not considered as an appropriate solution for closed-loop implementation since the predefined calculations are required. SHE-PWM that is proposed by Patel in 1973 [52] is based on fundamental frequency switching theory and depends on the elimination of defined harmonic orders. The main approach of this method focuses on defining the switching angles to eliminate specific harmonic orders. The Fourier expansion of an 11-level inverter is calculated as given in Eq. (35) in order to determine the output voltage:

$$V(wt) = \sum_{n=1,3,5,..}^{\infty} \frac{4V\mathrm{dc}}{n \cdot \pi} \cdot (\cos(n \cdot \theta_1) + \cos(n \cdot \theta_2) + \cdots + \cos(n \cdot \theta_5)) \cdot \sin(n \cdot wt) \tag{35}$$

where n denotes the harmonic order injected to the output. The switching angles of an 11-level inverter that are required to eliminate 5th, 7th, 11th, and 13th harmonics are calculated at the fundamental switching frequency as shown in Eq. (36):

$$\left.\begin{array}{l}\cos(\theta_1)+\cos(\theta_2)+\cos(\theta_3)+\cos(\theta_4)+\cos(\theta_5)=5.m_a\\ \cos(5\theta_1)+\cos(5\theta_2)+\cos(5\theta_3)+\cos(5\theta_4)+\cos(5\theta_5)=0\\ \cos(7\theta_1)+\cos(7\theta_2)+\cos(7\theta_3)+\cos(7\theta_4)+\cos(7\theta_5)=0\\ \cos(11\theta_1)+\cos(11\theta_2)+\cos(11\theta_3)+\cos(11\theta_4)+\cos(11\theta_5)=0\\ \cos(13\theta_1)+\cos(13\theta_2)+\cos(13\theta_3)+\cos(13\theta_4)+\cos(13\theta_5)=0\end{array}\right\} \quad (36)$$

The switching angles of θ_1, θ_2,..., θ_5 should be determined to minimize voltage THD ratio, while m_a defines the modulation index of the modulator. The exact angles are obtained using Newton–Raphson iterations since the parameters of Eq. (36) are nonlinear. The calculated angles of Eq. (36) are $\theta_1 = 6°$, $\theta_2 = 18°$, $\theta_3 = 27°$, $\theta_4 = 45°$, and $\theta_5 = 62°$ by assuming m_a as 0.8 and solving with Newton–Raphson Iteration [17].

In SPWM, a sinusoidal reference waveform is compared to a triangular carrier waveform to generate switching sequences for switches. The earliest fundamental frequency SPWM method was proposed to minimize the switching losses occurred in hard switching applications. The latest multicarrier SPWM methods that are classified according to vertical or horizontal arrangements of carrier signal are implemented to increase the efficiency of the MLI. The vertical carrier distribution techniques are phase disposition (PD), phase opposition disposition (POD), and alternative phase opposition disposition (APOD), while horizontal arrangement is phase-shifted PWM (PS-PWM) method [17]. Another prevailing control method for multilevel inverters is space vector PWM (SVM) that considers each switching vector as a point in complex space of (α, β). The SVM yields better harmonic elimination and fundamental voltage ratios compared to other methods. Furthermore, the maximum peak value of the output voltage is 15 % greater than triangular carrier-based modulations. The sector detection and look-up table that are required for all vectors make the SVM method quite complicated. Although the difficulty in determining sectors and switching sequences for increased n-level of inverter, the digital signal processor (DSP) and/or microprocessor implementations provide proper solution. The SVM method uses a number of level-shifted carrier waves to compare reference phase voltage. Any three-phase n-level space vector diagram consists of six sectors that all contain $(n-1)^2$ vector combinations per sector and n^3 switching states. Figure 12 shows the space vector diagram of a three-phase three-level DC-MLI inverter in which a phase leg is depicted in Fig. 9a. Each phase leg of inverter includes four switching devices and has three different switching states that are represented as 1, 0, or −1 to illustrate positive, zero, and negative switching sequences.

The V_1, V_2, and V_8 voltage vectors are calculated by assuming that the reference voltage vector V_{ref} is located in the second region (Δ_2) of S_1 sector during the sampling period T_s. The reference voltage also depends on the dwelling times of voltage vector. Hence, the equation for switching time of the voltage vectors constituting the reference voltage is given as in Eq. (37):

$$V_{\text{ref}} \cdot T_s = V_1 \cdot t_a + V_2 \cdot t_b + V_8 \cdot t_c \quad (37)$$

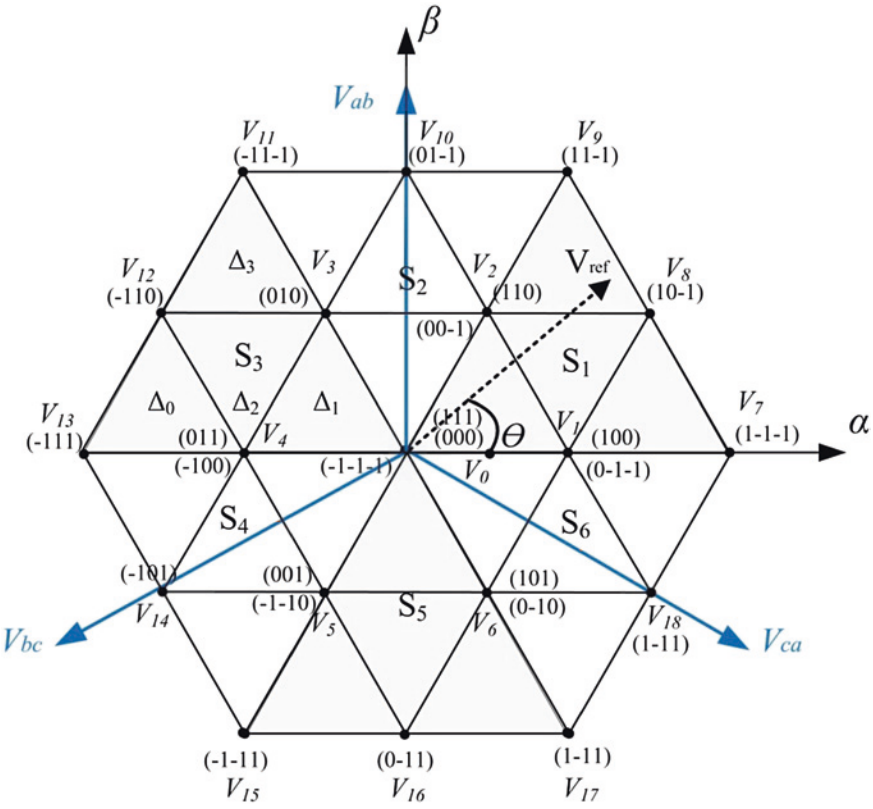

Fig. 12 Space vector diagram of a three-level diode-clamped inverter

The switch in intervals of voltage vectors is determined using Eqs. (37) and (38):

$$\begin{aligned} t_a &= T_\mathrm{s} - 2n\sin\theta \\ t_b &= 2n\sin\left(\frac{\pi}{3}+\theta\right) - T_\mathrm{s} \\ t_c &= T_\mathrm{s} - 2n\sin\left(\frac{\pi}{3}-\theta\right) \end{aligned} \tag{38}$$

in which

$$n = \left(\frac{4\sqrt{3}}{3}\right)(V_\mathrm{ref}/V_\mathrm{dc})T_\mathrm{s} \tag{39}$$

The calculations given above are done to obtain the first V_ref in a sector where it is required to be repeated to determine each switching sequence. By this way, the calculated values are stored in a look-up table and are applied to switches

according to a predefined switching calculation. This is the main deficiency of SVM that creates confusion when the voltage level is increased over three.

Several other modulation methods are implemented to decrease the switching losses and to increase the efficiency. Further reading about inverter topologies and control methods can be found in various textbooks about power electronic theory and in reference [17].

3 Control Methods in Solar Systems

Edmund Becquerel, a French physicist, firstly discovered the PV energy by generating electricity when he illuminated an electrode in electrolyte solution in 1839. Adams and Day applied the PV energy to solid materials around 40 years later, and this study is assumed as the first practical PV application. The primary PV cells made of selenium provide almost 1 or 2 % efficiency. Probably, Einstein was the most important contributor of PV by explaining theoretical PV effect in 1904 that brought a Nobel Prize to him in 1923. The first-generation silicon PV cells were produced in 1940s and 1950s by Czochralski, a Polish scientist. The solar panels that consist of numerous PV cells were commercially available in 1963 when Sharp Corporation succeeded in producing practical silicon photovoltaic modules. First applications of solar cells are seen in Vanguard I space satellite, Explorer III, Vanguard II, and Sputnik-3 in 1958 and 1959. The world's first largest PV array was built in Japan with 242 Wp rated power in 1963 [45, 69].

The bounce of solar energy was occurred by obtaining higher efficiency and lower cost of doped silicon cells in late 1980s. The analytical model of a PV cell is designed using the mathematical equations given in the literature. The electrical power obtained from a PV cell depends on the short-circuit current (I_{sc}), the ideality factor of the diode (η_I), the shunt resistance (R_{sh}), and the series resistance (R_S) parameters given in Fig. 13a. The current–voltage *I-V* characteristic of a PV panel is determined using Eq. (40) [32, 69]:

$$I_o = I_L - I_{Rs}\left(\left[\exp\left(\frac{V_O + I_o R_s}{\eta_I V_T}\right) - 1\right] - \frac{V_O + I_O R_S}{R_{sh}}\right) \tag{40}$$

where

I_o output current of the panel,
I_L current generated by irradiation value,
I_{Rs} current of output resistor,
V_T thermal voltage,
V_o output voltage,
η_I diode's ideality factor.

The current–voltage and output power analyses of a 170-W PV panel that is designed using Eq. (39) are shown in Fig. 13b, c, respectively [32]. The verification

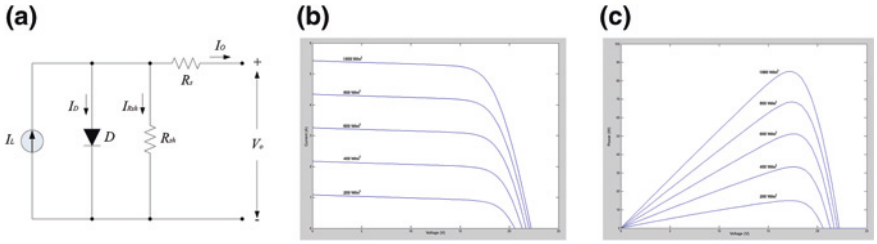

Fig. 13 Design and analysis of a PV cell: **a** equivalent circuit model of a PV cell, **b** current–voltage characteristic, and **c** generated power characteristic

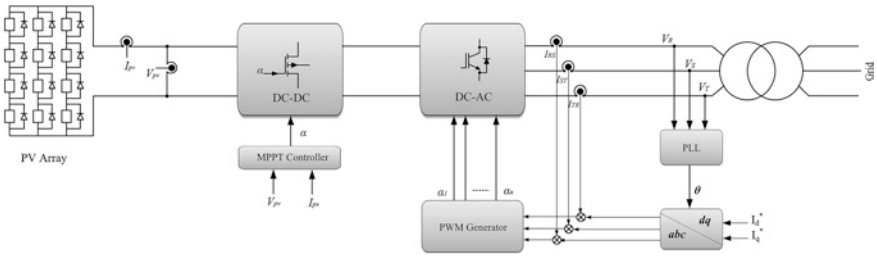

Fig. 14 A comprehensive block diagram of a solar energy system

tests are performed by increasing the irradiation level from 200 W/m^2 to 1,000 W/m^2. The obtained curves verify the reference PV module of manufacturer under same irradiation values [58].

A complete block diagram of a solar system is illustrated in Fig. 14 with its energy conversion and control units in which a converter and an inverter are controlled using current and voltage values. The solar panels in Fig. 14 are assumed to be arranged in a string array structure. A dc–dc converter is the main component of a solar energy conversion system in which an inverter and grid integration are preferably contained. Besides this configuration, the converter of a grid-connected solar system can be arranged using a central converter that contains an inverter and a string converter with the connection of all the PV arrays to a unique converter or a multistring inverter with parallel connection of string inverters. The outstanding control method used in dc–dc converters is known as maximum power point tracking (MPPT) that is based on several algorithms.

The MPPT algorithm controls the dc–dc converter to adapt the dc voltage across the PV array, and hence, maximum power transfer is obtained. On the other hand, MPPT algorithms are used in PV inverters in order to increase the obtained ac power. Several inverter control methods are implemented using MPPT, proportional–integral (PI), and proportional–integral–derivative (PID). The control methods used in solar energy conversion systems are introduced according to MPPT algorithms, power flow control regarding to current control methods, grid synchronization, and power quality control that is related to inverter control in this section.

3.1 Maximum Power Point Tracking Algorithms

MPPT is an essential part of a solar system owing to its incremental effects on the harvested total energy. The MPPT algorithms are being researched since a few decades, and several control approaches are widely adopted by many manufacturer and researchers. The MPPT algorithms are compared through their complexity, convergence time, sensor requirements, implementation costs, and response stability. The "perturb and observe" (P&O) and "incremental conductance" (InCon) algorithms where both are based on the hill-climbing method are outstanding MPPT algorithms among others. Besides these algorithms, numerous MPPT algorithm collections are introduced by researchers [20, 21, 30].

The power–voltage and current–voltage characteristic curves of a PV panel are shown in Fig. 15a, b, respectively. The MPPT algorithm is intended to find the maximum voltage V_{MPP} or the maximum current I_{MPP} to generate the maximum power output P_{MPP} for a given temperature and irradiance value. The hill-climbing method that is the main idea of MPPT provides to adjust duty ratio of switch in a converter. On the other hand, P&O and InCon algorithms that are based on hill-climbing method control the perturbation of the voltage or conductance of PV panel, respectively [20, 21].

The P&O algorithm implies modifying the voltage difference between PV array and the power converter by perturbing the duty cycle. The flow chart of P&O algorithm is shown in Fig. 16a in which the voltage and current variations of PV array are instantly measured. The latest perturbation of the obtained power is compared to the previous perturbation, and the difference is used to determine the increment or decrement ratio in this control method. In the next step, the determined difference is used to indicate the next duty cycle rate of PWM signal. The implemented algorithm seeks the increment of power perturbation and keeps the duty cycle in the same direction in order to reach the MPP, and if there is a decrement in the power, then the algorithm reverses the perturbation. The algorithm repeats this seeking until the MPP is reached, and algorithm generates stable duty cycle when the system reaches to the MPP. The oscillation at the MPP is requested to be minimized in order to increase the stability [20, 21, 30].

The InCon algorithm is established upon the fact that the differential value on the MPP is zero, while it is positive on the left-hand side and is negative on the right-hand side that is obviously shown in Fig. 15a. The change occurred in the MPP is determined by comparing the alteration in power and/or conductance. Once the algorithm seizes the MPP, the duty cycle is intended to be kept at actual value until any change occurs in ΔI. The algorithm decreases or increases the reference voltage V_{ref} regarding to alteration.

Both MPPT algorithms, P&O and InCon, have a main drawback on tracking the MPP under rapid atmospheric changes since they are based on hill-climbing method. Numerous methods have been proposed to overcome this drawback [20]. The fuzzy logic control and neural network-based MPPT controller are

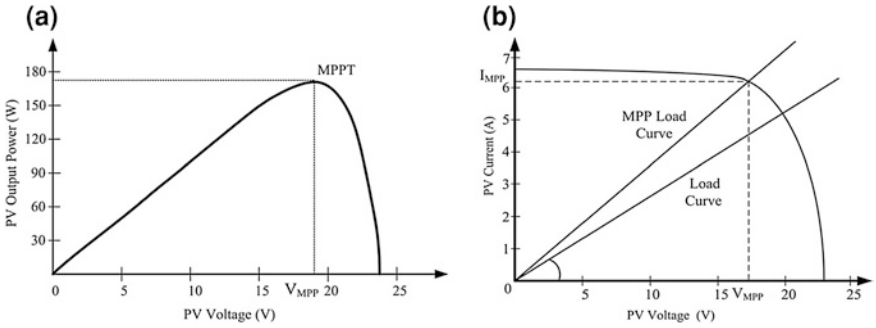

Fig. 15 Characteristic curves of MPPT: **a** power–voltage curve and **b** current–voltage curve

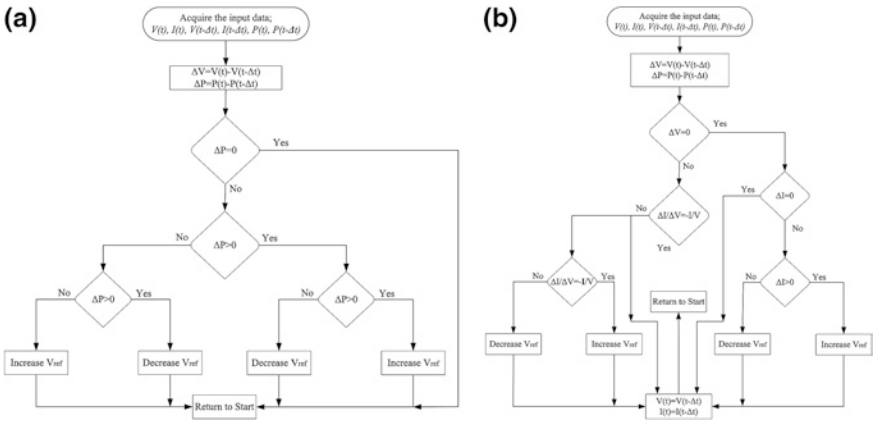

Fig. 16 Flow chart of MPPT algorithms: **a** perturb and observe and **b** incremental conductance

implemented to generate precise output even against the rapid changes in irradiance and temperature [30, 71, 73].

3.2 Current Control Methods

The power flow of a grid-connected solar system is performed with several current control methods. One of the most widely known current control methods is based on PI control that can be found almost in all industrial applications. The PI control of a grid-connected converter pursues the reference current and supplies the desired current value to the grid. This control is executed by converting natural frame *abc* to synchronously rotating reference frame *dq*. The transfer function of a PI controller is given in Eq. (41) in which K_P and K_I are the proportional and integrative gains.

$$T_{\mathrm{PI}}(s) = K_{\mathrm{P}} + \frac{K_{\mathrm{I}}}{s} \tag{41}$$

The voltage and currents can be described in various reference frames for the three-phase power system that involves the controller to be designed in different coordinate schemes. The natural *abc* reference system can be described as shown in Eq. (42) in which V_{m} is the peak value of the voltage and θ is the phase of the voltage.

$$\begin{bmatrix} V_a \\ V_b \\ V_c \end{bmatrix} = \begin{bmatrix} V_{\mathrm{m}} \cos(\theta) \\ V_{\mathrm{m}} \cos(\theta - \frac{2\pi}{3}) \\ V_{\mathrm{m}} \cos(\theta + \frac{2\pi}{3}) \end{bmatrix} \tag{42}$$

The space vector transformation, namely three-phase to two-phase conversion, that is widely used in PWM generation can be adopted with the term of stationary frame or $\alpha\beta$ frame. The voltage space vector v'_{s} is presented using the instantaneous values of v_a, v_b, and v_c instead of phasors.

$$v'_{\mathrm{s}} = v_\alpha + jv_\beta \tag{43}$$

$$v'_{\mathrm{s}} = k(v_a + \alpha v_b + \alpha^2 v_c) \tag{44}$$

in which α, α^2, and k are

$$\alpha = e^{-j\frac{2\pi}{3}} \quad \alpha^2 = e^{-j\frac{4\pi}{3}} \quad k = \frac{2}{3}$$

The *abc*-to-$\alpha\beta$ transformation matrix is obtained as given in Eq. (46) regarding to Eq. (45);

$$\begin{bmatrix} v_\alpha \\ v_\beta \end{bmatrix} = T_{\alpha\beta} \begin{bmatrix} v_a \\ v_b \\ v_c \end{bmatrix} \tag{45}$$

$$T_{\alpha\beta} = \frac{2}{3} \begin{bmatrix} 1 & -\frac{1}{2} & -\frac{1}{2} \\ 0 & -\frac{\sqrt{3}}{2} & \frac{\sqrt{3}}{2} \end{bmatrix} \tag{46}$$

Since the v_α and v_β values that are presented by Eq. (45) are functions of time, the space vector v'_s is a rotating frame. The reference frame considering v'_s provides to achieve synchronously rotating reference frame that is also called the *dq* reference frame. The block diagram of a PI controlled inverter is shown in Fig. 17 [75].

The natural frame to stationary frame is performed using the measured three-phase current, and the current controller blocks generate reference voltages supplied to PWM generator. The phase-locked loop (PLL) is involved in decreasing the error rate between the reference voltage and the actual voltage V_{q} as shown in Fig. 18. The park transformation determines the voltage level of the measured

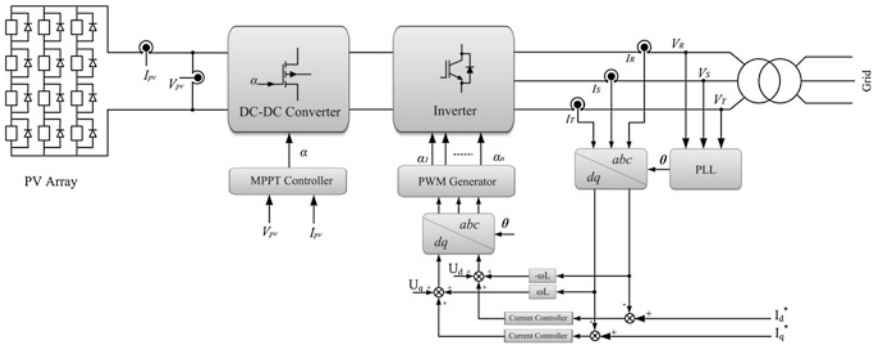

Fig. 17 Block diagram of a PI current control in grid-connected inverter

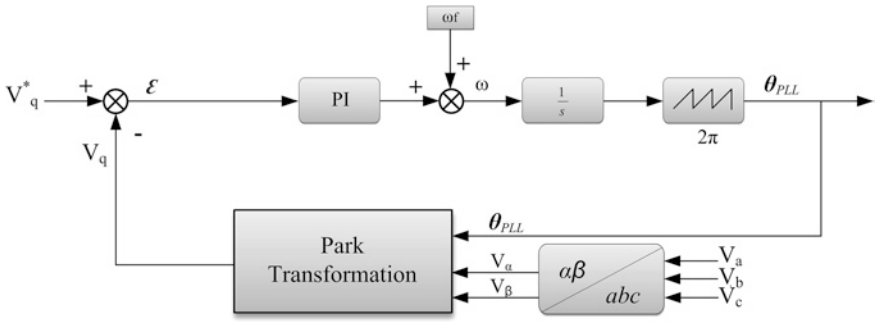

Fig. 18 Block diagram of a three-phase PLL

value, and feedback signal is applied to a comparator to detect the accurate error rate ε. In the next step of operation, the PI controller generates updated signals to minimize the error regarding to natural frequency ω_f.

The output voltage of a grid-connected inverter should be synchronized to amplitude, phase angle, and frequency of the grid voltage that are the most significant parameters. The grid synchronization is dependent on accurate, fast, and precise detection of the required parameters. The grid synchronization of the inverter involves robust algorithms to succeed a perfect match through the generated and the utility voltage at unity power factor. Two synchronization algorithms that are zero-crossing detection (ZCD) and phase-locked loop (PLL) outshine among others.

The ZCD depends on the detection of zero-crossing instants, while PLL is based on feedback signals that are generated referring to the phase shift of inverter voltage and grid voltage. A PLL control block consists of a phase detection unit that generates the instant error signal, a loop filter, and a voltage-controlled oscillator (VCO). Phase detection unit measures the phase difference between the reference and feedback signal that is acquired from the output voltage. The generated error signal is supplied to the loop filter in order to detect the dc component of

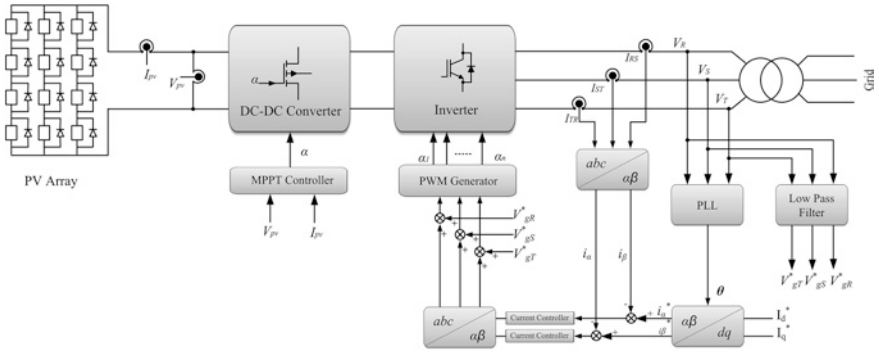

Fig. 19 Block diagram of a PR current control in grid-connected inverter

phase error. The amplified dc component is fed to VCO that particularly consists of a PI controller to generate frequency using the voltage input. This loop seeks for locking operation of output signal by minimizing the error signal. The block diagram of a three-phase PLL is depicted in Fig. 18. The principal idea of the PLL is to change the inverter current frequency ω_i when the inverter current and the grid voltage are out of phase [13, 53, 67].

The linearized transfer function of PLL $T_{\mathrm{PI}}(s)$ given in Eq. (48) is calculated using the form equation of the PI that is given in Eq. (47) [41, 54, 75].

$$\mathrm{PI}(s) = K_{\mathrm{p}}\left(\frac{K_{\mathrm{I}}s + 1}{K_{\mathrm{I}}s}\right) \tag{47}$$

$$T_{\mathrm{PI}}(s) = \left(\frac{K_{\mathrm{p}}s + \frac{K_{\mathrm{P}}}{K_I}}{s^2 + K_{\mathrm{P}}s + \frac{K_{\mathrm{P}}}{K_{\mathrm{I}}}}\right) \tag{48}$$

One of the most popular controllers used in grid-connected systems is the proportional resonant (PR) controller that regulates the current injected to the grid. The PR controller, the block diagram for which is given in Fig. 19, is developed to eliminate steady-state error of PI controller that occurs at the fundamental frequency. A PR controller consists of a proportional unit and a resonant unit as presented in Eq. (49) in which ω is the resonant frequency:

$$T_{\mathrm{PR}}(s) = K_{\mathrm{P}} + K_{\mathrm{I}}\frac{s}{s^2 + \omega^2} \tag{49}$$

This controller provides a high gain around the resonance frequency, and hence, it assures to eliminate the steady-state error that occurs in PI control. Besides the high-gain advantage, the PR controller contains a harmonic compensator to improve the performance by decreasing the THD ratio of the inverter. The transfer function of the harmonic compensator in which the harmonic order h can be easily added to PR control is given in Eq. (50) [6, 57, 75].

$$T_{\mathrm{HC}}(s) = \sum_{h=3,5,7,\ldots} K_{\mathrm{Ih}} \frac{s}{s^2 + (\omega h)^2} \tag{50}$$

The *abc-to-*$\alpha\beta$ block transforms the line currents to $\alpha\beta$ components i_α and i_β. In a balanced system, the α component stands for phase R, while the β component is combination of the S and T phases. On the other hand, the *dq-to-*$\alpha\beta$ transformation is for PLL controller that generates the phase information of grid voltage [57, 75].

Several control methods are also improved to increase the power quality in more accurate ways. The voltage H^∞, current H^∞, and current repetitive control methods are based on the control of the mutual active and reactive power flow between converter and the grid. H^∞ and repetitive control techniques use all the three phases in *abc-to-*$\alpha\beta$ and *dq-to-*$\alpha\beta$ transformations in order to minimize the possible steady-state errors in unbalanced systems. Therefore, the control system copes with unbalanced grid voltages and voltage sags within the limit given by the nature and predefined waveform quality requirements [75].

4 Control Methods in Wind Systems

A wind turbine (WT) is an electromechanical system itself that the propulsion is coped by the kinetic energy of the wind. The air density of wind that passes through the blades makes the rotor to turn owing to the rotation of the blades. The professional wind turbine systems (WTS) started to be implemented in the early 1980s with a few kilowatts (kW) rated power. However, the actual rated power of WTSs reached to multi-MW. The first technology that is also known as Danish concept is based on squirrel-cage induction generator (SCIG) directly connected to grid. This concept later classified as fixed-speed wind turbine or Type A with the advantage of simple and robust technology that assured the reliable operation conditions that are shown in Fig. 20a. Besides these advantages, it is mostly preferred because of its low-cost electrical and mechanical components. However, several disadvantages are faced such as lower power quality, mechanical stress on rotor bar, and uncontrolled active and reactive power consumption that is particularly required for generator. Furthermore, all the fluctuations of the wind speed are converted to mechanical torque and electrical energy by the generator and are supplied to the grid. This situation may cause large voltage fluctuations when it is connected to weak grids [3, 8, 12, 29].

4.1 Wind Turbine Dynamics

The developments seen in power electronic also affected the operation characteristics of wind turbine. The novel concept that is developed owing to the latest power electronic is known as variable-speed WT technology. The variable-speed WT is

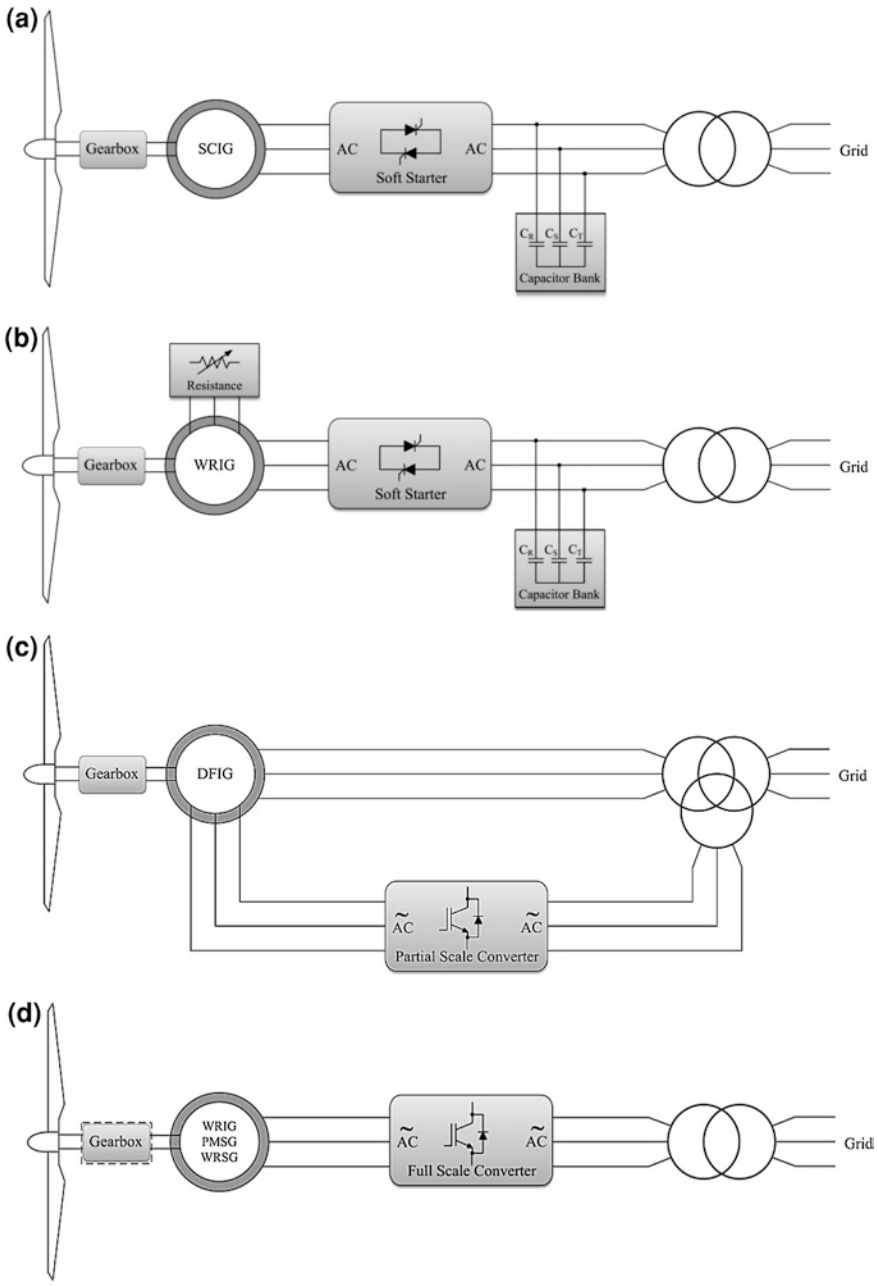

Fig. 20 Wind turbine configurations: **a** Type A: Fixed-speed wind turbine system with soft starter, **b** Type B: Variable-speed wind turbine system with soft starter, **c** Type C: Variable-speed wind turbine system with partial-scale AC-AC converter, and **d** Type D: Variable-speed wind turbine system with full scale AC-AC converter

implemented to acquire increased efficiency and quality in terms of power and waveforms. The most widely used and accepted variable-speed configurations are named Type B, Type C, and Type D that are, respectively, shown in Fig. 20b, c, d. The variable-speed WTs operate in a wide range of wind speed (v) and are able to accelerate or decelerate the rotational speed (ω) mechanically or electrically.

The control of ω allows us to obtain stable tip-speed ratio λ at a predefined value regarding to the maximum power coefficient. For a given wind speed, the rotor efficiency C_p varies owing to λ, which is defined as follows [33]:

$$\lambda = \frac{r\omega}{v} \tag{51}$$

where

r = radius of the rotor (m),
ω = rotational speed (rad/s)
v = wind speed (m/s).

In order to acquire high-power output at increased wind speeds, the rotor speed should be fixed to high values as possible by keeping the λ constant at the optimum limit. On the other hand, the output power of a WT is equalized depending on many parameters such as wind speed, air pressure, pitch angle, and so on. The mechanical output power of a WT is determined using Eq. (52) [33],

$$P_m = \frac{1}{2} C_p(\alpha, \beta) \cdot \rho \cdot A \cdot v^3 \tag{52}$$

where

P_m = mechanical output power of the wind turbine,
C_p = power coefficient (the rotor efficiency),
α = pitch angle (degree),
β = peak velocity ratio,
ρ = air density (kg/m^3),
A = rotor swept area (m^2),
v = wind speed (m/s).

The Type B concept that is also known as limited variable-speed WT consists of wounded rotor induction generator (WRIG) and used since 1990s. The capacitor bank provides the reactive power compensation, while the soft-starter prevents inrush current during the grid connection. The typical feature of the Type B is related to rotor winding of generator. The resistances serially connected to rotor winding are essential to change the torque characteristic of the generator in a limited range that varies up to 10 % over the synchronous speed. This feature is known as OptiSlip® that is a trademark of Vestas.

Another variable-speed WT configuration Type C, namely doubly fed induction generator (DFIG) concept, is configured with partial-scale converter and a WRIG that increases the limited range of Type B up to 30 % owing to the energy generated in the rotor circuit. The partial-scale converter also handles the reactive power

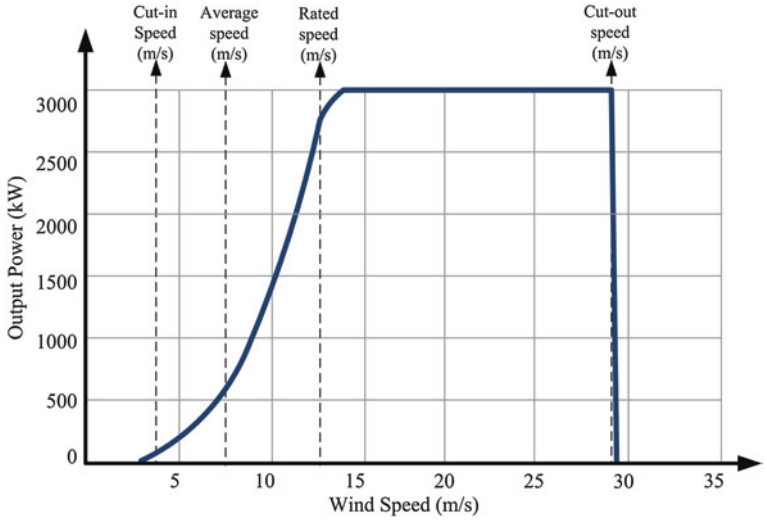

Fig. 21 Power curve of a WT

compensation instead of capacitor bank. Although this concept has been used extensively in 2000s, the novel WT configuration Type D is now the most widely preferred concept that corresponds to the full variable-speed wind turbine. The generator in Type D is connected to the grid through a full-scale frequency converter that manages the reactive power compensation and provides smoother grid connection. The generator can be one of the wound rotor synchronous generators (WRSGs), the WRIG, or the permanent magnet synchronous generator (PMSG) [3, 12, 14, 33].

4.2 Power Control Methods of Wind Turbines

The power curve of a WT is obtained using Eq. (52). The significant variables of the power curve are cut-in wind speed, average wind speed, rated wind speed, and cut-out wind speed that are illustrated for a 3-MW WT in Fig. 21. The cut-in speed describes the minimum speed that starts the rotor in order to rotate and generate power, and it is typically 3 m/s. The average wind speed defines the region between cut-in and rated speed range. The rated output power of a WT is achieved around 12–17 m/s.

The output power reaches to the maximum limit of generator from rated speed to cut-off speed. The cut-off limit prevents the probable damages that may occur at higher wind speeds. The cut-off speed range is fixed around 25–30 m/s. The significant parameters in terms of power control intervals of a WT are shown in Fig. 21 together in which cut-in speed is set to 4 m/s, while average speed is set at 8 m/s, rated speed at 12 m/s, and cut-out speed at 28 m/s [3, 14].

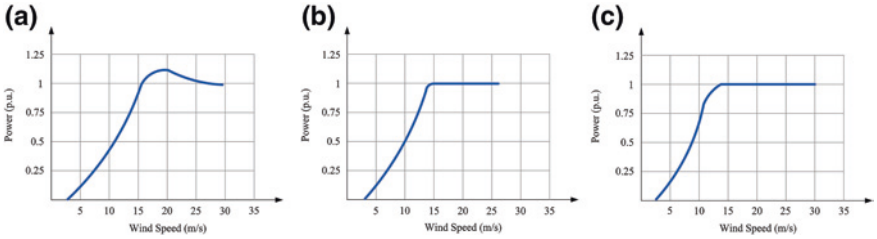

Fig. 22 Power control methods of WTs: **a** stall control, **b** active stall control, and **c** pitch control

Table 1 Power control methods corresponding to WT configuration [3]

WT configuration		Power control		
		Stall	Pitch	Active stall
Fixed speed	Type A	Type A0	Type A1	Type A2
Variable speed	Type B	Type B0	Type B1	Type B2
	Type C	Type C0	Type C1	Type C2
	Type D	Type D0	Type D1	Type D2

There are several methods to control the aerodynamic forces on the rotor and to limit the power in stormy winds in order to prevent damage to the wind turbine. The outstanding control methods are stall control, active stall control, and pitch control that are classified as Type 0, Type 1, and Type 2, corresponding to WT configurations. The characteristic curves of the methods are illustrated in Fig. 22. The stall control known as passive control is the cheapest and robust method where the rotor blades of wind turbines are fixed on the hub at a fixed angle. The aerodynamic design of rotor blades decelerates the WT at higher wind speeds. The improved stall control is defined with the term of active stall control where the rotor blades are pitched to increase the efficiency at lower wind speeds. The pitched blades are moved to opposite direction at higher wind speeds, and the air density is compensated itself. The pitch control method is used to adjust the rotor blades to the inner or outer, corresponding to the wind speed.

This control method provides assisted start-up and immediate stop features. At high wind speeds, the generated output power is limited around the rated power as shown in Fig. 22c [3, 38].

The power control methods and appropriate matching to WT configurations are depicted in Table 1. All the control methods are used in Type A WTs appropriately, while the variable-speed configurations require fast pitch control. The grey-shaded cells in the table define the abandoned power control methods.

4.3 Power Electronic Control of Variable-Speed Wind Turbines

The most widely used generator types of wind turbines are induction generator and synchronous generator. The SCIG is generally used in the fixed-speed wind turbines owing to its damping effect. The reactive power required to magnetize the

generator circuit is obtained from parallel capacitor bank. The WRIG that is the another type of induction generator supports only partial variable-speed operation by connecting external resistors to rotor winding that provides a limited increased energy acquisition up to 10 % of synchronous speed and reduced mechanical load to the grid. This configuration is essential for decreasing the reactive power requirement and obtaining increased energy output at wind speed lower than the rated speed. Two different exciting methods used for synchronous generators are obtained by externally applied dc excitation and by permanent magnets.

The wind turbines that use synchronous generator cannot be directly connected to the grid due to damping requirements. Most of the pioneer WT producers implemented multi-MW wind turbines using a PMSG or a DFIG in generator part. The gearbox is used to obtain high torque mechanical power at low wind speed. Besides this advantage, there are several risk factors such as periodic maintenance, misalignment at wind gusts, limited lifetime, and malfunction that exists for gearbox systems. Therefore, several operation methods are extensively researched to obtain gearless WTs that are based on direct-drive characteristic. There is also noticeable interest on multipole synchronous generators that remove the gearbox requirement [14, 38].

As a result of trade-off analyses conducted through generator types, the variable-speed WTs are implemented using PMSGs in Type D or DFIGs in Type C configurations. Consequently, the power electronic control methods of variable-speed WTs are examined corresponding to these generator types. PMSG has several advantages such as gearless configuration opportunity, fully controllable power electronics and grid interconnection, removed external dc excitation, and fault ride through control. On the other hand, the reliability and efficiency indexes of the inverter used in a PMSG are greater than the other used in a DFIG. The full-scale voltage source converters (VSC) are more preferred than the partial-scale VSC of DFIG configuration. The block diagram of a variable-speed WT consisted of PMSG is shown in Fig. 23 with its power electronic sections and control signals. The full-scale converter of WT contains two separate converters where one is used as rotor-side converter (RSC), while the other is used as grid-side converter (GSC). The high efficient configuration of PMSG WT consists of fully controlled and IGBT-based bidirectional converter. The most recently developed control technology is considered as direct-current vector control technology that increases reliability, efficiency, and stability compared to conventional vector control.

The vector control of a Type D WT requires the dynamic model of PMSG in the rotating reference frame that is given in Eqs. (53) and (54) [14, 38, 62]:

$$V_{\mathrm{q}} = R_{\mathrm{s}} i_{\mathrm{q}} + L_{\mathrm{q}} \frac{\mathrm{d}i_{\mathrm{q}}}{\mathrm{d}t} + \omega_r L_d i_d + \omega_r \lambda_m \tag{53}$$

$$V_{\mathrm{d}} = R_{\mathrm{s}} i_{\mathrm{d}} + L_{\mathrm{d}} \frac{\mathrm{d}i_{\mathrm{d}}}{\mathrm{d}t} - \omega_r L_q i_q \tag{54}$$

The electromagnetic torque of a PMSG and its reduced expression for cylindrical PMSG are presented, respectively, as follows:

$$T_{\mathrm{e}} = \frac{3}{2}\frac{P}{2}\left[\left(L_{\mathrm{d}} - L_{\mathrm{q}}\right) i_{\mathrm{q}} i_{\mathrm{d}} - \lambda_{\mathrm{m}} i_{\mathrm{q}}\right] \tag{55}$$

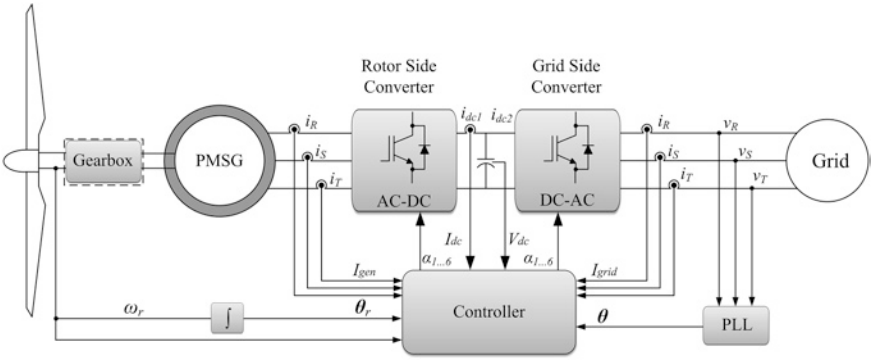

Fig. 23 Configuration of a variable-speed WT with PMSG, Type D

$$T_{\mathrm{e}} = \frac{3}{2}\frac{P}{2}\lambda_{\mathrm{m}} i_{\mathrm{q}} \tag{56}$$

where

V_{q} = voltage in quadrature axis,
R_{s} = rotor resistance,
L_{q} = inductance in the quadrature axis,
i_{q} = current in the quadrature axis,
ω_{r} = rotor speed,
L_{d} = inductance in the direct axis,
i_d = current in the direct axis,
λ_{m} = magnetic flux,
P = the number of poles of the generator.

Although there are several types of power electronics used in variable-speed WTs, the highest efficiency and reliability are assured by self-commutated converters that consist of IGBT or MOSFET and enable bidirectional power flow. The PMSG is connected to the grid over ac–dc and dc–ac converters. Hence, the generated power is primarily converted to dc that forms the dc-link voltage and then converted to ac using dc-link voltage to be supplied to the grid. The line currents generated during the conversion are indicated as I_{dc1} and I_{dc2} in Fig. 23 in which the calculations are given in Eqs. (57) and (58) [14, 38, 62]. P_{gen} stands for output power of generator, while P_{a} is the active power and P_{l} is the power losses.

$$I_{\mathrm{dc1}} = \frac{P_{\mathrm{gen}}}{V_{\mathrm{dc}}} \tag{57}$$

$$I_{\mathrm{dc2}} = \frac{P_{\mathrm{a}} + P_{\mathrm{l}}}{V_{\mathrm{dc}}} \tag{58}$$

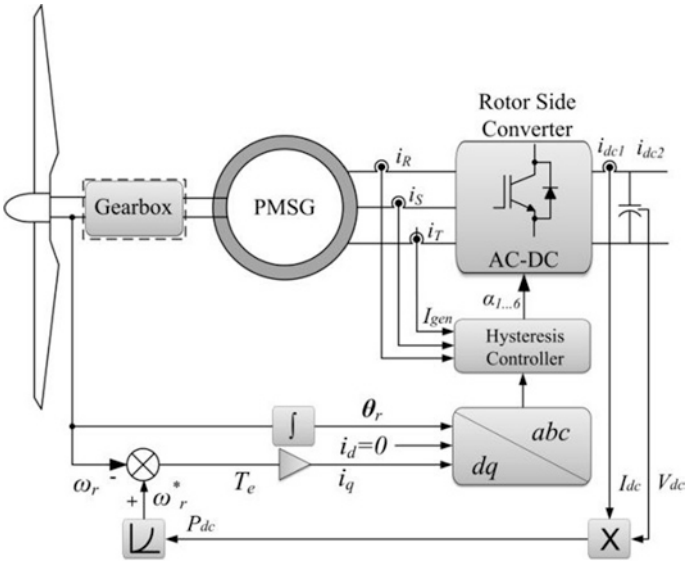

Fig. 24 Block diagram of RSC and controller of a Type D WT

The block diagram of RSC and its controller are depicted in Fig. 24. Since the maximum power of a variable-speed turbine is similar to a cubic function at various wind speeds, the rotor speed should be controlled corresponding to the power–speed characteristic. Therefore, current and voltage of dc link is required to generate a reference value using the power–speed curve of the generator. The current and voltage are measured on the right-hand side of the figure which are used to calculate the dc power of RSC. The electromechanical torque that is calculated in *dq* synchronously rotating reference frame is converted to *abc* natural frame regarding to pitch angle θr of the rotor blades. The hysteresis current controller is implemented using a closed-loop control system where an error signal $e(t)$ is generated inside the controller block.

The error signal is used to determine the current difference through the reference current i_{ref} to be tracked, and then, switching angles are adjusted again to the actual values to increase or decrease the output current. The duty cycle is reduced when $e(t)$ is higher than the reference or vice versa [38, 50, 62]. The detailed block diagram of GSC and its controller are shown in Fig. 25. The operation principle of GSC is derived from shunt active power filter where VSI is controlled regarding to harmonic compensation current and line currents. The vector control of GSC requires nested-loop structure containing a faster inner current control loop and a slower outer current control loop. The Δv_{d} and Δv_{q} of the inner loop are acquired corresponding to Eqs. (53) and (54), which are assumed as the state equation between the voltage and current on *d*- and *q*-axis loops. The voltage equations in the *dq* synchronously rotating reference frame are obtained using Eqs. (59) and (60) [38, 50, 62].

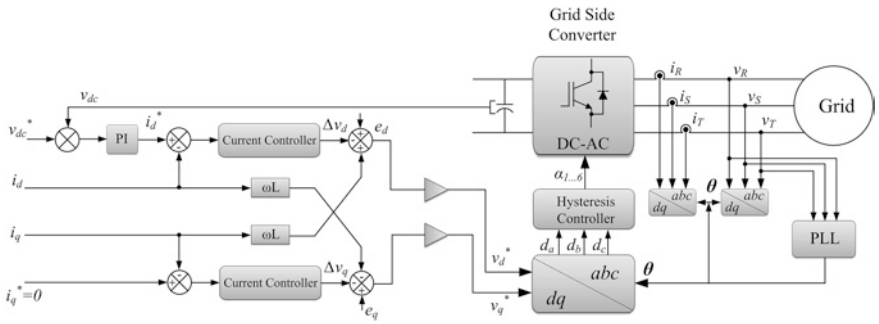

Fig. 25 Block diagram of GSC and controller of a Type D WT

$$e_{\mathrm{d}} = L\frac{\mathrm{d}i_{\mathrm{d}}}{\mathrm{d}t} - \omega L i_{\mathrm{q}} + v_{\mathrm{d}} \tag{59}$$

$$e_{\mathrm{q}} = L\frac{\mathrm{d}i_{\mathrm{q}}}{\mathrm{d}t} + \omega L i_{\mathrm{d}} + v_{\mathrm{q}} \tag{60}$$

The DFIG is essentially used in WTs owing to advantages of its rotor winding where it is connected parallel to the grid over back-to-back converters. The maximum output power is achieved by adjusting the electromagnetic torque and rotor speed and then converter to fixed-frequency electrical power. On the other hand, the partial-scale converters that have rated power around 30 % of the WT decreases the losses and cost. In addition to these advantages, the active and reactive powers on the stator side can be controlled separately.

The conventional control method of a DFIG-based WT is based on the flux-oriented vector control or voltage-oriented control of the stator, and the rotor current vector is disintegrated into two different components in the synchronously rotating reference frame. Electromagnetic torque and flux can be separately controlled by this way. The vector control method requires several sensors to determine the actual rotor position and speed values in order to enable us to transform the rotor current vector to $\alpha\beta$ and/or dq reference frames.

However, sensorless control of DFIG that is based on the possibility to measure the rotor current of generator, which is not possible in SCIG, is the most extensively studied topic. The direct torque control (DTC) is another control method that is widely used in DFIG because of the discrete operation of voltage source inverters. The direct power control (DPC) is another control method proposed for DFIG-based WT that is derived from DTC method. DPC provides notable improvements in the control of unbalanced operation that are caused by the configuration of the DFIG. Several studies are noted in the literature to eliminate power oscillations, torque oscillations, or unbalanced current output applying a factor that prioritizes the variable to be compensated [1, 22, 28, 59, 63, 74].

The generator equations of a DFIG are presented as follows:

$$V_s = R_s I_s + j\omega L_s I_s + j\omega_1 L_m (I_s + I_r + I_{rm}) \tag{61}$$

$$\frac{V_r}{s} = \frac{R_r}{s} I_r + j\omega L_r I_r + j\omega_1 L_m (I_s + I_r + I_{rm}) \tag{62}$$

$$0 = R_m I_{rm} + j\omega_1 L_m (I_s + I_r + I_{rm}) \tag{63}$$

where

V_s = stator voltage,
R_s = stator resistance,
V_r = rotor voltage,
R_r = rotor resistance,
I_s = stator current,
R_m = magnetizing resistance,
I_r = rotor current,
L_s = stator leakage inductance,
L_r = rotor leakage inductance,
I_{rm} = magnetizing resistance current,
ω_1 = stator frequency,
L_m = magnetizing inductance,
S = slip.

The electromagnetic torque of DFIG is represented as given in Eq. (64):

$$T_e = \frac{3}{2} n_p \frac{L_m}{L_s} \mathrm{Im}\{\psi_s i_r^*\} \tag{64}$$

where n_p is the pole pair, ψ_s is the stator flux, and i_r^* is the complex conjugate of rotor current. The instantaneous power of the stator in the dq reference frame is presented in Eqs. (65) and (66):

$$P_s = \frac{3}{2}\left(v_{ds} i_{ds} + v_{qs} i_{qs}\right) \tag{65}$$

$$Q_s = \frac{3}{2}\left(v_{qs} i_{qs} - v_{ds} i_{ds}\right) \tag{66}$$

Figure 26 shows the detailed configuration of a DFIG-based variable-speed WT with its control features. The wind turbine varies the rotational speed ω corresponding to the wind speed during the lower speeds and keeps the pitch angle θ_r at a fixed value. The rotational speed is adjusted at the attainable maximum slip at deficient wind speeds to obviate the over voltage at the output of the generator. The pitch angle controller that is illustrated at the lower part of Fig. 26 is used to limit the excessive output power. The RSC of the turbine regulates the total output power. The control ability of the GSC is based on the stable dc-link voltage [7, 63].

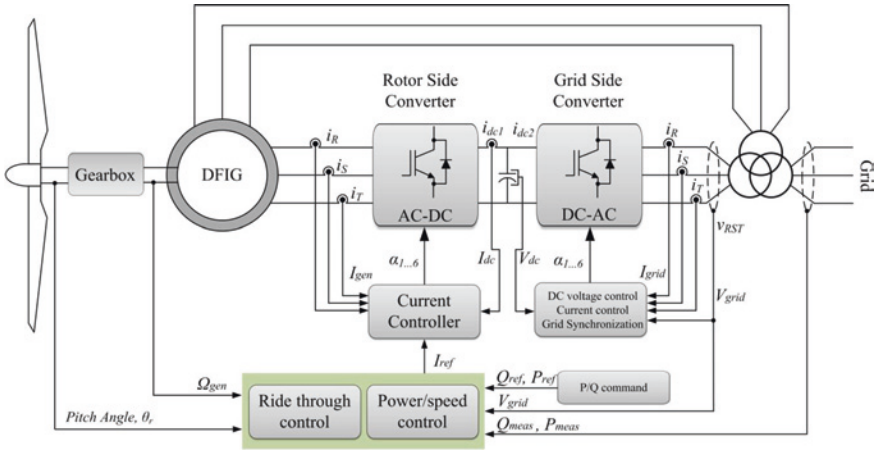

Fig. 26 Configuration of a variable-speed WT with DFIG, Type C

Although the active power is notably considered in power systems, the reactive power defines the characteristic property of the system as well. The generator inherits the required reactive power from grid in the grid-connected system, while the island-mode operation involves external reactive sources such as capacitor banks. Therefore, active and reactive power control is also quite important in DFIG-based wind systems. The sliding-mode controllers (SMC) are based on controlling the error of active and reactive powers. The active and reactive powers of stator are measured to generate P/Q command in SMC method and are supplied to DPC control block in the stator stationary reference frame. The inherited data are then converted to the rotor reference frame since V_{dc} controls the output voltage. This control method does not require any transformation to synchronous reference frame.

5 Control Methods in Fuel Cells

Fuel cells (FC) that are static energy conversion devices supply electrical energy to the systems by converting the chemical reaction to the electrical energy. The exhausted gas of a FC consists of hydrogen and oxygen that together produce water. A simple diagram of a FC is shown in Fig. 27 in which the left-hand side illustrates the fuel input, while the right-hand side shows the oxidant input. The anode and cathode leads are directly connected to loads where anode stands for positive output and cathode stands for the negative output.

Since this section is dedicated to the control methods, the FC types and chemical structures will not be introduced here. Further reading that can be found in several survey articles [9, 23, 24, 35, 39, 66] are recommended to readers who are not familiar to this source type. The FC is assumed as a dc voltage supply with delayed power response characteristic. The dc-link stabilization problem constitutes the most

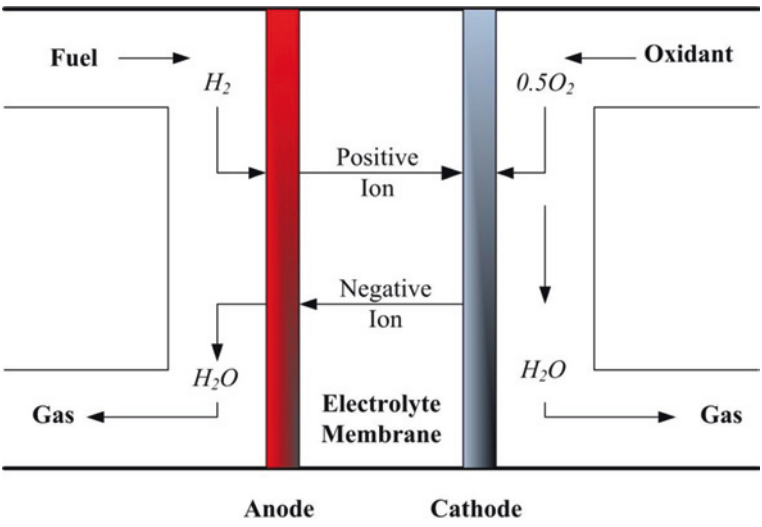

Fig. 27 Diagram of a fuel cell during energy generation

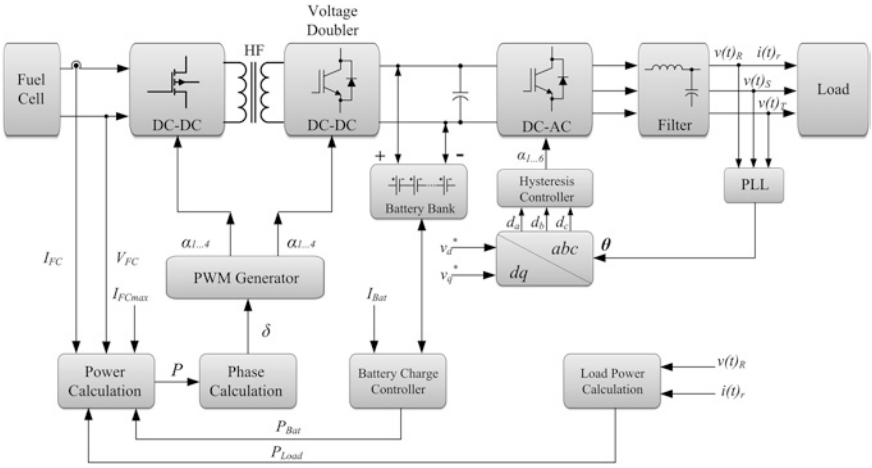

Fig. 28 Block diagram of a typical FC control system

important part of FC control studies. The conventional control methods are based on a linear transfer function of the converter and PI or PID controller feedback. Some novel approaches are also proposed to increase the system response using a supercapacitor in parallel with FC [66]. This kind of configuration requires cascaded controller for current and dc bus voltage. When a power system that is built with a fuel cell is connected to a single-phase inverter, it generates the ac ripple current twice that of the output frequency that decreases the utilization factor, efficiency, and lifetime of the FC due to the hysteresis effect [39].

Several active ripple reduction or elimination methods are proposed to tackle this problem. The commercially available FCs draw rated power from 2 W to 5,000 W, where the nominal dc output voltage varies from 13.2 to 72 V corresponding to power rate. A detailed control block diagram of a FC-supplied power system is illustrated in Fig. 28. The controller of dc–dc converter is operated corresponding to the load voltage and load current that are used to calculate the required output power P_L. The dc–dc converter is generally configured in H-bridge structure, and each switch of the converter is independently controlled. Since the FC-powered systems are assisted with parallel battery bank in order to regulate the system response, the battery voltage and current are also tracked simultaneously and the power involved to charge or to discharge the battery P_B is calculated by the controller. The total value of P_{L} and P_{B} yields the power rate that should be supplied by the FC. The required current that is provided by the FC is calculated using the output voltage and output power of FC. In case the required current output is greater than or equal to attainable maximum FC I_{FCmax}, the phase calculation block increases the phase-shift angle δ in order to provide the required current by cooperating with FC and battery bank. If the required current is lower than I_{FCmax}, the FC supplies the output current by itself.

This kind of measurement and sensing strategy allows obtaining fully controlled operation and the inverter side is safely operated owing to stable supply voltage [15, 26, 37, 48, 65, 72]. The inverter control strategy can be selected using one of the control methods that are introduced in the previous sections of this chapter.

References

1. Abad G, Rodriguez MA, Iwanski G, Poza J (2010) Direct power control of doubly-fed-induction-generator-based wind turbines under unbalanced grid voltage. IEEE Trans Power Electron 25(2):442–452
2. Acha E, Agelidis V, Anaya O, Miller TJE (2002) Power electronic control in electrical systems, 1st edn. Newnes power engineering series
3. Ackermann T (2005) Wind power in power systems. Wiley, New York
4. Andújar JM, Segura F (2009) Fuel cells: history and updating. A walk along two centuries. Renew Sustain Energy Rev 13(9):2309–2322
5. Bizon N, Dascalescu L, Tabatabaei NM (2013) Autonomous hybrid vehicles: intelligent transport systems and automotive technologies. University of Pitesti. ISBN: 978-606-560-327-1
6. Blaabjerg F, Teodorescu R, Liserre M, Timbus A (2006) Overview of control and grid synchronization for distributed power generation systems. IEEE Trans Industr Electron 53(5):1398–1409
7. Blaabjerg F, Ma K (2013) Future on power electronics for wind turbine systems. IEEE J Emerg Sel Top Power Electron 1(3):139–152
8. Blaabjerg F, Liserre M, Ma K (2012) Power electronics converters for wind turbine systems. IEEE Trans Ind Appl 48(2):708–719
9. Boscaino V, Miceli R, Capponi G, RiccoGalluzzo G (2014) A review of fuel cell based hybrid power supply architectures and algorithms for household appliances. Int J Hydrogen Energy 39(3):1195–1209
10. Bose BK (2002) Modern power electronics and AC drives. Prentice Hall Inc, Englewood Cliffs. ISBN 978-0130167439

11. Bull SR (2001) Renewable energy today and tomorrow. Proc IEEE 89(8):1216–1226
12. Burton T, Sharpe D, Jenkins N, Bossanyi E (2001) Wind energy handbook. Wiley, New York
13. Ciobotaru M, Teodorescu R, Agelidis VG (2008) Offset rejection for PLL based synchronization in grid-connected converters. In: 23rd annual IEEE applied power electronics conference and exposition. Austin, Texas, USA, 24–28 Feb 2008, p 1611
14. Chen Z, Guerrero JM, Blaabjerg F (2009) A review of the state of the art of power electronics for wind turbines. IEEE Trans Power Electron 24(8):1859–1875
15. Choe SY, Ahn JW, Lee JG, Baek SH (2008) Dynamic simulator for a PEM fuel cell system with a PWM DC/DC converter. IEEE Trans Energy Convers 23(2):669–680
16. Chow TT (2010) A review on photovoltaic/thermal hybrid solar technology. Appl Energy 87(2):365–379
17. Çolak I, Kabalcı E, Bayındır R (2011) Review of multilevel voltage source inverter topologies and control schemes. Energy Convers Manag 52:1114–1128
18. El Chaar L, Lamont LA, El Zein N (2011) Review of photovoltaic technologies. Renew Sustain Energy Rev 15(5):2165–2175
19. Erickson RW, Maksimovic D (1997) Fundamentals of power electronics. Chapman and Hall, London. ISBN 0-412-08541-0
20. Esram T, Chapman PL (2007) Comparison of photovoltaic array maximum power point tracking techniques. IEEE Trans Energy Convers 22(2):439–449
21. Femia N, Petrone G, Spagnuolo G, Vitelli M (2005) Optimization of perturb and observe maximum power point tracking method. IEEE Trans Power Electron 20(4):963–973
22. Fernandez LM, Garcia CA, Jurado F (2008) Comparative study on the performance of control systems for doubly fed induction generator (DFIG) wind turbines operating with power regulation. Energy 33(9):1438–1452
23. Giddey S, Badwal SPS, Kulkarni A, Munnings C (2012) A comprehensive review of direct carbon fuel cell technology. Prog Energy Combust Sci 38(3):360–399
24. Grasser F, Rufer AC (2006) A fully analytical PEM fuel cell system model for control applications. In: IEEE IAS annual meeting industry applications conference vol 5. Tampa FL, USA 8–12 Oct 2006, pp 2162–2168
25. Grigsby LL (2007) The electric power engineering handbook. CRC Press, Taylor & Francis Group, Boca Raton
26. Harfman Todorovic M, Palma L, Enjeti PN (2008) Design of a wide input range DC–DC converter with a robust power control scheme suitable for fuel cell power conversion. IEEE Trans Industr Electron 55(3):1247–1255
27. Hau E, von Renouard H (2005) Wind turbines: fundamentals, technologies, application. Springer, Economics
28. Hu J, Nian H, Hu B, He Y, Zhu ZQ (2010) Direct active and reactive power regulation of DFIG using sliding-mode control approach. IEEE Trans Energy Convers 25(4):1028–1039
29. Iov F, Blaabjerg F (2009) power electronics control of wind energy in distributed power systems. In: Hammons TJ (ed) Renewable energy. InTech, Winchester. Available from: http://www.intechopen.com/books/renewable-energy/power-electronics-control-of-wind-energy-in-distributedpower-systems
30. Jain S, Agarwal V (2007) Comparison of the performance of maximum power point tracking schemes applied to single-stage grid-connected photovoltaic systems. IET Electr Power Appl 1(5):753–762
31 Johansson TB, Burnham L (1993) Renewable energy: sources for fuels and electricity. Island Press, Washington
32 Kabalcı E, Kabalcı Y, Develi I (2012) Modelling and analysis of a power line communication system with QPSK modem for renewable smart grids. Int J Electr Power Energy Syst 34(1):19–28
33 Kabalcı E (2013) Design and analysis of a hybrid renewable energy plant with solar and wind power. Energy Convers Manag 72:51–59
34 Khatib T, Mohamed A, Sopian K (2013) A review of photovoltaic systems size optimization techniques. Renew Sustain Energy Rev 22:454–465

35 Kirubakaran A, Jain S, Nema RK (2009) A review on fuel cell technologies and power electronic interface. Renew Sustain Energy Rev 13(9):2430–2440
36 Kurzweil P (2009) History, fuel cells. In: Garche J (ed) Encyclopedia of electrochemical power sources. Elsevier, Amsterdam, pp 579–595
37. Lee JG, Choe SY, Ahn JW, Baek SH (2008) Modelling and simulation of a polymer electrolyte membrane fuel cell system with a PWM DC/DC converter for stationary applications. IET Power Electron 1(3):305–317
38. Li S, Haskew TA, Swatloski RP, Gathings W (2012) Optimal and direct-current vector control of direct-driven PMSG wind turbines. IEEE Trans Power Electron 27(5):2325–2337
39. Liu C, Lai JS (2007) Low frequency current ripple reduction technique with active control in a fuel cell power system with inverter load. IEEE Trans Power Electron 22(4):1429–1436
40. Long H, Li X, Wang H, Jia J (2013) Biomass resources and their bioenergy potential estimation: a review. Renew Sustain Energy Rev 26:344–352
41. Lorenzani E, Franceschini G, Bellini A, Tassoni C 2009) Single-phase grid connected converters for photovoltaic plants. In: Hammons TJ (ed) Renewable energy, InTech, Winchester. doi:10.5772/7374
42. Lucia U (2009) Overview on fuel cells. Renew Sustain Energy Rev 30:164–169
43. Luo FL, Ye H, Rashid MH (2005) Digital power electronics and applications. Elsevier, Academic Press. ISBN: 978-0120887576
44. Manwell JF, McGowan JG, Rogers AL (2010) Wind energy explained: theory, design and application. Wiley, New York
45. Masters GM (2004) Renewable and efficient electric power systems. Wiley-IEEE Press, New York
46. Mohan N, Undeland TM, Robbins WP (1995) Power electronics-converters, application and design. Wiley, New York
47. Nami A, Zare F (2009) Multilevel converters in renewable energy systems. In: Hammons TJ (ed) Renewable energy. InTech, Winchester. doi:10.5772/736
48. Palma L, Enjeti PN (2009) A modular fuel cell, modular DC–DC converter concept for high performance and enhanced reliability. IEEE Trans Power Electron 24(6):1437–1443
49. Pansini AJ, Smalling KD (2002) Guide to electric power generation. The Fairmont Press, Inc
50. Parker MA, Ng C, Ran L (2011) Fault-tolerant control for a modular generator–converter scheme for direct-drive wind turbines. IEEE Trans Industr Electron 58(1):305–315
51. Parida B, Iniyan S, Goic R (2011) A review of solar photovoltaic technologies. Renew Sustain Energy Rev 15(3):1625–1636
52. Patel HS, Hoft RG (1973) Generalized harmonic elimination and voltage control in thyristor converters: part I—harmonic elimination. IEEE Trans Ind Appl 9:310–317
53. Pozzebon GG, Goncalves AFQ, Pena GG, Mocambique NEM, Machado RQ (2013) Operation of a three-phase power converter connected to a distribution system. IEEE Trans Industr Electron 60(5):1810–1818
54. Rashid MH (2010) Power electronics handbook. Academic Press, London. ISBN-13: 978-0123820365
55. Rech C, Pinheiro JR (2007) Hybrid multilevel converters: unified analysis and design considerations. IEEE Trans Ind Electron 54(2):1092–1104
56. Sahin AS (2012) Modeling and optimization of renewable energy systems. InTech, Winchester
57. Sera D, Kerekes T, Lungeanu M, Nakhost P, Teodorescu R, Andersen GK, Liserre M (2005) Low-cost digital implementation of proportional-resonant current controllers for PV inverter applications using delta operator. In: 31st annual conference of ieee industrial electronics society. Raleigh, NC, USA, 6–10 Nov 2005, p 6
58. Sharp NE-170UC1 (2014) Multipurpose module, Sharp, USA. Available from: http://files.sharpusa.com/Downloads/Solar/Products/sol_dow_NE170U1.pdf. Accessed January 204
59. Shen B, Mwinyiwiwa B, Zhang Y, Ooi BT (2009) Sensorless maximum power point tracking of wind by DFIG using rotor position phase lock loop (PLL). IEEE Trans Power Electron 24(4):942–951
60. Shepherd W, Zhang L (2004) Power converter circuits. CRC Press, Boca Raton

61. Singh R, Shukla A (2014) A review on methods of flue gas cleaning from combustion of biomass. Renew Sustain Energy Rev 29:854–864
62. Singh M, Khadkikar V, Chandra A (2011) Grid synchronisation with harmonics and reactive power compensation capability of a permanent magnet synchronous generator-based variable speed wind energy conversion system. IET Power Electron 4(1):122–130
63. Tazil M, Kumar V, Bansal RC, Kong S, Dong ZY, Freitas W, Mathur HD (2010) Three-phase doubly fed induction generators: an overview. IET Electr Power Appl 4(2):75–89
64. Teodorescu R, Liserre M, Rodriguez P (2011) Grid converters for photovoltaic and wind power systems. Wiley IEEE, New York
65. Thounthong P, Raël S, Davat B (2009) Energy management of fuel cell/battery/supercapacitor hybrid power source for vehicle applications. J Power Source 193(3):76–85
66. Thounthong P, Tricoli P, Davat B (2014) Performance investigation of linear and nonlinear controls for a fuel cell/supercapacitor hybrid power plant. Int J Electr Power Energy Syst 54:454–464
67. Timbus AV, Teodorescu R, Blaabjerg F, Liserre M, Dell'Aquila A (2006) Independent synchronization and control of three phase grid converters. In: International symposium on power electronics, electrical drives, automation and motion. Taormina, Italy 23–26 May 2006, p 1246
68. Twidell J, Weir T (2005) Renewable energy resources. Taylor & Francis, London
69. Twidell J, Weir T (2006) Renewable energy sources. Taylor & Francis, London
70. Veenstra M, Rufer A (2003) Control of a hybrid asymmetric multi-level inverter for competitive medium-voltage industrial drives. IEEE Trans Ind Appl 41(2):655–664
71. Veerachary M, Senjyu T, Uezato K (2003) Neural-network-based maximum-power-point tracking of coupled-inductor interleaved-boost converter-supplied PV system using fuzzy controller. IEEE Trans Industr Electron 50(4):749–758
72. Wang J, Peng FZ, Anderson J, Joseph A, Buffenbarger R (2004) Low cost fuel cell converter system for residential power generation. IEEE Trans Power Electron 19(5):1315–1322
73. Wilamowski BM, Li X (2002) Fuzzy system based maximum power point tracking for PV system. In: Proceedings 28th annual conference of the ieee industrial electronics society (IECON 2002). Seville, Spain, 5–8 Nov 2002, p 3280
74. Yang S, Ajjarapu V (2010) A speed-adaptive reduced-order observer for sensorless vector control of doubly fed induction generator-based variable-speed wind turbines. IEEE Trans Energy Convers 25(3):891–900
75. Zhong QC, Hornik T (2013) Control of power inverters in renewable energy and smart grid integration. Wiley–IEEE, New York

Low-Cost Hybrid Systems of Renewable Energy

Petronio Vieira Jr.

Abstract This chapter is focused on research and development of low-cost technologies for attending small and medium energetic demands. The results of such development are related to the use of hybrid systems combining different sources of renewable energy (RE). To obtain the smallest cost of a system, it is necessary to obtain the smallest cost of each one of their parts and a better control strategy integrating the operation of these parts. Besides, it is necessary to obtain the best project than it relates the best cost so much benefit in relation to installation as for operation and maintenance. In this chapter, the constituent elements of a hybrid system will be presented initially, followed by a presentation of the technological progresses of these elements. Later the control strategies will be explained to obtain the maximum efficiency of these elements and connection arrangements among them. Finally, project methodologies will be presented for the optimization of the sizing of a project of hybrid system, and they will be described through examples of their application.

1 Hybrid Renewable Energy Systems

Sources of renewable energy (RE), such as sun, wind, geothermal, ocean, and biomass, has one characteristic in common which is that they are not available all the time. This intermittent nature of RE resources is a reason for employing hybrid systems combining different sources [4]. The hybrid renewable energy systems (HRES) consist of two or more renewable sources of energy [3]. A very important and typical application of these combinations is therefore oriented to assist

P. Vieira Jr. (✉)
Federal University of Pará, Belém, Brazil
e-mail: petronio@ufpa.br

M. A. Sanz-Bobi (ed.), *Use, Operation and Maintenance of Renewable Energy Systems*, Green Energy and Technology, DOI: 10.1007/978-3-319-03224-5_8,

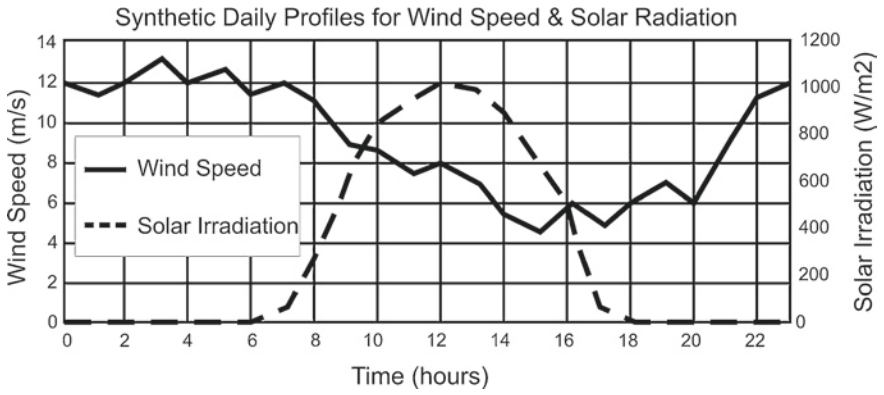

Fig. 1 The complementary power sources [36]

the demand of energy in isolated facilities (off-grid mode) or without a connection to the public network of energy. Another application is the association of renewable sources to a common connection point making energy available for a group of loads (on-grid mode), constituting a hybrid system, as can usually be observed in urban facilities (distributed energy resources—DER).

In remote areas, where it is difficult or costly to be connected to the power grid, stand-alone PV and wind power systems are gaining commercial attention [14]. Hybrid schemes can be especially beneficial when complementary RES are used. An example of complementary power sources is the energy harnessed from wind and solar irradiation. Wind turbine generators (WTG) generally have higher generation rates during night hours, due to the better wind conditions (stronger and more constant winds). Photovoltaic (PV) cells, on the other hand, can only produce power during daylight hours. Combining sources such as WTGs and PV cells, however, may not be sufficient to satisfy reliability requirements, as can be seen in Fig. 1 [36].

The installation of hybrid systems connected to the grid happens naturally in studies where the cost turns the use of the competitive RE with conventional generating units either due to the decrease in the cost of the generation originating from renewable sources or due to the increase in the costs of the conventional sources [21]. To obtain the smallest cost of a system, it is necessary to obtain the smallest cost in each one of their parts, to develop a control strategy and to integrate the operation of their parts. Besides, it is necessary to develop a project that has the best relationship cost benefit considering, besides the cost of the installation, the cost of operation and maintenance. In this chapter, the constituent elements of a hybrid system will be initially described, followed by a presentation of the technological progresses of these elements. Next, the strategies to obtain the maximum efficiency of these elements through control and connection arrangements among them will be presented. Finally, different methodologies used in real projects will be presented for optimization of the size of a hybrid system.

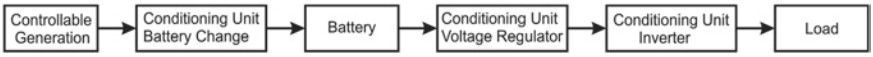

Fig. 2 Block diagram of connection series

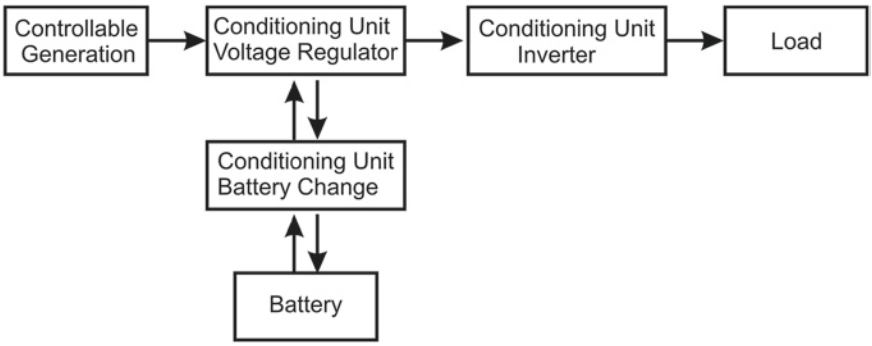

Fig. 3 Block diagram of connection parallel

2 Topology for Modulated Controlled Hybrid Renewable Energy Systems

The conversion systems of renewable sources of energy for electric power generation can be schematically presented through three elements. The first element converts the energy obtained from natural resources, or primary source of energy, into electric power energy called the controllable generators [3], a second element corresponds to the power conditioning units that conform this energy (energy conditioner), and a third constituent part is the backup devices. It can be mentioned as examples of controllable generators the photovoltaic generations (PV), wind turbines (WT), and microhydropower turbines [6]. Some examples of backup devices include as follows: fuel cells (FCs), batteries, ultracapacitors (UCs), or diesel generations (DGs) sets [4]. The conditioning units (or energy conditioner) have the DC regulators (Buck/Boost converters, battery chargers) and the DC–AC converters (inverters). The conditioning connected units in the controllable generation exit should add the function of obtaining the maximum power transfer. Usually, the cascade of two DC–DC converters consists of one for maximum power tracking and another one for voltage regulator [4]. These converters searching to reach a maximum power use controllers that execute algorithms called maximum power point tracking (MPPT) and are important to obtain the maximum efficiency of the system. In order to connect these elements (controllable generators, conditioning units, and backup devices), two topologies can be distinguished. A connection with all the elements in series (see Fig. 2) or part of the elements in parallel (see Fig. 3).

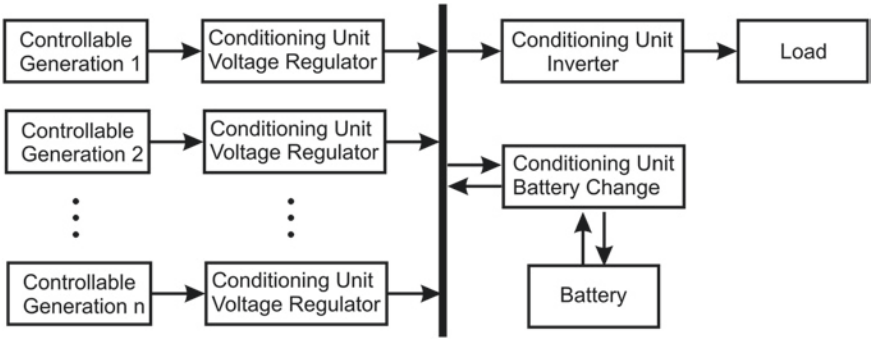

Fig. 4 Modulation in hybrid systems

The connection in series includes the generations maintained at a voltage and the circuit of connected load control in series with the battery (regulated line). This connection provides a direct transfer of energy (DET) with a bank of batteries. DET with a bank of batteries, without a doubt is considered to be the simplest topology. This system is chosen due to its reduced number of elements, however, it has an interface regulator switching element for load. This system type, although it seems to be desirable for use in small consuming loads, is a false economy, because the direct junction of the battery voltages and the controllable generators result in the need for greater generation.

The connection in parallel with the connected battery directly in parallel with generation (line not regulated) has its main advantages, a better adaptation of the load end and the good compatibility with the modular concepts and standardization. This second form has some advantages with relation to the configuration series, mainly due to the fact that the bank of batteries, after being completely loaded, can be disconnected from the system, making it possible for the load to just be fed by the energy generated by the constituted generators of independent modules as shown in the Fig. 4. This configuration is employed for HRES.

A generalized model of HRES described in [4] is presented in Fig. 5. The net of data is observed between the control of the converters and a central control. In this outline, the author introduces the generation diesel (DG) the backup device for understanding that, in spite of not being renewable, this unit offers the advantage of guaranteeing continuity in the provisioning of energy. Each slave controller (SC) receives its set points from a master controller (MC). The MC optimizes the operation based on distributed generator sources, forecasted wind speed, and forecasted solar irradiation.

The general model described in [4] is implemented in [24] for a stand-alone installation (off-grid mode) and shown in Fig. 6. In this figure, the MC is responsible for stabilizing the bus DC starting from the information of the conditions of operation of the controllable generations and using the levels of load from the backup devices. In the DC–DC converters of the generators, the control uses a searching algorithm of MPPT. It must be observed that the storage devices (backup devices) are considered to be non-controllable.

When the generation is distributed (DG), the control needs a network for data transmission, constituting one micro-grid (MG), which is an effective solution

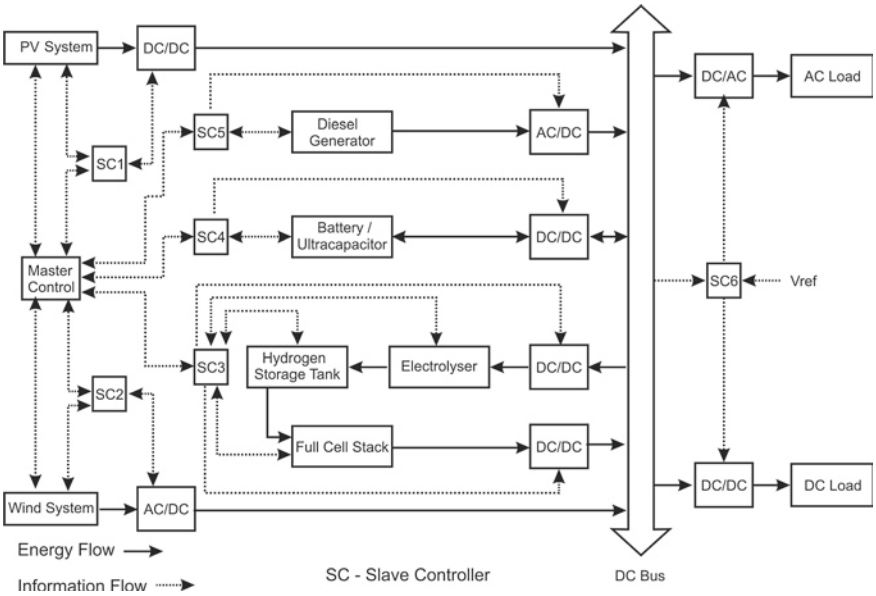

Fig. 5 A generalized model of HRES showed in [4]

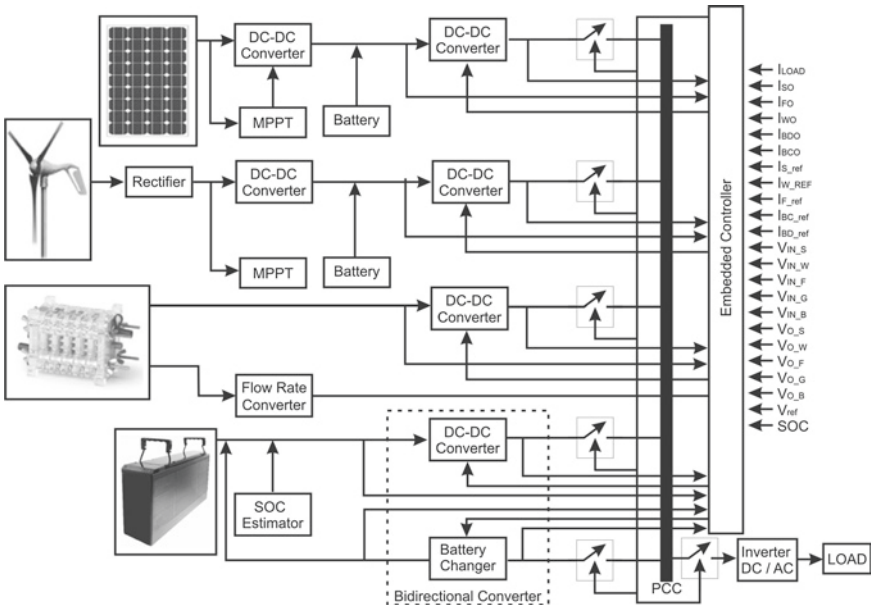

Fig. 6 Solar/WTG/fuel cell-fed hybrid stand-alone power supply showed in [24]

to incorporate DER into power systems realizing environmental and economical network operation goals. One of the most important applications of the MG generators is the utilization of small-modular residential or commercial generators

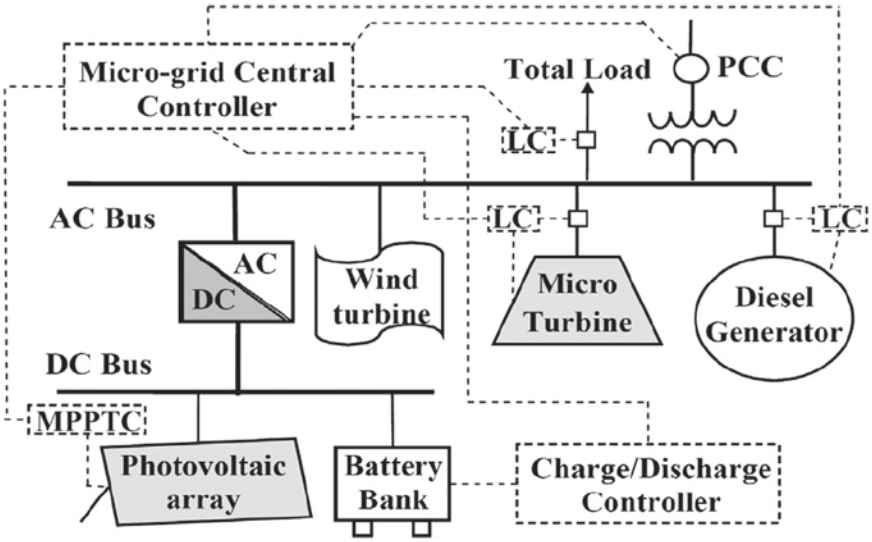

Fig. 7 Configuration of the MG in [12]

for onsite service. In [12], an implementation of an MG is presented, as shown in Fig. 7. In this installation, different from the off-grid or stand alone, the generation of a renewable source, WT, and PV generators consists of controllable and non-controllable micro-sources. The diesel engine generator (DEG) and the micro turbine (MT) constitute the controllable micro-sources. The point where the MC (Micro-grid central controller—MGCC) is connected, called the point of common coupling (PCC), is normally an AC bus. The slave controller presented in the generalized model of HRES of Fig. 5 is called the local controller (LC) in Fig. 7 associated with units/load. MGCC optimizes the MG operation based on distributed generator sources, forecasted wind speed, forecasted solar irradiation, forecasted loads, and operation policies send dispatch signals to the LCs [12]. The PV has a controller with a MPPT, which is called the maximum power point tracking controller (MPPTC).

3 Technologies of Low Cost for Generation Controllable

Hybrid systems of RE contain more than one source of energy type that should be complementary in order to try to guarantee the continuity of the energy supply. The wind and solar generations have this characteristic, for example, during the night time, the best profiles of wind occur, and during the daytime, the best conditions for solar generation are obviously found [36]. This configuration of generation is frequently employed, and for this reason, the technology of these two types of energy generation will be presented in the next sections of this chapter.

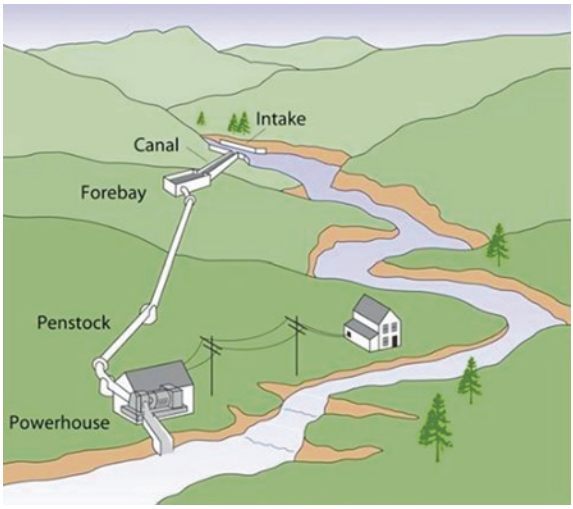

Fig. 8 Illustration of a micro hydroelectric plant using water from a river (taken from: http://engiobra.com/micro-usinas-hidreletricas)

3.1 Technologies for Microhydropower

Hydroelectricity is one of the most mature forms of RE, providing more than 19 % of the world's electricity consumption from both large and small power plants. Countries such as Brazil, the USA, and Norway produce significant amounts of electricity from very large hydroelectric facilities. However, there are also many regions of the world (e.g., China) that have a significant number of small hydropower plants in operation. There is no universally accepted definition of the term "microhydro" which, depending on local definitions, can vary from a few kilowatts up to 100 kW [6].

In Brazil, the hydroelectric plants can be classified according to the fall of water and the generation power as:

- Micro: with power <100 kW
- Mini: between 100 and 1,000 kW
- Small: among 1 and 30 MW.

Micro, mini, and small hydroelectrics power plants are becoming more and more a focus of interest due to having the smallest environmental impact, particularly for installation referred to as the river's thread. These do not use dams, they capture water from the rivers through piping (penstock), and through these they channel along until the turbine, as displayed the Fig. 8.

This system employs an axial flow hydraulic (semi-Kaplan) turbine with fixed blades and fixed-position wicket gates as described in [6] and called microhydropower Plant (MHPP) (see Fig. 9a). The same structure for a smaller fall of water using turbine Francis is presented in Fig. 9b. Although this type of installation is costs less, it also is less efficient and they are only used when the reservoir with a dam does not allow the stabilization of the water flow. During a season of drought,

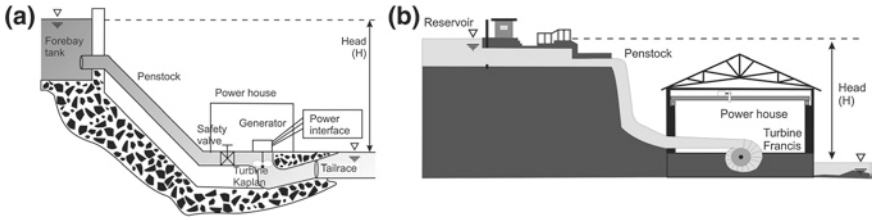

Fig. 9 Diagram representing the MHPP. **a** Diagram representing the MHPP [6]. **b** MHPP using turbine Francis

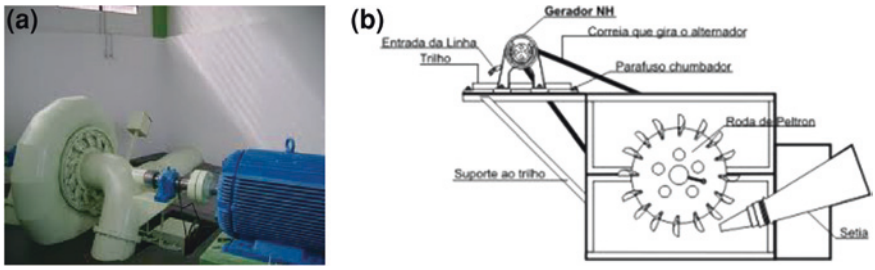

Fig. 10 Turbines of low cost for low power. **a** Francis turbine for low power http://www.alterima.com.br/. **b** Pelton turbine for low power http://www.nhgeradores.com.br/mini_usina.html

this causes a smaller available flow than the capacity of the turbines and, many times, this can cause damage to the hydroelectric plant, increasing the cost of the energy.

Turbines of the Francis type are employed to assist the low height of the fall and the low flow. These turbines are used with water falls of 10 up to 650 m, to speeds from 80 to 1,000 rpm. The generated power ranges between less than 10 and 750 MW. A Francis turbine that is well projected can extract up to 90 % of the potential energy of the water. In general, turbines of small capacity are installed in horizontal axis (see Fig. 10a), and the ones of medium or large size are installed with the vertical axis.

The Pelton turbines can also be used for hydroelectric generation of low cost, as is shown in Fig. 10b. These turbines work at the atmospheric pressure, and they are constituted by a wheel and one or more beak injectors guiding the drainage for the shovel that has the shape of a spoon, on the wheel. It is used for water falls from 350 up to 1,100 m and with rotation speeds above 1,000 rpm. A Pelton wheel, with a cross-flow turbine as a prime-mover and squirrel-cage induction generator (IG) as an electromechanical power converting medium, is quite popular due to its simple and robust technology [11].

Another low-cost installation can also be water pumps employed as turbines for generation of energy as shown in Fig. 11.

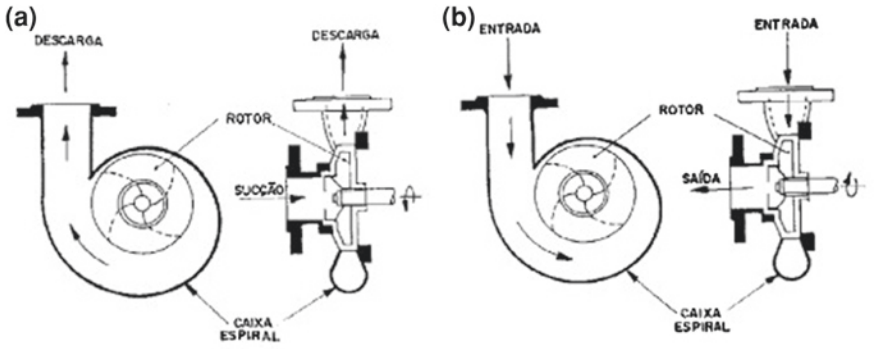

Fig. 11 Reversible hydraulic machines. **a** Working as pump. **b** Working as turbine

Fig. 12 Hydrokinetic turbines (Site: http://www.cerpch.unifei.edu.br/hidrocinetica.php). **a** Hydrokinetic helical-type turbine (Darreus turbine). **b** Hydrokinetic helical-type turbine (Gorlov turbine)

Another turbine type able to generate electricity without using a dam is the hydrodynamic. These are turbines developed to generate electric power using the flow of the river without the need to construct dams or use costly pipes. The turbine is constituted by a weather vane, with a smaller number of shovels, submerged into the water, as presented in Fig. 12a. The rotor, through a belt, allows the installed generator to work strategically on floats. The group is anchored, using cables, taking the best advantage of the current of the river. The turbine of helical rotor shown in Fig. 12a allows for greater efficiencies and generation of electrical energy in both directions, reaching a power of 25 kW. Another proposal is to install the rotor in a vertical position facilitating the installation of the generator or pulleys in order to multiply the speed and maintaining the characteristics to produce energy in both directions of the river flow.

Among the technological progresses of the hydrodynamic turbines, there is the turbine of the helical type, shown in Fig. 12b developed by Alexander. Gorlov that presents greater efficiency and smaller vibrations. These are hydraulic

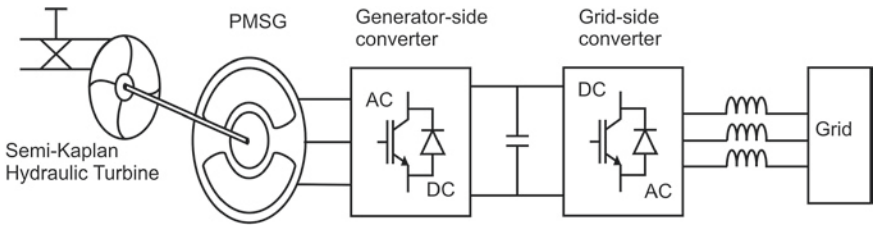

Fig. 13 Structures of MHPP generation system speed [6]

turbines able to generate up to 5 kW, operating independently of the direction of the flow. This turbine, keeping a free drainage, can obtain 35 % as maximum efficiency.

The technological progress is introducing power electronics into hydroelectric plants for a larger range of the water flow and volume. Figure 13 shows a series scheme that uses a voltage rectifier and a power inverter, this allows for a convenient electric generation at almost all of the range of speeds [6].

3.2 Technologies for Wind Turbine

There is a widespread use of wind turbine systems in power distribution networks as well as an increasing number of wind power stations connected to the transmission networks. Denmark, for example, has a high wind energy power capacity penetration over 30 % in major areas of the country, and today 28 % of all electrical energy consumption in the country is covered by wind energy [10]. It is expected that the global total wind power generation will supply around 12 % of the total world electricity generation at the end of 2020 [18].

The wind energy conversion system (WECS) consists of a turbine to capture the energy from the wind, a drive train to speed up the rotational speed of the shaft, and a generator to convert the mechanical energy into electrical energy [35].

Depending on the wind, the WT can have different diameters of the rotor. In locations with high wind speed, smaller rotor diameters are used. They usually could reach the maximum efficiency among 14–16 m/s. In locations with weaker gusts of wind, larger rotors are being used to reach the maximum efficiency among 12–14 m/s. Nowadays, turbines of three blades connected to power networks are more often used. They possess a larger inertia, and besides they produce a smaller noise level than the turbines with two blades. However, turbines with two blades have the advantage of the smallest weight and lower cost [21]. The WECS possess two different parts: the mechanical one (mechanical power) and the electroelectronic (electrical power) (Choi [10]) machine is robust and requires little maintenance as presented in Fig. 14. The mechanical part converts the kinetic energy from the wind into available mechanical energy in the axis coupled with the axis of an electric generator. The installation of gearboxes among these axes

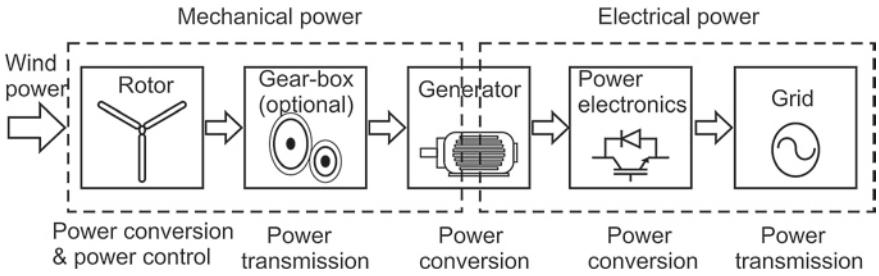

Fig. 14 Basic power conversion principle in a wind power system [10]

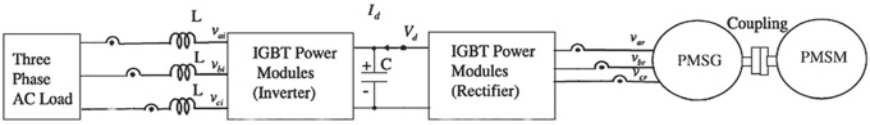

Fig. 15 Diagram of PM synchronous generator system using PM synchronous servo motor [17]

allows for a better use of the energy for the different range of speed of the wind. The electrical part allows for the electromagnetic conversion of the energy, and it conditions the form of wave of the appropriate voltage for feeding of apparels of final use of the electric power (load end).

The permanent magnet synchronous generator system (PMSGS) used in wind power generation does not require the use of a gearbox and has advantages such as simpler structure, better reliability, lower maintenance, and higher efficiency. Therefore, the PMSGS stands for a significant trend in progress of wind power applications [17]. In this reference, the wind turbine was emulated with a PM synchronous servomotor (PMSM) controlled by the variable speed of the PM synchronous generator (PMSG), which is directly driven as shown in Fig. 15.

The electric generation from wind can be further divided into fixed speed and variable-speed WT. In addition, considering the conditioning of the energy using power electronics, there are several configurations for WECS. Conventionally, there are three structures of energy conditioning for wind power system [10]. Simplified power converter structures for WT are presented in Fig. 16a and b, full power converter structures are presented in Fig. 16c, d, and multi-cell full power structures are included in Fig. 16e, f. The generators can be IGs with a wounded rotor, doubly fed induction generators with a wounded rotor (DFIG), asynchronous or synchronous electrically excited, Wound Rotor Synchronous Generator (WRSG), permanent magnet-excited synchronous (PMSG) such as a multi-pole or multi-wound rotor synchronous generator [10].

A wind turbine is connected directly to the grid, and the generator is "synchronized" to the power network. This technology is called "fixed" rotational speed wind turbine because the IG allows small mechanical speed variations [26].

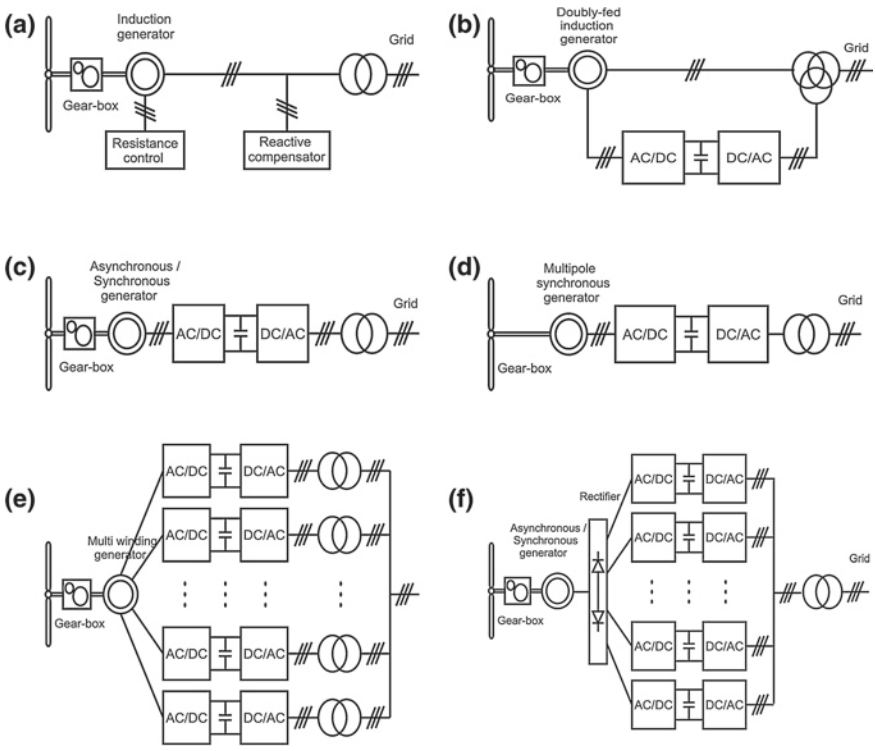

Fig. 16 Structures of power systems in WT [10]. **a** Rotor resistance converter structure. **b** Doubly fed induction generator (DFIG). **c** IG with gearbox. **d** Multi-pole synchronous generator. **e** Parallel connection and interleaved on the grid side, and **f** n-leg diode bridge producing a shared high DC voltage

This is the arrangement allows for a decrease in cost, however, there are also greater losses.

The high rotational speed requirement of an IG has already limited its applications and also caused extra energy loss during speedup and load, as shown in Fig. 17. The conventional wind turbine electric generator with fixed NRP actually loses a great amount of energy, especially in the slow wind speed field. To convert the unstable wind energy to more stable output electricity, the DFIGs are widely used in WT today, which use some control strategies to allow for output voltage with constant amplitude and frequency [34].

Nowadays, the favorite configuration for generation of wind turbine induction generator is fed doubly (DFIG). The characteristics of DFIG are high efficiency, flexible control, and low investment [32]. There are many advantages for variable-speed operation at medium applications. The advantages of variable-speed turbines are that their annual energy production is about 5 % greater than the fixed-speed technology and that the active and reactive powers generated can be easily controlled [9]. The machine is robust and requires little maintenance. The power electronics interface, usually consisting of two back-to-back PWM voltage

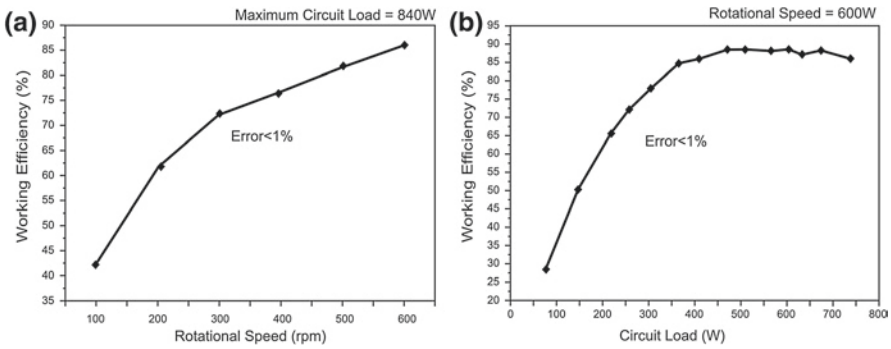

Fig. 17 The typical efficiency for the wind IG [34]. **a** Relationship of rotational speed versus working efficiency. **b** Relationship of the output power versus working efficiency

source inverters, is connected between the stator and rotor and, for restricted speed range applications, is rated at only a fraction of the machine nominal power [30]. Another advantageous characteristic is that this configuration reduces the mechanical stresses, as a result it improves the quality and stability of the energy [18]. Besides, they maximize the efficiency of the conversion of energy, because they operate at optimal rotational velocity for each given wind speed. It is worth noting, in contrast to the WT with full power converter, that its converter connected between the rotor windings and the grid is in part rating power, with a VA rating of typically 25 % of total system power. In general, no flicker problems occur with variable-speed turbines. Variable-speed turbines also allow the grid voltage to be controlled, as the reactive-power generation can be varied. One disadvantage, which must be pointed out, is that variable-speed WT need a power converter that increases the component count and make the control more complex.

The direct-drive applications are increasing because the gearbox can be eliminated. As compared to a conventional gearbox-coupled wind turbine generator, a direct-drive generator has reduced the overall size, has lower installation and maintenance cost, and has a flexible control method and quick response to wind fluctuations and load variation. For small WT, permanent magnet synchronous machines are more popular because of their higher efficiency, high-power density, and robust rotor structure when compared with induction and synchronous machines [9].

The multilayer magnetic cutting electric generator automatically adjusts its normal-rated power to match various wind speeds and reaches the maximum working efficiency. It is introduced in [34]. The results show that the total working efficiency of the full-field wind electric generator has increased 3 %.

The global efficiency depends on the control strategy because it acts on each type of electric generators. Figure 18 shows a general scheme to control the wind generation emulated by a PMSM.

An optimal control contributes to the maximum use of the generation because it guarantees stability, continuity, and quality in the supply of energy. It has been proposed in [32], through an analysis approach based on both trajectory and frequency

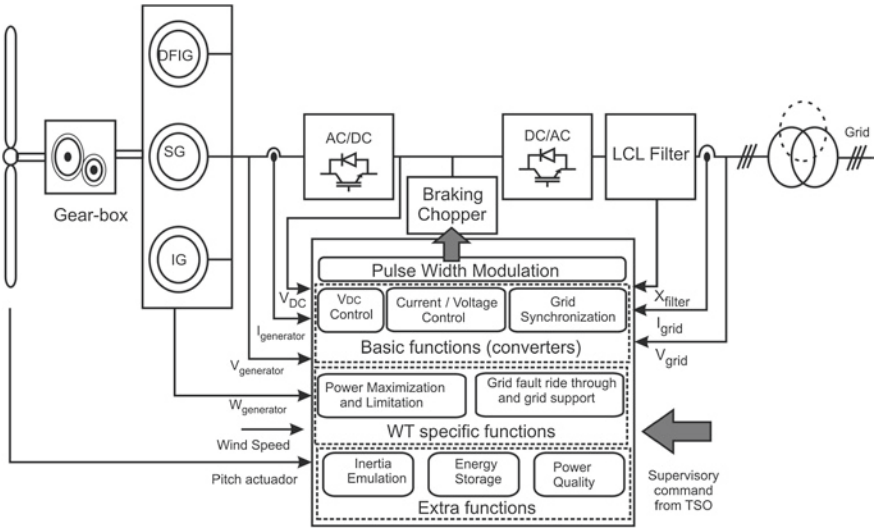

Fig. 18 General scheme of wind turbine control [10]

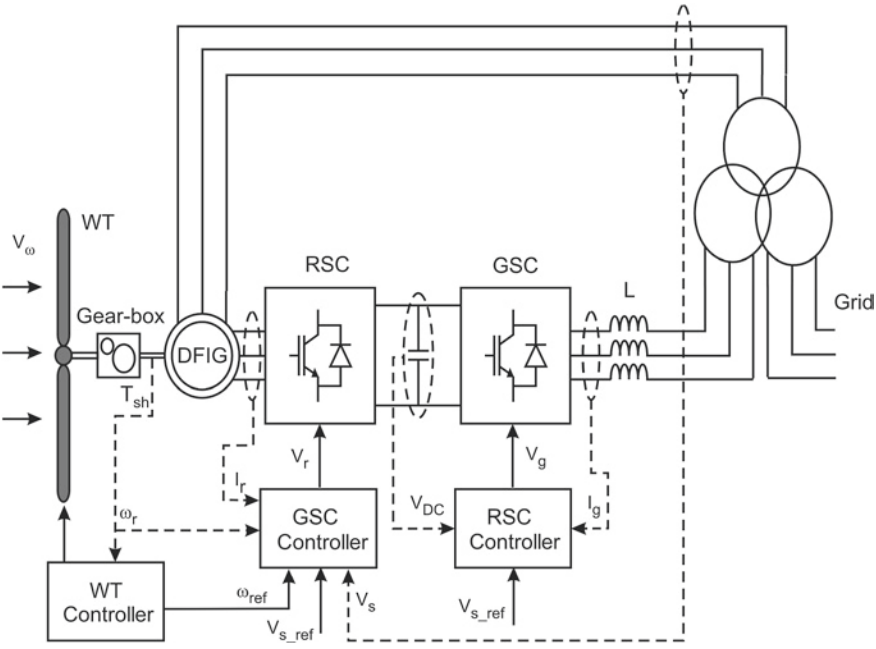

Fig. 19 Schematic diagram of DFIG wind turbine system [32]

domain information integrated with an evolutionary algorithm in order to achieve the optimal control of DFIG-based wind generation. Instead of optimizing all the control parameters, the key idea is to use a sensitivity analysis to first identify the critical

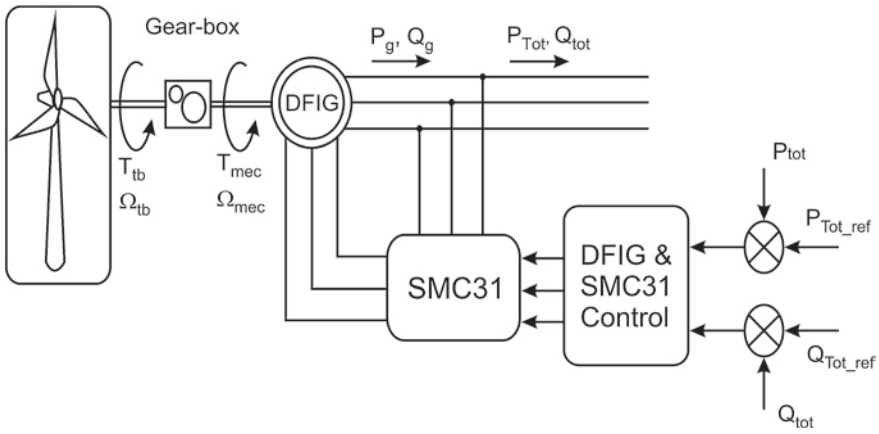

Fig. 20 Schematic diagram for a control proposal used in SMC3l [30]

parameters, the unified dominate control parameters (UDCP), in order to reduce the optimization complexity. Based on such selected parameters, a particle swarm optimization (PSO) algorithm was used to find the optimal values to achieve the control objective [32]. The schematic diagram of a wind turbine system is presented in Fig. 19. The back-to-back converter consists of three parts: the rotor side converter (RSC), the grid side converter (GSC), and the DC-link capacitor. The controllers of the converter have a significant effect on the stability of grid-connected DFIG.

According to [18], the WT should stay connected to the grid for a certain voltage range of time in case of a grid failure. This reference examines the transient behavior of the WT with DFIG during voltage faults using the scheme in Fig. 19 that includes power electronics in the RSC and in the GSC.

Another control proposal applies a sparse matrix converter (SMC3l) algorithm driving a three-level associated SMC3l to a grid-connected variable-speed wind generation (VSWG) scheme using a DFIGs for medium- and high-power application [30]. This controls the active and reactive power and uses a reference frame oriented along the stator flux vector for operation above and below synchronous speed, as shown in Fig. 20.

The reduction in the cost of generation begins in sizing. The load of a power system is a major source of uncertainty in power system planning. The variations of loads are considered in renewable DG locations. The hourly load profile over a one year period will be obtained as a percentage of the annual peak load [37]. The location of integrated DG for medium-power generation influences in the amount of losses that were caused. A methodology based on weighting factors is proposed in [37] to minimize energy losses by finding the optimal sizes of WT.

3.3 Technologies for Photovoltaic Generation

Solar energy can be utilized through two different conversion methods: solar thermal conversion and solar electric or solar-PV conversion. Solar thermal conversion uses the

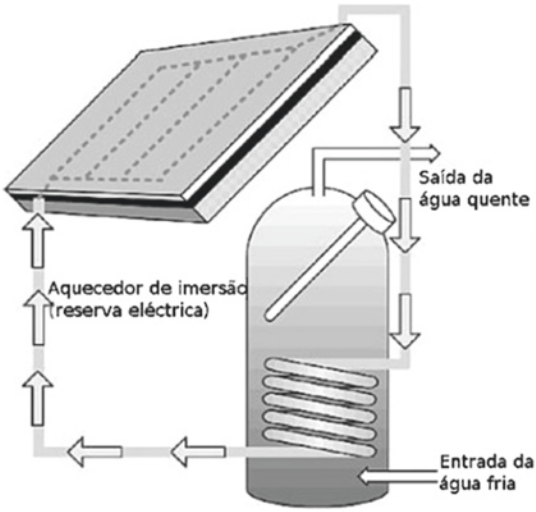

Fig. 21 Solar thermal conversion producing hot water in domestic installations

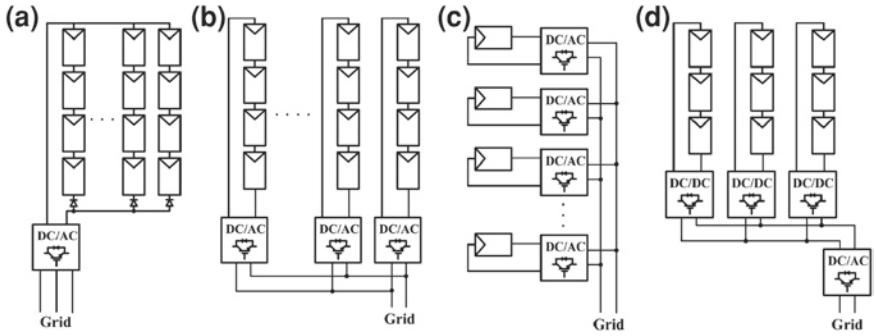

Fig. 22 Structure of different PV systems [10]. **a** Centralized inverter. **b** String inverter. **c** Module inverter. **d** Multi-string inverter

heat of the sun to produce hot water or air, cook food, dry materials etc. Solar-PV uses the heat from the sun to produce electricity for lighting houses and buildings, running motors, pumps, electric appliances, and lighting. Solar-PV systems are ideally suited for distributed resource applications [26]. The facilities of lower cost using the solar energy are applied for direct heating of water through solar panels, as displayed in Fig. 21.

A PV module without any mechanical parts has a lifetime of more than 25 years. However, aging may reduce its power generation capability to 75–80 % of the nominal value. A typical PV module is made up of around 36 or 72 cells connected in series, encapsulated in a structure made of, for example, aluminum [10].

There are three arrangements used to interconnect PV modules. One is the centralized inverter configuration (see Fig. 22a) that reaches high power, but has significant

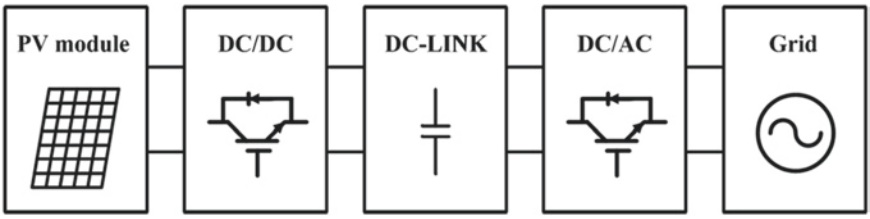

Fig. 23 Typical structure of PV systems [10]

disadvantages, such as a need for high voltage DC cables between PV panels and the inverter, power losses due to common MPPT, power losses due to module mismatch, losses in the string diodes, and the fact that the reliability of the whole system depends on one inverter. Another arrangement is the string inverter configuration, shown in Fig. 22b. It is a reduced version of the centralized inverter. If the string voltage is high enough, voltage boosting is not necessary and the efficiency can be improved. The advantages of the string inverter when compared with the centralized are no losses in the string diodes, separate MPPTs for each string, better yield due to separate MPPTs, and lower price due to the ease of mass production. The last arrangement is the module inverter configuration that is shown in Fig. 22c. It has the advantage that the losses are significantly reduced and it is possible to maximize the power production of each separate MPPT. This results in better optimization of power extraction than in the case of the string inverter. However, it has a low efficiency due to the high-voltage amplification, low-power conversion, and the price per watt is still higher compared with the previous inverters. The multi-string inverter, shown in Fig. 22d, combines the advantages of both string and module inverters by having many DC–DC converters with separate MPPTs that feed energy to a common DC–AC inverter. The multi-string concept is a flexible solution, having a high overall efficiency of power extraction because it is possible to control each PV string individually [10].

A typical structure of a PV system is presented in Fig. 23. The generated DC voltage is boosted by the DC–DC converter, and the current is converted to a suitable AC current by the DC–AC inverter [10].

A PV array or battery-operated DC–DC boost converter improves the quality in the distribution system. The PV array or battery-operated boost converter is used to maintain the desired voltage across the DC-bus capacitor to provide continuous compensation.

A PV control contributes to the maximum use of generation because it guarantees stability, continuity, and quality in the supply of the energy. The generalized block diagram control for PV generation is presented in Fig. 24.

Devices known as Custom Power can aid in providing continuous source harmonic reduction, reactive-power compensation, and load compensation. In [16], the use of DSTATCOM is proposed, and the scheme of it is presented in Fig. 25. It consists of three-leg VSC with a DC-link capacitor. The operation of VSC is supported by a DC-link capacitor with proper DC voltage across it. Here, a PV module or battery-interfaced boost converter is connected to the DC-bus capacitor

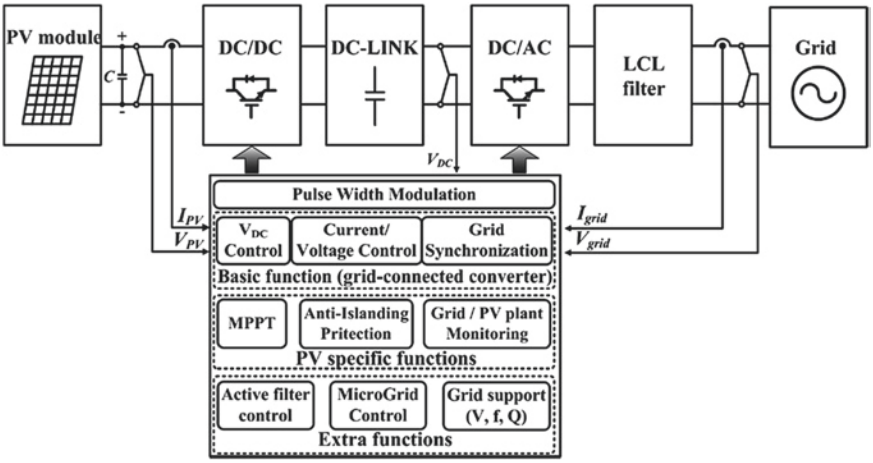

Fig. 24 Generic control structure for PV generation [10]

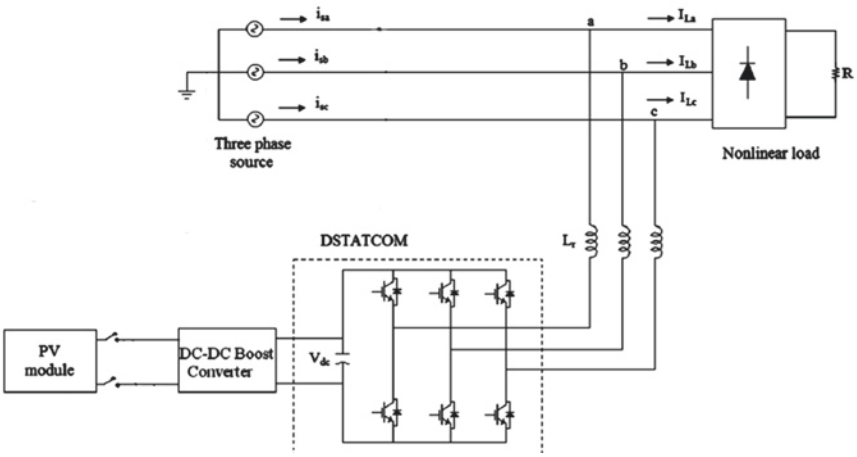

Fig. 25 Circuit diagram of proposed DSTATCOM in [16]

of VSC which is used to maintain the desired voltage across the DC bus for providing continuous source current harmonic reduction, reactive-power compensation, and load compensation throughout the day [16].

3.4 Maximum Power Point Tracking

There is a relationship between power produced and rotor speed both in microhydropower and in WT. This relationship influences the output voltage of

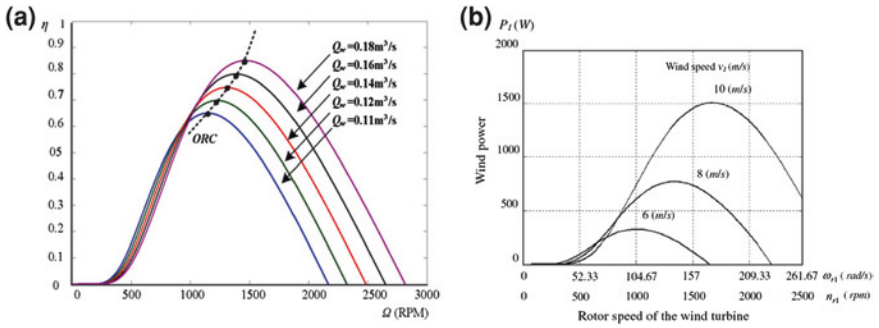

Fig. 26 Characteristic curves for controllable generation used to find the maximum power. **a** Semi-Kaplan (or propeller) steady-state characteristics: efficiency versus rotor speed [6]. **b** Characteristic curves of wind power versus rotor speed for wind turbine model at different wind speeds [17]

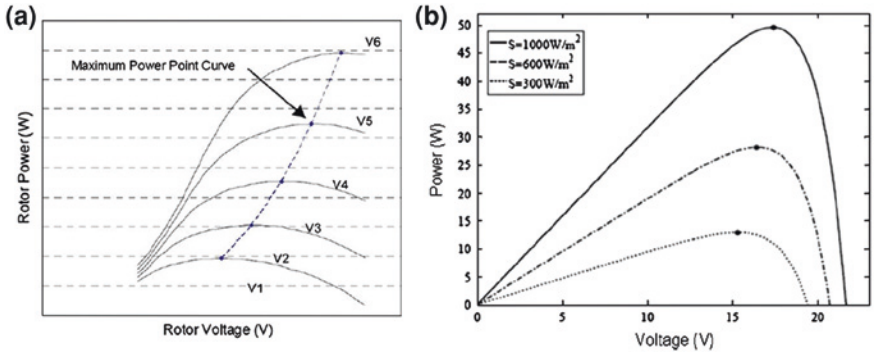

Fig. 27 Point where the derivative of the ratio between the power variation and the voltage variation is equal to zero for wind turbine and solar panel [15]. **a** P–V graphic of a wind turbine. **b** P–V graphic of a 50 W solar panel

the machine, as shown in Fig. 26a. Also in solar energy systems, there is a direct proportion between the output power and the voltage produced as can be seen in Fig. 26b. On the other hand, the output power does not directly increase proportionally with the voltage for several energy source [15].

The maximum power point refers to a special point where the derivative of the ratio between the power variation and the voltage variation is equal to zero as can be observed in Fig. 27. MPPT operation is required to efficiently use the energy produced by several energy sources [15].

She [25] proposes a control algorithm to be used as a "universal controller" for similar types of variable-speed wind turbine with minimal modifications. The modularity of the proposed controller is compliant with a plug-and-play property that will be helpful in distributed the control of smart grids.

An optimal operation of a grid-connected variable-speed wind turbine, based on a doubly fed IG is presented in [1]. The proposed control algorithms focus on

Table 1 Extracted energies during experimental tests (kWh) in [13]

Algorithm used	April 3	April 4	April 5	April 9	April 11	April 12
P&O	2.53	1.59	0.53	0.68	1.73	2.36
INC	2.56	1.61	0.55	0.69	1.76	2.39
ImP&O	*2.57*	*1.63*	*0.57*	*0.71*	*1.79*	*2.41*
FL	2.55	1.6	0.53	0.68	1.76	2.38

two main goals: a permanent track of the available maximum wind power, and a smooth regulation of the stator active and reactive powers exchanges between the machine and the grid.

An integrated voltage regulation system including MPPT Algorithm (MPPT) for solar generation is introduced in [15] to store and efficiently use of the energy produced by renewable sources using a dsPIC to obtain a rapid and stable operation. In order to minimize the oscillations on the output voltage, a cuk converter is used that can be operated as both buck and boost modes.

MPPT algorithms for solar generation with the classical linear voltage control the current-based sliding-mode approach ensures a wider regulation band but, unfortunately, in the presence of a fast irradiance variation, the sliding conditions might be violated, so that the operating point, which should be the maximum power point, might not be the expected one. In order to prevent such a drawback, a voltage compensation loop, developed in [7], is used to interface the current-based sliding mode with the MPPT algorithm.

Some direct MPPT (not requiring a priori evaluation of the PV panel, or not based on mathematical relationships or database) can also be classified according to the method by which the command variable is changed. Thus, fixed-step MPPT algorithms and variable-step MPPT algorithms can be differentiated. The most frequently used fixed-step MPPT algorithms methods are as follows: perturb and observe (P&O) and incremental conductance (INC). The most often used variable-step MPPT algorithms methods are those based on Fuzzy Logic. Additionally, an improved P&O algorithm (ImP&O) is also described in [13]. Using four identical PV, under strictly the same set of technical and meteorological conditions, an experimental comparison of these four algorithms is done in [13]. The results are presented in Table 1 from where it can be seen that the maximum of energy is extracted by the ImP&O algorithm.

4 Technologies of Low Cost for Backup Devices

In remote areas, where it is difficult or costly to connect to the utility power grid, stand-alone PV and wind power systems are gaining commercial attention. The power source of such RE is intermittent. Hence, in order to deliver continuous power to the loads, energy storage is required in many stand-alone power systems [14].

The intermittent behavior of many renewable energy sources (RESs) and distributed generation sources (DGs) due to their strong dependency on climatic and meteorological conditions, generate electrical energy that fluctuates especially

in a localized small capacity microgrid (MG) in more than 10 % of the RES occupation [31]. According to this, it is necessary to use energy storage systems (ESS) to backup generators and to aid in the stability of the electric net.

The quality of renewable resources is unpredictable at best and, as such, energy storage is seen to be vital to a RES system [36]. An ESS is presently the indispensable equipment in a MG as the smart way to suppress probable power fluctuation and deal with arduous imbalance challenges between the demand side and the supply side.

An ESS ideally encompasses the following key properties: a quick response time, the ability to store all spilled energy, and to release energy for a required amount of time. It must also be able to fully supplement the power generators in order to meet the maximum load demand. The costs, lifetime, and power characteristics all play important parts in the selection of ESS.

An MG may work at either a grid-connected mode or an islanded mode. When a failure in the utility grid is detected or the requirements for power quality are not satisfied, the MG will be disconnected from the utility grid and start to operate at islanded mode. Then, the instant power shortfall as the MG transferring from the grid-connected mode to the islanded mode can be compensated by the ESS boost. ESS can implement a seamless transfer of the MG between different modes. In addition, ESS may act as an emergency power buffer for critical customers during a fault situation and also facilitates a black start of the entire power systems [31].

Energy storage technologies can be classified into capacity-oriented (pumped hydroelectric systems, compressed air, hydrogen), and access-oriented storage devices (batteries, flywheels, supercapacitors, and superconducting magnetic energy storage) [35].

Different possibilities of technologies of electric power storage compared with different operation conditions based on time are presented in Table 2. Applications of storage in which there are possible replacement of conventional electricity systems for large-scale and long-duration storage (days and months duration) are expensive. The duration of storage up to a few hours is used low-cost installations. When considering the technologies of energy storage for low-cost facilities, it is necessary to take into account an efficiency comparison, application and the costs shown in Table 3.

The total annual costs and energy efficiencies have been used to calculate a cost of storage per kilowatt-hour discharged from the store as shown in Fig. 28. The costs of the electrical losses have been added at a typical UK wholesale price of 0.05/kWh. Only the lowest cost technologies have been included in this figure. Lead-acid batteries have been omitted from the figure. Their cost per kilowatt-hour is very similar to that of sodium sulfur batteries at timescales less than 1 h, while at longer timescales, they are more expensive than sodium sulfur and nickel–metal hydride batteries [5].

An electrochemical battery is one of most cost-effective energy storage technologies and has high-energy density (50–130 Wh/kg for lithium (Li)-ion batteries and 30–80 Wh/kg for nickel–metal hydride (NiMH) batteries); however, it is poor in power density [14]. The estimated overall efficiency of battery storage is in the range of 60–80 %, depending on the operational cycle and the electrochemistry type within the batteries. Lead–acid, Nickel–iron, Nickel–Cadmium (NiCd), Nickel–Metal Hydride (NiMh), and Lithium-Ion batteries are the four principal types of battery storage. Figure 29 shows a steady increase in the energy density of batteries [31].

Table 2 Storage technologies and application [5]

Full power duration of storage	Application of storage and possible replacement of conventional electricity system control	Biomass	Hydrogen. Electrolysis + full cell	Large hydro	Compressed air energy storage (CAES)	Heart or cold energy storage	Pumped hydro	Redox flow cells	Battery technologies	Flywheel	Superconducting magnetic energy storage (SMES)	Supercapacitor	Conventional capacitor or inductor
4 months	Annual smoothing of load, PV, wind, and small hydropower plants	X	X	X									
3 weeks	Smoothing weather effects: load, PV, wind, and small hydropower plants	X	X	X									
3 days	Weekly smoothing of load and most weather variations	X	X	X	X	X	X	X					
8 h	Daily load cycle, PV, wind, transmission line repair	X	X	X	X	X	X	X	X				

(continued)

Table 2 (continued)

Full power duration of storage	Application of storage and possible replacement of conventional electricity system control	Biomass	Hydrogen. Electrolysis + full cell	Large hydro	Compressed air energy storage (CAES)	Heart or cold energy storage	Pumped hydro	Redox flow cells	Battery technologies	Flywheel	Superconducting magnetic energy storage (SMES)	Supercapacitor	Conventional capacitor or inductor
2 h	Peak load lopping, standing reserve, wind power smoothing	X	X	X	X	X	X	X	X				
20 min	Spinning reserve, wind power smoothing, clouds on PV		X	X	X	X	X	X	X	X			
3 min	Spinning reserve, wind power smoothing of gusts		X				X	X	X	X			
20 s	Line or local faults							X	X	X	X	X	X

Table 3 Comparison of several typical ESSs [31]

Type	Efficiency (%)	Energy density (Wh/kg)	Power density (W/kg)	Response (ms)	Cycle life (time)	Cost ($/kWh)
Battery	60–80	20–200	25–1,000	30	200–2,000	150–1,300
SMES	95–98	30–100	1e4–1e5	5	1e6	High
Flywheel	95	5–50	1e3–5e3	5	>20,000	380–2,500
Supercapacitor	95	>50	4,000	5	>50,000	250–350
NaS	70	120	120	<100	2,000	450

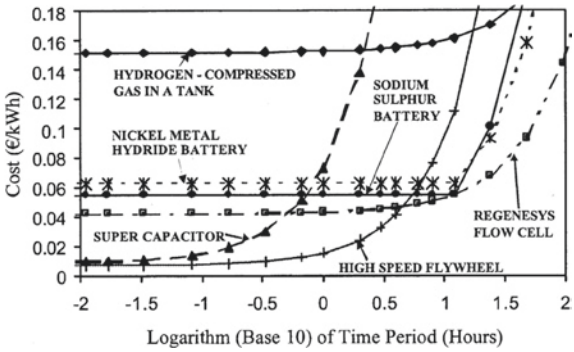

Fig. 28 Cost of energy storage technologies [5]

Frequent maintenance requirements, limited charging, and discharging cycles are also the bottleneck of this technology; and hence, it has become a less attractive option for the future. Among others, recent advancement in FC and electrolyzer (ELZ) technologies has opened the promising solution by utilizing H_2 as the intermediate and long-term storage medium [11].

A fuel cell is an electrochemical device that converts chemical energy into electrical energy. It produces electricity and heat when fuel is supplied. Unlike a battery, EC do not need to be recharged. The by-products of a fuel cell are water and heat, therefore, it is considered a clean source of energy. There are different types of FC depending on the electrolyte they use. The electrolyte defines the catalyst used, the operation temperature and the fuel required [27]. The electrolysis of water using cells with a polymer electrolyte membrane (PEM) is a very efficient method of producing hydrogen. PEM electrolyzers are very simple and compact and have demonstrated higher current density capability than conventional alkaline water ELZs. The reverse equivalent to a PEM electrolyzer is a PEM fuel cell, which is thus modeled similar to the PEM electrolyzer. Chemical energy from the hydrogen fuel is converted into electricity through a chemical reaction with oxygen. The by-products of this reaction are water and heat [35]. To improve efficiency, a higher voltage should be used, but the output power will be diminished, as shown in Fig. 30. Based on this, it is reasonable to say that a good operating point would be at an efficiency of approximately 40 %, where the voltage is 0.6 V and the power density is 315 mW/cm^2.

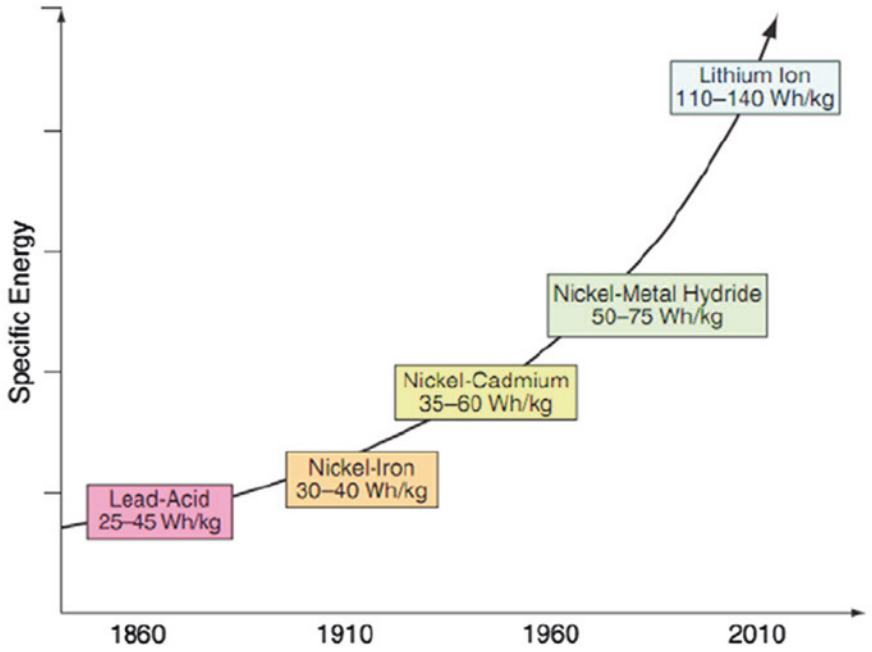

Fig. 29 Increment in the density of energy of the batteries along the years [31]

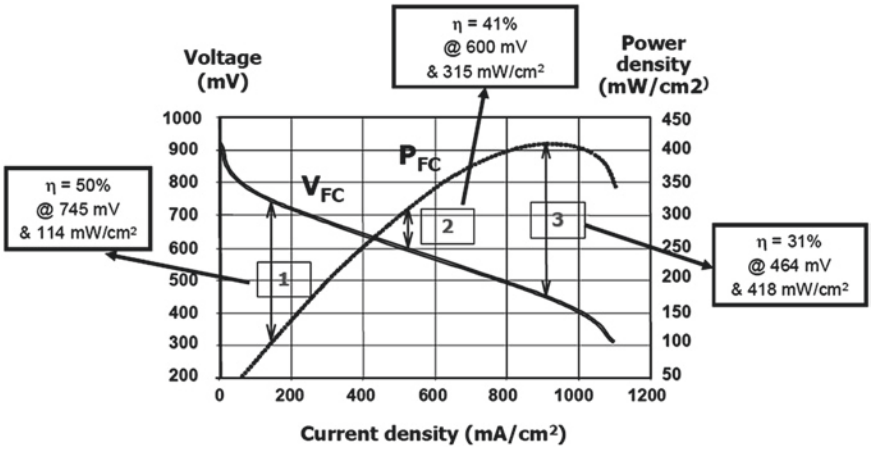

Fig. 30 Fuel cell performance [27]

A supercapacitor, also referred to as an ultracapacitor or electric double layer capacitor (EDLC), stores energy in two series capacitors of an electric double layer (EDL), which is formed between each of the electrodes and the electrolyte

ions. Without chemical processes, electrical energy can be stored directly, and thus, the response time is very small [31]. Supercapacitor has higher power density of 300–500 W/kg, and a long life cycle exceeding 500,000 cycles [14].

An ESS consists of one or more renewable storage technologies. A control strategy has been proposed to reduce battery stress and reduce charge/discharge cycles to extend battery lifetime within the Battery/Supercapacitor hybrid system. The basic principle is to use the battery to support system energy while the supercapacitor meets the power requirements. This can avoid frequent charging/discharging cycles and a long discharge current from the battery. This battery/Supercapacitor hybrid system has been introduced in stand-alone RE power systems, achieving outstanding system performance [14].

The output power response in a fuel cell is delayed due to the processing time through subsidiary equipment and their slow internal electrochemical and thermodynamic characteristics. Therefore, in order to supply electric power to fluctuating loads by a hybrid FC system, an electric energy storage system is needed to compensate the gap between the output from the FC and the load. Previous research has shown that the hybridization of FC with batteries, with supercapacitors, and with batteries/supercapacitors provides cost, performance, and operational improvements, as well as fuel economy benefits that are attractive [33].

An electrolyzer may be used to convert excess energy to produce hydrogen, which can act as an energy carrier. FC may be used as power sources to convert the chemical energy of hydrogen into electrical energy when power demand is higher than that which is instantaneously available from renewable sources. A battery pack is usually used to maintain a constant DC-bus voltage and to store or supply short-term energy deficits. The emphasis of such systems is not only on improving the performance of existing hydrogen production, storage and utilization technologies, but also on the effective integration of various subsystems to RES using system-level power management strategies (PMS) [38], as is presented in Fig. 31.

5 Technologies of Low Cost for Conditioning Units

Power electronics are needed in almost all types of RE systems to achieve high efficiency and performance in control. They control the renewable source and interfaces with the load effectively, which can be grid connection or working in a stand-alone mode [10]. In order to produce electric power, the renewable sources require conditioning units to reach the conformation and quality requirements demanded by the costumers of the power network. This conformation and quality are demanded even in isolated facilities because the apparels that use this energy were manufactured for the characteristics of the public power network. Therefore, a renewable source of energy is associated to a conditioning structure of energy as was previously mentioned in Sect. 3 of this chapter. The conditioning structures of energy represent a significant aspect for the improvement in the use of the RE and can commit to the process of the generation.

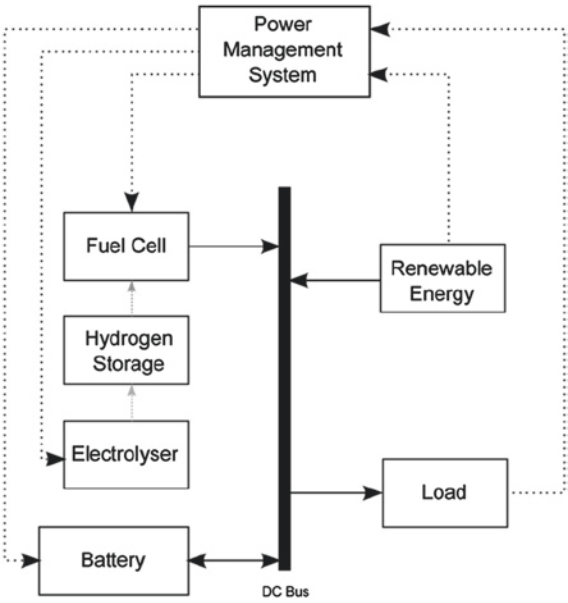

Fig. 31 Storage and utilization technology showed in [38]

Power electronics are used in all of the necessary aspects for direct use of the renewable sources in the electric system of energy. They are needed in the generation step, in devices for energy storage or in the integration of the several energy sources and end loads. Therefore, the selection of the power electronics to be used is related directly with the efficiency and smaller costs of the RE [23].

5.1 Power Electronics in Wind Energy Generation

The major advantage of the DFIG, which has become popular, is that the power electronic equipment only has to handle a fraction (20–30 %) of the total power system [26]. Several studies have been carried out concerning this topic in order to reduce losses in the structures and to increase energy use. For example, the converter applied in the WECS tries to enhance the efficiency control of the whole power system generation characterized by the power generated. It is obtained with a high quality of rotor voltages and currents that depend on the conditioning units (converters). The typical power electronic arrangement for WECS is back-to-back, as shown in Fig. 32. This scheme allows, on one hand, a vector control of the active and reactive powers of the machine, and on the other hand, a decrease in a high percentage of harmonic content injected into the grid by the power converter. The overall cost of power electronics is about 7 % of the whole wind turbine [9].

A structure of a low-cost back-to-back single-level converter is provided in Fig. 33. The main characteristics of this topology are the reduction in losses for

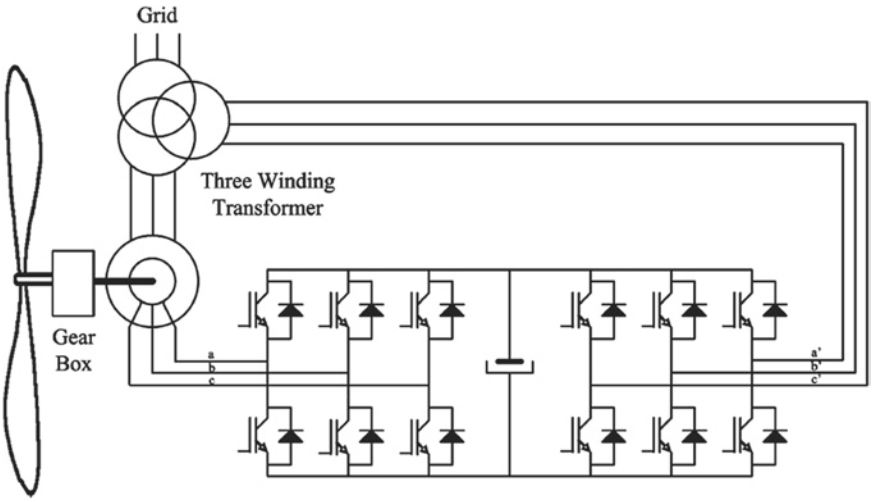

Fig. 32 Single doubly fed induction machine with reduced power converter structures using two fully controlled AC–DC power converters [9]

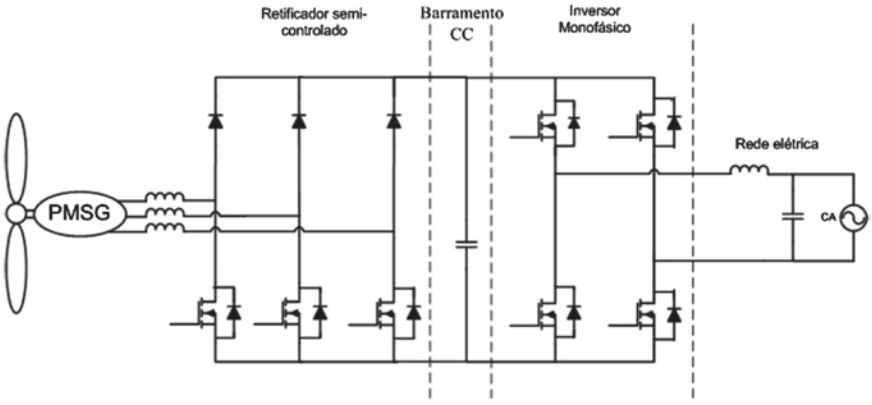

Fig. 33 Low-cost back-to-back single-level converter

transport, since cascaded converters are not used, a reduction in costs for using a smaller number of switches than the conventional topologies, and increased safety, because a short circuit possibly does not even exist among the top group and bottom group switches. Such characteristics cause the cost of larger harmonic distortion and smaller potency factor, although this is satisfactory in small load systems.

The multi-level converters (see Fig. 34) have the lowest demands for the input filters or alternatively reduced number of commutations. For the same harmonic performance as a two-level converter, the switching frequency of a multi-level

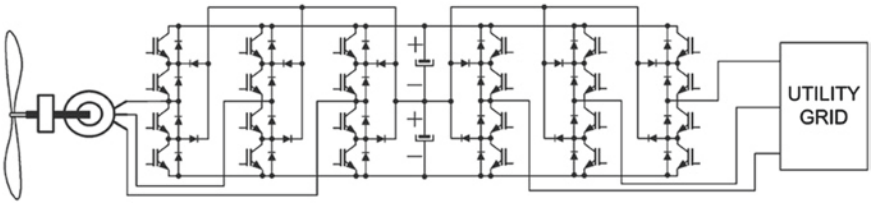

Fig. 34 Multi-level back-to-back converter for a direct connection of a wind turbine [9]

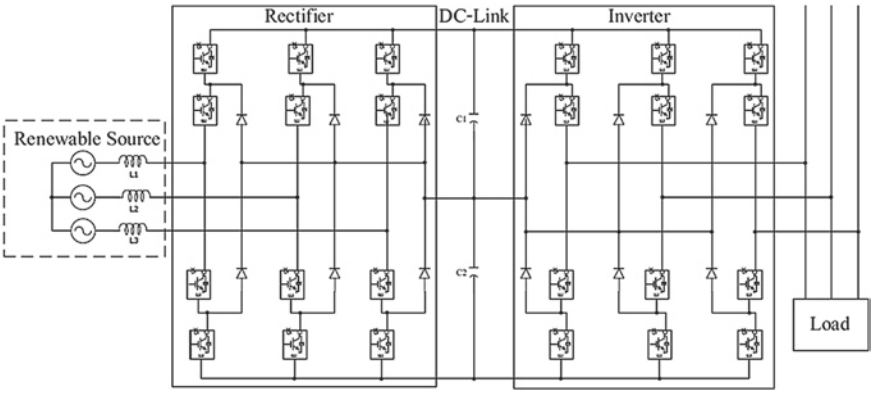

Fig. 35 Full power converter structures using back-to-back three-level converter [20]

converter can be reduced to 25 %, which results in the reduction in the switching losses. Even though the conducting losses are higher in the multi-level converter, the overall efficiency depends on the ratio between the switching and the conducting losses. The most commonly reported disadvantage of the multi-level converters with split DC link is the voltage unbalance between the capacitors that are integrated within it [9].

The structure presented in Fig. 35 is a three-level inverter using the space vector pulse width modulation method. It can improve the control system with fast response and stabilization of the DC voltage [20].

Nowadays, there is an increasing interest in AC–AC direct power conversion schemes without passive components in the DC link existing in rectifier–inverter-based systems as presented in Fig. 36. This topology has similar characteristics such as the direct matrix converter, but the existence of a DC link offers some other possibilities such as multi-drive operation, a change in the DC-link voltage magnitude, operating at different switching frequencies in the input and output stages to reduce losses and essentially upgrading voltage level numbers at the output stage [30]. There are applications that do not need a full input–output voltage ratio, such as WTG, that operate at a reduced speed range where the rated rotor voltage, i.e., the output voltage of the voltage source inverter, can be adjusted depending on the maximum slip velocity and the stator to rotor turn ratio (Table 4).

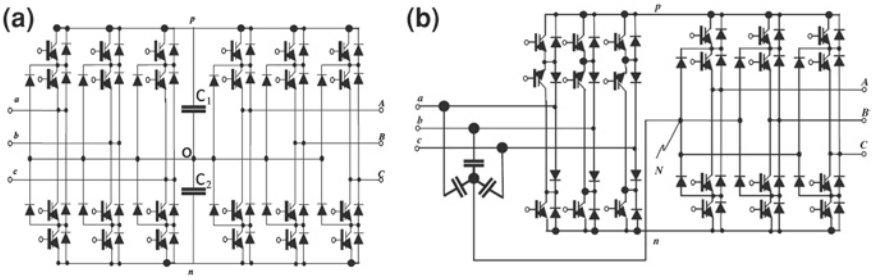

Fig. 36 Comparison between three-level topologies [30]. **a** Back-to-back three-level topology. **b** Three-level sparse matrix converter (SMC) topology

Table 4 Comparison between the proposed structure and back-to-back three-level converter [30]

Parameters	Back-to-back three-level converter	SMC
Number of IGBT	24	21
Number of diodes	36	30
Number of gate driver power supply	19	13
DC-bus capacitor	2	0
Output phase-to-phase voltage level	3	3
Input power factor controllability	Yes	Yes
Compact sight	No	Yes
Four-quadrant operation	No	Yes

5.2 Power Electronics in PV Generation

The module-integrated converter topology uses on the AC side one converter per PV module and a parallel connection. It requires a central measure for main supervision. Although this topology optimizes the energy yield, it has a lower efficiency than the string inverter (see Fig. 37). This concept can be implemented for PV plants of about 50–100 W [9].

In most energy systems, converters are used for regulating the output voltage; thus, the stability of the converter is an important factor to improve energy efficiency. If any power system uses either only buck or only boost converters, the energy produced can be stored only in certain levels. For this reason, using a cuk converter is a better solution for this issue because it can be operated at both buck and boost modes. In cuk converter-based systems, if the voltage produced by the source is lower than the desired level, the converter operates in boost mode. Otherwise, if the voltage produced is higher, the converter operates in buck mode. Therefore, the energy produced can be used without any interruption, and thus efficiency of the system is increased [15].

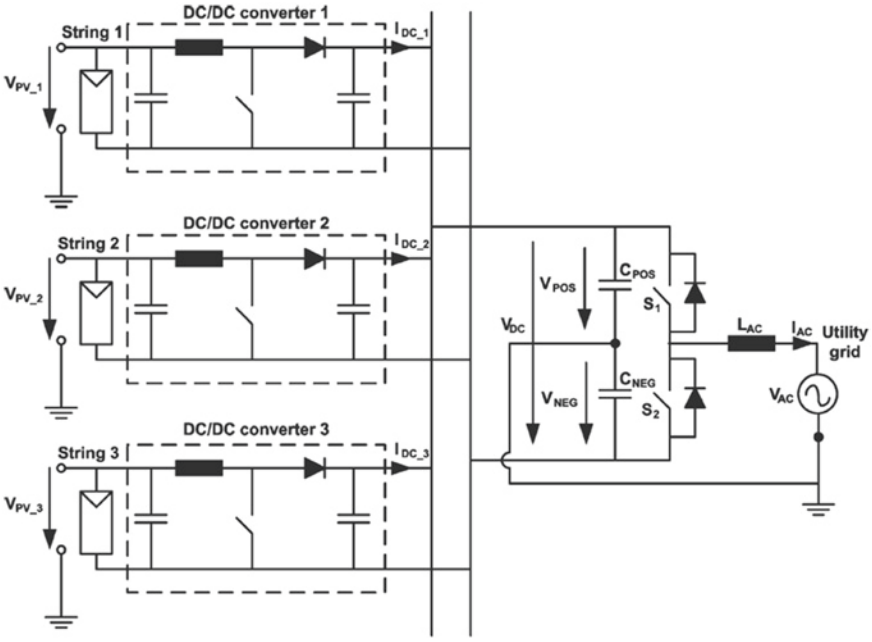

Fig. 37 Multi-string converter with a single-phase inverter stage [9]

The usual classification of PV topologies considers two major categories: PV inverters with DC/DC converter (with or without isolation) and PV inverters without DC/DC converter (with or without isolation). The isolation used in both categories is acquired using a transformer that can be placed on either the grid or low-frequency (LF) side or on the high frequency side (HF). PV systems without transformers would be the most suitable option in order to minimize the cost of the total system. On the other hand, the cost of the grid-connected inverter is becoming more visible in the total price system [9].

The transformerless PV converters increase the total efficiency of a PV system and have other advantages such as reduction in costs, size, and weight. Some topologies have been proposed such as the H-bridge, H5-bridge, HERIC, neutral-point clamped (NPC), and Conergy NPC. They are presented in Fig. 38 [10].

PV panel outputs have fluctuating power due to the variation in solar irradiation and temperature. An energy storage system could be added in the system to smooth the fluctuation of grid-injected power, where the battery is connected to the system either by an extra DC/DC converter on the DC side or by an extra DC/AC converter on the AC side. These structures make the power generation system more complex and expensive, causing low efficiency and low reliability. Figure 39 presents a new PV interface inverter by integrating quasi-Z-source inverter (qZSI) with a battery that can smooth the grid-injected power when PV power fluctuates [29].

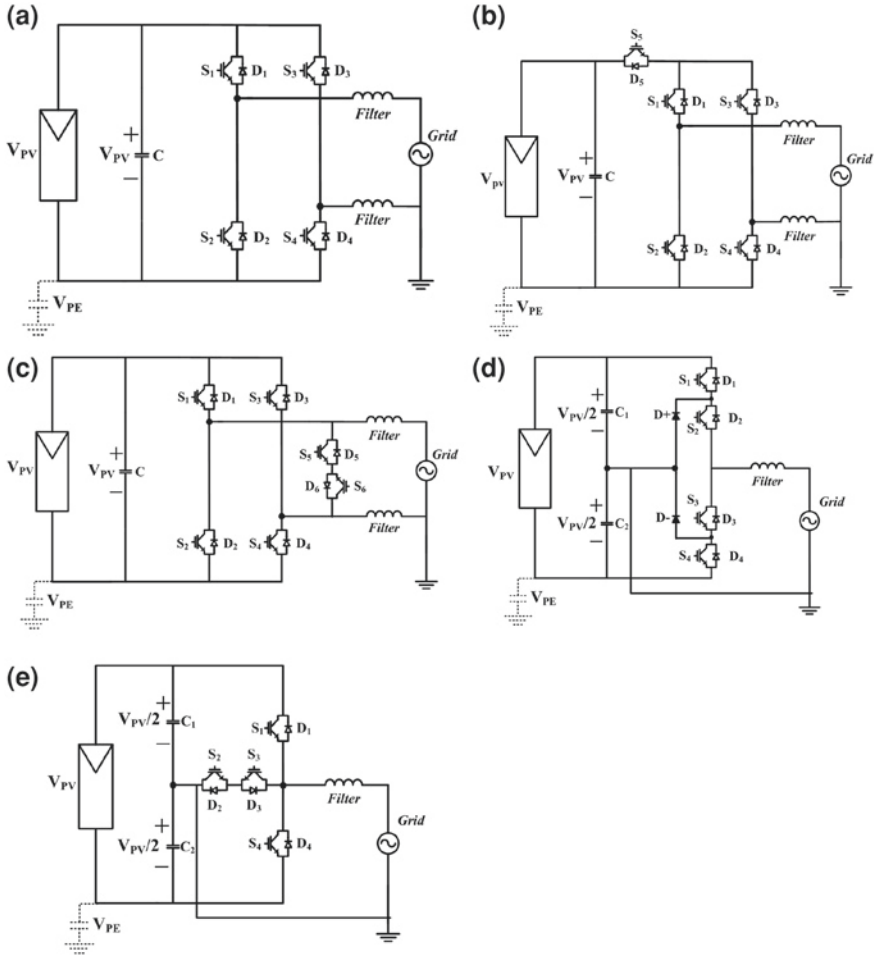

Fig. 38 Topologies of converters for PV system [10]. **a** H-bridge. **b** H5-bridge. **c** HERIC. **d** NPC. **e** Conergy NPC

5.3 Power Electronics in Energy Storage

According to [28], the following functions can be expected from a fuel cell power conditioning system:

- Regulation of the unregulated DC voltage output for different load current conditions during lifetime of the system.
- Matching of the voltage level of the inverter with the load.
- Conversion of the DC output voltage to demanded AC voltage with desired frequency.

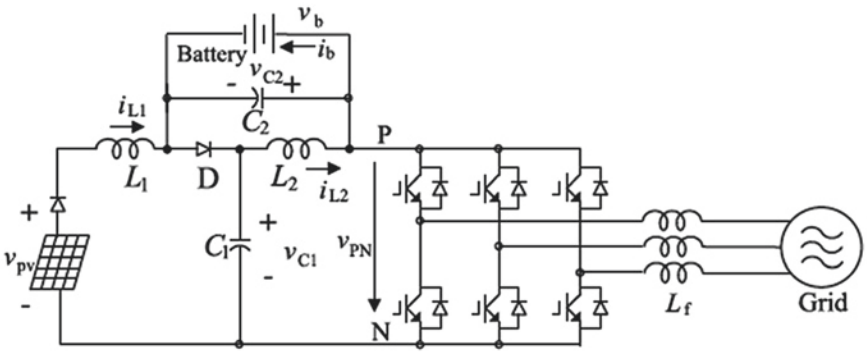

Fig. 39 qZSI with battery for a PV system proposed in [29]

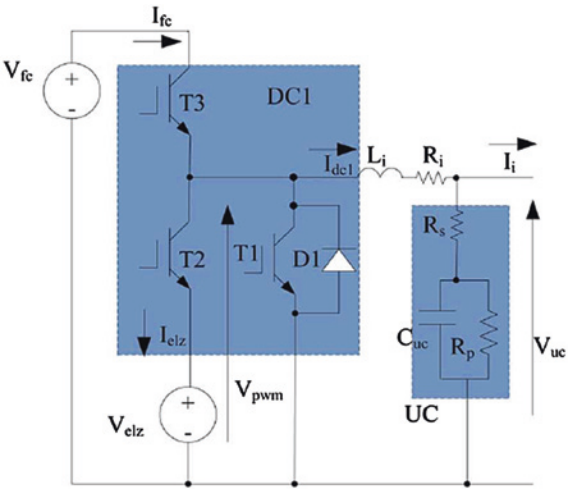

Fig. 40 Electrical diagram for **a** bidirectional DC–DC chopper [11]

Unlike other converters that operate only when the primary source is available, the interface for ESS will operate continuously to support the MG over a long period of time. Therefore, reliability and efficiency are the key issues to be considered in choosing topologies of the converters [31].

Many DERs and ESSs must be connected in series and in parallel in order to achieve high power and voltage requirements, where modular design is the best approach. Bidirectional DC/DC converters, such as phase shift controlled dual active bridge (DAB) converter and dual half bridge (DHB) converter, are promising in modular power converter synthesis.

A bidirectional DC/DC, as described in [11], is used in an integrated fuel cell, ELZ, and ultracapacitor system in a stand-alone microhydro plant (see Fig. 40).

5.4 Power-Integrated Hybrid Systems

Power converters can be used to couple or decouple the different components of the system, greatly simplifying its design and operation and yielding increased system reliability, reduced cost, and improved system performance.

In general, there exist three techniques to connect hybrid systems based on RES [28]: DC-coupled hybrid system, AC-coupled hybrid system, and combined DC/AC hybrid system. All are presented in Fig. 41. Table 5 lists the main advantages and disadvantages of the coupling methods before mentioned.

Rodriguez [23] proposes a power management system based on identical power modules, each one capable of interfacing a variety of loads or energy sources upon appropriate configuration. Each module has two electrical interfaces: the device side and the bus side (see Fig. 42).

The maximum power per module is chosen to be 500 W, and no limit is established a priori to the number of modules that can be connected to the same bus. The non-inverting four-switch buck-boost topology was selected to implement each module due to its bidirectional power flow and voltage step up/down capabilities, which offer the required versatility for the application. Very high efficiency over a wide range of operating voltages has already been demonstrated using this topology (see Figs. 43 and 44).

6 Examples of Applications

The penetration of the RE resources such as photovoltaic generations or WT is rapidly growing, and the concern about the influence on power systems, such as stability issues, is increasing. On the other hand, the low-operating cost of RE resources is a major advantage in rural areas or remote islands, where electricity cost is high because of a lack of transmission lines or high delivery cost of diesel fuel [3]. This section will present different cases around the world of low-cost installations based on RS of energy using hybrid systems.

6.1 Case A: Hybrid Diesel/Solar/Hydro/Fuel Cell Energy Schemes for a Rural ICT Telecenter

This case presents the rural electrification of an ICT telecenter located in the Kelabit Highland of Sarawak, in East Malaysia, which is 400 km west from the town of Miri (see Fig. 45a) [2]. Its height above sea level is approximately 1,000 ft, and the highland is essentially surrounded by dense jungle and mountains (see Fig. 45b). As such, it is isolated from other parts of the world. The rural electrification to provide means of ICTs and Internet access to the remote areas in order

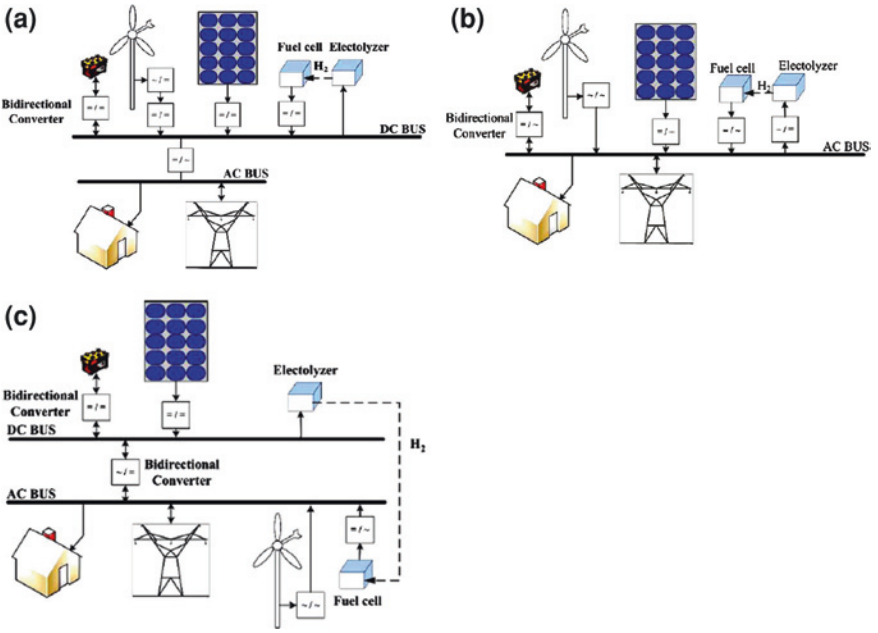

Fig. 41 Techniques to connect RES [28]. **a** DC-coupled hybrid system. **b** AC-coupled hybrid system. **c** Combined DC/AC hybrid system

Table 5 Advantages and disadvantages in coupling method in RE

Method of coupling	Advantageous	Disadvantageous
DC coupling	Simplest method of integration	Hybrid diesel/solar/hydroLow reliability of AC power due to high dependency on proper operation of AC/DC converter
	No need for synchronization	
	Balanced operation through single-wire connection	Non-modular structure, due to AC/DC converter. Thus, problems in future system capacity enhancement
	Compatible with DC loads	
AC coupling	High reliability, due to modular structure	Not compatible for DC loads
		Requirement for synchronous operation
	Easy future capacity enhancement	Power factor and harmonic distortion correction
	Ready for grid connection	
Combined coupling	Includes benefits of both previous systems	More cost for power electronics interface and complexity in control

to keep abreast of external developments. The object of bringing Internet access to Bario was to provide opportunities for social development available from the deployment of information and communication technologies within the remote communities.

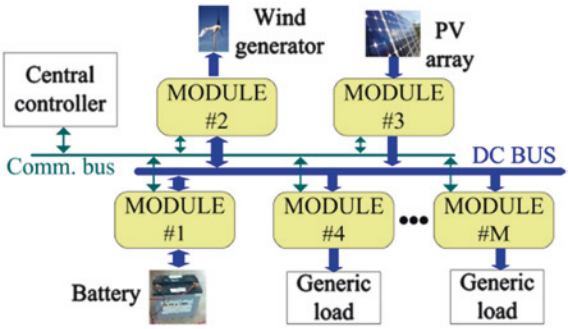

Fig. 42 Architecture of the proposed reconfigurable DC power management system [23]

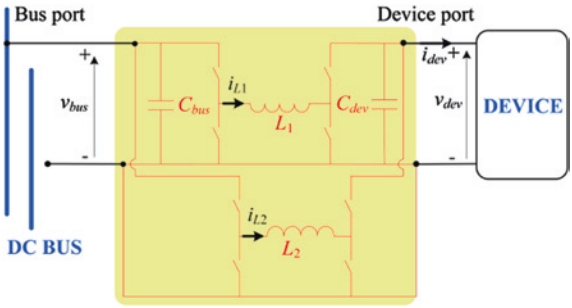

Fig. 43 Schematic diagram of the bidirectional module

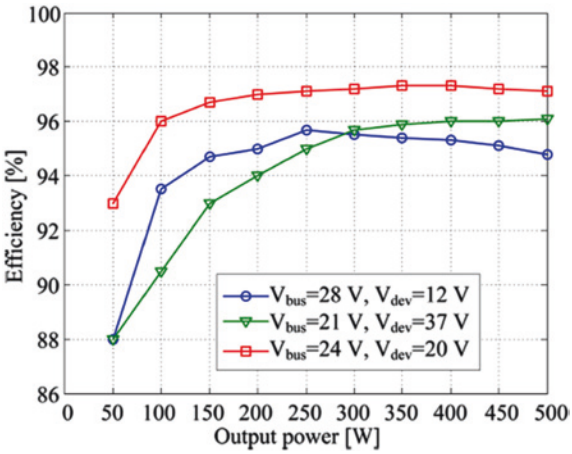

Fig. 44 Measured efficiency of the four-switch buck-boost prototype

The energy consumption load is 0.6 kW in the telecenter, whose plant is shown in Fig. 45d and whose energy consumption is according to Table 6. Initially, a diesel generator was brought in and used but it was utilized just for a few hours per day as diesel fuel is very expensive (with average price over US$ 2/l), limited in quantity and has to be flown in from a few hundred kilometers away. With

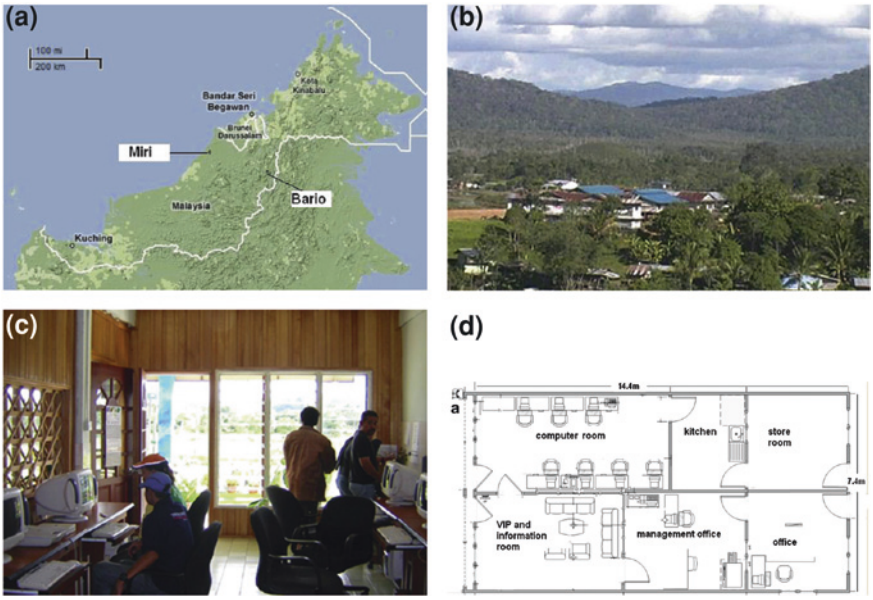

Fig. 45 Localization and plan of the ICT center. **a** Map of the area of Bario, Kelabit Highland, Sarawak, East Malaysia. **b** Photograph of the beautiful Bario village and its ICT telecenter at the valley of the Kelabit Highland. **c** Partial view of Zone A in the e-Bario ICT telecenter. **d** The floor plan of the ICT center

Table 6 Energy consumption load for the e-Bario ICT telecenter

Appliances/load	Quantity	Energy consumption (W)	Percentage (%)
PCs	8	360	60
Lighting	6	180	30
Other	–	60	10
Total load	–	600	100

escalating fuel cost and delivery difficulties, the sustainability of the e-Bario telecenter available for continuous community usage becomes an enormous task. Apart from this, the diesel-powered system needs frequent maintenance that is too expensive for the ICT telecenter.

As an alternative, solar-PV panels were brought in and implemented at the ICT in two stages in 2002 and 2005, respectively (Table 7).

The results demonstrated that hybrid systems are less costly than diesel generation from a net present cost perspective even with the high diesel fuel price subsidies. Although higher capital costs are incurred for the hybrid systems, their low-operating costs work in their favor. Also it was concluded that a diesel–wind hybrid was a most economical option for the area studied. However, lowering the capital cost of the PV system, its replacement cost, and its O&M cost by only 10 % would help a PV penetration into hybrid systems in remote areas.

Table 7 The alternative energy deign schemes for the e-Bario ICT telecenter

Alternative power schemes	Year of implementation	No. of PV panel	Total power
Diesel generator	1999	–	5 kW
Hybrid diesel generator-PV	2002	12	80 W/Panel × 12 + 5 kW = 5,960 W
PV stand-alone	2002	12	80 W/Panel × 12 = 960 W
Additional PV	2005	12 + 7	960 W + 175 W/Panel × 7 = 2,185 W
Hybrid PV-hydro	2007	19	2,185 W

6.2 Case B: Making Isolated Renewable Energy Systems More Reliable

The supply of electricity to isolated communities in Brazil and other developing countries, in general, is still done in a precarious way, using diesel generators, which operate for 3 or 4 h per day [22]. This has happened mostly due to the high cost associated with the expansion of the conventional power grid to these communities. In stand-alone systems, these solutions have been shown to be appropriated for areas of difficult access, dispersed, with environmental restrictions or with a population formed by low-income people, even when these adverse characteristics represent a difficulty for the sustainability of the designed generation system.

A practical example is the system installed on the Island of Lençóis in the northeast of Brazil. This autonomous system was projected to provide electrical power 24 h per day for a community formed by approximately 390 inhabitants distributed among 90 homes. At the end of 10 years of operation, the full power consumption of the Island was estimated to be approximately 6,800 kWh a month. This estimation takes into account the residential, small businesses, public agencies (school and health center) consumptions, and the consumption of a small ice factory with an average of 720 kg/day. Figure 46 shows a panoramic view of the Island and the installations of sub-systems and distribution network.

The simplified block diagram of the proposed system is presented in Fig. 47. It is formed by a solar sub-system, a wind sub-system, a battery bank, a backup diesel generator, an inverter system, and a sub-system of control and management based on a programmable logical controller (PLC).

The solar sub-system consists of 9 PV strings in parallel, each one formed by 18 PV modules, with 130 W each on in series. The strings were installed on the roof of the powerhouse as illustrated in Fig. 46c. Each string has a controller to provide the correct charging of the battery bank. The total maximum power of this sub-system is approximately 21 kW.

The wind sub-system is formed by three small WTs, each one with 3 blades up wind. These turbines were installed near the sea, on towers that are 30 m

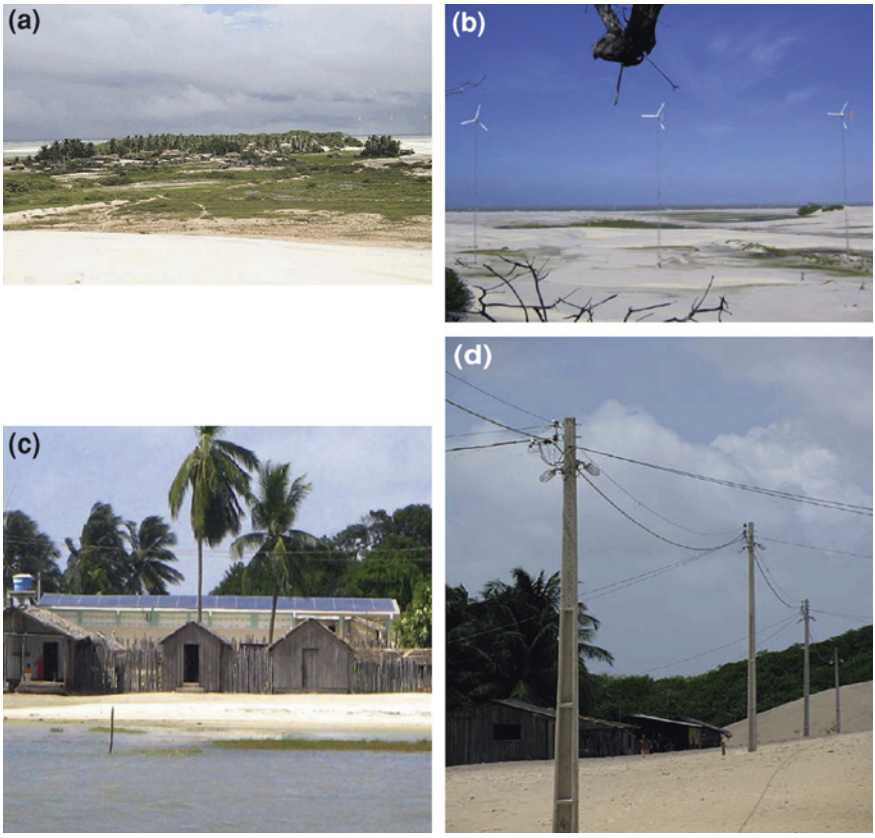

Fig. 46 Panoramic view of the Island and the installations of sub-systems and distribution network. **a** View of the island of Lençóis, Maranhão Brazil. **b** The wind sub-system (tower height: 30 m). **c** The solar sub-system. **d** View of the aerial distribution network

high, as shown in Fig. 46b. The wind generators are three-phase permanent, with 7–8.5 kW, magnet synchronous type, with an exterior rotor drum type with 38 poles. The AC output voltage is rectified to charge the battery bank.

The solar and wind sub-systems operate in parallel to charge a bank composed of 120 batteries, arranged in 6 parallel strings, each formed by 20 batteries of 150 Ah in series. The nominal voltage of the bank is 240 VDC.

There is also a 53 kVA diesel generator as a backup unit to be used eventually during the lack of primary energy sources or when the renewable power generation sub-systems are on maintenance.

The automatic management of the system is done by a programmable logic controller (PLC), which is responsible for the coordination of the parallel operation of all sources, with special attention paid to the system efficiency.

Figure 48 illustrates the individual contribution of renewable resources and battery bank charge in August 8, 2009. Negative values indicate that the battery bank

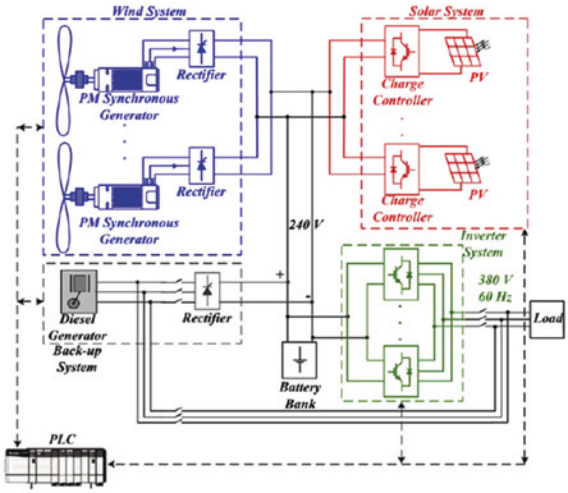

Fig. 47 Block diagram of the hybrid power system

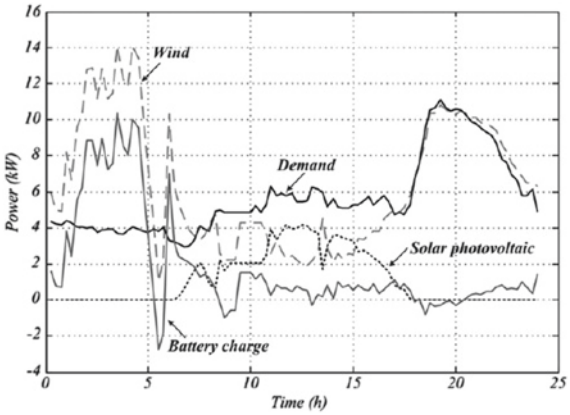

Fig. 48 Daily participation of renewable sources and battery bank

in discharging, i.e., it is complementing the load balance. For this day, a slight complementary behavior among solar and wind energies is observed. In general, this behavior cannot be sustained over several months. Typically, hot and sunny days are accompanied by winds.

Since July 20, 2008, the system has been in operation. The first year—160 days—was considered as a testing period, and 2009–2011 as steady-state operation. There are many indices for measuring reliability. The most common are referred to as SAIFI and SAIDI defined in IEEE Standard 1,366 as system average interruption frequency index and system average interruption duration index, respectively. These indices are equivalent to FEC and DEC, respectively, which are used in Brazil. Table 8 shows the value of these indexes in the case example.

Table 8 System operation indexes

System operation	SAIFI	SAIDI	Renewable energy operation (%)	Diesel operation (%)
First year (3,936 h)	3	72	99.39	0.61
Second year (8,760 h)	0	0	95.43	4.56
Third year (8,760 h)	2	48	92.30	7.70

6.3 Case C: Demonstrating Cost-Effective Low-Energy Buildings

This case is focused on an example of cost-effective low-energy buildings described in [19]. This case is a project that started in 2007 as a class 1 project. Originally, 442 dwellings were to be designed and constructed as "low-energy class 1" houses according to requirements set by the municipality of Egedal in Denmark. This means that the energy consumption should be 50 % below the existing energy regulations (BR08—Danish Building Regulations 2008). Sixty-five dwellings and about 30 single-family houses were constructed. Currently, because of the financial crisis, only about 200 new dwellings will actually be constructed. Therefore, a contingency plan (plan B) has been developed replacing some of the new dwellings with renovation projects for public buildings. Simultaneously, the original planned district heating network supplied from a relatively small bio-gasification plant has been substantially enlarged to cover a large part of the existing Stenloese town as well as a large wood-chip heating plant was added. The project demonstrates the benefits of ultra-low-energy buildings integrated with biomass and a solar heating energy supply. This case describes the class 1 project in Stenloese Syd settlement (see Fig. 49).

The municipality of Egedal advertised the construction sites for sale at the new settlement area Stenloese Syd with special energy requirements for all buildings to be built according to the Danish low-energy standard class 1 or better. Furthermore, the usage of solar energy for domestic hot water production and heat pumps for heating in the single-family houses is required. The class 1 project encompasses five different types of building demonstration projects:

- 65 ultra-low-energy social housing units—the KAB social housing project, whose cross section is shown in Fig. 49d.
- A kindergarten.
- A center for senior citizens.
- About 90 single-family houses.
- Four dense low-rise building areas.

Heating is primarily provided by a heating element in the ventilation system. As a backup, the air heating is supplemented by a radiator, which is placed in the living room in each apartment. The dwellings are planned to be supplied from a district heating network. As this is not in place yet, a boiler has been placed temporarily to supply the houses via the established district heating supply pipes. To reduce the water consumption in the houses, toilets have water-saving measures and there are thermostatic valves for the showers.

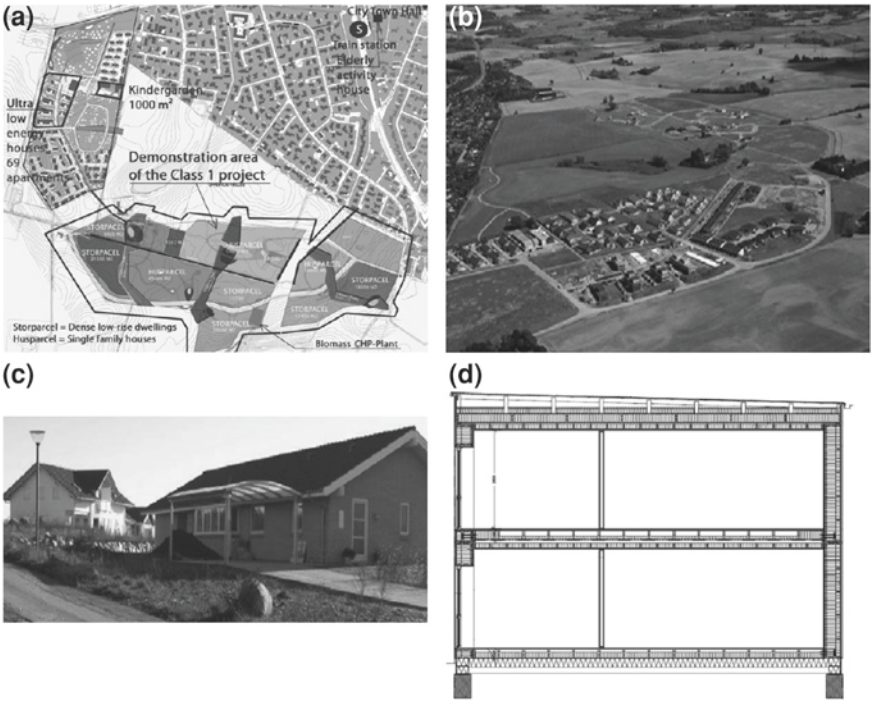

Fig. 49 Demonstration area and construction of Class 1 project in Stenloese Syd settlement. **a** Overview of the Stenloese Syd settlement. **b** Photograph of the Stenloese Syd settlement. **c** Photograph of two single-family houses. **d** Cross section of social housing units

The house was heated by a floor-heating system with a flow temperature of 35 °C and return temperature of 30 °C. The heating system was a 2.0 kW ground heat pump with a corresponding 2.0 kW electric cartridge. An 80-m-long ground loop for ground heat pumps was laid down, see Fig. 50. The nominal coefficient of performance (COP) of this heat pump was 3.4, and the relative COP at 50 % load was 0.9. The gross energy consumption of the single-family house was calculated to be 40.5 kWh/m^2/year. The low-energy class 1 frame for the house was 42.3 kWh/m^2/year, and thus, it complies with the requirement proposed.

6.4 Case D: Renewable Rural Electrification: Sustainability Assessment of Mini-Hybrid Off-Grid Technological Systems in the African Context

The project integrates wind, solar, and lead–acid battery energy storage technologies that were implemented as a mini-hybrid off-grid electrification system for a rural village in the Eastern Cape Province of South Africa (see Fig. 51) [8].

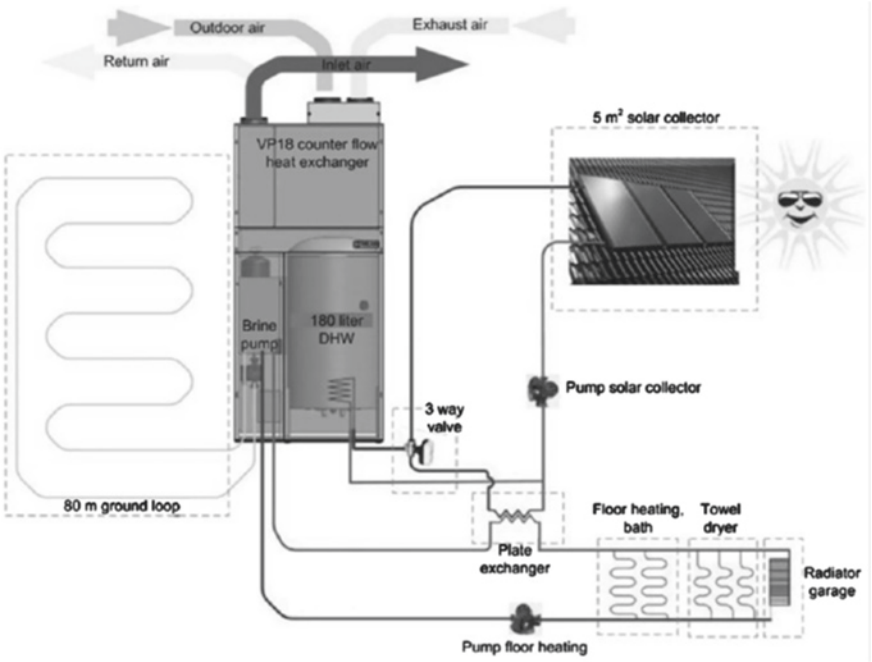

Fig. 50 Schematic diagram of plant with heating system and solar-heating system

Fig. 51 The Lucingweni Village mini-hybrid off-grid system

The useful energy that can be provided by six WT (6 kW-peak) and 540 solar panels (0.113 kW-peak) of the minihybrid off-grid technological sub-system is determined from the available wind and sun. The strongest local wind is located on the edge of an escarpment, and polycrystalline Si collectors are located adjacent to the WT (see Fig. 51).

Table 9 Projected average wind and sun energy, and capacity factors

Wind	Wind velocity	6.32	m/s (10 year average)
	Turbine output	9.00	kW
	Output/day	147	kwh/day
	Capacity factor	25	%—Output power/peak power
Sun	Solar radiance	4.67	kWh/m^2/day (10 year average)
		3.48	h full sun/day
	Efficiency Si PV	11	%—Output power/input power
	Output/day	190	kWh/day
	Capacity factor	19	%—Output power/peak power

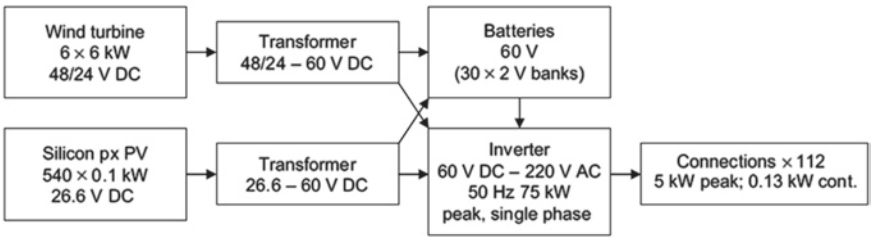

Fig. 52 Energy flows from generators to users

Table 10 Net system power availability for the 97 kW-DC system is 125 WAC per household

Energy generators	Power peak	Capacity factor	Conversion losses	Usable power in grid		Usable power/peak power	Power per household per day	
	kW-DC	% of kW-DC peak (%)	% kW p	kWh AC/ day	kW cont.	kW-AC/ kW-DC (%)	kWh AC kW-AC	
Wind turbines	36	25	32	146.9	6	17	1.311	0.055
Silicon photovoltaic	61	19	32	190.4	8	13	1.700	0.071
Total wind and solar	97	–	–	337.3	14	15	3.012	0.125

Table 9 presents the available wind and sun energy per day. This daily energy takes up on average an estimated 25 % of the maximum capacity of the WT and 19 % of the photovoltaic cells.

The flow of energy through the electrical system is shown schematically in Fig. 52. The amount of useful energy that can be obtained at the household connections can be determined from the input energy from the turbine and the photovoltaic and subtracting the energy losses in each of the components of the 220 VAC 50 Hz distribution system.

The useful energy from the 97 kW-peak system that is available at the 112 household connections is about 125 W continuous (see Table 10). This provides energy per household connection of just over 3 kWh per month.

The comparison of the outcomes of the project with a South African sustainable development framework shows that the specific village renewable off-grid electrification system is not viable. The main reason is that charges for electricity supply costs in village grids are too high for available subsidies. The economies of scale for RE supply technologies favor national grids. The failure of the integrated system may also be attributable to the complexity of the social–institutional subsystem, which resulted in uncertainty for project planners and system designers, and the lack of resilience of the technological system to demands from the socio-economic and institutional sub-systems.

References

1. Abdeddaim S, Betka A (2013) Optimal tracking and robust power control of the DFIG wind turbine. Electr Power Energy Syst 49:234–242
2. Abdullah MO, Yung VC, Anyi M, Othman AK, Hamid KB, Tarawe J (2010) Review and comparison study of hybrid diesel/solar/hydro/fuel cell energy schemes for a rural ICT Telecenter. Energy 35:639–646
3. Aki H (2010) Independent hybrid renewable energy systems: example applications around the world. IEEE Power Energy Soc Gen Meet 2010:1–4
4. Bajpai P, Dash V (2012) Hybrid Renewable energy systems for power generation in stand-alone application: a review. Renew Sustain Energy Rev 16:2926–2939
5. Barton JP, Infield DG (2004) Energy storage and its use with intermittent renewable energy. IEEE Trans Energy Convers 19(2):441–448
6. Belhadji L, Bachan S, Munteanu I, Rumeau A, Roye D (2013) Adaptive MPPT applied to variable-speed microhydropower plant. IEEE Trans Energy Convers 28(1):34–43
7. Bianconi E, Calvente J, Giral R, Mamarelis E, Petrone G, Ramos-Paja CA, Spagnuolo G, Vitelli M (2013) Perturb and Observe MPPT algorithm with a current controller based on the sliding mode. Electr Power Energy Syst 44:346–356
8. Brent AC, Rogers DE (2010) Renewable rural electrification: Sustainability assessment of mini-hybrid off-grid technological systems in the African context. Renewable Energy 35:257–265
9. Carrasco JM, Garcia Franquelo L, Bialasiewicz JT, Galván E, Portillo Guisado RC, Martín Prats MA, León JI, Moreno-Alfonso N (2006) Power-electronic systems for the grid integration of renewable energy sources: a survey. IEEE Trans Industr Electron 53(4):1002–1016
10. Choi UM, Lee KB, Blaabjerg F (2012) Power electronics for renewable energy systems: wind turbine and photovoltaic systems. In: international conference on renewable energy research and applications (ICRERA), Nagasaki, Japan, 11–14 Nov 2012
11. Gyawali N, Ohsawa Y (2010) Integrating fuel cell/electrolyzer/ultracapacitor system into a stand-alone microhydro plant. IEEE Trans Energy Convers 25(4):1092–1101
12. Hemmati M, Amjady N, Ehsan M (2014) System modeling and optimization for islanded micro-grid using multi-cross learning-based chaotic differential evolution algorithm. Electr Power Energy Syst 56:349–360
13. Houssamo I, Locment F, Sechilariu M (2013) Experimental analysis of impact of MPPT methods on energy efficiency for photovoltaic power systems. Electr Power Energy Syst 46:98–107
14. Hu X, Tseng KJ, Srinivasan M (2011) Optimization of battery energy storage system with super-capacitor for renewable energy applications. In: 8th international conference on power electronics–ECCE Asia, p 1552, The Shilla Jeju, Korea, 30 May–3 June 2011

15. Irmak E, Güler N (2013) Application of a high efficient voltage regulation system with MPPT algorithm. Electr Power Energy Syst 44:703–712
16. Kannan VK, Rengarajan N (2014) Investigating the performance of photovoltaic based DSTATCOM using I cosϕ algorithm. Electr Power Energy Syst 54:376–386
17. Lin CH (2013) Recurrent modified Elman neural network control of PM synchronous generator system using wind turbine emulator of PM synchronous servo motor drive. Electr Power Energy Syst 52:143–160
18. Ling Y, Cai X (2013) Rotor current dynamics of doubly fed induction generators during grid voltage dip and rise. Electr Power Energy Syst 44:17–24
19. Morck O, Thomsen KE, Rose J (2012) The EU CONCERTO project Class 1—demonstrating cost-effective low-energy buildings—recent results with special focus on comparison of calculated and measured energy performance of Danish buildings. Appl Energy 97:319–326
20. Phankong N, Yuktanon N, Bhumkittipich K (2013) Three-level back-to-back converter simulation for wind turbine energy source. Energy Procedia 34:449–458
21. Poullikkas A (2007) Implementation of distributed generation technologies in isolated power systems. Renew Sustain Energy Rev 11:30–56
22. Ribeiro LA, Saavedra OR, Lima SL, de Matos JG, Bonan G (2012) Making isolated renewable energy systems more reliable. Renewable Energy 45:221–231
23. Rodriguez M, Stahl G, Corradiniand L, Maksimovic D (2013) Smart DC power management system based on software-configurable power modules. IEEE Trans Power Electron 28(4):1571–1586
24. Saravanan S, Thangavel S (2014) Instantaneous reference current scheme based power management system for a solar/wind/fuel cell fed hybrid power supply. Electr Power Energy Syst 55:155–170
25. She Y, She X, Baran ME (2011) Universal tracking control of wind conversion system for purpose of maximum power acquisition under hierarchical control structure. IEEE Trans Energy Convers 26(3):766–775
26. Shinde SM, Patil KD, Khairnar ss, Gandhare Wz (2009) The role of power electronics in renewable energy systems research and development. In: 2nd international conference on emerging trends in engineering and technology, ICETET-09, p 726
27. Simoes MG, Uriarte CS, Chakraborty S, Farret FA (2006) Cost considerations on fuel cell, 41st IAS annual meeting. In: Conference record of the industry applications conference 2006. vol 5. p 2169
28. Siraki AG, Curry N, Pillay P, Williamson SS (2009) Power electronics intensive solutions for integrated urban building renewable energy systems. In: Industrial electronics, 2009. IECON'09. 35th annual conference of IEEE, p 3998
29. Sun D, Ge B, Rub HA, Peng FZ, de Almeida AT (2011) Power flow control for quasi-Z source inverter with battery based PV power generation system. In: IEEE energy conversion congress and exposition (ECCE), p 1051, 17–22 Sept 2011
30. Taib N, Metidji B, Rekioua T (2013) Performance and efficiency control enhancement of wind power generation system based on DFIG using three-level sparse matrix converter. Electr Power Energy Syst 53:287–296
31. Tan X, Li Q, Wang H (2013) Advances and trends of energy storage technology in microgrid. Electr Power Energy Syst 44:179–191
32. Tang Y, HaiboHe PJ, Qin C, Wu F (2013) Optimized control of DFIG-based wind generation using sensitivity analysis and particle swarm optimization. IEEE Trans Smart Grid 4(1):509–520
33. Thounthong P, Tricoli P, Davat B (2014) Performance investigation of linear and nonlinear controls for a fuel cell/supercapacitor hybrid power plant. Electr Power Energy Syst 54:454–464
34. Ting CC, Yeh LY (2014) Developing the full-field wind electric generator. Electr Power Energy Syst 55:420–428
35. Trifkovic M, Sheikhzadeh M, Nigim K, Daoutidis P (2014) Modeling and control of a renewable hybrid energy system with hydrogen storage. IEEE Trans Control Syst Technol 22(1):169–179

36. Tucker S, Negnevitsky M (2011) Renewable energy micro-grid power system for isolated communities. In: 21st Australasian Universities power engineering conference (AUPEC) 2011, pp 1–7
37. Ugranli F, Karatepe E (2013) Optimal wind turbine sizing to minimize energy loss. Electr Power Energy Syst 53:656–663
38. Zhang F, Thanapalan K, Procter A, Carr S, Maddy J, Premier G (2013) Power management control for off-grid solar hydrogen production and utilisation system. Int J Hydrogen Energy 38:4334–4341

Design for Reliability of Power Electronics in Renewable Energy Systems

Ke Ma, Yongheng Yang, Huai Wang and Frede Blaabjerg

Abstract Power electronics is the enabling technology for maximizing the power captured from renewable electrical generation, e.g., the wind and solar technology, and also for an efficient integration into the grid. Therefore, it is important that the power electronics are reliable and do not have too many failures during operation which otherwise will increase cost for operation, maintenance and reputation. Typically, power electronics in renewable electrical generation has to be designed for 20–30 years of operation, and in order to do that, it is crucial to know about the mission profile of the power electronics technology as well as to know how the power electronics technology is loaded in terms of temperature and other stressors relevant, to reliability. Hence, this chapter will show the basics of power electronics technology for renewable energy systems, describe the mission profile of the technology and demonstrate how the power electronics is loa ded under different stressors. Further, some systematic methods to design the power electronics technology for reliability will be given and demonstrated with two cases—one is a wind power and the other is photovoltaic application.

1 Introduction

The installed capacity of the renewable energy has been growing fast in the last decade, by the end of 2012, the worldwide non-hydropower generation based on renewables has exceeded 480 gigawatts (GW), which supplies 5.2 % of the global electricity consumption and accounts for almost half of the newly established generation capacity [1]. Among various renewable energy resources, the wind power and solar photovoltaic (PV) have already accounted for 80 % of the total power

K. Ma (✉) · Y. Yang · H. Wang · F. Blaabjerg
Aalborg University, Aalborg, Denmark
e-mail: kema@et.aau.dk

M. A. Sanz-Bobi (ed.), *Use, Operation and Maintenance of Renewable Energy Systems*, Green Energy and Technology, DOI: 10.1007/978-3-319-03224-5_9,

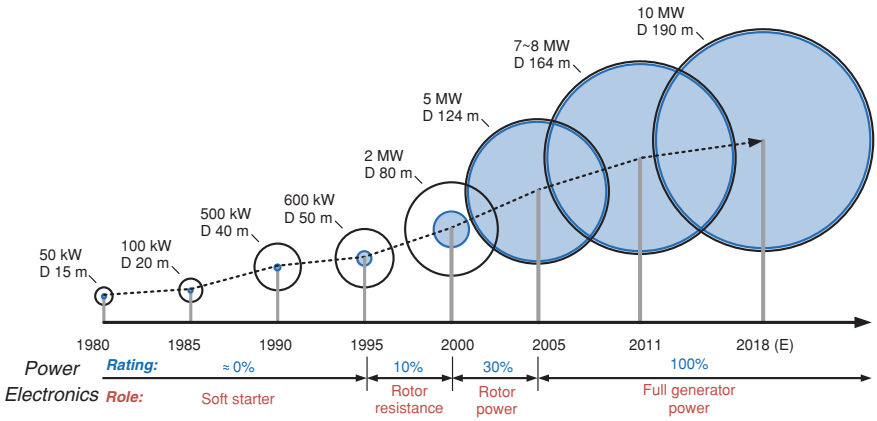

Fig. 1 Evolution of wind turbine size and the power electronics seen from 1980 to 2018 (estimated); *blue circle* indicates the power capacity coverage by power electronics [7]

production by non-hydrorenewables. Moreover, the worldwide wind and PV power generation achieved the fastest growth rate of all with 25 and 60 % increase in the last five years. Therefore, these two renewable technologies are the main focus in this chapter.

Accompanied with the capacity growth, the impacts by renewables to the power grid are also becoming significant. Unfortunately, the fluctuated and unpredicted behaviors of the renewable energies are unpreferred for power grid operations; thereby, technologies which can ensure more reliable and controllable power generating/converting are crucial. In the last two decades, the power electronics technology gradually becomes more and more advanced and brings significant performance improvements for the renewable energy production—not only to improve the energy capturing efficiency, but also to enable the whole renewable energy system to act as a controllable electrical power source in order to be better integrated into the power grid, and thus take active part of the grid control. A good example can be seen from the evolution of the wind turbine technology, as shown in Fig. 1 [2, 3], in which the covered power and played role by power electronics are both indicated. It is clear that the power electronics converter already achieved 100 % power coverage in the wind turbine system since 2005; actually in most of the newly established wind turbines and PV panels, power electronics converters have become essential components carrying all of the generated power up to multi-megawatts (MW), also illustrated by the examples of wind turbine shown in Fig. 1.

With respect to a modern renewable energy conversion chain, the power electronics technology is the core of the entire system, as it is shown in Fig. 2. Underpinned by advanced and intelligent control strategies, power converters are capable of ensuring a reliable and efficient power conversion from the wind and solar. As shown in Fig. 2, the power converters have to cope with both stressors from the generator side (e.g., induced by the mission profiles) and the grid side (e.g., related to grid conditions).

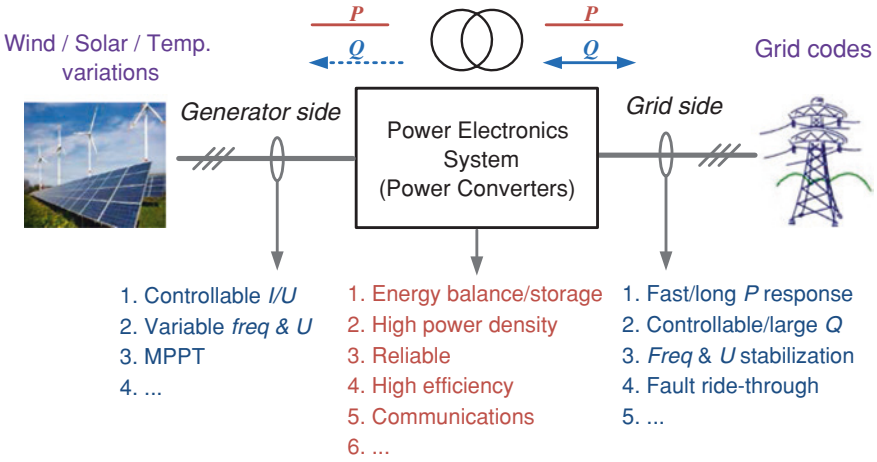

Fig. 2 Demands for renewable energy systems integrated into the power grid

When benchmarking such a renewable energy technology, the cost issue is the most important consideration, and it will determine the feasibility of certain energy technologies to be widely utilized in the future. The competitive cost advantage is one of the reasons why the wind and solar power generation has shown the most significant growth in the last few decades compared to the other renewable energy sources. Another reason is the national incentive schemes which have been put up. In order to quantify and compare the cost for different energy technologies, the Levelized Cost of Energy (LCOE) index is generally used as a parameter [4]. LCOE represents the price at which the electricity is generated from a specific energy source over the whole lifetime of the generation unit. It is an economic assessment of the cost of the energy—generating system including all the costs such as initial investment, development cost, capital cost, operations and maintenance cost, fuel cost, etc. LCOE is defined in a single equation as:

$$LCOE = \frac{C_{\mathrm{Dev}} + C_{\mathrm{Cap}} + C_{\mathrm{O\&M}}}{\mathrm{E}_{\mathrm{Annual}}} \tag{1}$$

It is noted that the initial development cost C_{Dev}, capital cost C_{Cap}, and the cost for operation and maintenance $C_{\mathrm{O\&M}}$ are first levelized to the annual average cost seen over the lifetime of the generation system, and then divided by the average annual energy production looking at the whole lifetime E_{Annual}.

As power electronics are almost essential with higher power rating and more advanced control features, on the one hand the cost for the power electronics itself is no longer ignorable and becomes critical in the whole energy conversion systems. On the other hand, the failures of power electronics will not only cause stability problems of the power grid due to sudden absence of a large amount of power capacity, but also it results in high cost for repairing and maintenance, especially for large and remote-located wind turbines or PV panels, where it takes time to repair. Additionally, it will cause production loss to the customer—leading to

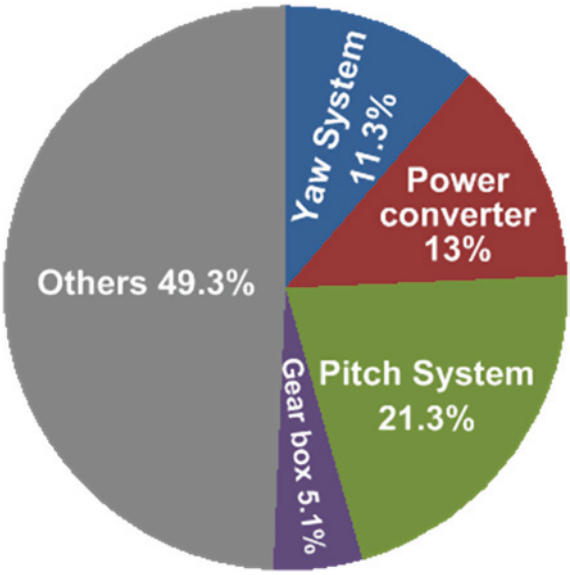

Fig. 3 Contribution of subsystems and assemblies to the overall failure rate of wind turbines measured in the time period of 10 years [5]

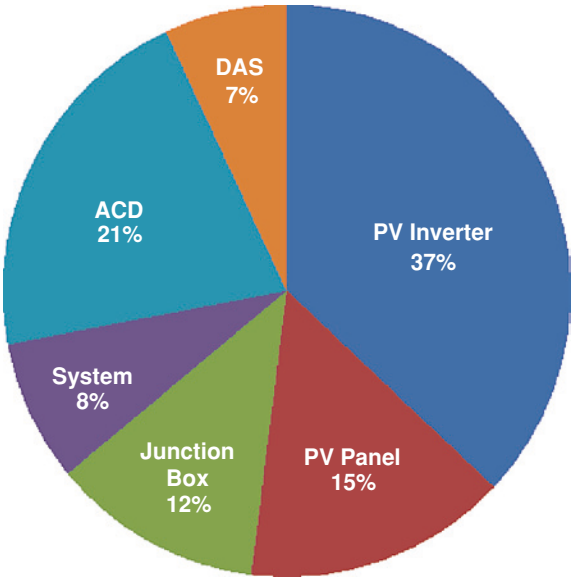

Fig. 4 Unscheduled maintenance events by subsystem in a PV power plant measured in the time period from 2001 to 2006 [6]

reduced total/annual energy production, and thus, it will increase the LCOE. As a result, the reliability performance is another critical factor for renewable energy applications in order to lower the cost of energy for the technology.

Nevertheless, the reliability of power electronics in renewable applications still seems to be challenged. As shown in Figs. 3 and 4, [5, 6], the failure rate and unscheduled maintenance for wind power converter and PV inverter account for

13 and 37 %, respectively, in the entire wind turbine and PV systems. Attentions should of course be given to the statistics of Figs. 3 and 4 as they are measured 5–8 years back in history, and based on the technology developed at least 10 years ago; also they are very application dependent. However, these data do reveal the importance of the power electronics reliability in the renewable energy systems. Therefore, the reliability improvements of the power electronics may effectively contribute to an extension of the energy production of renewable energies—and thus be a very helpful approach to further reduce the cost of energy, either for the technologies such as onshore wind power where the remaining potential for cost reduction is not so large, or for those technologies such as offshore wind power and solar PV power where the cost of energy is still relatively high.

2 Power Converters for Renewable Energy Systems

The development of the power electronics technology for renewable energy conversion has been in a steady progress for the last 35 years [7–10]. In the following, some of the state-of-the-art converter solutions for wind turbine and PV systems are going to be introduced.

2.1 Power Converters for Wind Turbines

Depending on the types of generator, power electronics, speed controllability, and the way in which the aerodynamic power is limited, the wind turbine designs can generally be categorized into several concepts [8, 11]. In these wind turbine concepts, the power electronics play quite different role and has various power rating coverage of the system. Up until now, the configuration of doubly fed induction generator (DFIG) equipped with partial-scale power converter is dominating on the market, as shown in Fig. 5a, but in very near future, the configuration with synchronous generator (SG) with full-scale power converter is expected to take over to be the dominant solution [7, 10], as shown in Fig. 5b. Each of the concepts has its suitable converter topologies to be used, and some of them are illustrated in the following.

2.1.1 Two-Level Power Converter

The Two-Level Pulse-Width-Modulation Voltage-Source-Converter (2L-PWM-VSC) is the most used converter topology so far for the application of doubly fed induction generator (DIFG)-based wind turbine concept as the power rating requirement for such a converter is limited. Normally, two 2L-PWM-VSCs are configured in a back-to-back structure in the wind turbine system, as shown in Fig. 5c, which is called 2L-BTB for convenience. A DC-link voltage capacitor C

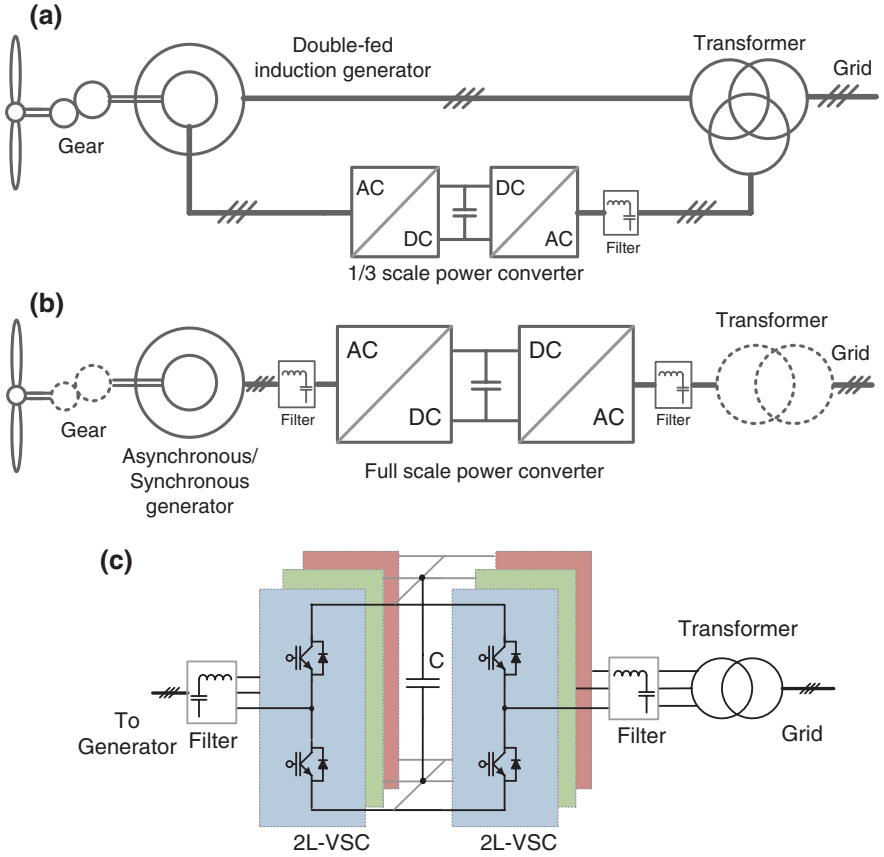

Fig. 5 Popular wind turbine concept. **a** Variable-speed wind turbine with partial-scale power converter and a doubly fed induction generator. **b** Variable-speed wind turbine with full-scale power converter. **c** Two-level back-to-back voltage source converter for wind turbine (2L-BTB)

"decouples" the two converters which normally are rated below 690 V AC voltage. A technical advantage of the 2L-BTB solution is the full power controllability (4-quadrant operation) with a relatively simple structure and few components, which contribute to a well-proven, robust, and reliable performances as well as the advantage of lower cost.

As the converter in this concept needs to carry all the generated power by wind turbines, e.g., up to 10 MW in the future, the 2L-BTB converter topology at this power level may suffer from large switching loss and many devices may need to be connected in parallel. Further, the cabling in the case of a low voltage level can be a great design/physical challenge. Consequently, it is becoming more and more difficult for a single 2L-BTB topology to achieve acceptable performance for the full-scale wind power converter, even though having a cost advantage. In addition, the safety issue is another obstacle for an even wider-scale adoption of 2L-BTB

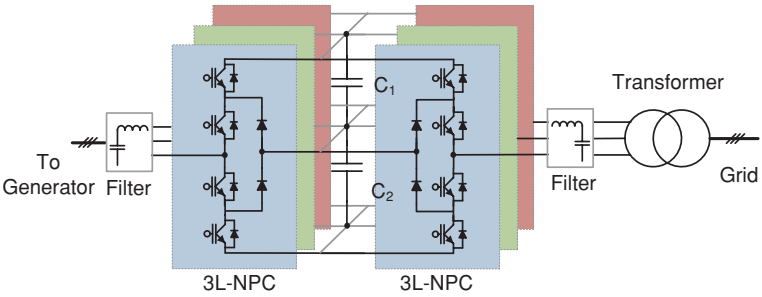

Fig. 6 Three-level Neutral Point Clamped back-to-back converter for wind turbine (3L-NPC BTB)

converters in wind turbine applications if the voltage level is increasing to reduce the conversion loss at MW power level.

2.1.2 Multi-level Power Converter

With the abilities to achieve higher voltage and power level, multi-level converters may become more preferred candidates in the full-scale converter-based concept [12–14]. The three-level neutral point diode clamped topology (3L-NPC) is one of the most commercialized multi-level topologies on the market. Similar to the 2L-BTB, it is usually configured as a back-to-back structure in the wind power application, as shown in Fig. 6, and it is called 3L-NPC BTB for convenience. Again, the capacitors (C_1, C_2) are adopted to "decouple" the generator and the grid. The 3L-BTB solution achieves one more output voltage level and less *dv/dt* stress compared to the counterpart of 2L-BTB; thus, it is possible to convert the power at medium voltage with lower current, less paralleled devices, and also smaller filter size to lower the current distortions. The midpoint voltage fluctuation of the DC bus can be a drawback of the 3L-NPC BTB. This problem has been extensively researched, and it is considered to be improved by controlling the redundant switching states [15–17]. However, it is found that the loss distribution is unequal between the outer and inner switching devices in a switching arm [18–20], and this problem might lead to a derated power capacity, when the power converter is practically used.

2.1.3 Other Solution for Higher-Power Wind Turbines

In order to handle the fast growing power capacity, some multi-cell converter configurations (i.e., parallel/series connection of converter cells) are also being developed and becoming widely adopted by the industry.

Figure 7a shows a multi-cell solution, e.g., adopted by Gamesa in the 4.5-MW wind turbines [21], which have 2L-BTB single-cell converters paralleled both on the generator side and on the grid side. It is possible to introduce the multi-cell

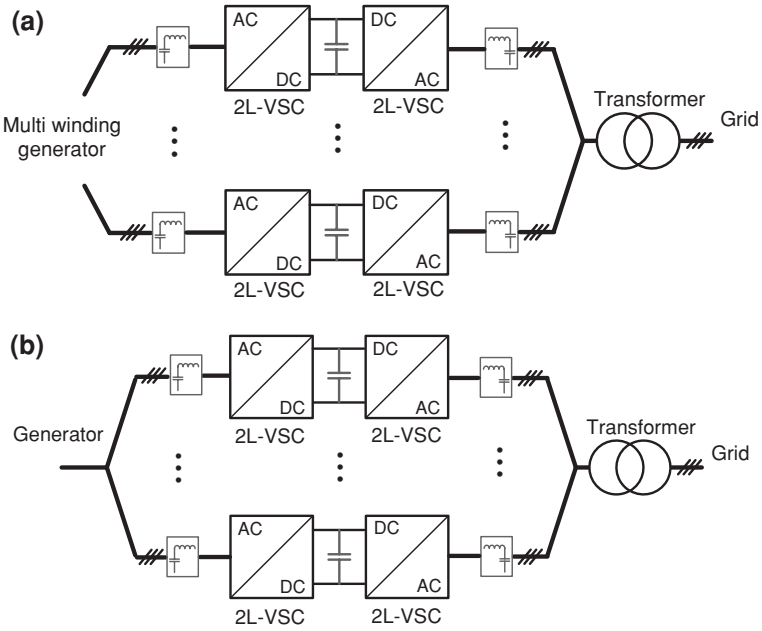

Fig. 7 Multi-cell converter with paralleled converter cells (MC-PCC): **a** variant 1 and **b** variant 2

solution in multi-MW wind turbines by paralleling a number of low-voltage power converters [22], as it is shown in Fig. 7b. The standard and proven low-voltage converter cells as well as redundant and modular characteristics are the main advantages. This converter configuration is the state-of-the-art solution in the industry for the wind turbines with power level higher than 3 MW.

2.2 Power Converters for PV Systems

Unlike the wind power technology, the solar PV produces much lower power per generating unit (e.g., individual PV panel or PV string), and thereby, the PV system is normally composed of many panels connected in parallel and/or in series to increase the output power within an acceptable range. To achieve higher efficiency and lower cost, transformerless inverters are introduced and used in many PV applications. The string inverters and multi-string inverters are adopted in those applications, where the single-phase grid connection configurations are the most commonly used. Due to the lack of galvanic isolation, leakage currents may appear between the PV panels and the ground, which will cause safety issues if not addressed properly. Thus, the transformerless inverters are required to reduce the leakage currents either by redesigning the topology or by modifying the modulation schemes toward the grid operation.

According to the state-of-the-art technologies, there are mainly four concepts [23, 24] to organize and deliver the PV power to the public grid, as shown in

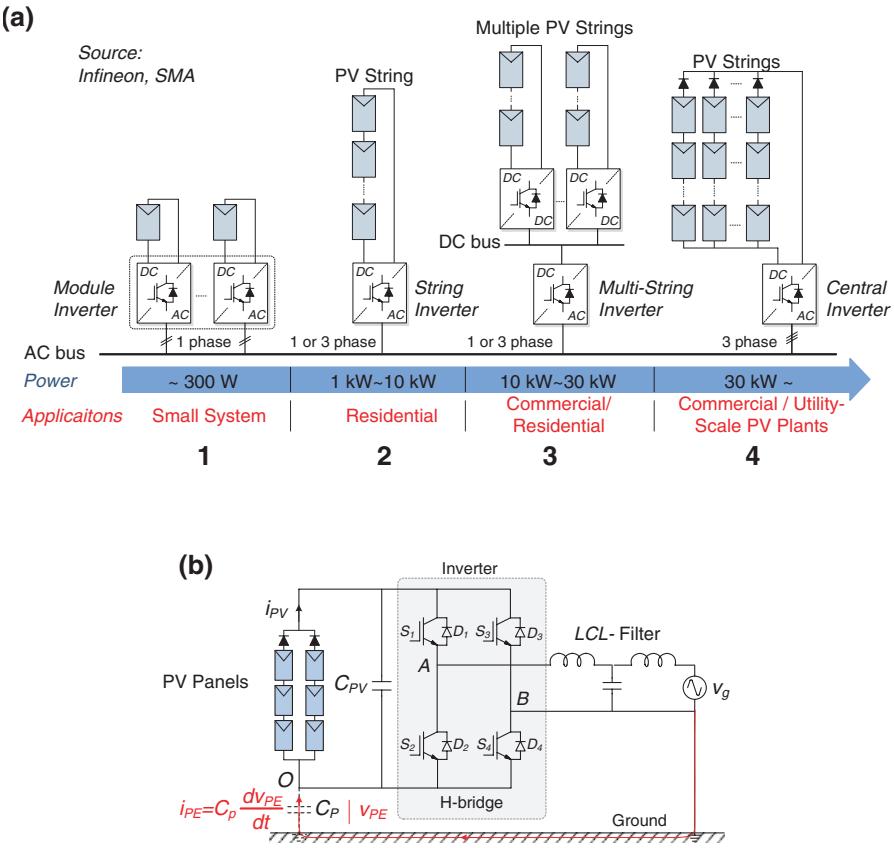

Fig. 8 **a** Different grid-connected PV inverter structures: 1 *module inverter*, 2 *string inverter*, 3 *multi-string inverter*, 4 central inverter **b** H-bridge transformerless topology for PV application (V_{PE}: common-mode voltage, i_{PE}: leakage current)

Fig. 8a, each of the concept consists of a series of PV panels or strings and a couple of power electronics converters (DC–DC converters and DC–AC inverters) configured in different structures. Depending on the output voltage level, a boost converter may be required by the string and multi-string inverters.

2.2.1 H-Bridge Topology

The H-Bridge inverter (Fig. 8b) is a well-known topology, and it is almost the standard solution for the single-phase DC–AC power conversion. It has been widely used in motor drives and UPS applications. However, in the case of the transformerless configuration for PV system, the PWM modulation strategies should be carefully evaluated, because some popular modulation methods like unipolar PWM may introduce abrupt change in the common-mode voltage (high

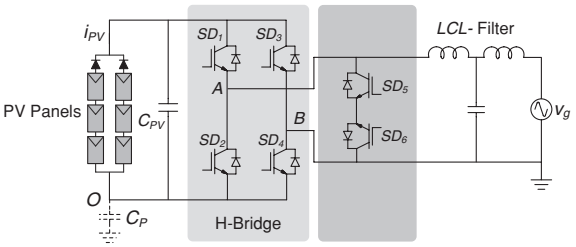

Fig. 9 HERIC transformerless topology for PV applications [80]

dv/dt) and thus lead to a large leakage current to ground, which are not preferable in transformerless PV systems and also in grid connection standards [25, 27]. The bipolar modulation scheme can be adopted in an H-bridge transformerless inverter with an effective elimination of leakage currents, but with a relatively low efficiency (<96.5 %).

In order to improve the common-mode behavior, but also further to increase the efficiency, and to keep all the other merits given by the H-bridge inverter, a number of modified topologies are proposed in the PV applications by adding bypass switches either on the DC side or on the AC side [27, 29, 30, 32–35, 79], as it will be more detailed in the following.

2.2.2 HERIC Topology

The Highly Efficient and Reliable Inverter Concept (HERIC) [80] includes two extra switches (SD_5–SD_6) on the AC output of the inverter, compared to the H-bridge topology, as it is shown in Fig. 9.

The common-mode behavior of the HERIC topology is similar to the H-bridge converter with bipolar PWM, where the voltage to ground of the PV array terminals will only have a sinusoidal shape, while the same high efficiency also can be achieved as the H-bridge converter with unipolar PWM. Therefore, the HERIC topology is more suitable for a transformerless PV system in terms of efficiency (up to 98 % reported) and is widely used for the power range of 2.5–5 kW for single-phase applications [81].

2.2.3 H6 Inverter

Another transformerless topology using the DC decoupling method is called the H6 converter [34, 35], which adds two extra switches and two extra diodes to the H-bridge topology as shown in Fig. 10.

The common-mode behavior of the topology is similar to the HERIC topologies, since the voltage to ground of the PV array has only a sinusoidal shape and the frequency is the grid frequency. It is another suitable solution for transformerless PV

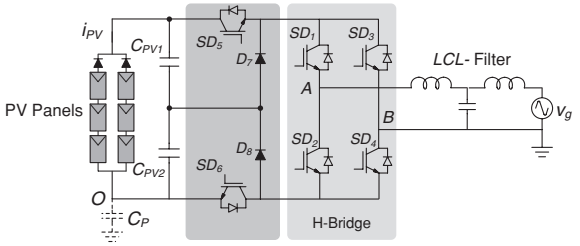

Fig. 10 H6 transformerless inverter topology for PV applications [34, 35]

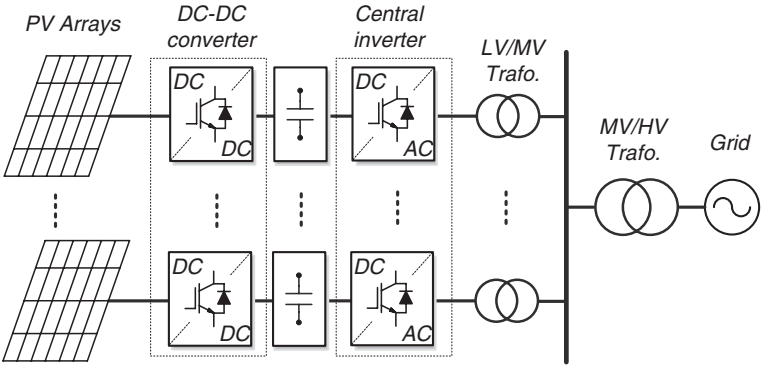

Fig. 11 Typical large-scale PV power plant based on central inverters for utility applications in the MW range

systems, and several commercial products are available on the markets with the efficiency of up to 97 %.

2.2.4 Solution for Higher-Power PV Strings

Although single-phase configurations are the most commonly used for PV applications, some companies such as SMA, Sunways, Kaco, and Danfoss are promoting the three-phase PV systems with central inverters for utility-scale applications [31, 73–75, 81]. For example, the Neuhardenberg solar power plant with a nominal output of 19.69 MWp in Germany uses Powador XP500-HV TL central inverters [73, 74]; the largest European thin-film PV power plant is equipped with 114 Sunny Central 900CP XT inverters from SMA, forming a PV plant of 128 MWp. Those large PV power plants, rated over tens and even hundreds of MW, adopt many central inverters with an individual power rating of up to 900 kW. A typical large-scale PV power plant is shown in Fig. 11, where DC–DC converters are also used before the central inverters in order to maximize the power capture.

3 Mission Profile for Renewable Energy System

The mission profiles for power electronics determine the loading of components, and thereby, they are closely related to the cost and reliability performances. In the renewable energy applications, the mission profiles for power electronics are relatively tough: They need to withstand large amount of power (even up to a few MWs), perform a series of complicated functions required from grid, and meanwhile, they also operate under harsh environment such as day–night temperature swings, dust, vibration, humidity, salty environments, etc. [1, 39]. On the other hand, the required operating hours for wind turbines can be up to 120,000 h, and for a PV inverter, it might need to be operating maybe 100,000 hours in a 20-year life span. Assuming, in each day, the PV inverter operates for 14 hours. . In this section, the typical mission profile for wind and PV applications is going to be addressed.

3.1 Operational Environment

3.1.1 Wind Speed

As the input of the whole wind turbine system, the wind energy quantified by the wind speed is an important factor that can determine the design, control, maintenance, energy yield, and also the cost of the whole system. During the construction and design phase, assumptions have to be made about the wind conditions that the wind turbines will be exposed to. Typically, wind classes are used which are determined by three parameters—the average wind speed, extreme 50-year gust, and turbulence [40]. Because the loading of power electronics converters are mainly caused by wind speed level as well as its variations, the knowledge of the wind class is of crucial importance for the reliability calculation and performances. In Table 1, the most adopted classifications of wind conditions are shown.

A field-recorded 1-year wind speeds are illustrated in Fig. 12 [41], which is based on 3 h averaged at 80 m hub height, and it was designated for the wind farm located near Thyborøn, Denmark, with latitude 56.71° and longitude 8.20°. The chosen hub wind speed belongs to the wind class IEC I-a with average wind speed of 8.5–10 m/s. It can be seen that the wind speed fluctuates largely from 0 m/s up to 28 m/s. Without proper controls of the mechanical and electrical parts, this significant fluctuation may be transferred to the grid and cause grid stability problems. Moreover, the components in the system may suffer from largely cyclical loadings which may quickly give reliability problems if not properly designed [42–46]. As a result, the roughness and fluctuation of the wind speeds should be carefully taken into account in the control and design of the power electronics converter [47].

Table 1 Wind classes according to IEC 61400 [40]

Wind class	I-a	I-b	II-a	II-b	III-a	III-b	IV-b
Turbulence[a]	18 %	16 %	18 %	16 %	18 %	16 %	16 %
Annual average wind speed (m/s)[b]	10		8.5		7.5		6
Extreme 50-year gust (m/s)[c]	70		59.5		52.5		42

[a]Turbulence is measured at 15 m/s wind speed, quantifying how much the wind varies within 10 min
[b]At hub height
[c]Based on the 3-s average wind speed

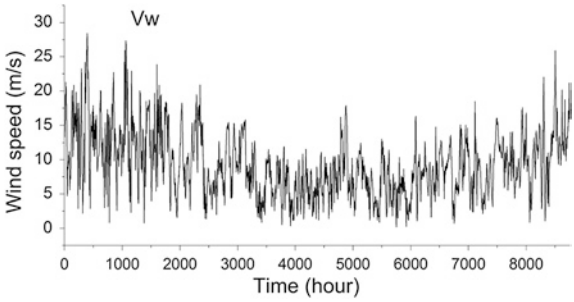

Fig. 12 One-year mission profile of wind speed from a wind farm of Denmark (3-h averaged) with roughness Class I according to IEC standard

3.1.2 Solar Irradiance and Ambient Temperature

Since the output power of a PV panel is significantly dependent on the environmental conditions, the knowledge of mission profiles, including solar irradiance level and ambient temperature, has become of high importance for the design, control, and operation of a PV conversion system. With the accumulation of field experiences and the introduction of more and more real-time monitoring systems, better mission profile data has been becoming available in various kinds of power electronic systems (e.g., PV inverters) [50]. This offers the possibilities to predict the lifetime of a PV inverter and the energy production of a PV system [50, 78].

Figure 13 shows yearly mission profiles for PV systems in Aalborg, Denmark, from October 2011 to September 2012. The original recorded data have a sampling frequency of 5 Hz [26]. In Fig. 13, the data are resampled every 5 min. It can be observed that both the solar irradiance level and the ambient temperature vary significantly through a year. Those fluctuations require dedicated maximum power point tracking (MPPT) control systems in order to increase the energy yield. Moreover, due to the intermittency, the resultant power, generated by a PV system and then transferred to the grid, may cause grid stability problems—especially when the PV penetration is getting larger and larger. It is also known that the reliability of a power electronics system has a strong connection with the temperature loading on the power electronics devices [41, 50, 77, 78], which is affected by the mission profiles. Hence, different time-scale mission profiles may have an influence on the consumed lifetime of a power electronics system [41].

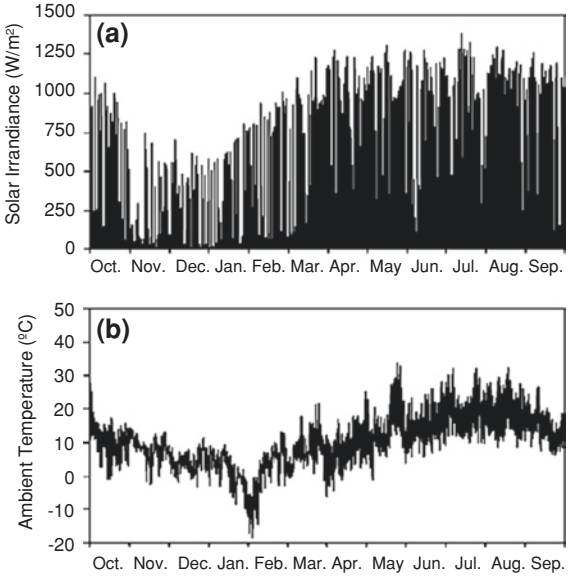

Fig. 13 Yearly mission profiles from recorded data (5 min per sampling data) for PV systems: (a) solar irradiance level and (b) ambient temperature

Consequently, those aspects related to mission profiles have to be carefully taken into considerations in the control and design of the power electronics converters for PV systems. With the development of power electronics technology, the advancement of monitoring techniques, and also intelligent control strategies, further improvement in the lifetime and reduction in energy cost for a PV system can be achieved.

3.2 Grid Codes

Most countries have dedicated grid codes for the connection of wind turbines to the grid, and they are updated regularly [5, 6, 53–55]; the trends can be also seen in the case of PV power generation. These requirements reflect, in most of the cases, the significant penetration of renewable energy into the grid system, and the requirements cover a wide range of voltage levels from medium voltage to very high voltage. Basically, the grid codes are always trying to make wind farms/PV plants to act as a conventional power plant from the viewpoint of electrical network. The generation system's power controllability, power quality, fault ride-through capability, and grid support ability during network disturbances are generally in high focus. Examples of grid codes by different countries for active and reactive power control, power quality, and ride-through capabilities are given in the following, and they are regulations either for each individual wind turbine or for a whole wind farm. Such regulations are dynamic and may change from year to year.

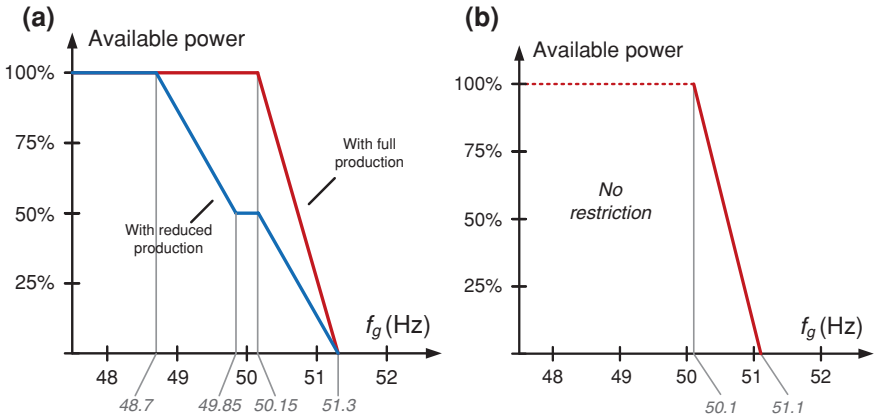

Fig. 14 Frequency control profiles for the wind turbines connected to the **a** Danish grid [54] and **b** German grid [55]

3.2.1 Active Power Control

According to most grid codes, the individual wind turbine must be able to control the active power in the point of common coupling (PCC) in a given power range. The active power is typically controlled based on the system frequency, e.g., Denmark, Ireland, and Germany, so that the power delivered to the grid is decreased when the grid frequency rises above 50.1 Hz. Typical characteristics for the frequency control (power versus frequency) in the Danish and German grid codes are shown in Fig. 14.

For the larger generation units at a wind farm scale—which is normally connected at the transmission line—the wind turbines shall act as a conventional power plant providing a wide range of controlled active power based on transmission system operator's (TSO) demands. Also they have to participate in primary and secondary control of the power system. Generally, these active power controls always require some reserved power capacity from the possible power generation by the wind farms—which will provide enough support in the case when extra active power is demanded and thereby maybe reduce the needs for the capacity of energy storage systems.

3.2.2 Reactive Power Control

During normal operation, the reactive power delivered by the wind turbine or the wind farm also has to be regulated by the grid codes in a certain range. The grid codes in different countries specify different reactive power control behaviors.

As shown in Fig. 15, both the Danish and German grid codes give a range for controlling the reactive power of the wind turbine system against the active power output. Also the TSOs will normally specify the reactive power range delivered by wind farms

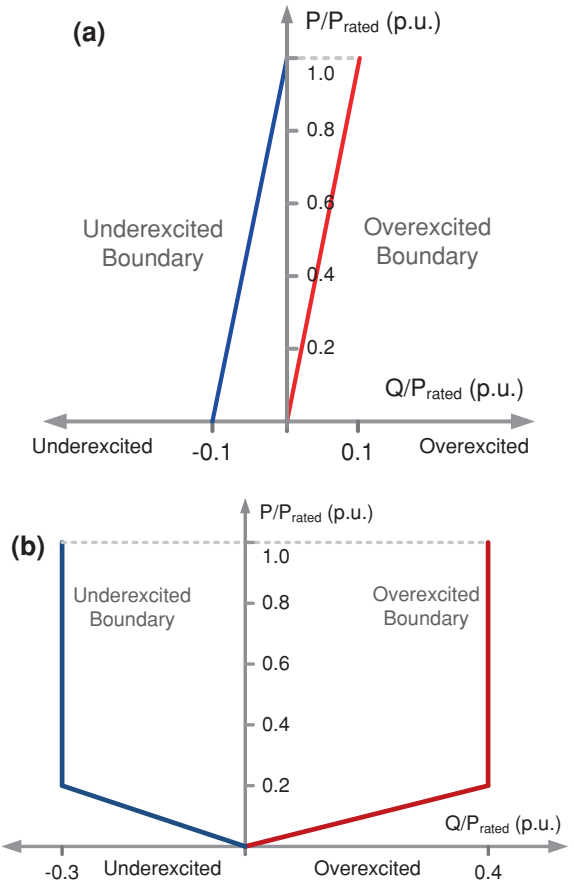

Fig. 15 Reactive power range under different generating powers **a** for a wind turbine specified by Danish grid codes [6] and **b** for a wind farm specified by German grid codes [55]

according to the grid voltage levels. It should be noted that this basic form of reactive power control should be realized slowly under a time constant of minutes [53].

3.2.3 Fault Ride-Through Capability

Besides the normal operation, the TSOs in different countries have issued strict low-voltage ride-through (LVRT) codes for wind turbines/wind farms. Fig. 16 shows the boundaries of various grid voltage dipping amplitudes as well the allowable disturbing time for a wind farm [5, 6, 53–55]. One of the uncertainties, which is still under discussion, is the definition for the voltage amplitude during unsymmetrical grid faults—it is not clearly specified in most of the grid codes.

Besides the fault ride-through ability, it is becoming a need that the wind power generation system should also provide reactive power (up to 100 % current capacity) to contribute to the voltage recovery, when the grid faults are present. Figure 17 shows the required amount of reactive current for wind farms against the grid voltage amplitude specified by the German [55] and Danish grid codes [54].

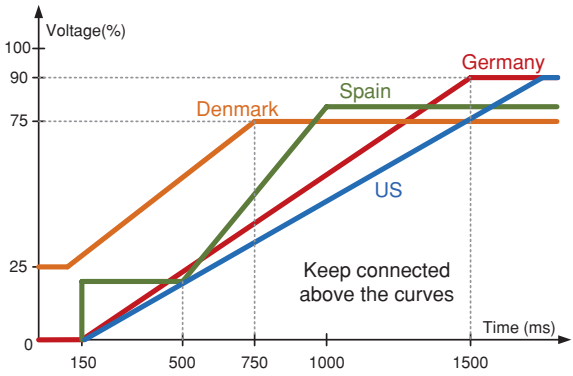

Fig. 16 Voltage profile for low-voltage fault ride-through capability of wind turbines [43]

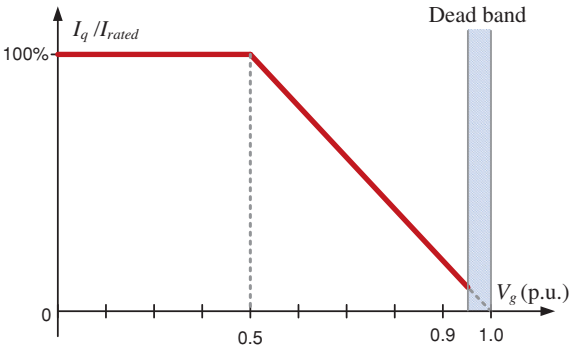

Fig. 17 Reactive current requirements for a wind farm during grid sags by the German and Danish grid code [54, 55]

The grid codes raise great challenges to the wind turbine system in the last decade and are pushing the technology developments of power electronics in wind power application. These requirements have on the one hand increased the cost per produced kWh but on the other hand made the wind power technology much more suitable to be utilized and integrated to the power grid. It can be predicted that the stricter grid codes in the future will keep challenging the wind turbine system and pushing forward the technology also for the use of power electronics.

As the penetration level of PV systems is continuously growing at a rapid rate, similar grid codes have been issued and imposed on grid-connected PV systems, especially of which the power ratings can be up to a few MWs for utility-scale applications. In fact, a shift of those grid codes, e.g., active power curtailment and reactive power injection, toward covering a wide range of applications (e.g., residential systems of several kWs to commercial PV plants of hundreds of kWs) is undergoing discussion in some countries [54–58]. Nonetheless, increasingly stringent grid requirements for renewable energy systems call for much more flexible controllability of grid-integrated systems, which could be enabled by the advanced power electronics technology.

4 Reliability Basics in Power Electronics

Power electronics enables efficient conversion and flexible control of electric energy by taking advantage of the innovative solutions in active and passive components, circuit topologies, control strategies, sensors, digital signal processors, and system integrations. While targets concerning efficiency of power electronic systems are within reach, the increasing reliability requirements create new challenges due to the following factors:

- Mission profiles critical applications (e.g., aerospace, military, more electrical aircrafts, railway tractions, automotive, data center, medical electronics).
- Emerging applications under harsh environment and long operation hours (e.g., onshore and offshore wind turbines, photovoltaic systems, air-conditions, and pump systems).
- More stringent cost constraints, reliability requirements, and safety compliances, e.g., demand for parts per million (ppm)-level failure rates in future products.
- Continuous need for higher power density in power converters and higher-level integration of power electronic systems, which may invoke new failure mechanisms and thermal issues.
- Uncertainty of reliability performance for new materials and packaging technologies (e.g., SiC and GaN devices).
- Increasing complexity of electronic systems in terms of functions, number of components, and control algorithms.
- Resource constraints (e.g., time and cost) for reliability testing and robustness validation due to time-to-market pressure as well as financial pressure.

4.1 Industrial Challenges and Lifetime Target in Typical Power Electronic Applications

Reliability is defined as the ability of an item to perform the required function under stated conditions for a certain period of time, which is often measured by the probability of survival and failure rate. It is relevant to the durability (i.e., lifetime) and availability of the item. The essence of reliability engineering is to prevent the creation of failures. The deficiencies in the design phase have an effect on all produced items, and the cost to correct them is progressively increased as the development proceeds.

Table 2 illustrates the industrial challenges in a reliability perspective of yesterday, today, and tomorrow. To meet the future application trends and customer expectations for ppm-level failure rate per year, it is essential to have better understanding of failure mechanisms of power electronic components and to explore innovative R&D approaches to build reliability in power electronic circuits and systems.

Table 2 The reliability challenge in industry seen before, today, and in the future [60]

	Yesterday	Today	Tomorrow
Customer expectations	Replacement if failure Years of warranty	Low risk of failure Request for maintenance	Peace of mind Predictive maintenance
Reliability target	Affordable market returns (%)	Low market return rates	ppm market return rates
R&D approach	Reliability test Avoid catastrophes	Robustness tests Improve weakest components	Design for reliability Balance with field load/ mission profile
R&D key tools	Product operating and function tests	Testing at the limits	Understanding failure mechanisms, field load, root cause Multi-domain simulation

Table 3 Typical lifetime target in different power electronic applications [60]

Applications	Typical design target of lifetime
Aircraft	24 years (100,000 h flight operation)
Automotive	15 years (10,000 operating hours, 300,000 km)
Industry motor drives	5–20 years (60,000 h at full load)
Railway	20–30 years (73,000–110,000 h)
Wind turbines	20 years (173,000 h)
Photovoltaic plants	5–31 years (22,000–130,000 h)

The performance requirements of power electronic products are increasingly demanding in terms of cost, efficiency, reliability, environmental sustainable materials, size, and power density. Of which, the reliability performance has influences on the safety, service quality, lifetime, availability, and life cycle cost of the specific applications. Table 3 summarizes the typical design target of lifetime in different applications. To meet those requirements, a paradigm shift is going on in the area of automotive electronics, more electrical aircrafts, and railway tractions by introducing new reliability design tools and robustness validation methods.

With the increasing penetration of renewable energy sources and the increasing adoption of more efficient variable-speed motor drives, the failure of power electronic converters in wind turbine, PV systems, and motor drives is becoming an issue. Field experiences in renewables reveal that power electronic converters are usually one of the most critical assemblies in terms of failure level, lifetime, and maintenance cost, as it is presented in Figs. 3 and 4.

4.2 Ongoing Paradigm Shift in Reliability Research

The reliability engineering has emerged as an identified discipline since 1950s with the demands to address the reliability issues in electronic products for military and space applications. Since then, much pioneer work has been devoted to various reliability

topics. One of the main streams is the quantitative reliability prediction based on empirical data and various handbooks released by military and industry. Another stream of the discipline focuses on identifying and modeling of the physical causes of component failures, which was the initial concept of physics of failure (PoF) presented in 1962. However, until the 1980s, the handbook-based constant failure rate models (e.g., Military-Handbook-217 series) have been dominantly applied for describing the useful life of electronic components. Since 1990s, with the increased complexity of electronic systems and especially the application of integrated circuits (ICs), more and more evidences were suggesting that constant failure rate models were inadequate. The Military-Handbook-217F [59] is therefore officially canceled in 1995. PoF approach has started to gain its more and more important role in reliability engineering.

In recent years, the initiatives to update the Military-Handbook-217F have turned to a hybrid approach, which is proposed for the planned version of Military-Handbook-217H. During the stage of program's acquisition–supplier selection activities, updated empirical models will be used for comparing different solutions. During the actual system design and development stage, scientific-based reliability modeling together with probabilistic methods will be applied. Intensive PoF research has been continuously conducted since 1990s in microelectronics. With the transition from pure empirical-based methods to more scientific-based approaches, the paradigm shift in reliability research is going on from the following aspects.

4.2.1 From Components to Failure Mechanisms

PoF approach is a methodology based on root cause failure mechanism analysis and the impact of materials, defects, and stresses on product reliability. It changes the analysis of system from a box of components to a box of failure mechanisms. The traditional handbook-based reliability prediction provides failure rate models for various components. PoF approach analyzes and models each failure mechanism induced by environmental and usage stresses. For a given component, there could be multiple failure mechanisms, which should be identified individually. Moreover, failure mechanisms are not limited to the component level. As discussed in the standard ANSI/-VITA 51.2 [60], there are various failure mechanisms at component level (i.e., single transistor level), package level, and printed circuit board (PCB) level. From this prospective, it is challengeable to apply PoF to a complex system of which limited number of models and their associated parameters are available. Therefore, it is important to identify and to focus on the critical failure mechanisms in specific applications.

4.2.2 From Constant Failure Rate to Mean Cumulative Function Curve

The conventional reliability metrics constant failure rate (defined as λ) and the corresponding mean time between failures (MTBF) (defined as $1/\lambda$) are found to be inappropriate to most practical cases. Therefore, the indiscriminate use of these metrics is discouraged.

The failure rate over operational time is not constant. An alternate technique to present the failure level and time is the mean cumulative function (MCF) curve. When analyzing repairable systems, it graphs the number of failures versus time (i.e., since installation). It is also possible to represent the behavior of the group of systems by an average number of failures versus time, which is known as MCF. The MCF curve is also an integration of the bathtub model [61], but here, it is possible to operate with quantitative figures, which can be broken down into budgets (e.g., the degradation budget).

4.2.3 From Reliability Prediction to Robustness Validation

Conventional empirical methodologies mainly attempt to determine the feasibility in fulfilling certain reliability goals and to predict the warranty costs and maintenance–support requirements. They provide limited insights into the design of the systems themselves to eliminate failures within targeted service life. Compared to them, the concept of PoF is to identify the root causes of different types of failure under environmental and operation stress conditions. Therefore, it helps to locate the weak links and formulate the corresponding guidelines on robustness design, process control, validation testing, and field operation. Products should be designed by considering the degraded parameters at the end of life with certain level of design margins.

4.2.4 From Microelectronics to also Power Electronics

The PoF approach has been extensively applied to microelectronic systems in the last two decades. Different failure mechanisms, lifetime models, and equivalent damaged circuit simulation models of electron devices are well presented. More and more new models are under development. One of the common driving factors from industry, academia, and military behind this is the demand for more reliable commercial-of-the-shell devices and systems.

In power electronic applications, reliability has been and will continue to be one of the important performance aspects in many applications. To address the challenges, power electronic engineers and scientists have started to apply various reliability tools for reliability prediction and reliability-oriented design of power electronic converters or systems. Last decade saw much pioneering work on the reliability of power converters for WTs and inverters for PV systems. It reveals that, unlike the case in microelectronics, conventional handbook methods are still dominantly applied nowadays for the reliability prediction in those studies.

While the pace of power electronics toward PoF approach is relatively slower than that of microelectronics, the need for this paradigm shift has been well recognized in automotive industry and then in other sectors. In particular, much interesting work from the semiconductor side investigates the failure

mechanisms of IGBT modules and physical-based lifetime models. The level of technology and scientific understanding are still highly evolving. The research in microelectronics could provide a very important foundation for the ongoing and future work in power electronics, especially seen from the methodologies' point of view. Nevertheless, it should be noted that most of the physical-based models are not scalable for power electronic components. System-level reliability problems (e.g., active thermal stresses, interconnections among components, and interaction of different components) are still of interest to be investigated.

4.3 Critical Stressors for Different Power Electronic Components

As discussed in Sect. 4.2.1, understanding of the reliability physics of components applied in power electronics is the most fundamental aspect. The PoF approach is based on analyzing and modeling each failure mechanism under various environmental and usage stresses. In practice, the PoF analysis focuses on critical components under critical stress conditions. Among other components, switching devices and capacitors are two of the most vulnerable components in terms of failure level and time. They are considered as the reliability-critical components in power electronic converters.

Focus point matrix (FPM) is a useful way to analyze the critical stressors that will kill the components. Based on the accumulated industrial experiences and future research needs, Table 4 shows the critical stressors for different components in power electronic systems. It can be noted that steady-state temperature, temperature swings, humidity, voltage, and vibrations have different level of impact on semiconductor devices, capacitors, inductors, and low-power control boards. It provides the information on determining the critical failure mechanisms. The interactions among different stressors are also of interest to be explored.

5 Overview and Practice of Design for Reliability

The important aspect of power electronics reliability is to build in reliability and sufficient robustness into the system design through design for reliability (DFR) process. Industries have advanced the development of reliability engineering from traditional testing for reliability to DFR. DFR is the process conducted during the design phase of a component or system that ensures them to be able to achieve required level of reliability. It aims to understand and fix the reliability problems up-front in the design process.

Table 4 Focus point matrix (FPM) in reliability of power electronic components [60]

Load			Focus points									
Climate + Design ≥ Stressor			Active power components			Passive power components		Control circuitry, IC, PCB, connectors, etc.				
Ambient	Product design	Stressors	Die	LASJ	Wire-bond	Cap.	Ind.	Solder Joint	MLCC	IC	PCB	Connectors
Relative humidity	Thermal system	Temperature swing ΔT	**X**	**X**	**X**			**X**				
$RH(t)$	Operation point	Average Temperature T	X	X	X	**X**		X	X	x	x	x
Temperature	ON/OFF	dT/dt	x	x	x	x						
$T(t)$	Power $P(t)$	Water								**X**	**X**	x
		Relative Humidity	x	x	x	X	x	x	x	**X**	**X**	x
Pollution	Tightness	Pollution						x			x	
Mains	Circuit	Voltage	x	x	x	**X**	X		x	x	x	x
Cosmic	Circuit	Voltage	x									
Mounting	Mechanical	Chock/vibration	x			x	x	x	x			x

LASJ large-area solder joint, *MLCC* multi-layer ceramic capacitor, *IC* integrated circuit, *PCB* printed circuit board, *Cap.* capacitor, *Ind.* inductor, level of importance (from high to low): **X**-**X**-X-x

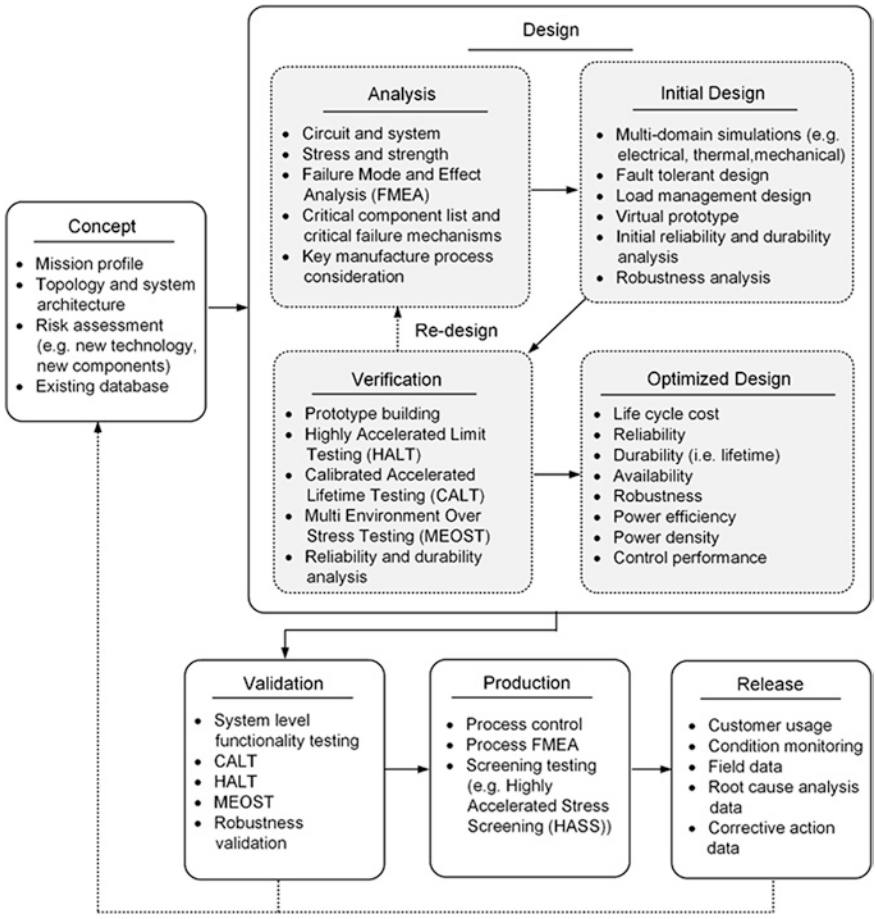

Fig. 18 State-of-the-art reliability design procedure for power electronics from concept to realization

5.1 A Systematic DFR Procedure in Power Electronics

A systematic DFR procedure which is specifically applicable to the design of power electronic products is shown in Fig. 18. By implementing the procedure, reliability is well considered and treated in each development phase (i.e., concept, design, validation, production, and release), especially in the design phase. The design of power electronic converters is mission profile based by taking into account large parametric variations (e.g., temperature swings, solar irradiance level changes, wind speed fluctuations, load changes, manufacturing process, etc.).

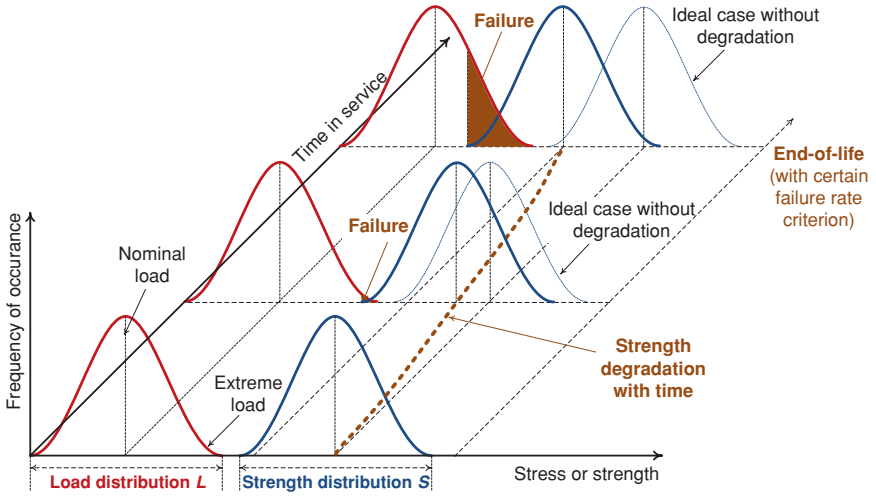

Fig. 19 Load–strength analysis to explain overstress failure and wear-out failure for a given power elctronics equipment

5.2 *Important Aspects of the DFR Procedure in Power Electronics*

5.2.1 Load–Strength Analysis

Load–strength analysis is an important method in the first step of the design phase as shown in Fig. 19. A component fails when the applied load L exceeds the design strength S. The load L here refers to a kind of stress (e.g., voltage, cyclic load, temperature, etc.), and strength S refers to any resisting physical property (e.g., hardness, melting point, adhesion, etc.). Figure 19 presents a typical load–strength interference which is evolving with time due to the degradation of the power electronic equipment. For most power electronic components, neither load nor strength is fixed, but allocated within a certain interval which can be presented by a specific probability density function (e.g., normal distribution). Moreover, the strength of a material or device could be degraded with time. Theoretically, the probability of failure can be obtained by analyzing the overlap area between the load distribution and the strength distribution. Practically, the exact distributions of load and strength are very often not available; then, Monte Carlo simulations can be applied to randomly select samples from each distribution and compared, and thus, the probability of failure for the specific converter can be roughly estimated.

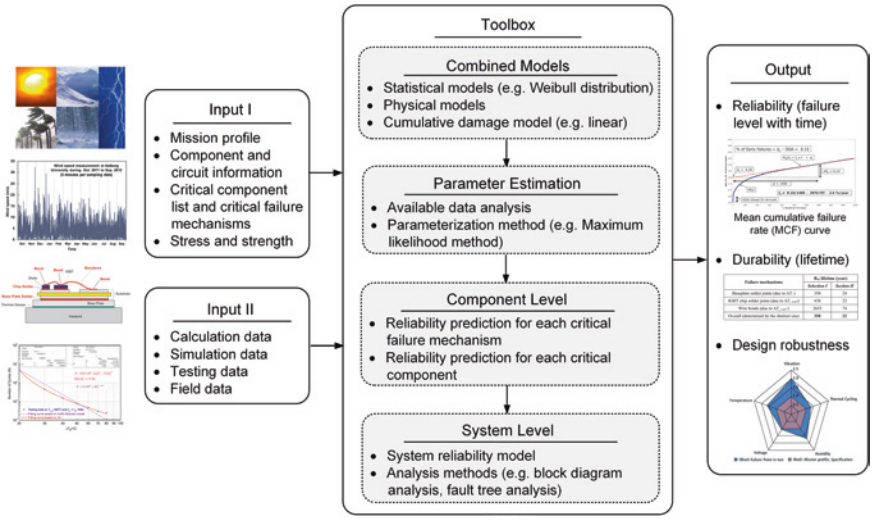

Fig. 20 Reliability prediction toolbox for power electronic systems

5.2.2 Reliability Prediction Toolbox

Reliability prediction (not based on constant failure rate λ) is also an important tool to quantify the lifetime, failure level, and design robustness based on various source of data and prediction models. Figure 20 presents a generic prediction toolbox based on the PoF approach. The toolbox includes statistical models and lifetime models and various sources of available data (e.g., manufacturer testing data, simulation data, and field data) for the reliability prediction of individual components and the overall system. The statistical models are well presented in the literatures, while the number of physical-based lifetime models available for power electronic components is still limited. Research efforts to both accelerated testing and advanced multi-disciplinary simulations will be beneficial in order to obtain those lifetime models.

To map the reliability from component level to the system level, reliability block diagram (RBD), fault-tree analysis (FTA), and state-space analysis (e.g., Markov analysis) are widely applied as summarized in Table 5.

It should be noted that the tabulated three methods are conventionally applicable to constant failure rate cases, which are corresponding to the handbook-based reliability prediction methods. The PoF-based system-level reliability prediction is still an open research topic even in microelectronics. The interactions among the different failure mechanisms will bring additional complexity into the analysis. Therefore, it was argued that the PoF approach is not practical for assessing an entire system. Moreover, it should be noted that the system reliability depends not only on components, but also on packaging, interconnections, manufacturing process, and human errors. The latter need also to be treated properly for a more accurate reliability assessment—from design to product.

Table 5 Summary of system-level reliability prediction methods

	Reliability block diagram (RBD)	Fault-tree analysis (FTA)	Markov analysis (MA)
Concepts	RBD is an analytical technique graphically representing the system components and their reliability-wise connections (from simple series–parallel to complex) by a logic diagram based on the system characteristics	FTA is an analytical technique using a top-down approach to analyze various system combinations of hardware, software, and human failures (i.e., subevents) that could cause the system failure (i.e., top event)	MA is a dynamic state-space analytical technique presenting all possible system states (i.e., functioning or failed) and the existing transitions between these states
Elements	Rectangle blocks	Events (i.e., initiating fault events, intermediate events, and top event)	States (i.e., functioning or failed)
	Direction lines	Logic gates (e.g., AND, OR, and more complex ones)	Transitions between states
	Failure level and time of the component/ subsystem represented by each blocks	Probability of each event	Transition rates based on failure rates and repair rates of components/ subsystems
Outcome	System-level reliability	System-level reliability	System-level reliability
		Identified all possible faults (similar to the results from FMEA)	System availability
Applications	For non-repairable systems	For non-repairable systems	Mainly for repairable systems
	Without redundancy	Without redundancy	Without redundancy
	With redundancy	With redundancy	With redundancy
Advantages	Simplicity and ease of application	All factors including human factors could be taken into account	Dynamic (i.e., represent state of every component at any time and the dependences among them)
		Useful also for identifying failure causes and design problems	Applicable for repairable systems

(continued)

Table 5 (continued)

	Reliability block diagram (RBD)	Fault-tree analysis (FTA)	Markov analysis (MA)
Disadvantages/ Limitations	Limitation in considering external events (e.g., human factor) and priority of events Dependencies among components/ subsystems are not well treated	Dependencies among components or subsystems are not well treated	State-based models easily get large (e.g., maximum 2^n states with n components) Primarily applicable for constant failure rate and constant repair rate (which works in theory only)

5.3 Challenges and Opportunities in the DFR of Power Electronics in Renewable Energy Systems

Joint efforts from engineers and scientists in the multiple disciplines are required to fulfill the research needs and promote the paradigm shift in reliability research in the area of power electronics for renewable energy applications. The major challenges and opportunities are summarized as follows for the renewable energy systems.

5.3.1 Challenges

- Pervasive and fast implementation of power electronics in a large variation of mission profiles with all kind of environmental exposures.
- Outdated paradigms and lack of understanding in the design for reliability process in power electronics.
- Uncertainties in mission profiles and variations in strength of components.
- Increasing electrical/electronic content and complexity.
- Lack of understanding in failure mechanisms and failure modes of reliability-critical components.
- Traditional system-level reliability prediction methods are based on constant failure rates. However, physics-of-failure-based component-level reliability prediction results in varying failure level with time.
- Resource-consuming testing for reliability prediction and robustness validation from components to entire systems.
- End up with ppm-level return rates for mass-manufactured power electronic products.
- Higher operating temperature (e.g., by using wide-band-gap power devices) which challenges the overall reliability and lifetime.
- Software reliability becomes an issue when more and more digital controllers are introduced in the power electronic systems, which should be treated adequately.

5.3.2 Opportunities

- The research in microelectronics provides an important foundation for the ongoing and future work in power electronics, especially from the methodologies' point of view.
- More and more mission profiles and online monitoring data from the field are available and accessible.
- Physics-of-failure approach provides insights to avoid failures in power electronic components, circuits, and systems.
- Active thermal control by controlling the power flow in power electronic circuits.

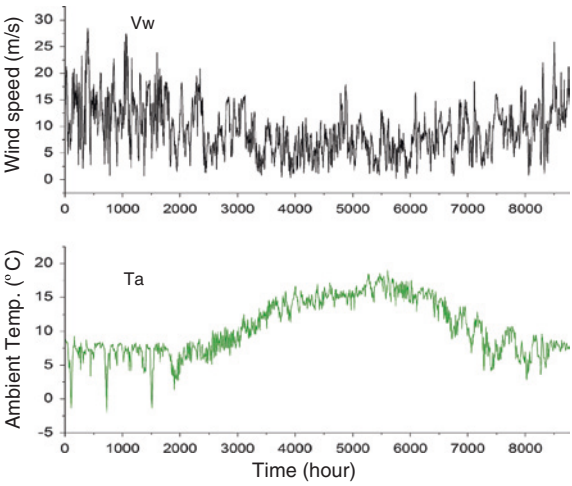

Fig. 21 One-year mission profile of wind speed and ambient temperature from a wind farm (3-h averaged)

- Component-level and system-level smart derating operation.
- Condition monitoring and fault-tolerant design, which allow extended lifetime and reduced failure rate.
- Emerging semiconductor and capacitor technologies enable more reliable power electronic components and systems.
- Computer-aided automated design software to save time and cost in the development process.
- Trends for modular design of power converters and standardized power electronic components and packaging technologies.

6 Cases for Lifetime Estimation of Power Electronics

6.1 A Case for 2-MW Three-Phase Wind Power Converter

A typical wind condition and wind turbine system has to be settled first as a study case. As shown in Fig. 21, a 1-year wind speed and an ambient temperature profile are used with 3 h averaged at 80 m hub height, which were designated for the wind farm located near Thyborøn, Denmark, with latitude 56.71° and longitude 8.20°. The chosen hub wind speed belongs to the wind class IEC I with average wind speed of 8.5–10 m/s [40, 62], and a 2.0-MW wind turbine [63] is chosen to fit the given wind condition.

With respect to the wind power converter, the most adopted two-level back-to-back voltage source converter topology is chosen, as shown in Fig. 22. Only the grid-side converter is chosen as a case study, whose parameters are basically designed according to Table 6, which is a state-of-the-art configuration for the two-level wind power converter. The generator-side converter can share a similar approach for the analysis.

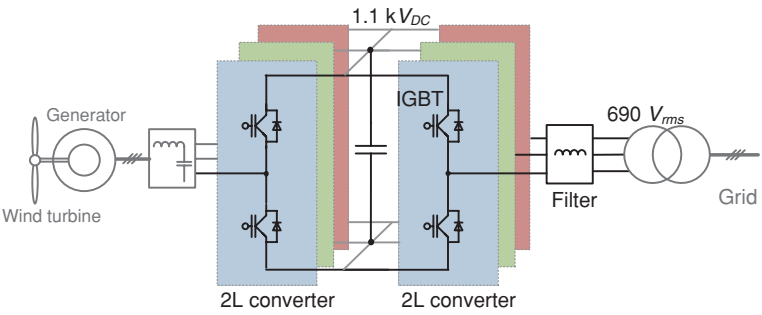

Fig. 22 Wind power converter for lifetime estimation

Table 6 Parameters of converter shown in Fig. 22

Rated output active power P_o	2 MW
DC bus voltage V_{dc}	1.1 kV DC
[a]Rated primary side voltage V_p	690 V rms
Rated load current I_{load}	1.93 kA rms
Fundamental frequency f_o	50 Hz
Switching frequency f_c	1950 Hz
Filter inductance L_f	132 μH (0.2 p.u.)

[a]Line-to-line voltage in the primary windings of transformer

As shown in Fig. 23, the operational flow for the lifetime estimation under a long-term time constant is straightforward: The wind profiles in Fig. 21 are directly fed into a series of wind turbine models in order to generate the corresponding thermal loading of the power devices. Then, the acquired thermal loading is processed for lifetime estimation. The analysis in this section is conducted with a time span of 1 year and step of 3 h, which is synchronized with the wind speed and ambient temperature profiles given in Fig. 21.

6.1.1 Long-Term Loading Profile Generation

In Fig. 24, a diagram for long-term loading profile calculation is indicated. It can be seen that multi-disciplinary models are included in order to map the mission profile of the wind turbines into the thermal loading of the power semiconductors.

The wind speed is sampled at 3 h, and only long-term thermal behaviors are in focus; the inertia effects of the wind turbine and generator can be ignored because the dynamics, which normally range with a time constant of seconds to minutes, are much smaller than the sampling rate. The output power of wind turbine can be looked up from the power curve provided by the manufacturer [63] and can be directly used as the delivered power of the converter.

Similarly, because the response time of converter power and corresponding losses are much smaller than the interested time constant, the loss on the power semiconductor can be directly acquired from lookup table in order to

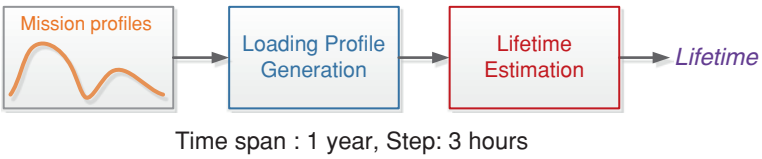

Fig. 23 Flowchart for lifetime estimation of power devices caused by long-term thermal cycles

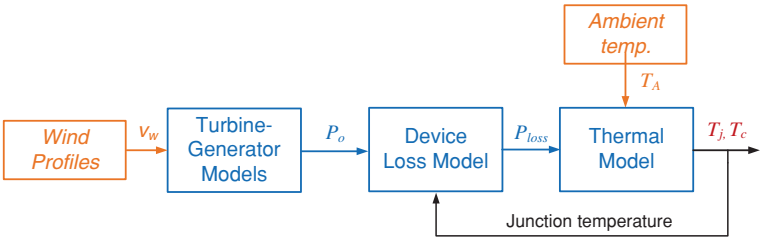

Fig. 24 Multi-domain models used for thermal profile generation of power devices in a 2-MW wind turbine

accelerate the analyzing speed. The IGBT module from a leading manufacturer (2.4 kA/1.1 kV/150 °C) [64] is chosen as power semiconductor devices, which in this chapter have maximum junction temperature at 115 °C when the liquid temperature of water-cooled heat sink is at 40 °C. In order to enable the temperature dependency of the device losses [65, 66], a 3-dimensional lookup table is established. As shown in Fig. 25, the losses consumed by the power devices are decided by the input power of the converter as well as device junction temperature. For the sake of accuracy, each of the point in the lookup table is simulated in a detailed circuit model with complete switching behaviors of the power devices, and the conduction loss, switching loss, and diode reverse recovery loss are also taken into account.

The thermal model (i.e., the network of thermal resistance and capacitance), which can transfer the acquired power loss in Fig. 25 to the corresponding temperature inside and outside the power devices, is an important consideration for the loading profile generation. Normally, the thermal capacitance of the power devices will lead to fast thermal changes ranging in the time constants of seconds to minutes [67]—which are still much smaller than the interested time constants for long-term thermal loading. As a result, the thermal capacitance inside the power device as well as the heat sink can be ignored and only thermal resistance is taken into account for long-term loading analysis. The used thermal network is shown in Fig. 26. It is noted that the fluid temperature of the water-cooled heat sink T_{fluid} is assumed to be maintained at 40 °C if the IGBT is generating power losses, and T_{fluid} is set to the nacelle temperature if the wind speed is below the cut-in speed more than 12 h. This is an operation-dependent parameter.

Based on the above-mentioned models and the 1-year mission profile shown in Fig. 3, the long-term thermal loading of the IGBT modules in the given wind power converter can be generated. As shown in Fig. 27, the junction temperature T_j of the IGBT chips and case temperature T_c of IGBT-based plate are shown,

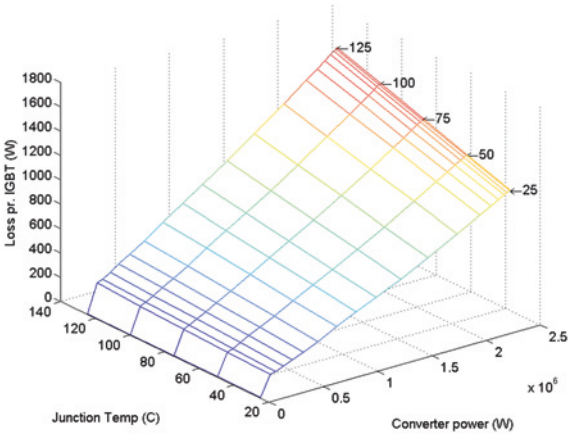

Fig. 25 3D lookup table for the IGBT loss in the given wind power converter

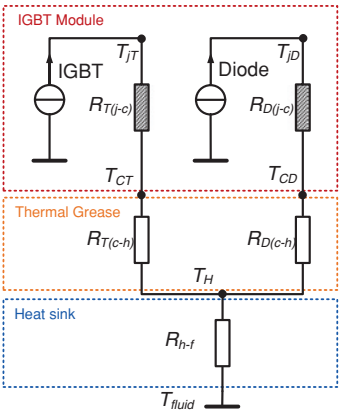

Note:

T_j: junction temperature

T_C: case temperature

T_H: heat sink temperature

T_{fluid}: Water-cooler fluid temperature

$R_{(j-c)}$: thermal impedance from junction to case

$R_{(c-h)}$: thermal impedance from case to heat sink

$R_{(h-f)}$: thermal impedance from heat sink to fluid

Fig. 26 Thermal network of power semiconductor devices for the long-term thermal profile generation

respectively, because they are closely related to the major failure mechanisms of the IGBT module [68].

6.1.2 Lifetime Estimation with Long-Term Thermal Loading

After the long-term thermal loading of the given IGBT is generated, a rain-flow counting method [69, 70] has to be applied in order to convert the randomly changed thermal profile to the regulated thermal cycles which are more suitable to be utilized by the lifetime models. It is becoming a common agreement that not only the amplitude ΔT_j and the mean value T_{jm} of thermal cycles, but also the cycling period t_{cycle}, all have strong impacts on the lifetime of the power devices. The counting results from the long-term thermal loading in Fig. 27 are shown in Fig. 28, where 460 thermal cycles are identified and each counted cycle with its corresponding ΔT_j, T_{jm}, and t_{cycle} are shown.

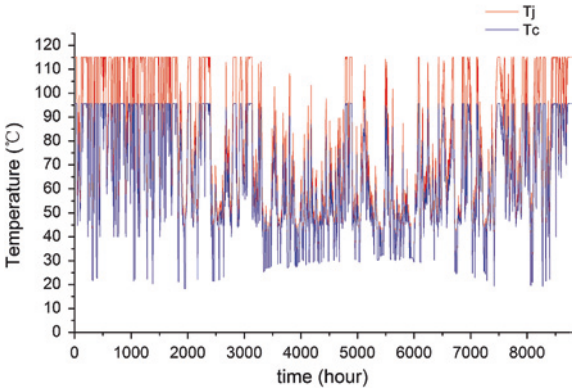

Fig. 27 One-year thermal profile under the given mission profile in Fig. 21. (Junction temperature T_j and case temperature T_c of the IGBT, time step of 3 h)

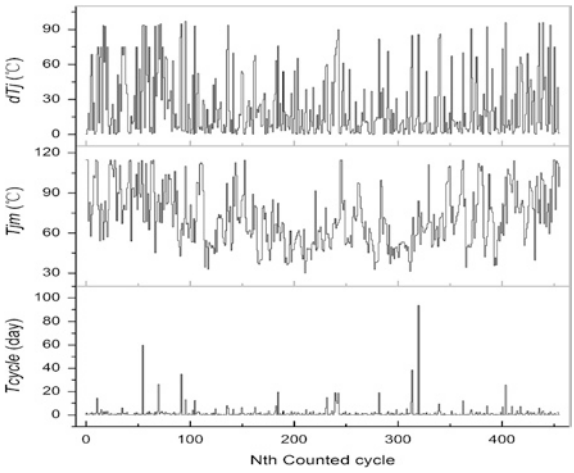

Fig. 28 Rain flow counting results of the junction temperature profile shown in Fig. 27

After the thermal profiles are counted and regulated, the lifetime models for power devices can be used. There are many different approaches for lifetime modeling of power semiconductor devices, but they are not concluded yet and updated regularly. Generally, the lifetime models provided by device manufacturers are more frequently used. These lifetime models are based on mathematical fitting of enormous aging test data, and normally, the numbers of thermal cycles N_{life} to a certain failure rate (B_X) is used as an indicator for the lifetime of power devices, which means an individual power device will have X % probability to fail (or a group of power devices have X % population to fail) after suffering N_{life} of the thermal cycles.

In this case study, the lifetime model provided by [71] is used for the lifetime estimation. This model is a series of lookup tables which can map the n_{th} counted thermal cycle in Fig. 10 to the corresponding number of cycles that the IGBT has 10 % probability of failure (N_{n_life} @ B_{10}). Then, the "consumed B_{10} lifetime" by each counted thermal cycle can be simply calculated in (1). And the total

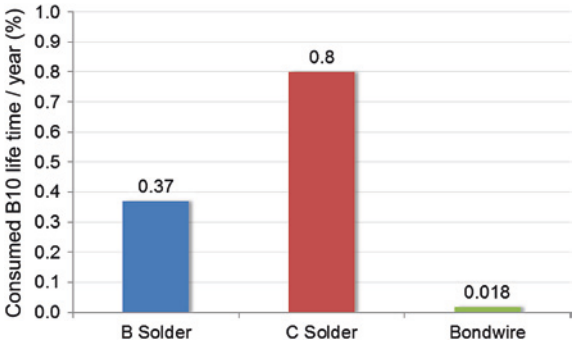

Fig. 29 Consumed B10 lifetime of IGBT by long-term thermal cycles for one year (considering thermal cycles ranging from 3 h to 1 year, *B solder* means baseplate solder, *C solder* means chips solder) under the mission profile shown in Fig. 21

"consumed B_{10} lifetime" by the counted 460 long-term thermal cycles in one year CL_{1year_long} can be accumulated in (2) according to the Miner's rule [72].

$$CL_n = \frac{1}{N_{n\_life}} \tag{1}$$

$$CL_{1year\_long} = \sum_{n=1}^{460} CL_n \tag{2}$$

The total 1-year consumed B_{10} lifetime of the IGBT module when applying the long-term thermal loading in Fig. 27 is shown in Fig. 29, in which three failure mechanisms such as the crack of baseplate soldering (B Solder, caused by case temperature cycling), crack of chip soldering (C solder, caused by junction temperature cycling), and bond-wire liftoff (bond wire, caused by junction temperature cycling) are shown, respectively. It can be seen that the junction temperature cycling on the chip soldering (C solder) consumes more lifetime (i.e., more quick to failure) than the other two failure mechanisms. It is worth to mention that this lifetime result only reflects the influence by long-term thermal cycles with a period larger than 3 h.

6.2 A Case Study with Single-Phase 3-kW PV Inverters

With the accumulative field experience and the introduction of more and more real-time monitoring systems, better mission profile data have become more available in various kinds of power electronic systems, like PV applications. This offers the possibilities to predict the lifetime of a certain inverter more accurately and provides possible estimation of energy production from PV power systems in certain applications. However, the solar irradiance together with the ambient temperature is variable with PV system locations and seasons, where the PV inverter efficiency changes. It is necessary to investigate the transformerless inverters not only in a short-term but also in a long-term duration in such a way to predict the PV energy production and the inverter lifetime. Hence, a mission profile-based

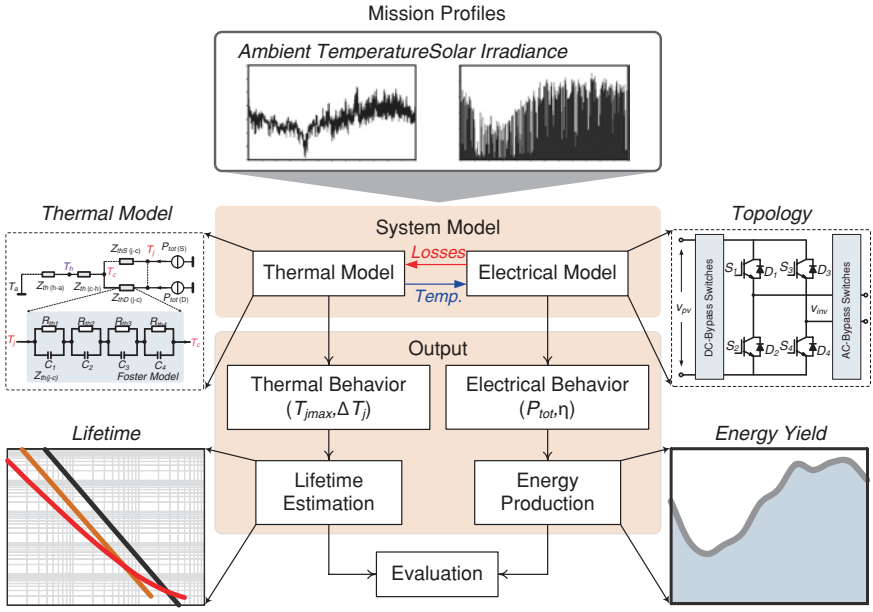

Fig. 30 Mission profile-based multi-disciplinary analysis method of single-phase transformerless PV inverters

multi-disciplinary evaluation method for single-phase transformerless PV systems is introduced. The analysis procedure of this method is shown in Fig. 30.

In the evaluation method, the mission profiles—solar irradiance and ambient temperature (yearly data, monthly data, and/or daily data)—are taken as the input variables like the case of wind turbines shown in Fig. 23. The selected different transformerless PV inverter topologies are simulated in PLECS based on the thermal model shown in Fig. 30. As it is shown in Fig. 30, the loss distribution in the power devices and the junction temperature of the power modules, including mean/max junction temperature (T_{jmax}) and temperature cycling (ΔT_{j}), can be obtained as the outputs of this proposed analysis method. Based on the resultant total losses and the thermal behavior, the energy production and the lifetime of a certain transformerless inverter can be obtained. Then, a benchmarking of different topologies could basically be done in terms of efficiency, energy production, and also reliability.

6.2.1 Analysis Approach Implementation

The mission profile-based analysis approach can be adopted for analysis of mission profiles at different time scales, e.g., a yearly mission profile and an hourly mission profile. As for short-term mission profiles within a range of milliseconds to several seconds, both power loss profile and temperature loading profile (junction

temperature) can directly be obtained from the simulations with a physical–electrical system model. However, for a long-term mission profile (normally longer than few minutes due to ambient or operating condition changes), especially with a high data sampling rate (e.g., 200 ms per sample), it will be a time-consuming process, and even impossible, to capture the full loading profile under this mission profile. Consequently, similar to the case of power losses shown in Fig. 25, lookup tables are adopted to accelerate the evaluation process [50, 77, 78], which requires appropriately decomposing the mission profile at different time scales. Figure 31 shows the decomposing procedure for a long-term mission profile.

In the following case study, a 600 V, 50 A IGBT module from a leading manufacturer has been selected as the power device in the potential transformerless topologies. The PV array consists of 46 BP 365-PV modules (2 strings, 23 modules of each string), being the rated maximum power of 2,990 W and the nominal voltage of 405 V at maximum power point under standard test conditions (25 °C, 1,000 W/m^2). The thermal parameters for the power devices are listed in Table 7. The efficiency of maximum power point tracking (MPPT) is assumed to be 99 %. Referring to Figs. 8 and 9, the single-phase FB topology with bipolar modulation (FB-bipolar) and the HERIC topology have been studied in terms of junction temperature behaviors under recorded mission profiles—yearly data, which are shown in Fig. 13, in order to evaluate the lifetime based on rain-flow analysis [46, 76]. Afterward, the lifetime (life consumption) can be calculated based a dedicated lifetime model.

6.2.2 Translated Stress Profiles for Lifetime Estimation

According to Figs. 30 and 31, the mission profile can be translated into stress profiles as shown in Fig. 32, including power loss profile and thermal loading profile, which are related to the lifetime prediction and should be appropriately extracted according to a specific lifetime model. For example, the well-known extended Coffin-Manson model [41, 44, 50, 77] may be applied for prediction of cycle-to-failure of IGBT modules. This lifetime model indicates that the number of cycles to failure N_f is only dependent on the temperature cycles, including cycle amplitude ΔT_j and mean junction temperature T_{jm}. Those values can easily be obtained under short-term or decomposed short-term mission profiles, as it is shown in Fig. 31.

However, it has been found in other lifetime models that N_f is also affected by the cycle period (t_{on}), bond–wire aspect ratio (ar), and the diode (f_{diode}) [44, 68, 82]. Hence, counting algorithms should be adopted to exploit the temperature loading profile shown in Fig. 32b, e.g., to acquire the information of cycle periods and cycle amplitudes. There are many cycle counting algorithms reported, e.g., level crossing counting, rain-flow counting, and simple range counting methods [76, 77, 83]. Then, the lifetime can quantitatively be calculated with the extracted information by applying it to a dedicated lifetime model.

The rain-flow counting results of the thermal loading profiles shown in Fig. 32 of the two transformerless PV inverters under a yearly mission profile are presented in Fig. 33. The results clearly indicate the number of cycles distributions

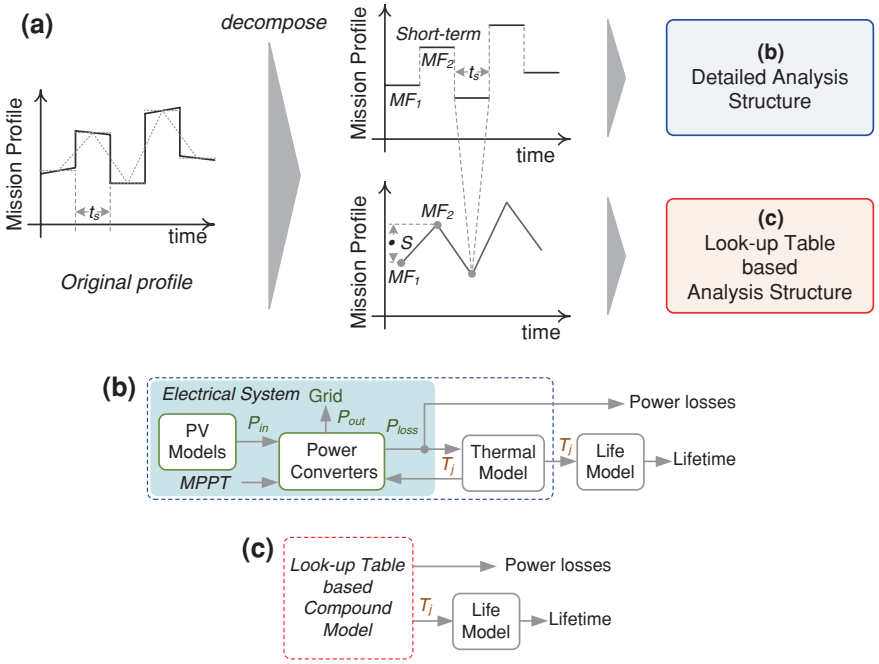

Fig. 31 Mission profile decomposition for the analysis approach: **a** decomposition procedure, **b** detailed structure for short-term mission profiles, and **c** lookup table-based structure for long-term mission profiles

Table 7 Thermal parameters for a 600 V/50A IGBT module

Impedance	$Z_{th(j\text{-}c)}$				
i		1	2	3	4
IGBT	R_{thi} (K/W)	0.074	0.173	0.526	0.527
	τ_i (s)	0.0005	0.005	0.05	0.2
Diode	R_{thi} (K/W)	0.123	0.264	0.594	0.468
	τ_i (s)	0.0005	0.005	0.05	0.2

on the junction temperature cycling amplitude ΔT_j and mean junction temperature T_{jm}. In addition, by applying the rain-flow counting algorithm to the thermal loading profiles, it is possible to get the cycle period information t_{on}, which may be required by a certain lifetime model. In this case, a detailed lifetime model for IGBT devices [82] has been adopted, and it is given as,

$$N_f = A \cdot \Delta T_j^{\alpha} \cdot (ar)^{\beta_1 \cdot \Delta T_j + \beta_0} \cdot \left(\frac{C + (t_{on})^{\gamma}}{C + 1} \right) \cdot \exp\left(\frac{E_a}{k_B \cdot T_{jm}} \right) \cdot f_{diode} \quad (3)$$

where k_B is the Boltzmann constant. The other parameters (A, α, β_0, β_1, γ, and E_a) of the model in (3) can be obtained through accelerating tests.

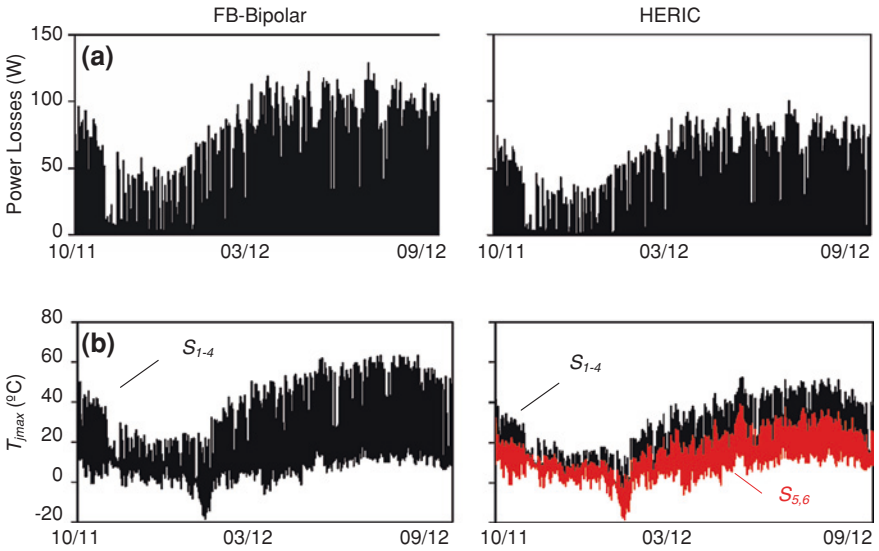

Fig. 32 Stress profiles of two single-phase 3-kW transformerless PV inverters (FB-bipolar and HERIC) under a yearly mission profile shown in Fig 13: **a** total power loss profile and **b** thermal loading profile of the power devices

According to the Miner's rule [50, 60, 77], the accumulated life consumption *LC* (i.e., damage) is linearly dependent on the contributions from different temperature cycles, which can be expressed as

$$LC = \sum_i \frac{n_i}{N_{fi}} \tag{4}$$

where n_i is the number of cycles at stress ΔT_{ji} and N_{fi} is the corresponding number of cycles to fail according to (3). Then, the lifetime of the power devices can be calculated as $LF = T_{mp}/LC$ under the mission profile with a duration of T_{mp}.

However, the parameters of the lifetime model in (3) are extracted under specific conditions, e.g., 0.07 s $\leq t_{on} \leq$ 63 s [82], and thus, they are not suitable to use for a quantitative calculation of the lifetime for the power devices used in this case (different power devices). Nevertheless, even though the parameters in those models are device dependent and their accurate values may not be available, the reliability performance of the switching devices in the PV inverters under the same environmental conditions could still be compared in a qualitative way by normalizing the life consumption so that the parameter dependency is reduced. The normalization of the life consumption can be given as

$$\overline{LC} = \frac{LC}{LC'} \tag{5}$$

in which $\overline{LC}$ is the normalized life consumption and *LC'* is the base *LC* for normalization.

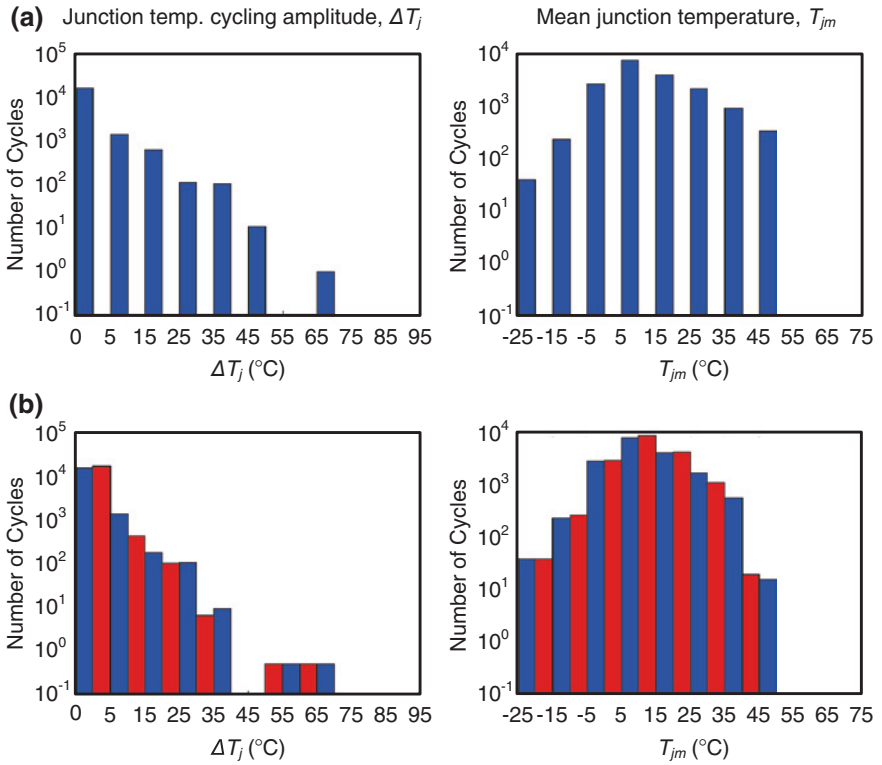

Fig. 33 Rain-flow counting results of the thermal loading profiles shown in Fig. 32 (*Blue* $S_{1–4}$, *Red* $S_{5,6}$): **a** FB-bipolar and **b** HERIC

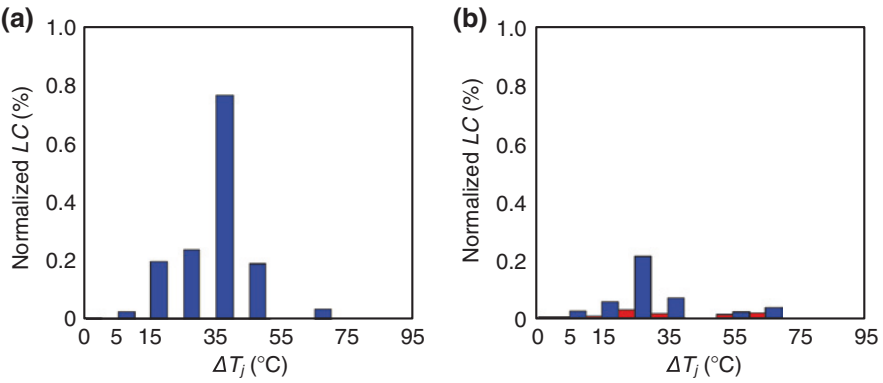

Fig. 34 Normalized life consumption (lifetime comparison) of the two inverters under the same mission profile shown in Fig. 13 (*Blue* $S_{1–4}$, *Red* $S_{5,6}$): **a** FB-Bipoar and **b** HERIC

According to (5) and the counting results presented in Fig. 33, the normalized *LC* of the two PV inverters under the same mission profile is shown in Fig. 34, where the life consumption of the power devices of the FB-bipolar inverter is chosen as the base value for normalization. It can be concluded for the results shown in Figs. 32 and 34 that the HERIC inverter would be the most promising solution for single-phase PV systems in terms of efficiency and also reliability. Another interesting conclusion that can be drawn is that although there are a few cycles of large temperature cycling amplitude induced by the mission profile (e.g., 10 cycles of 45–55 °C for the devices $S_{1\sim4}$ in Fig. 33a), they do contribute much more damage (e.g., 0.2 % in Fig. 34b).

7 Summary

The chapter illustrates the developments and requirements for the power electronics technology in the renewable energy systems, where the importance of reliability performance is especially focused. Afterward, a few state-of-the-art converter solutions for wind power and photovoltaic power generations are presented, respectively. Then, some principles, concepts, paradigm shifts, and practices about how to achieve more reliable power electronics are summarized and discussed. Finally, two examples which demonstrate how to translate the mission profiles of the converter into the lifetime of power semiconductor devices are given based on wind and PV applications.

It is concluded that as the development of renewable energy technology is quick, the reliability performance of power electronics is getting more and more critical. And there are many emerging challenges as well as technology opportunities to achieve more reliable power electronics in various applications like renewable energy conversion. It worth to mention that right now reliability calculation and analysis for power electronics are undergoing revolutionary advancements; many other issues besides power semiconductors and thermal loading are also important factors to be taken into account in the final product.

References

1. REN21 (2012) Renewables 2012 global status report. Available at http://www.ren21.net
2. Website of Vestas Wind Power (2011) Wind turbines overview. Available at http://www.vestas.com/
3. UpWind project (2011) Design limits and solutions for very large wind turbines. Available at http://www.ewea.org/fileadmin/ewea_documents/documents/upwind/21895_UpWind_Report_low_web.pdf
4. Lesnicar A, Marquardt R (2003) An innovative modular multilevel converter topology suitable for a wide power range. In: Proceedings of IEEE Bologna powertech conference, pp 1–6
5. Faulstich S, Lyding P, Hahn B, Tavner P (2009) Reliability of offshore turbines–identifying the risk by onshore experience. In: Proceedings of European offshore wind, Stockholm

6. Hahn B, Durstewitz M, Rohrig K (2007) Reliability of wind turbines—Experience of 15 years with 1,500 WTs, wind energy. Spinger, Berlin
7. Blaabjerg F, Ma K (2013) Future on power electronics for wind turbine systems. IEEE J Emerg Sel Top Power Electron 1(3):139–152
8. Blaabjerg F, Chen Z, Kjaer SB (2004) Power electronics as efficient interface in dispersed power generation systems. IEEE Trans Power Electron 19(4):1184–1194
9. Chen Z, Guerrero JM, Blaabjerg F (2009) A review of the state of the art of power electronics for wind turbines. IEEE Trans Power Electron 24(8):1859–1875
10. Blaabjerg F, Liserre M, Ma K (2012) Power electronics converters for wind turbine systems. IEEE Trans Ind Appl 48(2):708–719
11. Blaabjerg F, Ma K (2013) High power electronics—Key technology for wind turbines. Power electronics for renewable energy systems, transportation and industrial applications, Wiley, Chap. 6
12. Rodriguez J, Bernet S, Bin W, Pontt JO, Kouro S (2007) Multilevel voltage-source-converter topologies for industrial medium-voltage drives. IEEE Trans Ind Electron 54(6):2930–2945
13. Kouro S, Malinowski M, Gopakumar K, Pou J, Franquelo LG, Wu B, Rodriguez J, Perez MA, Leon JI (2010) Recent advances and industrial applications of multilevel converters. IEEE Trans Power Electron 57(8):2553–2580
14. Faulstich A, Stinke JK, Wittwer F (2005) Medium voltage converter for permanent magnet wind power generators up to 5 MW. Proc EPE 2005:1–9
15. Celanovic N, Boroyevich D (2000) A comprehensive study of neutral-point voltage balancing problem in three-level neutral-point-clamped voltage source PWM inverters. IEEE Trans Power Electron 15(2):242–249
16. Srikanthan S, Mishra MK (2010) DC capacitor voltage equalization in neutral clamped inverters for DSTATCOM application. IEEE Trans Ind Electron 57(8)
17. Zaragoza J, Pou J, Ceballos S, Robles E, Jaen C, Corbalan M (2009) Voltage-balance compensator for a carrier-based modulation in the neutral-point-clamped converter. IEEE Trans Ind Electron 56(2):305–314
18. Ma K, Blaabjerg F, Xu D (2011) Power devices loading in multilevel converters for 10 MW wind turbines. In: Proceedings of ISIE 2011, pp 340–346
19. Ma K, Blaabjerg F (2011) Multilevel converters for 10 MW wind turbines. In: Proceedings of EPE' 2011, Birmingham, pp 1–10
20. Rodriguez J, Bernet S, Steimer PK, Lizama IE (2010) A survey on neutral-point-clamped inverters. IEEE Trans Ind Electron 57(7):2219–2230
21. Andresen B, Birk J (2007) A high power density converter system for the Gamesa G10x 4.5 MW Wind turbine. In: Proceedings of EPE' 2007, pp 1–7
22. Jones R, Waite P (2011) Optimised power converter for multi-MW direct drive permanent magnet wind turbines. In: Proceeding of EPE' 2011, pp 1–10
23. Kjaer SB, Pedersen JK, Blaabjerg F (2005) A review of single-phase grid-connected inverters for photovoltaic modules. IEEE Trans Ind Appl 41(5):1292–1306
24. Kjaer SB (2005) Design and control of an inverter for photovoltaic applications. PhD thesis, Department of Energy Technology, Aalborg University, Aalborg, Denmark
25. Teodorescu R, Liserre M, Rodriguez P (2011) Grid converters for photovoltaic and wind power systems. IEEE/Wiley, NY
26. Photovoltaic Research Group, Department of Energy Technology, Aalborg University. Available at http://www.et.aau.dk/research-programmes/
27. Yang Y, Blaabjerg F, Wang H (2014) Low voltage ride-through of single-phase transformerless photovoltaic inverters. IEEE Trans Ind Appl 50(3). doi:10.1109/TIA.2013.2282966
28. Papanikolaou NP (2013) Low-voltage ride-through concept in flyback inverter-based alternating current—photovoltaic modules. IET Power Electron 6(7):1436–1448
29. Koutroulis E, Blaabjerg F (2013) Design optimization of transformer-less grid-connected PV inverters including reliability. IEEE Trans Power Electron 28(1):325–335
30. Meneses D, Blaabjerg F, García O, Cobos JA (2013) Review and comparison of step-up transformerless topologies for photovoltaic AC-module application. IEEE Trans Power Electron 28(6):2649–2663

31. SMA, SUNNY CENTRAL-High tech solution for solar power stations. Products category brochure. Available at http://www.sma-america.com/
32. Meinhardt M, Cramer G (2001) Multi-string-converter: the next step in evolution of string-converter technology, In: Proceedings of EPE'01, pp P.1–P.9
33. Araujo SV, Zacharias P, Mallwitz R (2010) Highly efficient single-phase transformerless inverters for grid-connected PV systems. IEEE Trans Ind Electron 57(9):3118–3128
34. Gonzalez R, Lopez J, Sanchis P, Marroyo L (2007) Transformerless inverter for single-phase photovoltaic systems. IEEE Trans Power Electron 22(2):693–697
35. Gonzalez SR, Coloma CJ, Marroyo PL, Lopez TJ, Sanchis GP (2008) Single-phase inverter circuit for conditioning and converting DC electrical energy into AC electrical. International patent application, Pub. No. WO/2008/015298, 7 Feb 2008
36. Bae Y, Vu T-K, Kim R-Y (2013) Implemental control strategy for grid stabilization of grid-connected PV system based on german grid code in symmetrical low-to-medium voltage network. IEEE Trans Energy Convers 28(3):619–631
37. Nabae A, Magi H, Takahashi I (1981) A new neutral-point-clamped PWM inverter. IEEE Trans Ind Appl 17(5):518–523
38. Knaup P (2007) International Patent Application, Pub. No. WO 2007/048420 A1, May 2007
39. Report of Danish Commission on Climate Change Policy (2010) Green energy—the road to a Danish energy system without fossil fuels. Available at http://www.klimakommissionen.dk/en-US/
40. Wikipedia (2013) IEC 61400. Avaiable at http://en.wikipedia.org/wiki/IEC_61400#cite_note-woeb-1
41. Ma K, Liserre M, Blaabjerg F (2013) Lifetime estimation for the power semiconductors considering mission profiles in wind power converter. In: IEEE Trans Power Electr 2014
42. Wolfgang E, Amigues L, Seliger N, Lugert G (2005) Building-in reliability into power electronics systems. The world of electronic packaging and system integration, pp 246–252
43. Hirschmann D, Tissen D, Schroder S, De Doncker RW (2005) Inverter design for hybrid electrical vehicles considering mission profiles. IEEE Conf Veh Power Propul 7–9:1–6
44. Busca C, Teodorescu R, Blaabjerg F, Munk-Nielsen S, Helle L, Abeyasekera T, Rodriguez P (2011) An overview of the reliability prediction related aspects of high power IGBTs in wind power applications. Microelectron Reliab 51(9–11):1903–1907
45. Wolfgang E (2007) Examples for failures in power electronics systems. Presented at ECPE tutorial on reliability of power electronic systems, Nuremberg, Germany
46. Yang S, Bryant AT, Mawby PA, Xiang D, Ran L, Tavner P (2011) An industry-based survey of reliability in power electronic converters. IEEE Trans Ind Appl 47(3):1441–1451
47. Isidori A, Rossi FM, Blaabjerg F, Ma K (2014) Thermal loading and reliability of 10-MW multilevel wind power converter at different wind roughness classes. IEEE Trans Ind Appl 50(1):484–494
48. Luque A, Hegedus S (2011) Handbook of photovoltaic science and engineering. Wiley, NY (second version)
49. Iov F, Ciobotaru M, Sera D, Teodorescu R, Blaabjerg F (2007) Power electronics and control of renewable energy systems. In: Proceedings of PEDS'07, pp P6–P28, 27–30 Nov 2007
50. Wang H, Liserre M, Blaabjerg F (2013) Toward reliable power electronics—challenges, design tools and opportunities. IEEE Ind Electron Mag 7(2):17–26
51. Ciobotaru M, Teodorescu R, Blaabjerg F (2005) Control of single-stage single-phase PV inverter. In: Proceedings of EPE'05, pp P.1–P.10
52. Koutroulis E, Blaabjerg F (2012) A new technique for tracking the global maximum power point of PV arrays operating under partial-shading conditions. IEEE J Photovol 2(2):184–190
53. Report of the International Renewable Energy Angency (IRENA) (2012) Renewable power generation costs in 2012: an overview. Released in 2013. Available at http://www.irena.org/
54. Kovanen KO (2013) Photovoltaics and power distribution. Renewable Energy Focus 14(3):20–21
55. Xue Y, Divya KC, Griepentrog G, Liviu M, Suresh S, Manjrekar M (2011) Towards next generation photovoltaic inverters. In: Proceedings of ECCE' 11, pp 2467–2474, 17–22 Sept 2011

56. Rosenwirth D, Strubbe K (2013) Integrating variable renewables as Germany expands its grid. Available at http://www.renewableenergyworld.com/. Accessed on 21 Mar 2013
57. Yang Y, Enjeti P, Blaabjerg F, Wang H (2014) Suggested grid code modifications to ensure wide-scale adoption of photovoltaic energy in distributed power generation systems. In: IEEE Industry Applications Magazine, accepted, in press, 2014
58. Kobayashi H (2012) Fault ride through requirements and measures of distributed PV systems in Japan. In: Proceedings of IEEE-PES general meeting, pp 1–6, 22–26 Jul 2012
59. Military Handbook (1991) Reliability prediction of electronic equipment, MIL-HDBK-217F, 2 Dec 1991
60. Wang H, Liserre M, Blaabjerg F, Rimmen PP, Jacobsen JB, Kvisgaard T, Landkildehus J (2014) Transitioning to physics-of-failure as a reliability driver in power electronics. IEEE J Emerg Sel Top Power Electron 2(1):97–114
61. Klutke GA, Kiessler PC, Wortman MA (2003) A critical look at the bathtub curve. IEEE Trans Reliab 52(1):125–129
62. Website of Vestas Wind Power (2013) Wind turbines classes. Available at http://www.vestas.com/
63. Website of Vestas Wind Power (2013) Wind turbines overview. Available at http://www.vestas.com/
64. Website of ABB semiconductor (2014) Avaiable at http://new.abb.com/products/semiconductors
65. User manual of PLECS blockset version 3.1, March 2011
66. Graovac D, Purschel M (2009) IGBT power losses calculation using the data-sheet parameters. Infineon application note
67. Infineon Application Note AN2008-03 (2008) Thermal equivalent circuit models
68. Kovacevic IF, Drofenik U, Kolar JW (2010) New physical model for lifetime estimation of power modules. In: Proceedings of IPEC, pp 2106–2114
69. ASTM International, E1049-85 (2005) Standard practices for cycle counting in fatigue analysis
70. Niesłony A (2009) Determination of fragments of multiaxial service loading strongly influencing the fatigue of machine components. Mech Syst Signal Process 23(8):2712–2721
71. Berner J (2012) Load-cycling capability of HiPak IGBT modules. ABB application note 5SYA 2043-02
72. Miner MA (1945) Cumulative damage in fatigue. J Appl Mech 12:A159–A164
73. Kaco, Powador XP500-HV TL central inverter. Available at http://www.kaco-newenergy.com/products/solar-inverters
74. Wikipedia (2013) List of photovoltaic power stations. Available at http://en.wikipedia.org/wiki/List_of_photovoltaic_power_stations
75. SMA news (2013) 114 Sunny central 900CP XT inverters from SMA. Available at http://www.sma.de/en/newsroom/current-news.html
76. Musallam M, Johnson CM (2012) An efficient implementation of the rainflow counting algorithm for life consumption estimation. IEEE Trans Reliab 61(4):978–986
77. Huang H, Mawby PA (2013) A lifetime estimation technique for voltage source inverters. IEEE Trans Power Electron 28(8):4113–4119
78. Yang Y, Wang H, Blaabjerg F, Ma K (2013) Mission profile based multi-disciplinary analysis of power modules in single-phase transformerless photovoltaic inverters. In: Proceeding of EPE ECCE Europe'13, pp P.1–P.10
79. Kerekes T, Teodorescu R, Rodriguez P, Vazquez G, Aldabas E (2011) A new high-efficiency single-phase transformerless PV inverter topology. IEEE Trans Ind Electron 58(1):184–191
80. Schmidt H, Christoph S, Ketterer J (2003) Current inverter for direct/alternating currents, has direct and alternating connections with an intermediate power store, a bridge circuit, rectifier diodes and a inductive choke. German Patent DE10 221 592 A1, 4 Dec 2003
81. Sunways, Yield-oriented solar inverters with up to 98 % peak efficiency. Product category. Available at http://www.sunways.eu/en/
82. Scheuermann U (2013) Pragmatic bond wire model. ECPE workshop, 3–4 Jun 2013
83. Bryant AT, Mawby PA, Palmer PR, Santi E, Hudgins JL (2008) Exploration of power device reliability using compact device models and fast electrothermal simulation. IEEE Trans Ind Appl 44(3):894–903

Part III
Renewable Energy Systems Supporting Industrial Applications

Use of Renewable Energy Systems in Smart Cities

Alvaro Sanchez-Miralles, Christian Calvillo, Francisco Martín and José Villar

Abstract Renewable energy sources (RES) used in small-scale distributed generation systems are a promising alternative for additional energy supply toward smarter and more sustainable cities. However, their proper integration as new infrastructures of the smart city (SMCT) requires understanding the SMCT architecture and promoting changes to the existing regulation, business models, and power grid topology and operation, constituting a new challenging energy supply paradigm. This chapter addresses the use of renewable energy systems on small scale, oriented to distributed generation (DG) for households or districts, integrated in an SMCT. In this context, the main renewable energies and companion technologies are reviewed, and their profitability investigated to highlight their current economic feasibility. A simplified architecture for SMCT development is presented, consisting of three interconnected layers, the intelligence layer, the communication layer, and the infrastructure layer. The integration and impact of distributed renewable energy generation and storage technologies in this architecture is analyzed. Special attention is paid to the grid topology for their technical and efficient integration, and to the business models for facilitating their economic integration and feasibility.

1 Introduction

Over the past few years, the *smart city* (SMCT) concept has gained increasing importance both in the scientific-research community and in worldwide public administrations and leading companies. Many projects have been proposed to

A. Sanchez-Miralles (✉) · C. Calvillo · F. Martín · J. Villar
Comillas Pontifical University, Institute for Research in Technology,
Santa Cruz de Marcenado, 26, 28015 Madrid, Spain
e-mail: alvaro@upcomillas.es

M. A. Sanz-Bobi (ed.), *Use, Operation and Maintenance of Renewable Energy Systems*, Green Energy and Technology, DOI: 10.1007/978-3-319-03224-5_10,

implement smart cities, and nowadays, several of them have even been materialized in cities such as Amsterdam, Dubai, or Copenhagen [1]. In a very simple way, the SMCT should be capable of bearing or mitigating the problems generated by rapid urbanization and the growth in population. An SMCT generally refers to a city with very advanced supervision, control, and decision-making systems, which improve the management of resources under normal and emergency situations (e.g., enhance the exploitation of facilities, use energy in a more efficient manner, cope with emergencies effectively, etc.). This in turn implies the existence of a large amount of different type of sensors installed for monitoring purposes all over the city facilities, interconnected with the intelligent applications tools with a highly developed information and communications technology (ICT) infrastructure. It is important to remark, however, that the conceptualization and definition of the SMCT are still emerging.

Energy plays a leading role in this conceptualization, as most of our everyday activities and most of our environment is related to some sort of energy source (electricity, fossil fuels, heat, etc.), even when not explicitly displayed. In the new SMCT paradigm, two characteristics should be attributed to energy: it has to be "clean and sustainable," and it has to be "available for all and all the time," keeping in mind the need of economic feasibility.

Although it is not easy to classify energy management in smart cities, this work proposes 5 main intervention areas: (a) generation, (b) storage, (c) infrastructure, (d) facilities, and (e) transport (mobility). All of these areas are related, but each one contributes to energy in a different way. Generation is one of the most important intervention areas, since energy supply is at the base of any other process or activity, but storage can also provide energy and is very effective to secure its availability, so both areas must be considered together for the design of optimal technology mixes. Infrastructure refers to energy distribution and interfaces with users, while facilities and transport systems are some of the main final receptors of energy, as they need it to operate. Energy supply sustainability should rely on renewable energy sources (RES) as a mid-long-term investment for energy self-sufficiency without compromising future generations [2], being at the strategic energy plans of most countries.

While it is accepted that conventional generation plants are generally more efficient than DG profiting from economies of scale, DG is gaining interest to support grid's reliability and resiliency. The benefits and requirements of the DG have been studied widely [3]. On the one hand, DG places generation sources closer to the loads, reducing losses, and improving reliability, and on the other hand, it helps to integrate small-scale renewable energy into the system. In addition, energy storage systems (ESS), such as batteries, are an important tool to facilitate the integration of renewable sources and demand response (DR) schemes. Hence, the study of performance and degradation of storage systems should not be overlooked [4].

This chapter provides an integrating overview of RES in an SMCT on a small-scale, oriented to DG for households or districts, looking at their economic feasibility and focusing on most relevant issues for their effective integration in the SMCT architecture.

This introduction reviews the SMCT concepts and outlines the main intervention areas from the point of view of an SMCT. Section 2 reviews some of the main RES to be used in small-scale distributed generation systems in an SMCT, whose economic feasibility is analyzed in Sect. 3. Section 4 proposes a possible SMCT architecture integrating physical facilities and infrastructures, measurements, communications, and control systems and analyzes how RES can be integrated and hierarchically controlled to contribute to the grid performance. Business models for facilitating their economic integration and feasibility are also reviewed and, several regulatory changes proposed. Finally Sect. 5 concludes the chapter.

2 Renewable Energy Sources

A renewable energy should be naturally regenerated over a short timescale and derived directly from the sun (such as thermal, photochemical, and photoelectric), indirectly from the sun (such as wind, hydropower, and photosynthetic energy stored in biomass), or from other natural movements and mechanisms of the environment (such as geothermal and tidal energy) and is excluded energy resources derived from fossil fuels, waste products from fossil sources, or waste products from inorganic sources [5].

Starting with solar power, photovoltaic (PV) panels have been extensively studied and highly preferred in low-scale generation; however, they have low efficiency and are still expensive at utility scale [6].

Thermal collectors (TC) have been proved as a reliable source to heat water or other heat transfer fluid for any kind of applications [7]. TCs have affordable prices at low scale and could be implemented as concentrated solar power (CSP) plants for electricity generation [8]. In addition, the photovoltaic thermal collectors (PV/T) work as regular PV cells, but also profit from the thermal energy delivered by the sun, using it to heat water or other fluid, increasing efficiency. However, there are few PV/T commercial modules and only on a small scale [9].

Wind turbines (WT) are a mature technology with a wide variety in system sizes, producing cheap energy at utility scale. However, they are expensive and voluminous for domestic scale and wind is generally highly unpredictable [10].

Biomass is a topic of increasing importance in recent years. It is a very versatile energy source capable of providing heat, electricity, and gaseous or liquid fuels at competitive prices [11]. However, unless coming from organic urban wastes, farming of biomass crops is needed and should be done responsibly in order to be sustainable. Indeed, new European directives cap the “first generation” biofuels, made with sugars and vegetable oils found in arable crops, while favouring the “second-generation” biomass compound by woody crops, agricultural residues, and waste [12].

Geothermal energy derives from the thermal energy flux flowing from the center of the earth. It can be used for thermal only production (heated fluid to low–medium temperatures) or cogeneration of heat and power (high temperatures).

Table 1 Comparison of most common renewable energy sources

Generator	Power[b]		Dispatchable	Efficiency[c]	Common application[d]
	e	*t*			
Solar PV	X	–	No	L	Hh, B
Solar TC	–	X	No	M	Hh, B,
Solar CSP	X[a]	X	Yes	M	(D)t/(D, P)e
Solar PV/T	X	X	No	M-H	Hh, B, D
Wind power	X	–	No	M	D, P
Poly-generation	X	X	Yes	H	B, D
Biomass	X	X	Yes	M	(Hh, B, D)t/(D, P)e
Geothermal	X'	X	Yes	H	(Hh, B, D)t/(D, P)e

[a]Indirect production
[b]*e* electric, *t* thermal
[c]*L* low(<30 %), *M* moderate (≤60 %), *H* high (>60 %)
[d]*Hh* household, *B* building, *D* district, *P* power plant

Geothermal electricity is very cheap when the proper ground conditions are met; nonetheless, many cities do not have those soil characteristics [13].

Finally, although strictly speaking not renewable, poly-generation or multi-generation appeared as an effort to use fossil fuels more efficiently: they can deliver different kinds of energy vectors from a single source of fuel (usually natural gas), reducing CO_2 emissions by this increased overall efficiency [14]. However, the disadvantage is the elevated cost on a very small scale [15].

Table 1 summarizes the main features and advantages of the different renewable energy sources. A more detailed review can be found in Calvillo et al. [16].

3 Profitability of Renewable Resources

Many RES can be potentially implemented in smart cities. However, important factors such as geo position characteristics, demand profiles, energy tariffs, and regulation need to be taken into account in order to select the optimal technology mix. Indeed, an adequate selection of technologies and the optimal scaling of the implemented systems are crucial for the economic feasibility of DG projects. This section shows a profitability analysis of small-scale renewable resources implementation, showing that under current pricing scenarios, renewable resources are feasible for a DG profitable expansion.

Given the great quantity of renewable sources, five very common technologies have been selected for the economic analysis of DG expansion and have been compared with the conventional case of no additional renewable generation installed. The selected costs and main characteristics of the considered technologies are provided in Table 2.

In order to develop a fair comparison among these technologies, a linear optimization problem, similar to the one proposed in Calvillo et al. [17], has been

Table 2 Costs and characteristics of the reviewed technologies

Generation technology	Installed cost (USD/W)	O&M cost (USD/kW/year)	Life span (years)	Energy losses (%)
PV panels	3.0	63	20	24
Thermal C	1.8	42	20	15
Heat pump	3.1	140	20	15
Batteries	0.5		8	10

Table 3 Considered energy tariffs and timetables

	Peak (18–22 h)	Off-peak (8–18 h)	Contracted power
Electricity tariff	0.2156 (USD/kWh)	0.0733 (USD/kWh)	27.9021 (USD/kW/year)
Natural gas tariff	0.0743 (USD/kWh)		0.3881 (USD/kW/day)

implemented to find the optimal scaling and technology mix. The optimization problem minimizes the total cost of the energetic needs, including the cost of investing and operating new facilities, and the cost of buying thermal and electric energy from the utility grid, providing the optimal technology investments. Operation costs are computed in an hourly base, considering the geographical characteristics of the city studied (in this case Madrid, Spain) and hourly gas and electricity tariffs. In this case, a flat tariff for natural gas and a "time-of-use" electricity tariff with two periods (see Table 3) have been selected. Hourly detail means that the model also provides the optimal hourly operation scheduling as a result.

The case study for the economic analysis considers a representative Spanish household with a yearly consumption of 3,100 kWh of electric energy and 12,400 kWh of thermal energy. Moreover, the average residential electricity demand curves and demand evolution of Spain REE [18] are also considered in the model, as shown in Fig. 1. Similarly, thermal requirements vary greatly along the year. In this study, thermal demand is considered to follow the same demand evolution illustrated in Fig. 1b. However, thermal generation systems very often include water tanks as thermal storage, decoupling to some extent the hourly relation of generation and energy usage. Therefore, hourly thermal demand patterns have not been considered.

For this economic feasibility analysis, a total period of 20 years has been considered, with an annual energy price increment rate of 5 % and a discount rate of 3 %.

The following combinations of the main five technologies have been selected for this analysis:

1. Nonrenewable DG installed (base case: energy bought from the utility grid)
2. Solar thermal collector (TC)
3. Air source heat pump (HP)
4. Air source HP with 30 % of total production in peak hours
5. PVs + Batteries
6. PV + Batteries + TC
7. PV + Batteries + HP

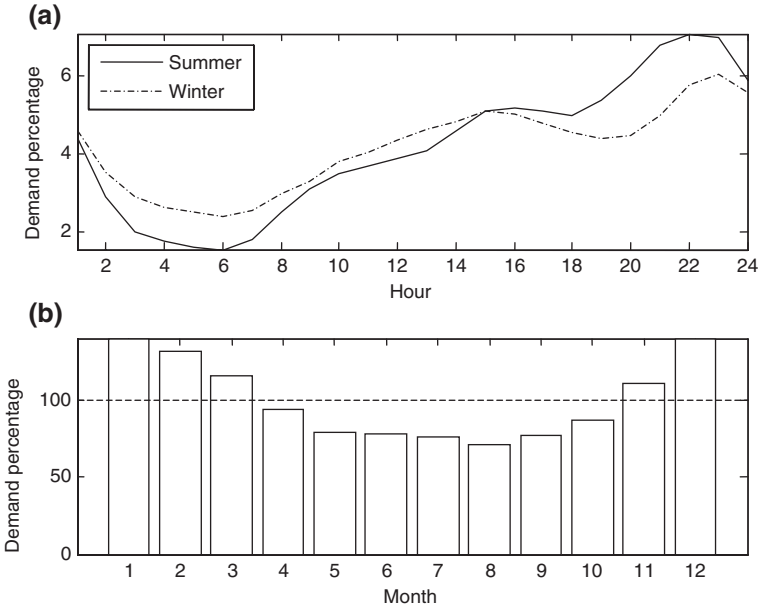

Fig. 1 Demand *curves* and annual evolution for residential sector in Spain. **a** Typical electric demand curves. **b** Annual demand evolution

8. PV + Batteries + HP with 30 % of total production in peak hours
9. PV + Batteries + HP with 30 % production in peak hours and battery cost incentives.

Case 1 considers only current conventional large-scale plants generation from the grid to supply the electric demand, and thermal energy is generated from a conventional gas boiler. It is used for comparison purposes.

In Cases 2 and 3, only the thermal demand is meet. While Case 2 does not affect the original electric demand, Case 3 does it since HP needs electricity for supplying thermal power.

Case 4 corresponds to a more realistic domestic production. A constraint to produce part of the total thermal energy requirement during the afternoon/evening (13–20 h) with higher electricity costs has been added to end up with a worse but more realistic comparison case.

In Case 6, PV is combined with batteries to address the electrical demand, getting the most out of the difference in the hourly discrimination tariff. Results of the optimization model developed show, see Fig. 2, how in the first hours of a typical day, when electricity price is low and there is no PV production, energy is bought from the grid to meet the demand and charge the batteries. When PV production increases, energy is no longer bought from the grid, and when PV generation diminishes and electricity price goes up, batteries supply their stored energy, minimizing the amount of energy bought at high price.

Cases 6 and 7 combine both electric and thermal generation. For the electric part, they include a combination of PV and batteries, while for the thermal side,

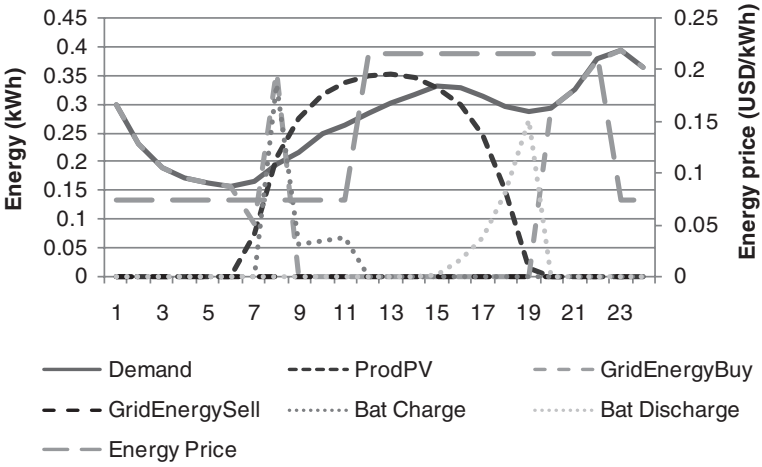

Fig. 2 PV energy production + battery management for a typical summer day

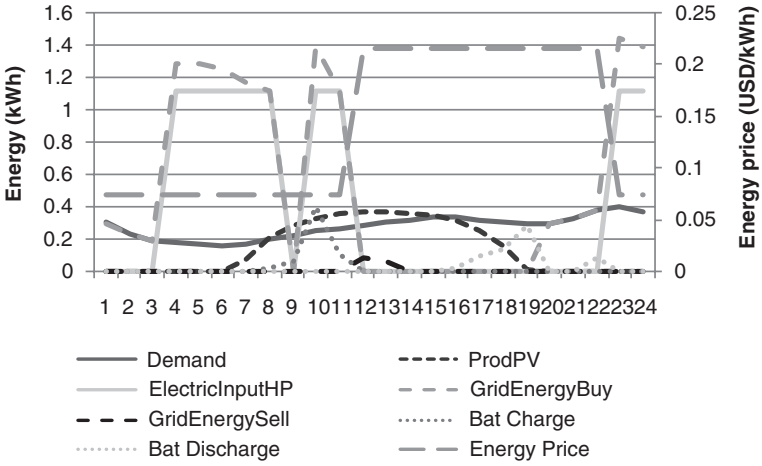

Fig. 3 PV production + battery + heat pump management for a typical summer day

they implement TC and HP, respectively. It is important to remark that the coefficient of performance (COP) selected is equal to 2.5 for all the cases including HP. An example of operation of Case 7 is illustrated in Fig. 3. It can be seen (as occurred in Case 5) how electricity from the grid is again bought mostly a low-price hour to charge batteries. Similarly, HP is also operated at low-price hours, to avoid consuming more expensive electricity at peak hours.

Case 8 is similar to Case 7 but tries to represent a more realistic operation. Indeed, even though thermal storage is considered, since it is unlikely that this storage has neither the capacity nor the performance to keep all the thermal energy produced in the early morning for later use, a constraint is added to force some thermal generation at peak hours (as in Case 4). Results are shown in Fig. 4.

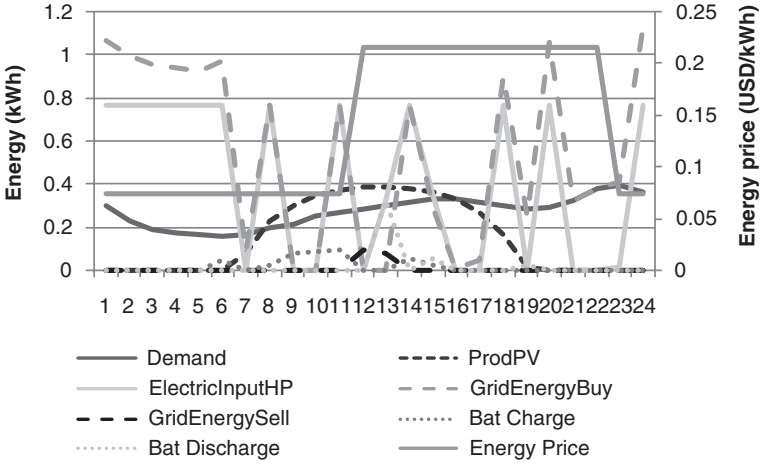

Fig. 4 PV production + battery + heat pump (30 % production in peak hours)

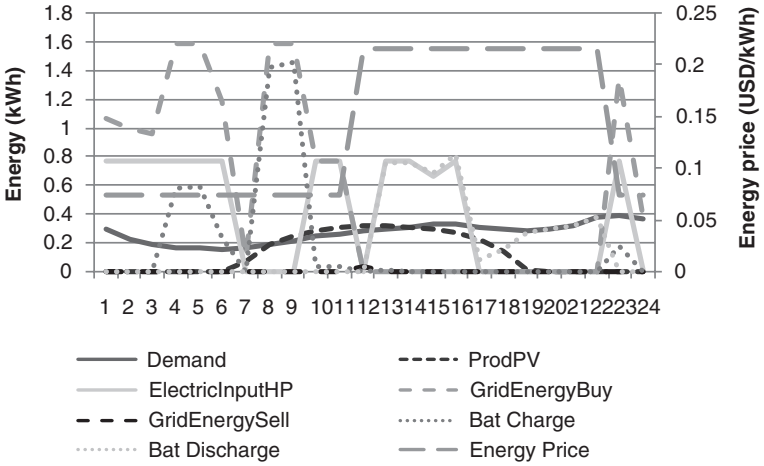

Fig. 5 PV production + battery + heat pump (30 % prod. in peak hours, 30 % battery discount)

It can be seen that the complexity of operation increases, although battery usage barely changes. This means that no additional cheap energy is stored in batteries to be used later instead of more expensive electricity. The former behavior is due to the high investment cost of batteries in current renewable DG systems, such as the hereby presented.

However, considering that economic incentives for renewable energies and storage systems are present in many countries, such scenario should be considered in this study, as it is for Case 9. If a 30 % discount is applied to the battery cost (0.35 instead of 0.50 USD/Wh), results, see Fig. 5, show a very different behavior.

Table 4 Economic feasibility analysis results

Scenario	PV (kW)	Batteries (kW)	Thermal (kW)	Total energy costs (USD)	Savings (%)
No renewable sources	0	0	0	33,819	0
TC	0	0	3.4392	30,681	9.28
Air source HP (COP = 2.5)	0	0	1.092	27,100	19.87
Air source HP (30 %)	0	0	0.7644	29,673	12.26
PV + batteries	0.6236	0.5198	0	32,635	3.50
PV + batteries + TC	0.6453	0.5654	3.4392	29,480	12.83
PV + batteries + HP	0.6474	0.5698	1.092	25,897	23.42
PV + batteries + HP (30 %)	0.6748	0.3255	0.7644	28,378	16.09
PV + batteries + HP (30 %) battery cost = 0.35 USD/Wh	0.5693	4.8451	0.7644	27,134	19.77

Indeed, battery capacity increases significantly, meeting most of the electric demand for peak hours with the stored energy.

Table 4 summarizes the optimal installed capacities and economic results obtained for each of the cases analyzed. It can be seen that the larger saving occurs when thermal generation technologies are also considered, due to the high energetic consumption of the base Case 1. Moreover, the air source HP presents about double the benefits in comparison with the thermal collector systems by taking advantage of the electricity off-peak price. While the combination of PV and batteries provides fewer saving, these increase slightly with a higher electric energy consumption, as for the case with the air source HP.

This analysis reveals that the technological combinations studied, including PV with batteries, are already profitable alternatives for supplying energy on a small scale, and, therefore, as efficiency and cost improvements are surely expected in the next future, RES have a very promising future and should be seriously considered as feasible alternatives for energy supply.

It is important to remark that, despite the apparent economic feasibility of the distributed renewable systems, many technical and regulatory challenges need to be addressed to successfully implement these systems. The next section reviews the main issues to be resolved and proposes an integration architecture for distributed RES systems.

4 Integration of Renewable Sources in the Smart City Architecture

Sections 2 and 3 have revealed that renewable energy sources, properly combined and managed, are a promising alternative for DG expansion and energy supply in the context of SMTCs. However, its proper integration as new SMCTs infrastructures requires changes to the existing regulation, business models, and power grid topology and operation, constituting a new challenging energy supply paradigm.

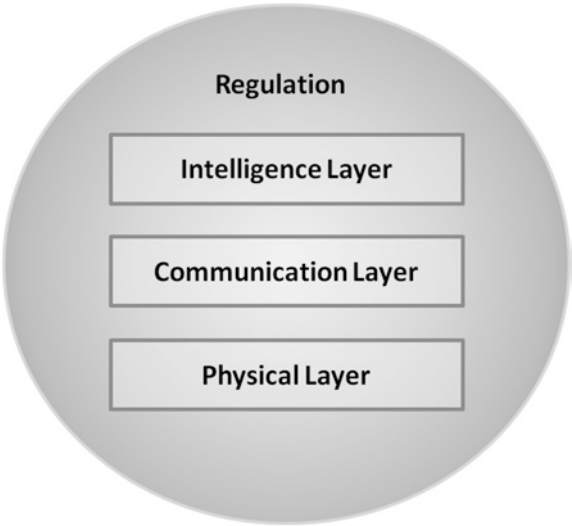

Fig. 6 Implementation model of SMCTs

This section proposes an implementation architecture for the development of SMCTs and analyzes how DG based on RES can be integrated and interacted with the proposed architecture. In addition, a business model for this architecture is proposed in this chapter.

The architecture for the development of SMCTs is based on three main layers and is shown in Fig. 6. Each layer refers to one of the following functionalities: intelligence, communications, and infrastructure with sensors and actuators. All of these layers should be built over an appropriate regulatory framework.

The lower-level layer is the physical layer and is composed by the physical elements needed in an SMCT. It must be able to support any kind of sensors and actuators distributed all over the city. Sensors are essential to measure the environment and detect the principal events that occur in the city, such as the behavior of basic services such as gas, cooling, irrigation, traffic, sewerage management, since they provide the information needed for decision making and taking intelligent actions. Actuators in turn are the way for the intelligence systems to influence on the city behavior and its main services, and these devices should also be spread over the SMCT. Actuators should accept local control from local control systems, or remote control from the centralized intelligent system.

The communication layer connects the physical and intelligence layers, giving support to the exchange of information between the sensors and actuators, located anywhere in the city, and the intelligence system located at the SMCT control center. It is made of any kind of ICTs, cabled or wireless, and is a critical component of the SMCT since all the rest of layers rely on its performance.

The last layer is the intelligence layer. It is made up of all the intelligent systems of the SMCT designed to process data from the sensor's measurements, make the appropriate decisions, and supply the corresponding outputs to the actuators, to optimize the performance of the SMCT main services. It uses the communication layer to establish connection with the distributed sensors and actuators.

It is important to notice that this implementation architecture does not specify the kind of intelligence system to choose. Indeed, for very simple problems, local intelligence approaches may be enough, rewarding the simplicity of the system, while for more complex problems, global intelligence systems, or hierarchical approaches may perform significantly better.

Finally, as Fig. 6 shows, the layer's diagram is immersed in the existing regulation of the country to which the city belongs to. This means that any implementation aspect of any layer cannot be decided without considering the existing laws and regulation of the country in which the SMCT is to be built. In turn, in most cases, proper modifications to the existing regulations may be advisable to encourage and facilitate a faster and easier implementation of this new SMCT paradigm to improve the quality and efficiency of the services provided to the citizens.

In following subsections, this chapter addresses the integration of RES on each of the three layers of the proposed implementation architecture of the SMCTs.

4.1 Integration with the Physical Layer (The Power System)

This layer is composed of the physical elements needed by a smart energy system. A smart energy system must provide the households with distribution grid connection and intelligent local and remote control, in order to optimize electricity consumption and provide peak shaving and regulating services to the grid.

It consists, among others, of intelligent or smart meters (SM) with appliance control capabilities, power electronics for renewables integration, power supply and regulation, and information and communication technologies for measurements gathering and decision making, to enhance the efficient use of energy and RES integration and control.

A smart grid is the result of this combination of the power distribution grid and the communication and information infrastructure. A two way communication system between the clients and the grids must be established by installing an advanced metering infrastructure at the distribution level. Indeed, optimal use of electric and thermal energy requires continuous metering of electricity and heat.

Heat meters are known as smart thermostats that are in charge of controlling the heating, ventilation and cooling systems which are the largest source of residential energy consumption. These systems will have presence and temperature sensors in order to operate more efficiently, saving energy when heat production is not needed.

Electricity meters, known as SM in the context of smart grids, are in charge of collecting the electricity consumption of the houses smart appliances, supplying it to the intelligence layer, and controlling their operation in response to the intelligence layer decisions to optimize energy usage. It should be noted that smart appliances are those designed to be controlled or operated by the SM. In addition, the use of SM involve a better understanding of the bills by the consumers, by supplying real-time information about prices and consumption.

This advanced metering infrastructure is also present at higher levels, and not only at households. For example, measuring voltage and currents of the distribution

lines is a way of controlling their correct operation, avoiding possible blackouts by adequately balancing production and demand.

When small-scale RES are used, power comes from a mix of DG or storage technologies combined with power from the grid. In order to produce electrical power with the frequency and amplitude needed by the appliances, power electronic devices are required. For example, the connection of solar arrays or electric batteries (from electric vehicles or as standalone ESS) requires two-stage converters, made up of a DC-DC converter stage and a single- or three-phase voltage source inverter stage for interfacing with the utility grid. However, since most appliances use DC internally, they need to implement AC/DC converters to transform standard AC supply into DC power. For this reason, some works (see for example Boroyevich et al. [19]) propose the use of household DC-nanogrids for more direct connection of DC appliances and generation and storage systems such as solar panels or electric batteries.

In general, using DC instead of AC has many advantages such as:

- Fewer power converters needed, reducing converter losses.
- DC currents do not have neither skin effects (allowing to use less width of wire) nor reactive power, avoiding the use of power factor corrector devices.
- No harmonic problems.
- No changes in the DC bus voltage after a blackout or voltage sag due to the stored energy of the capacitor and the control of the AC/DC converter.
- Current existing wires could still be used if they support the required DC voltage levels.

However, DC household supply protection systems are more complex since DC currents do not have zero-crossing point and the need of high voltages due to the lack of current if the levels of DC are low such as 24 or 48 V which are secure voltages, but they need higher currents for the same power in AC. So the net benefits of using DC in households are still being discussed.

Some works like Adda et al. [20], Ray and Mishra [21], propose converters able to provide both AC and DC currents at the same time. The main advantage is that a single converter can supply both DC and AC loads from a single DC input, the AC output can be lower or higher than the DC source voltage, it shows better electromagnetic noise immunity than the voltage source inverter, and it does not need dead-time circuit because it allows shoot-through (both switches in one leg are ON) in the inverter legs, something that in traditional VSI causes damages due to the short-circuit current.

These converters, sensors, and actuators deployed all over the city can be grouped in different levels forming a hierarchical structure. This hierarchical approach goes from households up to the distribution networks. Picogrids, nanogrids, and microgrids are the electricity grids corresponding to households, buildings, and neighborhoods, respectively, and are at the end connected to the power distribution grid, as shown in Fig. 7 (where VSC stands for “back-to-back voltage source converter,” ECU for “electronic control unit,” and PV for “photovoltaic panels”).

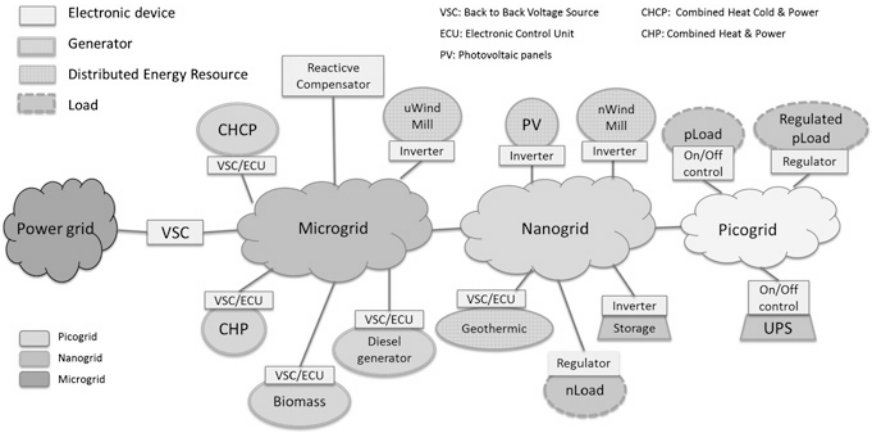

Fig. 7 Vision of the smart electric power grids

Picogrids control all the household manageable devices connected as picoloads to the network, including low-capacity local storage systems, such as uninterruptable power systems or UPS. This level does not include generation systems.

Nanogrids are intended to control nano-generation (nano wind turbines and PV panels), and manageable nano-loads and the picogrids themselves. Nanogrids may also include energy storage, for example batteries from the electric vehicles parked in a building.

At the third level in the grid hierarchy is the microgrid. Microgrids control nanogrids and microgeneration (micro wind turbines, biomass boilers, combined heating, cooling and power-CHCP) and also support distributed energy management with a market-based approach when operated in Island mode. Microgrids are directly connected to the electricity distribution power network, at least at one connection point. The connection and energy flows to and from the distribution power network must also be controlled to permit either energy supply or consumption, depending on the microgrid and distribution grid energy statuses at each moment. The smart power grid can be decomposed in several microgrids with their own controls, with small-scale generation sources close to the demand nodes. Microgrids in turn can also be interconnected through the power distribution network.

This distributed and hierarchical approach has the following advantages over the centralized approaches:

- Better integration of local DG and storage, optimizing CHP, and CHCP.
- Provision of different voltages, including DC, with higher supply reliability and quality.
- Microgrid isolated operation easier to implement.
- Control mechanisms easier to develop.
- Less bandwidth required for data exchanged.

- Hierarchical approaches are more deployable, flexible, cost-effective, and functional.
- Picogrids facilitate a gradual, cheaper, and faster grid development than the smart grid, although they can coexist. Picogrids, requiring lower investments, can be deployed in the households at the first stages and be integrated latter on into the emerging nanogrids, providing more immediate benefits.

4.2 Communications Layer

Integrating RES and DG into the power network implies changes in the way energy generation must be scheduled. Indeed, RES are hard to control, and balancing generation and demand requires knowing almost instantaneously consumption and generation. For this reason, the communication layer connects the physical layer with the intelligence layer. The intelligence layer needs to gather consumptions and other relevant data (like production of the DG and state of charge of energy storages, or existing bids for energy trading) from the physical layer.

In addition, real-time information has to be transmitted through the system. Firstly, consumers can consume and produce energy, so the directions of the power flows have to be known by the intelligence layer in order to correctly operate the protection systems if a fault or a blackout happens. Secondly, the intelligent layer needs measurements for applying its smart capabilities such as peak demand shaving to improve the efficiency and stability of the power supply. Finally, to provide the adequate economic signals to consumers, market prices have to be shown in their SM, so the intelligence layer has to provide this information along with DR programs information.

The following subsection reviews the architecture proposed for the communication layer for picogrids, nanogrids and milligrids, with special emphasis on the most common protocols.

4.2.1 Communication Area Networks

The communication structure can be defined in parallel with the physical layer structure.

Inside a picogrid, the home area network (HAN) is in charge of the communication with the appliances and other devices in the house. At the next level, inside the nanogrid, a building area network (BAN) for residential or office buildings, or an industrial area network (IAN) for factories, is responsible of the communication among the different picogrids, nano-energy storages, and nano-generation sources connected to the nanogrid [22].

When several buildings are grouped together, or when they are in a neighborhood forming a microgrid, the communications among the different nanogrids and with the microgeneration are performed through the neighborhood area network (NAN) [23].

The communication with the different elements of the power grid such as the market, transmission system operator (TSO), and the distribution system operator (DSO) is performed through a wide area network (WAN), where information about consumption of each microgrid, market prices, operation modes (islanded or grid-connected), and other operation data is exchanged [24].

The selected protocol used for the WAN should be able of transmit data along big distances with high data rates. Most current communications drivers used for these networks are LTE [25], cellular communications (EDGE, GPRS, etc.) [26], WiMAX [26], or optical fiber [24].

In the NAN, medium distances are required. Nowadays, most common communications drivers are Wi-fi or cellular communications [22, 26].

In the lowest levels of the area networks, HANs and BANs require low data rates and distances lower than 100 m. In these systems, the communications must support home energy management systems (HEMS) which include graphical user interfaces where the consumers can see their consumption, and SCADA systems to store the consumption information for future use. In these systems, most used protocols are ZigBee [27], ZigBee smart energy protocol (SEP) [28], 6LowPAN [22], or PLC [23].

In particular, 6LowPAN and the ZigBee SEP are two protocols based in the standard IEEE 802.15.4 but incorporate IP protocol in their network layer in order to support TCP/IP, one of the most extended protocols. Other less common protocols with similar characteristics are mDNS or ROLL [29, 30].

Table 5 summarizes the main uses that some common protocols could have in the coming smart grids.

The communications with advanced metering infrastructure systems allow to acquire data from the networks such as power quality measures, DG production, and power consumption of household appliances. Smart grids need also know the current state of the power grid over a wide area to predict the evolution of the power grid state in order to planning the operation of different units with the final objective of balancing the consumption with the demand, this is called, wide area situational awareness (WASA).

Similarly, the distribution management system (DMS) of the DSO need to know the behavior of the prosumers (final users who can produce energy) and the state of DG and storages in order to report abnormalities in the system and to balance the generation with the demand. Also, in substation automation systems, the communications play an important role to avoid power disturbances and outages.

Multiple protocols and standards can be used for the same functions, as shown in Table 5. In addition, new standards are being developed with the similar purposes. For example, ISA 100 Committee is proposing new standards for implementing wireless systems in the automation and control environment [31]. For this reason, the gateways among the different area networks have to be compatible with different standards and protocols to allow intercommunication among them.

The interoperability among different standards and various applications (HEMS, SM, etc.) is essential in order to share the smart grid information about them. In the customer level, the open platform OGEMA (Open Gateway Energy Management

Table 5 Main uses of different standards and protocols [22, 24, 50]

		Technologies										
		Wired			Wireless							
		PLC	Optical fibers	DSL	IEC 61850	WPAN 802,15 WPAN + IPv6 (6LowPAN)	WPAN 802,15 ZigBee and ZigBee SEP (IEEE 802.15.4)	Wi-fi (IEEE 802.11)	WiMAX (IEEE 802.16)	GSM/GPRS/ EDGE	3G/4G (IEEE 802.21)	Satellite
Applications	HEMS	✓				✓	✓	✓				
	Advanced metering infrastructure (AMI)	✓	✓	✓			✓[a]	✓	✓[b]	✓[b]	✓[b]	✓[b]
	Demand response management		✓	✓			✓[a]		✓[b]	✓[b]	✓[b]	
	Substation and distribution automation and protection	✓			✓[c]			✓				
	Outage management								✓			
	Electric vehicle						✓	✓			✓	
	Wide area situational awareness (WASA)		✓		✓				✓	✓		✓
	Distribution network management				✓		✓		✓		✓	
	Asset and meter management											
	Distributed energy resources and storage				✓			✓			✓	

[a]for appliances, [b]for backhaul, [c]main objective

Alliance) is an example of this idea OGEMA [32]. OGEMA has been created by Fraunhofer IWES for ensuring the device interoperability and the use of different protocols in the same software. This platform based on Java and OSGi (Open Services Gateways Initiative) is being used in projects such as the Model City of Mannheim, Germany [33] where the iteration with the clients uses OGEMA apps such as consumption data, price-based control of loads, and displays [32].

4.3 Intelligence Layer

This layer consists of all the decision-making and control systems, local or centralized, that process the information coming from the sensors and meters located on the different components of the physical layer of the SMCT energy system (loads, DG, picogrids, nanogrids, microgrids, etc.), and decides the right control actions to minimize the cost of the consumed energy and to maximize the profit of the generated energy. It uses the communication layer to connect with sensors, metering systems, and actuators located in the physical layer. Each grid has its own objectives:

- The picogrid tries to perform load levelling and load shifting for minimizing the cost of the consumed energy. Taking into account the end user's preferences and price signals the picogrid tries to manage its loads optimally. Optimal solutions consider minimizing the cost and maximizing the achievement of end user's preferences, which are much related with comfort levels.
- The main goals of the nanogrid are load levelling, load shifting, obtaining the maximum of the renewable resources, and reducing losses. Taking into account the picogrid's requirements and price signals, the nanogrid tries to manage the generation and the storage optimally. Optimal solutions have to do with maximizing the profit.
- Microgrids have two different running modes: isolated or connected to the power grid. When isolated, the microgrid tries to achieve a zero-energy balance with a local-market-based approach. When connected to the power grid, the microgrid tries to optimize the profit of all of the prosumers, aggregating their behaviors to interact with the wholesale markets.

Microgrids energy management systems can be organized under centralized or decentralized approaches. While centralized approaches profit from economies of scale, decentralized approaches seem to be more flexible and easier to implement. In addition, management and control systems are more and more compliant with multi-agent system (MAS) techniques, leading to the multi-agent system control technique. A MAS is a system where entities called agents cooperate one with another to reach a certain objective. The agents have the ability to perceive aspects of their environment and to take decisions in order to reach their goal. In addition, some agents may have social abilities that allow their mutual interaction. Thus, an intelligent agent has proactivity, reactivity, and social ability, so that it can act alone or with other agents [34]. Next subsections review these concepts in more detail.

4.3.1 Centralized Versus Decentralized Energy Management Systems

The control objectives of a microgrid can be reached with either centralized or decentralized control systems. In a centralized control, the decisions are taken by a central control system after gathering all the information in a centralized database, which is analyzed as a whole. In a decentralized control, the decisions are made locally in the distributed control systems without seeing the rest of the systems, which exchange information about their decisions in order to reach an agreement about their behavior as a whole.

The main differences between the two methods are explained for example in Colson and Nehrir [35], Su and Wang [36] and are summarized in Table 6.

The centralized control has some advantages such as a more economic implementation (profiting from lesser redundancies and economies of scale in costs of installation and operation for a basic energy management system) and simplified communication protocols. In addition, decisions are made considering the system as a whole, leading to higher speeds and more optimized decisions, but decision-making tools are much more complex. In addition, they are very dependent on communications (and therefore on the communication layer performance) because all the information has to reach the central controller in order to make the decisions. They also imply much higher complexity to implement plug-and-play facilities, one of the key elements in the smart grids concepts, because new elements connected to the network must be notified to the central controller, which has to include them into its decision-making process. There are some test beds for centralized control like in Kythnos Island in Greece or DEMOTEC in Kassel, Germany [37].

In decentralized control approaches, the prosumers have intelligence and communication capabilities that allow them to control their RES or theirs loads, with two main advantages. The first one is the less bandwidth requirements for the communication layer, because most communications take place among the local agents of neighborhoods. The second one is the system robustness, because if the central controller fails, the rest of the systems can still continue working due to its local control autonomy. Furthermore, they are based on asynchronous operations which allow them to face unanticipated events and have slower times of local decision making. However, this could imply more time for global decisions until the local agents reach a consensus. In addition, controllers and communication costs are higher because the existing communication networks do not support to exchange data directly between consumers which produce an expensive initial upgrading cost. There are some examples of decentralized control that can be found in Mannheim Wallstadt, Germany, by More microgrids project and in Groningen, Netherlands, by KEMA [37].

4.3.2 Using MAS in the Control of a Microgrid

MAS can be implemented to balance demand and supply in distribution networks in order to maximize the production of DG, minimizing the cost of the purchases

Table 6 Centralized versus decentralized control

	Characteristics	Advantages	Disadvantages
Centralized control	• Local agents that depend on a central controller for decision making	• Operational knowledge of the whole system to make decisions	• Requires high data interchanges
		• Central Controller that allows an economic implementation and is easier to maintain	• Lack of plug-and-play capability
		• Communications and controls actions occur synchronously	• Single point of failure • Difficult to expand
Distributed control	• Local agents make decisions collectively without a central controller	• Minimum communications requirements	• Need communications to operate in a coordinated way
		• Plug-and-play capabilities, so network expansion is easier	• Lower control of the entire system
		• System survivability. Increased reliability and robustness	• Need more time to reach consensus. Lack of prioritization
		• Distributed decision makers, more suitable for complex systems	

of energy from the grid and maximizing exports to the grid, according to the market prices and operation costs. The design of MAS consists in solving larger problems using agents that specialize on partial problems, combining individual solutions to obtain a coherent whole.

Due to the hierarchical structure of the power grid, centralized and distributed control approaches have to cope with three hierarchical levels of the grid using different agents:

- DSO and market operator (MO)—power grid
- Microgrid operator (MGO) and prosumer aggregator (PA) (see Sect. 4.4)—microgrid
- Prosumers and final consumers (see Sect. 4.4)—nanogrid and picogrid, respectively.

The transition to smart energy systems implies the transformation of traditional passive consumers into active prosumers, seeking to profit from the new energy paradigm, and participating into the security of supply be means of agreements with the PA from the previous level of the grid hierarchy.

PAs are in charge of managing prosumers that are responsible for controlling their renewable energy sources, storages, and controllable loads of their houses with HEMS, and also of optimizing power exchanges with the power grid, maximizing local production based on market prices and security constraints using their own energy management system. In centralized control systems, prosumers can only execute orders from the PA when the microgrid is connected to the power grid,

while in decentralized approaches, each prosumer using their energy management systems makes its own local decisions on how to consume and supply to the grid.

Finally, at the higher level of the grid hierarchy is the DSO, responsible among other tasks of the managing and controlling of the distribution network, and of interconnecting the microgrids connected to the distribution grid. In addition, there can be one or more MOs responsible of the wholesale market. The MGO in a centralized control is in charge of optimizing the production and consumption inside the microgrid with the market prices and data from the PA sending back the results to them using their management systems. However, in a decentralized control, the MGO continues exchanging market prices and it take part in cases of contingencies or failures inside the microgrid.

While the energy management systems and the control systems of the prosumers are in charge of collecting the local information of their energy storages and RES and controlling the voltage and the frequency of the microgrid, the PA is in charge of maximizing the microgrid value using market prices and requests of the MO and DSO. Here, there are two possible strategies for the PA. The former consists in satisfying the local energy demand using its local production without exporting power to the upstream distribution grid, behavior known as "good citizen" [38]. In the latter, the behavior is known as "ideal citizen" [38], and the PA takes part in the market between microgrids buying and selling power in order to maximize their revenues. The PA works together with the MGO in order to operate the overall distribution system in an economical and secure manner.

In Sect. 4.4, new business models using these agents are proposed. The centralized MAS approach corresponds to a management model based on aggregators, where the prosumers cannot operate independently but represented by a PA. The decentralized MAS corresponds to a decentralized management model, where prosumers can operate by themselves with the grid without the need of intermediate entities.

Other approaches in hierarchical control for microgrids could be based on the use of decentralized multi-agent systems where the agents could negotiate energy exchanges among picogrids, nanogrids, and microgrids.

4.3.3 Using MAS in the Nanogrid Level

The concept of MAS (using agents to solve smaller problems in order to reach a global common objective) can be implemented in a lower level like the nanogrid. Energy management systems using agents for smart buildings have been proposed in Smitha and Chacko [39], Wang et al. [40], Zhao et al. [41].

Taking into account that a smart building is integrated into the grid and it is made up of distributed renewable energy sources, energy storages, sensors, and actuators, the management for the building control and automation is focused on energy use and comfort factors. Different structures using three or four agents can be used for this purpose.

References [39, 40] propose centralized MAS with four levels of agents. A switch agent is responsible for connecting or disconnecting the building to/from

the grid. Another agent called Central Coordinator has the objective of maximizing the overall comfort and minimizing the power consumption required, using genetic algorithms or particle swarm optimization. The third level of agents is known as local control agents, and each one controls a comfort factor (temperature, lighting, CO_2 quality, etc.). The last agents are the load agents responsible of controlling all the appliances which are not connected with the comfort factors.

However, Zhao et al. [41] proposes a semi-centralized decision-making system with three agents and a central system (in charge of the optimization) for controlling a commercial building. The agents are in charge of the electric, heating, and cooling system, respectively. The electric agent receives the energy prices and DR information and sends the recovered-heat and electricity available to the other agents. All of them send their local optimized data to the central system that minimize the whole energy cost of the building.

4.4 A New Business Model

A business model is a logical and organizational framework by which the opportunity to address a need is identified and exploited to deliver value to customers. A business model is defined as the set of the involved agents and the business relationships among them.

With the introduction of the DG, new agents, management systems, and equipment are appearing. Retailers will not only have the role of trading energy but also of providing new type of services to their customers (such as energy management, aggregation, etc.), while consumers will transform into prosumers due their new generating role. These are some of the main new agents of the coming business:

- *Prosumers*: they are consumers who adopt a more participative role in the system by, not only consuming energy in more efficient ways, but also generating, or even interacting with DSOs and aggregators. Consumers will progressively become prosumers, to profit from the new energy paradigm, optimizing their consumption and services provided to the grid.
- *Prosumers Aggregator (PA)*: these are agents who act on behalf of their represented prosumers, to interact as a unit at the microgrid level or the power grid level. They trade energy in energy markets, sell services in ancillary service markets, and provide load-levelling services to DSOs and/or MGOs. By grouping prosumers, they profit from the benefit of larger sizes and market power, and deviation compensations among prosumers energy and ancillary services schedules compromised in wholesale markets.
- *MGO*: these agents operate the microgrids. For that purpose, a market-based approach can be created at the microgrid level to provide the economic framework for managing the energy flows and to maintain the grid stability, in particular for Island operation.

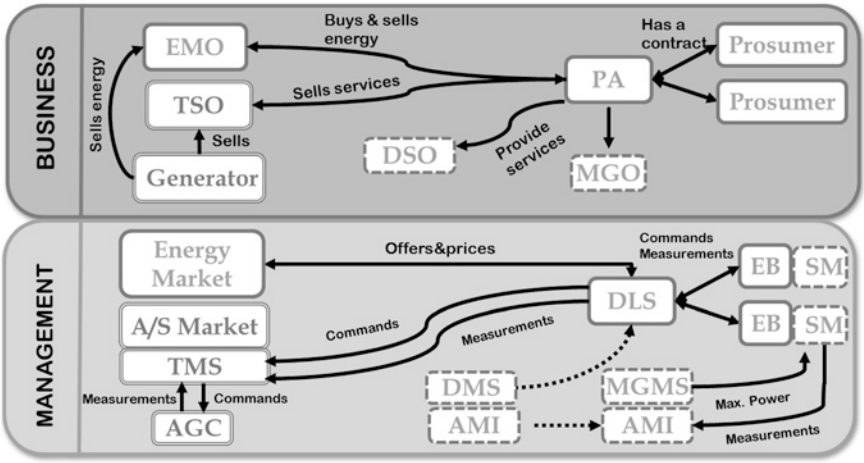

Fig. 8 New business model vision with the introduction of DG

Figure 8 represents these agents and the main relationships among them.

Two layers (see Fig. 8) can be identified in this new business model, the business layer and the management layer.

In the *business layer*, the TSO is the agent that owns and operates the transmission grid. The two main activities of the generators are selling energy at the energy market operated by the energy market operator (EMO), and selling ancillary services to the TSO. DSOs own and operate the distribution grid, while MGOs operate the microgrid. Prosumers consume and supply (thanks to their own DG and ESS) electricity and can be represented by PAs. In this case, PAs sell or buy electricity to prosumers and also aggregate the behavior of their represented prosumers located in one or several microgrids. In addition, PAs could sell ancillary services to the TSO and could also sell distribution energy services to DSOs or MGO to optimize their networks. Prosumers pay their PAs for the net services provided, while PAs supply them with the required energy and pay regulated tariffs to the DSOs for the grid services and other system-regulated costs. A key aspect of this context is that the distribution activity is unbundled from supply.

In the *management layer*, two different types of markets are considered: the energy market and the ancillary services market (AS Market). In the energy market PAs typically buy or sell energy while generators sell energy. The energy price and energy exchanges are set on the energy market. In the ancillary services market, generators and PAs sell ancillary services to the TSO for contributing to the system security. Agents have to implement different management systems to aid in their decision-making process:

- DSOs need, among other systems, a DMS, which controls the distribution grid operation.
- MGOs have a microgrid management system (MGMS) to operate the grid connected to the power grid or in Island mode. This MGMS communicates with SM owned by the MGO which meter hourly and peak energy consumptions. They include bidirectional communications for sending periodical measurements as well as receiving power commands in real time.
- The TSO needs a transmission management system (TMS) to manage the transmission power network.
- Generators have an automatic gain control (AGC) connected to their generation units, to obey the grid stabilizing settings provided by the TSO.
- PAs own the energy boxes (EB) that manages the bidirectional energy flow of the prosumers and the distributed local system (DLS). In addition, EB and SM must have wired communication to send the power references from the SM to the EB. The DLS is in charge of controlling each EB individually and aiding in the decision making for participating in the markets. To this end, PAs could have stochastic models of their prosumers in order to optimize their profits as a unique stochastic entity.

Given this business model, there are different ways to implement it:

- *Island model*: This model is driven by the idea that prosumers want to be self-sufficient and not dependent on the utilities, being MGO responsible of the microgrid stability. In this model, any prosumer could have renewables sources and storage systems. The stability of the grid is guaranteed thanks to a power market, operated by the MGO that regulates power exchanges among prosumers.
- *Aggregator model*: In this model, the PA manages the resources of the prosumers through to the EB installed at the prosumer's side. Prosumers obtain profit because PAs allocate part of their own profit to the prosumers.
- *Prosumers model*: PA creates a dynamic price structure for the energy exchange with its prosumers, typically consisting of three or four price levels (low, normal, high, extreme), based on the market prices for energy. Prosumers get information day-ahead, and the EB manage the resources of its prosumer to optimize the profit.

4.5 Regulatory Framework

Current regulations are not adapted to the future needs of the coming structure of the power grids made from microgrids, nanogrids, and picogrids. Traditional distribution networks are passive networks with unidirectional power flows where DG is considered as a passive element connected to the grid according to a "fit and forget" paradigm.

For this reason, the business models of the DSO needs a change in the existing regulatory context. Furthermore, the role of the prosumers has to be clarified.

In the picogrid, final consumers will have the capability of changing their consumption through DR programs. The benefits from DR programs will be for the retail companies; however, the consumers will obtain these benefits only when changes in the current laws are established Conchado and Linares [42].

Currently, the majority of the EU member states are changing their traditional regulation to new schemes based on incentives and penalties. This transition is caused by the penetration of RES at the distribution level. This section deals with the new laws, tariffs, and the economic effects related to higher levels of DG in the traditional distribution system.

4.5.1 Financial Effects on DSO Costs

The regulations of the EU countries do not address the role of the DSO in the active management that would allow to obtain benefits from DG for the grid, such as voltage support, reduction of power losses, network infrastructure upgrades, and improved power quality and reliability [43].

In the DG-GRID project, [44] reports a number of financial effects produced by the increase of DG in the UK and Finnish systems, divided in two groups:

- Network costs (CAPEX): These costs include all the network reinforcements needed when high amounts of DG are connected to the grid [45]. Costs increase faster at higher levels of DG penetration than at lower levels where the costs are almost negligible. This fact is due to the increase in the number of violated feeders [44]. Active network managements imply lower costs than passive network managements in any case, as shown in Cao et al. [44]. However, electricity flows from higher voltage levels are reduced, and therefore, lower investments in equipment replacement are required [45].
- Operational costs (OPEX): The energy losses decrease with low DG penetration because the generation is consumed by the local demand, but they can rise for higher penetration where the generation exceeds the local consumption [44]. When the active network management is applied, this tendency is intensified due to the smaller sizes of the feeder lines. Furthermore, with an active network management and high DG penetration, the operational costs increase because of the curtailment payments (payments to curtail DG in order to balance demand and generation), see for example [43].

These results mean that DG penetration involves expenditures in the power system, and thus, compensation mechanisms for DSO have to be developed taking into account the level of penetration of DG.

The conclusion extracted from Jansen et al. [43] is that passive approaches involve oversized distribution networks because the reinforcements are done for the worst operation conditions, and this implies more interventions of the DSO. However, an active management approach is better from the DSO perspective because planning and operation are considered together, and thus, OPEX and CAPEX can be reduced.

4.5.2 Distribution Network Planning and Charges

The successful expansion of DG based on RES relies on the existence of the appropriate business models that clarifies the roles of the different agents and regulates and facilitates the existent business opportunities, since badly designed models could make potential investments as non profitable.

In this sense, the penetration of RES involves the variation and regulation of the functions of many of the main involved agents.

DSOs should adapt their planning and operational procedures to deal with the appearance of active users or prosumers (consuming or generating with DG) in the network. For example, in Spain, the DSOs have currently the obligation to connect all the DG units to the network. For this reason, upgrades of the network are built to overcome the worst conditions, whose costs are recovered through the connection charges [46].

Future expansion plans of DSOs should consider at least two scenarios according to CNE [47]: peak generation and peak demand. In addition, DSOs should compute the net benefit of integrating DG at each possible grid location. New distribution grid codes can provide DSOs with the right economic signals in terms of incentives or penalties to promote an efficient grid expansion, for example to reduce losses, minimize ancillary requirements, or improving the quality of service.

According to Trebolle et al. [48], this incentives and penalties could be achieved using bilateral contracts between DG and DSOs where some references values should be set. These agreements, where the DG offers a number of hours per year to be curtailed, could be done in organized local markets at DSO level. In this case, the regulator should design standards contracts to increase the transparency of the system.

DSO revenues are explained in Cossent et al. [49] where the revenues are separated in two concepts: connection charges and use of systems (UoS) charges. Connection charges do not include now upstream grid reinforcements and they are paid just once. Hence, the rest of the connection charges are paid by use of system charges which are periodically paid by consumers, or if the country laws allow it, by DG. These UoS charges allow including time and geographical differentiations. The large penetration of solar or other DG could increase the DSO costs, but customer's storages or DR might reduce networks costs. Hence, DG UoS charges could be either positive or negative. Thus, for instance, in certain times and in certain areas, there could be a DG being paid by the DSOs for the reduction in the distribution system costs. The different voltage and consumption levels at the point of connection allow time differentiation in UoS charges. Geographical differentiation charges could be done if the country legislation allows charging with different tariffs to the end users.

As mentioned in Cossent et al. [49], there are three types of connection charges: the connection charges that only include the cost of connecting the DG unit to the nearest point in the distribution network, known as shallow connection charges, the connection charges called deep connection charges that include the

costs of grid reinforcements at distribution and transmission levels, and a mix of both types, commonly referred as shallowish connection charges. This last type contains direct connection costs and a proportional part of the reinforcement costs. A trade-off position between incentivizing the DG penetration with shallow connection charges, and a purely cost position with deep connection charges have to be reached.

4.5.3 Changes for Demand Response

In the active distribution grids (networks with demand participation), the consumers play an important role through DR programs. DR programs can only work if a large-scale deployment of SM and an advanced metering infrastructure is installed [50]. Hence, the regulatory framework needs to offer incentives in order to make attractive the replacement of the old meters with SM by DSOs. Once the SM have been installed replacing the old devices, DR programs involving DSOs, consumers, retailers, and regulator must be put in place.

In addition, a change in consumers' behavior is needed. This change of mind of the consumers could be achieved with home energy management and home automation systems. Information programs have to be developed by retailers to promote an active role of the consumers. Another key issue to obtain an active participation from the consumers is to provide them with real electricity prices, showing up end users incentives to flatten the demand curve.

The policy-makers have to develop a new regulation at the same time as the new business models take place, in order to increase the development of the smart grid paradigm.

5 Conclusions

In this chapter, a comparison of different common RES has been carried out and an analysis of the renewable economic feasibility inside the SMCT has been performed.

Many renewable energy (RE) technologies can be successfully implemented in the SMCT. For these projects, solar PV panels and WT are the preferred choices for electric production. Solar thermal collector and air source HP are frequently used for thermal energy needs. Nevertheless, other relevant renewable and nonrenewable yet efficient sources, such as combined heat and power (CHP), should not be overlooked.

Energy storage in distributed generation systems not only tries to mitigate the problems caused by the intermittency of renewable sources, but also gives new opportunities of interaction with the grid, such as load balancing and demand response, further improving the benefits of the renewable technologies. However, battery price is still relatively high, and under static tariff scenarios, little benefit

can be achieved from these systems. In this study, an hourly discrimination tariff was considered, allowing the battery system to charge with cheap energy and use it when the price increases. Similarly, profitability of HP technologies is highly dependent on energy prices. The COP in the HP must be higher than the ratio between electricity/natural gas prices in order to be economically feasible.

The constant decrement of costs in RE systems, in addition to the increasing price of energy, has derived in the profitability of RE in many applications; however, the adequate scaling of these systems, given the demand and geographical characteristics, is of prime importance in the economic feasibility analysis.

Results shown in this chapter have proved that the use of DG such as PV and batteries is profitable with the integration of RES in cities. However, high penetration of RES requires changes in the structure of the power system. A new paradigm is needed to compensate the transition to this new structure, which includes changes that goes from new business models and new regulatory frameworks to new topologies of the power grid.

In the physical layer, it is necessary to deploy advanced metering infrastructure in order to obtain more knowledge about the energy flows inside the electric system. In addition, power electronics is necessary to obtain the correct senoidal form, although, there is a debate about the use of DC inside the households. Using the concepts of picogrid, nanogrid, and microgrid, the use of RE in the distribution level will be possible and provide benefits. The main advantages of the future power system will be allowing isolated operations, cost reduction, and more reliability and quality of supply as well as more flexibility.

The communication layer is a key factor in the concept of SMCTs. The exchange of information inside the smart grid is essential to improve the real-time knowledge of the grid. The use of different area networks at the different levels of the future structure helps to manage the big amount of data. In addition, the transmission and security characteristics of the communication protocols have to be investigated with the objective of choosing the best one for each network.

The last layer is the intelligence layer where the support decision systems are located. These systems could be local systems or global intelligence systems depending on the complexity of the problems faced. These systems are preferably implemented as MAS where each agent has a set of defined tasks. The advantages and disadvantages of the centralized and distributed control have been explained, mainly showing that distributed systems are easier to develop gradually, more flexible and easier to maintain, but do not profit of economies of scale and tend to perform less optimally.

New structures require new business models. New agents such as prosumers, PA, and MGOs will appear, and thus, new business models need to be developed for these agents. A business model has been proposed in this context where the main aspect is that the distribution activity is unbundled from supply. Unbundling these two sectors is a key aspect which allows the business of the PAs, key agents for selling and buying energy to prosumers, selling ancillary services, and providing load-levelling services. Two business models are proposed, based on a centralized PA centered approach, or in a more decentralized approach more prosumers centered.

Finally, the integration of RES in the SMCT entails changes in the current laws and associated financial effects. The development of a smart grid needs changes in the regulation at the same time that new business models (or agents) appear. For instance, incentives and penalties have to be developed in order to increase the penetration of DG and to promote DR programs. These changes will transform the current distribution grid into an active distribution grid where RES will play a key role.

References

1. Anthopoulos L, Fitsilis P (2010) From digital to ubiquitous cities: defining a common architecture for urban development. In: Sixth international conference on intelligent environments, Kuala Lumpur, Malaysia, pp 301–306, 19–21 Jun 2010
2. Parkinson S, Wang D, Djilali N (2012) Toward low carbon energy systems: the convergence of wind power, demand response, and the electricity grid. In: IEEE innovative smart grid technologies—Asia (ISGT Asia), Tianjin, China, 21–24 May 2012
3. Méndez VH, Riviera J, de la Fuente JI, Gómez T, Arceluz J, Marín J, Madurga A (2006) Impact of distributed generation on distribution investment deferral. Int J Electr Power Energ Syst 28(4):244–252
4. Fernández IJ, Calvillo CF, Sánchez-Miralles A, Boal J (2013) Capacity fade and aging models for electric batteries and optimal charging strategy for electric vehicles. Energy 60:35–43
5. TREI (2013) Texas renewable energy industries association. http://www.treia.org/renewable-energy-defined. Accessed Jan 2014
6. Giraud F, Salameh ZM (2001) Steady-state performance of a grid-connected rooftop hybrid wind-photovoltaic power system with battery storage. IEEE Trans Energ Convers 16(1):1–7
7. Kalogirou A (2004) Solar thermal collectors and applications. Prog Energ Combust Sci 30(3):231–295
8. Usaola J (2012) Operation of concentrating solar power plants with storage in spot electricity markets. IET Renew Power Gener 6(1):59–66
9. Braunstein A, Kornfeld A (1986) On the development of the solar photovoltaic and thermal (PVT) collector. IEEE Trans Energ Convers EC-1 4:31–33
10. Brenden RK, Hallaj W, Subramanian G, Katoch S (2009) Wind energy roadmap. In: Portland international conference on management of engineering technology, PICMET 2009, Portland, Oregon USA, pp 2548–2562, 2–6 Aug 2009
11. Karekezi S, Lata K, Coelho ST (2004) Traditional biomass energy-improving its use and moving to modern energy use. Secretariat of the international conference for renewable energies. http://www.ren21.net/Portals/0/documents/irecs/renew2004/Traditional%20Biomass%20Energy.pdf. Accessed Jan 2014
12. European Biofuels Technology Platform (2013) Biofuels legislation in Europe. http://www.biofuelstp.eu/ legislation.html. Accessed Jan 2014
13. Hammons TJ (2003) Geothermal power generation worldwide. In: Proceedings of the power tech conference, Bologna, Italy, 23–26 Jun 2003
14. Mancarella P, Chicco G (2011) CO_2 emission reduction from sustainable energy systems: benefits and limits of distributed multi-generation. In: The second international conference on bioenvironment, biodiversity and renewable energies, Venice/Mestre, Italy, 22–27 May 2011
15. EPA (2013) US CHP technologies. http://www.epa.gov/chp/technologies.html. Accessed Jan 2014
16. Calvillo CF, Sánchez-Miralles A, Villar J (2013) Distributed energy generation in smart cities. In: International conference on renewable energy research and applications (ICRERA), Madrid, Spain, 20–23 Oct 2013

17. Calvillo CF, Sánchez-Miralles A, Villar J (2013) Evaluation and optimal scaling of distributed generation systems in a smart city. In: 8th international conference on urban regeneration and sustainability, Putrajaya, Malaysia, 2–6 Dec 2013
18. REE (1998) Red Eléctrica de España Proyecto INDEL: Atlas de la Demanda Eléctrica Española. http://www.ree.es/sites/default/files/downloadable/atlas_indel_ree.pdf. Accessed Jan 2004 (In Spanish)
19. Boroyevich D, Cvetkovic I, Dong D, Burgos R, Wang F, Lee F (2010) Future electronic power distribution systems a contemplative view. In: 12th international conference on optimization of electrical and electronic equipment (OPTIM) 2010, Brasov, Romania, p 1369, 20–22 May 2010. doi:10.1109/OPTIM.2010.5510477
20. Adda R, Ray O, Mishra SK, Joshi A (2013) Synchronous-reference-frame-based control of switched boost inverter for standalone DC nanogrid application. IEEE Trans Power Electron 28(3):1219–1233
21. Ray O, Mishra S (2013) Boost-derived hybrid converter with simultaneous DC and AC outputs. IEEE Trans Ind Appl doi:10.1109/TIA.2013.2271874. Accessed Jan 2014
22. Ancillotti E, Raffaele B, Conti M (2013) The role of communication systems in smart grids: architectures, technical solutions and research challenges. Comput Commun 36(17–18): 1665–1697
23. Niyato D, Xiao L, Wang P (2011) Machine-to-machine communications for home energy management system in smart grid. IEEE Commun Mag 49(4):53–59
24. Gungor VC, Sahin D, Kocak T, Ergut S, Buccella C, Cecati C, Hancke GP (2013) A survey on smart grid potential applications and communication requirements. IEEE Trans Ind Inf 9(1):28–42
25. Brown J, Khan JY (2013) Key performance aspects of an LTE FDD based smart grid communications network. Comput Commun 36(5):551–561
26. Usman A, Shami SH (2013) Evolution of communication technologies for smart grid applications. Renew Sustain Energ Rev 19:191–199
27. Dae-Man H, Jae-Hyun L (2010) Smart home energy management system using IEEE 802.15.4 and ZigBee. IEEE Trans Consum Electron 56(3):1403–1410
28. ZigBee Alliance (2013) ZigBee smart energy standard [Online]. http://www.zigbee.org/Standards/ZigBeeSmartEnergy/Overview.aspx. Accessed Jan 2014
29. Yu L (2011) Multicast DNS in wireless ad-hoc networks of low-resource devices techniche universiteit Eindhoven, Department of mathematics and computer science. http://alexandria.tue.nl/extra1/afstversl/wsk-i/luyu2012.pdf. Accessed Jan 2014
30. ROLL (2008) Working group routing over low power and lossy networks. http://datatracker.ietf.org/wg/roll/charter/. Accessed Jan 2014
31. ISA (2013) International society of automation ISA. http://www.isa.org//MSTemplate.cfm?MicrositeID=1134&CommitteeID=6891. Accessed Jan 2014
32. OGEMA (2013) OGEMA (open gateway energy management alliance). http://www.ogema.org. Accessed Jan 2014
33. E-Energy (2013) Modellstadt Mannheim model city Mannheim project. http://www.modellstadt-mannheim.de/moma/web/en/home/index.html. Accessed Jan 2014
34. Wooldridge M, Weiss G (1999) Intelligent agents. In: Multi-agent systems. MIT Press, Cambridge, p 3
35. Colson CM, Nehrir MH (2011) Algorithms for distributed decision-making for multi-agent microgrid power management. IEEE power and energy society general meeting, Detroit, Michigan, USA, 24–29 July 2011
36. Su W, Wang J (2012) Energy management systems in microgrid operations. Electr J 25(8):45–60
37. Planas E, Gil-de-Muro A, Andreu J, Kortabarria I, Martínez de Alegría I (2013) General aspects, hierarchical controls and droop methods in microgrids: a review. Renew Sustain Energ Rev 17:147–159

38. Hatziargyriou ND, Dimeas A, Tsikalakis AG, Oyarzabal J, Pecas Lopes JA, Kariniotakis G (2005) Management of microgrids in market environment. In: International conference on future power systems, Amsterdam, Netherlands, 16–18 Nov 2005
39. Smitha SD, Chacko FM (2013) Intelligent energy management in smart and sustainable buildings with multi-agent control system. In: 2013 international multi-conference on automation, computing, communication, control and compressed sensing (iMac4s), Kerala, India, pp 190, 195, 22–23 Mar 2013
40. Wang L, Wang Z, Yang R (2012) Intelligent multiagent control system for energy and comfort management in smart and sustainable buildings. IEEE Trans Smart Grid 3(2):605–617
41. Zhao P, Suryanarayanan S, Simoes MG (2013) An energy management system for building structures using a multi-agent decision-making control methodology. IEEE Trans Ind Appl 49(1):322–330
42. Conchado A, Linares P (2008) Gestión activa de la demanda eléctrica doméstica: beneficios y costes. http://gad.ite.es/docs/20100121_iit_comillas.pdf. Accessed Jan 2014 (in Spanish)
43. Jansen JJ, Welle AJ, Joode J (2007) The evolving role of the DSO in efficiently accommodating distributed generation. DG-GRID: intelligent energy Europe. http://www.ontario-sea.org/Storage/28/1950_The_Evolving_Role_of_the_DSO_in_Efficiently_Accommodating_Distributed_Generation_.pdf. Accessed Jan 2014
44. Cao DM, Pudjianto D, Strbac G, Martikainen A, Kärkkäinen S, Farin J (2006) Costs and benefits of DG connections to grid system, DG grid report D8. https://www.ecn.nl/fileadmin/ecn/units/bs/DG-GRID/Results/WP3/d8_cao_costs-and-benefits-of-dg-connections-to-grid-system.pdf. Accessed Jan 2014
45. Frías P, Gómez T, Rivier J (2008) Integration of distributed generation in distribution networks: regulatory challenges. In: 16th power systems computation conference, Glasgow, Scotland, UK, 14–18 July 2008
46. Cossent R, Gómez T, Olmos L (2011) Large-scale integration of renewable and distributed generation of electricity. Energ Policy 39:8078–8087
47. CNE (2009) Proposal for basic electricity distribution grid codes. http://www.cne.es/cne/doc/publicaciones/cne112_09.pdf. Accessed Jan 2014
48. Trebolle D, Gomez T, Cossent R, Frias P (2010) Distribution planning with reliability options for distributed generation. Electr Power Syst Res 80(2):222–229
49. Cossent R, Gómez T, Frías P (2009) Towards a future with large penetration of distributed generation: is the current regulation of electricity distribution ready? Regulatory recommendations under a European perspective. Energy Policy 37:1145–1155
50. Conchado A, Linares P (2012) The economic impact of demand-response programs on power systems. A survey of the state of the art. In: Sorokin A, Rebennack S, Pardalos PM, Iliadis NA, Niko A, Pereira MVF (eds) Handbook of networks in power systems I. Springer, Berlin Heidelberg, pp 281–301
51. MIT Energy Initiative (2011) The future of the electric grid. http://web.mit.edu/mitei/research/studies/documents/electric-grid-2011/Electric_Grid_Full_Report.pdf. Accessed Jan 2011

Analysis of the Impact of Increasing Shares of Electric Vehicles on the Integration of RES Generation

Andres Ramos, Kristin Dietrich, Fernando Banez-Chicharro, Luis Olmos and Jesus M. Latorre

Abstract This chapter analyzes the medium-term operation of a power system in several future scenarios that differ in the level of penetration of electric vehicles (EVs) and how renewable energy sources (RES) can be safely integrated in the former. The analysis is performed for different vehicle charging strategies (namely dumb, multi-tariff, and smart). The analysis is based on results produced by an operation model of the electric power system where the charging of EVs is being considered. Vehicles are regarded as additional loads whose features depend on the mobility pattern. The operation model employed is a combination of an optimization-based planning problem used to determine the optimal day-ahead system operation and a Monte Carlo simulation to consider the stochastic events that may happen after the planning step. The Spanish electric system deemed to exist in 2020 is used as the base-case study for conducting the numerical analyses. Relationships among the share of EVs (relative to the overall number of vehicles), the amount of RES generation integrated, and relevant system performance indicators, such as operation cost, reliability measures, and RES curtailment, are derived in the case study section.

Keywords Electric vehicles • Medium-term operation planning • Operating reserves • Renewable energy sources • Wind • Photovoltaic

1 Introduction

The commitment to turn our economy into a low-carbon one and the increase in the share of energy consumption coming from renewable energy sources (RES) is one of the European priorities in the long term. Limitation of fuel availability,

A. Ramos (✉) · K. Dietrich · F. Banez-Chicharro · L. Olmos · J. M. Latorre
Instituto de Investigación Tecnológica, Universidad Pontificia Comillas,
Alberto Aguilera 23, 28015 Madrid, Spain
e-mail: Andres.Ramos@upcomillas.es

M. A. Sanz-Bobi (ed.), *Use, Operation and Maintenance of Renewable Energy Systems*, Green Energy and Technology, DOI: 10.1007/978-3-319-03224-5_11,

climate change, and foreign resources dependency are major drivers of these priorities. Supporting schemes at national level have been used for promoting RES integration. Thus, solar photovoltaic and, mainly, wind generation have strongly increased their production in many European countries, see in [1, 2] the latest production data. However, these generation resources have an important restriction: their intermittency (i.e., variability and uncertainty) and limited controllability. The availability of some types of resources is hard to predict and to control, especially for wind generation, see [3, 4].

The integration of RES in the electric power system can be facilitated by the use of batteries (i.e., EV) that combine flexibility in their electricity consumption and storage capability. They can adapt their load profile to different system conditions and even provide some other energy services to the system [5].

In this chapter, we analyze the operation of an electric power system with a high percentage of RES generation and the impact that EV operation may have on improving the integration of this generation. The analysis is based on the use of a medium-term operation model that allows determining the technical and economic impact of EVs, see [6]. The model reproduces the competitive market system operation over a year. In particular, EVs are modeled as additional electricity consumers that can flexibly charge their batteries.

The focus of the chapter is to present a detailed quantitative analysis of the relationships between the levels of EV penetration and RES integration achieved. The operation model employed considers RES forecast errors and different EV charging strategies. Relationships derived concern how increasing shares of EVs and RES generation integrated affect relevant system performance indicators, such as operation cost, reliability measures, and RES curtailment. This quantitative analysis focuses on the large-scale Spanish power system. Results show that, in general, EVs contribute to decrease RES energy curtailment, especially for larger amounts of EVs. Curtailment levels are even further reduced when smart charge of EV batteries is considered. System operation costs augment due to the demand increase caused by EV consumption, but this increase is limited if smart charge is in place.

The remainder of this chapter is structured as follows. Section 2 provides an overview of the medium-term operation model which is used to simulate system operation as well as EV and RES impact on this system. Section 3 elaborates on the methodology applied to examine the improvement in RES integration due to EV electricity consumption. The case study and the results are presented in Sect. 4. Finally, Sect. 5 concludes.

2 Operation Model Description

The introduction of EVs and RES generation in the electric system operation is simulated by means of a medium-term model: the Reliability Operation Model (ROM) for RES (http://www.iit.upcomillas.es/aramos/ROM.htm). The detailed description of the model can be found in [6, 7]. In this section, we just give a brief overview of it.

This optimization model computes the *unit commitment* (UC) and *economic dispatch* (ED) of the system throughout a year (scope), considering the day as the time frame and an hour as the time unit. Computing the hourly operation of the system is required to appropriately represent the time variation of consumption and output of the generation technologies (including RES). As we consider that the system operation variables are constant within an hour, power is converted into the amount of energy corresponding to a time unit by multiplying this power by 1 h. Therefore, power and energy per time unit values are the same. The chronology of daily operation decisions over the whole year is kept. Consequently, the initial states of the generating units for every day are those in the last hour of the previous day.

The model follows a unique combined modeling approach that replicates the sequence of planning and real-time operation decisions that are made in power systems, from the system operator's (SO) point of view. Figure 1 presents an overview scheme of the model implementation. A daily optimization problem is solved to compute the UC and the ED for each day, considering the demand and forecasted (expected) RES power production one day in advance. This represents the outcome of the day-ahead market. Day-ahead estimates may differ from realizations of uncertain parameters (e.g., electricity demand, RES generation forecast error, and forced outages of thermal generators), which are taken into account by a Monte Carlo simulation model that modifies the day-ahead schedule to correct power imbalances caused by stochastic events. The outcome of this stage represents the real-time operation of the system. The model considers the chronology in the system operation over the whole year, running sequentially the 365 days of it, and being able to capture RES variability and forecast errors.

Weekly hydro scheduling, such as the daily hydro production or pumping, is determined endogenously by the model following an heuristic criterion. Although the model can consider the transmission network, for the purpose of the analyses presented in this chapter, it is assumed that the network is not affecting the system operation.

Results of the model include, among others (thermal and hydro) generation output, RES curtailment, pumped storage hydro usage, reliability measures, system marginal costs, fuel consumption, and CO_2 emissions.

2.1 Optimization Model Formulation

The operation planning step has the structure of a mixed-integer optimization problem that decides the optimal operation of the system including EV consumption and RES generation power production.

The main variables are commitment, start-up and shutdown of thermal units, electric energy output, upward and downward reserve power of each thermal and hydro generator, energy not served, consumption of pumped storage hydro plants, reservoir level and spillage of each hydro reservoir, and RES generation output and curtailment.

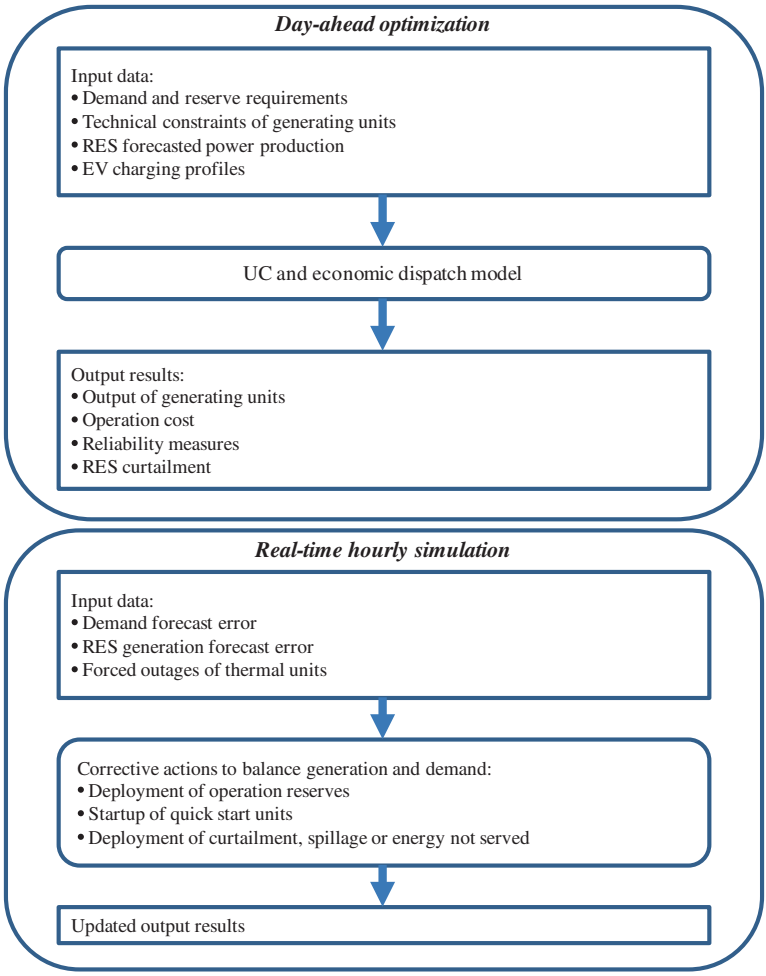

Fig. 1 General overview of the ROM model

Objective function

The objective function is to minimize the operation costs plus some penalty costs associated with the violation of some constraints.

Demand and reserve constraints

The balance of generation and demand for each hour involves the output of thermal, hydro, pumped storage hydro, and RES on the generation side, and the consumption of pumped storage hydro plants and EVs on the demand side.

Upward and downward reserve constraints

The operation reserve for each hour is provided by thermal units, hydro and pumped storage hydro plants. A reserve deficit variable is introduced that is penalized in the objective function.

Thermal unit constraints

The commitment, start-up, and shutdown of thermal units are linked by a logical constraint that sets the state of each unit as a function of these variables.

The power production offered in the energy market plus the power reserve offered as operating reserve by each thermal unit is bounded by the maximum output of the unit.

The unit variation output, including the mobilization of upward and downward power reserves, are limited by up and down hourly ramps relating the unit output in consecutive hours.

Hydro plant constraints

The output, including the mobilization of the upward power reserve, of each hydro plant is bounded by the maximum output of the plant. The model ensures that a hydro plant cannot be generating while it is pumping.

The inventory of the hydro reservoir is updated considering natural inflows, consumption and generation of the storage hydro plant, and possible water spillages.

3 Methodology Applied in the Analysis

In order to quantify the effect that the use of EVs has on the share of RES in the electric system, we have identified some key performance indicators (KPI) that follow as the most relevant:

- System production and operation cost, mainly associated with the variable production cost of thermal units.
- System reliability, measured by the expected energy not served (EENS) and the loss of load probability (LOLP).
- RES curtailment, as an indicator of the level of RES integration.

We have studied two different scenarios regarding the EV penetration levels, namely one featuring 0.3 and another one featuring 1.7 million EVs, which correspond to about 1 % of the total vehicle fleet and to future estimates by the Spanish Government of existing EVs in the year 2020, respectively.

EVs are considered as additional demand in the electric system and are provided as input data. Different EV charging strategies are employed for the quantitative analyses presented in this chapter:

- Smart strategy. The SO decides when EVs can be recharged, taking into account their feasible connection profiles. For this strategy, it is assumed that total EV consumption is centrally managed by aggregators (or energy services providers) that represents the SO point of view. These aggregators are able to manage the EV charge to minimize their costs, thus maximizing the efficiency of the power system operation, while allowing EVs to satisfy their mobility requirements[1] (time and distance of trips to be made).
- Multi-tariff strategy. The EV charge is directed to off-peak hours, when electricity tariffs are cheaper.
- Dumb strategy. The EV charge is mainly performed when arriving at home.

A similar quantitative analysis of the impact on the system operation of the EV charging strategies for several European countries, including Spain, is done in [8].

The power system operation is computed considering always the same system requirements but several amounts of EVs and charging strategies. A first set of analyses is made to compute the main impacts of EV integration on the KPIs defined. Then, several combinations of increases in EV penetration and installed RES generation capacity that result in constant values for the KPIs previously selected are identified. The latter results allow us to draw four types of curves depending on the indicator that is kept constant with the increase in the level of EVs and RES generation installed: iso-operation-cost curve, iso-EENS curve, iso-LOLP curve, and iso-RES-curtailment curve. In other words, these curves indicate the amount of EVs that is necessary to integrate more RES generation while the corresponding indicators remain constant.

4 Case Study

A case study focused on the Spanish electric system in 2020 is analyzed to determine the operation and economic impact of different EV shares in the system. The contribution of the EV to the integration of RES is also determined. The Spanish system is paradigmatic due to the significant RES share it features. For example, wind generation represented 22.2 % of the installed generation capacity and 21.1 % of the electric energy generated in 2013, see [9]. This is more than for any other generation technology. Moreover, Spain has limited cross-border interconnection capacity with neighbors, which means that the system is essentially operated as isolated.

[1] The mobility requirements are established by the vehicle owners, which decide when they need to travel in their vehicles.

Table 1 Main characteristics of the electric system

Demand and reserve		
Annual energy	331	TWh
Winter peak	58,000	MW
Summer peak	53,000	MW
Minimum load	28,450	MW
Peak/off-peak ratio	2.0	p.u.
Max upward reserve required	5,530	MW
Max downward reserve required	1,160	MW
Net installed capacity		
Nuclear	7,000	MW
Coal	7,113	MW
CCGT	24,491	MW
Gas turbines	301	MW
Hydro	16,692	MW
Pure pumped storage hydro	5,185	MW
Combined pumped storage hydro	2,884	MW
Wind generation	34,820	MW
Solar PV	6,250	MW
Solar thermal	3,810	MW
CHP	10,310	MW
Other RES	4,460	MW
Annual natural hydro inflows	27.9	TWh
Price		
Nuclear	0.002	€/Mcal
Coal	124.7	$/short tons
Natural gas	11.0	$/MMBTU
CO_2	30	€/t CO_2

The big impact that RES variability has on the operation of the system is taken into account by considering hourly series of RES generation. Separate series are taken for wind, solar photovoltaic and solar thermal, combined heat and power (CHP), and other RES (such as biomass and small hydro plants). For wind generation, which is the main RES technology, the forecast error is also taken into consideration. RES generation output series are estimated using hourly historical production profiles which are extrapolated to the year 2020 based on the forecasted installed generation capacity of each RES technology. Hourly demand profiles are also estimated extrapolating historical data to the year 2020 based on its forecasted energy and peak demand. The main data of the case study are based on the electric system forecast by the Government for 2020 [10].

Table 1 summarizes the main characteristics of our case study. As aforementioned, three EV charging strategies are analyzed: smart, dumb, and multi-tariff. Smart charging can improve the electric system operation conditions by increasing off-peak loads (essentially from 3 to 7 a.m. acting as a valley filling mean) and thus allowing the achievement of higher RES integration levels. Dumb strategy application results in charges of EVs from 17 up to 23 h. In the multi-tariff scheme, EVs are charged in off-peak hours, with a sudden peak at 2 a.m.

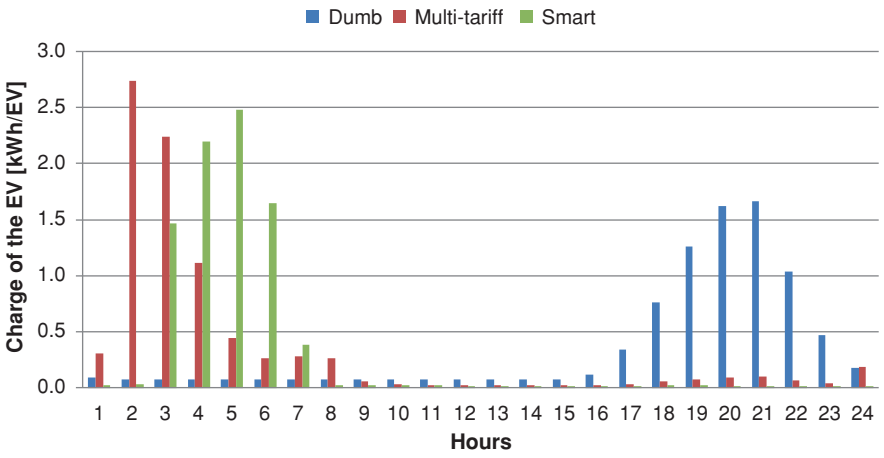

Fig. 2 EV charging strategies

Figure 2 presents the profile of these three charging strategies for a single EV on weekdays, when the user behavior is more predictable. However, over the weekend, due to the unpredictability of EV user constraints, only the multi-tariff strategy is applied.

System operation and cost

The increase in the amount of electric energy produced by the different technologies for 1.7 million EVs considering a smart charge of these, with respect to the situation where 0 EVs exist, is represented in Fig. 3. As it can be observed, mainly CCGTs, but also coal thermal units, increase their power production due to EV additional consumption. Also, small increases occur in wind generation output and in the use of pumped storage hydro plants.

Figure 4 shows changes in power production by technology for dumb and multi-tariff charging strategies with respect to the smart charging one, for 1.7 million EVs. The major changes are observed in pumped storage hydro production and consumption, and coal and CCGT power generation. Pumped storage hydro plants are used to improve system operation conditions, fundamentally by filling the valleys and clipping the peaks of the net load curve. EV smart charge has a valley filling effect. Therefore, pumped storage hydro plants are used more for dumb and multi-tariff EV charging strategies than for the smart one. The growth in pumped storage hydro usage implies an energy loss due to the fact that the efficiency of the pumping cycle is below 1 (about 0.7). This is covered by a net increase in coal and CCGT generation output, especially for the dumb charge strategy. CCGT generation is flexible and therefore is able to increase its production, while coal units reduce it.

The average cost of the electric energy produced increases by 4.7 % with 1.7 million EVs with respect to the case where no EV exists. This cost decreases

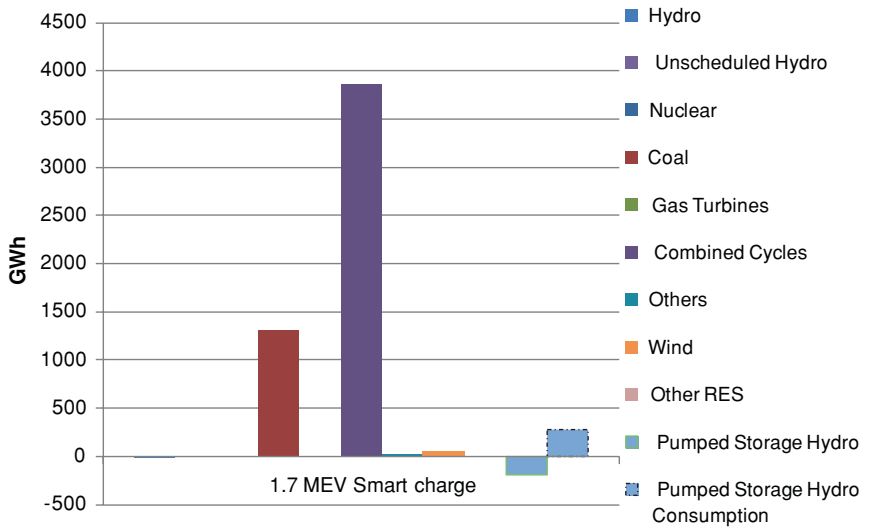

Fig. 3 Impact of smartly charged EVs on energy produced by different technologies

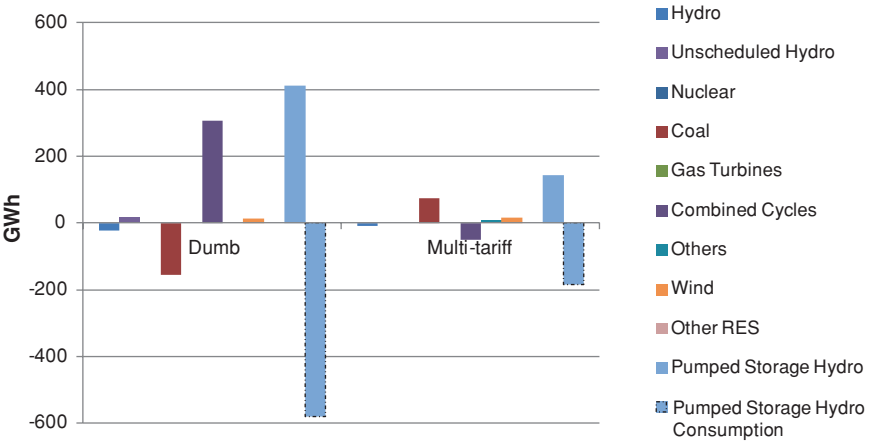

Fig. 4 Impact on energy production by technology of the dumb and multi-tariff charging strategies with respect to values for the smart charge one, for 1.7 million EVs

with the efficiency of the EV charge process (for example, from dumb to smart), as can be seen in Fig. 5.

As previously mentioned, in order to create an iso-operation-cost curve, we have run the model for different combinations of EV penetration and installed wind generation capacity levels to identify those combinations that resulted in the same variable production cost. Additional wind generation installed has exactly

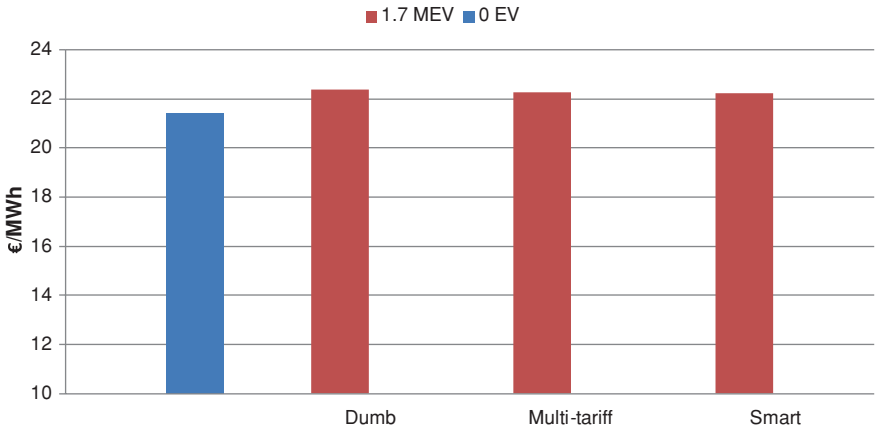

Fig. 5 Average cost of electric energy produced for each charging profile

the same characteristics as the one in the base case. Then, we have plotted the regression line linking these combinations. According to Fig. 6, the increase in the variable operation cost caused by 1 million EVs is compensated by the addition of about 425 MW of wind generation capacity (i.e., the slope of the regression line).

System reliability

Figures 7 and 8 show iso-EENS and iso-LOLP curves whose interpretation is similar to that of the iso-operation-cost curve above. The increase in the EENS caused by 1 million EVs can be offset by the addition of around 350 MW of wind generation capacity according to the iso-EENS curve, or 320 MW of this capacity according to the iso-LOLP curve.

RES and hydro energy integration

RES and hydro generation are renewables based and, therefore, all their primary energy resource must be used to the extent possible. RES energy curtailment is an indicator of how much renewable generation can be integrated into the system as EV shares increase. The extra annual amount of renewable generation that can be integrated into the system by increasing the number of EVs is shown in Fig. 9. Renewable generation output curtailment represents 0.8 % of total RES energy available when no EVs exists, and around 0.7 % for 1.7 million EVs. One can observe that each extra EV is enabling the integration, into the electric system, of around 80 kWh extra RES-based electricity, on average,[2] though numbers depend on the charging strategy. This compares with 3100 kWh of electricity consumed annually by each EV.

[2] It is computed as the ratio of the difference between renewable generation output curtailment with and without EVs to the number of EVs.

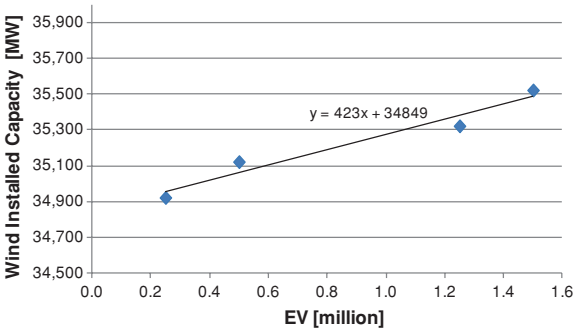

Fig. 6 Iso-operation-cost curve for different scenarios

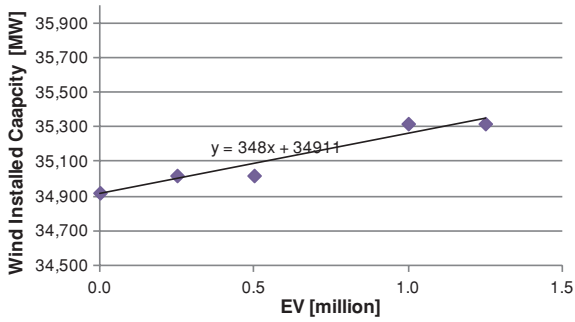

Fig. 7 Iso-EENS curve for different scenarios

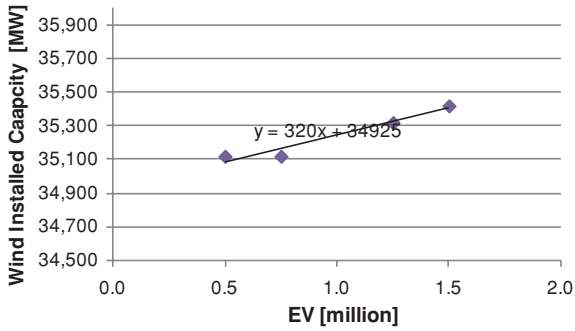

Fig. 8 Iso-LOLP curve for different scenarios

In Fig. 10, one can observe the profiles of the RES energy curtailment for the several charging strategies on (Monday–Friday) and (Saturday and Sunday) in the base case. They have been determined as the mean value, for each of the hours of the day, of the curtailment for the set of days classified as weekdays and weekends, respectively. It is clear that curtailment happens mainly at the weekend, when low demand coincides with high wind production.

Given that only on weekdays several charging strategies have been applied (at the weekend, the multi-tariff strategy is always used), we are comparing curtailment

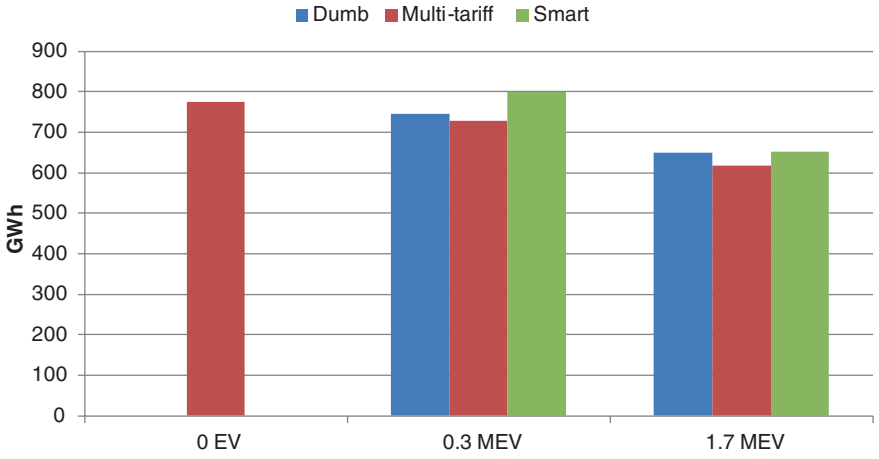

Fig. 9 Annual renewable generation output curtailment for different number of EVs and different strategies

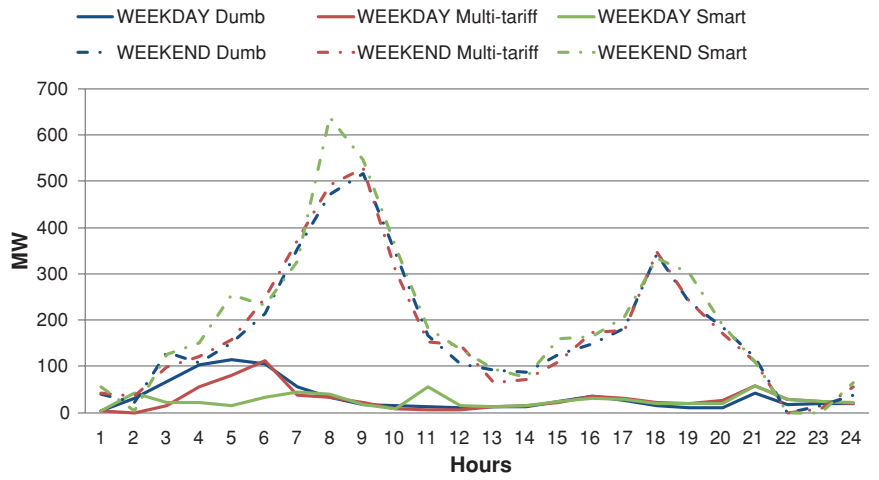

Fig. 10 Profile of renewable generation curtailment for weekends and weekdays, and the three charging strategies, in the base case

levels only for weekdays. One can observe in Fig. 11 the strong influence that the charging strategy has on spillages levels. As one could expect, curtailment levels decrease with the smartness of the charging strategy, i.e., from dumb to multi-tariff to smart charge.

We have also analyzed another case study characterized by a decrease in electricity consumption due to an increase in the efficiency of the use of energy. In this case, annual demand is 310 TWh compared to 331 TWh in the base case, though

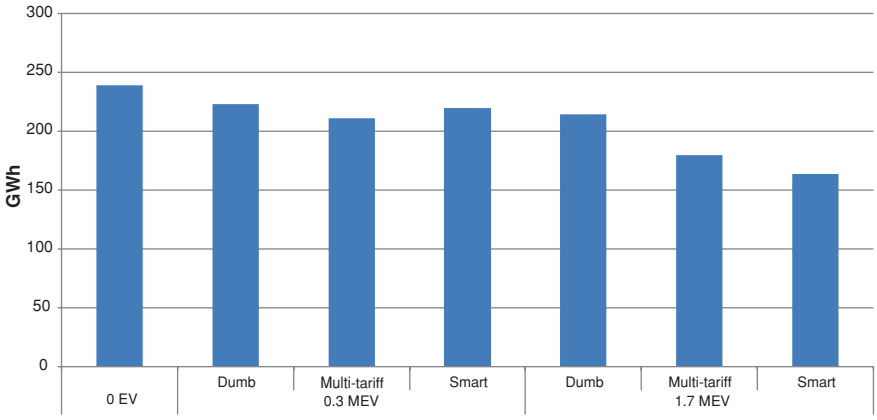

Fig. 11 Renewable generation curtailment on weekdays for the three charging strategies

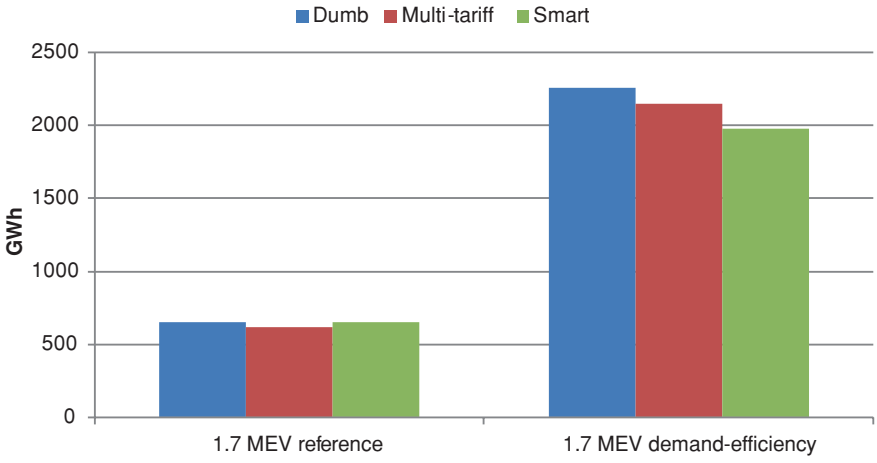

Fig. 12 Renewable generation curtailment for the reference case and the demand-efficiency case

the same winter and summer peaks exist. Figure 12 shows that curtailments in the demand–efficiency case increase significantly, from values of about 650 GWh for the reference case up to about 2100 GWh for the demand–efficiency case. As a consequence of the decrease in demand, the number of hours when thermal generation is at its minimum load increases and therefore the curtailment of renewable generation.

As expected, in the demand-efficiency case, the effect of EVs on the amount of renewable generation that can be safely integrated is stronger. One can observe in Fig. 13 that each extra EV is able to integrate in the electric system about 1,050 kWh of RES-based electricity, with specific levels depending on the charging strategy, instead of 80 kWh in the reference case.

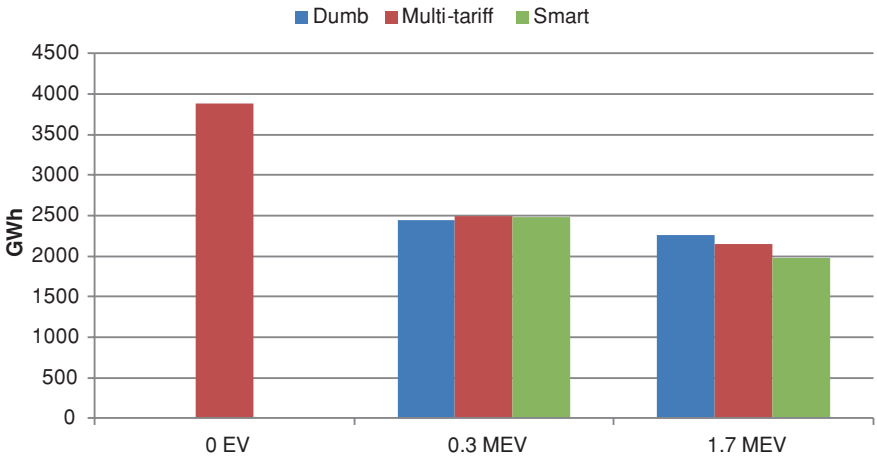

Fig. 13 Renewable generation curtailment for the demand-efficiency case

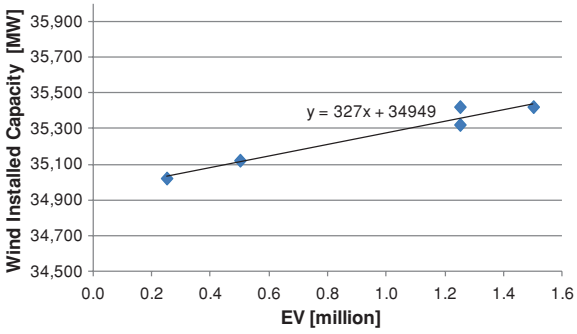

Fig. 14 Iso-renewable generation curtailment curve

From Fig. 14, one can draw the conclusion that 1 million EVs can integrate about 325 MW of additional wind generation capacity while the renewable generation curtailment is kept constant for the reference case.

5 Conclusions

This chapter has presented the results of the use of a medium-term operation model to analyze the impact of increasing shares of EVs on the system operation, including how the former can increase the amount of renewable generation integrated into the system.

System operation costs augment due to the demand increase caused by the EVs, but this increase is limited if smart EV charge is in place. Another important effect of EVs is the decrease in renewable generation output curtailment caused by the former. However, a relatively high number of EVs is required to notice such effect. RES energy curtailment diminishes when smart charging is applied.

From the point of view of the system operation cost, the renewable generation output curtailment, and reliability measures, the addition of 1 million EVs can be offset by the installation of 320–425 MW additional wind generation capacity, depending on the indicator.

Numbers computed are specific to the Spanish system, but they reflect the potential benefit that the addition of EVs may have for the integration of RES.

Acknowledgments This research has been partially funded by the Spanish CENIT-VERDE (http://cenitverde.es/) and European MERGE (http://www.ev-merge.eu/) projects.

References

1. EREC-European Renewable Energy Council (2009) Share of renewable electricity. http://www.erec.org/statistics/res-e-share.html. Accessed Jan 2014
2. EWEA-European Wind Energy Association (2013) Wind in power: 2012 European statistics. http://www.ewea.org/fileadmin/files/library/publications/statistics/Wind_in_power_annual_statistics_2012.pdf. Accessed Jan 2014
3. Fabbri A, Gómez San Román T, Rivier J, Méndez VH (2005) Assessment of the cost associated with wind generation prediction errors in a liberalized electricity market. IEEE Trans Power Syst 20(3):1440–1446
4. Smith JC, Milligan MR, DeMeo EA, Parsons B (2007) Utility wind integration and operating impact state of the art. IEEE Trans Power Syst 22(3):900–908
5. Kempton W, Tomić J (2005) Vehicle-to-grid power implementation: from stabilizing the grid to supporting large-scale renewable energy. J Power Sources 144(1):280–294
6. MERGE (2011) Functional specification for tools to assess steady state and dynamic behavior impacts, impact on electricity markets and impact of high penetration of EV on the reserve levels. Task 2.4 Deliverable 2.2. http://www.ev-merge.eu/. Accessed 2014
7. Ramos A, Latorre JM, Bañez-Chicharro F, Hernandez A, Morales-España G, Dietrich K, Olmos L (2011) Modeling the operation of electric vehicles in an operation planning model. In: 17th Power systems computation conference—PSCC'11, Stockholm, Sweden, 22–26 August
8. Banez-Chicharro F, Latorre JM, Ramos A (2014) Smart charging profiles for electric vehicles. Comput Manag Sci 11(1):87−110. doi: 10.1007/s10287-013-0180-8
9. REE-Red Eléctrica de España (2013) Avance del informe del Sistema Eléctrico español 2013 December 2013. http://www.ree.es/sites/default/files/downloadable/avance_informe_sistema_electrico_2013.pdf. Accessed Jan 2014
10. MIET-Ministerio de Industria, Energía y Turismo (2010) Plan de Acción Nacional de Energías Renovables de España (PANER) 2011–2020. http://www.mityc.es/energia/desarrollo/EnergiaRenovable/Paginas/paner.aspx. Accessed Jan 2014